A Genomic and Proteomic Investigation of the Plant Pathogen *Armillaria mellea*: Buried Treasure or Hidden Threat?

Cassandra Collins B.Sc.

NUI MAYNOOTH

Ollscoil na hÉireann Má Nuad

In fulfilment of the degree of

Doctor of Philosophy

Thesis submitted to the

National University of Ireland

Department of Biology

August 2013

Head of Department:

Professor Paul Moynagh

Supervisors:

Professor Sean Doyle

Dr. David Fitzpatrick

Table of Contents

Declaration of Authorship

This thesis has not previously been submitted in whole or in part to this or any other University for any other degree. This thesis is the sole work of the author, with the exception of:

A. mellea DNA extraction and species identification by Dr. Grainne O'Keeffe[a], genome sequencing by Dr. Thomas Keane[b] and Dr. Daniel Turner[b] and *A. mellea* gene identification and phylogenetic tree, genomic and proteomic database construction, by Dr. David Fitzpatrick[a].

[a]NUI Maynooth, Co. Kildare, Ireland.

[b]The Wellcome Trust Sanger Institute, Hinxton, Cambridge CB10 1SA, United Kingdom

Acknowledgements

I would like to thank my supervisor Professor Sean Doyle for all his help and mentoring from the time I first applied to study as an undergraduate, and who I regarded as a friend over the intervening years. Thanks to David Fitzpatrick for all his work on *Armillaria mellea* genomic and proteomic databases and whose door was always open to me. I would like to thank Thomas Keane and Daniel Turner from the Wellcome Trust, for their work on the sequencing of *A. mellea.*

Thanks to both the John and Pat Hume Scholarship and National University of Ireland Travelling Studentship, for funding my study and thanks to the HEA and HRB for LC-MS/MS facilities and HEA PRTLI-4 funding, necessary for completion of the project. Thanks to Dr. Kevin Kavanagh for supplying the human pathogenic species used in the course of this project.

Many thanks to Grainne O'Keeffe for her work on DNA extraction from *A. mellea* and for her help and encouragement when I started this study and throughout my PhD. Thanks are also due to Rebecca Owens who was so supportive during my study and during the writing of this thesis, and was another head helping me to get the best from our favourite machine. Many thanks to Karen and Lorna, although they are no longer in the lab, whose friendship is greatly appreciated, especially so while I was writing. Thanks to Lara for her support and encourgement although she was the "baby" in the lab, to Stephen (new), who appreciated my pivot tables, and Stephen (middle?) in Gary's lab. Thanks to all past members of the Biotech lab, including Stephen (old) who had six weeks to teach me everything, Luke, Carol, Natasha, and nearly Biotech people John Fallon and Karen Tomkins. Many thanks to the technical staff, especially Caroline, whose help went above and beyond the call of duty, and to Nick, who I could always call on to fix stuff. Thanks also to all of the lecturers who were always ready to help and to answer questions. Thanks are due to everyone in all of the other labs, always generous with their time, with "loans" of materials, and good fun at parties.

Thanks to my Mum and Dad, all my family and friends for their support and encourgement especially to Jody and Mark, who put up with me over the last few years, and thanks also to my favourite outlaws, Paddy and Caryn. Of course, my greatest appreciations is reserved for Dave, my wingman, without whom none of this would have happened, and who knows almost as much about *A. mellea* as I do.

Publications and Presentations

Research Publications

Collins, Cassandra; Keane, Thomas M.; Turner, Daniel J.; O'Keeffe, Grainne; Fitzpatrick, David A.; and Doyle, Sean (2013). Genomic and Proteomic Dissection of the Ubiquitous Plant Pathogen,*Armillaria mellea*: Towards a New Infection Model System. *Journal of Proteome Research* **12.** 2552-2570.

Oral Presentations

1. *Armillaria mellea* – Fruit Producers Nightmare or Buried Treasure? Society of Irish Plant Pathologists' Spring Scientific Meeting. NUI Maynooth, Friday 9th April 2010 Oral presentation.

2. Collins C. (2010) *Armillaria mellea* – Fruit Producers Nightmare or Buried Treasure? NUI Maynooth – 1st Year PhD Student Presentation. Maynooth, Co. Kildare. Date 27th May 2010. Oral presentation.

3. Life is sweet; new insights from protein mass spectrometry of *Armillaria mellea*. Waters Postgraduate Prize Symposium 2010.University College Dublin.27th January 2011. Oral presentation.

4. A shotgun BLAST to *Armillaria mellea's* secrets. NUI Maynooth – 2nd Year PhD Student Presentation. 2nd June 2011. Oral presentation.

5. Sweet secrets from a proteomic investigation of the honey fungus *Armillaria mellea*. Irish Fungal Society meeting, Trinity College, Dublin.16th June 2011. Oral presentation.

6. A Shotgun BLAST reveals *Armillaria mellea'*s Proteomic Secrets. Computational Biology and Innovation PhD Symposium UCD, Dublin. 6th December 2011. Oral presentation.

7. *Armillaria mellea* a plant pathogen under stress. Biology Research day. NUI Maynooth, 20th July 2012. Oral and poster presentation.

8. CSI Fungi. Laboratory seminar series, NUI Maynooth 19th February 2013. Oral presentation.

Poster Presentations

1. High-throughput DNA Sequencing and Proteomic Analysis of *Armillaria mellea* – Fruit Producers Nightmare or Buried Treasure? IMC9, Edinburgh. 5th August 2010. Poster presentation.

2. *Armillaria mellea* a plant pathogen under stress. 2nd Irish Fungal Society Meeting. Belfast City Hospital, 21st - 22nd June 2012. Poster presentation.

Abbreviations

◦C	Degrees centigrade
2-DE	2-Dimensional Polyacrylamide Gel Electrophoresis
4-HCCA	cyano-4-hydroxycinnamic acid
B2G	Blast 2 GO
BCA	Biocontrol agent
BLAST	Basic Local Alignment Search Tool
bp	Base pairs
BSA	Bovine serum albumin
CAZy	Carbohydrate active enzymes
cDNA	Complementary Dexoyribonucleic Acid
DMSO	dimethyl sulfoxide
DNA	Deoxyribonucleic acid
h	Hour
IEF	Isoelectric Focussing
IPS	InterProScan
Kb	Kilo-base
kDa	Kilo-Dalton
LC-MS/MS	Liquid chromatography mass spectrometry
MALDI-ToF	Matrix Assisted Laser Desorption Ionisation-Time of Flight
MEA	Malt extract agar
min	Minute
MM	Minimal Media
NCBI	National Centre for Biotechnology Information
OD	Optical Density
ORF	Open reading frame
PAGE	Polyacrylamide gel electrophoresis
PBS	Phosphate Buffered Saline
PBST	Phosphate Buffered Saline 0.05 % Tween
PCR	Polymerase Chain Reaction
PDB	Potato dextrose broth
Pfam	Protein families database of alignments
RNA	Ribonucleic acid
RP-HPLC	Reverse phase high performance liquid chromatography
SDS	Sodium Dodecyl Sulphate
TCA	Trichloracetic acid
TFA	Trifluoroacetic acid
TIGR	The Institute of Genomic Research
v/v	Volume per volume
WGS	Whole genome sequencing
w/v	Weight per volume

Summary

Armillaria mellea is a major plant pathogen of timber and agronomic crops. Yet, no large-scale "-omics" data are available to enable new studies, and limited experimental models are available to investigate basidiomycete pathogenicity. Herein it is revealed that the *A. mellea* genome comprises 58.35 Mb, contains 14473 gene models, of average length 1575 bp (4.72 introns/gene). A novel, large-scale proteomic shotgun analysis method, was developed for high-throughput proteomics, applicable to other *Armillaria* spp. and basidiomycete studies. Tandem mass spectrometry identified 951 mycelial (n = 629 unique) and secreted (n = 183 unique) proteins from *A. mellea*. Almost 100 mycelial proteins were either species-specific or previously unidentified at the protein level. Signal sequence occurrence was 4-fold greater for secreted (50.2%) compared to mycelial (12%) proteins. Analyses revealed a rich reservoir of carbohydrate degrading enzymes, laccases, lignin peroxidases and large cytochrome P450ome in the *A. mellea* proteome, reminiscent of both basidiomycete and ascomycete glycodegradative arsenals. Under oxidative stress, *A. mellea* underwent extensive proteome remodelling within 3 hours and comparative proteomics detected differentially regulated proteins (n = 14). Expression of proteins involved in methionine and polyamine biosynthesis (n = 2) and proteins (n = 2) involved maintenance of cellular homeostasis by regulation of homocysteine levels were significantly upregulated. This response may mitigate against oxidative cellular damage. Proteins (n = 2) putatively involved in the regulation of biosynthesis of specific polyamines were also identified. Remarkably, *A. mellea* exhibits a specific and significant killing effect against *Candida albicans* during co-culture. Proteomic investigation of this interaction revealed 205 secreted proteins, with the unique expression of defensive and potentially offensive *A. mellea* proteins (n = 30). Four proteins expressed in co-cultures were specific to *A. mellea*, or previously unidentified either by homology or at the protein level. Overall, the data reveal new insights into the origin of basidiomycete virulence, and a new model system for further studies aimed at deciphering fungal pathogenic mechanisms is presented.

Chapter 1 Introduction

1.1 General introduction

Recent developments in genome sequencing, RNA profiling, large-scale protein studies (proteomics), and the study of small molecules resulting from metabolic processes in organisms, have been enabled by new high-throughput technologies (Figure 1.1). These technologies, known as "-omics", when used together, can provide a dynamic profile of a microorganism; at different stages of its lifecycle, under stress conditions or when subject to nutritional restrictions, as well as a wider view of interactions between organisms (Jerez, 2007, 2008). This knowledge, combined with information in publicly available data repositories, informs our general understanding of biological processes, disease states, microorganism pathogenicity and virulence (Vincent *et al.*, 2012; Idnurm *et al.*, 2005; Yajima and Kav, 2006), and is used in many areas to facilitate drug discovery, develop pathogen-resistant plant varieties and aid the manufacture of industrial biotechnology products (Marchitti *et al.*, 2008; Perazzolli *et al.*, 2010; Hadibarata *et al.*, 2013). Fungi, in particular, have been the focus of study in recent years, as they are a potential source of novel enzymes and metabolites with demonstrable potential to satisfy the demand for new drugs, more eco-friendly industrial processes, bio-fuel production and bio-remediation (Bouws *et al.*, 2008; Lorenz and Zinke, 2005; Schuster and Schmoll, 2010; Grigoriev *et al.*, 2011). Consequently, this Introduction will comprise (i) a description of the fungal kingdom, (ii) recent outputs from high-throughput analysis of fungi from the phyla Ascomycota and Basidiomycota, (iii) Basidiomycota virulence and pathogenicity mechanisms, (iv) a detailed description of enzymes required for wood degradation by Basidiomycota, and (v) finally, relevant information on the current knowledge of *Armillaria* spp., and in particular, *Armillaria mellea*.

Fungi are large group of eukaryotes, estimated to comprise around 1.5 million species, yet less than 7% have been described in detail (González-Fernández and Novo, 2010). They are ubiquitous organisms which live in air, soil or water, and they may be associated with plants, animals or other fungi, where they can be symbiotic, pathogenic or saprophytic (Fisher *et al.*, 2012). There are about 15000 known pathogenic species, and these may have very broad host specificity, as in the case of the phytopathogen *Armillaria mellea*, which has more than 600 host species (Raabe, 1962); or, as seen in *Ophiocordyceps unilateralis* an entomopathogen, fungi may have a single host (Pontoppidan *et al.*, 2009) or they may be heteroecious parasites, that is parasites that

require two different host species, at different stages of their lifecycle. Pathogenic fungi may depend on a particular host tissue type to complete their lifecycle (Barrett and Heil, 2012) and they be classed biotrophic, hemibiotrophic or necrotrophic. Biotrophs derive their nutrition from the host without killing it, hemibiotrophs initially feed on live host cells, but eventually kill the host and live on dead tissue and necrotrophs kill their hosts and feed on them (González-Fernández and Novo, 2010; de Oliveira *et al.*, 2012; Amselem *et al.*, 2011). Understanding the molecular mechanisms underlying host-pathogen interactions is necessary to predict and control pathogenic organisms.

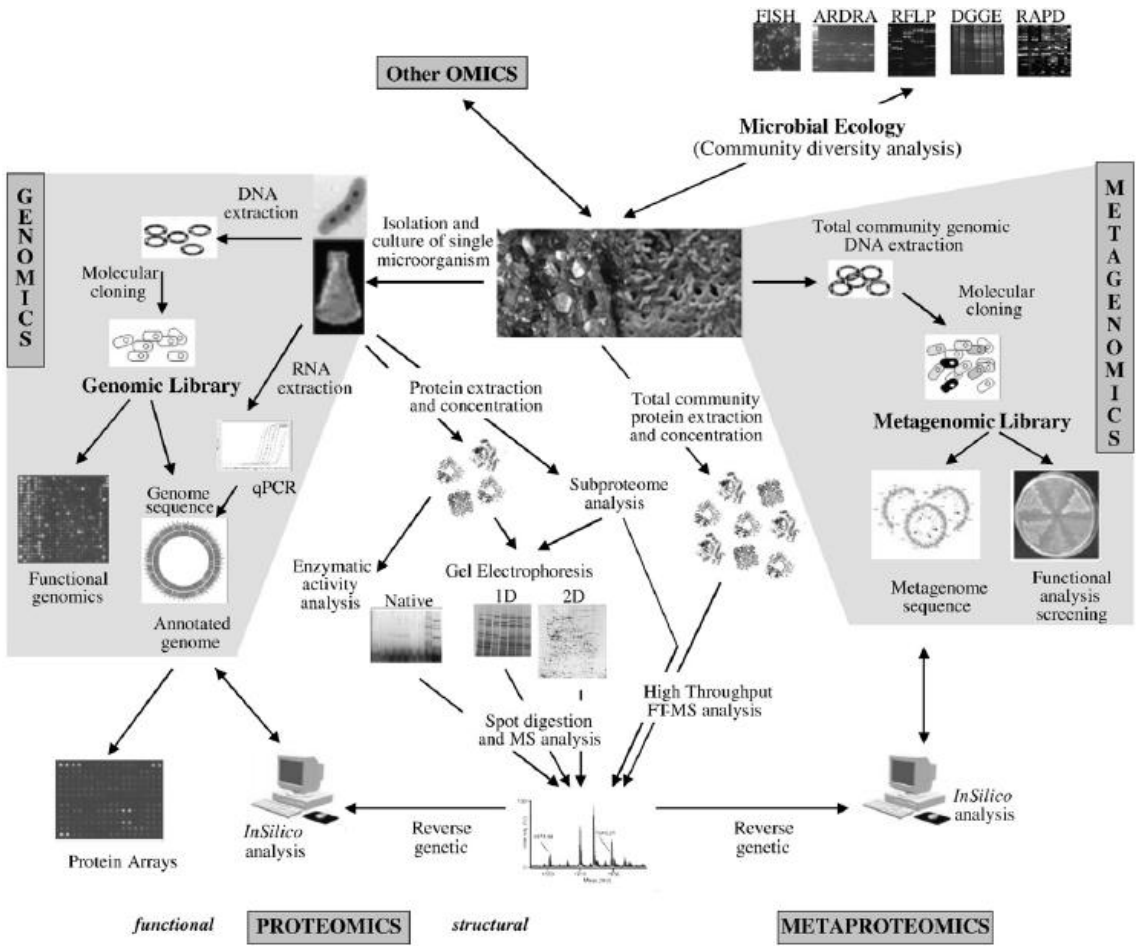

Figure 1.1. Overview of "Omics" technologies. Encompassing all perspectives of organisms and eco-systems, it includes genomics, proteomics, and metagenomics and metaproteomics, "other Omics", includes metabolomics (Jerez, 2008).

Pathogenic fungi are Janus-faced organisms. As parasites, they acquire nutrition from their hosts, killing them or undermining their viability, but the very enzymes and metabolites that they utilise to obtain nutrients, are bioactive and have hydrolytic or toxic properties, which can be extracted or synthesised as valuable compounds for

industrial and biomedical application. Indeed, the most virulent pathogens often provide the most useful compounds (Lee *et al.*, 2010; Misiek *et al.*, 2009; Baldrian and Valásková, 2008).

Fungi were classified by their morphology until the second half of the 20th century, and many are known by a second name during their anamorphic or asexual stage, but with the advent of molecular technologies and whole genome sequencing, more accurate phylogenomic classification has become possible (McLaughlin *et al.*, 2009). The fungal kingdom has seven phyla, Ascomycota and Basidiomycota (Hibbett *et al.*, 2007) are two phyla, that make up the Dikarya or higher fungi, which have been the subject of most study. Figure 1.2 shows Dikarya and phylogenetically related groups, with the sub-phyla (Ascomycota and Basidiomycota phyla) and phylum Agaricomytina underlined. *A. mellea*, the subject of this study, is a member of this phylum.

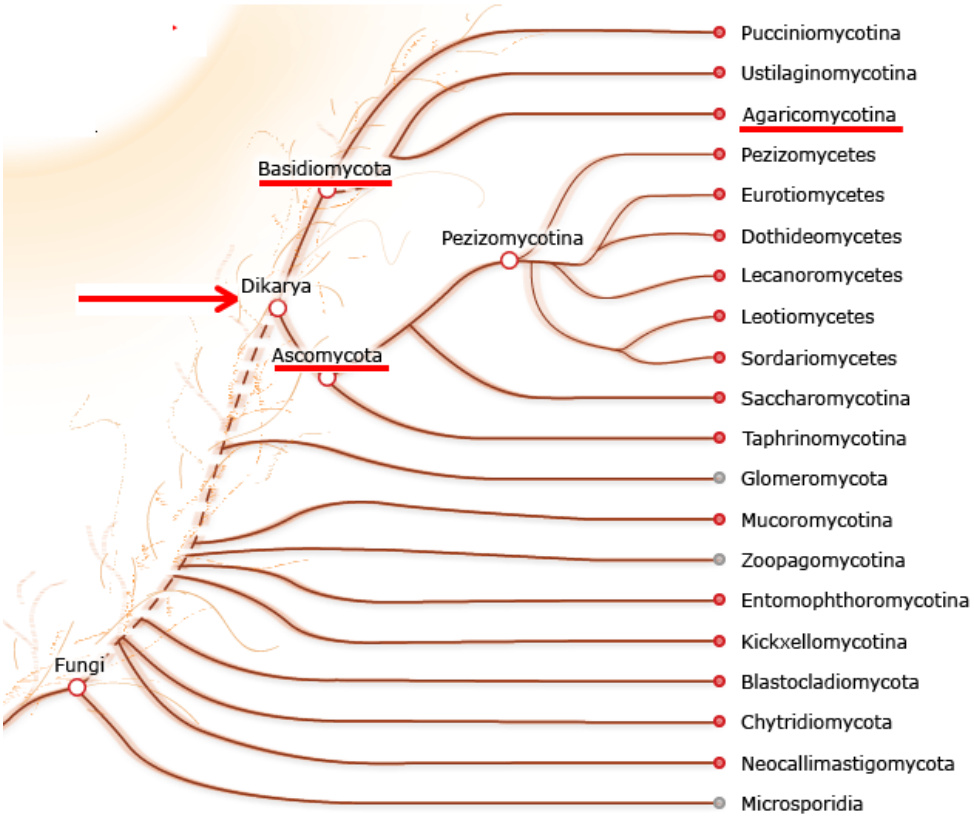

Figure 1.2. Cartoon representation of the Fungal tree of life showing phylogenetically related groups. Arrow indicates Sub-kingdom Dikarya, and underlined, the sub-phyla Ascomycota and Basidiomycota, and phylum Agaricomycotina of which *A. mellea* is a member (Grigoriev *et al.*, 2012).

1.1.1 Ascomycota

Ascomycota is the best studied of the fungal phyla for several reasons: (i) their lifecycles are less complicated than basidiomycetes making them easier to study, (ii) they cause damage to a wide range of agronomic plant species and many species are human and animal pathogens and thus are targets for therapeutic control measures and (iii) ascomycetes also secrete metabolites with bioactive properties, which themselves are potential therapeutic compounds of interest to pharmaceutical companies (Kniemeyer, 2011). Genome sequence data exists for 323 ascomycete species, there are 678 sequencing projects currently listed on the NCBI genome database (http://www.ncbi.nlm.nih.gov/genome Accessed 22/04/2013) and 129 genomes are publicly available for download from the Joint Genome Institute (http://genome.jgi.doe.gov Accessed 22/04/2013). A more informal synonym for Ascomycota, ascomycete, will be used in this study. Ascomycetes have single cell (yeast), hyphal (filamentous) or both (dimorphic) morphology. Ascomycota are defined by an ascus formed during sexual reproduction which contains eight haploid ascospores, however, ascomycetes also reproduce asexually by budding, or form conidia from hyphae which are also known as mitospores (Figure 1.3); (Taylor *et al.*, 2006). Heterothallic mating occurs between organisms and homothallic, or self mating, is also possible and is organism specific.

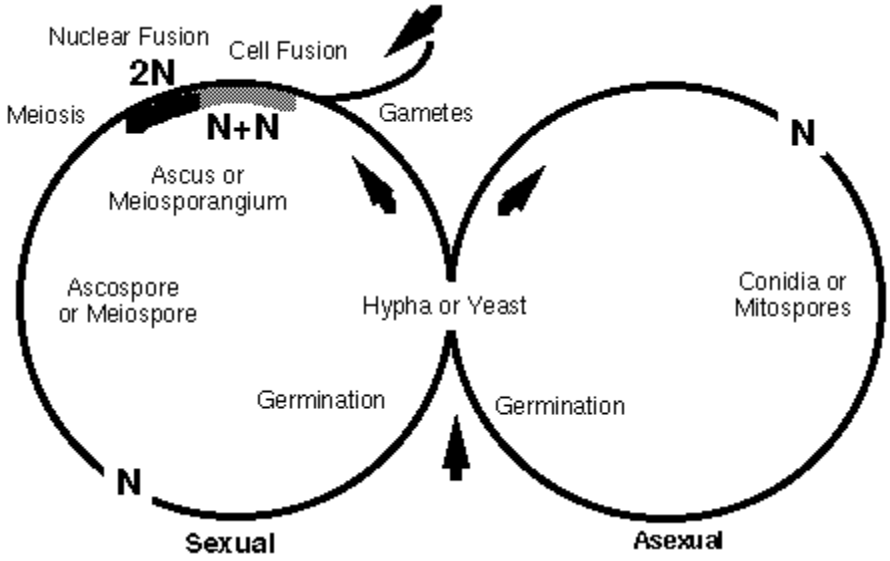

Figure 1.3. Ascomycota lifecycle showing both sexual and asexual reproduction, **Sexual reproduction:** Haploid ascospores germinate. Two compatible hyphae form an ascogonium (female) or antheridium (male) which fuse, and a dikaryote hypha is formed containing two haploid nuclei. During karyogamy, the nuclei fuse, forming a diploid cell which undergoes meiosis, forming eight haploid ascospores. **Asexual**

reproduction: Haploid ascopores germinate and hyphae grow and form conidiophores which produce haploid conidia which can germinate and form haploid hyphae. Arrows indicate the direction of the cycle (Taylor *et al.*, 2006).

1.1.1.1 Ascomycete genomes and proteomes

Fungi are more closely related to animals than to plants (Wainright *et al.*, 1993; Baldauf and Palmer, 1993), which poses problems for control, particularly of animal pathogens, as antifungals are often toxic to animals (Rossman and Palm-Hernandez, 2008). Therefore, use of genomic and proteomic techniques in combination, can broaden our understanding of systems biology and provide focus for research at the molecular level. The *Candida albicans* genome, sequenced in 2004, by whole genome shotgun (WGS) sequencing sequencing (Jones and Federspiel, 2004), was one of the first human pathogens to be sequenced. Its genome was compared to *Saccharomyces cerevisiae* and *Saccharomyces pombe* and 22% of its genes did not have matches to the other species; however many genes related to pathogenesis were identified, including genes relating to adhesion to host cells, iron transport genes, and secreted proteinases and lipases (Jones and Federspiel, 2004).

The genome of *Aspergillus fumigatus*, an opportunistic human pathogen, ubiquitous in the environment, which causes systemic infection and is life-threatening to immunocompromised patients was sequenced in 2005 (Nierman *et al.*, 2005). An investigation of the role played by thermotolerant proteins in pathogenicity of *A. fumigatus* found only one gene, a catalase, which was associated with temperature and pathogenicity, thus temperature was judged not to be the single pathogenic trigger. However the study did identify fifty-eight allergens, more than had been identified previously in any fungal species, and a large number of genes encoding secondary metabolites (Nierman *et al.*, 2005).

Aspergillus oryzae, whose genome was also sequenced in 2005, is used in production of fermented foods in Japan and has been used for production of industrial enzymes (Christensen and Kolomiets, 2011). *A. oryzae* does not produce aflatoxin, a toxic carcinogen produced by *A. fumigatus* and *A. nidulans*, and its genome is considerably larger than both of the other species, by 34% and 29%, respectively (Machida *et al.*, 2005). Genomic comparison of species was carried out, to determine what the differences were between the species, and whether *A. fumigatus* and *A. nidulans* had lost genes or whether genes had been gained by *A. oryzae* (Machida *et al.*, 2005). Comparative genomics between these related pathogenic and non-pathogenic

species, found that *A. oryzae* had acquired additional genes for metabolism and secondary metabolism which were hydrolytic and were required for nitrogen acquisition under the acidic fermentation conditions in which this species has been used. *A. fumigatus,* on the other hand, had more carbohydrate active enzymes (CAZy) (Cantarel *et al.*, 2009); enzymes specialised for metabolism and catabolism of carbohydrates, glycoproteins, glycolipids, and other glycoconjugates, necessary for nutrient acquisition in rotting vegetation. Paradoxically, while the *A. oryzae* genome does contain putative aflatoxin genes, there was no evidence that they are expressed, leading to the conclusion that *A. oryzae* may have been originally selected for domestication because it was non-toxic (Machida *et al.*, 2005). Thus, there was no environmental pressure to maintain a large number of CAZy in *A. oryzae*.

High-throughput DNA sequencing has become relatively inexpensive, enabling larger comparative genomic studies (Liu *et al.*, 2012). A case in point is a recent study in which eighteen species of *Dothideomycetes,* a large group of ascomycetes, which includes pathogens of agronomic crops, trees, saprophytic species and soil fungi, were compared (Ohm *et al.*, 2012). The genomes of fourteen of these species were newly sequenced and described for the first time, enabling profiles of variation in genome sizes, nutrient acquisition strategies and metabolites to be combined to present a catalogue of genes consistent with lifestyle and also to define core genes in this group (Ohm *et al.*, 2012).

Proteins may only be expressed in particular conditions and mRNA presence is not always coincident with functional proteins, thus proteins must be identified to positively prove their existence (Wright *et al.*, 2009). Functional proteomics therefore is vital in providing the complete profile of a biological system. An early functional proteomics approach in *A. fumigatus* was undertaken by Carberry *et al.* (2006); intracellular proteins were identified by protein mass spectrometry after separation by 2 dimensional gel electrophoresis (2-DE). Most of the proteins identified in this study related to energy production, but heat shock, signalling, protein biosynthesis, transcription and structural proteins were also identified. Some proteins differed from their theoretical molecular mass which is consistent with post-translational modification, and transcriptome analysis would not have identified these modifications. Glutathione (GSH) is an antioxidant and mitigates against oxidative stress and five GSH binding proteins were identified after mass spectrometric analysis in one of the first studies of *A. fumigatus* at sub-proteome level (Carberry *et al.*, 2006).

In a technology advance, an immunoproteomic study of secreted *A. fumigatus* proteins was undertaken to assess the immunoreactivity of *A. fumigatus* proteins against IgE. This technique, combines gel electrophoresis with immunoblotting prior to analysis, and is a focussed proteomic study. Seventy-five IgE immunoreactive proteins were identified, an increase of 48 proteins on those previously described (Gautam *et al.*, 2006). In a further advance in proteomic technology, a technique which multiplexes fluorescently stained samples from different conditions, differential 2D-gel electrophoresis (DIGE), used to not only visualise and analyse proteins but also to quantify proteins, was used to identify proteins differentially regulated under heat shock. *A. fumigatus* was subjected to temperatures of 48 °C, and ninety-one proteins were identified as differentially regulated under this condition. Previously unknown heat-shock proteins, indicators of organism stress were identified (Albrecht and Guthke, 2010).

A 2D-DIGE quantatitive proteomics approach was also used to compare yeast and hyphal morphology. of the dimorphic *C. albicans.* Cytoplasmic proteins were compared, from yeast and hyphae, but additionally, samples were prefractionated, and low pH proteins were enriched before being separated and identified. There were 2974 protein spots visualised and 106 of these were differentially regulated, thus providing quantitative differential analysis and acidic subproteomic identification of proteins associated with yeast or hyphae, in this dimorphic microorganism (Monteoliva and Martinez-Lopez, 2011).

Shotgun proteomics, a relatively recent innovation for high-throughput proteomics, which identifies all of the proteins in a complex sample, was used to identify secreted proteins in *A. niger.* Proteins were separated by gel electrophoresis in one dimension, and divided into five fractions, analysed and compared with *in silico* predictions (Braaksma *et al.*, 2010). Two hundred secreted proteins were identified and the results compared to three other *Aspergilli,* this information was used to update annotation of an *in silico* database by validating signal peptides in these proteins. Signal peptides are short peptide sequence at the N-terminal of proteins, a signal which targets the proteins for secretion (Braaksma *et al.*, 2010; Petersen *et al.*, 2011).

In the environment, fungal species are in competition with many other organisms and in order to survive they secrete bioactive small metabolites which have antibiotic and antifungal properties, and as such are potential therapeutics (Pelaez, 2005). A study was undertaken to determine the effect of competitive interactions

between different *Aspergilli* on the production and activity of these metabolites. No consistent increase or decrease of metabolites in any particular species was apparent, although bioactive metabolites were detected. Some metabolites were active against the species which had produced them, leading to the conclusion that metabolite production was dynamic and multifactorial, but that this method of investigation was a cost-effective method of inducing novel enzymes and an effective means of investigation of pathogenicity and virulence in fungi (Losada *et al.*, 2009).

A review by Johnson (2013) discusses the biotechnological use of ascomycetes and application of genetic techniques for their manipulation. *Kluyveromyces lactis* a species which has a GRAS status, can be used for production of food ingredients and flavours (van Ooyen *et al.*, 2006). Lipid accumulation in oleaginous yeast species including *Candida*, *Cryptococcus* and *Pichia* has applications not only in the synthesis of bio-diesel but also in synthesis of lipid-soluble carotenoids, surfactants and flavourings (Papanikolaou *et al.*, 2002; Papanikolaou and Aggelis, 2011; Dai *et al.*, 2007). *Debayomyces hansenii* another oleaginous ascomycete species, can produce xylitol from wood, and also toxins against yeast species which can be used to maintain sterility in industrial fermentations (Breuer and Harms, 2006; Biswas *et al.*, 2013; Buzzini and Martini, 2001).

1.1.2 Basidiomycota

Genomic sequence data for 126 Basidiomycota species, from 595 projects, is currently listed on the NCBI genome database (http://www.ncbi.nlm.nih.gov/genome Accessed 22/04/2013) and 74 genomes are publicly available for download from the Joint Genome Institute website (http://genome.jgi.doe.gov). Basidiomycota, a phylum of the Dikarya subkingdom, is divided into three subphyla which are best known by the morphology of their fruiting bodies (i) Ustilaginomycotina, whose best studied member is *Ustilago maydis*, a pathogen of maize which forms tumours on host plants containing diploid teliospores (Figure 1.4), (ii) Pucciniomycotina, known as rust, with more than 7000 different species, are pathogens of grasses and damage cereal crops causing major economic losses; they have a complicated lifecycle, with different spore types formed on two different host species (Figure 1.5), and (iii) Agaricomycotina, nearly all of which are mushroom-forming fungi, colonise forest litter, soil and wood; their fruiting bodies evidence of their location, they may be ectomycorrhizal, saprophytic or pathogenic (Figure 1.6). A more informal term for all Basidiomycota is basidiomycetes which will be used in this study.

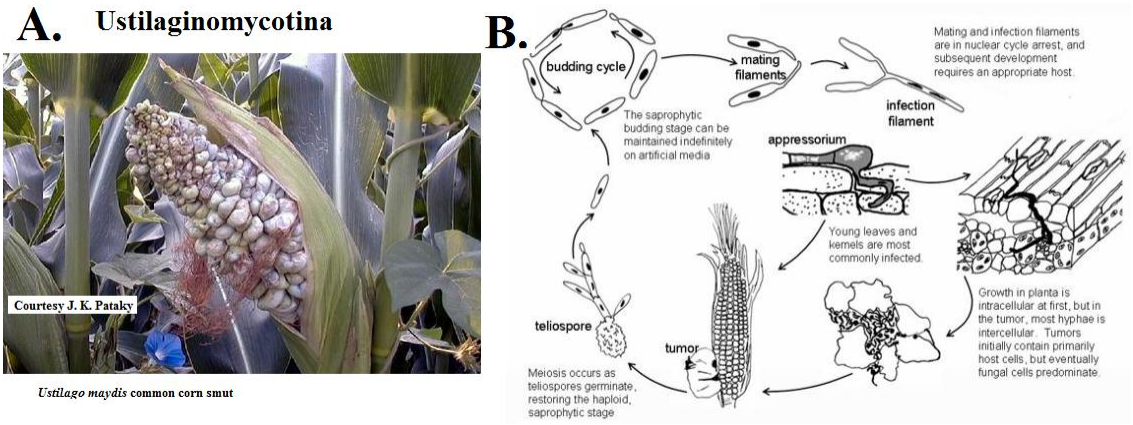

Figure 1.4. Reproductive structures and lifecycle of Ustilaginomycotina **A**. *Ustilago maydis* smut tumour on corn. **B.** Life cycle: Haploid spores germinate into monokaryote infection mycelia, grow and mate, generating mycelia with two unfused nuclei, dikaryote mycelia (plasmogamy), which invade host plants and grow intracellularly before forming a tumour of fungal cells. This is followed by spore formation through fusion of nuclei (karyogamy) and then meiosis which generates haploid spores (monokaryotic) (Feldbrügge *et al.*, 2004).

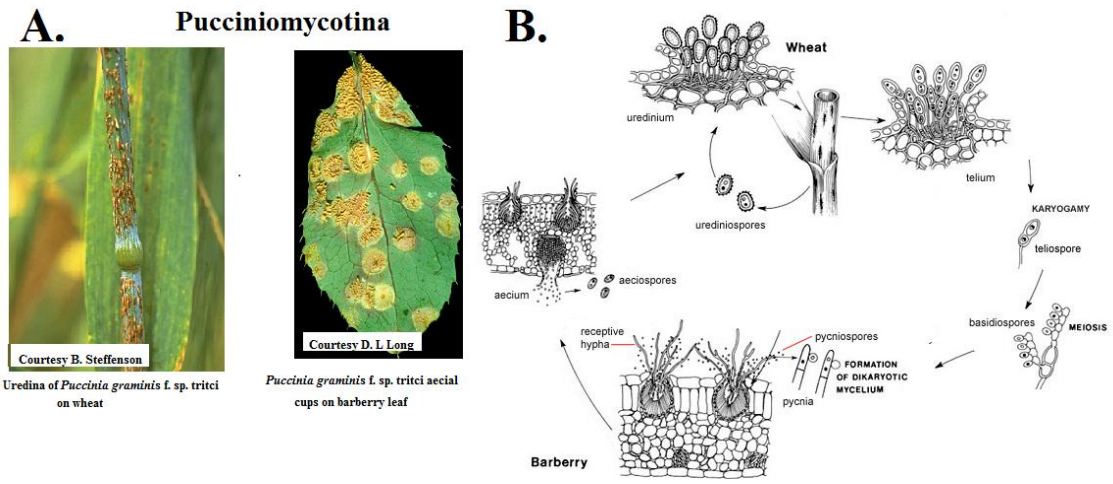

Figure 1.5. Reproductive structures and lifecycle of Pucciniomycotina **A.** *Puccinia tritci*, reproductive structures on two hosts, uridina on wheat, and aecial cups on barberry leaf. **B.** These fungi have the most complicated fungal life cycle and require two hosts of different species. Dikaryote uridinospores dispersed by wind, germinate on the stems of wheat (primary host) and invade the plant. They obtain nutrients from the plant and generate uridinia with prolific spore production and release causing devastation to wheat crops. At the end of the growing season structures called telia are formed from dikaryotic cells containing two celled teilospores. The nuclei fuse and dipoid teliospores are formed, and remain dormant over winter. In spring teliospores germinate and undergo meiosis which generates haploid basidiospores (monokaryotic). The basidiospores are released and germinate on barberry (secondary host). They invade the leaf and form spermogonia which release haploid spermatia which are released and transported by insects to compatible mates. These fuse and form dikaryotic mycelia from which aecia are formed. These structures contain aeciospores which are released into the air and infect wheat (primary host) (**http://archive.bio.ed.ac.uk/jdeacon/FungalBiology/rust.htm**).

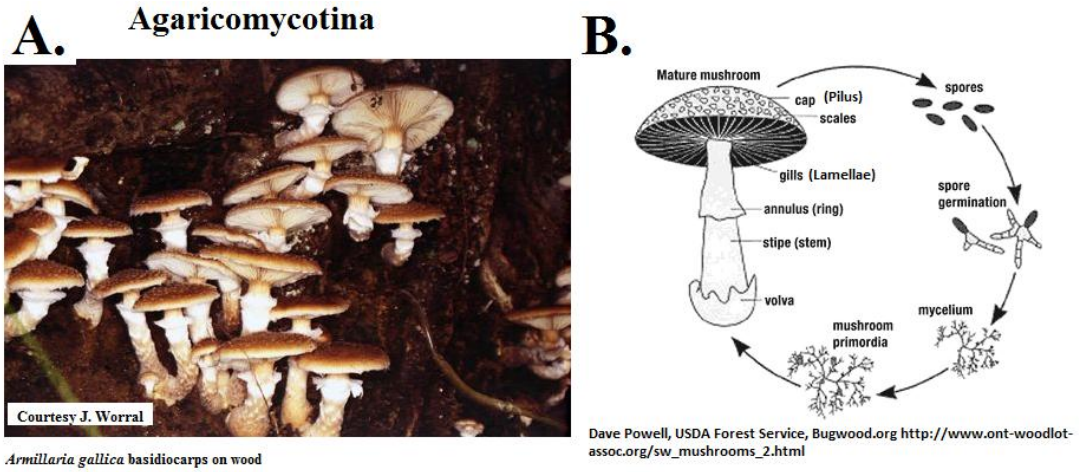

Figure 1.6. Reproductive structures and lifecycle of Agaricomycotina **A.** *Armillaria gallica* basidiocarp on tree stump. **B.** Lifecycle: Haploid spores germinate into hyphae which fuse and form dikaryote mycelia, fruiting bodies, basidiocarps are formed from mycelia. They have a large surface area due to the formation of gills from which structures called basidia grow. Karyogamy occurs in basidia this is followed by meiosis which generates haploid spores which move to the the tips of the basidia, and are then released into the air and wind dispersed. These germinate into monokaryotic mycelia which mate, forming dikaryotic mycelia. (Illustrations and photographs from the website of The American Phytopathological Society http://www.apsnet.org/edcenter/intropp/lessons/fungi/Basidiomycetes/Pages/default.aspx**,** except for the lifecycle of the agricarales, Dave Powell USDA **www.ont-woodlot-assoc.org/sw_mushrooms_2.html**).

In addition to complicated lifecycles, the basidiomycete mating system is also complicated. They may be self-mating, homothallic, or out-crossing, heterothallic. Some species have bipolar mating systems, with two haploid mating types akin to male and female, but other species have tetrapolar mating systems where each haploid cell has two mating factors which generate four haploid mating types (Findley *et al.*, 2012) (Figure 1.7). The persistent lifecycle phase of basidiomycetes is vegetative, in a state called plasmogamy. Fruiting bodies are formed for a short period of the lifecycle and are ephemeral. Spores grow into hyphae which fuse, although nuclei remain separate, forming a dikaryon, or even a heterokaryon (more than two nuclei). Sexual reproduction by fusion of two nuclei (karyogamy) occurs in a fruiting body structure called a basidium, the cell quickly undergoes meiosis, producing four haploid spores (Figure 1.7). Basidia are formed on gills and basidiospores are formed on the basidia and released into the air, where they are dispersed by wind (James, 2012). Vegetative

mycelia grow and reproduce by means of clamp connections. Two nuclei in the cell at the hyphal tip divide by mitosis forming two pairs of nuclei; one of the nuclei migrates to an outgrowth called a clamp connection which loops backwards from the hyphal tip. Two nuclei move to the hyphal tip and the nucleus in the clamp connection moves through the hyphal wall close to the single nucleus and a septum grows separating the two sets of nuclei into two discrete cells (Korhonen and Hintikka, 1974), (Figure 1.7).

Basidiomycetes are a very diverse group of organisms and their varied lifestyles which depend on their abilities to evade detection, colonise or kill other organisms and forage for nutrients requires them to have a supportive arsenal of proteins. Fungal secretomes were described by Bouws *et al.* (2008), as "natures toolbox for white biotechnology". Basidomycetes have been less studied than ascomycetes, as few of them are animal pathogens and because they are more complex organisms than ascomycetes. Indeed, genetic manipulation of ascomycetes and their use as "cell factories" to synthesise proteins of medical and industrial relevance, has been used for many years, and *A. niger* is one of the most prominant species used for this purpose (Punt *et al.*, 2002; Pel *et al.*, 2007; Mapari *et al.*, 2009). However with the advent of new technologies such as whole genome sequencing (WGS), transcriptome sequencing (RNA-seq), RT-qPCR and high throughput "shotgun" proteomics, basidiomycetes have been targeted as subjects for investigation, both for the study of compounds they produce, and to explore their use as overexpression systems for valuable enzymes (Alves and Record, 2004), particularly as the quantity and activity of secreted enzymes in basidiomycetes is greater that that of other phyla (Alves and Record, 2004). However, transformation in many basidiomycete species is more difficult than ascomycetes (Godio *et al.*, 2004; Baumgartner, Fujiyoshi, *et al.*, 2010; Abbott *et al.*, 2013).

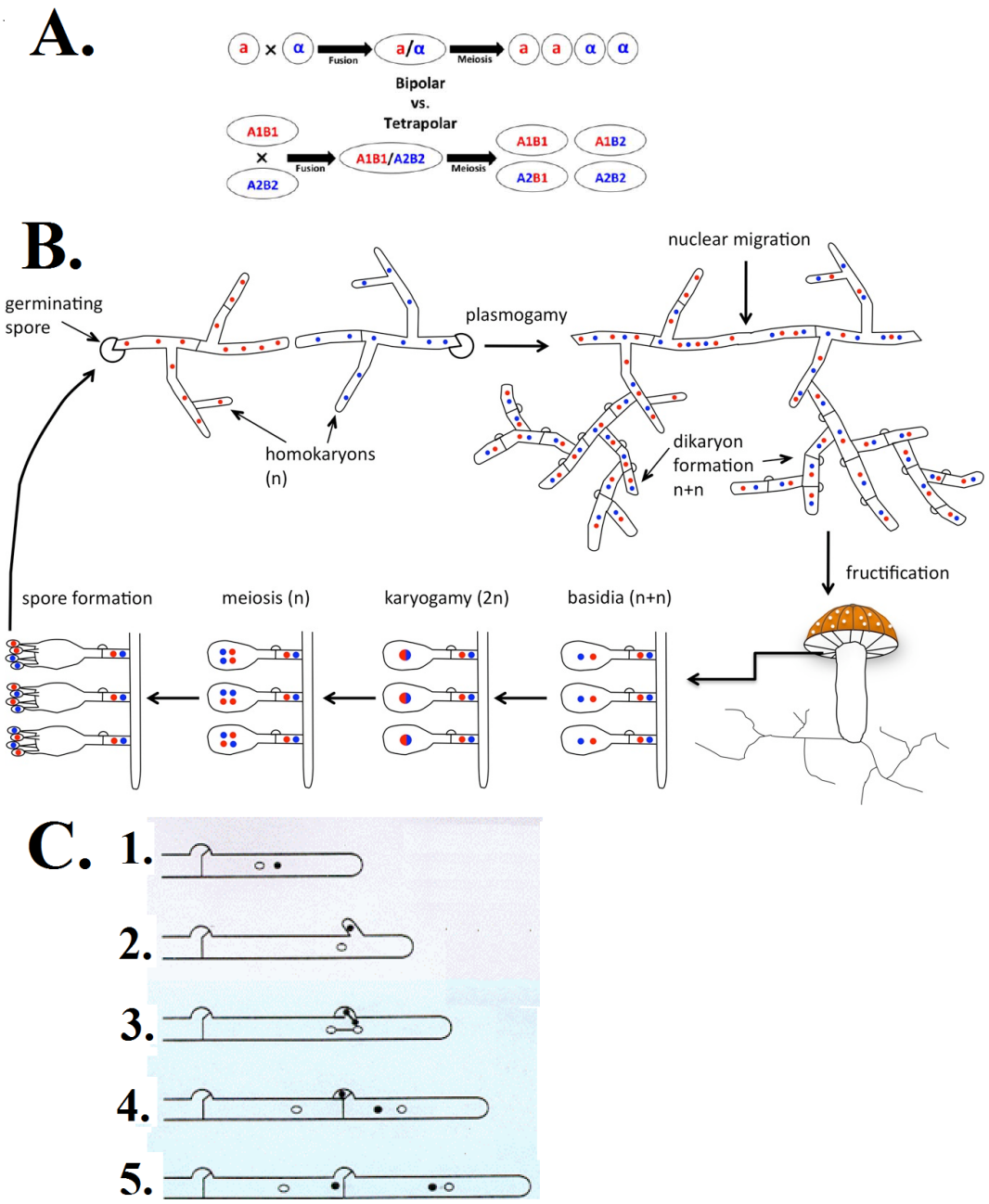

Figure 1.7. A. Basidiomycetes have may bipolar or tetrapolar mating systems which generate either two or four different mating types respectively (Findley *et al.*, 2012). **B.** Life cycle of agricarales. Spores germinate and form monokaryote hyphae which mate and amalgamate forming dikaryote mycelia, the most persistent form. Diploid cell are formed in basida, undergo meiosis and haploid spores are formed (James, 2012) (Illustration: T. Y. James http://www.umich.edu/~mycology/research.html). **C.** Clamp connection, growth of dikaryote mycelia. **1.** Cells elongate in the direction of growth. **2.** One nucleus migrates to an outgrowth of the hypha which loops backwards. **3.** The two nuclei divide by mitosis generating 4 nuclei**.** A bridge is formed and two dissimilar nuclei associate but do not fuse. **5.** Septum forms in the hypha between the two pairs of

nuclei and also between the bridge (clamp) and the leading cell **5.** Clamp wall dissolves and nucleus migrates into cell (Korhonen and Hintikka, 1974) (Image JW Deacon, 1997, *Modern Mycology*, Blackwell Science).

1.1.2.1 Basidiomycete genome sequencing and proteomics.

The genome of *Phanerochaete chrysosporium*, a saprophytic basidiomycete, sequenced, initially in 2002 and resequenced in 2004 by WGS, was the first genome sequence of this phylum to be determined. Gene modelling was difficult as previously-sequenced fungi were only distantly related to *P. chrysosporium* (Martinez *et al.*, 2004). Gene finding software and computational analysis identified many protein families in the organism related to degradation of plant cell walls, including peroxidases and cytochrome P450s. Genes encoding short-chain dehydrogenases/reductases, aspartyl proteases and Ras small GTPase domains were more abundant than in *S. cerevisiae,* and the genome was larger, its complexity due to the morphology and lifestyle of the organism (Martinez *et al.*, 2004). This fungus degrades two of the most abundant organic polymers on earth, cellulose and lignin, which are components of plant cells and wood. As expected in a fungus which not only degrades lignin, but also cellulose and hemicellulose, an array of hydrolytic enzymes was identified, as were enzymes with secretion signals and proteins putatively involved in secondary metabolite and polyketide synthesis. A further computational analysis of the genome was carried out by gel electrophoresis and shotgun proteomics to analyse secreted proteins from the fungus (Vanden Wymelenberg *et al.*, 2006). The genome of *Coprinopsis cinerea,* which was sequenced in 2003 (Stajich *et al.*, 2010), has served as a model organism for study of this phylum, it is a platform for genetic and molecular study of morphology and hyphal growth, DNA repair and mating in basidiomycetes, as it is easy to culture on defined media, has a short lifecycle and can be transformed easily (Stajich *et al.*, 2010). Its study enabled early comparative genomic studies between both basidiomycete species and between basidiomycetes and ascomycetes and other organisms (Hoegger *et al.*, 2004), as few eukaryotic organisms had been sequenced, WGS was prohibitively expensive and few eukaryotic genomic sequences were available for comparison (Hoegger *et al.*, 2004).

Laccaria bicolor is an ectomycorrhizal basidiomycete whose genome was sequenced in 2008 (Martin *et al.*, 2008). This fungus forms a symbiotic relationship with plants, colonising their roots. The genome of this fungus encodes a large number of small secreted proteins, similar to signalling molecules, whose functions are

unknown, but which are expressed in hyphae proliferating on symbiont roots (Martin *et al.,* 2008). The *L. bicolor* genome had an unexpectedly low number of cell wall degrading enzymes, but contained many genes encoding other polysaccharide degrading enzymes, revealing a dual lifestyle, both saprotrophic and biotrophic, enabling the fungus to grow in the soil as well as on plant roots, thus providing insight into mechanisms of fungal symbiosis (Martin *et al.*, 2008).

The genome of *Schizophyllum commune*, a fungus that is mostly saprophobic but is also known to be an animal and plant pathogen, was sequenced in 2010 (Ohm *et al.*, 2010). Its fruiting bodies are used as a food source in Africa and Asia and like *C. cinerea,* it has a short lifecycle. The genome of *S. commune* contains a comprehensive suite of enzymes involved in carbohydrate degradation, and is particularly rich in cellulose-degrading, hemicellulose-degrading and pectin-degrading enzymes. It also contains laccases which degrade aromatic compounds such as lignin (Ohm *et al.*, 2010). A comparison with other fungal genomes (Martinez *et al.*, 2009), showed that the mechanisms used by *S. commune* for the degradation of wood, were different to *P. chrysosporium, L. bicolor* and *C. cinerea,* in that no peroxidases were encoded in the genome, which was also the case in the *Postia placenta* genome (Martinez *et al.,* 2009), while wood-degrading laccase enzymes were encoded in the *S. commune* genome, which were missing from *P. chrysosporium.* Comparative genomics and proteomics have been enabled by the wealth of genomic information which is extensive and growing. Sequence comparisons between different species of the same genus (Suzuki *et al.*, 2012) or different genera (Fernandez-Fueyo *et al.*, 2012) to elucidate fungal growth mechanisms is important, as it would have been expected that *P. chrysosporium* would encode laccases, based on its substrate in the wild, whereas, *L. bicolor* and *S. commune* might be expected to share the same mechanisms of cell wall degradation. Therefore, information from each newly sequenced organism contributes to inform on the overall systems biology of fungi.

1.1.2.2 Investigation of basidiomycete pathogenicity and virulence strategies

Many basidomycetes are phytopathogens which cause extensive damage to food crops, particularly grains, but also to fruit trees and timber plantations; and some basidiomycetes are animal pathogens (Duplessis *et al.*, 2011; Rampitsch *et al.*, 2006; Djamei and Kahmann, 2012; Zheng *et al.*, 2013; Martinez *et al.*, 2009; Eastwood *et al.*, 2011; Liu *et al.*, 2010; Raja *et al.*, 2013). It is important to elucidate precise molecular mechanisms used by pathogenic basidiomycetes, to infect their hosts, in order to control

these organisms. Genomic and proteomic techniques assist in identification of virulence factors and pathogenic strategies and recent approaches using one or more techniques will be discussed.

Ustilago maydis is a smut fungus which causes major damage to grasses of agronomic value such as maize, wheat and sugar cane (Djamei and Kahmann, 2012). *U. maydis* is a biotroph and requires a host for completion of its sexual cycle. Plant infection is not systemic, and affects only aerial parts of the plant. The fungus penetrates plant cells and fungal hyphae are invaginated, an interaction between the two is established and the fungus forms tumours on the plant (Djamei and Kahmann, 2012; Kämper *et al.*, 2006). Comparative genomics of *U. Maydis* with *C. cinerea*, *P. chrysosporium* and *Cryptococcus neoformans* showed that *U. maydis* has a relatively small genome, with fewer introns than in the other species, and fewer genes known to confer pathogenicity than are present in other phytopathogens (Djamei and Kahmann, 2012). Effectors are small secreted proteins that bind to host proteins and moderate their activity. They enable fungi to evade plant defences by silencing plant defences triggered by fungal penetration (Stergiopoulos and de Wit, 2009; De Wit *et al.*, 2009). One gene for an effector protein, chorismate mutase, reduces the levels of chorismate which is used to generate salicylic acid, a plant defence compound (Djamei and Kahmann, 2012; Kämper *et al.*, 2006; Jonkers *et al.*, 2012). This protein is highly expressed during *U. maydis* colonisation of plants, and was the first identification of an effector which is internalised by host cells, diffuses into adjacent host cells and alters host metabolic processes (Djamei *et al.*, 2011).

Metabolic and transcriptomic profiles of *Fusarium verticillioides*, an ascomycete soil fungus, was grown in co-culture with *U. maydis* to study their interaction mechanisms, and to investigate potential strategies for *U. maydis* biocontrol. Transcriptomic changes were identified over 7 days and single and co-culture metabolic profiles were examined (Jonkers *et al.*, 2012). *U. maydis* growth was completely inhibited by *F.verticillioides* after 7 days. Moreover, there were a number of *U. maydis* proteins upregulated in co-cultures which related to pathogenicity and stress, including multidrug transporters, which are known to excrete toxic compounds from cells. In this case, they are likely to extrude toxic metabolites secreted by *F.verticillioides. U. maydis* specific proteins, which are found in genomic clusters which also encode effector proteins, were also upregulated (Kämper *et al.*, 2006; Jonkers *et al.*, 2012). This study provides potential targets for investigation of biocontrol of *U. maydis*.

Rhizoctonia solani is a basidiomycete which causes rice sheath blight and stem canker of potato. Current control measures for the fungus are limited to chemical control, as molecular strategies have been largely ineffective, although inoculation of plants with non-pathogenic *Rhizoctonia* spp. as biocontrol agents (BCA) has had limited success (Thind and Aggarwal, 2008). Therefore, if pathogenic genes and molecular mechanisms can be established, a harmless strain could be developed as a BCA against the fungus. *R. solani* from one host type (potato) was shown to be only slightly pathogenic to other host species (rice), and could therefore be used a biocontrol inoculant with a different host (Pannecoucque and Höfte, 2009; Rioux *et al.*, 2011). A genome mining study of *R. solani* on infected tissue from rice and potato was carried out to determine genes common to virulence and pathogenicity of the fungus in interactions with the two host species (Rioux *et al.*, 2011). Infection strategies were broken into three stages: penetration and early interaction which involved appressorium formation (Figure 1.8), host defence suppression, and detoxification of host resistance compounds (Rioux *et al.*, 2011). A further genomic study of this fungus found that there were key glycoside hydrolases, secreted proteins and effectors, which have important roles in pathogenicity, and although *R. solani* possesses a large suite of CAZy and secreted metabolites, most are not necessary for pathogenicity (Zheng *et al.*, 2013). In a comparison of *Trichoderma* spp., used as BCA against *R. solani*, the strategies employed by the *Trichoderma* species in co-cultures with *R. solani*, were found to differ. *T. virens* secreted a phytotoxin, gliotoxin, against *R. solani*, whereas *T. atroviride* was found to secrete both antibiotic compounds and a polysaccharide degrading enzyme against *R. solani* cell wall. Other responses in co-cultures included upregulation of proteases, proteins involved in detoxification and stress response by *Trichoderma* spp. as antagonists against *R. solani*. Stress response proteins were also identified in *T. reesei*, which do not inhibit *R. solani* (Atanasova *et al.*, 2013). This study demonstrates the diversity of fungal-host responses even within species of the same genera and the importance of elucidating molecular mechanisms in fungal contol.

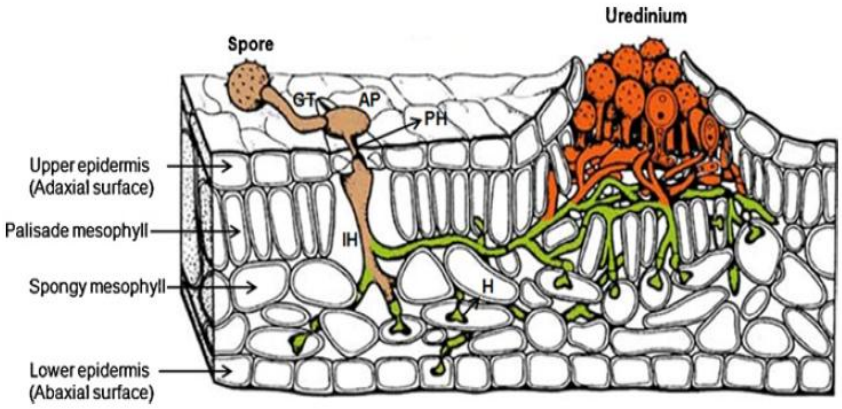

Figure 1.8. Schematic of the infection structures of fungi during fungal infection of dicotyledon leaf. AP, an appressorium is an external structure formed on leaf surface for fungal penetration; H, haustoria are internal structures fungal structures inside leaf; GT, germ tube; PH, penetration hyphae; IH, infection hyphae (Hahn, 2000; Tremblay *et al.*, 2010).

Puccinia triticina infects cereal crops, causing widespread damage worldwide and control of these species is economically important. Drafts of the genomes of *Puccinia* spp. have only recently become publicly available (http://www.broadinstitute.org/annotation/genome/puccinia_group/MultiHome.html) which has impeded investigation of these pathogens. Expressed Sequence Tag (EST) sequences have been used for gene discovery in spores generated from sexual reproduction, spores generated by asexual reproduction and haustoria from *P. triticina* by comparison with *U. maydis* and other rust fungi. More than 40% of the *P. triticina* genes from these structures did not have homologs in other organisms, and as the genome sequence has not been finalised, this information will be a resource for verification of genome annotation (Xu *et al.*, 2011).

Haustoria (Figure 1.8), the internal infective structures of *P. triticina,* militate against plant defences by production of effector molecules, although how these are delivered into the plant is still a matter for investigation (Rafiqi *et al.*, 2012). Gel electrophoresis followed by LC-MS/MS was employed to identify 260 haustorial proteins from infected wheat. These haustorial proteins had a range of biological functions, and 17 were hypothetical proteins, meaning they were predicted *in silico* in other organisms, but there is no experimental evidence that they are expressed. Secretion signals were also identified in seven of the 17 proteins. Identified proteins

included proteins with homology to haustorial proteins from other species (Song *et al.*, 2011).

Genome mining of *P. tricitina* identified genes which may confer putative pathogenicity, including a MAPK kinase, a cyclophilin and a calcineurin B, which were silenced *in planta* using a novel *Agrobacterium tumifaciens* RNA interference (RNAi) technique; which although previously used in dicots, was used for the first time by Panwar *et al.* (2013) in wheat leaves, to silence *P. triticina* genes by RNAi. RNA silencing generated by the host is dependent on genes in the pathogen which enable this mechanism. Not all fungi possess this mechanism and without an annotated genome it was not known if *P. triticina* had such a mechanism. Transfer DNA (T-DNA) delivered by *A. tumefaciens*, into the host (wheat) expresses hairpin RNA in wheat which triggers gene silencing by generating small interfering RNA molecules, targeted to the pathogen (*P. triticina).* Using this novel technique, downregulation of the three targeted genes (63 - 70 %) was achieved (Panwar *et al.*, 2013), and represents a possible strategy for investigation of other putative virulence genes. Thus, comparative genome mining, coupled with other molecular techniques, enabled determination and activity of putative virulence genes.

C. neoformans, is one of a few virulent human pathogenic basidiomycete species, has yeast morphology in its vegetative form, and is found in trees and in bird guano (Kozubowski and Heitman, 2012). However, its sexual cycle induces a hyphal morphology which produces spores. These spores, and desiccated yeast cells, can colonise human lungs especially in immunocompromised hosts. These migrate into the bloodstream, cross the blood-brain barrier and cause meningoencephalitis which can be fatal (Idnurm *et al.*, 2005). The yeast morphology persists during infection and *C. neoformans* sexual reproduction does not occur during animal infection. Kozubowski and Heitman (2012) used RNAi to determine that the pheromone receptor Ste3, usually associated with mating, increases the size of some fungal cells in the lungs of infected animals by tenfold. These cells resist phagocytosis and this may be a mechanism to evade immune response, especially as these large cells reproduce faster than smaller cells (Kozubowski and Heitman, 2012). One mechanism of virulence in the organism seems to be copper acquisition (Kozubowski and Heitman, 2012) and the organism sequesters copper in both copper limited and copper replete environments. In media enriched with copper, it sequesters much higher levels of copper than observed for other fungi. In mutant strains where the copper-dependent regulator is deleted, the organism

was less virulent, thus copper may play a role in pathogenicity of *C. neoformans* (Raja *et al.*, 2013) and this copper-dependent regulator is a possible target for antifungal drugs.

In a resequencing study of *Heterobasidion annosum senso lato,* a basidiomycete phytopathogen with both a saprophytic and parasitic lifestyle, RNA microarray analysis of genes differentially regulated from tissue obtained from infected plants, compared to cultures on defined media was carried out (Olson *et al.*, 2012). The study found transcription of fewer carbohydrate degrading enzymes (CAZys), upregulation of pectinolytic enzymes, polyketide synthases (PKS), a non-ribosomal peptide synthetase (NRPS), and enzymes involved in generation of ROS and host metal scavenging, in necrotic tissue - compared to culture on defined media (Olson *et al.*, 2012).

1.1.2.3 Enzymes with biotechnological application

Genome sequencing, together with proteomic data, has led to identification of proteins expressed under various fungal culture conditions. Proteins may be induced in liquid cultures that are not expressed in solid substrate fermentation and *vice versa* (Imanaka *et al.*, 2010), or novel proteins may be expressed in response to biotic, abiotic or xenobiotic-induced stresses (Sasidharan *et al.*, 2011). These proteins may be of mycelial origin or may be secreted. Gel electrophoresis, the separation of proteins by molecular mass/iso-electric point has been used to date; to identify proteins, but only subsets of fungal proteins can be identified by this method. A high throughput proteomic technique, called shotgun proteomics, has recently been used to attempt to identify all proteins expressed in an organism (Doyle, 2011; Gonzalez-Fernandez and Jorrin-Novo, 2012; Weckwerth, 2011). Integration of genomic and proteomic data with comparative proteomics is used to identify expressed proteins with biotechnological applications.

Medically relevant enzymes from the ergosterol biosynthesis pathway which is not present in all fungi, but is specific to fungi, have also been identified and purified from several fungi (Thorpe *et al.*, 2004; Herath *et al.*, 2012; Xu *et al.*, 2011; Kristan and Rižner, 2012). As the ergosterol pathway is unique to fungi, it has been a target for antifungal drugs, but in addition, enzymes in the ergosterol pathway are constituents of the cytochrome P450 superfamily of monoxygenases and modify steroids. Ergosterol serves as a precursor for steroid drugs, and fungal oxidoreductases and hydroxylases which are used in anti-inflammatory drugs, anti-depressants, progestins, and heart medication, have medical applications (Kristan and Rižner, 2012). Polyketides are a

class of metabolites with medicinal applications and genome mining has been used to identify polyketide synthases in sequenced fungi which encode polyketides with antibiotic, cytotoxic and cholesterol-reducing properties (Lackner *et al.*, 2012).

The substrate which enables growth of many fungi is plant material. Plant cell walls are composed of many interlinked and crosslinked polymers, and are some of the most abundant compounds on earth. Cellulose is an unbranched polysaccharide of glucose monomers and is the most abundant organic polymer (Baldrian and Valásková, 2008). Hemicellulose can be comprised of a variety of hexose and pentose saccharide polymers in a random heteropolymeric structure which is branched and binds other components of the cell wall (Del Bem and Vincentz, 2010). Lignin is a heterogenic polymer the second most abundant compound in wood. It is comprised of aromatic monomers crosslinked randomly, is hydrophobic and recalcitrant to degradation (Boerjan *et al.*, 2003). Lignin crosslinks and binds the other components of the plant cell wall and strengthens the structure (Sticklen, 2008; Boerjan *et al.*, 2003) (Figure 1.9). Fungal genomes encode hundreds of carbohydrate active hydrolytic enzymes (CAZy) (Martin *et al.*, 2008; Fernández-Fueyo *et al.*, 2012). which degrade plant cell walls and these enzymes, which have lignocellulolytic properties, are especially interesting for biotechnological applications. For example, pectinolytic enzymes are used in food processing, and cellulases, xylanases and laccases have applications bio-fuel production (Grigoriev *et al.*, 2011).

Production of enzymes by fungi represents a cost effective method of producing compounds of biotechnological interest and comparative studies identifying novel enzymes or enzymes with increased activity are being used a “green” alternative to chemical synthesis (Weckwerth, 2011), either overproduced in the original organism or in organisms which have been genetically modified to produce the enzymes in question.

1.1.2.4 Wood degradation in basidiomycetes

Wood-degrading basidiomycetes are considered to have a huge potential in industrial biotechnology (Himmel and Bayer, 2009; Lynd *et al.*, 2008; Sticklen, 2008; Chapple *et al.*, 2007). Precise understanding of the molecular mechanism employed by these organisms to degrade wood, promises cheap bio-fuels from the degradation of agro-industrial waste products (Grigoriev *et al.*, 2011). There are two types of wood degrading basidiomycetes, brown-rot fungi and white-rot fungi. Brown-rot fungi and their molecular systems of degradation are less studied than those of white-rot fungi.

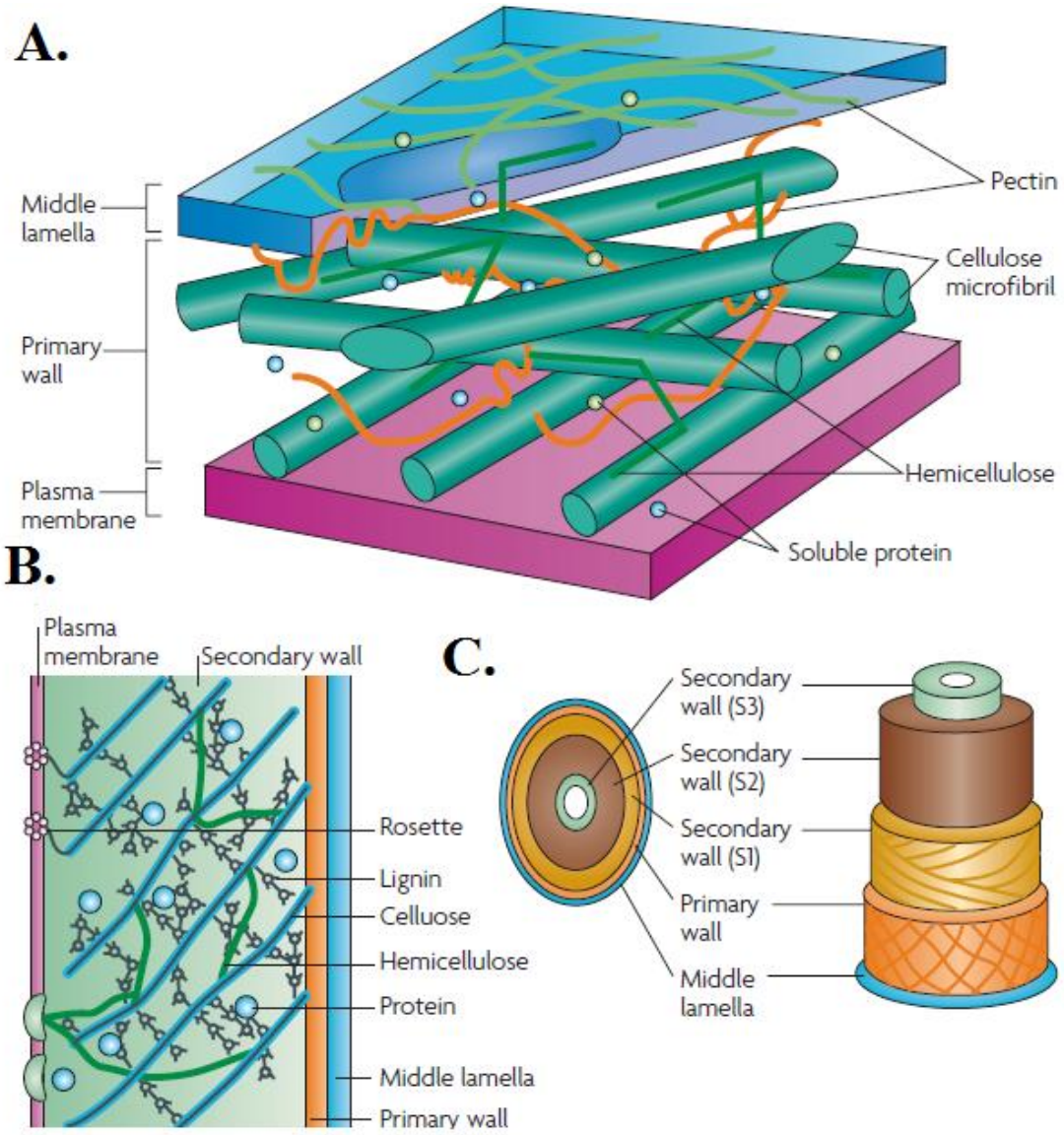

Figure 1.9. The plant cell wall. **A.** Cellulose, polymers comprise the largest proportion of the plant cell wall, pectin and hemicellulose polysaccharides extend from the middle lamella to the plasma membrane and soluble proteins are contained in this matrix. **B.** Lignin is a polymer which crosslinks the components of the cell wall and is its second most abundant component. Lignin is recalcitrant to degradation due to its aromatic heteropolymeric structure and strengthens the cell wall. **C.** The S1, S2 and S3 layers of the plant cell wall are lignified (Adapted from Sticklen (2008)).

1.1.2.5 Brown-rot basidiomycetes

Brown-rot fungi comprise less than 10% of wood-degrading species but are the largest group in boreal forests (Arantes *et al.*, 2012). *Postia placenta* (Martinez *et al.*, 2009) and *Serpula lacrymans* (Eastwood *et al.*, 2011) are two brown-rot fungi whose genomes have been sequenced. During brown-rot degradation, cellulose is initially depolymerised without loss of weight. In later stages of brown-rot, only lignin is left,

cellulose and hemicellulose oligosaccharides having been hydrolysed by glycodegradative enzymes (Arantes *et al.*, 2012). Brown rot saphrotrophs are thought to have lost lignin-degrading enzymes which are retained by white rot species. They appear to have evolved a strategy for cellulose degradation and lignin modification, without expending energy, by non-enzymatic initial degradation of cellulose by Fenton chemistry which generates extracellular hydroxyl radicals by the following reaction:

$$Fe^{2+} + H_2O_2 + H^+ \rightarrow Fe^{3+} + {\cdot}OH + H_2O$$

these radical species then oxidise substrates (Arantes *et al.*, 2012; Halliwell, 1965; Koenigs, 1974). Brown rot fungal genomes encode cellulases, but none are exo-cellulases, so although they depolymerise cellulose, they produce insoluble oligomers and not soluble sugars (Ryu *et al.*, 2011). *P. placenta* has only four cellulose-acting enzymes and 34 glycoside hydrolases, which was quite unexpected when the *P. placenta* genome was first sequenced, as it was thought that many cellulase and other hydrolytic enzymes would be encoded therein (Martinez *et al.*, 2009). Brown-rot fungi also modify lignin, although its aromatic units remain after degradation of celluloses and hemicelluloses (Martinez *et al.*, 2009). A combination of endo-cellulases and small cellulolytic oxidants are thought to degrade cellulose (Ryu *et al.*, 2011), and this is supported by the fact that more than 300 cytochrome P450 monoxygenases were identified in the *P. placenta* genome (Ide *et al.*, 2012). Phenolate moieties synthesised by *S. lacrymans* reduce Fe^{3+} to Fe^{2+} and *S. lacrymans* appear to have the same non-enzymatic Fenton chemistry mechanisms for lignocellulose degradation, as that of *P. placenta* and other brown-rot fungi (Eastwood *et al.*, 2011; Ichinose, 2013). It was originally thought that the small molecules which diffused into the inner plant cell wall (S2, S3, Figure 1.9) during cellulose degradation were enzymes, but it is now known that H_2O_2 is the catalytic agent in cellulose degradation. A proposed mechanism for wood degradation by brown-rot fungi has been described by Arantes *et al.* (2012). Degradation is initiated in the inner cell wall, away from the fungal hyphae in the lumen of wood cells. Fungal hyphae secrete high levels of oxalic acid and H_2O_2, and iron (Fe^{3+}) in the lumen of wood cells, at low pH, forms a complex with the oxalic acid. The Fe-oxalate complex remain stable, and reduction of iron by H_2O_2 is prevented by the low pH. The complex diffuses into the cell wall where the pH increases, the lignocellulose matrix buffers and maintains the increased pH. The hyphae, which remain in the lumen are thus unaffected by this change in pH. Iron is chelated in the cell

wall by an iron reducing compound and Fe^{3+}, in the Fe-oxalate complex, is reduced to Fe^{2+} which reacts with the H_2O_2 secreted by the fungus, generating hydroxyl radicals, by the Fenton reaction, which oxidise the components of the cell wall (Figure 1.10). Cellulose is fragmented and subjected to oxidative cleavage; hemicellulose undergoes oxidative cleavage; and lignin is demethylated and side chains oxidised, remodelling and repolymerising the lignin (Figure 1.10). Oxidation of cellulose produces partly degraded oligo-cellulose fragments, but more importantly, remodelling of lignin and hemicellulose removal opens up the structure to enzymatic degradation as this open structure allows enzyme access to sugars, this making them available for industrial bioprocessing (Arantes *et al.*, 2012).

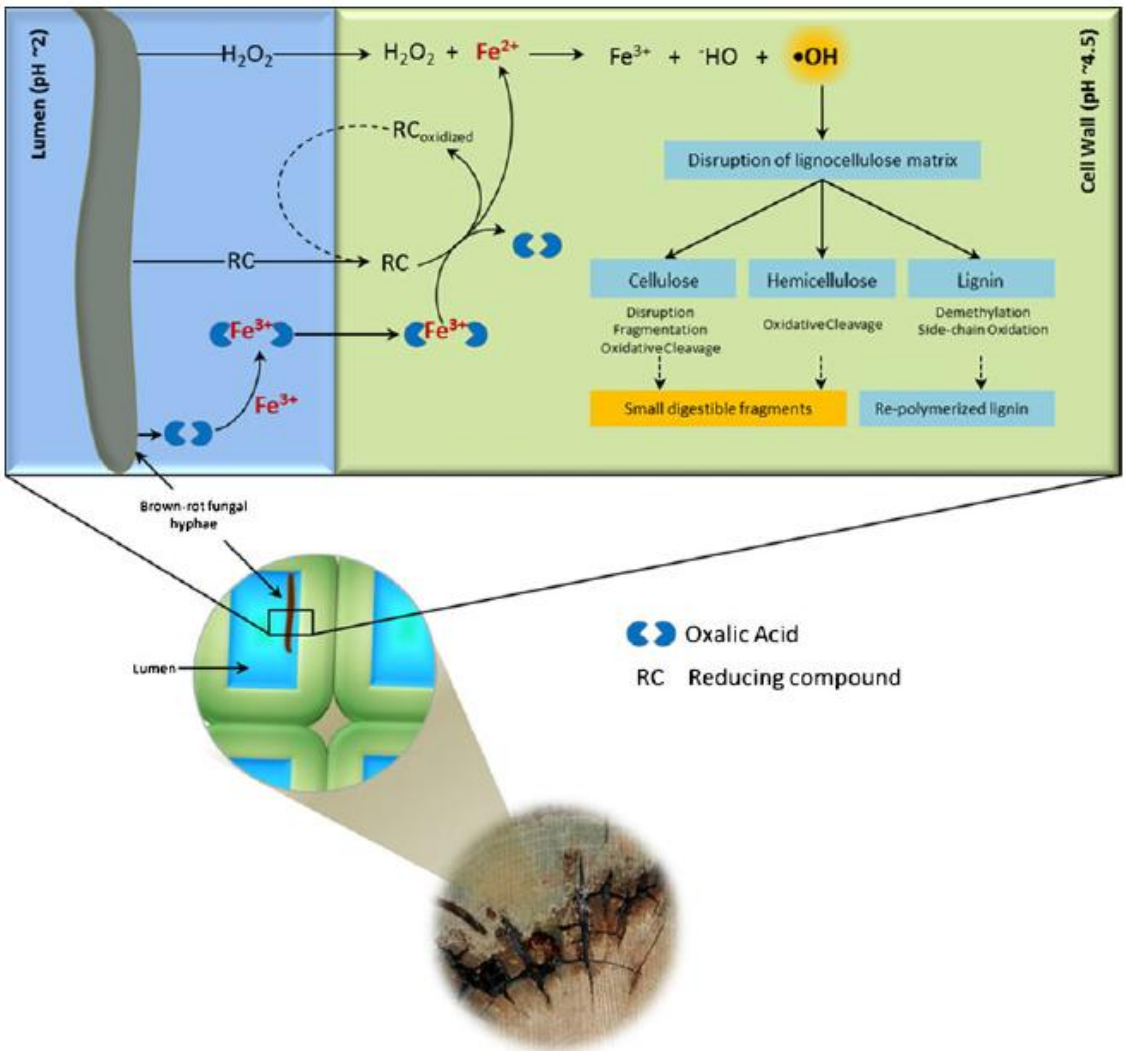

Figure 1.10. Proposed mechanism for oxidative cleavage of lignocellulose by brown-rot fungi via the Fenton Reaction. Fungal hyphae in the lumen of wood produce oxalic acid, iron-reducing compounds and H_2O_2. Oxalic acid forms a complex with plant-derived iron which diffuses into the cell wall, where the iron is sequestered. Increased pH in the cell wall enables a reducing compound to reduce Fe^{3+} to Fe^{2+} and

by means of the Fenton reaction, Fe^{2+} reacts with H_2O_2 forming hydroxyl radicals which react with cell wall components, glycoside bonds in cellulose and hemicellulose undergo oxidative cleavage and lignin is depolymerised and subsequently repolymerised and thus remodelled (Arantes *et al.*, 2012).

1.1.2.6 White-rot basidiomycetes

Lignin, one of the most abundant aromatic polymers in nature is a coloured polymer, composed of phenylpropanoid units crosslinked by ether and carbon-carbon bonds, whose heterogenous structure makes it recalcitrant to degradation (Figure 1.11), (Ruiz-Dueñas and Martínez, 2009). In contrast to brown-rot fungi, which do not utilise enzymes in plant cell wall degradation and leaves lignin in situ, white-rot degradation requires a suite of powerful enzymes to degrade lignin to CO_2 and H_2O (Vanden Wymelenberg *et al.*, 2010; Ichinose, 2013). Initial white-rot degradation removes lignin, leaving colourless cellulose which appears white, hence the name white-rot. Fungal pretreatment of wood by white-rot fungi is used in the manufacture of paper, as a more cost-effective and environmentally friendly means of bio-pulping than use of chemical or electrical methods (Hakala *et al.*, 2004). Although white-rot fungi do not grow on lignin alone (Vanden Wymelenberg *et al.*, 2010), they mineralise lignin, and a range of enzymes, and other compounds are required to achieve this degradation. Lignin peroxidase (LiP), manganese peroxidase (MnP), versatile peroxidase (VP), laccases, organic acids and veratryl alcohol (a secondary metabolite) are all involved in lignin degradation (Lundell *et al.*, 2010). However, not all fungi utilise this complete range but according to Dwivedi *et al.* (2011), minimum requirements for lignin degradation are a MnP and laccase or MnP and LiP and many isoforms of these proteins have been identified in plants and fungi (Gavnholt *et al.*, 2002; Dwivedi *et al.*, 2011; Tuomela *et al.*, 2000; Hatakka, 1994).

Lignin peroxidases (LiPs) are haem peroxidases, which are highly reactive enzymes that enable the oxidation of non-phenolic aromatic compounds by generating radicals that interact with the heterogeneous polymer (Figure 1.11). LiPs are oxidised by H_2O_2 to give an oxidised intermediate (Compound I) with Fe^{4+} and a radical on a tetrapyrrole ring. Compound I oxidises a substrate, generating a substrate-free radical and Compound II which still has Fe^{4+} but no radical. Compound II oxidises another molecule of substrate generating a second substrate-free radical and native peroxidase as shown Figure 1.12 (Hammel and Cullen, 2008), these radicals degrade in the

presence of molecular oxygen. VP also oxidises non-phenolic polymers by means of this catalytic cycle.

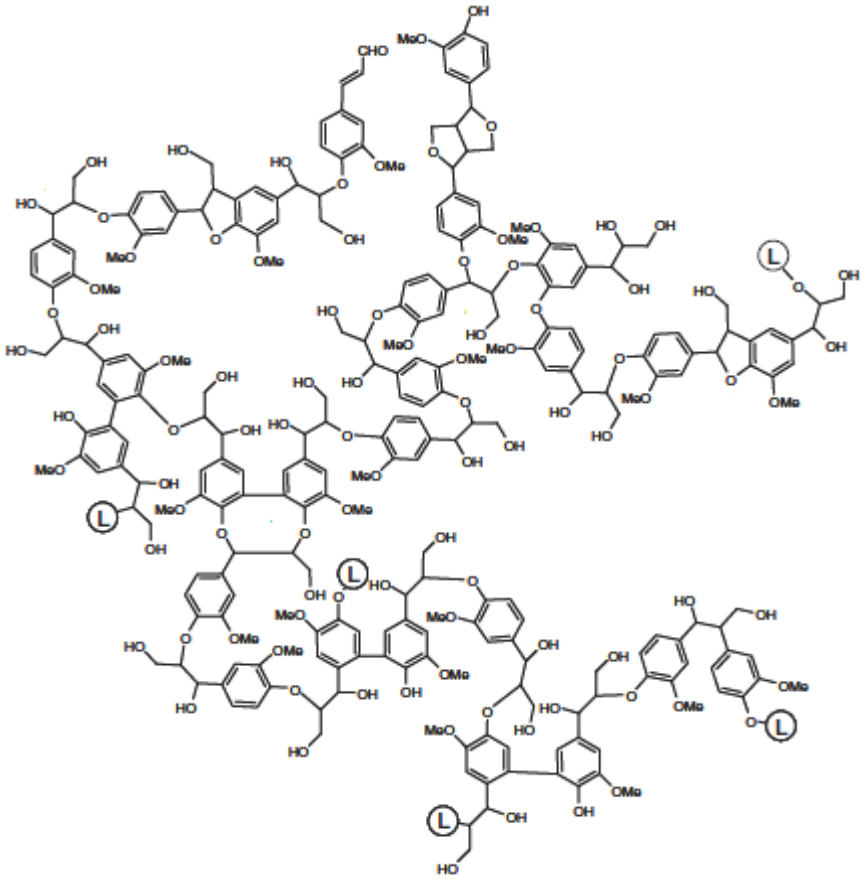

Figure 1.11. Heterogeneous structure of a lignin polymer. L indicates attachment sites of additional lignin polymers (Adapted from Ruiz-Dueñas and Martínez, 2009).

A general catalytic cycle of peroxidases is shown in Figure 1.12. Cleavage of aliphatic side chains of lignin between C-α and C-β, forms benzaldehydes, which results in a build-up of benzoic acid residues observed in lignin that has been degraded by white-rot fungi (Hammel and Cullen, 2008). The cleavage site in lignin residues is shown in Figure 1.12.

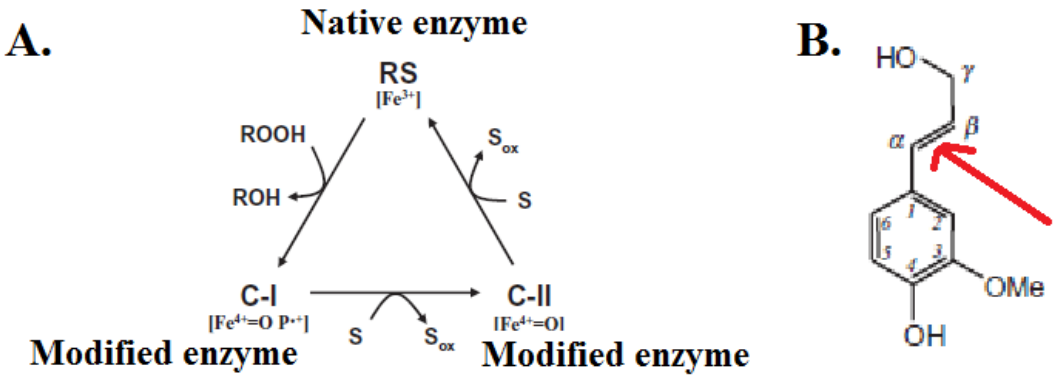

Figure 1.12. A. Catalytic cycle of peroxidases. The enzyme (LiP, MnP or VP), which contains Fe^{3+} in a resting state (RS) is oxidised by hydroperoxide forming compound I (C-I; Fe^{4+}-oxo and a porphyrin cation radical), which is reduced in two one-electron steps yielding an intermediate compound II (C-II; Fe^{4+}=O after porphyrin reduction) the resting state is restored by concomitant oxidation of two substrate molecules S (S; in the case of LiP, substrate are low-redox potential phenols or in the case of MnP and VP Mn^{2+}) (Dunford, 1999; Ruiz-Dueñas and Martínez, 2009) **B.** Cleavage site of aliphatic side chains in lignin forms benzaldehydes. Lignin cleavage site by the enzyme (LiP, MnP or VP), between C-α and C-β is shown by red arrow (Hammel and Cullen, 2008).

The catalytic cycle of MnP is similar to LiP, but uses a Mn^{2+} co-factor, which is omnipresent in lignocellulose and is chelated by an organic acid such as oxylate. MnP is activated by H_2O_2 and forms a Fe-MnP complex (Compound I) with a Fe^{4+} radical complex, water is released and MnP Compound II is formed. Mn^{2+} is oxidised to Mn^{3+}, Compound II is reduced and a second Mn^{3+} is formed from Mn^{2+} regenerating the native enzyme (Figure 1.12). VP, which combines features of both LiPs and MnPs, can also oxidise Mn^{2+} to Mn^{3+}. MnP catalyses the formation of a range of radicals, from a variety of aromatic and non-aromatic substrates, some of which are shown in (Figure 1.13) (Bao *et al.*, 1994; Hofrichter, 2002).

The role of veratryl alcohol, a secondary metabolite, mentioned earlier as being involved in lignin degradation, is not well understood and there are a number of theories about its activity. In one theory, LiP oxidises veratryl alcohol to a veratryl alcohol radical cation which can diffuse into lignin and cleave it oxidatively by electron transfer (Hunt *et al.*, 2013). For large polymers, oxidative cleavage requires the presence of veratryl alcohol, and a veratryl alcohol cation would be able diffuse into lignin, due to its small size, to catalyse the oxidation of substrate. This supports the argument for this role for veratryl alcohol. An alternative theory proposed for veratryl alcohol concerns its

inactivation of H_2O_2, preventing the oxidation of LiP. The veratryl alcohol cation has a long half life at low pH, and lignin is a bulky substrate, thus LiP may require some time to cleave the polymer and would be oxidised by H_2O_2, if it were not protected by veratryl alcohol (Cai and Tien, 1992).

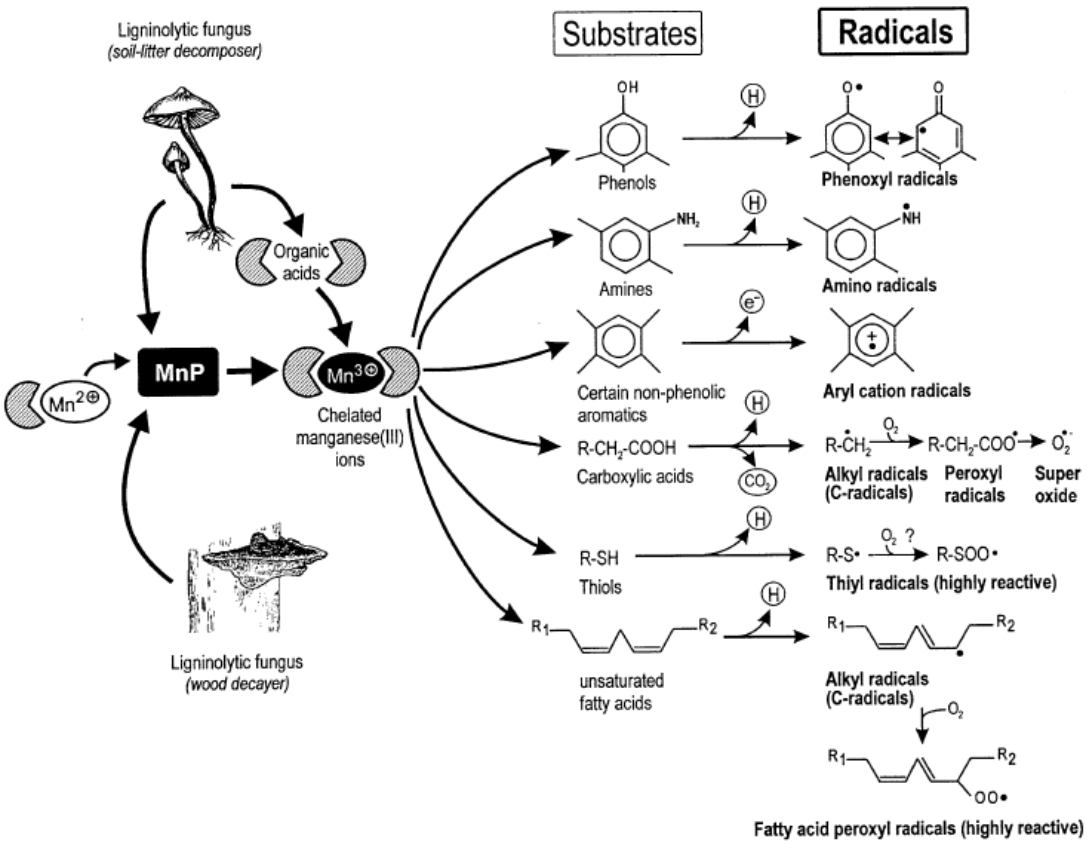

Figure 1.13. Substrates of MnP and the radicals generated by its activity (Hofrichter, 2002).

Laccase catalyses the reduction of O_2 to H_2O from many compounds (Baldrian, 2006). Laccase, polyphenol oxidase (multicopper oxidase), catalyses the reduction of O_2 to water and oxidises a wide range of phenolic and non-phenolic substrates, with the exception of tyrosine, using them as hydrogen donors and redox mediators (Figure 1.14) (Strong and Claus, 2011; Hammel and Cullen, 2008). Laccases are extracellular glycoproteins and usually consist of isoenzymes with unique substrate specificity, and a pH range of 3 - 7 (Dwivedi *et al.*, 2011; Baldrian, 2006).

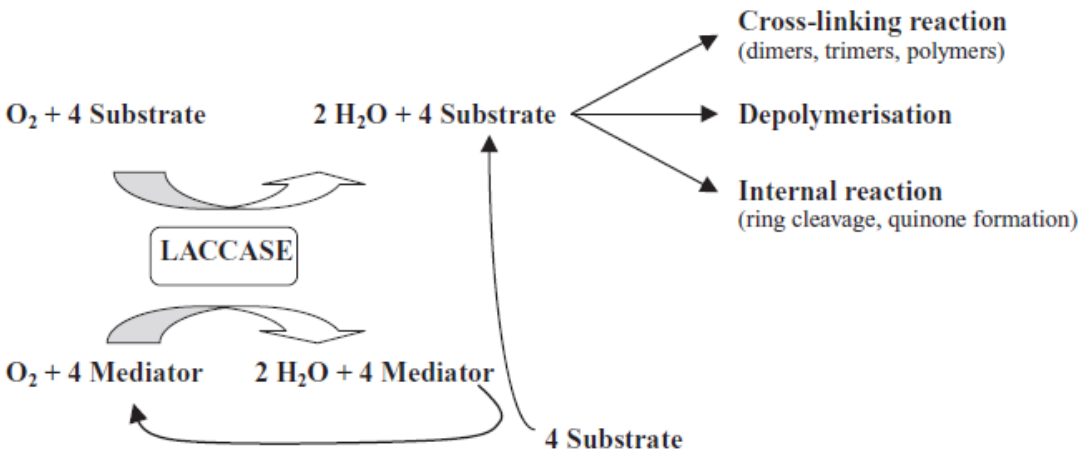

Figure 1.14. Laccase reaction. Laccase catalyses the reduction of O_2 to water, by oxidation of substrate, and formation of unstable radicals. These radicals further react with substrate, forming dimers, trimers and polymers; they can also depolymerise substrate or cleave aromatic rings, forming quinones. Substrates of laccase are numerous and isoenzymes many specificities have been identified in all organisms that possess laccases. Diphenols, aromatic amines, polyphenols, and methoxy substituted phenols are all substrates of laccase. There over 100 synthetic mediators, used in industrial applications of laccase (Johannes and Majcherczyk, 2000), and naturally occurring mediators include: *p*-coumaric acid, ferrulic acid or synapic acid, derivatives of phenylalanine and putative precursors of monolignols (Strong and Claus, 2011; Boerjan *et al.*, 2003) these mediators can improve the effacacy of laccases (Kang *et al.*, 2002).

Due to their broad substrate specificity laccases have perhaps the widest range of biotechnological applications of any enzyme. Laccases have been used to remove toxins from industrial wastes, and to degrade agro-industrial waste, polyaromatic carbons and carcinogenic compounds (Keum and Li, 2004; Hadibarata *et al.*, 2012; Hadibarata and Kristanti, 2012a; Moreira-Neto *et al.*, 2013; Chapple *et al.*, 2007; Alcalde *et al.*, 2002; Yang *et al.*, 2009; Kang *et al.*, 2002), and have been used to polymerise compounds in the personal care and cosmetic industry (Jeon *et al.*, 2010; Markussen and P.E. Jensen, 2006). They have been used in food and drink industries to clarify beer, juice and wine and improve products containing gluten (Osma *et al.*, 2010; Rodríguez Couto and Toca Herrera, 2006; Renzetti *et al.*, 2010). Their medical applications include use as biosensors, sterilising agents and in immunochemical and enzymatic assays (Dwivedi *et al.*, 2011; Liu and Dong, 2007; Orndorff, 1984; Murao *et al.*, 1985).

1.1.2.7 Other cell wall component degradation by basidiomycetes species.

Cellulose, the most abundant component of the plant cell wall is an unbranched polysaccharide polymer composed of β-1,4-linked glucose monomers which form microfibrils of parallel polymers be composed of up to 15,000 glucose monomers. The structure of cellulose is shown in Figure 1.15 (Sticklen, 2008).

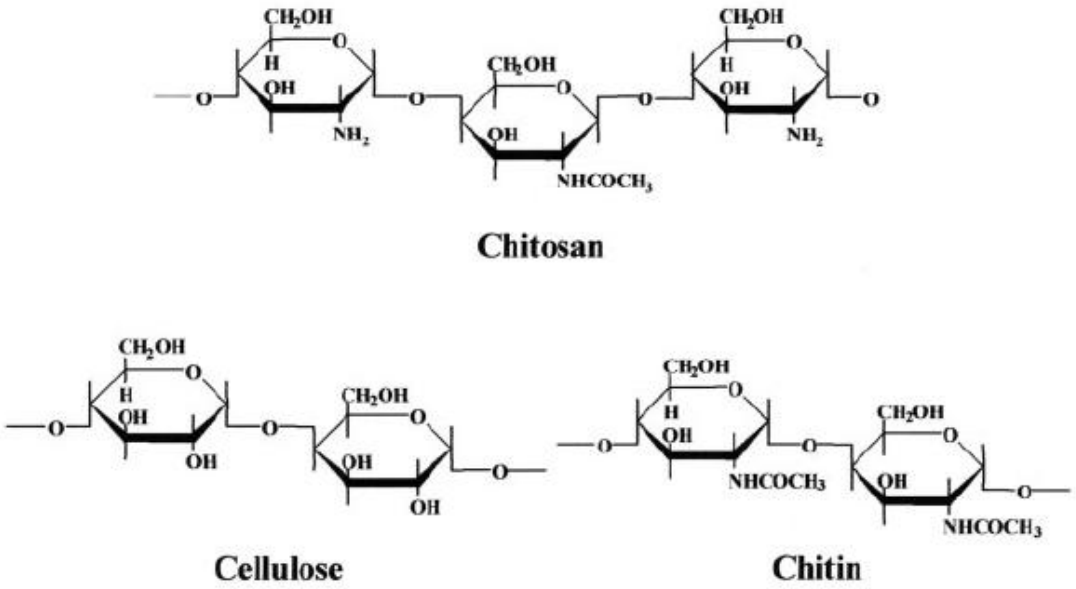

Figure 1.15. Structures of cellulose, chitin and chitosan (Jang *et al.*, 2004).

Hemicellulose is comprised of short polysaccharides composed of different saccharide monomers, and has a random structure which links other cell wall components (Sticklen, 2008), some possible structures of hemicellulose are shown in Figure 1.16. Pectins are heterogeneous polysaccharides found in the primary cell wall, which are branched and highly hydrated and comprise one third of primary cell wall molecules (Wong, 2008). The structure of pectin is made up of homogenous regions and other regions which are composed of many different polysaccharides, and pectin from different organisms varies in composition, one such structure is shown in Figure 1.16 (Huisman *et al.*, 2001). In addition, the fungal cell wall is comprised of chitin, a (1-4)-linked N-acetyl-β-D-glucosamine polysaccharide, similar to cellulose except for an acetamide group, in place of the hydroxyl at the C-2 position of the glucose unit (Jang *et al.*, 2004). Fungal cell walls must constantly be remodelled and may undergo acetylation (to chitosan) (Figure 1.15) as the fungus forages for nutrition, which requires degradative enzymes (Feofilova, 2010; Vincent *et al.*, 2012).

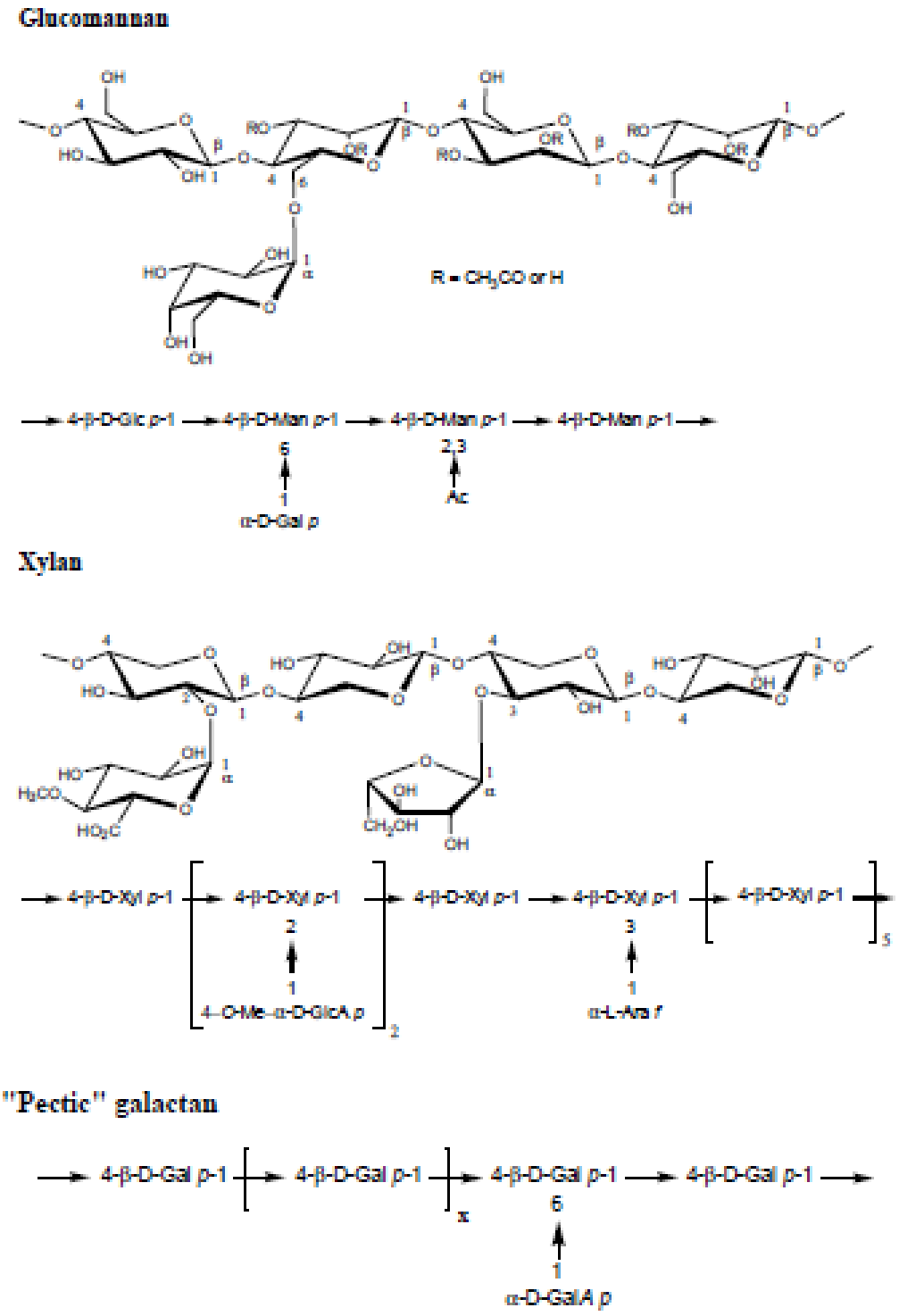

Figure 1.16. Structure of hemicelluloses from softwood and pectin. Man, mannopyranose; Gal, galactopyranose; GlcA, glucuronic acid; Ara, arabinose;Xyl, xylose; (Laine, 2005)

Degradation of these heterogenous polysaccharides by fungi requires a wide range of hydrolytic enzymes with specificity for cleavage of particular glycosidic bonds. These enzymes are broadly categorised into (i) glycoside hydrolases, (ii)

glycosyltransferases, (iii) polysaccharide lyases and (iv) carbohydrate lyases. Some of these enzymes may also have carbohydrate binding modules which bind polysaccharides and present them for lysis by glycolytic enzymes (Cantarel *et al.*, 2009). These categories are further subdivided into families based on substrate specificity and catalytic mechanism. Briefly, glycoside hydrolases cleave bonds between two carbohydrates or between carbohydrate and non-carbohydrate moieties; glycosyltransferases transfer saccharides from a donor which is phosphor-activated, to an acceptor forming glycosidic bonds; polysaccharide lyases cleave polymers that contain uronic acids, to form unsaturated hexenuronic residues and polymers with new reducing ends; carbohydrate esterases cleave esters in mono-, oligo- or polysaccharides (Cantarel *et al.*, 2009).

1.2 *Armillaria* spp.

Armillaria (Agaricales, Physalacriaceae), species were first described by a Danish mycologist Martin Vahl in 1790, and in 1857 Fredrich Staude characterised the generic rank of *Armillaria* (Watling *et al.*, 1982). *Armillaria mellea* was characterised by Paul Kummer a German mycologist in 1871 (Kummer, 1871). The genus *Armillaria* (Fr.) Staude, and type species *Armillaria mellea* (Vahl) P. Kumm., are taxonomically recognised classifications today. A former synonym for the genus was *Armillariella* (Singer, 1986).

Armillaria species are some of the largest organisms on earth and persist in the soil for many years. One *A. ostoyae* specimen, in a forest of mixed conifers in Oregon, U.S.A., is reputed to be millennia old and estimated to cover 965 ha. (Ferguson *et al.*, 2003). *Armillaria* spp. are both saprophytic and parasitic and are pathogens of more than 600 plant species (Raabe, 1966). Pathogenicity is dependent on both the *Armillaria* species and the host species, and in addition, individual isolates may be more or less virulent on different species (Raabe, 1972). The descending order of virulence in pathogenic species, is *A. mellea*, *A. ostoyae* (Morrison, 1982, 1991), *A. gallicia*, *A. cepistipes* (Redfern, 1975; Morrison, 2004; Gregory, 1985), although in North America, *A ostoyae* is more widespread. *A. mellea*, the most virulent of *Armillaria* spp. infects fruit, timber, and agronomic crops, as well as ornamental species and weeds (Baumgartner *et al.*, 2011; Raabe, 1962; Robinson-Bax and Fox, 2002; West and Hughes, 2000; Sainz-Oses, 2004; Pertot *et al.*, 2008; Morrison, 2004; Choi *et al.*, 2011; Korhonen, 1978). *A. mellea* was listed by the American Phytopathological Society as a

high priority species for genomic sequencing, due to its virulence and pathogenicity on forest trees and the corresponding impact this has on global CO_2 levels (APS, 2008).

The numbers of *Armillaria* species now identified is more than 50 (Coetzee *et al.*, 2011). There is one holarctic group comprised of three subgroups, Europe, North America and Asia (Table 1.1), and three non-holarctic groups (i) Austrialia, South America and New Zealand; (ii) Africa and India; and (iii) Central America (Table 1.2) (Coetzee *et al.*, 2011). There are a number of species in each group which may be compatible. For instance, *A. mellea* is known as North American Biological group (NABS) VI, European Biological Species (EBS) D, and Chinese biological species (CBS) K, but has no compatible group from Japan. On the other hand, *A. cepistipes*, EBS B and NABS XI crosses, are infertile (Baumgartner *et al.*, 2011).

Table 1.1 The *Armillaria* species which occur the Holarctic Floral Kingdom.

Species	Western North America	Eastern North America	Europe	China	Japan
A. borealis			A	CBS M	
A. calvescens		NABS III			
A. cepistipes	NABS XI	NABS XI	B		NAG D
A. ectypa			*		*
A. gallica	NABS VII	NABS VII	E	CBS B	NAG A
A. gemina		NABS II			
A. jezoensis					H
A. mellea	NABS VI	NABS VI	D	CBS K	
A. mellea ssp. *nipponica*				CBS G	NAG Am
A. nabsnona	NABS IX				NAG B
A. ostoyae	NABS I	NABS I	C	CBS D	NAG C
A. sinapina	NABS V	NABS V		CBS A	F
A. singula					G
A. tabescens	*	*	*	CBS I	T
Undescribed species					
NABS X	*				
CBS C				*	
CBS F				*	
CBS H				*	
CBS J				*	
CBS L				*	
CBS N				*	
CBS O				*	
NAG E					*

NABS, North American biological species; CBS, Chinese biological species; NAG, Nagasawa, Japan; *, a species is present (Baumgartner *et al.*, 2011).

1.2.1 Taxonomy

Armillaria spp. were originally classified by the morphological characteristics of their fruiting bodies, pathogenicity and ecological niche, but this was unsatisfactory, as over 274 species were classified taxonomically as *Armillaria mellea* (Volk and Burdsall, 1995), due to their white spores and gill shape (Fukuda *et al.*, 2003). Additionally, basidiocarps are short-lived in the field, these fruiting bodies are not always produced and basidocarp and hyphal morphology may be influenced by nutrition source, basidiocarps are not easily induced in the laboratory and may have altered

morphology in cultures (Kile and Watling, 1988; Grillo *et al.*, 2000; Baumgartner *et al.*, 2011).

Species recognition, using mating studies as a basis for biological identification, was used in the 1970s and a number of different *Armillaria* species were identified in Europe and North America by this method (Anderson and Ullrich, 1979; Korhonen, 1978; Baumgartner *et al.*, 2011). Mating studies are not satisfactory as a means of identification. The morphology of haploid mycelia, which is white initially, after successful mating becomes brown and crustose which is the morphology of the diploid (Korhonen and Hintikka, 1974), but diploid/haploid mating results can be ambiguous (Harrington *et al.*, 1992; Korhonen, 1978). However, this method still is used to identify species in Europe, where biological and morphological *Armillaria* species coincide (Baumgartner *et al.*, 2011).

Table 1.2. *Armillaria* species and equivalent species in the non-Holarctic Floral Kingdoms.

Species	Central America	South America	Africa	Australia	New Zealand	Other regions
A. affinis	*					
A. camerunensis			*			
A. duplicata						India
A. fellea						New Guinea
A. fumosa				*		
A. fuscipes			*			
A. griseomellea		*				
A. heimii			SIG II			
A. hinnulea				*	*	
A. limonea					*	
A. luteobubalina				*		
A. mellea			SIG I			
A. mellea ssp. *nipponica*						Bhutan
A. melleo-rubens	*					
A. montagnei		*				
A. novae-zelandiae		*		*	*	New Guinea, Sumatra, Malaysia, Fiji
A. omnituens						India
A. pallidula				*		
A. paulensis		*				
A. pelliculata			*			
A. procera		*				
A. puiggarii		*				
A. sparrei		*				
A. tabescens	*					
A. tigrensis		*				
A. umbrinobrunnea		*				
A. viridiflava		*				
A. yungensis		*				
Undescribed species						
BPS I						Bhutan
NZ *Armillaria* sp.					*	

BPS, Bhutan Phylogenetic Species; NZ, New Zealand; SIG, Somatic Incompatibility; *, a species is present (Baumgartner *et al.*, 2011).

Molecular approaches have improved species identification, and DNA based identification has been used in recent years to determine the origins of different *Armillaria* species, their phylogeny, geographical origins and distribution (Coetzee *et al.*, 2011). Several molecular methods have been employed. Amplification fragment

length polymorphism (AFLP) was one of the first of the molecular methods to be used (Motta, 1985; Smith *et al.*, 1990; Pérez-Sierra *et al.*, 2004). Restriction fragment length polymorphisms (RFLP) (Otieno *et al.*, 2003; Anderson *et al.*, 1987; Coetzee *et al.*, 2000), with identification of intergenic sequence (IGS) of rDNA has enabled species comparisons (Mwenje *et al.*, 2006; Jahnke *et al.*, 1987; Sicoli *et al.*, 2003; Anderson and Stasovski, 1992; Kim and Klopfenstein, 2000; Coetzee *et al.*, 2001; Coetzee, Wingfield, Kirisits, *et al.*, 2005; Otieno *et al.*, 2003; Cox *et al.*, 2006), this has been combined with internal transcribed region (ITS) of rDNA profiling (Schulze and Bahnweg, 1995; Otieno *et al.*, 2003; Coetzee *et al.*, 2001; Coetzee, Wingfield, Kirisits, *et al.*, 2005; Sicoli *et al.*, 2003). Some species have very similar ITS sequences, and although IGS sequences can differentiate between European species, some isolates of *A. cestipes* and *A. gallica* cannot be distinguished (Chillali *et al.*, 1998).

An approach taken by Antonin *et al.* (2009), combining ITS and IGS profiling with sequencing of elongation factor 1-α (EF1-α) gene, of *A. cepistipes* and *A. gallica*, was used successfully to differentiate between these species. Another combination method used IGS with fatty acid methyl-ester profiling of species, to confirm the identity of different *Armillaria* species in a single area (Cox *et al.*, 2006). Pectic enzyme profiles (isozyme profiles) from different *Armillaria* species was used successfully to distinguish between a number of African species and some European species (Mwenje and Ride, 1997; Mwenje *et al.*, 2006), and in a larger study of 36 isolates, from different hosts and geographic regions, 17 *Armillaria* species were identified by pectic isozyme profiling (Coetzee *et al.*, 2009).

Positive species identification is vital to prevent the introduction of pathogenic species into agronomic crops and timber forests (Rossman and Palm-Hernandez, 2008). Holarctic *Armillaria* strains from Europe appear to have been introduced into South Africa, and have not caused damage to agronomic crops, but are restricted to gardens in urban areas (Coetzee *et al.*, 2001). This contrasts with the introduction of Asian species to Africa, where their spatial distibution is extensive, compatibility with African strains is evident, and they have been identified in locations 4000 km apart. Basidiospores are thought to be the mode of dispersal of these species, possibly derived from an initial infection of infected plants imported from Asia (Baumgartner *et al.*, 2011).

1.2.2 Lifecycle of *Armillaria* spp.

The vegetative state of *Armillaria* spp. is diploid, not dikaryote, which is unusual among basidiomycetes (Korhonen and Hintikka, 1974). *A. mellea* is unusual,

both among basidiomycetes and also among *Armillaria* spp. in that its vegetative mycelia do not have a dikaryotic stage during fruiting (Figure 1.17) (Ota *et al.*, 1998; Lamoure, 1985). In *A. mellea* single spore matings, dikaryotic mycelia form, but these dikaryote cells are unstable, and either die within a few days or become diploid (Lamoure, 1985). Most *Armillaria* species have two dikaryotic stages, the first occurs after mating of monosporus mycelia, and the second in the subhymenium, or gill tissue, before meiosis and the generation of haploid basidiospores (Figure 1.17). A sub-species of *A. mellea* identified in Japan has an unusual type of homothallism, whereby tetraploid cells undergo meiosis twice and haploid cells are generated. These cells fuse and migrate to the basidiospores either singly or in pairs where basidiospores are either diploid, anucleate, or dikaryotic and diploid (Figure 1.17) (Ota *et al.*, 1998).

Armillaria spp. grow as saprophytic rhizomorphs, comprised of thousands of hyphae surrounded by a protective melanin containing sheath which look similar to plant roots (Schweiger *et al.*, 2002; Mihail and Bruhn, 2005; Motta, 1969; Yafetto *et al.*, 2009). These rhizomorphs grow through the soil, foraging for nutrients (Mihail and Bruhn, 2005) and colonising plant roots. Rhizomorphs may have dichotomous branching, similar to adventitious root systems in plants, or monopodial branching, similar to tap root systems in plants, and species with dichotomous branching are generally more virulent (Morrison, 2004). Mycelial hyphal fans infect plants by growing between the bark and cambium eventually killing the plant.

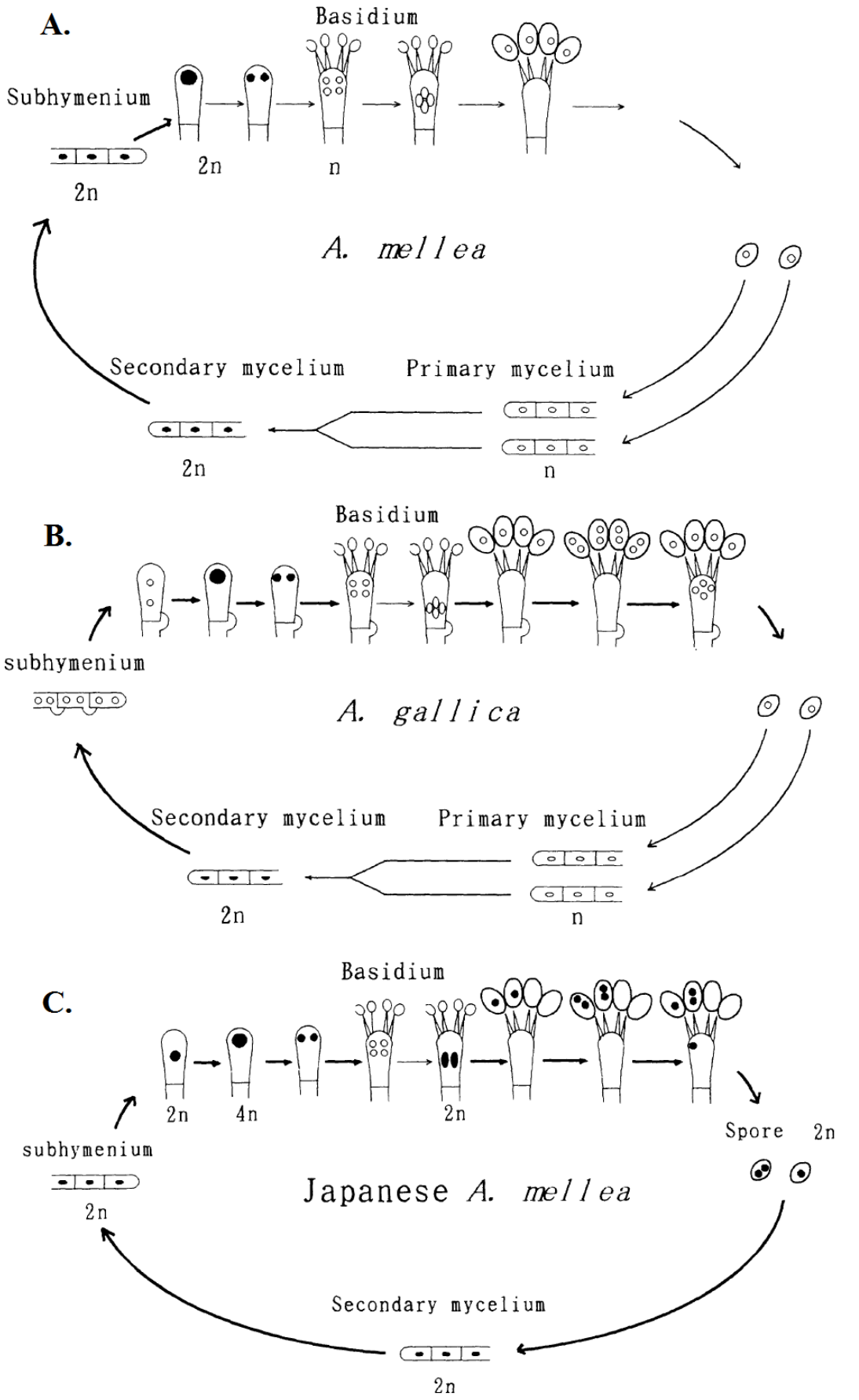

2n indicates diploid mycelia **n indicates haploid mycelia**

Indicates diploid nuclei **Indicates haploid nuclei**

Figure 1.17. Lifecycles of selected *Armillaria* spp. **A**. *A. mellea* lifecycle: The most persistent mycelia are vegetative diploid brown crustose mycelia. During fruiting, basidiocarps are formed which contain basidia with diploid nuclei that undergo meiosis, generating haploid basidospores. The basidiospores are wind-dispersed and germinate into white fluffy haploid mycelia (primary mycelia) with a tetrapolar mating system. Mating produces dikaryotic mycelia which becomes diploid and forms secondary mycelia, or die within a few days (Lamoure, 1985; Korhonen and Hintikka, 1974; Ota *et al.*, 1998). **B**. *A. gallica* lifecycle: Vegetative mycelia, the persistent form of the fungi, are diploid but in the gill tissue (subhymenium), dikaryotic mycelia form, these develop by unknown means into dikaryotic basidia that undergo mitosis and meiosis forming haploid basidiospores, which are wind-dispersed and germinate into primary mycelia. Heterothallic mating produces diploid secondary mycelia. **C.** Japanese *A. mellea:* Vegetative diploid mycelia become tetraploid (4n) and undergo meiosis, haploid cells are generated, two pairs fuse and migrate to basidiospores either singly, in pairs, or not at all. Basidiospores are wind-dispersed and germinate into diploid mycelia. This is a form of homothallism and known only in this species (Ota *et al.*, 1998).

1.2.3 *Armillaria mellea* pathogenicity and virulence.

A. mellea is known by several names, such as honey fungus, root rot, butt rot, or bootlace fungus, the latter a reference to the black rhizomorphs found under the bark of diseased trees and in the soil. Basidiospores are not widely implicated in the spread of the fungus (Williams *et al.*, 1989), however a study by Travadon *et al.* (2011) has suggested that the role of basidiospores in infection is greater that was thought heretofore, and this supports studies of *A. novae-zealandiae* that found basidiospores were responsible for colonisation of tree stumps (Hood *et al.*, 2002; 2008). Most plant infections by *A. mellea*, occur through contact with rhizomorphs in the soil, or by contact between roots of infected plants. In the wild, *A. mellea* mostly affects trees that have been subjected to stress, by insects, competition or environmental conditions but can it also kill healthy trees (Williams *et al.*, 1989). However, in land that has been cleared for planting of agricultural or timber crops, rhizomorphs remain in the soil and on tree stumps, serving as innocula for new foci of infection (Baumgartner, 2004; Baumgartner *et al.*, 2011). *A. mellea* rhizomorph systems are dichotomous, and variable in volume and length (Morrison, 2004). White mycelial fans grow between bark and wood, in the vascular cambium (Shaw III and Kile, 1991) and mechanical activity as well as enzyme hydrolysis of plant tissue, cause host tissue penetration, although the

precise nature of enzyme-mediated degradation of plant tissue is not known. Clearly much work remains to be done on identifying the *A. mellea* "degradome".Vascular destruction and necrosis of cambium and secondary xylem follow (Shaw III and Kile, 1991; Yafetto *et al.*, 2009; Mwenje *et al.*, 2006) and once a plant has been girdled by *A. mellea* mycelia, it inevitably dies (Williams *et al.*, 1989). In a virulence study of *Armillaria* spp., 66% of Douglas Fir seedlings exposed to *A. mellea* became infected by the fungus within one year and 81% of these died. Fifty-one percent of all seedlings in the study were dead within two years (Morrison, 2004). This virulence is mirrored by a study of vineyards in Northern Italy where it was found that replanting of vines had no effect on the total number of infected vines (Pertot *et al.*, 2008), although more resistant species can be grown in areas infected with *A. mellea* to alleviate its effects (Baumgartner and Rizzo, 2006; Thomas *et al.*, 1948).

1.2.3.1 Signs and symptoms of infection by *A mellea*.

Signs of infection by *A. mellea* infection are usually disease foci that expand radially, with dead and dying plants forming circular openings in forest canopies (Figure 1.18), or discoloured red patches of vines within vineyards due to discolouration of leaves (Figure 1.18), (Baumgartner *et al.*, 2011; Ferguson *et al.*, 2003; Pertot *et al.*, 2008). Individual trees within an area may become infected more rapidly within an infection locus (Baumgartner *et al.*, 2011). Infected trees exhibit wilting and defoliation with gradual loss of vigour and stunted growth, fruit quality deteriorates, and death of the plant follows, either from loss of vascular tissue, susceptibility to attack from other pathogens and insects, or wood loss which causes the plant to collapse (Baumgartner and Rizzo, 2001b; Baumgartner *et al.*, 2011; Pertot *et al.*, 2008; Thomidis and Exadaktylou, 2012). Large amounts of resin are exuded by infected plants, particularly coniferous trees (a protective mechanism by the host) root collars may be swollen, or may have cavities (Williams *et al.*, 1989; Brazee and Wick, 2009), and *A. mellea* rhizomorphs can be seen growing on roots and in soil around plants. *A. mellea* fruiting bodies which grow in clumps, a habit known as caespitose, (Figure 1.18), can be seen in the soil or around the base of infected plants in Autumn, particularly under moist conditions (Williams *et al.*, 1989; Coetzee *et al.*, 2001; Otieno *et al.*, 2003; Baumgartner *et al.*, 2011). Dark-coloured *A. mellea* rhizomorphs are visible on wood underneath the bark of roots and at the root collar (Figure 1.18) and white mycelial fans are visible beneath tree bark spreading upward from the roots, (Figure 1.18). Wood from infected

trees has a water-soaked appearance and dark coloured wood decay lines are visible on wood in advance of mycelial fans (Williams *et al.*, 1989; Baumgartner *et al.*, 2011).

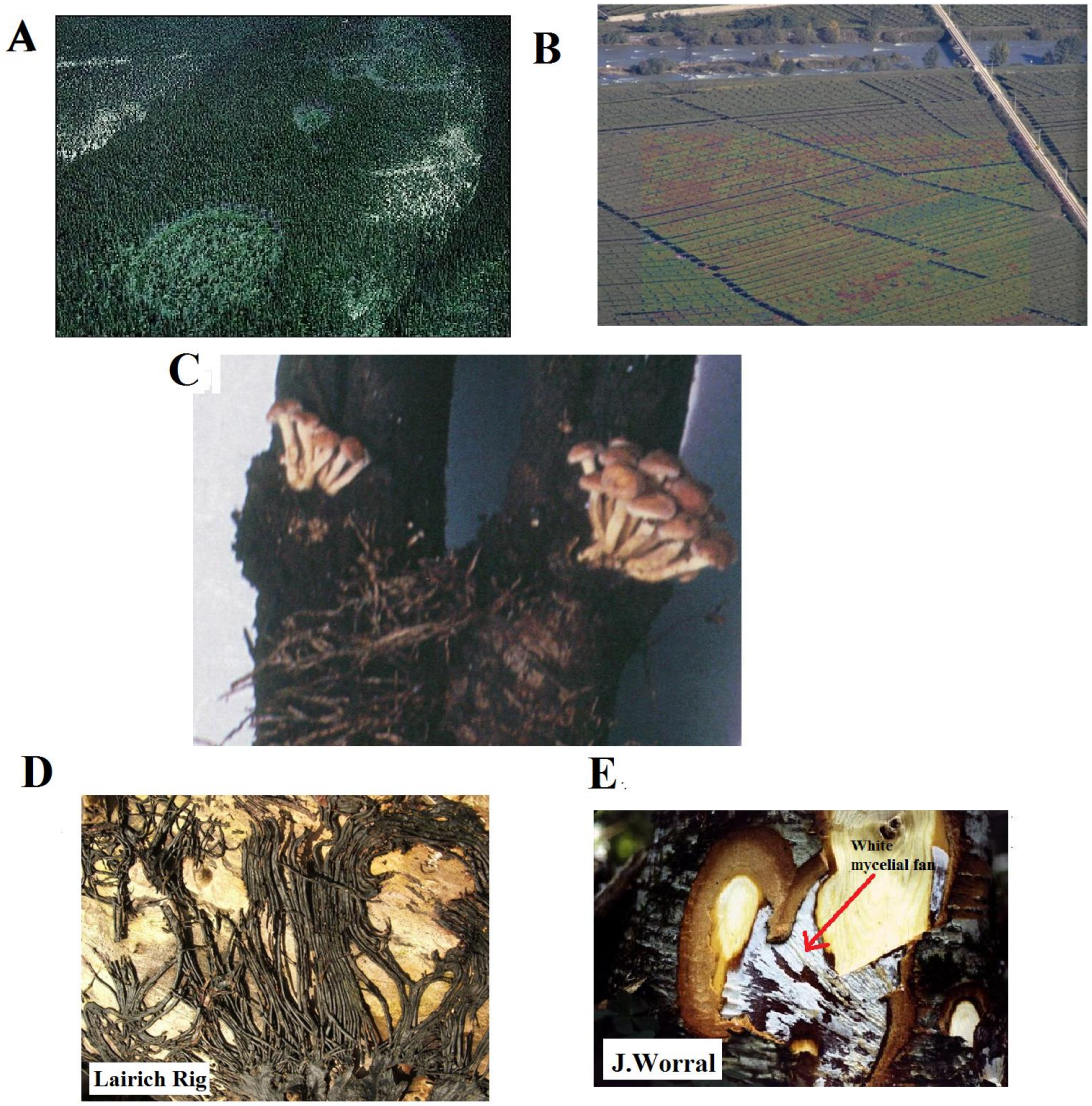

Figure 1.18. Anatomy of infection by *A. mellea* **A.** Virgin forest in Montana, U.S.A. Aerial view shows several disease centres indicated by light coloured patches, which are gaps in the forest canopy (Williams *et al.*, 1989). **B.** Aerial view of vineyards in Northern Italy, where red patches indicate areas affected by *A. mellea* infection (Pertot *et al.*, 2008) **C.** *A. mellea* rhizomorphs and basidiocarps on tea plant, showing caespitose basidiocarps (Otieno *et al.*, 2003). **D.** Black *A. mellea* rhizomorphs found between the bark and the wood of trees. (Photograph, Lairich Rig [CC-BY-SA-2.0 (http://creativecommons.org/licenses/by-sa/2.0)]. **E.** White mycelial fan of *A. mellea* beneath the bark of a birch tree where it has destroyed the vascular cambium and secondary xylem. (Photograph J. Worral **http://www.apsnet.org/edcenter/intropp/lessons/fungi/Basidiomycetes/Pages/Armillaria.aspx)**.

1.2.3.2 Damage caused by *A. mellea*

Although damage to plants by *Armillaria* spp. worldwide has been recorded for many years, confusion arising from lack of positive identification of the infecting species has obscured the damage done by each particular species. Qualitative data are available, but quantitative data less so, and the range of host species parasitised by *A. mellea* (Raabe, 1962, 1966; Robinson-Bax and Fox, 2002) means that no cohesive estimates are available of the total cost of damage caused by the fungus. Perhaps its ubiquitous existence precludes quantification, as a study of *A. mellea* reported it to be highly pathogenic on a range of deciduous trees and conifers in the United Kingdom (Rishbeth, 1982), but this study only assessed the species causing pathogenicity, rather than the cost in economic and ecological terms. In Europe, *A. mellea* is prevalent throughout the continent, especially in the more northern regions (Guillaumin *et al.*, 1985). There is widespread *A. mellea* infection in California on many hosts, its occurrence has been reported in indigenous forests, urban areas, vineyard and orchards, with higher incidences observed in vineyards and orchards than in other locations (Baumgartner and Rizzo, 2001a,b). In Californian mixed-hardwood forests, a survey found *A mellea* infections in more than 12% of dead trees and over 9% living trees (Baumgartner and Rizzo, 2001a,b). Bhutan, a kingdom in the Himalayas, is highly forested (64%), which is ecologically important, but the forests are also of significant local economic importance. The forests have shown a decline in Fir populations attributed to *Armillaria* spp. infection, but due to the transient nature of basidoicarps, the species responsible have not been identified (Coetzee *et al.*, 2005). *A. mellea* has been identified as responsible for oak forest decline in Pennsylvania (Marcais and Wargo, 2000) and Missouri (Bruhn *et al.*, 2000) in the U.S.A., and in Iran (Davari and Askari, 2005). Infections of *Alnus glutinosa* were reported in the Czech Republic (Antonin *et al.*, 2009) and *Pinus* and *Eucalyptus* in Africa (Wingfield and Knox-Davies, 1980) (Wingfield1980 Knox). *A. mellea* was found to be present in most areas of Greece, in uncultivated areas, and was also found to be highly pathogenic to olive trees (Tsopelas, 1999).

Some quantitative data on the scale of *A. mellea* infections have been published. A survey of *Pinus* spp. in timber stands in South Africa, showed 20% tree mortality within the first 15 years after planting due to *Armillaria* infection (Lundquist, 1993). In the Rift Valley of Kenya, forested land has been cleared for tea plantations, and

A. mellea infection has been reported, infecting not only tea plants but also indigenous trees, particularly *Acacia* spp., adjacent to plantations. *A. mellea* infection occurs wherever tea is grown in Kenya causing up to 50% crop losses on small farms (Onsando *et al.*, 1997). In Zimbabwe, *A. mellea* is most prevalent in the eastern highlands and infects pine plantations and orchards. It is not very prevalent or virulent among indigenous tree species, but is virulent in orchards where land is cleared and rhizomorphs serve as inocula. It has been reported from one disease location, where two orchards were infected by *A. mellea*, 80% of plum trees in an orchard of 2 ha., and 60 % of peach trees in a 1.5 ha orchard, were killed by the fungus and 20 % of the remaining peach trees were symptomatic with chlorotic leaves (Mwenje *et al.*, 1998). *A. mellea* also infects cassava an important food crop which is vital for the local economy in Zimbabwe, and *A. mellea* infection has been responsible for up to 30% of Cassava crop losses (Mwenje *et al.*, 1998). In a survey of vineyards of northwest Spain, 2% of plants were infected by *Armillaria* spp. One vineyard had a 17% infection rate and two years later the infection rate had risen to 43% of plants from that vineyard (Sainz-Oses, 2004), an indication that once an area has an infection locus *A. mellea* spreads rapidly. A 4-year assessment of vineyards of Piana Rotalina in Northern Italy where viticulture is of great economic importance, found that 25% of the vineyards (36 ha.) were infected by *Armillaria* spp. and that 2% of the cultivated vines exhibited disease (Pertot *et al.*, 2008). Fir trees in the subalpine region of Colorado are particularly susceptible to *A. mellea* and quickly succumb to infection. The annual loss of timber from Fir species in this area is estimated to be 10,500 m^3 (Williams *et al.*, 1989; Shaw III and Kile, 1991; USDA Forest Service, 2011). Wood destruction by *A. mellea* on walnut timber in one Iranian forest represented up to 10% of wood weight (Dalili *et al.*, 2010). In Canandan prairie provinces where conifer regeneration has been undertaken, *A. mellea* killed trees 5 to 25 years after planting with mortality rates of up to 25% (Mallett, 1985). The annual loss caused by *Armillaria* spp. to the peach industry in South Carolina was $3.86 million in the years 1987 to 1992 and in Georgia in 2000 *Armillaria* spp. caused $660,000 damage to the peach industry (Miller, 1994; Williams-Woodward, 2001; Cox *et al.*, 2006).

Most studies into pathogenic aspects of *A. mellea* control have focussed on control measures (Baumgartner and Warnock, 2006b; Baumgartner and Rizzo, 2006; Baumgartner and Warnock, 2006a; Baumgartner *et al.*, 2013; Adaskaveg *et al.*, 1999; Dalili *et al.*, 2010; Marcais and Wargo, 2000; Pellegrini *et al.*, 2012; Raziq, 1998; Redfern, 1975; Veness, 1991a; Aguín *et al.*, 2006). These include bio-controls by use of

a proprietory inoculant (Baumgartner and Warnock, 2006b) and application of microorganisms (Pellegrini *et al.*, 2012; Raziq, 1998). Chemical treatments, however, have been largely ineffective (Adaskaveg *et al.*, 1999; Veness, 1991b; Marcais and Wargo, 2000; Aguín *et al.*, 2006), whereby the one chemical control which is most effective, methyl bromide, is about to be banned for use in the U.S. (Baumgartner *et al.*, 2011) although some recent success has been demonstrated using cyproconazole (Thomidis and Exadaktylou, 2012). Development of resistant host strains is also a route under investigation in the development of *A. mellea* control measures (Baumgartner and Rizzo, 2006). Pear trees were thought to be resistant to *A. mellea,* and were the species of choice in Californian orchards for this reason, but the incidence of infection has increased and many disease foci have been identified, putatively spread through clearing of oak forests for orchards (Rizzo *et al.*, 1998). This makes investigation of the pathogen at molecular level more urgent, in order to develop more effective controls for *A. mellea*.

A. mellea is a symbiont of *Gastrodia elata*, a member of the orchid family and penetrates the roots of *G. elata* which derives its nutrition from fungal digestion of wood (Gao *et al.*, 2009; Sekizaki *et al.*, 2008; Park *et al.*, 2010). *A. mellea* can also be parasitised by other species and *Entoloma abortivum,* another Agricaricales species, is one such organism, which causes *A. mellea* fruiting bodies to become mis-shapen carpophoroids, which are fruiting bodies comprised of *Armillaria* spp. hyphae (Czederpiltz *et al.*, 2001; Fukuda *et al.*, 2003). Moreover, an ascomycete, *Wynnea*, is also thought to parasitise *A. mellea* (Fukuda *et al.*, 2003).

1.2.4 Bioluminescence, secondary metabolites, and known protein activities

A. mellea has been known to be bioluminescent and to secrete a range of bioactive compounds many of which are sesquiterpene aryl-esters, that were identified in the thirty years between 1970 - 2000, but there has been remarkably little investigation of the fungus since the advent of high-throughput genomic and proteomic technologies. Little is known about mechanisms of *A. mellea* infection, inoculation of plants with *A. mellea* and detection of infection is difficult under laboratory conditions, which hampers investigation into mechanisms pathogenicity and virulence (Baumgartner *et al.*, 2010).

1.2.4.1 Bioluminescence in *A. mellea*

A. mellea mycelia are known to be luminescent at 520 – 530 nm, when the fungus is actively growing on wood, in moist, acid (pH 5.7 – 6) conditions, with an adequate supply of oxygen, at moderate temperatures; and light continues to be emitted until active growth is nutrition-limited (Coder and Daniel, 1999). Luminescence is enhanced by growth in a dark environment (Mihail and Bruhn, 2007), and *in vitro,* optimum conditions for the induction of luiminescence of *A. mellea* grown on agar, is 22 °C and pH 3.5 – 7 (Weitz *et al.*, 2001). *A. mellea* luminescence, although previously reported only in mycelia, has been detected in both basidiocarps and rhizomorphs (Mihail, 2013). This attribute was used as a toxicity biosensor for 3,5-dichlorophenol (3,5-DCP), pentachlorophenol (PCP), copper and zinc, with a putative application as a bioassay, to detect environmental pollutants, as the level of luminosity corresponds to metabolic activity, thus toxic levels of pollutants are indicated by reduced luminosity (Weitz *et al.*, 2002).

1.2.4.2 Diketopiperazines

A 2,5-diketopiperazine was extracted from A. *mellea* (Wang *et al.*, 2013). Diketopiperazines are bioactive compounds and are known to have wide-ranging activities with antibiotic, antifungal and cytotoxic properties (Martins and Carvalho, 2007). Diketopiperazines are synthesised by non-ribosomal peptide (NRP) synthetases; large multimodular enzymes, whose modules incorporate specific amino acids into a growing peptide, and synthesise a wide range of secondary metabolites and bio-active compounds (O'Hanlon *et al.*, 2012). Peptides may be modified as the NRP is synthesised, and the monomers incorporated into the peptide are diverse,with more than 500 types identified to date (Caboche *et al.*, 2008), including non-proteinogenic amino acids, fatty acids and α-hydroxy acids (Strieker *et al.*, 2010). The existence of NRPS-like genes in *A. mellea* which could synthesise diketopiperazines was first confirmed in 2011, but this is the first identification of one of these metabolites in *A. mellea* (Misiek *et al.*, 2011; Wang *et al.*, 2013).

1.2.4.3 Anti-inflammatory activity

Two compounds were extracted from *A. mellea* and identified by NMR as ergosterol (Macaulay, 1988; Guo and Guo, 2008) and ergosterol peroxide (Gao *et al.*, 2001; Kim *et al.*, 1999; Guo and Guo, 2008), although there was no quantitation of the levels of ergosterol or ergosterol peroxide. Both of these compounds have been shown to inhibit nitric oxide production in stimulated macrophages, indeed ergosterol is

particularly active in this regard, and ergosterol peroxide additionally has cytotoxic activity against human prostate and breast cancer cell lines (Ma *et al.*, 2013). *A. mellea* extracts were shown to have a very high levels (22.8 %) of lipid peroxidation inhibition, an indication of antioxidant activity, against rat liver microsomes, in a comparison of 20 fungal species, and the active compound was identified as ergosterol peroxide (Kim *et al.*, 1999). Extracts from mycelia of *A. mellea* were shown in assays to have anti-inflammatory activity against lipopolysaccharide induced stress in human cell lines by inhibiting nitic oxide and prostaglandin production and protecting against pro-inflammatory cytokine production. *A. mellea* extracts showed significant levels of protection of THP-1 cells against cell death during LPS-induced stress (Wu *et al.*, 2007).

1.2.4.4 Antimicrobial activity

Mycelial, organic extracts from *A. mellea* environmental isolates, had activity against several microbes, including *Escherichia coli*, *Salmonella typhimurium*, *Sarcina lutea*, and *Candida albicans.* Although *A. mellea* antimicrobial activity was less than that of other fungal species, extracts also exhibited antioxidant activity as determined by scavenging of reactive oxygen species however, the bioactive components of the extracts were not determined (Kalyoncu *et al.*, 2010).

1.2.4.5 Antioxidant activity

Intracellular and secreted extracts from *A. mellea* show high antioxidant activities, with high levels of Fe^{2+} chelating activity, and scavenging activity ROS and superoxide anions, which protects cells against universal damage by harmful molecular species (Lung and Chang, 2011). Polysaccharides which comprised 27% (w/w) of the water soluble fraction of mycelial extracts from *A. mellea* had high levels of antioxidant properties and were shown to scavenge ROS, inhibit DNA damage and lipid peroxidation in murine hepatic microsomes (Gao and Wang, 2012). Exopolysaccharide extracts from *A. mellea* of undetermined structure, but with molecular mass ranging 1850 to 2140 kDa, also had antioxidant properties. Activity of the exopolysaccharides, which also had proteinaceous content, was related to mass, protein/polysaccharide ratio, and higher activities were seen in high mass polysaccharides (Lung and Hsieh, 2011).

Ergothionine (Figure 1.19), derived from histidine, has two tautomeric forms but is found mainly in its thione form rather than its thiol form. Ergothioneine is very stable and is not easily oxidised, it scavenges ROS and chelates metals (Cheah and Halliwell,

2012). It is found ubiquitously in organisms, and in mammals it accumulates particularly in cells prone to high levels of oxidative stress, such as the liver (Cheah and Halliwell, 2012). It is very potent antioxidant and cytoprotectant and is found in high levels in the mycelia of *A. mellea* (Lee *et al.*, 2009; Park *et al.*, 2010).

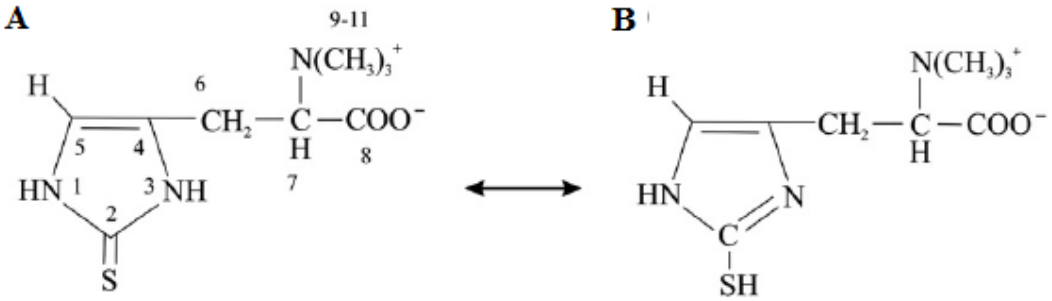

Figure 1.19. Ergothioneine tautomer structures. **A.** Thione tautomer; this conformation is more stable than thiols such as glutathione. **B.** Thiol tautomer; a less stable conformation. In physiological conditions, in solution, the thione is predominant (Cheah and Halliwell, 2012).

1.2.4.6 *A. mellea* immunostimulating activity

Polysaccharide extracts from fruiting bodies of *A. mellea* were purified by size-exclusion chromatography and characterised by NMR. The polysaccharide was composed of (1-6)-linked-α-D-glucopyranosyl, (1-2,6)-linked- α -D-glucopyranosyl and (1-6)-linked- α-D-galactopyranosyl residues in the ratio of 3:1:1, and terminated with one single terminal (1-)-β-D-glucopyranosyl at the O-2 position of (1-2,6)-linked- α -D-glucopyranosyl. The polysaccharide had stimulating effects on murine lymphocyte production induced by lipopolysaccharide and concanavalin A. The extract, termed *A. mellea* polysaccharide (AMP), has potential as an immunopotentiating agent (Sun *et al.*, 2009). Unidentified water-soluble components from *A. mellea* were found to induce the maturation of human dendritic cells, without inducing upregulation of pro-inflammatory cytokines (Kim *et al.*, 2008).

1.2.4.7 *A. mellea* indole compounds

Three indole compounds, the amino acid L-tryptophan, and its derivatives tryptamine and serotonin, were isolated and purified from *A. mellea.* The levels of these compounds were higher than those found in other basidiomycetes, particularly L-tryptophan which was 19-fold higher than previously determined in basidiomycete species and serotonin which was shown to be 4-fold higher than found in other

basidiomycete species (Muszyska *et al.*, 2011). Indole compounds are bio-active and psychoactive and L-tryptophan and serotonin have been used in the treatment of depression (Young, 2007; Thomson *et al.*, 1982).

1.2.4.8 *A. mellea* known proteins and their activities

An endo-exonuclease purified from *A. mellea*, was found to cleave both single-stranded DNA and double-stranded DNA, exhibiting more activity towards dsDNA, but had no activity against RNA (Healy *et al.*, 1999). A fibrinolytic enzyme, *A. mellea* metalloprotease (AMMP), has been extracted and purified (Lee *et al.*, 2005; Healy *et al.*, 1999) from *A. mellea* fruiting bodies. It cleaves the amino side of lysine residues and has been used in sequence analysis of proteins (Lewis *et al.*, 1978a) and was patented as a possible treatment for thrombosis (Broadbent *et al.*, 1972; Lee *et al.*, 2005). Two laccases have been identified and purified from *A. mellea*, both had optimal activity at pH 4 and it was not determined if the two laccases were different products of the same gene. Laccases were only secreted during rhizomorph formation, and growth media was found to influence the production of each laccase type (Billal and Thurston, 1996; Rehman, 1992). In a survey of lignin-degrading enzymes in eight *Armillaria* spp., *A. mellea* had low levels of laccase production compared to *A. tabescens* which has a more saprophytic lifestyle (Stoytchev and Nerud, 2000). Laccase activity was determined to be a key step in the bioremediation of a range of polyaromatic hydrocarbons by *Armillaria* spp., although activity was only apparent after a substantial amount of biomass had been generated (Hadibarata and Kristanti, 2012a, b; Hadibarata *et al.*, 2013, 2012). *Armillaria* spp. could utilise PAH as sole carbon sources, although addition of polysaccharide co-substrate enhanced laccase activity (Hadibarata and Kristanti, 2012b).

1.2.4.9 Sesquiterpene aryl-esters

The most well-known metabolites of *A. mellea* are sesquiterpene aryl-esters and fifty-one distinct sesquiterpenes have been identified of which fifteen have been shown to have antibiotic activity (Donnelly *et al.*, 1982; Momose *et al.*, 2000; Arnone *et al.*, 1988; Misiek and Hoffmeister, 2010), three have antifungal activity (Cremin *et al.*, 1995; Donnelly, *et al.*, 1985c; Donnelly and Hutchinson, 1990; Macaulay, 1988), and six have cytotoxic activity against lymphatic, breast and colorectal cancers (Donnelly, *et al.*, 1985; Misiek *et al.*, 2009). The structures of some of these compounds is shown in Figure 1.20 (Misiek *et al.*, 2009). The sesquiterpene is a protoilludanol alcohol which is esterified by an orsellinic acid derived from polyketide synthase metabolism. *Armillaria*

spp. sesquiterpene aryl-esters are tricyclical, comprised of fused ring structures, specifically a five membered ring is fused to a six membered ring which is fused to a four membered ring, and wide range of functional groups are bonded to this last structure. The central six membered ring contains a double bond and this, coupled to the lipophilic properties of the compounds, is thought to determine the bioactivity of the sesquiterpenes and the antibiotic activity of the compounds (Misiek and Hoffmeister, 2010).

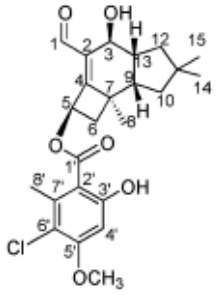

1 (arnamial)

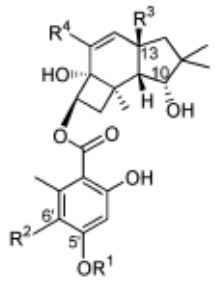

	R^1	R^2	R^3	R^4
2 (melledonol):	H	H	OH	CH_2OH
3 (melleolide C):	CH_3	H	OH	CH_2OH
4 (melleolide D):	CH_3	Cl	OH	CH_2OH
5 (melledonal A):	H	H	OH	CHO
6 (melledonal C):	CH_3	Cl	OH	CHO
7 (10α-hydroxymelleolide):	H	H	H	CHO

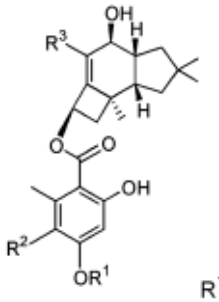

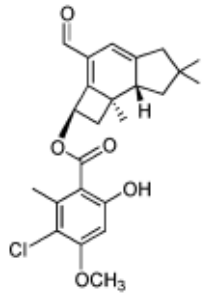

11 (armillaribin)

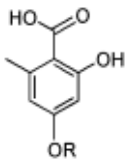

	R^1	R^2	R^3
8 (arnamiol):	CH_3	Cl	CH_2OH
9 (armillyl orsellinate):	H	H	CH_2OH
10 (oxidized armillyl orsellinate):	H	H	CHO

	R
12 (orsellinic acid):	H
13 (orsellinic acid 5-*O*-methyl ester):	CH_3

Figure 1.20. Structures of eleven sesquiterpenes extracted from *A. mellea* mycelia and culture supernatants (Misiek *et al.*, 2009).

1.2.5 Recent molecular studies on *Armillaria mellea*.

1.2.5.1 Processing sites involved in intron splicing of *Armillaria* natural product genes

A. mellea has long been known to produce secondary metabolites and small molecules, probably in response to competition, or as virulence compounds against host species (Sonnenbichler *et al.*, 1994). Following *A. mellea* culture in conditions

conducive to secondary metabolite production, cDNA synthesis was undertaken, and four genes whose products were anticipated to be involved in secondary metabolism were analysed to verify *in silico*-predicted splice sites. The four open reading frames of interest were identified as *orf1* (an open reading frame similar to a non-ribosomal peptide synthetase (NRPS) and transcription regulator). NRPS are modular proteins containing adenylation, condensation, thiolation and optional epimerisation domains, involved in synthesis of secondary metabolites, as mentioned earlier. *orf1* had homology to zinc finger motif genes, but was unusual in that it two zinc finger motifs and appeared to be the first time it had been identified in basidiomycetes. This zinc finger is a transcription activator in *Magnaporthe grisea* and *Aspergillus* spp. for secondary metabolite production. *orf2* and *orf3* had 48% sequence similarity to each other, and had homology to the sequences of major facilitator efflux transporters putatively involved in small molecule transport. While the whole proteins for *orf2* and *orf3* showed homology to a *Coprinopsis cinerea* hypothetical protein, motifs from within the sequence had homology to efflux pumps, a drug resistance protein in *C. neoformans* and an aminotriazole resistance protein in *Neurospora crassa* with similarity of 31% and 37% respectively. Homology to other proteins which facilitate self-resistance to antibiotic-producing organisms was also identified. The homologs usually have extensive transmembrane regions, and *orf2* had 12 and *orf3* had 14 transmembrane helices. *orf 4* was homologous to a putative laccase, several alternative splice sites for this gene were determined, with alternative and acceptor splice junctions which appeared to be allele specific (Misiek and Hoffmeister, 2008).

1.2.5.2 Structure and Cytotoxicity of Arnamial and Related Fungal Sesquiterpene Aryl Esters

A new compound, arnamial, which was structurally related to sesquiterpene aryl esters previously identified, was extracted and isolated from the liquid supernatant of *A. mellea* cultures. The structure of arnamial was elucidated (Figure 1.20), and arnamial, together with six previously identified related sesquiterpenoids was tested for cytotoxicity against colorectal carcinoma, breast adenocarcinoma and lymphoblastic leukemia cell lines. Four of the seven compounds tested: arnamial, melleolide D, melledonal C, and 10α-hydroxymellolide, showed cytotoxicity against the cancer cell lines, and the newly identified arnamial, had the highest levels of cytotoxicity compared to the other cytotoxic compounds, against all cell lines. The unique position of a double bond which changed the conformation of the sequiterpene aryl-ester was determined to be responsible for conferring cytotoxic properties to arnimal. Furthermore, the

cytotoxicity was established to be caspase related, and cytotoxicity was by the apoptotic pathway (Misiek *et al.*, 2009).

1.2.5.3 *Agrobacterium tumefaciens*-Mediated Transformation for Investigation of Somatic Recombination in the Fungal Pathogen *Armillaria mellea*.

A. mellea mating can occur in the environment between diploid and haploid mycelia and a recombinant diploid organism can be generated without meiosis. While this is thought to contribute to the pathogenicity of *A. mellea,* no reliable method had been developed to study this phenomenon. A novel transformation system for *A. mellea* was developed using *Agrobacterium tumefaciens* to generate somatic recombinants using a hygromycin phosphotranserase gene (*hph*). Transformation of the fungus was confirmed by growth on selective media, Southern blotting and RT-PCR. Markers of mitochondrial and nuclear inheritance were developed to identify transformants, and wild type diploids were crossed with hygromycin-resistant haploids, which conferred hygromycin resistance on the recombinants. Recombinant *A. mellea* used as inocula for grape plants, showed no difference in fungal biomass compared with wild type. This was the first time *A. mellea* transformation had been carried out and represented a major advance in study of the pathogen (Baumgartner *et al.*, 2010)

1.2.5.4 A rapid infection assay for *Armillaria* and real-time PCR quantitation of the fungal biomass in planta

An *A. mellea* infection study in the laboratory was developed to expedite detection of infected plants, as plants *in vitro* are slow to exhibit signs of infection, which may take 18 months to appear, and inocula may not infect all plants. Susceptible and non-susceptible plants were used in the assay and infection with *A. mellea* was carried out over eight weeks. Infected plant roots were subjected to separate qPCR of a single copy fungal gene EF1α and a single copy grape gene, UDP-glucose: flavonoid 3-O-glucosyl transferase (UFGT). A ratio of fungal biomass:plant biomass was calculated and the infection of plants determined by qPCR was confirmed by confocal microscopy. The study confirmed EF1α as a single copy gene in *A. mellea*, the first time that this had been determined, and also the 150 bp section of the gene amplified by PCR was invariant among North American *Armillaria* species, whereas other PCR primers were designed to be able to differentiate between species (Baumgartner *et al.*, 2010).

1.2.5.5 Characterisation of the ArmA adenylation domain implies a more diverse secondary metabolism in the genus *Armillaria*.

In a follow-on study of Misiek and Hoffmeister (2008), *A. melle*, cDNA was synthesised and data were interrogated for proteins involved in secondary metabolite biosynthetic pathways. A gene encoding encoding a quinone synthetase-like gene, *armA*, was identified from cDNA. The substrates of these quinine synthetase proteins are 2-oxo acids, but no aminotransferase genes were detected close to this gene, as might have been expected; instead two halogenase genes, *armH1* and *armH2* were adjacent to the gene, whose product is referred to as ArmA (Figure 1.21). Other open reading frames, *orf1 – orf11*, had homology to heat shock proteins (*orf5*) glycoside hydrolase family 79 proteins (*orf9*), transcription regulators (*orf1* and *orf6*) and hypothetical proteins in other organisms (*orf 6, 7, 8, 10* and *11*). ArmA has three domains, and biochemical analysis of its function indicates that it does not have functions similar to quinine synthetase, nor was it similar to furanone synthetase, a bacterial protein which has a 2-oxo acid substrate specificity. ArmA had similarity to an NRPS, and L-leucine was found to be the optimal substrate for ArmA and the adenylation domain of this NRP synthetase was identified. A modified diketopiperazine composed of L-leucine was identified in *A. ectypa*. This would imply that ArmA is an NRPS lacking a condensation domain and is the first biochemical characterisation in a basidiomycete, of an NRPS amino acid-adenylating enzyme (Misiek *et al.*, 2011).

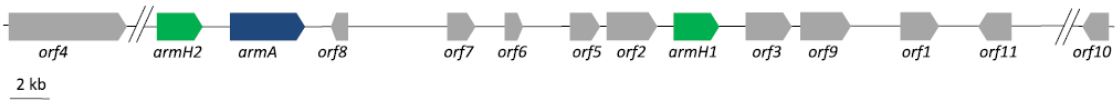

Figure 1.21. Open reading frames and genes identified from the genome of *A. mellea* encoding an NRPS-like cluster. *armA*, quinine synthetase-like enzyme; *arm*H1, halogenase; *armH2*, halogenase; *orf1*, transcription regulator; *orf2*,efflux protein; *orf3*efflux protein; *orf4* laccase; *orf5* unknown; *orf6* transcription regulator; *orf7* unknown; *orf8* unknown; *orf9* glysoside hydrolase; *orf10* unknown; *orf11* unknown (Misiek *et al.*, 2011).

1.2.5.6 Genome mining reveals the evolutionary origin and biosynthetic potential of basidiomycete polyketide synthases

A genome library of *A. mellea* clones (unpublished) was screened for polyketide synthase genes and one cosmid contained a fragment of a ketosynthase gene. This gene, *armB*, was sequenced and cDNA obtained. Comparative bioinformatic analysis of this

sequence against the genomic sequences of thirty-five recently sequenced fungi was carried out, to determine the phylogenetic chacteristics of the polyketide synthase (PKS) genes. A phylogenetic tree was constructed and showed that 114 PKS genes were identified. Analysis of PKS genes deduced that they evolved prior to the divergence of Ascomycota and Basidiomycota. Comparison of genomic and metabolomic data revealed that there may be many more putative polyketide metabolites than have been empirically identified to date. An average of four PKS genes in Agaricomycotina genomes was revealed and reveals that these organisms are targets for identification of novel metabolites. *In silico* analysis of these genes, and similarity clusters apparent after phylogenetic analysis, will inform future predictions of basidiomycete PKS gene functions (Lackner *et al.*, 2012).

1.2.6 Knowledge deficiency of *A. mellea* biology

Although online resources and software tools are available for investigation of *A. mellea* and other fungal species (Table 1.3), there is a dearth of relevant experimental data. Thus, since there have been so few genomic studies on basidiomycete species and little genomic information on *A. mellea* in particular, genomic sequencing and annotation of the *A. mellea* genome would provide a platform for study of the pathogen. The genomic sequencing and annotation of *A. mellea* would also substantially add to the general knowledge of basidiomycete and *Armillaria* spp. and *A. mellea* in particular. The fact that the genome has not been sequenced to date has hampered the investigation of the proteome of *A. mellea*. Indeed, no large scale proteomic study of *A. mellea* has been undertaken, neither of intracellular or of secreted proteins (secretome), but with a complete genome, the hugh diversity of biosynthetic enzymes and their putative products can to be determined. Furthermore, protocols and techniques for the implementation of proteomic studies in basidiomycetes, and more particularly in *A. mellea*, have not been developed, and high-throughput technologies have not been utilised hithertofore for investigation this virulent pathogen. Development of techniques and high-throughput strategies would contribute to the body of knowledge of the integrated biological system of *A. mellea*.

Furthermore, molecular studies of *A. mellea* in stress or pathogenic environments have never been undertaken, thus, study of the proteins differentially expressed by the pathogen under oxidative stress or uniquely expressed in an infection model would also greatly contribute to discovery of the pathogenic and virulence mechanisms of *A. mellea*.

Table 1.3. Online resources and software tools for investigation of *A. mellea* and other basidiomycete species.

Website address	Description
http://armillariamellea.com/	Database of *A. mellea* nucleotide and protein models.
http://botit.botany.wisc.edu/toms_fungi/	Webpage of Tom Volk of the University of Wisconsin-La Crosse fungal information links and resources
http://fungi.ensembl.org/index.html	Database of fungal species with genome assembly information, comparative genomics, regulation, annotation and gene variation.
http://fungidb.org/fungidb/	FungiDB Database of fungal sequences and software tools for functional analysis of genes and proteins.
http://genome.jgi.doe.gov/programs/fungi/index.jsf	MycoCosm, JGI. 1000 Fungal Genomes project to sequence 1000 genomes and a database of fungal genome sequences and software tools for analysis and promotion of function studies into species with relevance to the environment and energy.
http://mycor.nancy.inra.fr/blogGenomes/?category_name=plant-biology	The blog of Francis Martin of the French INRA Forestry Center MycorWeb Genomics blog is a portal with postings about about the increasing amount of data generated on the genomes of fungi and plants, and how to access it through the tools, databases and resources that are publicly available.

Website address	Description
http://tolweb.org/Basidiomycota/20520	Tree of Life A collaborative project of biologists and nature enthusiasts worldwide to provide information on biodiversity and phylogeny of organisms.
http://www.broadinstitute.org/scientific-community/science/projects/fungal-genome-initiative/fungal-genome-initiative.	Joint Genome Initiative Database of sequence data and analysis of organisms of bio-medical, agricultural and industrial relevance.
http://www.genomesonline.org/cgi-bin/GOLD/index.cgi	Genomes Online Database (GOLD) provides access to data from genomic and metagenomic sequencing projects worldwide.
http://www.ncbi.nlm.nih.gov/genome/browse/	Database of all genomes deposited with the NCBI
http://www.sanger.ac.uk/resources/downloads/fungi/	Wellcome Trust database of fungal genomes sequenced by the organisation.
https://sbi.hki-jena.de/FungiFun/FungiFun.cgi	FungiFun is an online tool for functional annotation of fungal genomic and proteomic data.

1.3 Thesis objectives

The objectives of the work presented in this thesis are the in-depth analysis of the genome of *Armillaria mellea* and proteomic analysis of *A. mellea* under a variety of conditions. This will identify protein families and individual proteins encoded in the genome of this pathogen. Development of methods for culture and extraction of protein from both the mycelia and culture supernatants of *A. mellea* will allow identification of proteins expressed under nutrient-replete, as well as nutrient-restricted conditions. Conditions of stress and infection should identify proteins putatively involved in virulence and pathogenicity of the organism.

To these ends the following approaches will be taken:

1. Genomic sequencing of *A. mellea* and construction of a cDNA database which will be annotated by bioinformatic analysis.

2. Methods will developed for *A. mellea* culture, protein extraction from both mycelia and culture supernatants, prior to separation and analysis by LC-MS/MS and interrogation of the cDNA database.

3. Novel method of analysis of complex *A. mellea* protein mixtures by LC-MS/MS will be developed to identify mycelial and secreted proteins.

4. Oxidative stress will be induced in *A. mellea* and proteins differentially regulated under two stressors will be identified by LC-MS/MS analysis.

5. An infection model for *A. mellea* will be developed to identify *A. mellea* proteins which may be uniquely-expressed during *A. mellea* infection.

Chapter 2 Materials and Methods

The following organisms were used in this study (Table 2.1).

Table 2.1. Organisms used in this study.

Organism	Strain
A. mellea (Vahl:Fr) Kummer	DSM 3731, DSMZ Sales, Germany.
Aspergillus fumigatus	Strain AF293.
Candida albicans	Clinical isolate from a patient with ocular infection.
Escherichia coli	Clinical isolate.
Pseudomonas aeruginosa	Strain 27853.
Methicillin resistant *Staphylococcus aureus*	American Tissue Culture Collection.
Staphylococcus aureus	Clinical isolate.

All chemicals were purchased from Sigma-Aldrich Chemical Co. Ltd. (U.K.), unless otherwise stated.

2.1 Materials

2.1.1 DNA isolation

ZR Fungal/Bacteria DNA kit (Zymo Research Group) containing: lysis solution, Zymo Spin IV spin filters, DNA binding buffer, Zymo-Spin IIC Column, DNA prewash buffer, Fungal/bacterial DNA wash buffer, DNA elution buffer.

2.1.2 3 M Sodium Acetate

Sodium acetate (258 mg) was added to 1 ml Milli-Q® H_2O.

2.1.3 Media and Agar

2.1.3.1 Potato dextrose broth (PDB)

Potato dextrose broth (4.8 g) was added to 500 ml Erlenmeyer flasks with 200 ml deionised (dH_2O). These were plugged with cotton wool, the top wrapped in aluminium foil and autoclaved (105 °C for 30 min).

2.1.3.2 Potato dextrose agar (PDA)

Potato dextrose broth (4.8 g) was added to 200 ml dH_2O and agar (5 g). The solution was autoclaved (105 °C for 30 min) and allowed to cool to 50 °C before being poured into 90 mm petri dishes, under sterile conditions and allowed to set. Stored at 4 °C.

2.1.3.3 Malt extract agar (MEA)

Malt extract agar (30 g) (Oxoid Ltd., U.K.) was added to 600 ml dH_2O, and dissolved. The solution was autoclaved (105 °C for 30 min), and allowed to cool to 50 °C. Agar (25 ml) was poured into 90 mm petri dishes, under sterile conditions and allowed to set. Stored at 4 °C.

2.1.3.4 Trace elements

$Na_2B_4O_7.7H_2O$ (40 mg), $CuSO_4.5H_2O$ (400 mg), $FeSO_4.2H_2O$ (800 mg), $Na_2MoO.2H_2O$ (800 mg) and $ZnSO_4.7H_2O$ (8 g) were added to 800 ml of distilled water (dH_2O) in sequence until each dissolved, before the next addition. The solution was brought to 1 L with dH_2O and autoclaved at 121 °C for 15 min. Stored in aliquots (50 ml) at −20 °C.

2.1.3.5 50 X Salt solution

KCl (26 g), $MgSO_4.7H_2O$ (26 g), KH_2PO_4 (76 g) and trace elements (50 ml) (Section 2.1.3.4) were added to 800 ml dH_2O and dissolved. The solution was brought to 1 L with dH_2O and autoclaved at 121 °C for 15 min. Stored at room temperature.

2.1.3.6 100 X Ammonium Tartrate

Ammonium tartrate (92 g) was dissolved in 1 L of dH_2O and autoclaved at 121 °C for 15 min. Stored at room temperature.

2.1.3.7 Sterilising Solution

11 % (w/v) Sodium hypochlorite solution (318 ml), was added to 1 L dH_2O to make a 3.5 % (w/v) solution.

2.1.3.8 300 mM L-glutamine

L-glutamine (43.8 g) was added to 800 ml dH_2O, HCl was added dropwise until it dissolved, then the solution adjusted to pH 6.5, the volume brought to 1 L with dH_2O, and filter sterilised. Stored at room temperature.

2.1.3.9 Carbon Sources

The following were used as discrete carbon sources for culture media: alkali lignin, xylan from beechwood, microgranular cellulose, rutin hydrate, yeast extract, glucose, malt extract (Sharlau, Spain).

2.1.3.10 Sterilised *Vitis vinifera (*grapevine)

A branch from grapevine purchased commercially and grown in Maynooth, Co. Kildare (100 g), was broken into 5 cm pieces, put into a container with enough sterilising solution (Section 2.1.3.7) to cover, sealed and agitated gently for 35 min. Under sterile conditions, the supernatant was poured off and replaced with sterile dH_2O and the agitation repeated. Pieces were rinsed with sterile dH_2O twice more, removed from dH_2O, gently shaken to remove excess dH_2O, ground in liquid N_2 and put into a sterile container. Stored −70 °C.

2.1.3.11 Culture of *A. mellea* on MEA with autoclaved *C. albicans*

Malt extract agar (30 g) (Oxoid Ltd., U.K.) was added to 600 ml dH_2O, and dissolved. *C. albicans* cells (4×10^5/ml final conc.) were added. The solution was autoclaved (105 °C for 30 min), and allowed to cool to 50 °C. Agar (25 ml) was poured into 90 mm petri dishes, under sterile conditions and allowed to set. Stored at 4 °C.

2.1.3.12 Minimal Media (MMA) agar

Ammonium tartrate (Section 2.1.3.6) 10 ml, salt solution (Section 2.1.3.5) 20 ml, and one carbon source from (Section 2.1.3.9) (10 g) were added to 800 ml dH_2O and dissolved, adjusted to pH 6.8 and brought to 1 L with dH_2O prior to the addition of agar (20 g). The solution was autoclaved (105 °C for 30 min) and allowed to cool to 50 °C. Where grapevine was the carbon source, it was added to cooled media after autoclaving (Section 2.1.3.10. Agar was poured into 90 mm petri dishes, under sterile conditions and allowed to set. Stored at 4 °C.

2.1.3.13 Minimal Media (MML) liquid

Ammonium tartrate (Section 2.1.3.6) 10 ml, salt solution (Section 2.1.3.5) 20 ml, were added to 800 ml dH_2O, adjusted to pH 6.8. and brought to 1 L with dH_2O. 200 ml was poured into 500 ml Erlenmeyer flasks and a single carbon source from (Section 2.1.3.9 (2 g) was added. Where grapevine (Section 2.1.3.10) was the carbon source it was added to cooled media after autoclaving. The solution was mixed and flasks plugged with cotton wool, the top wrapped in aluminium foil and autoclaved (105 °C for 30 min).

2.1.3.14 Phosphate Buffered Saline (PBS)

One PBS tablet was added to 200 ml of dH_2O dissolved by stirring and autoclaved at 105 °C for 30 min. Stored at room temperature.

2.1.3.15 Phosphate Buffer Saline 0.05 % Tween (PBST)

Tween-20 (0.5 ml) was added to 1 L PBS (Section 2.1.3.14) prior to autoclaving at 105 °C for 30 min. Stored at room temperature.

2.1.3.16 Bradford Solution

One part BioRad dye reagent was added to four parts PBS and mixed. This was stored at 4 °C for one week

2.1.4 Solutions for pH Adjustment

2.1.4.1 5 M Hydrochloric Acid (HCl)

36-38 % Hydrochloric acid (43.64 ml) was added slowly to a glass graduated cylinder containing with dH_2O (50 ml) and the volume adjusted to 100 ml with dH_2O. Stored at room temperature.

2.1.4.2 5 M Sodium Hydroxide (NaOH)

NaOH pellets (20 g) were added to dH_2O (80 ml) and dissolved using a magnetic stirrer and the volume adjusted to 100 ml with dH_2O. Stored at room temperature.

2.1.5 *A. mellea* protein extraction

2.1.5.1 Lysis buffer 1 – *A. mellea* 2-DE protein extraction

Tris-HCl (12.5 g), NaCl (2.9 g), EDTA (7.44 g), Glycerol (100 ml) were added to 800 ml of Milli-Q® H_2O, adjusted to pH 7.5 using 5 M HCl and volume brought to 1 L with Milli-Q® H_2O. Storage: 4 °C. DTT (4.63 mg/ml), 1 µg/ml (final) each pepstatin A, leupeptin and aprotinin were added directly before use.

2.1.5.2 Lysis Buffer 2 – *A. mellea* whole cell lysate (WCL) protein extraction

Tris-HCl (394 mg), Guanidine HCL (57.32 g), DTT (154 mg) were dissolved in 80 ml Milli-Q® H_2O adjusted to pH 8.6, brought to 100 ml with Milli-Q® H_2O. Stored at 4 °C.

2.1.5.3 50 mM Tris Buffer pH 7.5

Trizma base (303 mg) was added to 40 ml Milli-Q® H_2O, dissolved using a magnetic stirrer, adjusted to pH 7.5 and brought to 50 ml.

2.1.5.4 100 mM ammonium bicarbonate (NH_4HCO_3)

Ammonium bicarbonate (AnalR Code 103025E), (395 mg), was added to a container and brought to 50 ml with Milli-Q® H_2O. For immediate use.

2.1.5.5 10 mM Ammonium bicarbonate (NH_4HCO_3)

Freshly made Ammonium bicarbonate (100 mM, 5 ml), (Section 2.1.5.4) was added to a container and brought to 50 ml with Milli-Q® H_2O.

2.1.5.6 50 mM Potassium phosphate (KH_2PO_4 pH 7.5)

Potassium phosphate (340 mg) was added to a container with dH_2O (40 ml), adjusted to pH 7.5 and brought to 50 ml with dH_2O.

2.1.5.7 1 M DL-Dithiothreitol (DTT) stock

DTT (154.2 mg) was added to dH_2O (1 ml).

2.1.5.8 1 M Iodoacetamide stock

Iodoacetamide (184.96 mg) was added to dH_2O (1 ml)

2.1.5.9 Trypsin Diluent

Acetonitrile (ACN), (1 ml), was added to ammonium bicarbonate (10 mM, 9 ml) (Section 2.1.5.5). Final ACN conc. 10 % (v/v).

2.1.5.10 Trypsin solution WCL (400 ng/µl)

Trypsin Diluent (Section 2.1.5.9), (50 µl), was added to a 20 µg vial of trypsin (Promega Sequencing grade modified trypsin V5111).

2.1.5.11 Trypsin solution WCL agar (65 ng/µl)

Trypsin Diluent (Section 2.1.5.9), (300 µl) was added to a 20 µg vial of trypsin.

2.1.5.12 Trypsin solution in-gel digestion (13 ng/µl)

Trypsin Diluent (Section 2.1.5.9), (1.5 ml), was added to a 20 µg vial of trypsin (Shevchenko *et al.*, 2007).

2.1.5.13 80 % (v/v) Glycerol solution

Glycerol (800 ml), was added to a container, brought to 1 L with dH_2O and mixed with a magnetic stirrer. The solution was autoclaved at 121 °C for 15 min. Stored at room temperature.

2.1.5.14 Supernatant organic extraction buffer

Ethyl acetate (50 ml), dichloromethane (33.3 ml) and methanol (16.7 ml) were added to a 1 L container (Smedsgaard, 1997). Stored at room temperature.

2.1.5.15 100 % (w/v) Trichloroacetic acid

A solution of 100 g solid TCA (Merck, Ireland), and dH_2O (45.4 ml) was made and mixed well to dissolve the TCA. Stored at 4 °C.

2.1.5.16 10 % (w/v) Trichloroacetic acid

TCA (100 %, (w/v) 100 ml), was added to 900 ml dH_2O. Stored at 4 °C.

2.1.6 Sodium dodecyl sulphate-polyacrylamide gel electrophoresis (SDS-PAGE) reagents

2.1.6.1 10 % (w/v) Sodium Dodecyl Sulphate

SDS (10 g) was added to 100 ml of Milli-Q® H_2O, and dissolved. Stored at room temperature. In the event of SDS precipitation solution was placed at 37 °C, until it redissolved.

2.1.6.2 1.5 M Tris Buffer, pH 8.8

Trizma base (18.15 g) was added to 75 ml Milli-Q® H_2O and dissolved using a magnetic stirrer and the pH adjusted to 8.8 using 5 M HCl or NaOH (Section 2.1.4.1 or 2.1.4.2). The volume was brought to 100 ml with Milli-Q® H_2O. Stored at 4 °C.

2.1.6.3 0.5 M Tris Buffer, pH 6.8

Trizma base (6.05 g) was added to 75 ml Milli-Q® H2O, dissolved using a magnetic stirrer, adjusted to pH 6.8 using 5 M HCl and the volume brought to 100 ml with Milli-Q® water. Stored at 4 °C.

2.1.6.4 30 % Acrylamide/Bis

Protogel® (30 %) (National Diagnostics, Dublin, Ireland).

2.1.6.5 10 % (w/v) Ammonium Persulphate (APS)

Ammonium persulphate (0.1 g) was added to 1 ml with Milli-Q® H_2O. Stored at 4 °C, and used within 24 h.

2.1.6.6 1 % (w/v) Bromophenol blue solution

Bromophenol blue (0.2 g) was added to Milli-Q® H_2O (20 ml). Stored 4 °C.

2.1.6.7 0.5 % (w/v) Bromophenol blue solution

Bromophenol blue (0.1 g) was added to Milli-Q® H_2O (20 ml). Stored 4 °C.

2.1.6.8 5 X Solubilisation buffer

Glycerol (8 ml) was added to Milli-Q® H_2O (4 ml), containing 1.6 ml of 10 % SDS (Section 2.1.6.1) and 1 ml of 0.5 M Tris-HCl (Section 2.1.6.3), (pH 6.8). 2-mercapthoethanol (0.4 ml) was added to the solution with 0.2 ml of 0.5 % (w/v) bromophenol blue solution (Section 2.1.6.7). Stored in 1 ml aliquots at −20 °C.

2.1.6.9 5 X Electrode running buffer

Trizma base (15 g), glycine (72 g) and SDS (5 g) were added to Milli-Q® H_2O (800 ml), and dissolved using a magnetic stirrer. The final volume was adjusted to 1 L. The solution was stored at room temperature.

2.1.6.10 1 X Electrode running buffer

200 ml 5 X electrode running buffer (Section 2.1.6.9) was put into a 1 L container and brought to 1 L with dH_2O.

2.1.6.11 Coomassie®Blue Stain Solution

Deionised water (600 ml), glacial acetic acid (100 ml) and methanol (300 ml) were added to a glass bottle, containing 1 g Brilliant Blue R. The solution was stored at room temperature.

2.1.6.12 Destain Solution

Glacial acetic acid (100 ml) was added to 600 ml Milli-Q® H_2O and 300 ml methanol. The solution was stored at room temperature.

2.1.6.13 Colloidal Coomassie® Fixing solution

Phosphoric acid (30 ml), was added to Milli-Q® H_2O (470 ml) and ethanol (500 ml). Made on day of use.

2.1.6.14 Colloidal Coomassie® Incubation buffer

Phosphoric acid (30 ml), was added to Milli-Q® H_2O (400 ml), methanol (340 ml) and ammonium sulphate (170 g), brought up to 1 L with Milli-Q® H_2O. Made on day of use.

2.1.6.15 Colloidal Coomassie® Stain solution

Phosphoric acid (30 ml), was added to Milli-Q® H_2O (400 ml), methanol (340 ml), ammonium sulphate (17 % (w/v) (170 g) brought up to 1 L with Milli-Q® H_2O. Stain

solution 100 ml was added to each gel. Colloidal Coomassie® Blue G-250 (Serva, Germany), (0.35 g/L) was sprinkled directly onto solution.

2.1.6.16 2-DE Focussing Buffer

Urea (48 g), Thiourea (15.2 g), CHAPS (4 g), Triton X-100 (1 ml), Tris base (0.12 g) added to 50 ml Milli-Q® H_2O and brought to 100 ml with Milli-Q® H_2O. Stock solution stored in 1 ml aliquots at −20 °C until use. After thawing, DTT (0.01 g, 65 mM final) was added to 1 ml of stock with IPG Buffer 3 - 11 (8 µl), 4 - 7 (5 µl) and 6 - 11 (5 µl) (Amersham Biosciences).

2.1.6.17 Equilibration Buffer

Glycerol (15 ml), SDS (1 g), Urea (18 g), Tris base (300 mg) were added to 40 ml Milli-Q® H_2O, adjusted to pH 6.8 and brought up to 50 ml. Stored in 10 ml aliquots at −20 °C.

2.1.6.18 2-DE Reduction buffer

DTT (200 mg), final conc. 2 % (w/v) was dissolved into 10 ml equilibration buffer (Section 2.1.6.17)

2.1.6.19 2-DE Alkylation buffer

Iodoacetamide (250 mg), final conc. 2.5 % (w/v)) was dissolved into 10 ml equilibration buffer (Section 2.1.6.17) and 1 % (w/v) bromophenol blue solution (Section 2.1.6.6), (100 µl), was added.

2.1.6.20 Agarose Sealing Solution

Trizma base (1.5 g), glycine (7.2 g) and SDS (0.5 g) were added to Milli-Q® H_2O (80 ml). 0.5 % (w/v) Agarose (0.5 g), 1 % (w/v) bromophenol blue (Section 2.1.6.6), 200 µl were added and volume brought to 100 ml.

2.1.7 0.1% (v/v) Trifluoroacetic acid

Aqueous trifluoroacetic acid (≥ 99 %), (5 µl) was added to 5 ml dH_2O for immediate use.

2.1.8 OFFGEL electrophoresis solutions

2.1.8.1 OFFGEL stock solution (1.25 X)

Urea (25.2 g), was put into a 50 ml container with thiourea (9.1 g), DTT (600 mg), and glycerol (6 ml). 3-10 IPG buffer (Amersham Biosciences), (600 µl), was added and volume brought to 50 ml with dH_2O. Stored frozen −20 °C.

2.1.8.2 OFFGEL strip rehydration solution

OFFGEL solution (Section 2.1.8.1) (1.25 X, 280 µl) was added to 70 µl dH_2O.

2.1.8.3 PepClean™ Sample Buffer

0.1% Formic acid (1 µl) was added to Milli-Q® H_2O (800 µl) containing ACN (200 µl).

2.1.8.4 PepClean™ Activation Solution

MeOH (3 ml) was added to Milli-Q® H_2O (3 ml).

2.1.8.5 PepClean™ Equilibration Solution

0.1% Formic acid (6 µl) was added to Milli-Q® H_2O (5.7 ml) containing ACN (300 µl).

2.1.8.6 PepClean™ Wash Solution

0.1% Formic acid (12 µl) was added to Milli-Q® H_2O (11.4 ml) containing ACN (600 µl).

2.1.8.7 PepClean™ Elution Buffer

ACN (200 µl) was added to Milli-Q® H_2O (180 µl).

2.1.9 Liquid Chromatography Mass Spectrometry reagents (LC-MS/MS)

2.1.9.1 50 mM Iodoacetamide

Iodoacetamide (46 mg) was added to 100 mM NH_4HCO_3 (Section 2.1.5.4) (5 ml). Made on day of use.

2.1.9.2 LC-MS/MS Buffer A

1 ml Formic acid (Fluka) was added to HPLC grade water 1 L and used within 7 days.

2.1.9.3 LC-MS/MS Buffer B

HPLC grade water (100 ml) and 1 ml formic acid were added to 899 ml ACN and used within 7 days.

2.1.10 Stain, assay buffers and reagents

2.1.10.1 100 mM Sodium acetate buffer pH 5.0

Sodium acetate (82 g) was added to 800 ml dH_2O, adjusted to pH 5.0 with 99 % acetic acid and brought to 1 L with dH_2O.

2.1.10.2 20 % (w/v) Bovine serum albumin (BSA)

BSA (2 g) was put into a container and brought to 10 ml with dH_2O and allowed to dissolve.

2.1.10.3 Fluorescein diacetate (FDA) stock solution

FDA (5 mg) was dissolved in 1 ml acetone. Stored frozen at −20 °C or at 4 °C in darkness for up to 4 weeks.

2.1.10.4 Fluorescein diacetate (FDA) working solution

FDA (40 µl) stock solution (Section 2.1.10.3) was added to 10 ml PBS (Section 2.1.3.14) and stored on ice in darkness prior to same day use.

2.1.10.5 Propidium Iodide (PI) stock solution

Sterile PBS (Section 2.1.3.14) (5 ml) was added to 10 mg PI. Stored in (200 µl) aliquots at −20 °C in darkness.

2.1.10.6 Propidium Iodide (PI) working solution

PI stock (10 µl) solution was added to 490 µl sterile cold PBS (Section 2.1.3.14) and stored on ice in darkness for same day use.

2.2 Methods

The schematic shown in Figure 2.1 illustrates the the genomic, proteomic, metabolic and bioinformatic workflows that were employed during this study of *A. mellea*.

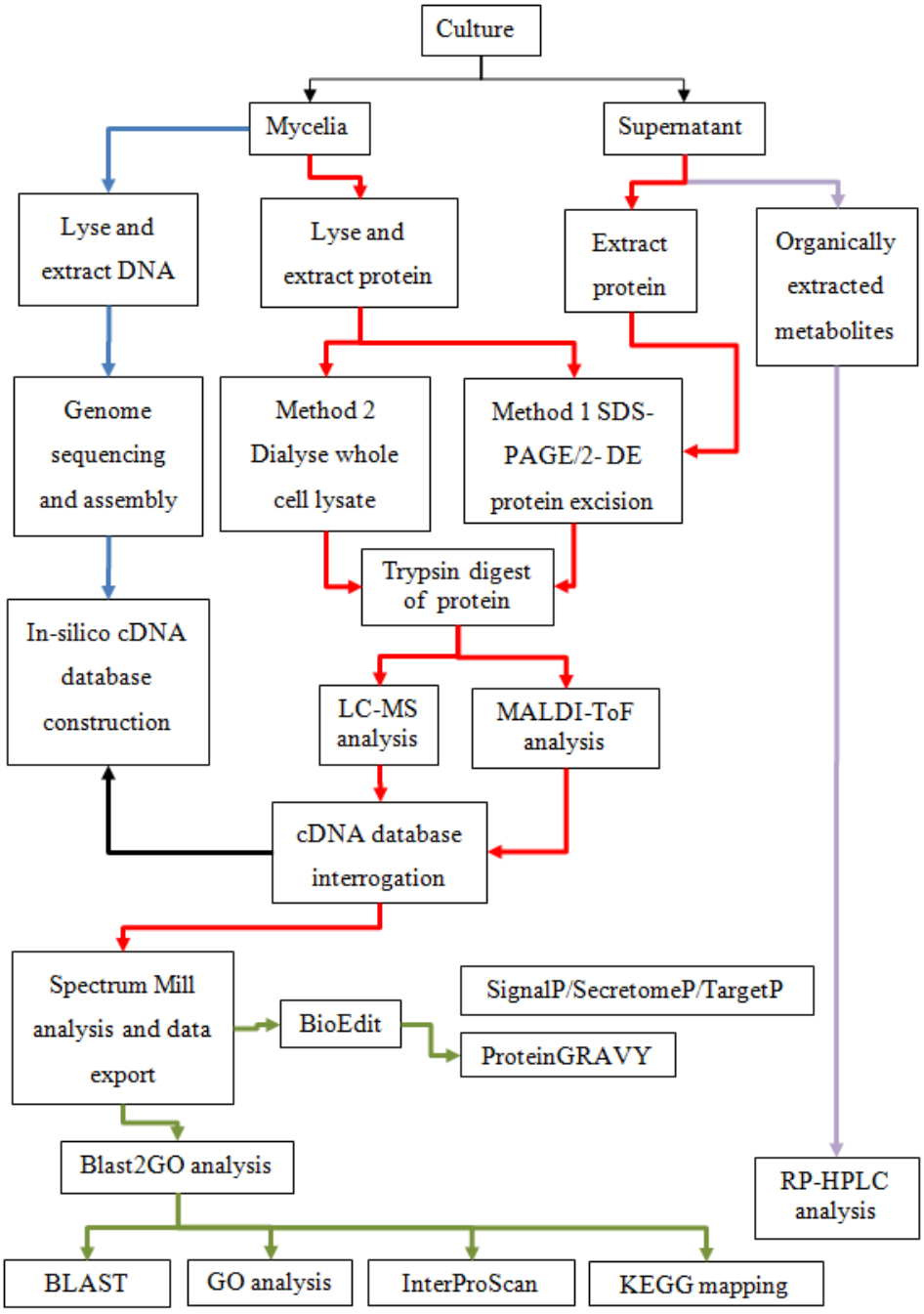

Figure 2.1. Schematic of *A. mellea* genomic, proteomic, metabolomic and bioinformatic workflows. Blue arrows illustrate genomic workflow; red arrows indicate proteomic workflow; purple arrows show metabolite analysis workflow (data will not be shown in this thesis); green arrows demonstrate the bioinformatic workflow and double-headed black lines show confirmation of the *in silico A. mellea* cDNA database through proteomic analysis.

2.2.1 DNA isolation

A. mellea DNA was extracted using a ZR Fungal/ Bacterial DNA Kit (Zymo Research Group) using a modified protocol. Mycelia were ground into a fine powder in liquid N_2, 300 mg added to tubes containing glass beads (200 mg, 0.4 mm). Lysis Solution (750 µl) was added, specimens were bead-beaten for 2 min at 20 Hz followed by centrifugation at 10,000 *g* for 1 min. Supernatants (400 µl) were transferred to Zymo-Spin IV Spin Filters and centrifuged for 1 min at 7,000 *g*. Fungal/ Bacterial DNA Binding Buffer (1200 µl) was added to the filtrates which were then passed through a Zymo-Spin IIC Column by centrifuging at 10,000 *g* for 1 min. DNA Pre-Wash Buffer (200 µl) was added to the Zymo-Spin IIC Column which was then centrifuged for 1 min at 10,000 *g*. Fungal/Bacterial DNA Wash Buffer (500 µl) was then added to the spin column which was again centrifuged at 10,000 *g* for 1 min. DNA was eluted from the column following the addition of DNA Elution Buffer (100 µl) and centrifuging for 30 s at 10,000 *g*. DNA was precipitated by adding 3 M sodium acetate ($^1/_{10}$ vol.) and 3 vol. ice-cold ethanol (100 % (v/v)). Following incubation at –20 °C for 3 h, specimens were centrifuged at 13,000 *g* for 10 min and supernatants removed. Pellets were washed again with ice-cold ethanol (75 % (v/v), 180 µl) followed by centrifugation at 13,000 *g* for 10 min. After supernatant removal, pellets were air-dried to remove traces of ethanol before resuspending in Milli-Q® H_2O (20 µl).

2.2.2 Genome Sequencing, Assembly and Annotation

A single no-PCR paired-end library was created from *A. mellea* genomic DNA according to the method of Kozarewa *et al.* (2009), with an estimated fragment size of 168 $\pm$ 92 bp (inferred by remapping the reads onto the assembly with the Maq software (http://maq.sourceforge.net/)). The library was run on three lanes of the Illumina GAII at 76 bp read length (Bentley *et al.*, 2008) producing a total of 6.72 giga base pairs (Gbp) Q20 bases. The reads were assembled with Velvet v0.7.53 (Zerbino and Birney, 2008) with a kmer of 53 bp. The raw sequence data have been submitted to the ENA under accession: ERP000894. Gene models were predicted using the *ab initio* gene finder AUGUSTUS (Stanke and Waack, 2003). Based on a close phylogenetic relationship, *Laccaria bicolor* was chosen as an appropriate training sequence. The minimum length of a gene was set to 300 nucleotides. A preliminary annotation of predicted gene models was performed using Blast2GO (Conesa *et al.*, 2005). Blast2GO (B2G) was also used to assign gene ontology (GO) (Ashburner *et al.*, 2000) terms to all gene models. Signal secretion peptides were predicted using SignalP ver3.0 (Bendtsen,

et al., 2004). *A. mellea* multigene families were located by performing an all against all BlastP database search (Altschul *et al.*, 1997) the resulting hits were clustered into families using the mcl algorithm (Enright *et al.*, 2002) with an inflation value of 2. A nucleotide sequence *in silico* cDNA database in FASTA format was generated and converted to a peptide sequence FASTA format database. This database was interrogated for all subsequent proteome investigations.

2.2.3 Phylogenetic supertree construction

Genome data was obtained from the relevant sequencing centres (Table 2.2) for phylogenetic supertree construction from 23 Basidiomycete and 2 Ascomycete species and a phylogenetic supertree was constructed byDr. David Fitzpatrick. Gene families were aligned using the multiple sequence alignment software Muscle v3.7 (Edgar, 2004) with the default settings. Using the default settings, misaligned or fast evolving regions of alignments were removed with Gblocks (Castresana, 2000). Permutation tail probability (PTP) tests (Archie, 1989; Faith and Cranston, 1991) were performed on each alignment to ensure that the presence of evolutionary signal was better than random ($P < 0.05$). Gene families that failed the PTP test were removed. Optimum models of protein evolution were selected using Modelgenerator (Keane *et al.*, 2004) and these were used to reconstruct maximum likelihood phylogenies in Phyml v3.0 (Guindon and Gascuel, 2003). Bootstrap resampling was performed 100 times on each alignment and majority rule consensus (threshold of 50%) trees were reconstructed.

2.2.3.1 Protein identification overview

As illustrated (Figure 2.1), two methods of protein identification were employed. Method 1, whereby protein was extracted from either mycelia or supernatant, separated by SDS-PAGE in one or two dimensions, excised from gels, digested with trypsin and analysed by liquid chromatography mass spectrometry (LC-MS/MS) and matrix assisted laser desorption ionisation time of flight (MALDI-ToF) before bioinformatic analysis. Method 2, whereby protein was extracted from either mycelia or supernatant, digested with trypsin and analysed by LC-MS/MS directly, with no further processing prior to bioinformatic analysis.

Table 2.2. List of Basidiomycota genomes used in phylogenetic supertree construction. Genome centre and subphyla are listed. The Ascomycetes, *Candida albicans* and *Saccharomyces cerevisiae* were used as outgroups.

Species	Centre	Subphylum
Dichomitus squalens	JGI	Agaricomycotina
Ganoderma	JGI	Agaricomycotina
Postia placenta	JGI	Agaricomycotina
Ceriporiopsis subvermispora	JGI	Agaricomycotina
Phanerochaete carnosa	JGI	Agaricomycotina
Phlebia brevispora	JGI	Agaricomycotina
Moniliophthora perniciosa	NCBI	Agaricomycotina
Agaricus bisporus	JGI	Agaricomycotina
Coprinopsis cinerea	BROAD	Agaricomycotina
Laccaria bicolor	JGI	Agaricomycotina
Coniophora puteana	JGI	Agaricomycotina
Paxillus involutus	JGI	Agaricomycotina
Serpula lacrymans	JGI	Agaricomycotina
Tremella mesenterica	JGI	Agaricomycotina
Cryptococcus neoformans	BROAD	Agaricomycotina
Cryptococcus gattii	BROAD	Agaricomycotina
Sporobolomyces roseus	JGI	Pucciniomycotina
Rhodotorula graminis	JGI	Pucciniomycotina
Puccinia graminis	BROAD	Pucciniomycotina
Melampsora laricis-populina	JGI	Pucciniomycotina
Malassezia globos	JGI	Ustilaginomycotina
Ustilago maydis	BROAD	Ustilaginomycotina

2.2.3.2 Bioinformatic Analysis of protein data

A FASTA format file of the cDNA protein database was saved with sequence alignment editor BioEdit (Hall, 1999). This file was then used as a query file to select subset data for discrete searches, whereupon a subset database was constructed for further analysis. The online software tool Blast2GO (B2G), a functional analysis and annotation tool, was employed initially (Götz *et al.*, 2008); a BlastP search of the National Centre for

Biotechnology Information non-redundant database (NCBInr) was run, with the number of hits set to ten and files saved in .xml format; a GO mapping step followed, after which annotation and annotation augmentation were implemented; InterProScan (IPS) (Figure 2.2) and "InterProScan GO's merge to annotation" was performed; enzyme code and KEGG mapping steps were run, after completion of which GO slim was executed and combined outputs generated.

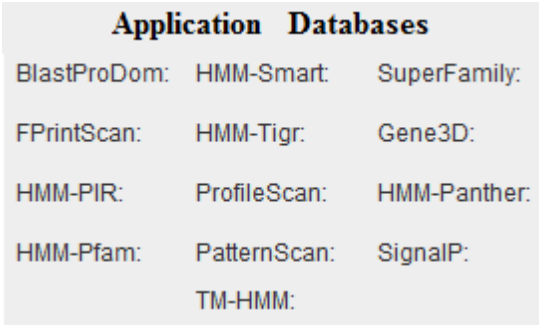

Figure 2.2. Application databases interrogated by InterProScan during Blast2GO analysis of proteins.

Subset databases were used to query Phobius (Käll *et al.*, 2004) which uses protein sequence data to model topography of proteins with regard to transmembrane regions. ProteinGRAVY (Stothard, 2000) interrogation with protein sequence data returns a number denoting the hydropathy of proteins: hydrophobic showing a positive number and hydrophilic showing a negative result. The Centre for Biosequence Analysis (Technical University of Denmark) SignalP (Petersen *et al.*, 2011) database was then searched with protein sequence data for signal peptides denoting a secretion signal and interrogation of a second database SecretomeP (Bendtsen *et al.*, 2005) with protein sequence data for non-classical secretion signals. TargetP interrogation of sequences returns sequences which show a mitochondrial target sequence together with a score denoting the likelihood of the protein being mitochondrial (Emanuelsson *et al.*, 2007). BioEdit (Hall, 1999) multiple sequence alignment tool ClustalW (Larkin *et al.*, 2007) was used to align sequences. All software used for data analysis is shown in Table 2.3.

2.2.3.3 Culture of *A. mellea* on solid media

Mycelia from culture of *A. mellea* on MEA (stored at 4 °C wrapped in parafilm) was used to inoculate petri dishes of agar (Section 2.1.3.3 or 2.1.3.12). A sterile loop was used to excise 3 – 5 mm mycelia that were placed into the centre of a petri dish. Cultures were incubated at 25 °C for 3 - 6 weeks, after which they were stored at 4 °C

wrapped in parafilm. Alternatively, plates intended for metabolite organic extraction were stored at −20 °C.

Table 2.3. Programs used for bioinformatic analysis.

Program	Function	Reference
BioEdit	A biological sequence alignment editor for alignment or editing of sequences in FASTA format with links to exteRNAl programs e.g. ClustalW	(Hall, 1999)
BLAST	Search of National Centre for Biotechnology Information, non-redundant database (NCBInr) for homology to input sequence.	(Altschul *et al.*, 1990)
Blast2Go	BLAST search, GO mapping, InterProScan annotation, enzyme code mapping and Kegg pathway mapping; consolidation of annotation and graphing of data in text or graphical format by biological process, cellular component or molecular function.	(Conesa *et al.*, 2005)
ClustalW	A multiple sequence alignment program	(Larkin *et al.*, 2007)
GO	A gene orthology classification scheme based on cellular component, molecular function, and biological process.	(Ashburner *et al.*, 2000)
InterProScan	European Bioinformatics Institute InterProScan database collection for protein signatures	(Zdobnov and Apweiler, 2001)
Kegg pathway mapping	Kyoto Encyclopedia of Genes and Genomes (KEGG) pathway mapping databases show protein interactions and reactions	(Kanehisa and Goto, 2000, Kanehisa et al., 2012)
Phobius	Protein topology and signal prediction i.e. membrane regions and signal peptides	(Käll *et al.*, 2004)
Protein GRAVY	Calculates the grand average of hydropathy	(Stothard, 2000)
SecretomeP	Predicts the presence of non- classical secretion signals	(Bendtsen, Jensen, *et al.*, 2004)
SignalP	Predicts the presence and peptide cleavage sites of secretion signal peptides	(Petersen *et al.*, 2011)
TargetP	Predicts the subcellular location based on mitochondrial targeting and secretory peptides	(Emanuelsson *et al.*, 2007)

2.2.4 *A. mellea* - maintenance and storage

A. mellea was maintained on MEA (Section 2.1.3.3), inoculated and grown as in Section 2.2.3.3. Plates wrapped in parafilm were stored at 4 °C.

2.2.4.1 Liquid Culture of *A. mellea*

Under sterile conditions, ethanol (300 µl) was added to flasks of autoclaved liquid media (Section 2.1.3.1 or 2.1.3.13) which was then inoculated with *A. mellea* mycelia as follows. Agar culture (25 ml) was broken up using a sterile loop, transferred to a sterile container with approx. 10 ml sterile dH_2O and shaken vigorously to break the mycelia into pieces. Aliquots of this liquid/agar were used to inoculate the flasks which were incubated at 25 °C, either static or shaking for 3-6 weeks. Flasks were also wrapped in foil to totally exclude light and grown in static conditions at 25 °C for 3 - 6 weeks. Cultures were also grown with ethanol omitted.

2.2.4.2 Harvest and storage of *A. mellea* liquid culture

Mycelia from *A. mellea* liquid culture were filtered through miracloth, washed with Milli-Q® H_2O (50 ml) dried thoroughly with absorbent paper, wrapped in aluminium foil and put immediately into liquid nitrogen (N_2). Stored at −70 °C or alternatively put into a container and lyophilised to dryness. Supernatant filtrates were stored at −20 °C in sterile containers.

2.2.4.3 Agar culture of *A. fumigatus*

Under sterile conditions, a loop of spores from a stock conidia solution of *A. fumigatus* was streaked onto culture plates of MEA (Section 2.1.3.3) and incubated at 37 °C for 3 days. To harvest the freshly grown spores, PBST (Section 2.1.3.15) 10 ml, was put onto the dish and the surface rubbed with a sterile bent glass rod to dislodge conidia. The liquid was pipetted into a sterile container and used for inoculation of plates. Conidial solutions were stored at 4 °C for up to two weeks.

2.2.4.4 Maintenance of *C. albicans*

Under sterile conditions a loop of culture from a stock solution of *C. albicans* was streaked onto culture plates of MEA (Section 2.1.3.3) and incubated at 37 °C for 2 days. To harvest cultures, glycerol solution (Section 2.1.5.13), (10 ml), was put onto the culture and a sterile bent glass rod used to wash colonies into the liquid. The liquid was pipetted into a sterile container and used for inoculation of plates. Solutions were stored at −70 °C.

2.2.4.5 Culture of *C. albicans* on MEA

Under sterile conditions, a loop of culture from a stock solution of *C. albicans* was streaked onto culture plates of MEA (Section 2.1.3.3) and incubated at 37 °C for 30 h. To harvest cultures, 2 ml of PBS (Section 2.1.3.14) was put onto the culture and a sterile loop used to wash colonies into the liquid. The liquid was pipetted into a sterile container. 100 µl was removed and serially diluted to 1:10, 1:100 and 1:1000. Cells were counted on a haemocytometer and stored at 4 °C for up to four weeks.

2.2.4.6 Liquid culture and storage of *C. albicans*

Under sterile conditions 100 µl of culture from a stock solution of *C. albicans* was put into 100 ml flasks containing 50 ml of autoclaved PDB (Section 2.1.3.1) and incubated with shaking (200 rpm) 37 °C for 24 h. Cultures were harvested by pipetting into a sterile container and centrifuging at 4000 *g* for 5 min. Liquid was removed and the cells were washed twice with sterile PBS (5 ml). Unused solution was stored at 4 °C.

2.2.5 Oxidative stress

Liquid static cultures of *A. mellea* (Section 2.2.4.1) were grown in PDB media for 28 days. Two discrete oxidative stress conditions were induced as follows: (a) H_2O_2 (9.79 M, 20 µl, 1 mM final) was added to cultures, an equivalent volume of sterile H_2O was added to controls, (b) Menadione (0.5 mM) in methanol plus $FeCl_3$ (1 µM final), were added to cultures, an equivalent volume of methanol was added to controls (Ruiz-Duenas *et al.*, 1999). Cultures were incubated at 25 °C for 3 h with stirring every 15 min, then placed on ice and harvested immediately. Mycelia were washed with dH_2O (50 ml) dried and flash frozen in N_2 before storage at −70 °C. Supernatants were frozen at −20 °C.

2.2.6 Co-cultures

2.2.6.1 Co-culture of *A. mellea* and *A. fumigatus* on MEA

Under sterile conditions, petri dishes of MEA (Section 2.1.3.3) were inoculated with *A. mellea* mycelia (Section 2.2.3.3) and also in four places with *Aspergillus fumigatus* Af293 (5 µl x 4) in PBST (Section 2.2.4.3) containing between 10^4 and 10^6 conidia per inoculation. Plates were incubated at 25 °C and grown for 2-4 weeks.

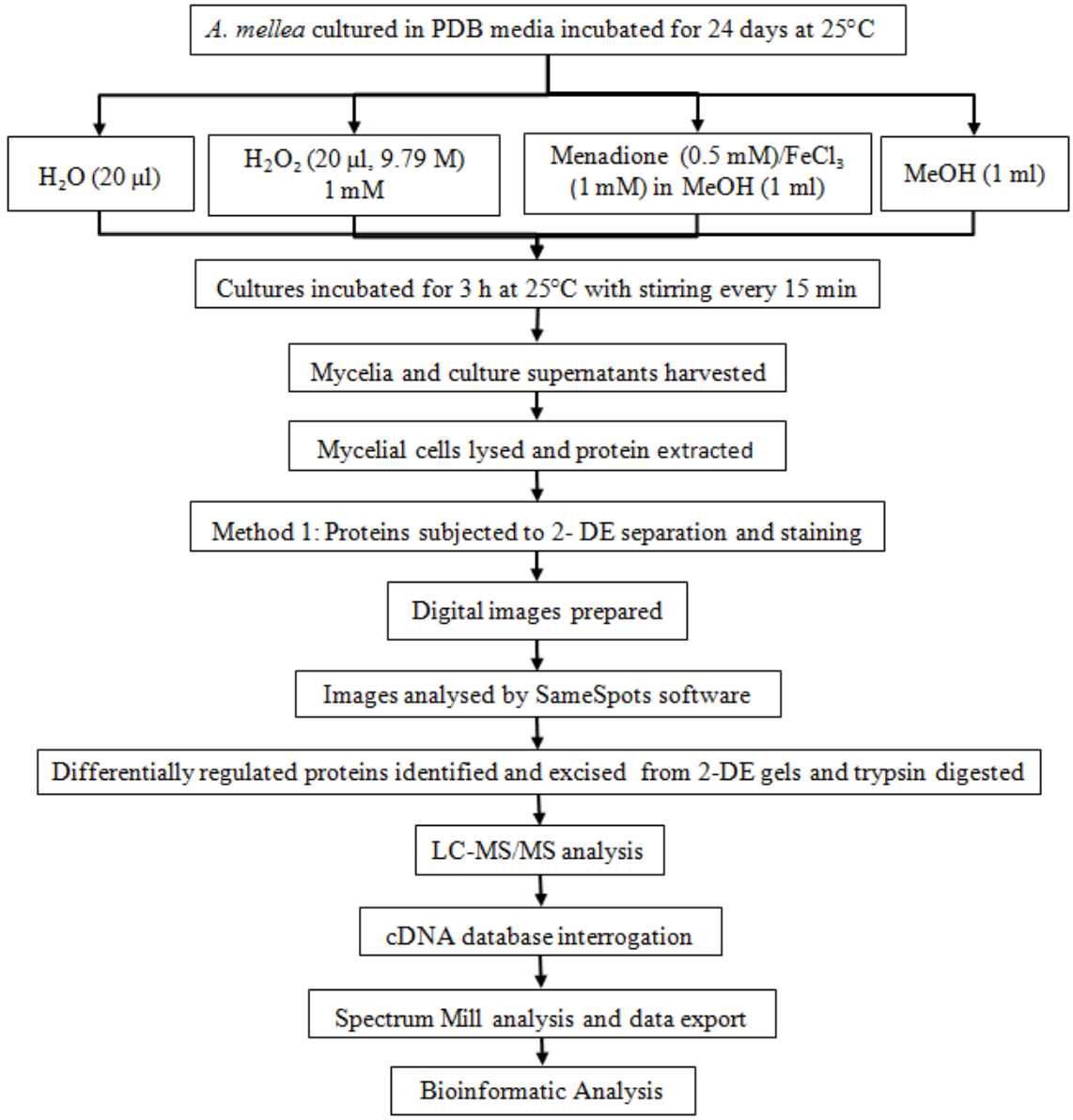

Figure 2.3. Workflow for oxidative stress, differential proteomics followed by LC-MS/MS analysis, identification and bioinformatic analysis of differentially regulated proteins.

2.2.6.2 Co-culture of *A. mellea* and *C. albicans* on MEA

Under sterile conditions, petri dishes of MEA (Section 2.1.3.3) were inoculated with *A. mellea* mycelia (Section 2.2.3.3) incubated at 25 °C for one week. Four discrete inoculations of *C. albicans* (Section 2.2.4.5) per plate were carried out each with the same number of cells ranging from 10^4 - 10^9 cells per inoculation. Cultures were incubated for a further 2-4 weeks at 25 °C.

2.2.6.3 Culture of plugs from *A. mellea* and *C. albicans* co-cultures on MEA

Under sterile conditions a cork borer was used to remove plugs from inoculation points of both *A. mellea* and *C. albicans* co-cultures and *C. albicans* controls. The plugs were

agitated in PBS (Section 2.1.3.14) (7 ml), to suspend *C. albicans* cells and dilutions were made 1/10, 1/100, 1/1000 and 1/10000. Cell suspension (100 µl) was pipetted onto MEA (Section 2.1.3.3) plates and spread using sterile inoculating loop. Cultures were incubated at 37 °C for 30 h.

2.2.6.4 Co-culture of *A. mellea* and *C. albicans* on PDA

Under sterile conditions, petri dishes of PDA (Section 2.1.3.2) were inoculated with *A. mellea* mycelia (Section 2.2.3.3) incubated at 25 °C for 8 days, inoculated with *C. albicans* from agar culture using a pipette tip (10^4 cells x 4) and grown for a further 16 days.

2.2.6.5 Co-culture of *A. mellea* and *Pseudomonas aeruginosa* on PDA

Under sterile conditions, petri dishes of PDA (Section 2.1.3.2) were inoculated with *A. mellea* mycelia (Section 2.2.3.3) incubated at 25 °C for 8 days, inoculated with *P. aeruginosa* glycerol stock (OD_{600} >3), (5 µl x 4) and grown for a further 16 days.

2.2.6.6 Co-culture of *A. mellea* and *Staphylococcus aureus* on PDA

Under sterile conditions, petri dishes of PDA (Section 2.1.3.2) were inoculated with *A. mellea* mycelia (Section 2.2.3.3) incubated at 25 °C for 8 days, inoculated with *S. aureus* glycerol stock (OD_{600} >3), (5 µl x 4) and grown for a further 16 days.

2.2.6.7 Co-culture of *A. mellea* and Methicillin-resistant *Staphylococcus aureus* (MRSA) on PDA

Under sterile conditions, petri dishes of PDA (Section 2.1.3.2) were inoculated with *A. mellea* mycelia (Section 2.2.3.3) incubated at 25 °C for 8 days, inoculated with MRSA glycerol stock (OD_{600} >3), (5 µl x 4) and grown for a further 16 days.

2.2.6.8 Co-culture of *A. mellea* and *Escherichia coli* on PDA

Under sterile conditions, petri dishes of PDA (Section 2.1.3.2) were inoculated with *A. mellea* mycelia (Section 2.2.3.3) incubated at 25 °C for 8 days, inoculated with *E. coli* glycerol stock (OD_{600} >3), (5 µl x 4) and grown for a further 16 days.

2.2.6.9 *A. fumigatus* with *A. mellea* supernatant on agar

Under sterile conditions, organic extract from *A. mellea* supernatant or methanol control (200 µl) was added to 12.5 ml MEA (Section 2.1.3.3) poured and allowed to set. Plates were inoculated with 5 µl harvested *A. fumigatus* conidia (Section 2.2.4.3) in quadruplicate and incubated at 25 °C for 120 h. Culture diameters were measured at 48 h post inoculation and every 24 h thereafter up to 120 h.

2.2.6.10 Co-culture of *A. mellea* and *C. albicans* in PDB

Under sterile conditions ethanol (300 µl) was added to flasks of autoclaved liquid media (Section 2.1.3.1 or 2.1.3.13) which were then inoculated with mycelia. Agar culture (25 ml) was broken up using a sterile loop, transferred to a sterile container with approx. 10 ml sterile dH_2O and shaken to break the mycelia. Aliquots of this liquid/agar were used to inoculate the flasks which were incubated at 25 °C either static or shaking for 1 week. Flasks were inoculated with *C. albicans* cells (1×10^9) returned to the incubator and grown for a further 13 days.

2.2.6.11 Lyophilised Supernatant in solvent

In accordance with a modified protocol from Coleman *et al.* (2011), flasks from mono-culture of *A. mellea* in PDB (Section 2.2.4.1) or co-culture of *A. mellea* and *C. albicans* in PDB (Section 2.2.6.10) were harvested and supernatant was gravity filtered through miracloth. The supernatant was lyophylised to dryness and resuspended in DMSO or MeOH at a rate of 200 mg/ml.

2.2.6.12 Plate assay of *C. albicans* with *A. mellea* mono-culture and *A. mellea* and *C. albicans* co-culture lyophilised supernatants

MEA plates were inoculated with *C. albicans* cells (10^4, 10^5 or 10^6) cells in PBST. The cells were spread with sterile tungsten beads to ensure confluence. Pads of filter paper (6 mm) were put on the surface. Supernatant resuspended in MeOH (Coleman *et al.*, 2011), was applied to the paper pads at range of supernatant concentrations (1 mg-10 mg/50 µl MeOH) from mono-culture and co-culture culture supernatants, 50 µl MeOH was added to one pad as control (Section 2.2.6.11). Cultures were incubated for 24 h at 37 °C.

2.2.6.13 Supernatant Organic extraction

Culture supernatant (Section 2.2.4.2) which had been stored at −20 °C was defrosted and extracted twice with organic extraction buffer (Section 2.1.5.14) 2:1 supernatant. The volatiles were removed under vacuum, and organic layer resolubilised in methanol $^1/_{100}{}^{th}$ original volume supernatant.

2.2.6.14 Assay of *Aspergillus fumigatus* Af293 growth with *A. mellea* culture supernatant extract in MML

A. mellea liquid cultures (10 ml) of MML (Section 2.1.3.13) with glucose as a carbon source were inoculated with *A. fumigatus* (Section 2.2.4.3), containing 10^4 or 10^6 conidia. *A. mellea* culture supernatant (100 ml) organic extract was resolubilised in 1 ml

methanol (Section 2.2.6.13). Inoculated media (400 µl) was put into each of four microfuge tubes. Organic extract (25 µl) each was added to 2 tubes and MeOH (25 µl) each was added to the other 2 as control. Tubes were vortexed briefly to mix.

Inoculated media (200 µl) was added to twenty further tubes, 10^4 conidia to ten and 10^6 conidia to a second ten.

Samples were diluted serially by withdrawing 200 µl from the microfuge tubes containing organic extract or methanol and adding it to one of the tubes containing inoculated media only, mixing well and withdrawing 200 µl and adding it to a tube containing media with the same cell concentration. Six dilutions were obtained. Duplicates from each dilution (100 µl) were added to a 96 well plate. The plate was incubated at 37 °C for 96 h. The optical density of wells (Abs 540 nm) was measured on a BioTec Synergy HT Plate reader running KC4 (V.3.3 Rev 10) at 24 h, 48 h and 96 h.

2.2.7 Protein Extraction

All protein extraction was carried out at 4 °C.

2.2.7.1 Bradford Protein Assay

Stock solution of BSA (10 mg/ml) was prepared and diluted in PBS (Section 2.1.3.14) to give solutions of known protein concentration (as well as a blank PBS control) to generate a protein standard curve. Samples of known concentration (20 µl) were mixed with Bradford solution (Section 2.1.3.16), (980 µl), to give a final volume of 1 ml. Protein samples to be assayed (20 µl), were mixed with Bradford solution (Section 2.1.3.16), (980 µl), to give a final volume of 1 ml. Following 10 min incubation, absorbances were determined using a spectrophotometer at A_{595nm} (Eppendorf Biophotometer). A graph of A_{595nm} versus BSA concentration was plotted and the protein concentration of the samples was calculated from the curve. All samples were prepared and analysed in duplicate.

2.2.7.2 Method 1 - *A. mellea* mycelial lysate protein extraction for 2-DE separation of proteins

A. mellea mycelia were harvested (Section 2.2.4.2), ground to very fine powder in liquid N_2 using a pestle and mortar and weighed. PMSF (100 mM) was added directly to mycelia at a final concentration of 1 mM. Lysis buffer (Section 2.1.5.1) was then added (2 ml/g). A probe sonicator (Bandelin Senoplus HD2200) Cycle 6, Power 10 % was used to generate lysates in six 10 s bursts, cooling the sample on ice for one min between bursts. Lysates were frozen in liquid N_2, thawed on ice and sonicated as before.

Mycelial lysates were centrifuged at 3,200 *g* for 15 min to remove cell debris. Samples were removed to clean tubes, sonicated on Fisher Scientific FB15050 Sonicating waterbath, centrifuged at 14,000 *g* for 15 min and again placed into a clean tube. Cold 100% (w/v) TCA (Section 2.1.5.15) stock solution was added so that it comprised 10 % (v/v) of the final solution. Samples were vortexed and kept on ice for 1 h. The samples were centrifuged at 14,000 *g* for 15 min. The liquid was removed and pellets were washed with ice-cold acetone. Samples were put on ice overnight. The wash step was repeated twice more with centrifugation at 10,000 *g* for 5 min each time. 2-DE focussing buffer (Section 2.1.6.16) was added to each tube at a rate of 1 ml/g of ground mycelia. Samples were centrifuged for 5 min at 13,000 *g*. Protein concentration was then quantified using the Bradford Protein Assay (Section 2.2.7.1).

2.2.7.3 Method 2A - *A. mellea* mycelial whole cell lysate (WCL) protein extraction for direct LC-MS/MS analysis

Mycelia were harvested (Section 2.2.4.2), ground to very fine powder in liquid N_2 using a pestle and mortar and weighed. WCL Lysis Buffer (Section 2.1.5.2) was added to mycelial mass at the ratio of 6 ml/g mycelia. A probe sonicator (Cycle 6, Power 10 %,) was used to generate a lysate in six 10 s bursts, cooling samples on ice 1 min between bursts to generate a whole cell lysate. Samples were centrifuged at 14,000 x *g* for 15 min and liquid removed to a clean tube. 50 µl was retained for determination of protein concentration using a Bradford assay (Section 2.2.7.1). After sonication, 1 M DTT stock (10 µl/ml lysate) was added. This was incubated at 56 °C for 30 min, allowed to cool to room temperature and 1 M iodoacetamide (55 µl/ml of lysate) was added. The solution was incubated in darkness at room temperature for 20 min. The lysate was dialysed twice using MW03115 dialysis tubing, against cold 100 mM ammonium bicarbonate (Section 2.1.5.4), (2 x 50 volumes), for at least 3 h on each occasion, with stirring, at 4 °C. The denatured protein was put into a clean tube. Precipitates of denatured protein was present after dialysis. Material was stored at −20 °C prior to trypsin digestion.

2.2.7.4 Method 2B Whole cell lysate (WCL) of lyophilised *A. mellea* mycelia protein extraction for direct LC-MS/MS analysis

Lyophilised mycelia (100 mg) were placed into microfuge tubes with a 3 mm tungsten bead and beaten at 30 Hz for 5 min. WCL lysis buffer (Section 2.1.5.2) (500 µl), was added to the tubes and beaten as before. A further (200 µl) WCL lysis buffer was added and samples incubated for 1 h on ice. Tubes were centrifuged at 15,000 *g* for 2 min and liquid removed to a clean tube. 1 M DTT (Section 2.1.5.7) (5 µl) was added and

incubated at 56 °C for 30 min. Samples were cooled to room temperature and 27.5 µl 1 M iodoacetamide (Section 2.1.5.8) was added. Tubes were incubated in the dark for 20 min. The liquid was transferred to dialysis tubing (MW03115). The lysate was dialysed twice using MW03115 dialysis tubing, against cold 100 mM ammonium bicarbonate (Section 2.1.5.4), (2 x 50 volumes), for at least 3 h on each occasion, with stirring, at 4 °C. The denatured protein was put into a clean tube; a precipitate of denatured protein was present after dialysis. Stored at −20 °C.

2.2.7.5 Extraction of secreted protein from culture supernatants prior to SDS-PAGE

This protocol was adapted from Fragner *et al.* (2009). Supernatant, frozen at −20 °C (200 ml) for a minimum of 12 h was defrosted and centrifuged on a at 48,000 *g* (4 °C) for 30 min. The supernatant was removed to a clean container and concentrated 10-fold by lyophilisation. 100 % (w/v) TCA stock solution (Section 2.1.5.15) was added to the concentrate so that it comprised 10 % (v/v) of the final solution. This was mixed and incubated on a roller overnight at 4 °C. Samples were centrifuged at 1,700 *g* (4 °C) for 45 min. Tris-buffer (Section 2.1.5.3) (50 mM, 2 ml) was added to ice-cold acetone (8 ml), final concentration of buffer 20% (v/v). The pellet washed with 1- 2 ml of this solution and was centrifuged for 3 min at 9,400 (4 °C). The wash step was repeated twice with 2 min centrifugation each time, after which it was washed with one ml of ice-cold acetone, centrifuged for 2 min, air dried and stored at −20 °C. Prior to separation by SDS-PAGE, 1 M DTT (Section 2.1.5.7) (10 µl), 10 % (w/v) SDS (Section 2.1.6.1) (10 µl) and 5 X solubilisation buffer (Section 2.1.6.8), (10 µl), were added to solubilise the protein.

2.2.7.6 Concentration of secreted protein from culture supernatants

This protocol was adapted from Fragner *et al.* (2009). Supernatant, frozen at −20 °C (200 ml) for at least 12 h, was defrosted and centrifuged at 48,000 *g* (4 °C) for 30 min. The supernatant was put into a clean container and lyophilised to dryness. Samples were stored −20 °C, resolubilised in dimethyl sulfoxide (DMSO) or MeOH at 10 mg/ml for use in plate assay.

2.2.7.7 Extraction of secreted protein from agar for SDS-PAGE or direct LC-MS/MS analysis (Methods 1 and 2)

This protocol was adapted from a combination of two protocols: Imanaka *et al*. (2010) and Fragner *et al*. (2009) . Cultures grown on an agar medium were ground gently using a pestle and mortar to break up the agar but not to grind mycelia. KH_2PO_4 (Section

2.1.5.6), (50 mM, 50 ml) was added gradually to a 25 ml agar culture. This was agitated overnight at 4 °C. The liquid was gravity filtered before being centrifuged at 48,000 *g* (4 °C) for 30 min and supernatants were put into clean containers. 100 % (w/v) TCA stock solution (Section 2.1.5.15) was added to the liquid so that it comprised 10 % (v/v) of the final solution. Samples were mixed and incubated on a roller overnight at 4 °C, followed by centrifugation at 1700 *g* (4 °C), 45 min. Tris-buffer (Section 2.1.5.3), (50 mM, 2 ml) was added to ice cold acetone (final concentration of Tris-buffer 20 % (v/v)). This solution (1 -2 ml) was used to wash the pellet. This was centrifuged for 2 min at 9,400 *g* (4 °C) and washed twice more with centrifugation for 1 min at 9,400 *g* (4 °C), after which it was washed with 1 ml of ice-cold acetone; air dried and stored at −20 °C.

Routinely, 10 µl 1 M DTT, 10 µl 10 % SDS (w/v) and 10 µl 5 X solubilising buffer (Section 2.1.6.8) were added to pellets prior to separation by SDS-PAGE. Alternatively, pellets were trypsin digested and protein was analysed directly by LC-MS/MS.

2.2.8 Sodium Dodecyl Sulphate Polyacrylamide Gel Electrophoresis (SDS-PAGE)

2.2.8.1 Gel Electrophoresis (SDS-PAGE)

SDS-PAGE gels, both stacking and separating, were prepared according to Laemmli (1970), (Table 2.4). The gels were cast using BioRad gel casting apparatus (BioRad, CA., USA) according to the manufacturer's guidelines.

Samples were prepared by adding 1 volume of 5 X solubilisation buffer (Section 2.1.6.9) to every 4 volumes of sample to a 1.5 ml microfuge tube. Tubes were pierced on the lid and boiled for 10 min before being loaded onto the gel with a Hamilton syringe. A prestained protein marker (BioLabs, UK) was loaded into one well. Electrophoresis was carried out initially at 60 V for 30 min, followed by Electrophoresis at 120 V for 1 h or more, depending on the nature of the sample, using 1 X Running Buffer (Section 2.1.3.8), until dye front was 0.5 cm from the bottom of the gel. Following electrophoresis, gels were either placed in (i) Staining solution (Section 2.1.6.11) overnight with gentle agitation and subsequently placed in de-stain solution (Section 2.1.6.12) for 30 min or (ii) submitted for Colloidal Coomassie® Blue Staining (Section 2.2.8.2).

2.2.8.2 Colloidal Coomassie® Blue Staining

Gels were fixed overnight in fixing solution (Section 2.1.6.13). This was followed by three 20 min washes in Milli-Q® H_2O. Gels were pre-incubated for 1 h in incubation

buffer (Section 2.1.6.14) before being stained for between 4-5 days in stain solution (Section 2.1.6.15). Gels were destained by repeated changing of Milli-Q® H_2O to remove background staining.

Table 2.4. Reagent volumes used for SDS-PAGE preparation.

Reagent	Stacking	Separating				
	Mini Gel	Mini Gel			Large Gel	
Acrylamide%	4%	7.50%	10%	12%	10%	12%
0.5M Tris HCL pH 6.8 (ml)	0.63	-	-	-	-	-
1.5 M Tris HCL pH 8.3 (ml)	-	1.75	1.75	1.75	15.75	15.75
10 % (w/v) SDS (µl)	25	70	70	70	605	605
30 % (w/v) Acrylamide/bis Acrylamide (ml)	0.33	1.73	2.33	2.83	20.93	25.35
Deionised H_2O (ml)	1.53	3.66	3.08	2.33	27.68	20.85
10 % (w/v) Ammonium persulphate (µl)	50	25	25	25	225	225
TEMED (µl)	5	5.75	5.75	5.75	52.2	52.2

2.2.8.3 Isoelectric Focussing (IEF) and 2-DE

Protein (250 - 300 µg) was resolubilised in 2-DE focussing buffer (250 µl) (Section 2.1.6.16), centrifuged at 12,000 *g* for 5 min to remove insoluble material and a few crystals of bromophenol blue added. A pipette was used to load samples along the length of 13 cm IPGphor strip holders. A forceps was used to place an IPG strip, gel-side down into the holder on top of the sample excluding any bubbles. The strips were then overlaid with 1 ml of Overlay fluid (GE Healthcare), the plastic cover was put on top, the IPGphor strip holders placed on IPGphor II IEF unit and subjected to isoelectric focussing according to the program in Table 2.5.

Table 2.5. IEF program.

	Voltage	Time (h)
Step	50	12
Step	250	0.25
Gradient	5000	2
Step	5000	5
Gradient	8000	2
Step	8000	1

Following IEF, IPG strips were equilibrated in 2-DE reduction buffer (Section 2.1.6.18) for 20 min, followed by equilibration in alkylation buffer (Section 2.1.6.19) for a further 20 min. IPG strips were then rinsed in 1 X Electrode Running buffer (Section 2.1.6.10) before being placed on top of a homogenous SDS-PAGE gel, using a forceps. Gels were overlaid with agarose sealing solution (Section 2.1.8.4), which was allowed set before the gels were placed into the PROTEAN Plus Dodeca Cell (BIO-RAD) according to the manufacturer's instructions. The upper and lower chambers were filled with 2 X electrode running buffer, 1 X electrode running buffer respectively. Gels were electrophoresed for 1 h at 30 V and 30 mA per gel for the remaining time until the dye front was 2 cm from the bottom of the gel. Following electrophoresis, gels were either placed in (i) Staining solution (Section 2.1.6.11) overnight with gentle agitation and subsequently placed in de-stain solution (Section 2.1.6.12) or (ii) Colloidal Coomassie® Blue Staining (Section 2.2.8.2) was carried out.

2.2.9 Comparative proteomics SameSpots software analysis

A. mellea liquid cultures which had been subjected to oxidative stress (Section 2.2.5) were harvested (Section 2.2.4.2), mycelia protein was extracted and separated by 2-DE (Table 2.4 and Section 2.2.8.3), and gels were stained with Colloidal Coomassie (Section 2.2.8.2). Digital images of gels were recorded using a CCD scanner. Image quality was inspected, images were aligned, normalised and replicates grouped using Progenesis SameSpots software in line with workflow recommended by software developer. Spots were selected for excision and LC-MS/MS analysis based on a $p < 0.05$ Anova value from SameSpots analysis and visual inspection.

2.2.10 Protein Digestion methods

2.2.10.1 Digestion of WCL mycelial samples

All microfuge tubes were siliconised with Sigmacote. Samples of whole cell lysate (Section 2.2.7.3) or lyophilised whole cell lysate (Section 2.2.7.4) were vortexed, and 100 µl put into microfuge tubes. Trypsin solution (Section 2.1.5.10) (400 ng/µl, 5 µl) was added and incubated overnight at 37 °C.

2.2.10.2 Digestion of agar samples for direct analysis by LC-MS/MS

Trypsin solution (Section 2.1.5.11), (65 ng/µl, 50 µl), was added to microfuge tubes of protein extracted from agar (Section 2.2.7.7), and incubated overnight at 37 °C.

2.2.10.3 In-Gel Digestion of SDS-PAGE samples

An in-gel digest protocol according to Shevchenko *et al.* (2007), was utilised. All microfuge tubes were siliconised with Sigmacote. One or two dimensional gels were rinsed in dH_2O, (a) SDS-PAGE gel bands were excised using disposable scalpels cleaned in methanol. Bands approx (2 mm x 4 mm) were transferred to microfuge tubes (b) selected gel spots from 2-DE gels were excised using a pipette tip from which the tapered end had been cut and transferred to microfuge tubes. 100 mM ammonium bicarbonate (Section 2.1.5.4) was added to the microfuge tubes to cover the gel pieces and incubated at room temperature for 1 h to destain the gel pieces; liquid was removed. If the gels were heavily stained, the pieces were destained a second time. Acetonitrile was added to cover the gel pieces and incubated for 20 min at room temperature and ACN removed. Trypsin solution (13 ng/µl) (Section 2.1.5.12), 50 µl was added and the microfuge tubes were left on ice for 30 min. The tubes were checked to ensure the gel pieces were covered with solution and returned to ice for a further 90 min with occasional vortexing, and incubated overnight at 37 °C. The samples were subjected to sonication on a waterbath for 10 min then centrifuged at 12,000 *g* for 10 min and the supernatants removed to a fresh tube. Gel pieces were stored at −20 °C. The samples were dried under vacuum (Thermo Scientific Savant DNA120 Speedivac) and stored at −20 °C for analysis by LC-MS/MS.

2.2.10.4 OFFGEL peptide digest

A whole cell lysate (2.2.10.1) (approx 500 µg) was put into a microfuge tube. Trypsin solution (Section 2.1.5.10) (400 ng/µl, 5 µl) was added and incubated overnight at 37 °C. 360 µl of the whole cell lysate tryptic digest was put into a clean microfuge tube with 1.25 X OFFGEL solution (2.1.8.1), (1.44 ml).

2.2.11 OFFGEL peptide electrophoresis

An Agilent 3100 Fractionator was used for electrophoresis. IPG 3-10 strips were placed into OFFGEL tray as per manufacturer's instructions. A twelve well frame was fitted and 40 µl rehydration solution (Section 2.1.8.2) was pipetted into each well. Two wetted electrode pads were put on each end of the strip. The gel was rehydrated for 15 min and 150 µl OFFGEL peptide digest (Section 2.2.10.4) was pipetted into each well and the cover seal fitted. dH_2O (10 µl) was pipetted onto the electrode pads. IPG cover fluid, (200 µl), was pipetted onto anode end of the IPG strip and 1 ml. onto the cathode end. An additional 200 µl was applied to both ends after 1 min and the tray fitted into the fractionator. Fractionation was started using the default peptide program OG122PE00.

Once fractionation was completed fractions were collected into separate microfuge tubes which were dried by vacuum centrifuge. PepClean™ sample buffer (67 µl) was added to each sample. Samples were sonicated on a water bath for 10 min twice, to ensure they were in solution. PepClean™ C_{18} spin columns (Pierce, U.S.A.) were prepared by tapping to settle resin. The caps were removed and columns placed into receiver tubes. PepClean™ Activation solution was added (200 µl) (Section 2.1.8.3) to each, washing the column walls and centrifuged at 1500 *g* for 1 min. Flow-through was discarded and this was repeated. PepClean™ Equilibration solution (200 µl) (Section 2.1.8.5) was added, tubes were centrifuged at 1500 *g* for 1 min. This was repeated. Samples were loaded on top of resin, clean receiver tubes were used and columns centrifuged at 1500 *g* for 1 min. Flow through was recovered and reloaded onto the resin to ensure sample binding and centrifuged at 1500 *g* for 1 min. PepClean™Wash solution (200 µl) (Section 2.1.8.6), was added to each tube which was centrifuged at 1500 *g* for 1 min and flow-through discarded. This washing step was repeated twice more. Columns were placed into new receiver tubes and PepClean™ Elution Buffer (Section 2.1.8.7) (20 µl) was added to each, centrifuged at 1500 *g* for 1 min and this was repeated using the same receiver tubes. Samples were evaporated under vaccum for storage or LC-MS/MS analysis.

2.2.12 MALDI-ToF Mass Spectrometry

2.2.13 MALDI ToF Matrix Preparation

Trifluoroacetic acid (Section 2.1.7), (0.1 % (v/v) in Milli-Q® H_2O, 500 µl) was added to an equal volume of ACN. To this solution, α-cyano-4-hydroxycinnamic acid (4-HCCA) (5 mg) was added. The mixture was vortexed for 2 min and allowed to stand at room temperature for 15 min. The mixture was vortexed for 30 s and centrifuged at 12,000 *g* for 1 min, the supernatant was retained. Internal calibrants Angiotensin fragment III and human ACTH 18-39 were added in sufficient concentration to be identified in mass spectra above background.

2.2.14 Target preparation and MS analysis.

Aliquots of peptide solution from in-gel digest of SDS-PAGE samples (Section 2.2.10.3) (2 µl) were diluted 1:1 with the matrix sample in siliconised microfuge tubes. Matrix/peptide sample (0.4 µl) was transferred to an individual position on the MALDI-ToF target slide and allowed to air dry. Samples were prepared in duplicate and each slide submitted for MALDI-ToF analysis contained at least one spot of external calibration mix (LaserBio labs, Proteomix C104) (0.4 µl) as well as each spot

containing internal calibrants, Angiotensin fragment III and human ACTH 18-39. All samples were subjected to delayed extraction reflectron MALDI-ToF analysis with a nitrogen laser (337 nm) at 20 kV using an Ettan MALDI-ToF Pro mass spectrometer (Amersham Bioscience). Spectra were calibrated, before mass (*m/z*) lists were interrogated against

(i) a FASTA version of *A. mellea in silico* cDNA protein database

(ii) the NCBInr database to search for protein hits by homology against proteins in other organisms.

Criteria were set as monoisotopic peptide tolerance 50 ppm and 2 missed cleavages, with variable modifications set as oxidation of methionine and carbamidomethylation, for all database searches.

2.2.15 Liquid chromatography mass spectrometry (LC-MS/MS)

An Agilent 6340 ESI ion trap with system software V6.2 was used to determine the identity of peptides or molecules. Agilent recommended settings were used. Bovine serum albumin (BSA) standard (10 fmol) was analysed, identified and used to verify accuracy of identification and optimum machine functionality before samples were analysed.

2.2.15.1 LC-MS/MS analysis of Whole cell lysate

Whole cell lysate digests from mycelia (Section 2.2.7.3), lyophylised mycelia (Section 2.2.7.4) or agar (Section 2.2.7.7), (20 µl) were spin filtered (Agilent Technologies 0.22 µm Cellulose Acetate) prior to LC-MS/MS analysis. Samples were diluted at a range of ($^{1}/_{100}$ – 1) in LC-MS/MS Buffer A (Section 2.1.9.2). Preliminary analysis was performed with serial dilutions ranging from $^{1}/_{100}$ to neat sample until spectral intensity was sufficiently high to identify proteins from background.

A high capacity loading 150 mm, 300 Å, C-18 chip with a 9 mm, 160 nl trap column (G4240-62010) was used for sample analysis. An initial 10 min gradient of LC-MS/MS Buffer B (Section 2.1.9.3) method was followed by gradient optimisation based on peptide retention time and spectral intensity of individual samples. Test gradients (A – G) are shown in Table 2.6.

2.2.15.2 LC-MS/MS analysis of SDS-PAGE samples

Samples from SDS-PAGE, 2-DE (Section 2.2.10.3) gel digests which had been dried by vacuum centrifuge were reconstituted in 20 µl Buffer A (Section 2.1.9.2); OFFGEL peptide electrophoresis samples (Section 2.2.11) reconstituted in 50 µl Buffer A (Section 2.1.9.2) were analysed using a ProID 150 (II), 150 mm, 300 Å, C-18 chip with a 9 mm, 40 nl trap column (G4240-62006). Analysis of bands or spots excised from polyacrylamide gels was by Program A. Program A followed by Program C was used for the analysis of OFFGEL peptide electrophoresis samples (Table 2.6).

Table 2.6. Seven test LC-MS/MS gradients showing %B vs time (min).

Program A		Program B		Program C		Program D		Program E		Program F		Program G	
Time (min)	Solvent B (%)	Time (min)	Solvent B (%)	Time (min)	Solvent B (%)	Time (min)	Solvent B (%)	Time (min)	Solvent B (%)	Time (min)	Solvent B (%)	Time (min)	Solvent B (%)
0	5	0	5	0	5	0	5	0	5	0	5	0	5
1	5	1	5	1	5	1	5	20	15	40	15	100	11
7	70	17	70	60	50	120	70	350	40	160	30	340	16
8	100	18	100	63	100	121	100	360	48	480	36	540	21
9	100	23	100	66	100	126	100	365	100	570	48	690	28
10	5	24	5	67	5	127	5	370	100	595	100	710	40
								375	5	600	100	715	100
										605	5	720	100
												725	5
Flow rate (µl/min)	0.6		0.6		0.4		0.6		0.4		0.4		0.4

2.2.15.3 LC-MS/MS Chromatogram analysis

Protein identification was performed using Agilent G2721AA Spectrum Mill MS Proteomics Workbench software (Rev A.03.03.084 SR4). An *A. mellea in silico* cDNA protein database (Section 2.2.2) in FASTA format was downloaded to the Spectrum Mill database folder. The database was renamed PA.A.mellea in accordance with Agilent instructions, the inital PA denoting a protein database. In the Spectrum Mill protein database utilities tab, indices were created for the newly downloaded database and the database list was updated. Raw MS/MS datafiles from LC-MS/MS analysis (.D format) were uploaded to the Spectrum Mill server for analysis. Data files were extracted using default criteria. MS searches were then performed using the following criteria: tryptic enzymatic digest, with fixed modification carbamidomethylation of cysteines and two variable modifications, deamination and oxidation of methionine. Two missed cleavages were allowed. The minimum scored peak intensity was set to 70; with precursor mass tolerance +/- 2.5 Da and product mass tolerance +/- 0.7. The maximum ambiguous charge was set to 3, with a sequence tag length > 3 and minimum detected peaks set to 4. Reversed database scores were calculated. Autovalidation was used to validate files using the Agilent default settings for proteins and then peptides. Figure 2.4 is a schematic of a worklow from Agilent and Table 2.7 shows peptide scoring system for validation of results (Spectrum Mill MS Proteomics Workbench).

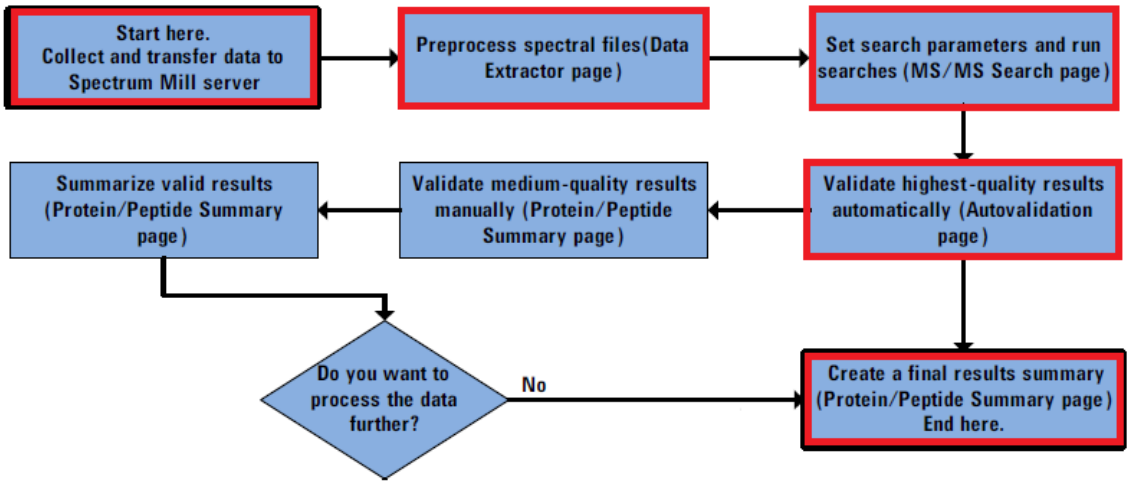

Figure 2.4 Schematic workflow from Agilent Spectrum Mill guidelines. The boxes outlined in red were used in this study.

Table 2.7 Agilent Spectrum Mill guidelines for validating ion trap results based on MS/MS Search scores

Peptide score	Quality	Peptide fragmentation	Likelihood of valid interpretation
13-25	Excellent	Extensive	When combined with **% SPI** of 70 or greater, very likely to be valid
9-13	Good	Substantial	When combined with % SPI of 70 or greater, likely to be valid
6-9	Mediocre	Moderate	Review results to determine whether interpretation is valid
3-6	Weak	Sparse	Not likely to be valid

2.2.15.4 Mycelial microscopy

Mycelia (1 mm) were excised and suspended in a drop of water on a glass slide, a cover slip placed on top and pressed with blotting paper to absorb excess liquid. Slides were sealed with a colourless lacquer and allowed to dry prior to microscopy

2.2.15.5 Live/dead cell staining of *C. albicans*

This protocol was adapted from Jones and Senft (1985). *C. albicans* cells (Section 2.2.4.5 or Section2.2.4.6) were harvested in PBS (Section 2.1.3.14) and 2 x 10^6 cells either live or dead by autoclaving for at 121 °C for 15 min, were placed in a microfuge tube. Cells were pelleted by centrifugation at 4000 *g* for 5 min at 4 °C. 100 µl (2 µg) of FDA working solution (Section 2.1.10.4) and 30 µl (0.6 µg) PI working solution (Section 2.1.10.6) was put directly onto cells which were incubated for 30 min in darkness. Tubes were centrifuged as before and stain removed. Cold PBS (1 ml) was added to the cells and vortexed. Tubes were centrifuged as before and liquid removed. 1 ml 20 % (w/v) BSA (Section 2.1.10.2) which had been kept on ice was put onto pellets, mixed to resuspend pellets, centrifuged as before and BSA removed, leaving approximately 50 µl. 1 - 3 µl was pipetted onto a large cover slide (76 x 26 x 0.17 mm), spread to an area of 10 mm^2 and allowed to dry at 4 °C. Samples were viewed dry; no cover slip was put on top as water causes cells to excrete fluorescein. Slides stored in the dark at room temperature for up to 1 week.

2.2.15.6 Live/Dead staining of *C. albicans* cells from co-culture

This protocol was adapted from Jones and Senft (1985). *C. albicans* cells from co-culture (Section 2.2.6.2) inoculation points excised using a sterile cork borer were suspended in PBS (7 ml) (Section 2.1.3.14) Cell suspension liquid (1.5 ml) was removed to a clean tube and pelleted by centrifugation at 4000 *g* for 5 min at 4 °C. 100 µl (2 µg) of FDA working solution (Section 2.1.10.4) and 30 µl (0.6 µg) PI working solution (Section 2.1.10.6) was put directly onto cells which were incubated for 30 min in darkness. Tubes were centrifuged as before and stain removed. Cold PBS (1 ml) was added to the cells and vortexed. Tubes were centrifuged as before and liquid removed. 1 ml 20 % (w/v) BSA (Section 2.1.10.2) which had been kept on ice was put onto the pellet, mixed to resuspend the pellet, centrifuged as before and BSA removed, leaving approximately 50 µl. 1 - 3 µl was pipetted onto a large cover slide (76 x 26 x 0.17 mm), spread to an area of 10 mm^2 and allowed to dry at 4 °C. Samples were viewed dry; no cover slip was put on top as water causes cells to excrete fluorescein. Slides stored in the dark at room temperature for up to 1 week.

2.2.15.7 Confocal microscopy

Olympus FluoView 1000 (FluoView FV10-ASW V.1.07 software) was used to visualise prepared mycelial slides (Section 2.2.15.4) or stained cells (Section 2.2.15.5, Section 2.2.15.6).

2.2.15.8 Data analysis

Data was exported from Spectrum Mill and analysed using Microsoft Excel® pivot tables.

Statistical analysis was carried out in Excel® using a t-test and graphs generated in Excel® unless stated otherwise.

Chapter 3 Genome sequence analysis of *A. mellea* and *in silico* cDNA database construction and annotation.

3.1 Introduction

3.1.1 Sequencing

Although *A. mellea* is a virulent pathogen, little is known about it at a molecular level (Baumgartner *et al.*, 2011) and genome sequencing is a first step in addressing this deficiency. Whole genome sequencing enables analysis of an organism and comparison across different phyla. A core proteome can be deduced, to provide insight into processes and development of an organism, compared with organisms of the same or different phyla (François *et al.*, 2010; Fernandez-Fueyo *et al.*, 2012). Where an organism is newly sequenced, protein functions can be inferred through homology. Comparison with protein networks in other organisms can establish possible interaction partners in protein complexes. Bioinformatic analysis of protein domains permits the preliminary appraisal of the functions of novel sequences. Sequence data can be mined for compounds with biotechnological application, such as proteins with bioactive properties (e.g. antibiotic, cytotoxic or fibrinolytic), or industrial relevance (lignolytic or cellulolytic enzymes) (Arantes *et al.*, 2012).

Since high-throughput DNA sequencing has played a major part in revealing fungal genome data (Fitzpatrick *et al.*, 2006; Vanden Wymelenberg *et al.*, 2006; Kämper *et al.*, 2006; Srivatsan *et al.*, 2008; Martin *et al.*, 2008; Ohm *et al.*, 2010), particularly from basidiomycetes, and because it was deployed for exploration of the *A. mellea* genome, the evolution and principles of the technique will now be described. Sanger sequencing, or first generation sequencing technology, was developed in 1977. It is based on fragmentation of template DNA and synthesis of complementary DNA strands from denatured template DNA, which are terminated by a fluorescent dideoxynucleotide detectable by laser (Shendure and Ji, 2008). This sequencing method is accurate (99.999%) and fragment lengths are long (400-900 bp). However, its throughput is low (1.9 ~ 84 Kb/run) and the cost of sequencing is high ($2,400/million bases), making this type of sequencing prohibitively expensive and slow, although recent improvements have increased the rates of data output. Three high throughput sequencing systems, also known as next generation sequencing (NGS) systems were reviewed by Liu *et al.* (2012). The systems were the Roche 454 sequencer, the AB SOLiD system and the Illumina GA/HiSeq system. This review details the NGS systems, their advantages, disadvantages and relative costs. The difference between

these systems and the older Sanger sequencing technology is that in NGS, many fragments are sequenced at the same time, known as parallel sequencing, resulting in very high throughput (0.7-120 Gb/run), low cost ($0.7 - $10/million bases) DNA sequencing. The disadvantages of the NGS parallel processing systems are shorter read lengths (50 – 700 bp) and reduced accuracy (98 – 99.9 %). However, as sequencing is considerably cheaper using these methods, more coverage and repeat sequencing can be carried out.

Illumina sequencing begins by randomly fragmenting DNA by sonication. Exposed ends are repaired by addition of dNTPs, DNA polymerase and polynucleotide kinase, which produce blunt ended DNA with phosphorylated 5' ends, after which the 3' ends are adenylated. Adapters are then ligated to each end by addition of oligonucleotides to phosphorylated and adenylated DNA fragments (Figure 3.1) (Shendure and Ji, 2008). The adapters have PCR and sequencing primer annealing sites, as well as an index sequence. This index allows different samples to be pooled (Illumina Inc., 2012) and electrophoresis is then used to sort DNA fragments by size.

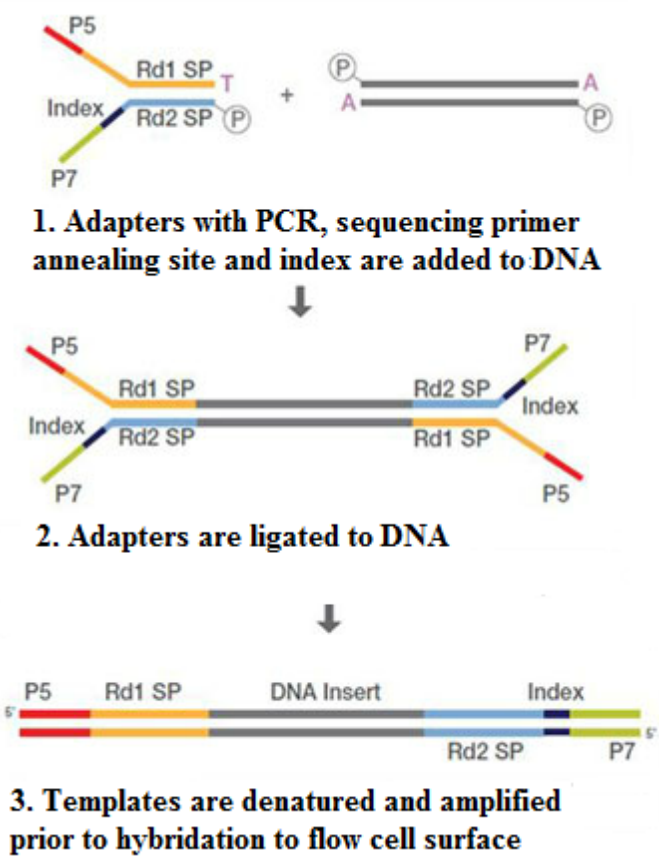

Figure 3.1. Template preparation for addition to a proprietary flow cell. Adapters with PCR, sequence primer annealing site and index sequences are ligated to DNA and

amplified. P5 oligo, red; P7 oligo, green; Rd1 sequencing primer site, yellow; Rd2 sequencing primer site, blue, Index, black; DNA, grey (Illumina Inc., 2011).

The template DNA fragments are denatured, and single stranded DNA templates added to an Illumina proprietary flow cell which has a carpet of oligos that bind the adapters, and consequently to the fragments of template DNA. These templates are duplicated by addition of unlabelled nucleotides and polymerase, and bind covalently to the flow cell surface. The templates are amplified to generate hundreds of millions of unique clusters through isothermal bridge amplication. The reverse strands, those attached to P5 oligos on the flow cell, are removed by washing, the template ends are blocked and DNA primers added to the templates (Illumina Inc., 2011; Ansorge, 2009).

Nucleotides modified with a chemically cleavable, specific reporter fluorophore for each of the four bases and a 3' hydroxyl modification, which acts as a reversible terminator are added to the flow cell with a polymerase adapted to accommodate these dNTP modifications. All four nucleotides are added at the same time and compete to bind to the template, thus complementary nucleotides are incorporated one at a time into the newly synthesised DNA and unincorporated nucleotides are washed away. A laser excites the fluorophores which emit at a wavelength specific to each base, thus identifying the newly added bases. This flow cell image is captured and the base added to each cluster determined. The 3'hydroxyl block and fluorescent label are removed chemically in preparation for the addition of the next base. Cycles of base incorporation, imaging and chemical cleavage follow until each DNA template has been sequenced (Figure 3.2 and Figure 3.3). Hundred of millions of clusters are sequenced in parallel, generating the very large datasets characteristic of Illumina sequencing (Shendure and Ji, 2008). A step-wise summary of this approach, known as sequencing by synthesis, is shown in Figure 3.2 and Figure 3.3.

Illumina sequencing is constrained by short read lengths, as more than one base can be incorporated, or the terminator may be defective and not block addition of bases (Dohm *et al.,* 2008; Voelkerding *et al.,* 2009). In both of these cases the sequence is out of phase with the other sequences in a cluster. A second error type where cleavage of either the terminator or the fluorescent moiety is not completed, generates signal decay or noise. As clusters are comprised of identical sequences, short reads are not problematic, but as reads become longer, errors accumulate, thus limiting read length. A read length of 150 bp has an error rate of less than 0.1% using this technology (Dohm *et al.*, 2008; Voelkerding *et al.,* 2009).

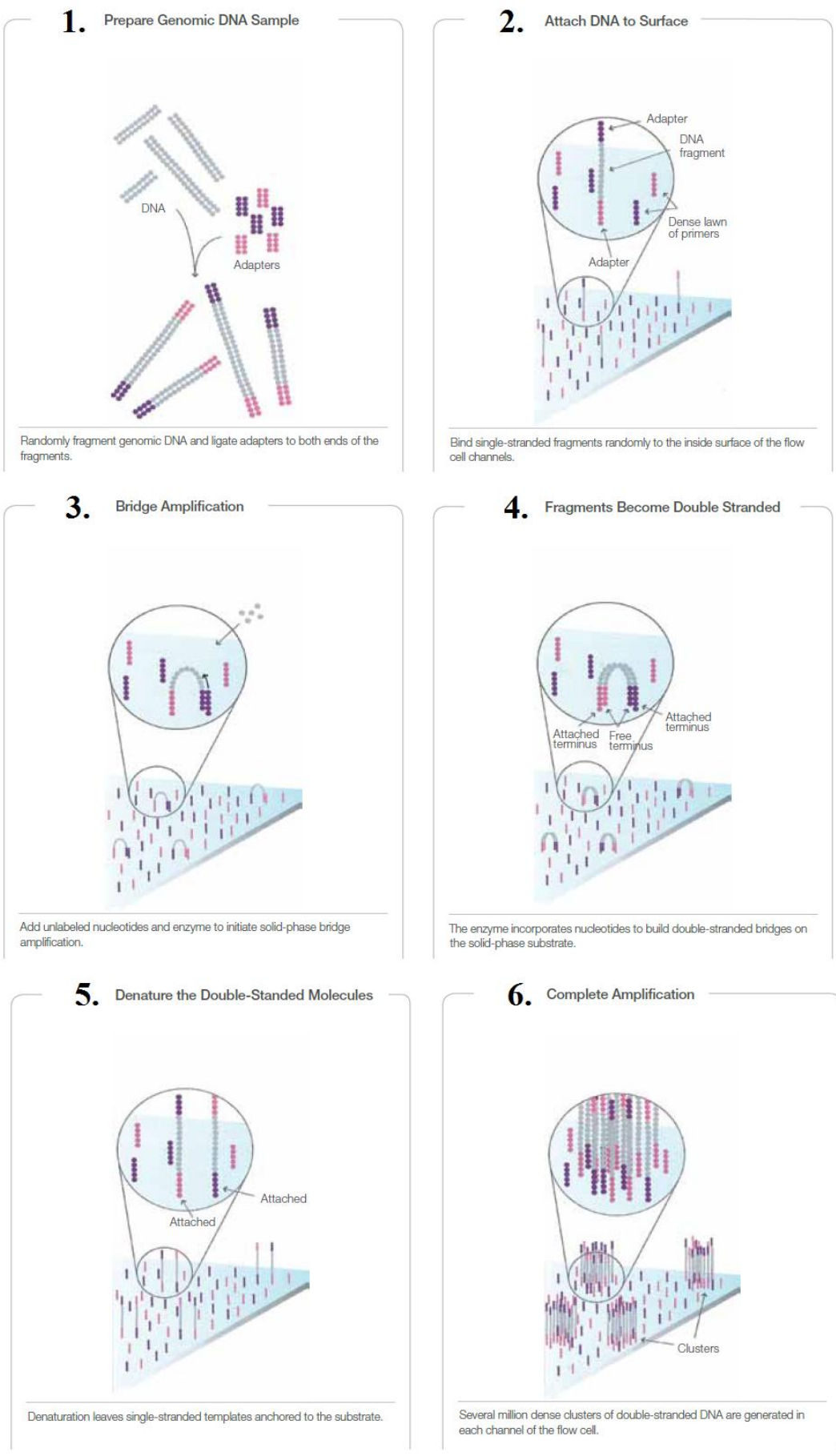

Figure 3.2. Illumina Sequencing, Steps 1- 6 (Illumina Inc., 2010).

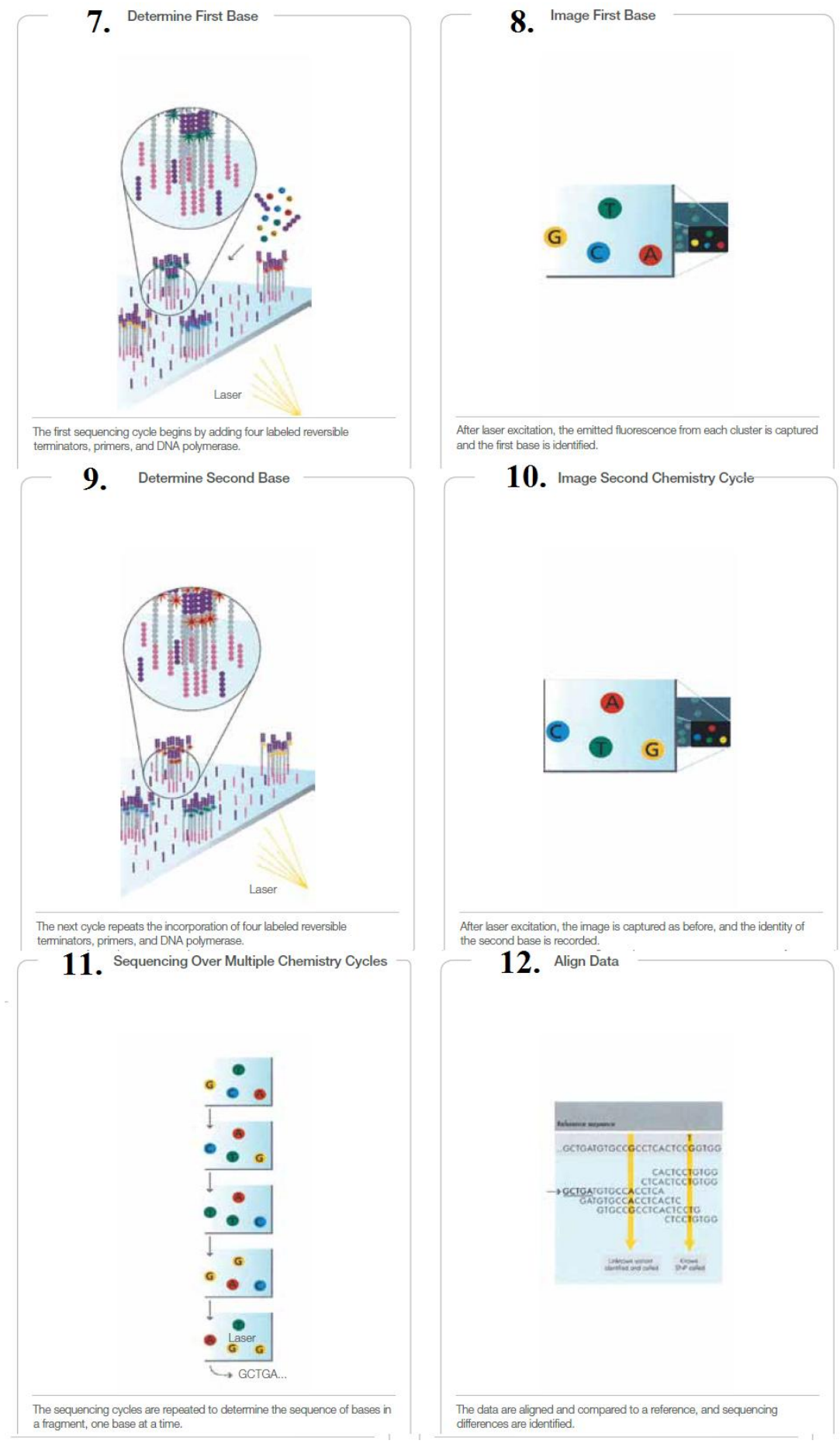

Figure 3.3. Illumina Sequencing, Steps 7-12 (Illumina Inc., 2010).

Millions of short sequence reads approximately 100 bp, are generated by NGS. These are aligned and assembly algorithms are used to compile the short read lengths into larger contiguous DNA sequences called contigs. Briefly, reads are aligned so that bases from one sequence overlap the same bases in another and thus contigs are built up from millions of overlapping reads, using bioinformatic software (Zerbino and Birney, 2008). Scaffolds are assembled from contig overlaps. A schematic of read alignment for contig assembly is shown in Figure 3.4. Where resequencing is being undertaken a reference genome may be used to align sequences (Illumina Inc., 2010) as shown in Figure 3.3 12, where the top line is the reference (purple) but in the case of *de novo* sequencing this is not an option.

Multiple assembly programs have been developed for NGS (Paszkiewicz and Studholme, 2010). Analysis of homopolymeric and repetitive sequences of short read length are problematic, although accurately sequenced, algorithims are required to assemble them into contigs.

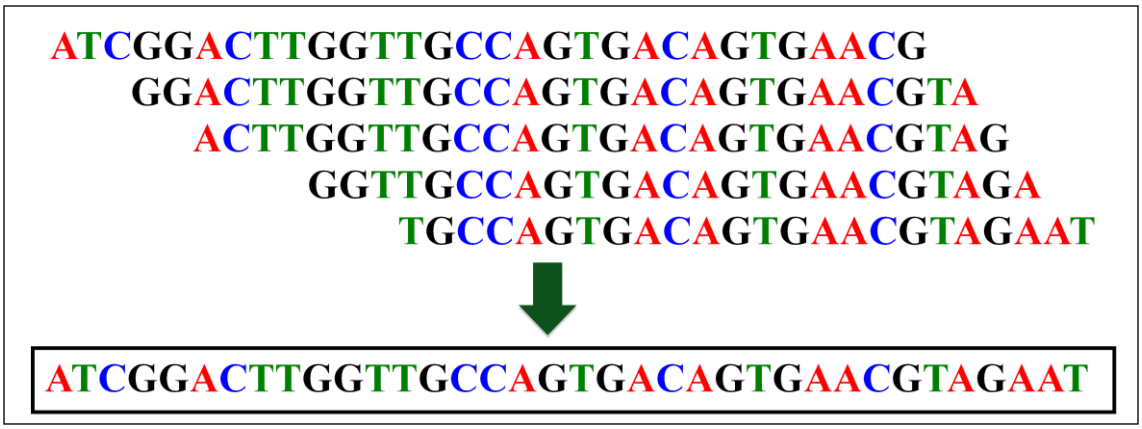

Figure 3.4. Schematic of read aligment and sequence assembly from sequencing reads.

On completion of this process contigs are subjected to interrogation by gene finding software, which searches the contigs for genes. AUGUSTUS was the program used in this study (Stanke and Waack, 2003). Mathematical models of biological signals such as translation start and stop sequences or splice sites are used by gene prediction software. Where *de novo* sequencing is undertaken, an already sequenced organism which might be expected to have a similar gene structure is used as a training set for mathematical models of gene structure in the organism being sequenced (Stanke and Waack, 2003). *Laccaria bicolor* was used in conjunction with AUGUSTUS software as a training set for *A. mellea* genome sequence annotation. Hidden Markov Models (HMM) are used to train software to recognise basidiomycete introns which may have

specific sequences or have similar lengths. Genomic data processing is then complete and a protein database is generated from genomic data. Genes and protein motifs from related organisms show general similarity, thus enabling genes and their structures to be deduced from newly sequenced data (Stanke and Waack, 2003).

3.1.2 Genome

The first basidiomycete genome sequence, that of *P. chrysosporium*, a white-rot fungus, presented difficulty in *ab initio* gene finding. Organisms from other kingdoms and phyla were used as comparative models to deduce homology, which was particularly difficult for more novel genes and approximately 10,000 genes were predicted (Martinez *et al.*, 2004). The genome of *L. bicolor* was sequenced in 2008 and was twice as big as that of *P. chrysosporium*, with approximately 20,000 genes. It lacked plant cell wall carbohydrate degrading enzymes which might have been expected in this fungus but retained the ability to degrade other polysaccharides, thus providing insight into the lifestyle of this symbiotic and saphrotrophic mycorrhizal fungus (Martin *et al.*, 2008).

Protein signature domains and motifs enable categorisation of proteins into families, and the number of protein families and the average number of proteins per family was shown to increase with the size of the genome (Martin *et al.*, 2008). Corresponding to sequencing technology acceleration, the number of sequenced organisms and accuracy of sequencing in recent years, bioinformatic and proteomic information has increased exponentially (Riffle and Eng, 2009). A recent study indicates that while the numbers of entries in the NCBI database since 2003 has remained fairly constant only about 50% of the entries in that build are represented in the current database, due to constant revision and updates (Sirota *et al.*, 2012). However Sirota *et al.* (2012), allude to the fact that a number of well studied proteins have been removed. Carbohydrate esterase (CE) family 10 proteins are one case in point, where the Carbohydrate-Active Enzymes site (www.cazy.org) no longer updates this class of protein as their activity is now known to be much broader that previously thought and this classification is obsolete, however a BLAST search still identifies proteins as CE10, but they cannot be annotated as a single functional class. Other databases such as IPS can be used to further identify protein domain signatures and motifs within their sequences enabling more accurate annotation.

It is against this background of rapidly developing technology, continuously emerging genome sequences and ever-changing data repositories, that the present work

was initiated. Given the importance of *A. mellea* as a plant pathogen, and dearth of knowledge regarding its biology and virulence, the objectives of the work presented in this chapter were:

1. To sequence and annotate the *A. mellea* genome, and construct an *in silico* cDNA database for detailed analysis, and subsequent proteomic investigations.
2. To undertake a phylogenetic analysis of *A. mellea* and to reveal its position, and near-relatives in the basidiomycete phyla.
3. To carry out a detailed bioinformatic analysis and survey of the *A. mellea* genome.
4. To identify, categorise and carry out a detailed bioinformatic analysis of the major protein families encoded by the predicted *A. mellea* cDNA database.
5. To illuminate that status of hypothetical and predicted proteins, in addition to detection of any *A. mellea*-specific proteins, encoded within the predicted *A. mellea* cDNA database.

3.2 Results

3.2.1 Sequencing and database setup

Illumina GA II sequencing system was used in this study, with read lengths of 76 bp which had a Q20 score, inferring 99% accuracy in base calling (Ewing and Green, 1998). NGS analysis of *A. mellea* DNA yielded 6.72 Gbp of sequence data. Nucleotide reads of k length (kmers) which overlap by k-1 nucleotides are used to assemble contigs (Zerbino and Birney, 2008). Kmers are shorter than sequence read lengths and 53 bp kmers were used in this study. VELVET, a program developed by Zerbino and Birney (2008), was used to assemble *A. mellea* contigs and results are shown in Table 3.1.

Table 3.1. Genome assembly statistics for *A. mellea* (Vahl:Fr) Kummer DSM 3731.

	Scaffolds	Contigs
N50	36,679 bp	5,485 bp
Largest	639,705 bp	154,911 bp
Count	4,377	15,215
Total Length	58,358,340 bp	71,738,977 bp

The initial genome assembly and corresponding *A. mellea* accession numbers is available from the following web address, http://armillariamellea.com/. *A. mellea* protein coding genes (n = 14473), with an average length of 1575 bp, had an average 1228 bp coding sequence length with average exon length of 218 bp, and on average 4.72 introns/gene. In the case of *A. mellea*, average intron length was found to be 73.62 bp. These data are comparable to the gene statistics from gene assembly data of two closely related fungi for which sequencing data is available (Table 3.2) (Martin *et al.*, 2008). A number of coding sequences (n = 957) were below the threshold for minimum gene length. The numbers of protein coding genes (n = 14473) is similar to that of *C. cinerea* (n = 13544) and somewhat lower than *L. bicolor* (n = 20614) (Table 3.2 and Figure 3.5) (Martin *et al.*, 2008). From these protein coding genes, nucleotide sequences were translated into their corresponding protein equivalents using an in-house perl program written by Dr. David Fitzpatrick. An *in silico* cDNA protein sequence database was thus generated in FASTA format and converted to a peptide sequence FASTA format database. Genes were numbered sequentially on contigs and corresponding proteins were given a unique numeric identifier, AmXXXXX.

Table 3.2. Gene statistics for *A. mellea* (Vahl:Fr) Kummer DSM 3731.

	A. mellea	*L. bicolor*	*C. cinerea*
Genome Assembly (Mb)	58.3	64.9	37.5
Number of protein-coding genes	14473	20614	13544
Coding sequence <300 bp	957	2191	838
Average gene length (bp)	1575	1533	1679
Average coding sequence length (bp)	1228	1134	1352
Average exon length	217.5	210.1	251
Average intron length	73.6	92.7	75
Average number of introns per gene	4.72	4.44	4.66

3.2.2 Phylogenetic supertree

A representative genome species tree consisted of 23 basidiomycete species and 2 ascomycete outgroups (Figure 3.6). In total, 8860 homologous gene families (containing 4 or more genes) were identified using a previously described randomised BlastP approach (Creevey *et al*., 2004, Fitzpatrick *et al*., 2006, Pisani *et al*., 2007). Gene families (n = 2,924) that failed the permutation tail probability (PTP) test (Archie, 1989; Fitzpatrick *et al*., 2006), were removed, leaving a dataset of 5,936 gene families. The number of gene families in *A. mellea* is considerably larger than the number of gene families in *C. cinera* and comparable to the number of families determined in *L. bicolor* (Martin *et al.*, 2008) (Figure 3.4).

Gene families were used to reconstruct supertrees using gene tree parsimony (Page, 1998; Slowinski and Page, 1999) implemented in the software DupTree version 1.48 (Wehe *et al.*, 2008). Figure 3.6 shows a basidiomycete supertree and the arrow indicates the position of *A. mellea* in the overall phylogenetic relationship.

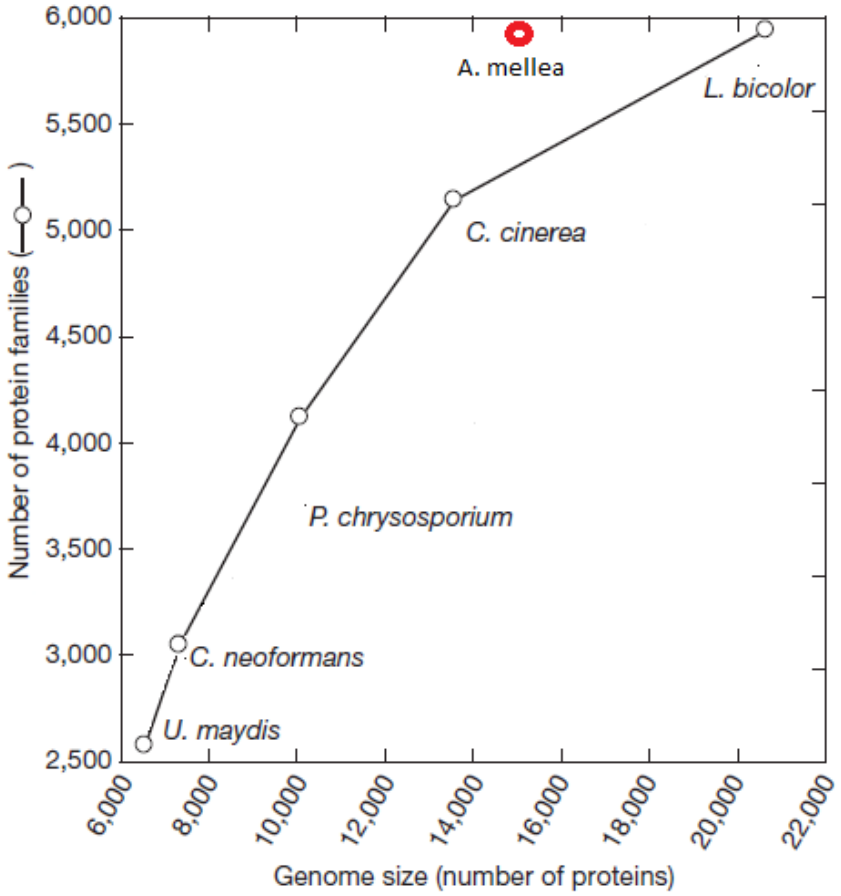

Figure 3.5. The number of protein families compared with numbers of protein coding genes in sequenced basidiomycete species (Adapted from Martin *et al*., 2008a). Number of *A. mellea* gene families shown is as a red circle. The number of A.mellea protein families is greater than expected given the genome size in comparison to other basidiomycetes.

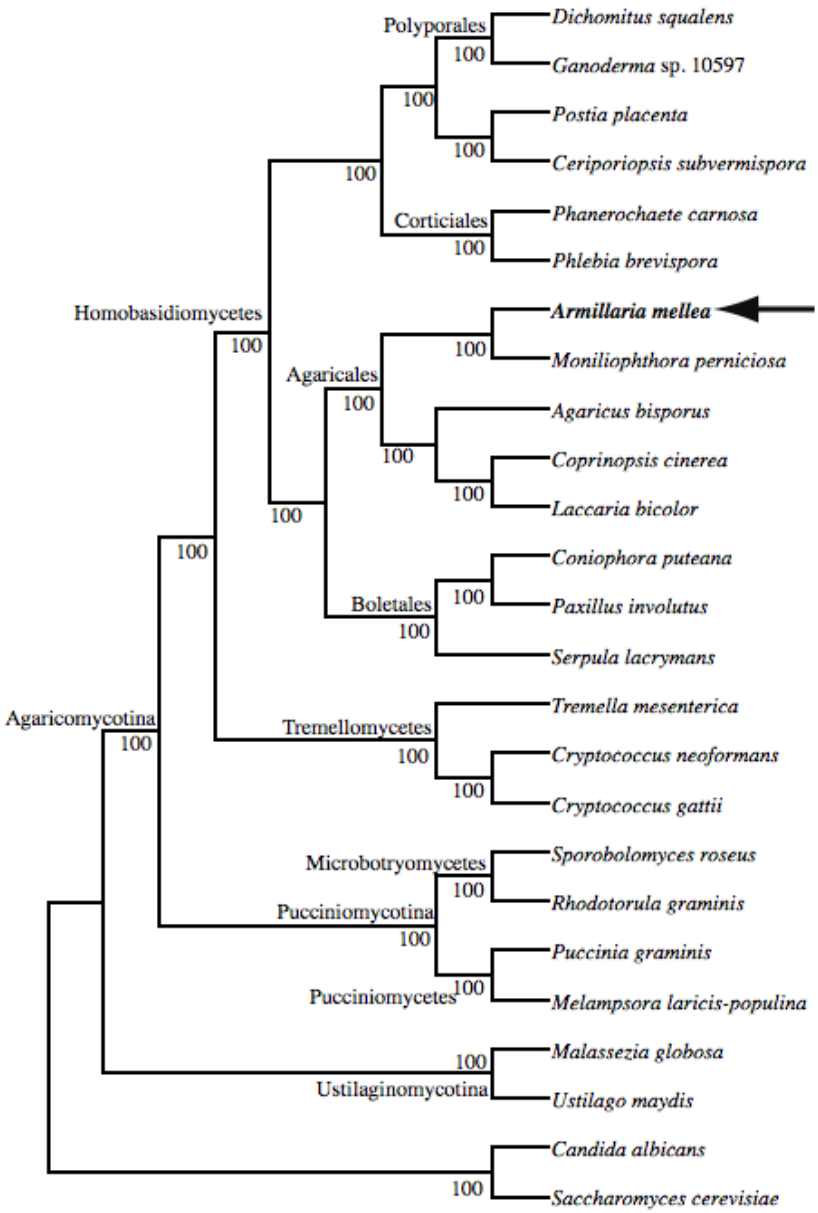

Figure 3.6. Basidiomycete phylogenetic supertree: Supertree is derived from 5,936 individual gene families. Basidiomycotina subphyla, class and orders are shown where applicable. Numbers along branches represent bootstrap support values. Two Ascomycete species (*Candida albicans* and *Saccharomyces cerevisiae*) have been chosen as an outgroup. Arrow indicates *A. mellea*.

3.2.3 Genome analysis and protein families

Analysis of the *A. mellea* genome has been undertaken using a range of bioinformatic and proteomic analysis tools, to identify all proteins encoded by the genome. As little *A. mellea* genomic and proteomic data has been published to date, homologous sequence information from other organisms was used to annotate the genome. Information which is publicly available include databases whose information is specific to particular types of protein (www.cazy.org) (Lombard *et al.*, 2010; Henrissat and Bairoch, 1993; Henrissat, 1991; Coutinho *et al.*, 2003; Cantarel *et al.*, 2009), to domain specific protein signature prediction (http://www.ebi.ac.uk/interpro) (Hunter *et al.*, 2012) or structural information which has been experimentally determined (http://www.rcsb.org) in other organisms. Cross-linked database information such as that retrieved by Blast2GO (B2G) (Conesa *et al.*, 2005), whereby all information pertaining to an individual protein taken from many different databases such as CAZy, the IUBMB Enzyme Nomenclature list, enzyme codes and KEGG pathway mapping may be viewed in tabular format and is invaluable in genome annotation.

The *in silico A. mellea* cDNA protein database was initially analysed using B2G (Conesa *et al.*, 2005) and data mining tools were used to visualise results in graphical format. B2G, a program which combines searches from different databases, initially interrogates the NCBInr database with sequences. *De novo* sequences are annotated by searching the NCBInr database (http://blast.ncbi.nlm.nih.gov) for homologous sequences. Conserved sequences within phyla will return annotation, however, for a newly sequenced organism such as *A. mellea*, less conserved sequences exhibit no BLAST homology. Figure 3.7A shows a breakdown of BLAST annotation: functional annotation, hypothetical proteins, predicted proteins and *A. mellea* specific proteins were 59%, 16%, 6% and 19%, respectively. Gene Ontology (GO) (http://www.geneontology.org/), from organisms sequenced *de novo* is less than from organisms which have already been sequenced, but complete genes are not necessary to identify attributes of (i) molecular function, (ii) biological process or (iii) cellular component associated with a sequence as illustrated in Figure 3.7B, where 57% of *A. mellea* proteins had GO annotation. IPS combines a number of protein recognition resources into a single tool, based on recognition of conserved protein domain signatures and motifs (Zdobnov and Apweiler, 2001) and Figure 3.7C illustrates IPS annotation percentages where only 8% of proteins did not have any annotation. Figure 3.7 illustrates the genome annotation percentages obtained from the three different

search methods. More proteins were annotated using IPS search, as thirteen discrete databases are searched for homology, protein motifs, protein fingerprints, signal sequences and mathematical protein models, thus parts of proteins can used to infer functionality (Zdobnov and Apweiler, 2001; Hunter *et al.*, 2012; Mulder and Apweiler, 2008) (Figure 3.7).

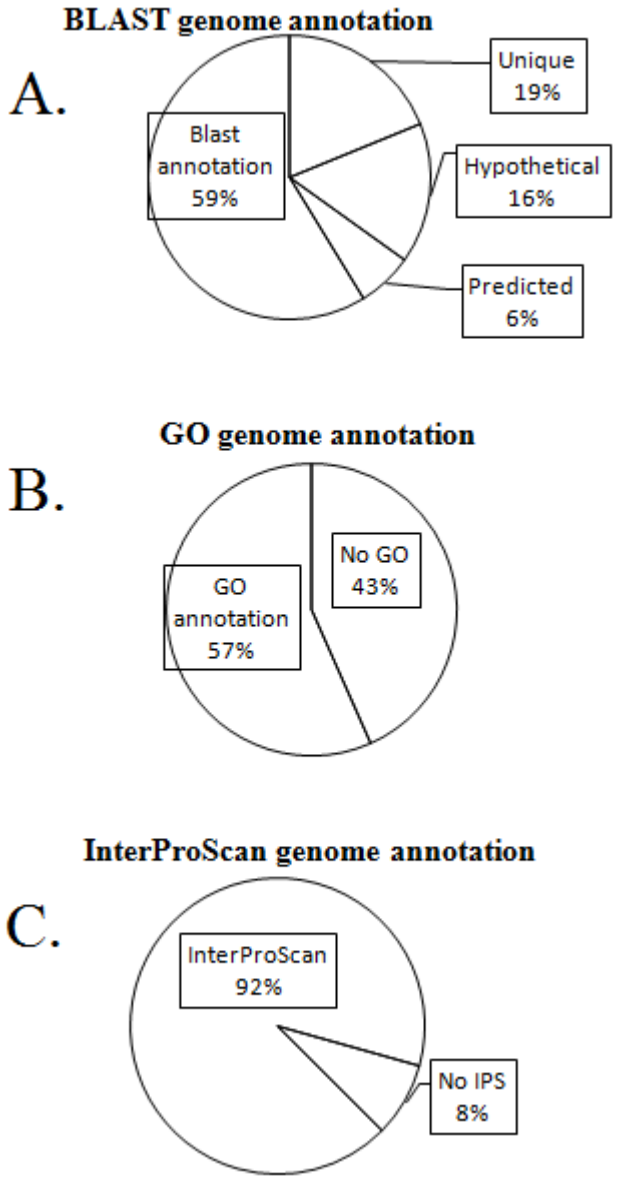

Figure 3.7. Genome analysis by Blast2GO annotation of *A. mellea* protein database. **A.** BLAST annotation: Protein sequences homologous to proteins with known functions 59%; Proteins homologous to proteins whose function have been predicted *in silico* and are "hypothetical" (16%); Proteins "predicted" from *in silico* analysis of ORF (6%), as well as *A. mellea*-specific proteins (19%). **B.** Gene ontology (GO) annotation: Proteins with GO in molecular function, biological process or cellular component 57%; Proteins

with no GO 43%. **C.** InterProScan (IPS) annotation: Proteins for which a domain signature or motif annotation was returned: 92%; Proteins with no IPS annotation: 8%.

3.2.3.1 Survey of *A. mellea* proteins

A. mellea cDNA data analysed by B2G was categorised by biological process, cellular component and molecular function to give an overview of broad protein categories. One feature of B2G analysis is generation of combined graphs for large datasets of complex data. These are directed acyclic graphs (DAG), which use GO annotation of sequences to determine molecular function, biological process and cellular component for sequences where these exist. These graphs are hierarchical and enable visualisation of complicated data by GO term association of sequences. Nodes which represent a GO term are generated and node scores are determined from the number of sequences associated with that term, moreover, colour intensity of nodes with high scores aids visualisation (Figure 3.8). From these DAG, more simplified multilevel graphs which show the statistical representation of genes from the lowest category at each node may be generated. The number of sequences belonging to a category is shown graphically (Conesa and Gotz, 2009). These visual outputs do not show all of the sequences in the dataset, as they would have too many components, rather, they give an overview of sequence distribution.

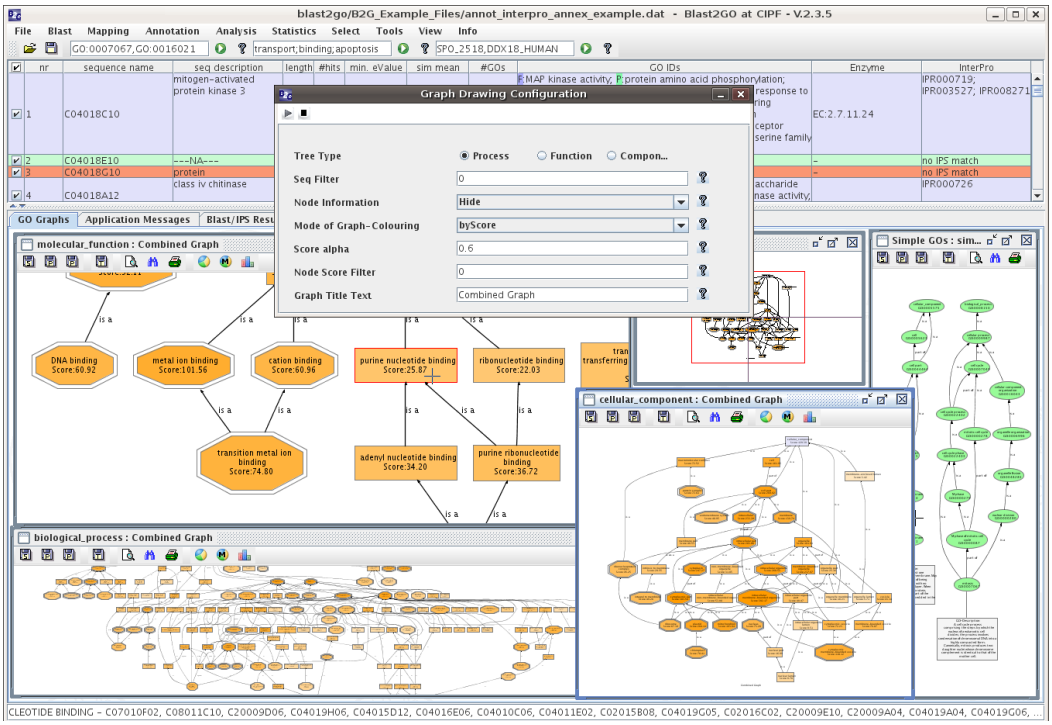

Figure 3.8. Combined graph screenshot of Blast2GO (Conesa and Gotz, 2009).

The largest proportions of *A. mellea* genes categorised by biological process (Figure 3.9), was DNA metabolic process (*n* = 1142). Research Collaboratory for Structural Bioinformatics protein data bank (RCSB – PDB, http://www.rcsb.org/pdb/home/, accessed 22.09.2012), lists 1606 different eukaryotic proteins associated with DNA metabolic process, the majority of which are transferases, but include hydrolases, lyases and oxidoreductases. *A. mellea* has representation in 71% of proteins in this category, indicating that these are highly conserved proteins. Processes involve DNA replication, repair, recombination and structure. As a proportion of all genes involved in biological processes, this category almost outweighs the next three categories: catabolism (*n* = 594), carbohydrate metabolism (*n* = 388) and protein modification (*n* = 376) together. This signifies the importance DNA processing to the organism as it supercedes the energy production and growth together. Protein modification genes (*n* = 376) are more numerous than amino acid metabolism (*n*= 319), indicating the importance of post-translational modifications (PTMs) in the organism. Cell signalling (*n* = 230) and regulation of downstream cellular process is next most important category. Transcription of DNA prior to protein synthesis and relevant genes (*n* = 217), is the next most abundant category. Lipid process genes (*n* = 197) encoding proteins which catalyse reactions and pathways involving hydrophobic molecules including fatty acids, sterols and glycerolipids functioning as cell membranes, energy storage and signalling molecules form the next most substantial class. Gene ontology for response to stress (*n* = 179) is next in rank, followed by ion transport (*n* = 122) and generation of precursor metabolites with the liberation of energy (*n* = 98). The smaller categories of bioprocess proteins are shown in Figure 3.9.

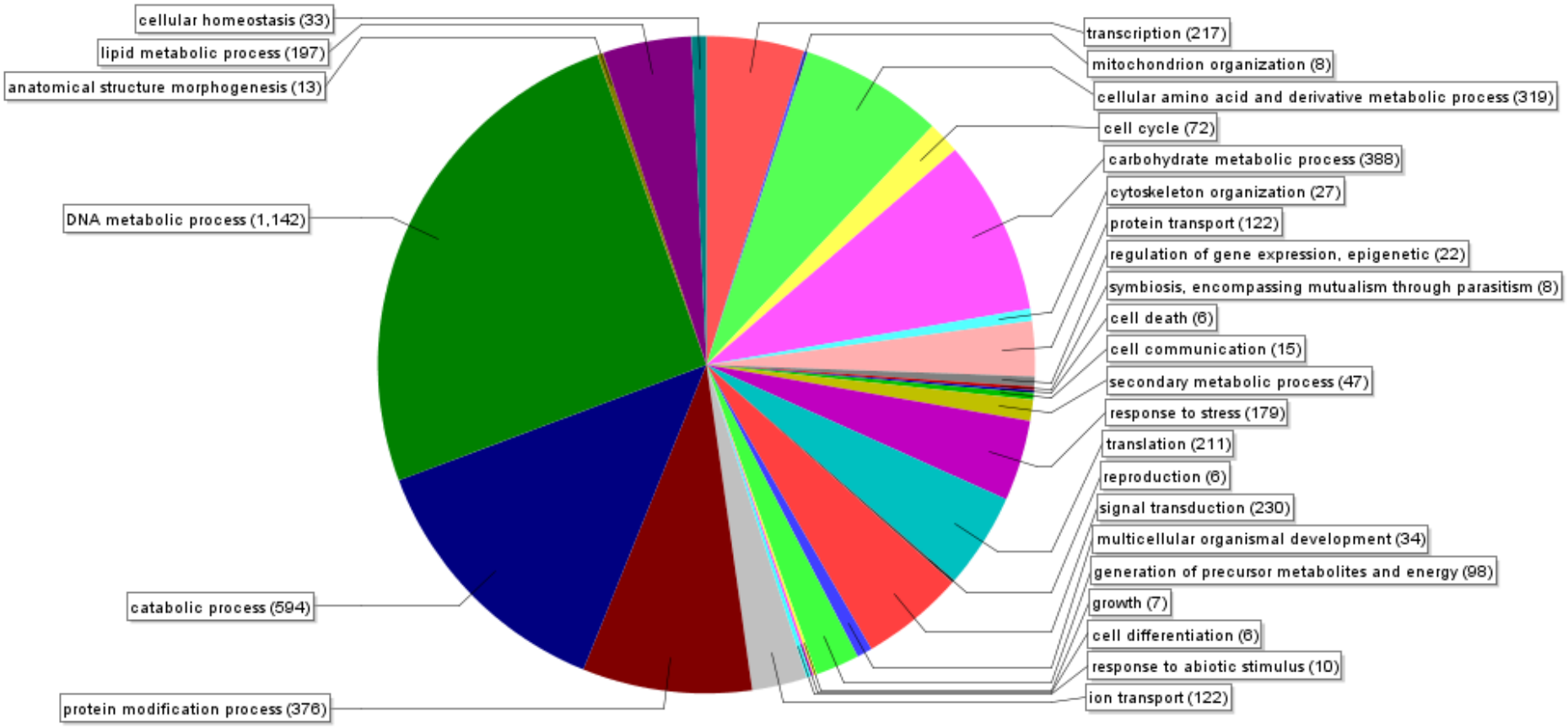

Figure 3.9. Biological process. GO multilevel representation of all proteins from the *A. mellea* cDNA database identified following Blast2GO annotation; identification of biological process property domains defined by http://www.geneontology.org. GO annotation from the lowest nodes of GO hierarchy in the category of molecular function is shown. Numbers in brackets indicate the number of proteins in each category.

A view of the genome cellular component classes (Figure 3.10) shows protein complexes (n = 403) as the largest class of cellular components. Ribosome proteins are the next most significant class. Proteins in the nucleoplasm form the next category (n = 112). Mitochondrial proteins (n = 100) have almost the same number as nuclear proteins signifying the importance of these proteins. Cytosolic proteins (n = 95) were lower than the previous categories and comprised 8 % of the total. The endoplasmic reticulum (ER) (n = 61) protein functions range from transport to chaperones and hydrolases. Nucleolar proteins (n = 42) which comprise those involved in DNA and RNA processing, cell cycle and cytoskeleton proteins are represented. Golgi apparatus proteins (n = 41) for processing, sorting and transporting proteins is the next most numerous class. A RCSB - PDB search for Golgi lists proteins with such diverse functions as lipid and peptide binding, transport and membrane proteins. Smaller classes of cellular component can be seen in Figure 3.10.

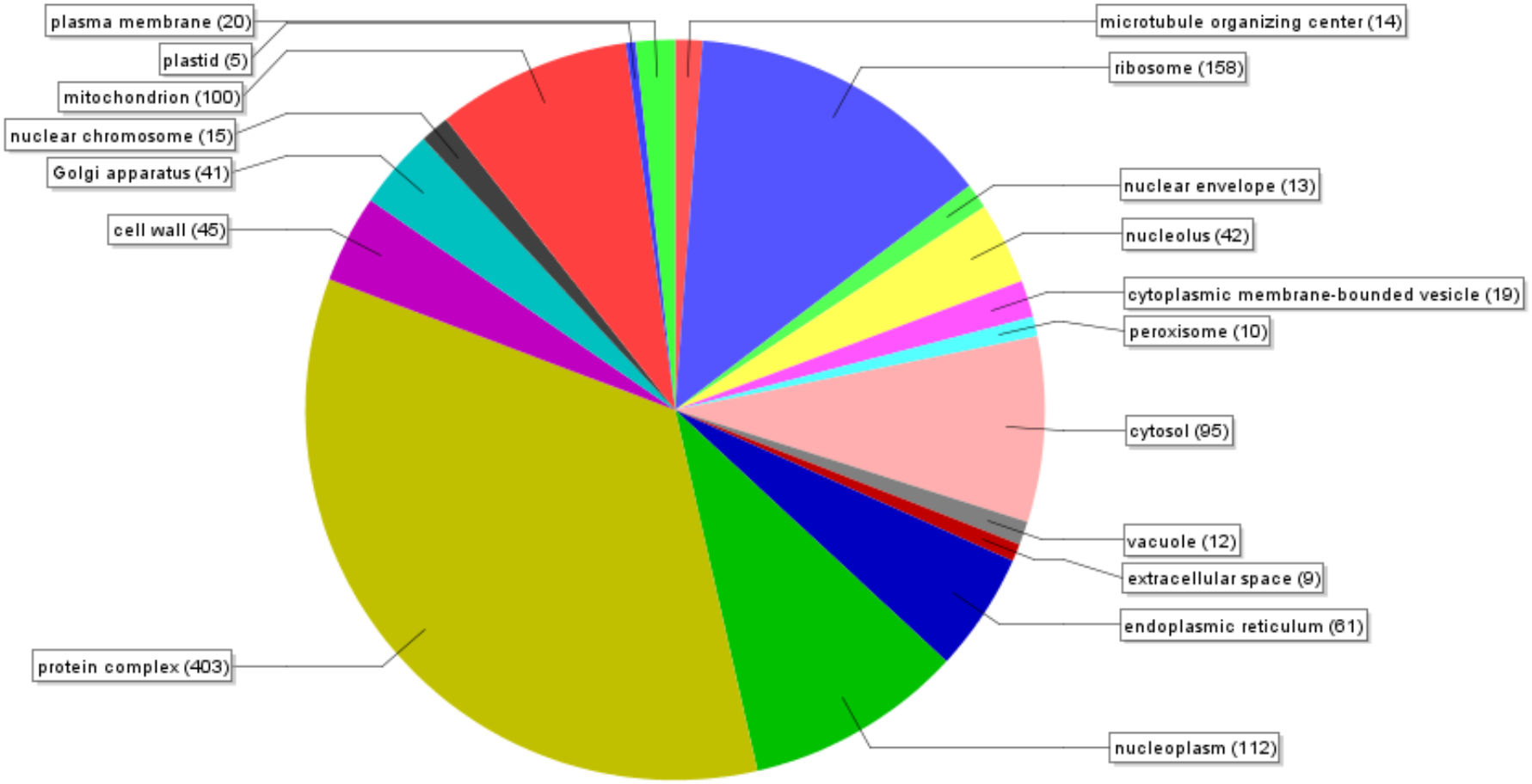

Figure 3.10. Cellular component. GO multilevel representation of all proteins from the *A. mellea* cDNA database identified following Blast2GO annotation; identification of cellular component property domains defined by http://www.geneontology.org. GO annotation from the lowest nodes of GO hierarchy in the category of molecular function is shown. Numbers in brackets indicate the number of proteins in each category.

A. mellea nucleotide binding proteins (*n* = 1206), are the most abundant class categorised by molecular function (Figure 3.11). This corresponds with the numbers in the DNA metabolic process genes in the biological process data (Figure 3.9). RCSB – PDB search of these proteins lists 2761 eukaryotic proteins in this category, which denotes that *A. mellea* is represented in 44% of proteins in this class. Taken together with the next most abundant group, RNA binding (*n* = 649), they account for a very large proportion of all molecular functions. These proteins are diverse and complex and form macromolecules that regulate transcription, translation, replication and modification of nucleic acids.

Electron carrier activity proteins (*n* = 314), are generally membrane bound, metal-containing proteins such as cytochrome C or flavoproteins accepting or donating electrons. They are involved in a broad range of molecular functions, cellular respiration, redox signalling and proteosome activity. Protein kinases (*n* = 229) are involved in signalling and regulating protein activity (Hamel *et al.*, 2012). Histone modification, cell cycle and stress signalling are some of the molecular functions of this group as classified by AmiGO, the GO browser and search engine (http://amigo.geneontology.org/). The structural molecule (*n* = 164), molecular function category includes such proteins as extracellular matrix structures, protein complex scaffolds, structural constituents of chromatin and ribosomes. AmiGO defines carbohydrate binding (*n* = 45) molecular function proteins as non-covalently binding and interacting selectively with carbohydrate moieties and AmiGO lists 6591 protein products conforming to this description, which include oligosaccharide, disaccharide and monosaccharide binding.

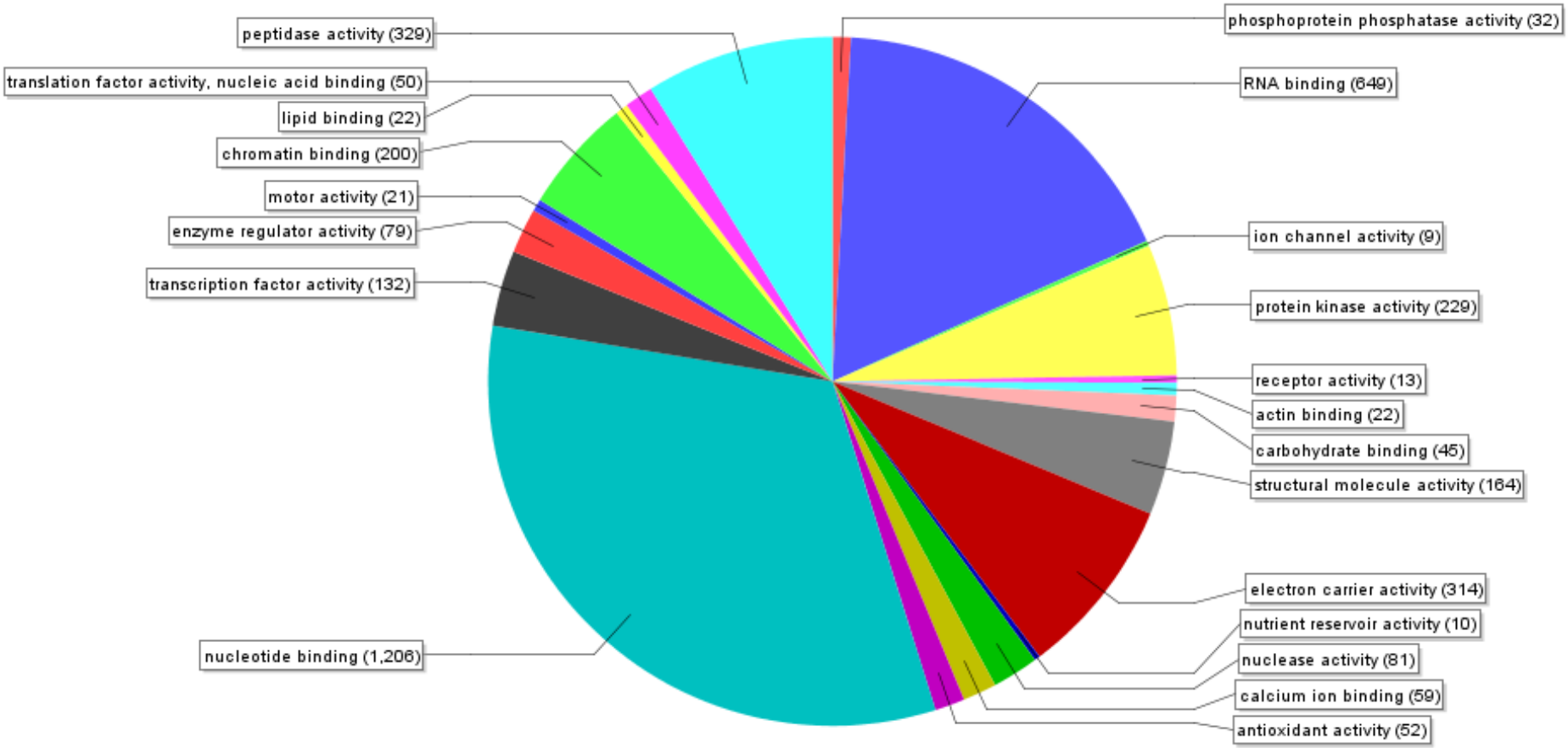

Figure 3.11. Molecular function. GO multilevel representation of all proteins from the *A. mellea* cDNA database identified following Blast2GO annotation; identification of molecular function property domains defined by http://www.geneontology.org. GO annotation from the lowest nodes of GO hierarchy in the category of molecular function is shown. Numbers in brackets indicate the number of proteins in each category.

A subset of proteins in the protein database which Blast2GO annotated as containing PFAM domains (http://pfam.sanger.ac.uk/; (Punta *et al.*, 2012) (*n* = 475) was surveyed and analysed. These included proteins determined by BLAST search to be *A. mellea* specific genes (*n* = 4), hypothetical (*n* = 56), predicted (*n* = 24) and proteins whose sole annotation were topological features (*n* = 130). This enabled a more specific analysis of proteins with functional regions than those identified by GO. There were twenty-seven PFAM functional domains which had more than 3 genes associated with a particular function (Table 3.3). The most abundant were F-box like domains (*n* = 119). Alpha-beta hydrolase folds 5 and 6 had seventy-two domains and ankyrin repeats twenty-eight.

Table 3.3. Summary of PFAM domains with annotation of greater than 3 genes showing numbers of *A. mellea* genes attributed to each domain.

Pfam Code	**Pfam Description**	***A. mellea* genes**
PF12937	F-box-like	119
PF12697	Alpha/beta hydrolase fold 6	67
PF12796	Ankyrin repeat	28
PF12706	Beta-lactamase superfamily domain	13
PF12710	Haloacid dehalogenase-like hydrolase	11
PF12874	Zinc-finger of C2H2 type	9
PF05729	NACHT domain	8
PF11895	Domain of unknown function (DUF3415)	8
PF06330	Trichodiene synthase (TRI5)	7
PF11790	Glycosyl hydrolase catalytic core	7
PF12770	CHAT domain	7
PF04193	PQ loop repeat	5
PF07691	PA14 domain	5
PF12695	Alpha/beta hydrolase fold 5	5
PF12799	Leucine-rich repeat	5
PF00637	Region in Clathrin and VPS	4
PF12708	Pectate lyase superfamily protein	4
PF02114	Phosducin	3
PF07534	Top-level domain (TLD)	3
PF10433	Mono-functional DNA-alkylating methyl methanesulfonate N-term	3
PF11700	Vacuole effluxer Atg22 like	3

Pfam Code	Pfam Description	*A. mellea* genes
PF11717	RNA binding activity-knot of a chromodomain	3
PF12352	Snare region anchored in the vesicle membrane C-terminus	3
PF12763	Cytoskeletal-regulatory complex EF hand	3
PF12783	Guanine nucleotide exchange factor in Golgi transport N-terminal	3
PF12848	ATP-binding domain of ABC transporters	3
PF12998	Inhibitor of growth proteins N-terminal histone-binding	3

3.2.3.2 Carbohydrate Active Enzymes (CAZy)

A survey of the *A. mellea* genome against the **C**arbohydrate **A**ctive En**Zy**me (CAZy) database was carried out (http://www.cazy.org; Cantarel *et al.*, 2009) and the data compiled into families (Table 3.4) (*A. mellea* accession numbers in accompanying CD file Seq_BLAST_IPS.xlsx). Interrogation of the CAZy database with sequences from the *A. mellea* cDNA database returned hits (n = 442) against proteins in the CAZy database. Further analysis by Center for Biological Sequence analysis (CBS) prediction server (http://www.cbs.dtu.dk) SignalP, identified 172 of these with classical secretion signals, of which 53 contained transmembrane regions. Prediction by TargetP targeted six of these to the mitochondrial membrane. Analysis by CBS SecretomeP identified proteins (n = 168) with non-classical secretion signals.

CAZy analysis of the genome followed by a comparative analysis of plant cell wall (PCW) degrading enzymes in *A. mellea* and other fungi with sequenced genomes was performed (Amselem *et al.*, 2011; Fernandez-Fueyo *et al.*, 2012; Martin *et al.*, 2008). When compared with other basidomycetes, shown in Table 3.5, *A. mellea* has 27% more PCW-degrading CAZys than average for this dataset while it has 1% more PCW-degrading CAZy than the average ascomycete, thus *A. mellea* has a CAZy enzyme array characteristic of both ascomycetes and basidiomycetes (Table 3.5). The number of *A. mellea* carbohydrate esterases was almost twice that of *C. cinerea*, a basidiomycete, the fungus with next highest abundance. The numbers of glycosyl transferases and pectin lyases both showed closer similarity to Ascomycetes, which are cellulose and pectin degrading, and do not degrade wood. Numbers of Glycoside Hydrolases (GHs) were comparable with fungi from both basidiomycete and ascomycete phyla. The number of *A. mellea* GH genes (n = 223) show greater similarity

to ascomycetes than to basidiomycetes as can be seen in Table 3.5. Among basidiomycetes *Schizophyllum commune* (*n* = 236) possessed more GH enzymes than *A. mellea*.

Table 3.4. CAZy annotation of *A. mellea* genome carbohydrate active enzymes. http://www.cazy.org (Cantarel *et al.*, 2009).

Carbohydrate Binding Modules									**Total**
Family	CBM1	CBM13	CBM21	CBM48	CBM48/GH13	CBM5/CBM12/GH18	CBM50		**7**
Number	3	4	2	1	1	1	3		**15**
Carbohydrate Esterases									**Total**
Family	CE1	CE4	CE8	CE9	CE9/GH128	CE10	CE10/GH1	CE14	**8**
Number	5	16	9	11	1	54	1	1	**98**
Glycoside Hydrolases									**Total**
Family	GH1	GH2	GH3	GH3/CBM1	GH5	GH6	GH6/CBM1	GH7	
Number	8	1	16	1	7	1	1	4	
Family	GH9	GH10	GH11	GH12	GH13	GH13/CBM20	GH15	GH15/CBM20	
Number	1	6	2	4	7	2	3	2	
Family	GH16	GH18	GH20	GH23	GH25	GH27	GH28	GH29	
Number	16	10	2	1	1	5	17	3	
Family	GH30	GH31	GH35	GH37	GH38	GH43	GH47	GH51	
Number	2	5	7	3	1	5	11	3	
Family	GH53	GH61	GH61/CBM1	GH63	GH71	GH72/CBM43	GH75	GH76	
Number	2	21	1	1	7	1	2	4	
Family	GH78	GH85	GH88	GH92	GH109	GH125	GH127	GH128	**48**
Number	1	1	3	4	8	1	2	6	**223**

Glycosyltransferases									**Total**
Family	GT2	GT3	GT4	GT4/GH13/GT5	GT8	GT15	GT17	GT20	
Number	38	1	7	1	3	5	1	4	
Family	GT22	GT24	GT28	GT32	GT35	GT39	GT48	GT49	
Number	1	1	1	2	2	4	2	1	
Family	GT50	GT57	GT58	GT59	GT61	GT66	GT69		**23**
Number	1	1	1	1	7	1	4		**90**
[a]Polysaccharide Lyases									**Total**
Family	[b]PL1	PL3	PL5	PL8					**[d]4**
Number	[c]5	8	2	3					**[e]18**

CAZy are families grouped according to structural domain and module similarity. Genes are grouped into CAZy classes and further subcategorised by family. Below each family is shown with the number of *A. mellea* genes encoding for each family. Totals represent the number of families and proteins in each class.[a]Protein class, polysaccharide lyase. [b]PL1, olysaccharide lyase family 1. [c]Number of *A. mellea* genes identified as belonging to polysaccharide lyase family 1 (n = 5). [d]Total number of polysaccharide lyase families identified from the protein database (n = 4). [e]Total number of *A. mellea* polysaccharide lyase proteins identified from the database (n = 18).

Table 3.5. *A. mellea* plant cell wall degrading enzymes compared with other fungi

Organism	Phylum	Attributes	[a]CE	[b]CBM	[c]GH	[d]GT	[e]PL	[f]EXPN
***Armillaria Mellea* (Vahl:Fr) Kummer DSM3731**	**Basidiomycete**	**Necrotroph/White rot -lignin**	**98**	**15**	**223**	**90**	**18**	**20**
Ceriporiopsis subvermispora	Basidiomycete	Non-phytopathogenic White rot -lignin	16	37	170	67	6	11
Coprinopsis cinerea Okayama 7 (#130)	Basidiomycete	Non-phytopathogenic	51	89	211	71	13	15
Laccaria bicolor S238N-H82	Basidiomycete	Mycorrhizal	19	26	163	88	7	12
Phanerochaete chrysosporium	Basidiomycete	Non-phytopathogenic White rot -lignin	17	48	177	66	4	11
Schizophyllum commune H4-8	Basidiomycete	Non-phytopathogenic White Rot-lignin	30	30	236	75	16	19
Postia placenta Mad-698-R	Basidiomycete	Non-phytopathogenic Brown Rot - cellulose	18	20	145	71	8	13
Aspergillus nidulans FGSC A4	Ascomycete	Non-phytopathogenic Model organism	31	41	251	92	21	1
Aspergillus niger CBS 513.88	Ascomycete	Necrotrophic	24	40	243	111	8	1
Podospora anserina S mat+	Ascomycete	Non-phytopathogenic Model organism	41	97	226	86	7	2

[a]CE carbohydrate esterase; [b]CBM carbohydrate binding module; [c]GH glycoside hydrolase; [d]GT glycosyl transferase; [e]PL pectin lyase; [f]EXPN expansins. *A. mellea* data is bold. Highlighted in yellow is the organism with the highest occurrence of this class of enzyme (Fernandez-Fueyo *et al.*, 2012; Martin *et al.*, 2008).

3.2.3.3 Glycoside hydrolases (GH)

Glycoside hydrolases degrade and modify cell wall components such as chitin, cellulose and pectin, with activity against the cell walls of fungi, plants and bacteria (van den Brink and de Vries, 2011). Glycoside hydrolases were the major group of CAZys (n = 223) and families (n = 48). A breakdown of the activities of *A. mellea* glycoside hydrolases and their associated families is shown in Table 3.6, (*A. mellea* accession numbers in accompanying CD file Seq_BLAST_IPS.xlsx). Protein families with differential abundance in the *A. mellea* genome compared with other fungi include a number of GH enzyme families. *A. mellea* had greater abundance of GH1 family (n = 8) than any of the comparative species in Table 3.5. GH3 family are β-glucosidases and degrade cellulose. *A. mellea* GH3 enzymes (n=17) are more numerous than in other basidiomycetes, for example, the white rot fungus *P. chrysosporium* in comparison has eleven (Table 3.5). GH15 a glucoamylase family *A. mellea* (n = 5), hydrolyses glucose polysaccharides such as starch, to glucose monomers. It has been widely described and characterised in bacteria and eukaryotes (Janeček *et al.*, 2011; van den Brink and de Vries, 2011). The number of GH15 family genes in *A. mellea* is greater than all other fungi in Table 3.5. GH27 family are multifunctional enzymes with arabinopyranosidase and galactopyranosidase activity (Sakamoto *et al.*, 2010), and are implicated in stress resistance and cell wall integrity (West *et al.*, 2009). Pectolytic enzymes would be expected to be more numerous in ascomycetes than basidiomycetes, but the *A. mellea* genome encodes more than twice the number of GH28 enzymes than any other basidiomycete listed in Table 3.5. GH28 enzymes showed correlation between the number of duplications in a genome and pathogenicity, in a 69 species comparison of non-pathogenic and biotrophic fungi which have fewer GH28 genes, with necrotrophic species which have greatly increased numbers (Sprockett *et al.*, 2011). The only fungus from Table 3.5 possessing more GH28 genes than *A. mellea* (n = 17) is *A. niger* which has n = 21 while other fungi in have an average of five GH28 enzymes. This observation supports the findings of Sprockett *et al.* (2011), as *A. mellea* is a virulent pathogen. Harris *et al.* (2010) showed that GH61 family has negligible hydrolase activity in fungi, but that GH61, in the presence of divalent metal ions, increased the lignocellulytic enzyme activity of other glycoside hydrolases, twofold. GH61 genes are highly abundant in *A. mellea*. In biofuel production, cocktails of enzymes are required to breakdown lignocellulose. In view the abundance of GH enzymes in *A. mellea*, it may be suitable as a single source of enzymes for biofuel production as it not only has abundant GH61 family enzymes, but also has many lignocellulytic enzymes. *A. mellea*

GH75 chitosanase (Am10471 and Am7009), identified in bacteria and ascomycetes but not to date in basidiomycetes, cleaves β-1,4 linkages between D-glucosamine residues of partly acetylated chitosan. During fungal growth, cell walls are continuously repaired and reconstructed by chitinases and chitosanases (Baker and Specht, 2009). *A. mellea* GH109 family, α-*N*-acetylgalactosaminidase has to date only been identified in prokaryotic exoglycosidases possesses an unusual mechanism using NAD^+ in a manner indicative of an oxidoreductase, but not requiring a divalent metal ion. The enzyme was characterised by Liu *et al.* (2007) in *Elizabethkingia meningosepticum.* A biotechnological application of this unique activity which cleaves GalNac, is synthesis of universal red blood cells from A and AB blood groups. GalNac is the A antigenic moiety of blood groups A and AB and enzymatic cleavage of this enabled Liu *et al.* (2007) to convert group A blood type to group O blood type.

Table 3.6. *A. mellea* glycoside hydrolase activities and associated families.

Uni-Prot/CAZy	**GH Family**	**No. genes**
α-1,6-mannanase	GH76	4
α-amylases,cyclomaltodextrin glucanotransferase	GH13	9
α-galactosidases, α-*N*-acetylgalactosaminidases, isomalto-dextranases	GH27	5
α-glucosidase; α glucoamylase; sucrase-isomaltases; α-xylosidase	GH31	5
α-L-arabinofuranosidases; endoglucanase	GH51	3
α-L-fucosidases; α-1,3/1,4-L-fucosidase	GH29	3
α-L-iduronidases; β-xylosidases; β-1,3-xylosidase; α-L-arabinofuranosidase; arabinanase; xylanase; galactan 1,3-β-galactosidase	GH43	5
α-L-rhamnosidase	GH78	1
α-mannosidases	GH47	11
α-mannosidases; mannosyl-oligosaccharide α-1,3-1,6-mannosidase; mannosyl-oligosaccharide α-1,3-mannosidase	GH38	1
α-*N*-acetylgalactosaminidase	GH109	8
β-1,3-glucanase	GH128	6
β-1,3-glucanosyltransglycosylase	GH72	1
β-galactosidases	GH2	1
β-galactosidases exo-β-glucosaminidase; exo-β1,4-galactanase	GH35	7
β-glucanases, xyloglucan:xyloglucosyltransferase	GH16	16
β-glucosidases	GH1	8
β-glucosidases; xylan 1,4-β-xylosidase ; β-*N*-acetylhexosaminidase	GH3	17
β-hexosaminidases and chitobiases; β-1,6-*N*-acetylglucosaminidase	GH20	2

Uni-Prot/CAZy	GH Family	No. genes
β-L-arabinofuranosidase	GH127	2
Chitinases, endo-β-*N*-acetylglucosaminidases, di-*N*-acetylchitobiases xylanase inhibitor; concanavalin B; narbonin	GH18	10
Chitosanase	GH75	2
D-4,5-unsaturated β-glucuronyl hydrolase	GH88	3
Endo-1,4-b-xylanase, Xylanases	GH10	6
Endo-1,4-β-galactanases	GH53	2
Endoglucanases	GH12	4
Endoglucanases and cellobiohydrolases	GH6	2
Endoglucanases and cellobiohydrolases;endo-b-1,4-glucanase; reducing end-Acting cellobiohydrolase; chitosanase; endo-b-1,3-1,4-glucanase	GH7	4
Endoglucanases; copper-dependent polysaccharide monooxygenases	GH61	22
Endoglucanases; endoglucanase; cellobiohydrolase; β-glucosidase; exo-β-Glucosaminidase	GH9	1
Endoglucanases; reducing end-acting cellobiohydrolase; endo-β-1,4-Glucanase; chitinase	GH5	7
Endo-β-*N*-acetylglucosaminidase	GH85	1
Exo-α-1,6-mannosidase	GH125	1
Glucan endo-1,3-α-glucosidases	GH71	7
Glucoamylases; glucodextranase α,α-trehalase	GH15	5
Glucosylceramidases, β-1,6-glucanase; β-xylosidase; β-fucosidase;	GH30	2
Lysozymes	GH25	1
Lysozymes type G; peptidoglycan lyase	GH23	1
Mannosyl-oligosaccharide glucosidases; a-glucosidase; a-1,3-glucosidase; a-Glucosidase	GH63	1
Mannosyl-oligosaccharide mannosidases; mannosyl-oligosaccharide α-1,2-mannosidase; mannosyl-oligosaccharide α-1,3-mannosidase ; mannosyl-oligosaccharide α-1,6-mannosidase; α-mannosidase; α-1,2-mannosidase; α-1,3-mannosidase; α-1,4-manno	GH92	4
Polygalacturonases; xylogalacturonan hydrolase; exo-polygalacturonosidase	GH28	17
Trehalases; α,α-trehalase	GH37	3
Xylanases	GH11	2

3.2.3.4 Carbohydrate Esterases (CE)

Carbohydrate esterases are accessory enzymes to facilitate cell wall degradation by GH in order to release saccharides (Cantarel *et al.*, 2009). There were eight CE protein families, totalling 98 proteins, encoded by the *A. mellea* genome which is a greater abundance than all the other species in Table 3.5. Indeed, *C. cinerea*, the next most abundant, has 51. These proteins can be modular, forming a protein complex with other CAZy. One CE9 (Am16040) was a module of a GH128 protein and a CE10 (Am18271) formed a module of a GH1 (Table 3.4) (*A. mellea* accession numbers in accompanying CD file Seq_BLAST_IPS.xlsx). CE are usually metal binding enzymes and have conserved motifs and domains (Blair *et al.*, 2005; Cantarel *et al.*, 2009; Caufrier *et al.*, 2003; http://www.cazy.org/Carbohydrate-Esterases.html (Accessed 18/12/2012)). Hemicelluloses are short heteropolymers which can crosslink to other cell wall polymers such as lignins, or form esters with phenolic acids involved in plant defence. CE1 family preferentially cleave 2-*O*-linked residues of which hemicellulose is composed (van den Brink and de Vries, 2011). Xylan, a hemicellulose, comprises 30% of plant cell walls. CE1 esterases cleave ester bonds enabling access by xylanases and pectinases and release of these defence molecules (Garcia-Conesa *et al.*, 1999; Faulds *et al.*, 1997).

CE4 family (n = 16), CAZy cleave 2-*O*-linked residues were identified in *A. mellea*. They are chitin deacetylases whose highly conserved catalytic and binding sties (Caufrier *et al.*, 2003; Blair *et al.*, 2005), were conserved in *A. mellea*. CE4, are secreted during hyphal penetration of plants by *Colletotrichum lindemuthianum*. Tsigos and Bouriotis (1995) hypothesised that chitin of invading pathogens triggers recognition by plant defences inducing plant chitinase activity which gives rise to formation of lignin and callus. Deacetylases modify plant chitinases thereby neutralising plant defences, and modify fungal chitin to chitosan which plant deacetylases are unable to modify, thus enabling the fungus to invade the plant.

A. mellea has greater abundance of CE enzymes than other fungi listed in Table 3.5, with more than double the number of the other fungi in total. CE families generally have been found to act as accessory enzymes to facilitate cell wall degradation by GH in order to release saccharides (King *et al.*, 2011).

3.2.3.5 Carbohydrate Binding Modules (CBM)

Carbohydrate binding modules are attached to other CAZys (Boraston *et al.*, 2004). They bind carbohydrates and act in concert with lytic enzymes, while not having lytic activity themselves. As these families are modules attached to other CAZys (Boraston *et al.*, 2004), their activity is carbohydrate binding, enabling other CAZy to lyse glycosidic bonds. Thus, as can be seen in Table 3.4 (*A. mellea* accession numbers in accompanying CD file Seq_BLAST_IPS.xlsx) CBM are regularly associated with other classes of CAZy. They are usually incorporated in a protein fold of another CAZy. There were fifteen proteins from seven families identified primarily as CBM. CBM48 was a modular attachment of GH13 (Am17455) and a CBM5 module was attached to a CBM12 module and GH18 protein (Am18922). CBM1 family proteins (n = 3) were attached to GH3, GH6 and GH61 proteins (Am13998, Am19553, and Am20347, respectively). CBM20 family (n = 4) were attached to GH13 (Am13041 and Am16197) and GH15 (Am14148 and Am14157). A CBM43 module was bound to a GH72 (Am15111).

CBMs bind carbohydrates and act in concert with lytic enzymes, while not having lytic activity themselves. CBM5 members have antifungal properties thought to be brought about by inhibition of chitin biosynthesis during cell division (Mehmood *et al.*, 2011). CBM12 previously only described in bacteria, is unusual in the specificity of its substrate, as many CBM bind non-specifically to polysaccharides. CBM12 binds very specifically to insoluble chitin but not to chitin oligosaccharides or glucose (Boraston *et al*., 2004) and acts in concert with chitinase. Chitinases have been investigated as biotechnological biocontrol for plant pathogenic fungi (Mehmood *et al*., 2010).

3.2.3.6 Glycosyl Transferases (GT)

This protein family catalyses the transfer of sugars from donor to sugar or non-sugar acceptor molecules and members are classed according to sequence similarity (Coutinho *et al.*, 2003). Ninety proteins from 23 families were identified in the *A. mellea* cDNA database by interrogation of the CAZy database (Table 3.4) (*A. mellea* accession numbers in accompanying CD file Seq_BLAST_IPS.xlsx). One protein (Am8629) had motifs from GT4, GT5 and GH13.

3.2.3.7 Polysaccharide Lyases (PL)

Eighteen PL from four families were identified in the *A. mellea* genome (Table 3.4) *(A. mellea* accession numbers in accompanying CD file Seq_BLAST_IPS.xlsx). Fungal PL are secreted, degrade pectin in the cell wall of plants and are phytopathogenic virulence factors (Herron and Benen, 2000; Creze *et al.*, 2008). Pectins are cleaved by PL and pectates are cleaved by metal-dependant PLs. Cleavage is by β-elimination of the non-reducing end of the polysaccharide.

PL5 family has alginate lyase activity. Alginates are heterpolysaccharides composed of β-D-mannuronate and its C5 epimer α-L-guluronate. The gel formed on brown seaweeds and produced by some bacteria is comprised of this and pathogenic bacteria use the gel as a protective biofilm (Yoon *et al.*, 1999).

3.2.3.8 Cytochrome P450 (P450)

A. mellea has a large (*n* = 248) P450ome (Table 3.7) (*A. mellea* accession numbers in accompanying CD file Seq_BLAST_IPS.xlsx), with monooxygenases ranging in size from 105 to 2505 residues. The active site of these enzymes is a cysteine-thiolate bound to a heme group. Seventy-eight percent (*n* = 193) of *A. mellea* P450 proteins are full length (≥ 300 residues). In contrast the white-rot fungus, *P. chrysosporium* only has 150 (Doddapaneni *et al.*, 2005), while the brown-rot fungus *P. placenta* has 184 (Ide *et al.*, 2012), and *Ganoderma lucidium* has 197 functional cytochrome P450s (Chen *et al.*, 2012). SecretomeP analysis of all the *A. mellea* P450 genes identified 112 with classical secretion signals (SignalP), a further 89 with non-classical secretion signals (SecretomeP), and a Phobius search predicted proteins with transmembrane regions (*n* = 92). Three proteins (Am14960, Am3421 and Am3841) with mitochondrial target signals were identified by TargetP.

Table 3.7. BLAST annotation of cytochrome P450 genes in *A. mellea.*

BLAST Description	No. of Genes
614 534 cytochrome p450	3
Benzoate 4'-monooxygenase cytochrome p450	3
Cytochrome p450	160
Cytochrome p450 11b1	1
Cytochrome p450 4f5	5

BLAST Description	No. of Genes
Cytochrome p450 cyp3 cyp5 cyp6 cyp9	1
Cytochrome p450 family protein	1
Cytochrome p450 monooxygenase	10
Cytochrome p450 monooxygenase pc'-1	4
Cytochrome p450 monooxygenase pc'-3	10
Cytochrome p450 oxidoreductase	1
Cytochrome p450 oxidoreductase '-	1
Cytochrome p450, putative [*Talaromyces stipitatus* ATCC 10500]	1
High nitrogen upregulated cytochrome p450 monooxygenase 2	4
P450 monooxygenase	2
Pah'-inducible cytochrome p450 monooxygenase pc'-pah 1	10
Pah'-inducible cytochrome p450 monooxygenase pc'-pah 4	30
Potential p450 cytochrome	1

Cytochrome P450 abundance in *A. mellea* has likely arisen from gene duplications and insertions with possible neofunctionalisation (Syed and Yadav, 2012). These enzymes are monooxygenases and detoxify many xenobiotic compounds *in vivo*. Their activity in fungi is both intracellular and extracellular. Particularly interesting is complete degradation to H_2O and CO_2 by fungi of polycyclic aromatic hydrocarbons (PAH) which are environmental pollutants and carcinogens (Peng *et al.*, 2008). It was thought that the ability of white rot fungi to degrade PAH was due to its laccases and peroxidases and that low nitrogen (lignolytic) conditions would be conducive to PAH degradation but Syed *et al.* (2010) have shown the ability of *P. chrysosporium* P450s to degrade high molecular weight PAHs (≥4 PAH rings) in rich media. White rot fungi, because of the number and varied specificity of their P450 monooxygenases are thought to be particularly good candidates for bioremediation of PAH (Doddapaneni *et al.*, 2005). The abundant cohort of P450 genes in *A. mellea* makes it likely that it has specificity for many PAH and recent studies into this have been conducted by Hadibarata *et al.* (2012) and Hadibarata and Kristanti (2012b). *A. mellea* was shown to degrade naphthalene, pyrene, benzo[a]pyrene, pyrene and anthracene although its catalytic activity was attributed to laccases rather than cytochrome P450 enzymes (Hadibarata *et al.*, 2012; Hadibarata and Kristanti, 2012a, 2012b; Hadibarata *et al.*, 2013).

3.2.3.9 Expansins

BLAST identified *A. mellea* expansin genes (n = 3) and InterProScan (IPR) identified a further seventeen (total: n = 20) with expansin motifs (Table 3.8). These proteins are involved the expansion and extension of plant cell walls during growth and differentiation. Expansin proteins disrupt the non-covalent interaction between cellulose microfibrils and hemicellulose (Cosgrove, 2000). They cause relaxation of cell wall turgidity enabling water and solutes to fill vacuoles thus enabling loosening and expansion of the cell wall. These enzymes have also been identified in many fungi (Verbeke *et al.*, 2009; Saloheimo *et al.*, 2002; Fernandez-Fueyo *et al.*, 2012). These proteins have a SignalP 20-30 aa from the N-terminal, several cysteines putatively involved in folding, a His-Phe-Asp catalytic site and conserved cellulose binding Trp residues near the C-terminal.

In a study of mycoparasite activity between the avirulent plant symbiont *Trichoderma atroviride* and *Rhizoctonia solani*, a plant pathogenic fungus, Reithner *et al.* (2011) identified an expansin like gene (SWO1) upregulated in *T. atrovirde* even before contact between the two fungi became visible, indicating signalling between the fungi, a function not usually associated with expansins.

Table 3.8. Proteins containing InterProScan expansin (IPR009009) domain signatures identified in an *A. mellea* genome survey. Nine proteins were identified by BLAST search as having homology to expansins. GO annotation identified protein signatures with varied biological processes, carbohydrate metabolism, symbiosis, defence.

[a]Accession No.	[b]BLAST description	[c]GO Biological Process
Am7435	Calcium-transporting atpase	biosynthetic process; nucleobase, nucleoside, nucleotide and nucleic acid metabolic process; ion transport;
Am14461	Cerato-platanin-related secreted protein	symbiosis, encompassing mutualism through parasitism
Am14586	Cerato-platanin-related secreted protein	-
Am18392	Eliciting plant response-like protein	-
Am16559	Endoglucanase v-like protein	protein modification process
Am18393	Epl1 protein	symbiosis, encompassing mutualism through parasitism
Am16042	Expansin family protein	-
Am19860	Expansin family protein	-
Am19903	Expansin family protein	defense response to fungus; defense response to bacterium
Am17252	Glycoside hydrolase family 16 protein	metabolic process; carbohydrate metabolic process
Am18844	Glycosyl hydrolase family 45 protein	carbohydrate metabolic process
Am7123	Glycosyl hydrolase family 45 protein	carbohydrate metabolic process; metabolic process
Am11610	Non-catalytic module family expn protein	-
Am18712	Non-catalytic module family expn protein	-
Am2584	Non-catalytic module family expn protein	-
Am6133	Non-catalytic module family expn protein	-
Am6783	Non-catalytic module family expn protein	defense response to fungus; defense response to bacterium
Am8597	Non-catalytic module family expn protein	chitin catabolic process; defense response to fungus; defense response to bacterium

[a]Accession No.	[b]BLAST description	[c]GO Biological Process
Am17698	Riboflavin aldehyde-forming enzyme	-
Am18718	Riboflavin aldehyde-forming enzyme	-

[a]Accession No. [b]BLAST description. [c]GO biological process

3.2.3.10 F-box and ubiquitin proteosome pathway proteins

F-box proteins (*n* = 71) were identified in the *A. mellea* cDNA database *(A. mellea* accession numbers in accompanying CD file Seq_BLAST_IPS.xlsx). A BLAST search identified fifteen, of which eight had IPS (IPR001810) F-box protein motifs, and the balance (*n* = 56) were identified by IPS (IPR001810) motif. These proteins have been identified in model systems and are involved in regulation of many processes including cell cycle, nutrition and transcription by labelling proteins with ubiquitin (Liu and Xue, 2011). F-box proteins have been studied in model systems for some time, but there have been recent studies of these proteins in other organisms. High numbers of F-box protein homologs have been found in pathogenic fungi: *C. albicans* (*n* = 21), *Cryptococcus neoformans* (*n* = 19), *Fusarium graminearum* (*n* = 62), *Fusarium oxysporum* (*n* = 53), *Botrytis cinerea* (*n* = 40) and *Magnaporthe oryzae* (*n* = 11) (Butler *et al.*, 2006; Jonkers *et al.*, 2011; Shieh *et al.*, 2005; Liu, Wang, *et al.*, 2011; Han *et al.*, 2007; Sweigard *et al.*, 1998). A number have been shown to be essential virulence proteins (Liu and Xue, 2011). Ubiquitin and ubiquitin proteosome pathway proteins (*n* = 78), in addition to F-box proteins, were identified in the *A. mellea* genome of which eighteen were ubiquitin ligases and seventeen were ubiquitin-conjugating enzymes.

3.2.3.11 Hydrophobins

Hydrophobins are morphogenetic and form an interface between fungi and host in both mutualistic and pathogenic interactions. They self assemble at hydrophobic and aqueous interfaces and have an ability to attract proteins due to their amphipathic character (Vincent *et al.*, 2012). Hydrophobins (*n* = 31) from *A. mellea* were annotated by BLAST (*A. mellea* accession numbers in accompanying CD file Seq_BLAST_IPS.xlsx). Hydrophobins are small molecular weight proteins found only in fungi (Sunde *et al.*, 2008) and *A. mellea* hydrophobins are between 87 and 203 residues long. Hydrophobins generally show little sequence similarity but all are hydrophobic, have four disulphide bonds (Figure 3.12) and are secreted. One of the hydrophobins identified from the *A. mellea* cDNA database (Am10069) has a SecretomeP motif while the others have SignalP motifs. Six have predicted transmembrane regions. These are divided into hydrophobin 1 (*n* = 6), hydrophobin 2 (*n* = 15) and other hydrophobins (*n* = 10). Hydrophobin gene products are insoluble polymers of two types: Hydrophobin 1 which form layers of parallel rodlets, are insoluble in organic solvents, detergents and alkali but soluble in 100% TCA and can be

repolymerised into rodlets. Hydrophobin 2 are aggregates of monomers soluble in some organic solvents and do not form rodlets. Sc3 hydrophobins of *Schizophyllum commune* coat the surface of hyphae. They attach to hydrophobic surfaces, decrease surface tension of aqueous substrates enabling submerged hyphae break the surface and become aerial mycelia, a second hydrophobin Sc4 provides these hyphae with air channels (Whiteford *et al.*, 2004; Wösten *et al.*, 1999). In a study of *Magnaporthe grisea* (Talbot and Kershaw, 1996), appressorium formation and pathogenicity were suppressed by deletion of a class 1 hydrophobin. Class 2 hydrophobins in an immunological study of *Cladosporium fulvum* by Whiteford *et al.* (2004) were secreted by the fungus onto substrate and neither growth or pathogenicity was affected in class 2 knock-out strains. Figure 3.12 shows *A. mellea* hydrophobin sequences which have been truncated for illustration and aligned using BioEdit and ClustalW. The alignment shows cysteine residues highlighted in yellow with the four predicted disulphide bonds in brackets underneath.

A review by Sunde *et al.* (2008) described hydrophobins in fungi whose genomes were sequenced at that time as families of between 2 and seven genes, the exception being *Coprinus cinereus* which has 23 genes. Since then, other genomes have been sequenced and comparison of *L. bicolor* strains S238N-H82 (n = 12) and 81306 (n = 9) strain by Plett *et al.* (2012) proposes that three extra hydrophobin genes in S238N-H82 arose through duplication as they are bordered by transposon rich regions. In *A. mellea* twenty-six residues comprised almost exclusively of proline and alanine near the N-terminus of Am12059 and forty-one close to the N-terminus of Am16941 may indicate similar duplication by TE's. There appear to be insertions (Am10727 Am11364 Am12059, Am16941 and Am16997) and deletions (Am5852) in hydrophobin genes.

Due to the unique properties of hydrophobins, they have wide ranging biotechnological applications: cleaning agents, surface coating of hydrophobic or hydrophilic materials such as silica, attachment of proteins to surfaces in cell culture and attachment of enzymes to biosensors in medical applications (Erjavec *et al.*, 2012; Cox and Hooley, 2009).

Figure 3.12. Alignment of hydrophobins illustrating the pattern of cysteine residues forming predicted disulphide bonds highlighted in yellow. Brackets indicate the cysteines which form bridges. [a] Hydrophobin 1; [b]Hydrophobin 2; [c]Hydrophobin motifs in *A. mellea* specific proteins. Only residues 140- 290 of the alignment are shown.

3.2.3.12 Metalloenzymes

The *A. mellea* genome encodes forty-five metalloenzymes. Seven have both transmembrane regions and SignalP motifs, with a further twelve and eleven containing transmembrane regions and SignalP motifs, respectively. There is very little sequence similarity between these enzymes, but about half of globally identified metalloproteins have a HEXXH motif. Others have a HExxHxxGxxHx or an abXHEbbHbc motif, where a is valine or threonine; b is an uncharged residue and c is any hydrophobic residue. The functions of metalloenzymes encoded by the *A. mellea* genome are many and varied and likely include protein processing and signalling, heavy metal transport, proteolytic activity, antibiotic activity, DNA polymerase activity and terpene synthesis (Table 3.9). In this study, 17 of the 45 metalloproteins have the HEXXH motif (Table 3.9). Nearly 50% of all enzymes require a metal co-factor (Waldron *et al.*, 2009). *A. mellea* enzymes specifically identified as metalloenzymes have a broad range of functions (Table 3.9). Four groups containing large regions with almost identical sequences, were identified among *A. mellea* metalloenzymes.

In pathogenic species, metalloproteins interfere with host defences, cleaving surface antigens of pathogens to evade host recognition (Hung *et al.*, 2005). They cleave host resistance proteins, such as plant chitinases (Naumann *et al.*, 2011) and sequester host metal in pathogenic interactions, thereby starving the host of vital nutrients (Agranoff and Krishna, 2002). Their activity varies; some synthesise clavulanic acid which inhibits β-lactamase activity (Iqbal *et al.*, 2010) and paradoxically some have β-lactamase activity which cleave antibiotics (Carfi *et al.*, 1995).

Metalloproteins involved in signalling, and cleave N-terminal signal sequences from mitochondrial peptides (Taylor *et al.*, 2001), have mitogen-activated protein (MAP) kinase activity with dual specificity which controls signal transduction in vital cellular functions (Camps *et al.*, 2000). Some metalloproteins whose normal function is growth regulation, degrade host tissue in pathogenic species (Hesami *et al.*, 2011; Laursen *et al.*, 2001). They control cellular influx and efflux of heavy metal ions (Higuchi *et al.*, 2009; Worlock and Smith, 2002).

While plant terpenes have been widely studied and more than 20,000 have been identified (Tholl, 2006), less is known about fungal terpenes particularly in higher fungi. *A. mellea* terpenes have been studied for quite some time and compounds with antibiotic, antifungal and cytotoxic properties have been extracted and identified (Fraga, 2012; Donnelly, Coveney, *et al.*, 1985; Donnelly *et al.*, 1987, 1990; Donnelly and

Hutchinson, 1990; Fraga, 2003, 2001, 1995; Cremin *et al.*, 1995, 2000; Donnelly *et al.*, 1986). Terpene synthases synthesise bioactive compounds, from a relatively small pool of substrates and chaperone the initial substrate through a process of cyclisation and modification. Köllner *et al.* (2006) identified fourteen different products from a maize terpene synthase (TPS4). Other enzymes such as P450 monooxygenases act in concert with these proteins to further modify their endproducts thus generating an as yet unidentified, vast range of bioactive metabolites. Technological advances in genome sequencing with resultant increases in availability of sequence information have enabled focussed investigation of potential bioactive metabolites. Terpene synthase genes are clustered with multifunctional P450 genes in *Fusarium* spp. catalysing the synthesis of mycotoxins (Tokai *et al.*, 2007). Very few genes from higher fungi have to date been cloned, their enzymes expressed and functionally characterised. Agger *et al.* (2009) transformed *E. coli* and *S. cerevisiae* with *C. cinerea* genes, and compounds which were expressed natively in *C. cinerea* were obtained. As sources of bioactive enzymes and metabolites, fungi are now coming to the fore with seven novel *A. mellea* sesquiterpenoids patented by Chen *et al.* (2011) as potential treatments for breast, lung, colon cancer and leukaemia.

Table 3.9. Metalloproteins encoded by the *A. mellea* genome.

[a]BLAST annotation	[b]Putative function	[c]Reference	[d]ID	[e]Group	[f]Motif
A'-pheromone processing metallopeptidase ste23	Cleavage of signal peptide	(Taylor *et al.*, 2001)	Am16706		
Cdf'-like metal transporter	Cation Efflux protein	(Higuchi *et al.*, 2009)	Am13812	1	M
			Am16286	1	
			Am16287		
			Am18263	1	M
			Am18300	1	
			Am18576		
			Am6025	1	
Deuterolysin m35 metalloprotease	Metallopeptidase, catalytic domain	(Li *et al.*, 2012)	Am2792	4	M
			Am3079		
			Am5511	4	M
			Am562	4	M
			Am9292	4	M
Divalent metal ion transporter with a broad specificity for di'-valent and tri'-valent metals	Metal ion homeostasis and intracellular parasitism.	(Agranoff and Krishna, 2002)	Am15078		

[a]BLAST annotation	[b]Putative function	[c]Reference	[d]ID	[e]Group	[f]Motif
Endoplasmic reticulum metallopeptidase	Amino peptidase M28	(Yoo *et al.*, 2010)	Am683		M
Extracellular elastinolytic metalloproteinase	Peptidase M36, fungalysin - chitinase	(Naumann *et al.*, 2011)	Am17617		M
Extracellular metalloproteinase 3	n/a		Am13991		
Family metal ion transporter	CorA-like/Zinc transport protein	(Worlock and Smith, 2002)	Am16868		
Metal homeostatis protein bsd2	GNAT protein from the clavulanic acid biosynthesis pathway	(Iqbal *et al.*, 2010)	Am17282		
			Am8109		
Metal ion binding protein	Dual specificity MAP kinase	(Camps *et al.*, 2000)	Am15489		
Metal resistance protein ycf1	ABC transporter		Am15778		
Metal'-dependent phosphohydrolase	HD-domain/PDEase-like superfamily DNA polymerase	(Aravind and Koonin, 1998)	Am8863		
Metallo-beta-lactamase superfamily protein	zinc metallo-beta-lactamase	(Carfi *et al.*, 1995)	Am13567		
Metallo-beta-lactamase superfamily protein	zinc metallo-beta-lactamase		Am13994	2	
Metallo-beta-lactamase superfamily protein	zinc metallo-beta-lactamase		Am15377	2	M
Metallo-beta-lactamase superfamily protein	zinc metallo-beta-lactamase		Am7220	2	M
Metallopeptidase	Zn-dependent exopeptidases superfamily		Am17787		

[a]BLAST annotation	[b]Putative function	[c]Reference	[d]ID	[e]Group	[f]Motif
Metallophosphatase domain-containing protein	Phosphoesterase domains associated with DNA polymerases of diverse origins	(Aravind and Koonin, 1998)	Am14387		
			Am14392		
			Am14449		
Metalloprotease	Cytophagalysin family – regulation of growth and destruction of host tissue by pathogen	(Laursen *et al.*, 2001; Hesami *et al.*, 2011)	Am13603		M
Metalloprotease mep2	Peptidase M36, fungalysin - chitinase	(Naumann *et al.*, 2011)	Am15013	3	
Metalloprotease mep2			Am16370	3	M
Metalloprotease mep2			Am3869	3	
Metalloproteinase 10	Peptidase M36, fungalysin - chitinase	(Naumann *et al.*, 2011)	Am10554	3	
Metalloproteinase 10			Am16276	3	
Metalloproteinase 10			Am20017	3	M
Metalloproteinase 10			Am9721		M
Metalloproteinase 10			Am9998	3	M
Mycorrhiza-upregulated terpene synthase metal binding domain protein	Terpene synthase metal binding domain	(Lesburg *et al.*, 1998)	Am18307		

[a]BLAST annotation	[b]Putative function	[c]Reference	[d]ID	[e]Group	[f]Motif
Mycorrhiza'-upregulated terpene synthase metal binding domain protein	Terpene synthase metal binding domain		Am20182		
Zinc metallopeptidase	The WLM (WSS1-like metalloprotease) domain is a globular domain related to the zincin-like superfamily of Zn-dependent peptidase.	(Mullen *et al.*, 2010)	Am15931		M
Zinc metallopeptidase	Metallo-dependent hydrolases superfamily		Am17835		
Zinc metalloprotease	ADAM/reprolysin	(Zhu *et al.*, 2009)	Am17506		M

[a]BLAST annotation. [b]Putative function [c]Reference, literature reference to BLAST annotation. [d]ID, Gene number from the *A. mellea* database. [e]Group, alignment of metalloproteins with similar sequences. [f]Motif, M, HEXXH motif of metal binding proteins.

In addition to the two terpene synthases in Table 3.9 which were identified as metalloproteins, a further thirty-six genes with terpene synthase motifs (IPR008949) were identified in the *A. mellea* protein database. Eight of these have at least one DDXXD motif and twelve have polyprenyl synthase motifs, denoting terpene precursor synthases (Agger *et al.*, 2009). IPS domain signatures annotate 21 predicted proteins as terpene synthase genes.

Table 3.10. Terpene synthase motifs (IPR008949) identified from *A. mellea* database interrogation of IPS.

Accession No.	BLAST description
Am16533	Calnexin precursor
Am14512	Decaprenyl-diphosphate synthase subunit 1
Am16904	Decaprenyl-diphosphate synthase subunit 1
Am14010	Farnesyl-diphosphate synthase
Am14280	Farnesyl-diphosphate synthase
Am14824	Farnesyl-diphosphate synthase
Am3697	Farnesyl-diphosphate synthase
Am9681	Farnesyl-diphosphate synthase
Am17869	Isoprenoid biosynthesis-related protein
Am2800	Isoprenoid biosynthesis-related protein
Am9680	Isoprenoid biosynthesis-related protein
Am9682	Isoprenoid biosynthesis-related protein
Am18307	Mycorrhiza-upregulated terpene synthase metal binding domain protein
Am20182	Mycorrhiza-upregulated terpene synthase metal binding domain protein
Am11113	Predicted protein [*Laccaria bicolor* S238N-H82]
Am16422	Predicted protein [*Laccaria bicolor* S238N-H82]
Am4705	Predicted protein [*Laccaria bicolor* S238N-H82]
Am11145	Predicted protein
Am11635	Predicted protein
Am12521	Predicted protein
Am12829	Predicted protein
Am12834	Predicted protein
Am12835	Predicted protein
Am13169	Predicted protein
Am14511	Predicted protein
Am14852	Predicted protein

Accession No.	BLAST description
Am15668	Predicted protein
Am16105	Predicted protein
Am16722	Predicted protein
Am16896	Predicted protein
Am19043	Predicted protein
Am19082	Predicted protein
Am3931	Predicted protein
Am4655	Predicted protein
Am9864	Predicted protein
Am3952	Squalene synthase
Am17358	Terpene cyclase
Am20210	Terpene cyclase

3.2.3.13 Nonribosomal peptide synthethase (NRPS)

Twelve NRPS genes were identified in the *A. mellea* genome. One was annotated by BLAST as an NRPS, nine as NRPS 12, and two as nonribosomal siderophore peptide synthetase proteins (Table 3.11). These proteins are large with diverse functionality and encode adenylation, condensation, thiolation and epimerase domains with variable architecture whereby domain order is specific to a particular NRPS and may be repeated (Nierman *et al.*, 2005; Stack *et al.*, 2007).

Table 3.11. *A. mellea* genes encoding nonribosomal peptide synthetase proteins identified from the genome.

Accession No.	BLAST description	Sequence Length	InterProScan annotation
Am8348	Nonribosomal peptide synthetase	955	AMP dependent synthetase/ligase; NAD(P) binding domain; AMP binding conserved site; Low complexity domain.
Am14132	Nonribosomal peptide synthetase 12	421	Low complexity domain, Transmembrane domain
Am14436	Nonribosomal peptide synthetase 12	370	AMP dependent synthetase/ligase
Am2619	Nonribosomal peptide synthetase 12	483	Low complexity domain, Transmembrane domain
Am2620	Nonribosomal peptide synthetase 12	478	Low complexity domain, Transmembrane domain
Am3994	Nonribosomal peptide synthetase 12	310	Classical secretion signal, Transmembrane domain

Accession No.	BLAST description	Sequence Length	InterProScan annotation
Am445	Nonribosomal peptide synthetase 12	670	Transmembrane domain
Am5760	Nonribosomal peptide synthetase 12	554	AMP dependent synthetase/ligase; Low complexity domain, Classical secretion signal
Am5761	Nonribosomal peptide synthetase 12	494	Low complexity domain, Transmembrane domain
Am9703	Nonribosomal peptide synthetase 12	765	AMP dependent synthetase/ligase; AMP binding domain; AMP dependent synthetase/ligase; NAD(P) binding domain; Low complexity domain, Classical secretion signal.
Am9594	Nonribosomal siderophore peptide synthetase	753	AMP dependent synthetase/ligase; Amino acid adenylation domain; AMP binding conserved site; Low complexity domain
Am18602	Nonribosomal siderophore peptide synthetase	4460	AMP dependent synthetase/ligase; Condenstaion domain; Phosphopantethine attchment site; Polyketide synthase phosphopantethine; Phosphopantethine binding domain; AMP binding conserved site; Low complexity domain

3.2.3.14 Polyketide synthase (PKS)

Eleven PKS were identified in the *A. mellea* genome (Table 3.12), these proteins are multi-domain although not all domains are present in every protein. Figure 3.13 shows the biosynthesis of polyketides and the domain organisation of polyketide synthases.

Table 3.12. *A. mellea* genes encoding polyketide synthase proteins identified from the genome.

Accession No	BLAST Description	Sequence Length	InterProScan Annotation
Am10848	Polyketide synthase	341	Alpha/beta hydrolase fold-3;
Am14527	Polyketide synthase	458	Beta-ketoacyl synthase; Acyl transferase/acyl hydrolase/lysophospholipase;
Am14528	Polyketide synthase	2043	Polyketide synthase, KR; Malonyl-CoA ACP transacylase, ACP-binding;

Accession No	BLAST Description	Sequence Length	InterProScan Annotation
Am14842	Polyketide synthase	2314	Beta-ketoacyl synthase; Acyl transferase/acyl hydrolase/lysophospholipase; Malonyl-CoA ACP transacylase, ACP-binding;
Am15264	Polyketide synthase	2227	Polyketide synthase, KR; Beta-ketoacyl synthase; Malonyl-CoA ACP transacylase, ACP-binding; Polyketide synthase/Fatty acid synthase, KR;
Am1558	Polyketide beta-ketoacyl-synthase	167	Acyl transferase domain; Acyl transferase/acyl hydrolase/lysophospholipase;
Am16405	Polyketide synthase	1180	Polyketide synthase/Fatty acid synthase, KR;
Am16406	Polyketide synthase	829	Beta-ketoacyl synthase; Malonyl-CoA ACP transacylase, ACP-binding;
Am315	Polyketide synthase	1475	Beta-ketoacyl synthase; Acyl transferase/acyl hydrolase/lysophospholipase; Malonyl-CoA ACP transacylase, ACP-binding; Thiolase-like, subgroup; Polyketide synthase, beta-ketoacyl synthase domain;
Am316	Polyketide synthase	1011	Polyketide synthase, phosphopantetheine-binding domain;
Am5437	Polyketide synthase	448	Thioesterase; Acyl carrier protein-like;

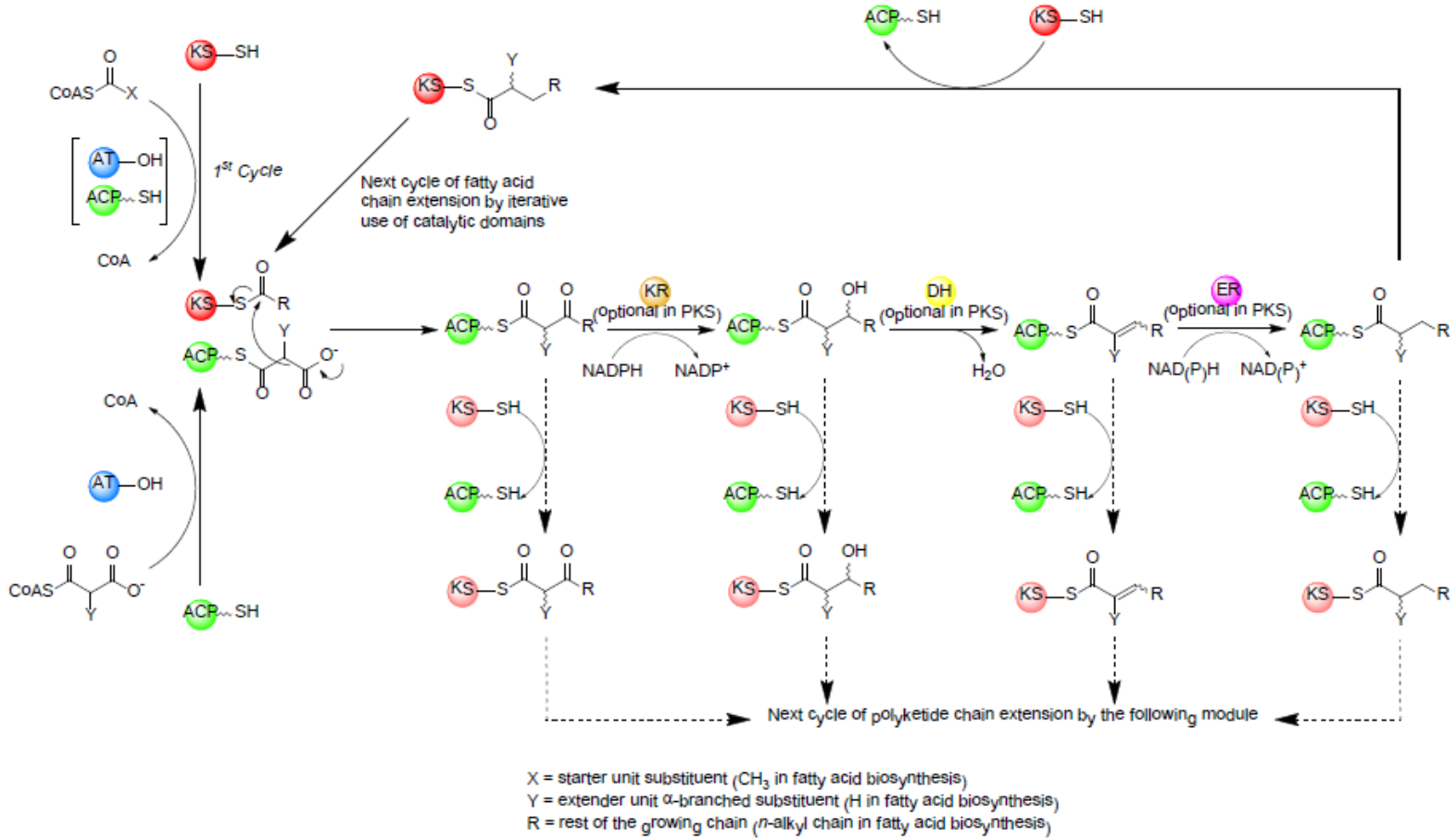

Figure 3.13. Biosynthesis of polyketides by polyketide synthases which are modular proteins that synthesise those secondary metabolites. AT, acyltransferase ; ACP, acyl carrier protein; KS keto-synthase; KR, ketoreductase; DH, dehydrogenase; ER, enoylreductase; MT, methlytransferase; SH. Sulfohydrolase;, TE, thioesterase (Kwan and Schulz, 2011)

3.2.3.15 Oxygenases

Genes encoding oxygenases (*n* = 92) were identified in the *A. mellea* genome (*A. mellea* accession numbers in accompanying CD file Seq_BLAST_IPS.xlsx). Nine have transmembrane regions. Sixty-eight percent exhibit secretion signals: SignalP (*n* = 21) and SecretomeP (*n* = 41). The defining characteristic of these oxidoreductases is the transfer molecular oxygen to a substrate (Hayaishi, 2005) and they are classed as monooxygenases or dioxygenases depending on whether they integrate one or both atoms of dioxygen into substrates. Oxygenases are involved xenobiotic degradation and metabolic pathways (Fetzner, 2002). Oxygenases are utilised by both bacteria and fungi and can degrade low molecular mass PAHs (Peng *et al.*, 2008). Cytochrome P450s discussed in Section 3.2.3.8, are a superfamily of monooxygenases, detailed separately in this study. BLAST annotations and the number of genes relating to each are shown in Table 3.13.

Table 3.13. BLAST annotation of oxygenases encoded within the *A. mellea* genome.

BLAST Description	No. of Genes
2'-nitropropane dioxygenase	6
2 OG-Fe oxygenase	6
3'-hydroxyanthranilate-dioxygenase	1
4'-hydroxyacetophenone monooxygenase	1
Alpha-ketoglutarate dependent xanthine dioxygenase	2
Alpha-ketoglutarate-dependent sulfonate dioxygenase	1
Alpha-ketoglutarate'-dependent taurine dioxygenase	3
Aromatic ring-opening dioxygenase	1
Catechol-dioxygenase	1
Coq6 monooxygenase	1
Delta 12 fatty acid epoxygenase	2
-Dihydroxy-3-keto-5-methylthiopentene dioxygenase	1
Dimethylaniline monooxygenase	3
Extracellular dioxygenase	16
Flavin-binding monooxygenase	6
Flavin-containing monooxygenase fmo family protein	2
Flavoprotein oxygenase	1
GPI anchored dioxygenase	1
Heme oxygenase	1
Hypothetical monooxygenase	12

BLAST Description	No. of Genes
Intradiol ring'-cleavage dioxygenase	3
Kynurenine 3'-monooxygenase	1
Leucoanthocyanidin dioxygenase	1
L'-lysine 6'-monooxygenase	1
Monooxygenase FAD-binding	1
Myo'-inositol oxygenase	2
Naringenin 3'-dioxygenase	1
-Oxoglutarate 3'-dioxygenase	1
Pentachlorophenol 4'-monooxygenase	1
Phytanoyl- dioxygenase	3
Protocatechuate dioxygenase	1
Salicylate 1'-monooxygenase	2
Squalene monooxygenase	1
Taurine catabolism dioxygenase	2
Thymine dioxygenase	1
TPA: 2OG'-Fe oxygenase (afu_orthologue AFUA_5g11160)	1
Trimethyllysine dioxygenase	1

3.2.3.16 Oxidases and peroxidases

BLAST interrogation of the *A. mellea* genome identified genes encoding oxidases (*n* = 118) (Table 3.14) (*A. mellea* accession numbers in accompanying CD file Seq_BLAST_IPS.xlsx) and peroxidases (*n* = 24) (Table 3.15) Eighty-six percent of these had secretion signals: SignalPs (*n* = 56), SecretomeP (*n* = 67). Transmembrane regions (*n* = 36) were identified in these proteins. Two laccase genes were identified (Table 3.14).

Table 3.14. BLAST annotation of oxidase genes from the *A.mellea* database

BLAST Description	No. Genes
Acyl- oxidase	9
Alcohol oxidase	2
Alcohol oxidase-like protein	6
Alternative oxidase 1	1
Amine oxidase	2
Amino oxidase domain protein	1
Aryl-alcohol oxidase	23

BLAST Description	No. Genes
Aryl-alcohol oxidase-like protein	2
C-4 methyl sterol oxidase	1
C-4 methylsterol oxidase	1
Conidial pigment biosynthesis oxidase arb2 brown2	1
Copper amine oxidase	2
Copper radical oxidase	6
Copper radical oxidase variant a	1
Coproporphyrinogen iii oxidase	2
COX16_crynb ame: full=cytochrome c oxidase assembly protein mitochondrial flags: precursor	1
Cytochrome c oxidase assembly protein cox11	1
Cytochrome c oxidase assembly protein cox15	2
Cytochrome c oxidase subunit v	2
Cytochrome-c oxidase chain vi	1
D-amino-acid oxidase	4
D-aspartate oxidase	1
Dihydroorotate oxidase	1
Diphenol oxidase-a2	1
FAD FMN-containing isoamyl alcohol oxidase -	1
Glucooligosaccharide oxidase	5
Glucose oxidase	2
Gulonolactone oxidase lgo1	1
Lac2, laccase-2 ame	1
Lac4, laccase-4 ame	1
L-amino acid oxidase	1
L-ascorbate oxidase	2
Lysyl oxidase	1
Multicopper oxidase	3
NADH:flavin oxidoreductase NADH oxidase	4
NADH:flavin oxidoreductase NADH oxidase family protein	1
NADPH oxidase	1
NADPH oxidase isoform 2	1
NADPH oxidase regulator	1
Peroxisomal copper amine oxidase	3
Polyamine oxidase	2
Protoporphyrinogen oxidase	1

BLAST Description	No. Genes
Pyranose 2-oxidase	3
Pyranose oxidase	1
Pyridoxamine 5 -phosphate oxidase	2
Pyridoxamine 5 -phosphate oxidase- fmn-binding	1
Pyridoxamine phosphate oxidase	1
Pyridoxamine-phosphate oxidase	1
Subunit vib of cytochrome c oxidase	1
Sulfite oxidase	1
X15341 cytochrome c oxidase subunit	1

Table 3.15. BLAST annotation of peroxidase genes from the *A. mellea* database

BLAST. Description	No. Genes
A chain crystal structure analysis of fungal versatile peroxidase from pleurotus eryngii	1
Chloroperoxidase-like protein	1
Cytochrome c peroxidase	1
Fungal peroxidase	2
Glutathione peroxidase	1
Heme peroxidase	4
Manganese peroxidase	4
Manganese peroxidase 3	1
Peroxidase	1
Peroxidase TAP	2
Thioredoxin-dependent peroxidase	2
Versatile peroxidase	4

3.2.3.17 Oxidoreductases

Oxidoreductases were identified from the *A. mellea* genome (n = 89) (Table 3.16) (*A. mellea* accession numbers in accompanying CD file Seq_BLAST_IPS.xlsx). Thirteen percent of the genes coding for these proteins had SignalP (n = 12), while none possessed SecretomeP motifs. Transmembrane regions were identified (n = 7) and only one protein (Am13557) had both SignalP and transmembrane domains.

Table 3.16. Oxidoreductases identified from a BLAST search of the *A. mellea* genome

Blast description	No of Genes
D-lactate dehydrogenase cytochrome oxidoreductase	2
FAD dependent oxidoreductase family protein	4
Flavoprotein NADH-dependent oxidoreductase	6
Glucose-methanol-choline oxidoreductase	15
NAD-binding rossmann fold oxidoreductase family protein	2
NADH ubiquinone oxidoreductase subunit	2
NADH:flavin oxidoreductase nadh oxidase family protein	5
NADH-dependent flavin oxidoreductase	1
Quinone oxidoreductase	16
Oxidoreductase	11
Oxidoreductase fad nad -binding protein	5
Oxidoreductase FAD-binding protein	1
Oxidoreductase htatip2-like	1
Oxidoreductase molybdopterin binding domain-containing protein	1
Quinate utilisation oxidoreductase	1
Quinone oxidoreductase	4
Related to NADH-dependent oxidoreductase	1
Short chain oxidoreductase	3
Sulfide-quinone oxidoreductase	1
Zinc-binding oxidoreductase	1
Zn-dependent hydrolase oxidoreductase family	6

3.2.3.18 Proline rich repeats (PPR)

Proteins with PRR's (n = 10) (Figure 3.14) are primarily structural proteins and are not usually found in globular proteins. They are also involved in binding and signalling (Williamson, 1994). IPS annotation of sequences in this category identified domains exhibiting signalling and localisation signatures and possessing characteristics of a superfamily associated with DNA repair and replication (CATH/G3DSA:3.40.50.10190 http://www.cathdb.info). These sequences have little in common except PRRs. Proline confers unusual properties including rigidity and steric hindrance of adjacent amino acids inhibiting α- helix formation, it cannot act as a hydrogen donor because it has a CH_2 on the amide group and is known as a "helix breaker", this rigidity also breaks β-sheets (Williamson, 1994). Structural proteins such as collagen contain proline while it is more unusual in globular proteins. PRRs form

long open structures which have a large surface area to which polyphenols are cross-linked by covalent or multivalent bonds, which are many but weak, and PRRs are thought to be have roles in phosphorylation. One well-characterised property is plant polyphenol binding (Williamson, 1994). Polyphenols are produced in response to infection by pathogens and Nicholson *et al.* (1986), showed that glycoproteins with PRR showed 26-fold greater binding affinity to polyphenolic molecules than to BSA and proposed that PRR glycoproteins should be considered fungal virulence factors.

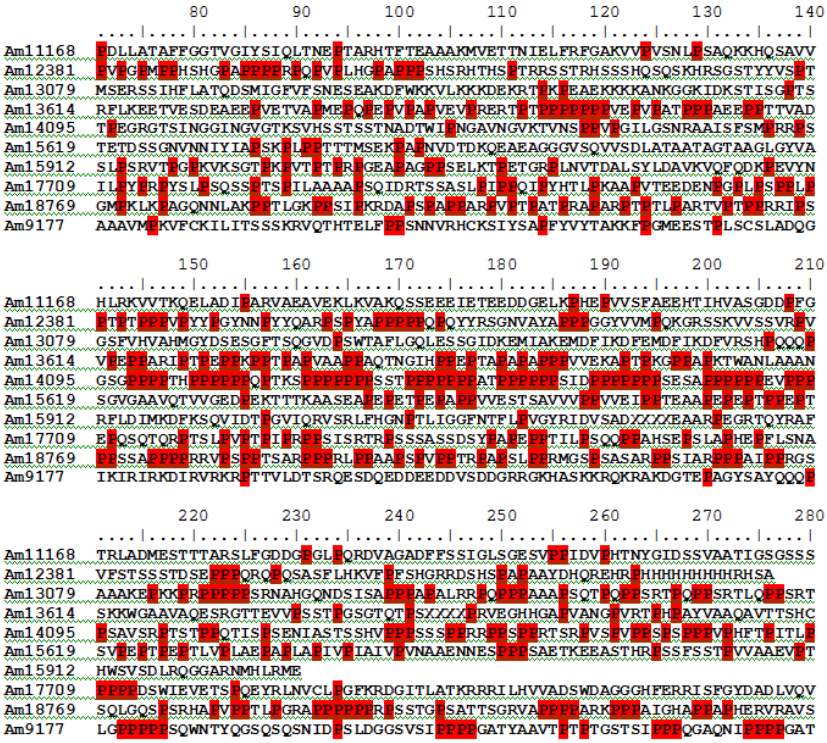

Figure 3.14. Truncated protein sequences of *A. mellea* proteins having proline rich repeat motifs. Residues shown in red are proline.

3.2.3.19 Retrotransposable elements

Rearrangement of DNA by transposable elements (TEs) increases genetic variation (Mieczkowski *et al.*, 2006; Plett *et al.*, 2012). Genes can be duplicated, deleted, inverted or moved either within a chromosome, or to other chromosomes, by TEs. These elements affect gene expression levels, inactivate genes or alter proteins. As well as gene inactivation, they are responsible for expansion of gene families and parasitic organisms can use this to their advantage (The *Schistosoma japonicum* Genome Sequencing and Functional Analysis Consortium, 2009). Genes encoding retrotransposable elements (n = 567) (Table 3.17) were identified in the *A. mellea*

genome comprising almost 4% of all *A. mellea* genes (*A. mellea* accession numbers in accompanying CD file Seq_BLAST_IPS.xlsx). Retrotransposable elements comprised 2.5% of *C. cinerea* genomic sequence (Stajich *et al.*, 2010). Almost 24% of the genome assembly of *L. bicolor* is comprised of TEs and while 9% were truncated sequences 15% were full length and their presence and may contribute to the size of the genome compared with *A. mellea* and *C. cinerea* (Labbé *et al.*, 2012). Ten *A. mellea* TEs had SignalP and ten had transmembrane domains, four retrotransposable elements exhibited coincident SignalP and transmembrane domains (Am12510, Am2070, Am8384 and Am8553). IPS domains identified in TEs were also identified in reverse transcriptase-ribonuclease H-integrase, RNA inhibitor and RNA helicase proteins, (Table 3.19). The most predominant domains were CHRromatin Organization MOdifier (CHROMO) domains which are thought to be important in chromosome segregation by silencing centromeric chromatin by alteration its structure (Piacentini *et al.*, 2003).

Table 3.17. Retransposable elements in the *A. mellea* genome.

Blast description	**No of genes**
Copia-like retrotransposable element	2
Copia-like retrotransposon family protein	1
Putative retrotransposon [*Serpula lacrymans* var. Lacrymans s7.9]	2
Retrotransposable element tf2 155 kDa protein type 1-like	416
Retrotransposable element tf2 155 kDa protein type 3- partial	1
Retrotransposable element tf2 155 kDa protein type 3-like	1
Retrotransposon like protein	1
Retrotransposon nucleocapsid protein	79
Retrotransposon polyprotein	1
Retrotransposon ty1-copia subclass	8
Retrotransposon ty1-copia sub-class	1
Retrotransposon ty3-gypsy subclass	24
Retrotransposon ty3-gypsy sub-class	1
Retrotransposon-derived protein peg10 isoform 1	6
Retrotransposon-derived protein peg10 isoform 2	13
Retrotransposon-derived protein peg10 isoform 4	5
Retrotransposon-derived protein peg10 isoform 6	1
Retrotransposon-derived protein peg10- partial	1
Retrotransposon-derived protein peg10-like	1
Retrotransposon-like 1	1

Blast description	No of genes
Retrotransposon-like protein 1	1

3.2.3.20 Ribonucleases

Of all ribonucleases (*n* = 424) in the *A. mellea* genome most are reverse transcriptase-RNase H-integrases (*n* = 392) (Table 3.18) (*A. mellea* accession numbers in accompanying CD file Seq_BLAST_IPS.xlsx). SignalPs were only identified in fourteen and only two had putative transmembrane domains. Reverse transcriptase-RNase H-integrase gene annotation by IPS identified fifteen different domain signatures (Table 3.19).

One particularly interesting RNase is an extracellular guanyl-specific ribonuclease (Am3791) and has a signalP sequence. It is a T_1/N_1 family endonuclease and cleaves phosphodiester bond of guanine. Some T_1 RNases are known to be cytotoxic as they cleave a guanine bond in a universally conserved domain of the large rRNA subunit, known as the sarcin/ricin loop (Lacadena *et al.*, 2007), which inhibits protein biosynthesis, as the protein no longer interacts with elongation factors and causes cell death by apoptosis (Szewczak *et al.*, 1993; Lacadena *et al.*, 2007). Cytotoxic RNases from *Aspergilli* were found to be unspecific and toxic at levels of 0.1 nM (Lacadena *et al.*, 2007). Other cytotoxic RNases with higher specificity have been used as anticancer therapies, and ranpirnase (Onconase®) extracted from amphibian eggs and embryos has been registered as an anticancer treatment. It causes apoptosis without DNA damage and is seen as an alternative to other therapies (Lee, 2008). Overexpression of *A. mellea* RNase has possible application as producing RNase N_1 for use in molecular biology or medical applications (Takahashi, 1988; Allgaier *et al.*, 2010).

Table 3.18. Ribonucleases identified by BLAST in the *A. mellea* genome

BLAST annotation	No. Genes
3 tRNA processing endoribonuclease	1
5 '-3 exoribonuclease 2	1
Exodeoxyribonuclease 1	1
Extracellular guanyl-specific ribonuclease	1
Mitochondrial exoribonuclease cyt-	1

BLAST annotation	No. Genes
Pab-dependent poly-specific ribonuclease subunit pan2	1
Poly-specific ribonuclease	1
Related to ribonuclease p protein subunit p30	1
Reverse transcriptase ribonuclease h	5
Reverse transcriptase-RNase H-integrase	392
Ribonuclease H	6
Ribonuclease H1	2
Ribonuclease H2 subunit a	1
Ribonuclease P mrp protein subunit	1
Ribonuclease P protein subunit p29	1
Ribonuclease t2	2
Ribonucleases p mrp protein subunit pop3 kda subunit	1
RNA helicase RNase	2
RNase h domain protein	1
RNase l inhibitor-type ATP binding cassette protein	1
TPA_exp: reverse transcriptase ribonuclease h	1

Retrotransposon abundant domains are the CHROMO domains. Ribonuclease genes have similar domains to those found in retrotransposable elements. Table 3.19 compares these genes to the number of genes in ribonucleases and retrotransposons. The CHROMO/shadow domains in retrotransposons are approximately four times more abundant in retrotranspons as in RNases. GAG (group specific antigen gene) protein domains (n = 80) identified among genes encoding transposable elements were more abundant compared to genes encoding RNases (n = 2). Other domains had comparable frequency in both.

Table 3.19. Domains identified by IPS in both ribonuclease and retrotransposable element genes.

IPS ID	Domain	Transposable Elements	Ribonuclease		
			RT-RNAse h-integrase	Inhibitor	Helicase
IPR001450	4 Fe -4S binding domain		1		
IPR017900	4Fe-4S ferredoxin, iron-sulphur binding, conserved site			1	
IPR017896	4 Fe-4S ferredoxin-type iron-sulphur binding domain			1	
IPR003593	AAA+ ATPase domain			1	
IPR013283	ABC transporter, ABCE			1	
IPR017871	ABC transporter, conserved site			1	
IPR003439	ABC transporter-like			1	
IPR023780	Chromo domain	170	52		
IPR000953	Chromo domain/shadow	196	54		
IPR016197	Chromo domain-like	204	58		
IPR000488	DEATH	9			1
IPR005034	Dicer double-stranded RNA-binding fold				1
IPR011545	DNA/RNA helicase, DEAD/DEAH box type N-terminal				2
IPR005135	Endonuclease/exonuclease/phosphatase		2		
IPR014001	Helicase superfamily 1/2 ATP-binding domain				2
IPR001650	Helicase, C-terminal		1		

IPS ID	Domain	Transposable Elements	Ribonuclease		
			RT-RNAse h-integrase	Inhibitor	Helicase
IPR001584	Integrase, catalytic core	188	186		
IPR001995	Peptidase A2A, retrovirus, catalytic	2			
IPR021109	Peptidase aspartic	36	35		
IPR005162	Retrotransposon gag protein	81	2		
IPR013242	Retroviral aspartyl protease	39	40		
IPR000477	Reverse transcriptase	102	116		
IPR013103	Reverse transcriptase, RNA-dependent DNA polymerase	9			
IPR002156	Ribonuclease H domain		5		
IPR012337	Ribonuclease H-like domain	209	207		
IPR000999	Ribonuclease III domain				1
IPR007209	Ubiquinol-cytochrome c chaperone, CBP3			1	
IPR013084	Zinc finger, CCHC retroviral-type	10	10		
IPR001878	Zinc finger, CCHC-type	16	9		
IPR015416	Zinc finger, H2C2-type, histone UAS binding	13	30		

3.2.3.21 Ribosomal proteins

The *A. mellea* database was annotated from a BLAST search with genes encoding ribosomal proteins (*n* = 115) (Table 3.20) (*A. mellea* accession numbers in accompanying CD file Seq_BLAST_IPS.xlsx). This dataset has SignalP (*n* = 6), SecretomeP (*n* = 69) and transmembrane regions (*n* = 9), and only in the case of Am7387, defined as a ribosomal RNA assembly protein mis3, were these coincident.

Table 3.20. Ribosomal protein classification from BLAST analysis of the *A. mellea* genome

BLAST Description	No. of Genes
30S ribosomal protein	1
37S ribosomal protein	1
39S ribosomal protein	1
40S ribosomal protein	28
50S ribosomal protein	8
54S ribosomal protein	2
60S ribosomal protein	43
Mitochondrial ribosomal protein	12
Other ribosomal proteins	12
Ribosomal processing proteins	7

3.2.3.22 Ribonuclease inhibitor proteins

Ribonuclease inhibitor proteins encompass a broad spectrum of proteins including F-box superfamily, discussed in Section 3.2.3.10. *A. mellea* cDNA database search by IPS returned motif annotation codes (*n* = 192) from the University College London Gene 3D database for these proteins. UCL's CATH protein structure classification database lists 2515 unique organisms and 1194 GO terms associated with ribonuclease inhibitor proteins http://www.cathdb.info/version/3.5.0/superfamily/3.80.10.10 (accessed 19-09-2012)

3.2.3.23 Hypothetical proteins

The hierarcy of predicted proteins used by SWISS-PROT for annotation is: probable, potential, putative and hypothetical in decreasing order of precision (Apweiler, 2001). Protein function prediction may be derived using sequence similarity, protein-protein interaction, phylogenetic analysis or by bioinformatic analysis using data mining tools,

machine learing, 3-D structure or genomic context approaches. Hypothetical proteins are proteins that have been predicted by nucleic acid sequence analysis, they are ambiguous as they may not encode proteins as they have no expressed sequence tags (EST) or cDNA and are not similar to known genes (Mohan and Venugopal, 2012). They may be homologous to genes of unknown function or "conserved hypothetical" if they have been assigned a function but they have not been experimentally characterised (Sivashankari and Shanmughavel, 2006; Lubec *et al.*, 2005). BLAST annotation identified 2333 hypothetical proteins potentially encoded by the *A. mellea* genome. Further information regarding the functionality of these genes was determined from other database searches. IPS analysis of these matched 88% to protein signatures, and 39% (*n* = 904) had GO annotation. Two hundred and sixty-two hypothetical proteins without IPS match have GO annotations. Within this dataset, SignalP peptides (*n* = 465) were predicted and transmembrane regions were predicted in 505 genes. Hypothetical proteins predicted by BLAST but with minimal information from other searches denoting 3-D structure such as a coil (non-α-helix non-β-strand) (Fitzkee *et al.*, 2005) or seg (low-complexity segment) (Wootton and Federhen, 1996) were also predicted (*n* = 425). Hypothetical proteins in *A. mellea* were homologous to hypothetical proteins in sixty-eight different species. Species with the greatest abundance of orthologs were *Serpula lacrymans* spp. (*n* = 874), *Coprinopsis cinerea* okayama 7#130 (*n* = 484), *Schizophyllum commune* H4-8 (*n* = 419) *Moniliophthora perniciosa* FA553 (*n* = 306). One hundred and sixty one proteins from the *A. mellea* database showed homology to a single hypothetical protein (CC1G_03488) from *Coprinopsis cinerea* okayama 7#130). Heterokaryon incompatibility motifs (*n* = 49) were identified by IPS in this group. SignalP (*n* = 15) and transmembrane domains (*n* = 5) were also identified in this group the transmembrane domains being coincident with SignalP. Homologs of hypothetical proteins from more than 50 species were identified in the *A. mellea* genome.

A. mellea genes encoding hypothetical protein homologs identified from other basidiomycetes: *M. perniciosa* FA553 (*n* = 306), *S. commune* H4-8 (*n* = 419) *C. cinerea* okayama7#130 (*n* = 484) and *S. lacrymans* spp. (*n* = 874) were highly abundant. However, genes encoding homologs from *L. bicolor* were in much lower abundance (*n* = 18). Hypothetical proteins annotated by BLAST functions (*n* = 92) are shown in Table 3.21 (*A. mellea* accession numbers in accompanying CD file Seq_BLAST_IPS.xlsx)

Table 3.21. Hypothetical proteins from the *A. mellea* genome which have BLAST functional annotation (*n* = 92).

BLAST Description	No of Genes
Conserved hypothetical amidohydrolase	1
Conserved hypothetical exported protein	1
Hypothetical acetylcholine esterase	1
Hypothetical adenylyl cyclase associated protein	1
Hypothetical amidohydrolase	1
Hypothetical arrestin	1
Hypothetical carboxylesterase	2
Hypothetical DNA photolyase	1
Hypothetical eukaryotic translation initiation factor eif1 sui1	1
Hypothetical FAD dependent oxidoreductase	12
Hypothetical fungal pheromone GPCR	2
Hypothetical GMC oxidoreductase	9
Hypothetical G-protein coupled receptor	1
Hypothetical histidine phosphotransferase	2
Hypothetical iron permease	1
Hypothetical iron reductase	4
Hypothetical iron transporter	1
Hypothetical iron transporter biosynthesis regulating transcription factor	1
Hypothetical iron uptake cluster protein	2
Hypothetical kinase	1
Hypothetical leucine-rich protein	2
Hypothetical lysophospholipase	1
Hypothetical magnesium -like protein	2
Hypothetical monooxygenase	12
Hypothetical mRNA turnover protein 4-like protein	1
Hypothetical NADH-ubiquinone oxidoreductase complex i lyr_b22_ndufb9 subunit	1
Hypothetical nucleolar complex-associated protein 3	1
Hypothetical pas domain protein	1
Hypothetical proline serine-rich protein	1
Hypothetical proline-rich protein	3
Hypothetical pyrophosphatase dcp2	1
Hypothetical response regulator receiver protein	2
Hypothetical RNA-binding protein	1
Hypothetical RTA 1-like protein	6

BLAST Description	No of Genes
Hypothetical transporter of the NRAMP family	3
Hypothetical triacylglycerol lipase	1
Hypothetical ubiquinone oxidoreductase 20 kd subunit	1
Hypothetical WD-repeat protein	1
Hypothetical zinc finger protein	1
TPA: aromatic-amino-acid hypothetical	1
TPA: conserved hypothetical protein [*Aspergillus nidulans* FGSC A4]	3

3.2.3.24 Predicted proteins

Predicted proteins are similar to hypothetical proteins and are predicted *in silico* from ORFs (open reading frames) of genomic sequences and show similarities to characterised protein conserved residues but not to significant protein regions (Sivashankari and Shanmughavel, 2006). Their functions may be inferred by motifs and domains from other organisms although enzyme function may differ between organisms. Functions may be predicted by (i) protein-protein interactions, where two proteins interact in another organism, (ii) comparative genomics and phylogeny where genes from metabolic pathways and structural complexes evolve together in different organisms, or (iii) annotation based on 3D structure (Sivashankari and Shanmughavel, 2006). From predicted proteins (n = 921) encoded by the *A. mellea* genome, 89% have IPS matches, some of these have only minimal structural information such as conserved protein coils, segments, SignalP or transmembrane regions (n = 436). There were GO annotations for 34% of genes encoding predicted proteins (n = 316). All proteins without IPS match had GO annotations. SignalP motifs (n = 144) and transmembrane (n = 194) regions were identified in these predicted protein sequences. Predicted protein encoding genes were homologous to predicted proteins from ten distinct species (Table 3.22) (*A. mellea* accession numbers in accompanying CD file Seq_BLAST_IPS.xlsx), with the greatest frequency being *L. bicolor* predicted protein homologs (n = 835), from 44 different superfamilies (Table 3.23), fourteen different protein families (PFAM) and 311 different IPS protein domains.

Table 3.22. *A. mellea* proteins homologous to predicted proteins in other organisms.

Seq. Description	No. of genes
Predicted protein [*Arthroderma otae* CBS 113480]	1
Predicted protein [*Aspergillus terreus* NIH2624]	7
Predicted protein [*Laccaria bicolor* S238N-H82]	815
Predicted protein [*Physcomitrella patens* subsp. Patens]	1
Predicted protein [*Postia placenta* Mad-698-R]	85
Predicted protein [*Pyrenophora tritici-repentis* Pt-1C-BFP]	1
Predicted protein [*Sclerotinia sclerotiorum* 1980]	6
Predicted protein [*Trichoderma reesei* QM6a]	2
Predicted protein [*Uncinocarpus reesii* 1704]	1
Predicted protein [*Verticillium albo-atrum* vams.102]	2

Table 3.23. *A. mellea* homologs in *L. bicolor*. Classification of superfamilies identified by IPS.

Superfamily ID	Description	No of Genes
SSF75011	3-carboxy-cis,cis-mucoante lactonizing enzyme	1
SSF54862	4Fe-4S ferredoxins	1
SSF53474	αβ hydrolase	13
SSF56801	Acetyl-CoA synthetase-like	2
SSF55753	Actin depolymerizing proteins	1
SSF55961	Bet v1-like	1
SSF57667	β -β-α zinc fingers	5
SSF54277	CAD & PB1 domains	1
SSF51197	Clavaminate synthase-like	2
SSF52096	ClpP/crotonase	1
SSF54001	Cysteine proteinases	1
SSF52467	DHS-like NAD/FAD-binding domain	1
SSF51905	FAD/NAD(P)-binding domain	5
SSF54373	FAD-linked reductases, C-terminal domain	2
SSF81901	HCP-like	3
SSF144232	HIT/MYND zinc finger-like	4
SSF52972	ITPase-like	1
SSF52058	L domain-like	2
SSF141091	L21p-like	1

Superfamily ID	Description	No of Genes
SSF56281	Metallo-hydrolase/oxidoreductase	2
SSF140361	MIT domain-like superfamily	1
SSF103481	Multidrug resistance efflux transporter EmrE superfamily	2
SSF51735	NAD(P)-binding Rossmann-fold domains	5
SSF54427	NTF2-like	2
SSF81301	Nucleotidyltransferase	1
SSF81631	PAP/OAS1 substrate-binding domain	1
SSF143870	PF0523-like	1
SSF50729	PH domain-like	2
SSF53254	Phosphoglycerate mutase-like	1
SSF88723	PIN domain-like	1
SSF52540	P-loop containing nucleoside triphosphate hydrolases	4
SSF140860	Pseudo ankyrin repeat-like superfamily	1
SSF57850	RING/U-box	3
SSF54928	RNA-binding domain, RBD superfamily	8
SSF52047	RNI-like	5
SSF53335	S-adenosyl-L-methionine-dependent methyltransferases	10
SSF82199	SET domain	1
SSF46966	Spectrin repeat	1
SSF54637	Thioesterase/thiol ester dehydrase-isomerase	1
SSF48452	TPR-like	3
SSF54236	Ubiquitin-like	4
SSF53300	vWA-like	1
SSF46785	"Winged helix" DNA-binding domain superfamily	9
SSF143990	YbiA-like	1

3.2.3.25 *A. mellea* specific proteins

A. mellea genes which revealed no BLAST homology (n = 2721) may be unique to the organism (*A. mellea* accession numbers in accompanying CD file Seq_BLAST_IPS.xlsx). Twenty three percent of these (n = 640) had no GO, IPS or enzyme annotation. Combined detail from the remainder (n = 2081) was obtained using various databases. Genes had IPS motifs (n = 2081), GO annotation (n = 64) and enzyme code mapping (n = 4) enabling initial putative annotation. Genes with structural features (n = 1899) and secretion signals (n = 398) only, comprised a large proportion of these. Genes encoding conserved protein segments or coil structures only (n = 274), and proteins with transmembrane regions (n = 336) were identified. Putative functions

of *A. mellea* specific genes were identified from protein coding motifs identified by IPS in this cohort (*n* = 112), homology to protein families (*n* = 6) and superfamilies (*n* = 19).

Retrotransposon gag protein motifs (*n* = 33) were identified among the *A. mellea* specific proteins. Three proteins (Am1367, 12059, and 16941), with homology to hydrophobin proteins were identified among *A. mellea* specific proteins (Figure 3.12), although Am12059 does not have a SignalP which would be expected. Alignments of these *A. mellea* specific genes with hydrophobin motifs and other *A. mellea* hydrophobins are shown in Figure 3.12. F-box protein motif annotations (*n* = 8) were identified by IPS (Am17860, 7008, 8001, 8058, 9370, 10484, 12259 and 12406). Proline rich extensin signature (*n* = 6), (Am18127, 12814, 13195, 13711, 15148 and 16024), were identified among *A. mellea* specific proteins. *A. mellea* specific genes (Am10137, 19420, 4742 and 6913) (*n* = 4) with motifs homologous to CHROMO domains were identified.

Protein motifs (*n* = 3) with characteristics described in an antigenic galactomannoprotein identified in cell walls of *A. fumigatus* (Yuen *et al.*, 2001) were identified (Am14278, 10612 and 16682). Also identified as *A. mellea* specific proteins, were highly conserved leucine-rich repeat motifs indicative of ribonuclease inhibitor proteins (*n* = 30). Zinc-dependent binding motifs (*n* = 21) which are found in a range of proteins, which bind DNA, RNA, lipids and other proteins were identified in *A. mellea* specific proteins.

3.3 Concluding remarks

The work presented in this Chapter encompasses the first detailed sequence investigation of *Armillaria mellea*. The findings reveal that the genome size is 58.3 Mb, and consists of almost 15000 genes, with each gene containing approximately 5 introns. *A. mellea* is most closely related to *M. perniciosa*. The data further detail the occurrence of a rich repository of carbohydrate-degrading enzymes, a large P450ome, and the presence of many *A. mellea*-specific genes. While the genome shows some characteristics reminiscent of other fungal genomes, it contains many unique aspects, and more importantly, its availability now sets the scene for detailed proteomic dissection of the organism - which will be elucidated in subsequent Chapters.

Chapter 4 Proteomic investigation of *Armillaria mellea* by electrophoresis and mass spectrometry.

4.1 Introduction

As so little *A. mellea* genome and proteome data has been published to date, this study represents the first attempt to address the deficit by analysis of a broad range of mycelial and secreted proteins using several proteomic techniques. The most widely established media for *A. mellea* culture is PDB (Lung and Chang, 2011; Donnelly *et al.*, 1997; Sonnenbichler *et al.*, 1997), in the case of liquid culture or in the case of solid culture, MEA (Raziq, 1998; Otieno *et al.*, 2003; Hadibarata and Kristanti, 2012a), and these were both used in this study. Mycelial proteins identified by a gel electrophoresis mass spectrometry approach were derived solely from PDB cultures, while secreted proteins were derived from culture on a variety of media.

The dynamic nature of protein and metabolite expression induced by environmental conditions makes the study of the global proteome more difficult and there is no universal method of analysis (Baginsky and Gruissem, 2006). To study the organism *in vitro*, defined media which restrict specific nutrients to particular carbon sources are utilised. However, proteins which may be induced by symbiotic or pathogenic interactions are excluded from consideration by use of defined media, resulting in knowledge gaps due to more favourable conditions than those found in nature, an issue which also pertains to plant studies (Collakova *et al.*, 2012). Defined media with restricted carbon sources have been used to induce expression of proteins in fungi (Martinez *et al.*, 2009; Vanden Wymelenberg *et al.*, 2009; Hori *et al.*, 2012; Fernández-Acero *et al.*, 2010). Lignocellulosic biomass degradation is of particular interest as agro-industrial waste disposal is costly, as well as causing environmental pollution (Strong and Claus, 2011). White rot fungi can completely degrade lignin substrates to H_2O and CO_2 (Martinez *et al.*, 2009), releasing sugars from plant cell walls which become available for bio-fuel generation (Strong and Claus, 2011). Thus, extracellular *A. mellea* enzymes may have potential for lignocellulosic material degradation in industrial and bio-medical applications (Kunamneni *et al.*, 2008).

The fungal cell wall is very robust (Bowman and Free, 2006) making cell lysis and protein retrieval difficult, and mechanical and chemical methods must be employed to achieve this. Gel electrophoresis which separates proteins by size, or in two dimensions by both charge and size is used to isolate either single or a small number of proteins. If there are any contaminants present, 2-DE is unyielding and proteins will not

focus and proteins cannot be isolated. Polysaccharides secreted into *A. mellea* culture media comprise up to 10% (w/w) (Gao *et al.*, 2009), many bioactive metabolites are also known to be secreted (Misiek *et al.*, 2009; Donnelly *et al.*, 1985; Herath *et al.*, 2012; Misiek *et al.*, 2011) as well as hydrolytic enzymes (Hadibarata and Kristanti, 2012a), and melanin. This makes it difficult to separate proteins of interest from the mixture, as concentration of the media also concentrates interfering compounds. Proteins are ultimately excised from polyacryamide gels and subjected to tryptic digestion into their component peptides for analysis.

MALDI-ToF is an analysis method whereby digested proteins are embedded in a matrix comprised of small UV absorbant molecules and subjected to a laser pulse. This pulse desorbs the matrix and in doing so protonates and ablates analytes which are accelerated into a flight tube by application of an electric field (Kaufmann, 1995; Yates, 1998). On exiting this field, analytes maintain their speed and drift to an analyser. The length of this drift is extended by an ion mirror, extending the time of flight (ToF) allowing for better resolution of individual peptides. This drift, their ToF, is measured in calculating their mass, as lighter particles move faster than heavier ones. Peptides which have been protonated have a single charge and a mass of MH^+, M being the mass of the peptide and H^+ the proton. The analyser identifies peptides based on their mass to charge ratio (*m/z*). MALDI control software compares this *m/z* to a database, in this case the *A. mellea* cDNA database, an *in silico* protein digest of this database is used to generate protein mass fingerprints and identification is derived from the *m/z* of component peptides (Kaufmann, 1995; Yates, 1998).

LC-MS/MS or liquid chromatography tandem mass spectrometry, is an analytical method whereby digested and protonated peptides are separated initially by HPLC (high performance liquid chromatography) based on their hydrophobicity by loading them onto a reversed phase C_{18} column and eluting peptides using a gradient mobile phase of organic solvent, for example, acetonitrile (Peng *et al.*, 2003). Eluted peptides in acidified liquid are sprayed into a nitrogen filled chamber at high temperature; electrostatic repulsion causes the charge to be pushed to the droplet surface causing the droplet to explode as the liquid evaporates due to Coulomb force. This fission is repeated until only the peptide which has acquired one or multiple charges from the liquid, is in the gas phase. The resultant precursor ion is trapped and its *m/z* is analysed, ions held in the trap take energy from the dipolar field, collide with helium gas and fragment, the fragment *m/z* are analysed in a second round of mass

spectrometry (MS^2). Thus, fragmentation data and a mass fingerprint are obtained for each peptide. Fingerprints are compared to a database to identify proteins (Yates, 1998; Gaskell, 1997; Fenn *et al.*, 1989).

There has to date, been no global protein study of *Armillaria* spp. proteins from either intracellular or extracellular locations, instead focus has been on bioactive metabolite analysis (Donnelly *et al.*, 1982; Yang, Su, *et al.*, 1989; Donnelly *et al.*, 1990, 1987; Yang, Chen, *et al.*, 1989; Donnelly, Coveney, *et al.*, 1985; Yang *et al.*, 1990; Misiek *et al.*, 2009; Cremin *et al.*, 1995; Donnelly, Abe, *et al.*, 1985; Sonnenbichler *et al.*, 1997; Bohnert *et al.*, 2011; Muszyska *et al.*, 2011; Misiek *et al.*, 2011), enzymatic activity (Healy *et al.*, 1999; Barry *et al.*, 1981; Hunneyball and Stanworth, 1975; Doonan and Fahmy, 1975; Lewis *et al.*, 1978; Billal and Thurston, 1996) lignocellulose degradation (Stoytchev and Nerud, 2000; Dhiman *et al.*, 2012; Birkinshaw *et al.*, 1948) and bioremediation (Hadibarata and Kristanti, 2012a; Hadibarata *et al.*, 2013; Hadibarata and Kristanti, 2012b; Hadibarata *et al.*, 2012).

The objectives of this chapter were to establish a comprehensive proteomic overview of *A. mellea*, taking the following approaches:

1. To optimise growth conditions mycelial biomass and culture supernatants generation.
2. To develop protocols for efficient protein extraction in order to construct the first 2-DE mycelial map of *A. mellea.*
3. To develop procedures for optimisation of protein retrieval from culture supernatants for SDS-PAGE,
4. To identity proteins from the *A. mellea* cDNA database following separation by gel electrophesis and analysis by MALDI-ToF and LC-MS/MS.
5. To carry out a bioinformatic analysis of the proteins identified from *A. mellea* mycelia and secretome to attribute functions to these proteins.

4.2 Results

4.2.1.1 Optimisation of growth conditions

A. mellea grown on solid media produced cultures which had fluffy white mycelia at its centre with rhizomorphs radiating outwards. The rhizomorphs initially had a white fluffy appearance, but were subsequently replaced by smoother darker brown sclerotial mycelia as growth proceeded, with aerial hyphae projecting above the culture surface (Figure 4.1).

Figure 4.1. Culture of *A. mellea* on MEA showing fluffy white mycelia in the centre, sclerotial rhizomorphs and some dark brown aerial hyphae can be seen at the edges. Brown exudates can be seen at the tips of some of these.

Two distinct morphologies were observed in liquid culture, both static and shaking; a floating form which had white fluffy aerial hyphae with brown branched sclerotial rhizomorphs under the liquid surface (Figure 4.2) and a submerged tough white translucent gelatinous form. The amount of *A. mellea* biomass generated was specific to individual cultures, but in all cases brown mycelia produced greater biomass than gelatinous morphology. Biomass generated under the same culture conditions was >10 times greater where brown mycelia developed than where cultures produced white mycelia.

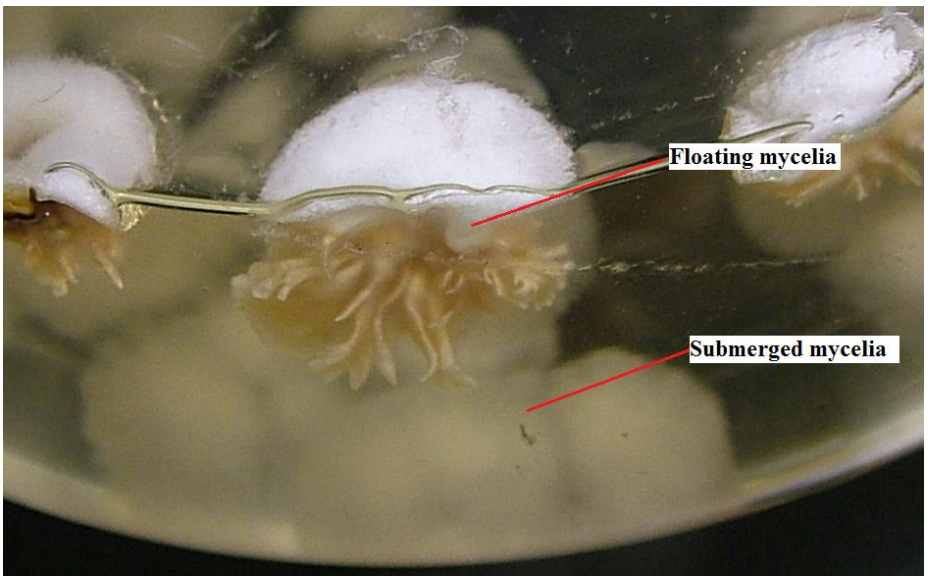

Figure 4.2. Liquid culture of *A. mellea* grown in PDB illustrating two distinct morphologies obtained from static cultures.

Basidiomycete cultures, including *A. mellea*, are known produce polysaccharides and melanin which are secreted into culture supernatants (Fragner *et al.*, 2009). This interferes with protein extraction. Mycelia from static and shaking cultures have different morphology and shaking cultures produce more melanin. Figure 4.3A illustrates the morphology and Figure 4.3B the light colour of supernatant recovered from static *A. mellea* cultures, compared with Figure 4.3C and Figure 4.3D which illustrate morphology and supernatant colour respectively, from shaking culture. The presence of melanin and polysaccharides interferes with efficient protein extraction from culture supernatants (Fragner *et al.*, 2009).

The most efficacious innoculation method and culture conditions for biomass generation, is described in Section 2.2.4.1. Briefly, this involved breaking a culture of *A. mellea* grown on agar (25 ml) into pieces with a sterile loop followed by vigorous shaking in a container of sterile H_2O (10 ml) to break the culture into very small pieces. Aliquots (~10 ml) were used to inoculate flasks of PDB to which 0.15% (v/v) ethanol had been added. Cultures under static conditions were incubated at 25 °C for 3 – 6 weeks.

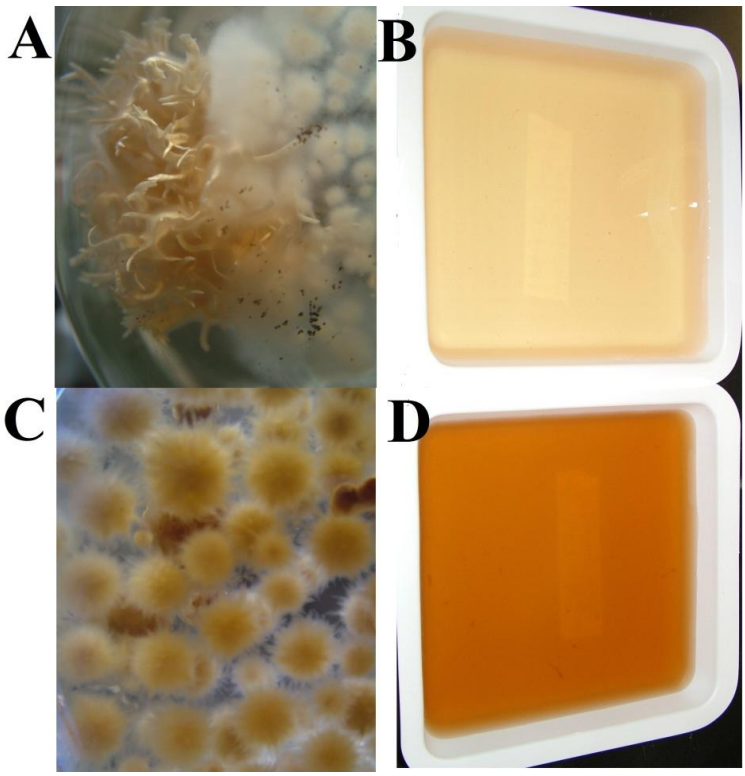

Figure 4.3. Comparison between mycelial morphologies and culture supernatant colours in static and shaking cultures of *A. mellea* in PDB. **A.** floating mycelia from static culture; **B.** supernatant from static culture; **C.** mycelia from shaking culture; **D.** supernatant from shaking culture.

4.2.2 Optimisation of protein extraction techniques for SDS-PAGE and 2-DE

Due to the dearth of research on the proteomics of *A. mellea* in particular and basidiomycetes in general, there are few established methods for intracellular and extracellular protein extraction. It was therefore necessary to develop techniques to separate intracellular proteins by 2-DE and extracellular proteins by SDS-PAGE (Fragner *et al.*, 2009).

4.2.2.1 Mycelial protein extraction

Static liquid cultures of *A. mellea* grown for 3 - 6 weeks (Section 2.2.4.1) were harvested (Section 2.2.4.2). Initally a method whereby mycelia were ground and 10% (w/v) TCA (Section 2.1.5.16) added to precipitate protein prior to sonication, followed by protein solubilisation in 2-DE focussing buffer (Section 2.1.6.16) was employed. This protocol was found to be unsuitable, due to the presence of contaminants which interfered with the focussing of the proteins in the first dimension and caused vertical streaking following 2-DE (Figure 4.4).

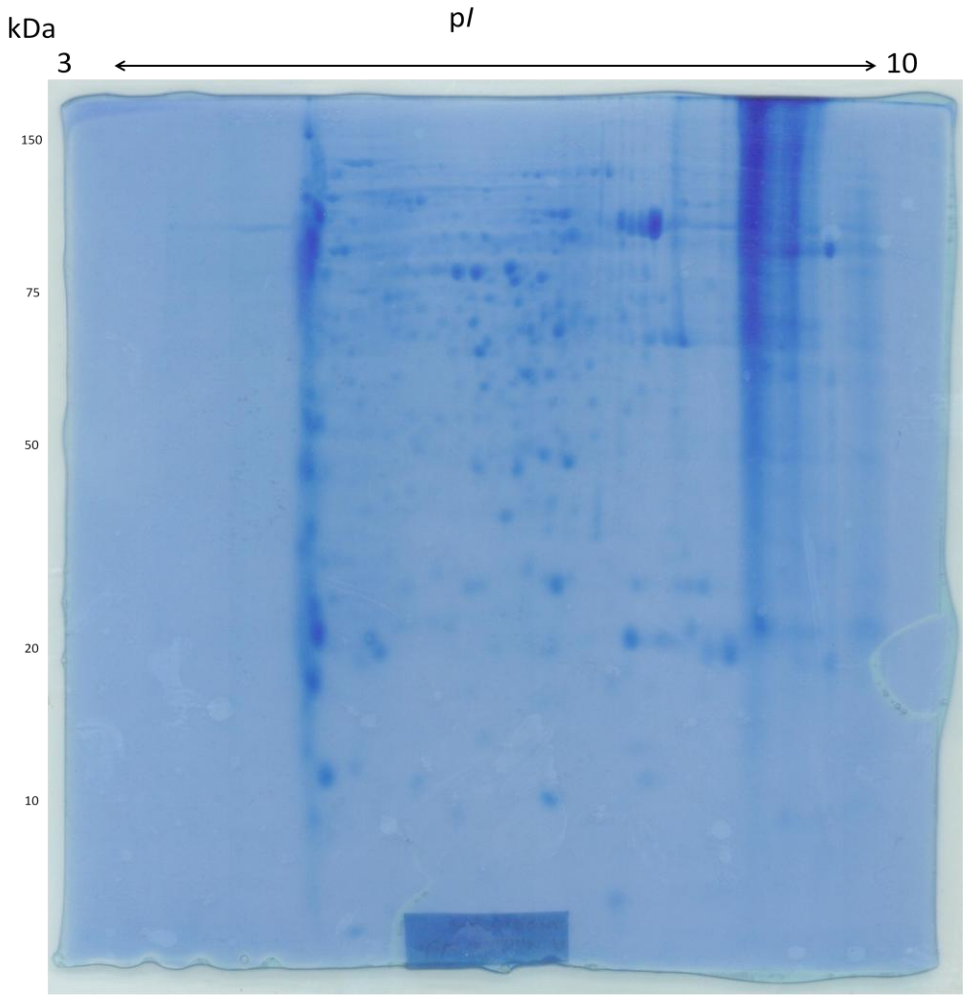

Figure 4.4. *A. mellea* mycelial 2-DE gel showing incomplete focussing and vertical streaking. Only the proteins in mid range have focussed properly.

An optimised method, Method 1 (Section 2.2.7.2), was developed whereby mycelia were ground and lysis buffer (Section 2.1.5.1) added prior to sonication and centrifugation. Cell debris was thus pelleted and removed. Soluble protein was precipated in TCA and resolubilised in 2-DE focussing buffer (Section 2.1.6.16). Protein concentrations were determined using the Bradford assay (Section 2.2.7.1). Proteins were separated by 2-DE (Section 2.2.8.3) and the resultant 2-DE gels stained (Figure 4.5). Individual protein spots were excised and digested (Section 2.2.10.3) prior to analysis by MALDI-ToF (Section 2.2.14) and LC-MS/MS (Section 2.2.15.2).

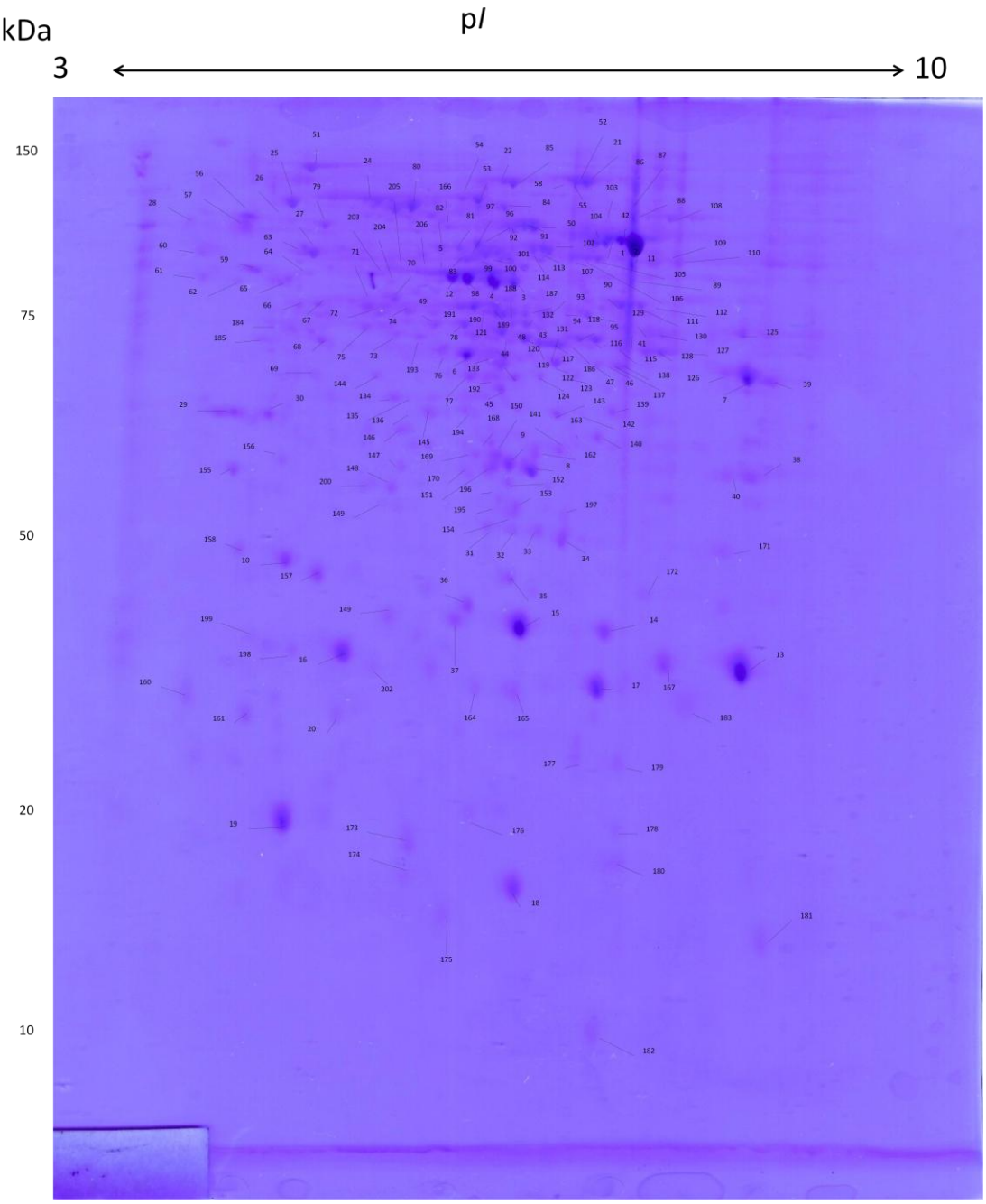

Figure 4.5. The first 2-DE map of *A. mellea* mycelial proteome, derived following culture in PDB media.

4.2.2.2 Supernatant protein extraction

A. mellea grown for 3 - 6 weeks (Section 2.2.4.1) was harvested (Section 2.2.4.2). *A. mellea* culture supernatants were frozen at -20 °C overnight, defrosted and centrifuged at 48,000 *g*, 30 min. This process induced polysaccharide precipitation which enabled retrieval of protein in the liquid fractions. An *A. mellea* specific protocol was designed (Section 2.2.7.5), whereby after addition of TCA (10% w/v), protein was precipitated and collected by centrifugation. The duration of this step was increased until there was

no further precipitation of protein. An initial time of 15 min was extended in 15 min increments to 45 min, which was found to be optimal. Even with this treatment, the colour of both precipitated and resolubilised protein was brown, indicating residual melanin, so 2-DE was not attempted. Due to the presence of residual contamination in resolubilised supernatant proteins, protein quantitation proved largely ineffective. Therefore, protein was resolubilised in 1 M DTT (10 µl), 10% (w/v) SDS (10 µl) and 5 X solubilisation buffer (10 µl), (Section 2.2.7.5) and fractionated by SDS-PAGE (Section 2.2.8.1).

The increased polysaccharide and melanin contamination in shaking cultures reduced the quantity of protein that could be retrieved, as a sticky dark brown pellet would not go into solution, and a brown residue remained in microfuge tubes. Figure 4.6 illustrates an exemplar SDS-PAGE analysis of proteins extracted from 200 ml *A. mellea* PDB liquid culture supernatants from shaking and static cultures respectively. Solubilised protein solution (80 µl) was obtained from static culture supernatants (200 ml), and solubilised protein solution (80 µl) was obtained from shaking culture supernatants (200 ml), and were loaded in aliquots (20 µl) onto gels (four lanes per each condition).

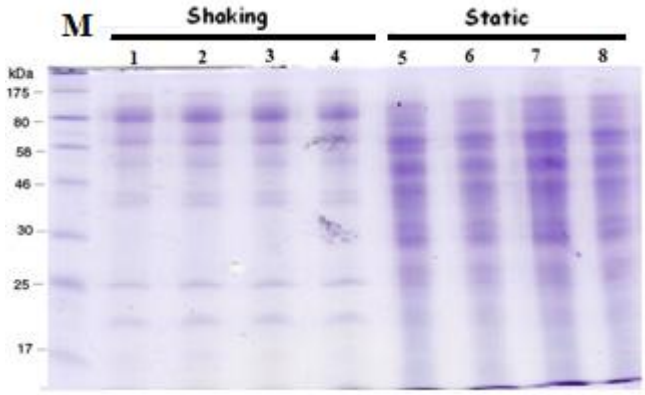

Figure 4.6. Comparative SDS-PAGE analysis of proteins extracted from *A. mellea* culture supernatants obtained after shaking and static culture. M, prestained marker; lanes 1 - 4, shaking cultures; lanes 5 - 8, static cultures. Each culture condition yielded solubilised protein solution (80 µl) which was loaded equally (20 µl) for SDS-PAGE. Static culture produced a higher protein yield than shaking culture conditions.

A range of media were used as carbon sources in order to explore if it was possible to induce specific enzyme expression: including lignin, xylan, cellulose, yeast extract and glucose (Section 2.1.3.9). Attempts were made to remove contaminating substances from protein in supernatants of *A. mellea* cultures grown on restricted carbon sources

but very little biomass was generated, with consequent reduction in the amounts of secreted protein. SDS-PAGE was carried out but in the case of xylan or lignin no clean banding pattern was visible on gels (Figure 4.7A, and B). Bands from both lignin and xylan culture supernatants were excised and trypsin-digested prior to LC-MS/MS analysis (Section 2.2.10.3).

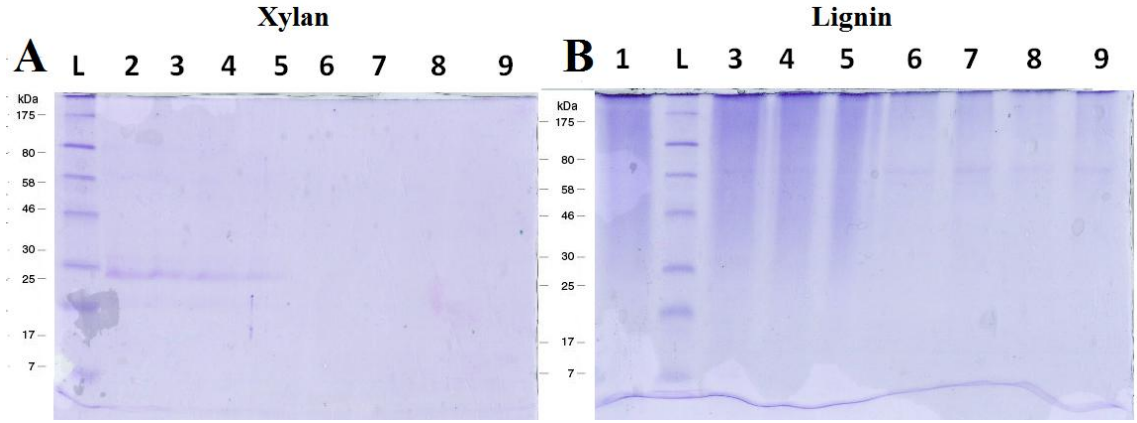

Figure 4.7. SDS-PAGE of supernatants from liquid cultures of *A. mellea* with (**A**) xylan and (**B**) lignin as carbon sources respectively. **A.** L, prestained marker; lanes 2 - 5 static culture and lanes 6 - 9 shaking culture. **B.** L, prestained marker; lanes 1, 3, 4, 5 shaking culture and lanes 6 – 9 static culture.

4.2.3 Mycelial protein identification by MALDI-ToF and LC-MS/MS following 2-DE.

A. mellea was grown for three weeks in PDB liquid culture (Section 2.2.4.1), harvested (Section 2.2.4.2), protein was extracted and subjected to 2-DE (Section 2.2.8.3). Protein spots (n = 206) from 2-DE shown in Figure 4.5 were excised and digested (Section 2.2.10.3) prior to MALDI (Section 2.2.14) and LC-MS/MS analysis (Section 2.2.15.2) using Program A (Table 2.6).

Proteins were identified by MALDI-ToF analysis (Table 4.1) in 47 2-DE spots with an E value ≤ 0.008 corresponding to 38 *A. mellea* genes from the *A. mellea* database. These proteins were also subsequently identified by LC-MS/MS with the exception of five proteins (Am1181, SH3 domain-containing protein; Am7248, unknown function protein; Am9971, phosphatidylinositol phosphate kinase, pipk5; Am13361, aldehyde dehydrogenase; Am16969, *A. mellea* specific protein of unknown function) which were identified solely by MALDI. Two proteins, alcohol oxidase-like proteins (Am13458, and Am9694) were identified from spot No. 79. Although homology of these two proteins is to an alcohol oxidase-like protein they have < 8 % similarity. There were

five proteins identified in more than one spot indicating the occurrence of protein isoforms or subunits of different molecular mass (Am17277, 5-methyltetrahydropteroyltriglutamate-homocysteine S-methyltransferase (cobalamin-independent methionine synthase), Spots 21 and 52; Am17600, peroxisomal catalase, Spots 1, 3 and 104; Am17796, phosphoglycerate kinase, Spots 2, 4 and 113; Am19381, 3-ketoacyl-CoA-thiolase (peroxisomal), Spots 115 and 117; Am6591, 1-cys peroxiredoxin, Spots 8 and 9). Sequence coverage ranged from 6 to 56% and only three proteins (Am1181, Am13458 and Am19464) had < 10 % sequence coverage. Five proteins (Am9971, Am12502, Am14558, Am16713 and Am18655) had transmembrane regions and two (Am10845 and Am9971) had classical secretion signals. A further seventeen possessed non-classical secretion signals.

Table 4.1. *A. mellea* mycelial proteins identified from by MALDI analysis subsequent to 2-DE (Figure 4.5).

[a]Accession No.	[b]BLAST description	Spot No.	[c]tM$_r$ (kDa)	[d]tp*I*	[e]MALDI E-value	Coverage (%)	[f]GRAVY Score	[g]TM	[h]SigP/ SecP	[i]Method	[j]Extraction
Am6591	1-cys peroxiredoxin	8	24.8	6.1	0	56.8	-0.404			MToF	M
Am6591	1-cys peroxiredoxin	9	24.8	6.1	0	44.5	-0.404			MToF	M
Am19381	3-ketoacyl-CoA-thiolase peroxisomal	115	40.32	6.3	0	20.4	0.088		SecP	MToF	M
Am19381	3-ketoacyl-CoA-thiolase peroxisomal	117	40.32	6.3	0	20.1	0.088		SecP	MToF	M
Am17277	5-methyltetrahydropteroyltriglutamate-homocysteine S-methyltransferase	21	84.5	6.4	0	25.6	-0.201			MToF	M
Am17277	5-methyltetrahydropteroyltriglutamate-homocysteine S-methyltransferase	52	84.5	6.4	0.001	20.3	-0.201			MToF	M
Am11823	Aconitate hydratase	22	84.59	6.2	0	10.8	-0.278		SecP	MToF	M
Am11275	Activator of Hsp70 and Hsp90 chaperones	23	64.89	5.8	0	24.8	-0.718			MToF	M
Am5210	Alanine transaminase	92	52.1	5.7	0.002	13.4	-0.139		SecP	MToF	M
Am13458	Alcohol oxidase-like protein	79	168.02	6.1	0	4.3	-0.313			MToF	M
Am9694	Alcohol oxidase-like protein	79	65.92	5.3	0	16.8	-0.286			MToF	M
Am13361	Aldehyde dehydrogenase	94	54.48	5.9	0.006	15.6	-0.125		SecP	MToF	M
Am19374	Aldehyde dehydrogenase	96	55.69	6.2	0.003	14.4	-0.227		SecP	MToF	M
Am19925	Aspartate ammonia lyase	100	54.69	7.2	0	13.6	-0.119		SecP	MToF	M
Am19833	Chaperone binding protein	149	22.05	5.4	0	48	-0.718		SecP	MToF	M

[a]Accession No.	[b]BLAST description	Spot No.	[c]tM$_r$ (kDa)	[d]tp*I*	[e]MALDI E-value	Coverage (%)	[f]GRAVY Score	[g]TM	[h]SigP/ SecP	[i]Method	[j]Extraction
Am8697	Glutamate carboxypeptidase	28	52.48	5	0	25.6	-0.218		SecP	MToF	M
Am19877	Glutamic oxaloacetic transaminase, aat1	41	45.79	8.6	0	21	-0.212		SecP	MToF	M
Am19877	Glutamic oxaloacetic transaminase, aat1	42	45.79	8.6	0	13.2	-0.212		SecP	MToF	M
Am12863	Glyceraldehyde-3-phosphate dehydrogenase	127	39.97	8.4	0.001	22.7	0.079		SecP	MToF	M
Am14651	Glycine hydroxymethyltransferase	105	52.32	6.8	0.001	10.6	-0.225		SecP	MToF	M
Am7160	Heat shock protein	53	74.69	5.5	0.002	16.2	-0.348			MToF	M
Am10845	Hsp70 chaperone	25	72.23	4.9	0	40	-0.391		SigP	MToF	M
Am18655	Ketol-acid reductoisomerase	49	90.56	9.6	0	17.8	-0.418	1		MToF	M
Am1779	Leucine aminopeptidase	83	51.18	5.6	0.002	17.2	-0.2			MToF	M
Am11036	Macrolide-binding protein fkbp12	18	11.58	6.1	0	64.8	-0.234			MToF	M
Am6119	Malate dehydrogenase NAD-dependent	7	33.81	8.8	0	53	0.291			MToF	M
Am6119	Malate dehydrogenase NAD-dependent	126	35.81	8.8	0.002	27.4	0.291			MToF	M
Am19464	mRNA transport regulator	99	148.89	5.3	0.005	6	-0.153			MToF	M
Am16969	*A. mellea* unknown function protein	45	39.89	6.5	0.004	15.2	-0.376		SecP	MToF	M
Am14790	P47 protein isoform c	65	41.01	4.8	0	30.4	-0.717		SecP	MToF	M
Am17600	Peroxisomal catalase	1	58.48	6.8	0.002	32.6	-0.587			MToF	M
Am17600	Peroxisomal catalase	3	58.48	6.8	0	26.4	-0.587			MToF	M
Am17600	Peroxisomal catalase	104	58.48	6.8	0.001	25	-0.587			MToF	M

[a]Accession No.	[b]BLAST description	Spot No.	[c]tM$_r$ (kDa)	[d]tp*I*	[e]MALDI E-value	Coverage (%)	[f]GRAVY Score	[g]TM	[h]SigP/ SecP	[i]Method	[j]Extraction
Am9971	Phosphatidylinositol phosphate kinase, pipk5	123	89.93	6.8	0	18.9	-0.586	2	SigP	MToF	M
Am17796	Phosphoglycerate kinase	2	45.91	5.9	0	16	0.006			MToF	M
Am17796	Phosphoglycerate kinase	4	45.91	5.9	0	41.2	0.006			MToF	M
Am17796	Phosphoglycerate kinase	113	45.91	5.9	0	27	0.006			MToF	M
Am20231	Phosphopyruvate hydratase	12	47.08	5.7	0	29.5	-0.108			MToF	M
Am12529	Potential stress response protein	61	45.46	4.3	0.004	13.7	-1.54			MToF	M
Am12502	Predicted protein [*Laccaria bicolor* S238N-H82]	114	58.67	6.2	0	17.4	-0.174	1		MToF	M
Am7248	Protein	24	67.43	5.5	0	33.6	-1.029			MToF	M
Am11784	Protein vip1	141	25.94	6.4	0.007	29.6	-0.458			MToF	M
Am19160	Ribose 5-phosphate isomerase	14	16.89	6.7	0.002	40.6	-0.003		SecP	MToF	M
Am8498	Set domain protein	13	50.74	5.4	0	19.5	-0.235			MToF	M
Am1181	SH3 domain-containing protein	95	105.42	8.2	0.005	8.9	-0.847			MToF	M
Am16713	Short-chain dehydrogenase	91	60.51	6.2	0	18.6	-0.032	1	SecP	MToF	M
Am14558	Valosin-containing protein	51	177.09	5.4	0	12.7	-0.258	3		MToF	M

[a]Accession number from *A. mellea* cDNA database; [b]Blast annotation following Blast2GO analysis of proteins identified from *A. mellea* cDNA database; [c]M$_r$, theoretical molecular mass; [d]tp*I*, theoretical isoelectric point; [e]MALDI E-value, expect value from MALDI analysis of proteins identified from *A. mellea* cDNA database; ; [f]GRAVY score, grand average of hydropathy (Negative score indicates hydrophilicity while Positive score indicates hydrophobicity); [g]TM, number of transmembrane regions; [h]SigP, classical secretion signal peptide; SecP, non-classical secretion signal; [i]Method, 2-DE proteins separated in two dimensions prior to MALDI ToF analysis, MToF; [j]Extraction: M, mycelia.

Excised spots from 2-DE were also analysed by LC-MS/MS. Chromatogram data was exported to Spectrum Mill for analysis and interrogation of the *A. mellea* database, applying settings described in Section 2.2.15.3. Two hundred and six spots were analysed and proteins identified from excised spots (n = 182). No proteins were identified from the remainder (n = 24). Spectrum Mill scores ranged from 11.05 to 433.00. Scores in the 9 – 13, range when combined with a SPI > 70 %, denote peptides of good quality with substantial peptide fragmentation according to Spectrum Mill guidelines (Table 2.7). Peptide score is a maximum of 25, therefore a score of 433 denotes a large number of high scoring peptides.

The number of proteins identified ranged from a single protein per spot up to ten proteins from a single spot (Spot No. 89) (Figure 4.5), and as with MALDI analysis protein isoforms were evident. Protein identification (n = 274) was supported by 1428 peptides after interrogation of the *A. mellea* database. Percentage coverage per protein ranged between 1% (n = 8) supported by 1 peptide and 81% (n = 1) supported by 11 peptides. Proteins in this dataset were supported by single peptide (n = 77), 2-5 peptides (n = 96), 6-10 peptides (n = 59) and 11-25 peptides (n = 27). The highest scoring mycelial proteins uniquely identified from LC-MS/MS are shown in Table 4.2.

Table 4.2. High scoring *A. mellea* mycelial proteins uniquely identified by LC-MS/MS analysis subsequent to 2-DE (Figure 4.5).

[a]Accession No.	[b]BLAST Annotation	[c]tM$_r$	[d]tp*I*	Coverage (%)	Unique Peptides	[e]SM Score	[f]GRAVY score	[g]TM	[h]SigP/ SecP	[i]TarP	[j]Method	[k]Extraction
Am14746	20S Proteasome Subunit	28961.1	7.02	28	8	127.39	-0.295		SecP		2-DE	M
Am18487	20S Proteasome Subunit	29717.2	8.9	7	2	26.31	-0.28				2-DE	M
Am19373	20S Proteasome Subunit	23637.2	5.38	23	3	49.03	-0.208				2-DE	M
Am11823	Aconitate Hydratase	84604.4	6.23	19	14	212.14	-0.278		SecP	Mt	2-DE	M
Am7572	Adenylate Kinase	36640.8	9.3	14	6	85.08	-0.402				2-DE	M
Am16947	Aldo Keto Reductase	78476.9	4.56	4	2	41.92	-0.457	1	SecP		2-DE	M
Am17876	Atpase V1 A1 Complex Subunit E	29102.4	7.82	34	7	109.55	-0.531				2-DE	M
Am18616	Citrate Synthase	50677	8.58	5	2	30.99	-1.025				2-DE	M
Am10545	Cytochrome-B5 Reductase	29149.7	8.79	10	2	39.44	-0.282				2-DE	M
Am18662	Dihydrodipicolinate Synthetase	33189.2	6.45	15	5	81.2	0.051				2-DE	M
Am19925	Fumarate Hydratase	54704.9	7.17	21	8	142.75	-0.119		SecP	Mt	2-DE	M
Am3968	Galactose Mutarotase-Like Protein	47051.2	5.43	9	3	47.07	-0.222				2-DE	M
Am7428	Heat Shock Protein 70	67452.9	5.51	43	22	390.54	-0.302				2-DE	M

[a]Accession No.	[b]BLAST Annotation	[c]tM$_r$	[d]tp*I*	Coverage (%)	Unique Peptides	[e]SM Score	[f]GRAVY score	[g]TM	[h]SigP/ SecP	[i]TarP	[j]Method	[k]Extraction
Am5827	Histone 2A	15403.9	10.69	11	1	14.03	-0.377		SecP		2-DE	M
Am11737	Hypothetical Protein Cmq 7689 [*Grosmannia clavigera* Kw1407]	31480.1	9.19	21	4	65.62	-0.316				2-DE	M
Am14390	Hypothetical Protein Serla73Draft_180097 [*Serpula lacrymans* Var. Lacrymans S7.3]	51109	4.8	6	2	32.75	-0.793		SecP		2-DE	M
Am9103	Hypothetical Protein Travedraft_26989 [*Trametes versicolor* Fp-101664 Ss1]	9374.6	9.15	43	2	39.82	-0.38		SecP		2-DE	M
Am15767	Mitochondrial Carrier	53645.5	6.21	4	2	37.65	-0.027				2-DE	M
Am14771	Mitochondrial Pyruvate Dehydrogenase E1 Component Beta Subunit	44318.5	6.25	14	6	110.57	-0.379			Mt	2-DE	M
Am17114	Mn Superoxide Dismutase	24551	7.94	12	3	44.61	-0.329		SecP	Mt	2-DE	M
Am14873	Monooxygenase FAD-Binding	43718.9	5.41	24	9	110.35	-0.325				2-DE	M

[a]Accession No.	[b]BLAST Annotation	[c]tM$_r$	[d]tp*I*	Coverage (%)	Unique Peptides	[e]SM Score	[f]GRAVY score	[g]TM	[h]SigP/ SecP	[i]TarP	[j]Method	[k]Extraction
Am17269	Mov34-Domain-Containing Protein	40774.1	5.75	6	2	28.4	-0.587				2-DE	M
Am9808	NAD -Binding Protein	37185.5	5.8	10	3	40.96	-0.181				2-DE	M
Am11624	NADH Dehydrogenase	43310.3	6.38	4	2	27.77	-0.281				2-DE	M
Am19009	O-Methyltransferase Family 3 Protein	24976.5	5.81	18	2	36.69	-0.142				2-DE	M
Am16589	Peptidyl-Prolyl Cis-Trans Isomerase	11653.6	5.84	20	2	30.28	0.011				2-DE	M
Am14569	Predicted Protein [*Laccaria bicolor* S238N-H82]	30523.7	6.86	8	2	25.97	-0.218				2-DE	M
Am12246	Predicted Protein [*Postia placenta* Mad-698-R]	24544	6.98	18	3	56.85	-0.38		SecP		2-DE	M
Am5361	Probable Ubiquitin-Like Protein Ubl1	8625.1	8.09	41	2	36.28	-0.36		SecP		2-DE	M
Am19014	Proteasome Subunit Alpha Type 4	62364.2	5.21	14	7	126.29	-0.27				2-DE	M
Am17973	Protein Disulfide Isomerase	56038.7	4.74	10	4	73.3	-0.449		SigP		2-DE	M
Am20247	Protein Disulfide Isomerase	81758.1	5.71	12	8	126.55	-0.364		SigP		2-DE	M

[a]Accession No.	[b]BLAST Annotation	[c]tM$_r$	[d]tp*I*	Coverage (%)	Unique Peptides	[e]SM Score	[f]GRAVY score	[g]TM	[h]SigP/ SecP	[i]TarP	[j]Method	[k]Extraction
Am17183	Proteolysis And Peptidolysis-Related Protein	24178.3	5.81	9	2	32.24	-0.359				2-DE	M
Am12194	PRTase-Like Protein, armadillo/beta-catenin/plakoglobin	26262.6	5.63	13	2	40.15	0.021				2-DE	M
Am6597	Related To Sodium-Calcium Exchangers	102126.5	6.26	7	4	67.88	0.026	1	SigP		2-DE	M
Am18435	Rhogap-Domain-Containing Protein [*Stereum hirsutum* Fp-91666 Ss1]	152887.8	9.17	2	3	52.97	-0.429				2-DE	M
Am15110	RNA-Binding Domain-Containing Protein	42099.1	9.22	5	2	30.3	-1.166	1			2-DE	M
Am8591	S-Adenosyl-L-Methionine-Dependent Methyltransferase	30909.1	6.01	35	8	133.71	-0.28				2-DE	M
Am7403	Serine Threonine Kinase Receptor Associated Protein	57616.5	7.46	6	2	36.64	-0.4		SecP		2-DE	M
Am19833	SGS-Domain-Containing Protein	22070.9	5.38	30	6	95.48	-0.718		SecP		2-DE	M

[a]Accession No.	[b]BLAST Annotation	[c]tM$_r$	[d]tp*I*	Coverage (%)	Unique Peptides	[e]SM Score	[f]GRAVY score	[g]TM	[h]SigP/ SecP	[i]TarP	[j]Method	[k]Extraction
Am13591	Short-Chain Dehydrogenase	30863.8	8.81	16	3	48.02	-0.119		SecP		2-DE	M
Am4143	Tautomerase Mif	13132.2	9.26	14	2	32.87	-0.055		SecP		2-DE	M
Am4272	Thiazole Biosynthetic Enzyme	33239.5	5.89	19	4	74.17	0.108		SecP		2-DE	M
Am10094	Thioredoxin Reductase	36226.3	5.35	22	6	96.61	-0.158				2-DE	M
Am19476	Transcription Factor	65206.1	5.93	4	2	29.42	-0.265				2-DE	M
Am17950	Ubc-Like Protein	15434.7	6.07	36	4	64.01	-0.475		SecP		2-DE	M
Am19982	Ubiquitin-Conjugating Enzyme E2-24 kDa	21115.1	6.31	23	4	74.78	-0.306				2-DE	M
Am16629	Urease Accessory Protein	23477.8	5.04	34	5	78.08	-0.11				2-DE	M
Am16451	Uridine Nucleosidase	72404.4	5.97	5	2	36.07	-0.234		SecP		2-DE	M

[a]Accession number from *A. mellea* cDNA database; [b]Blast annotation following Blast2GO analysis of proteins identified from *A. mellea* cDNA database; [c]M$_r$, theoretical molecular mass; [d]tp*I*, theoretical isoelectric point; [e]SM score, Spectrum Mill protein score; [f]GRAVY score, grand average of hydropathy (Negative score indicates hydrophilicity while Positive score indicates hydrophobicity); [g]TM, number of transmembrane regions; [h]SigP, classical secretion signal peptide; SecP, non-classical secretion signal; [i]TarP, subcellular location of proteins, Mt, mitochondrial targeting peptide; [j]Method: 2-DE prior to LC-MS/MS analysis, 2-DE proteins separated in two dimensions prior to LC-MS/MS analysis, [k]Extraction: M, mycelia.

Figure 4.8 provides an overview of the total number of proteins identified after 2-DE fractionation (Figure 4.5) and mass spectrometry. The superiority of LC-MS/MS over MALDI-ToF analysis for protein identification is clearly evident. Data pertaining to identification of each protein spot in Figure 4.5 are outlined in Appendix A.1 (Accompanying CD file Master Tables Appendices.docx).

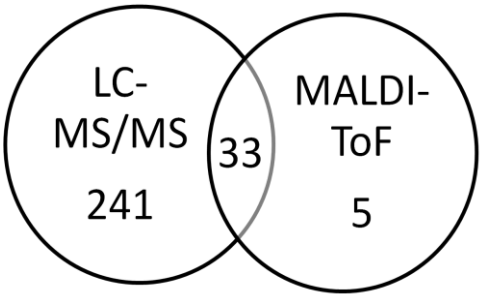

Figure 4.8. Identification of *A. mellea* mycelial proteins following 2-DE and mass spectrometry analysis. Overall, 279 proteins were identified, five uniquely by MALDI, 33 by both methods and 241 proteins were only detected by LC-MS/MS.

All details of proteins identified from 2-DE are shown in Appendix A.2 and A.3 (Accompanying CD file Master Tables Appendices.docx). Eight percent of these proteins (n = 23) possess transmembrane regions, 54% have secretion signals (SignalP (7%) and SecretomeP (46%); (n = 20 and 128, respectively) and 12% (n = 35) exhibit GRAVY scores denoting hydrophobic proteins. The number of transmembrane domains per protein ranged between one (n = 16 proteins), two (n = 4) three (n = 1) and five (n = 1).

B2G analysis generates hierarchical graphs, directed acyclic graphs (DAG) of GO annotated proteins (Götz *et al.*, 2008). Scores are assigned to nodes based on the number of sequences and distance from the parent node. This is illustrated by DAG analysis of molecular functions of *A. mellea* mycelial proteins (Figure 4.9). Further B2G analysis was used to reduce the complexity of large datasets and give an overview of combined annotation. Multilevel graphs were generated from combined data analysis whereby the lowest ranked nodes on each branch are visualised together. The numbers of proteins in a multilevel chart represent the numbers of proteins with a particular GO designation. Thus peptidase activity is a subset of hydrolase activity, but does not include all proteins involved in hydrolysis (Figure 4.9). Therefore the number of proteins in a multilevel chart does not represent all of the proteins in a dataset, only the

lowest hierarchical level and serves to give a broad overview of the data. Data in Figure 4.9 is shown as a multilevel chart in Figure 4.10.

B2G multilevel datasets were produced for molecular function (Figure 4.10), biological process (Figure 4.11) and cellular component (Figure 4.12). When categorised by molecular function, GO analysis revealed that nucleotide binding proteins (44%) were most abundant. Protein binding proteins (22%), peptidase activity (10%), and kinase activity (6%) were lower. Proteins with transporter (5%) and DNA binding functions were also identified, as well as RNA and electron carrier activity proteins (Figure 4.10) each accounting for 4%, respectively.

The largest cohort in biological process is catabolic process (27%), carbohydrate metabolic process (18%) was next ranking, succeeded by generation of precursor metabolites and energy, which give the same percentage as nucleic acid metabolic processes (14%). Regulation of biological process (8%) ensues in ranking and secondary metabolic process (5%) is next. Translation and response to stress have the same with 4% each, respectively. Ion transport and lipid metabolic process (3%) are the lowest ranking GOs in this category (Figure 4.11).

When categorised by cellular component, the largest grouping are proteins involved in protein complexes (40%). Nuclear protein representation was 20%, cytoskeleton and mitochondrial proteins were 12% each. Ribosome (9%) and cytosol (7%) proteins were lowest in this category (Figure 4.12).

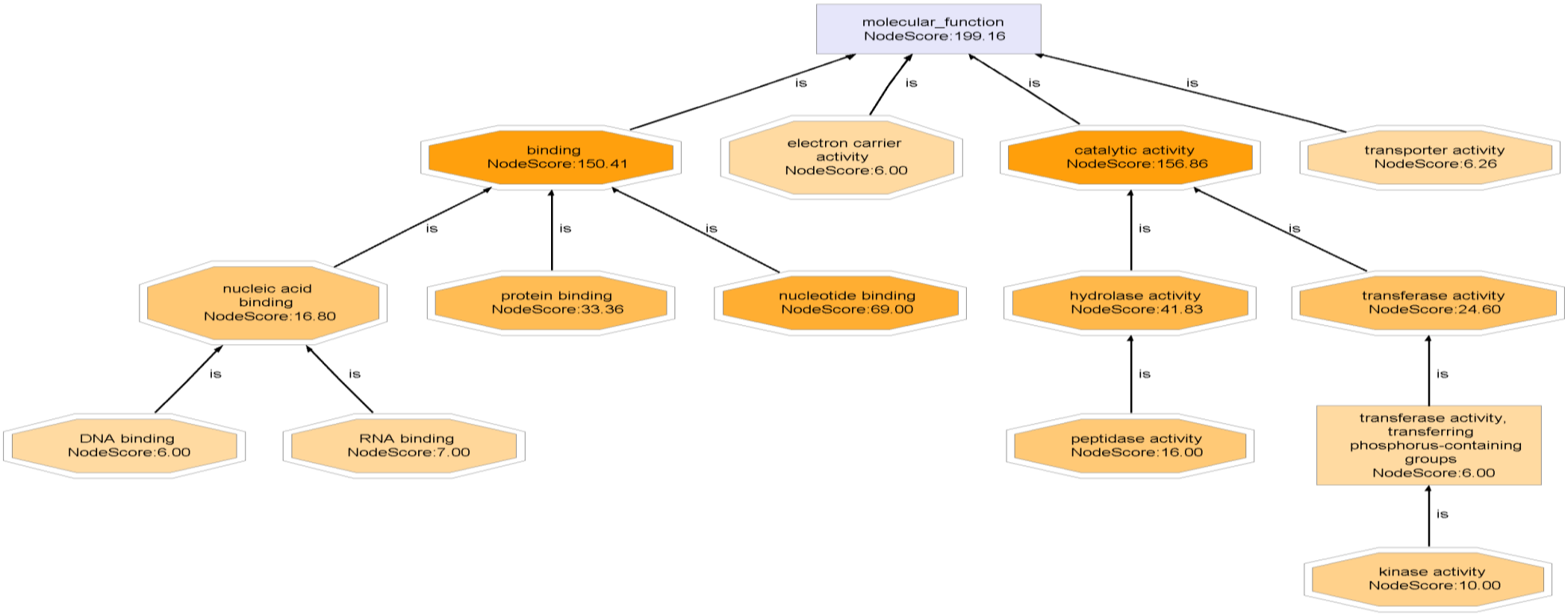

Figure 4.9. Directed acyclical graph (DAG) of *A. mellea* mycelial analysis of GO annotation identified from MALDI-ToF and LC-MS/MS analysis. Nodes associated with < 6 sequences have been eliminated for enhanced clarity. GO annotation hierarchy of protein molecular functions from this dataset is illustrated Scores are based on the number of sequences and proximity to parent nodes. Colour intensity varies with the proportionality of the score the more intense colours denoting more proteins. Data from the lowest node on each branch can be grouped in a multilevel chart enabling less complicated visualisation of data (Figure 4.10).

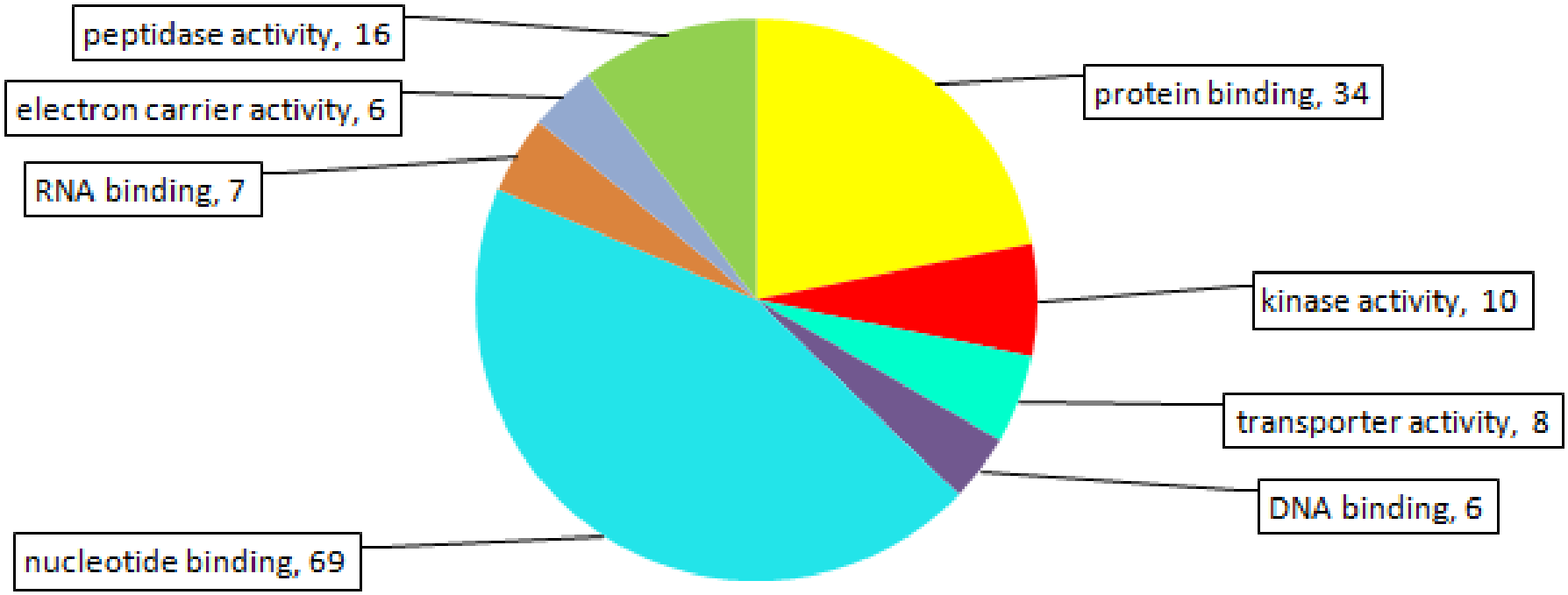

Figure 4.10. Molecular Function. GO multilevel representation of *A. mellea* mycelial proteins fractionated by 2-DE followed by MALDI-ToF and LC-MS/MS analysis; identification of molecular function property domains defined by http://www.geneontology.org. GO annotation from the lowest nodes of GO hierarchy in the category of molecular function is shown. Numbers indicate the number of proteins in each category. A DAG of this data is shown in (Figure 4.9).

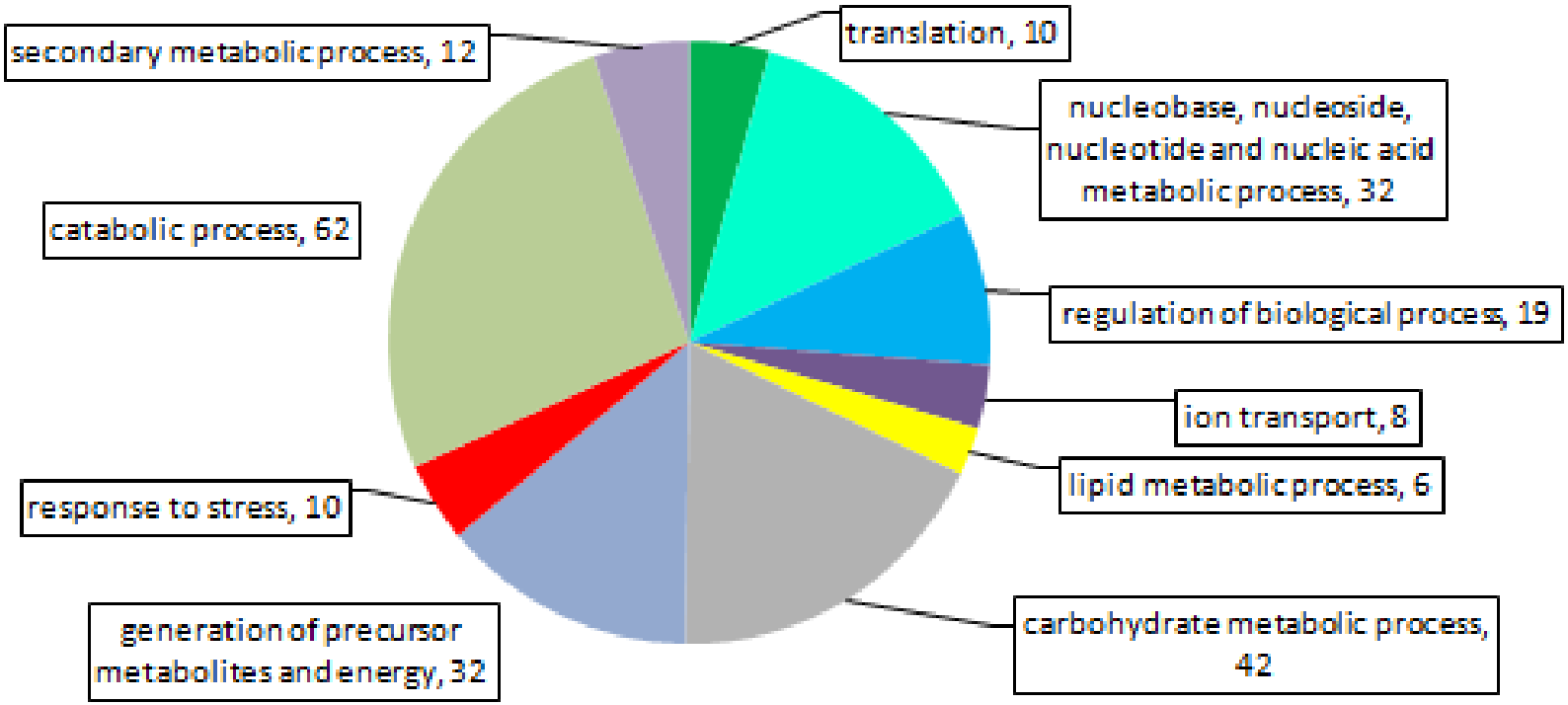

Figure 4.11. Biological process. GO multilevel representation of *A. mellea* mycelial protein fractionated by 2-DE followed by MALDI-ToF and LC-MS/MS analysis; identification of biological process property domains defined by http://www.geneontology.org. Visualisation of GO annotations is from the lowest nodes of GO hierarchy, in the category of biological process. Numbers indicate the number of proteins in each category.

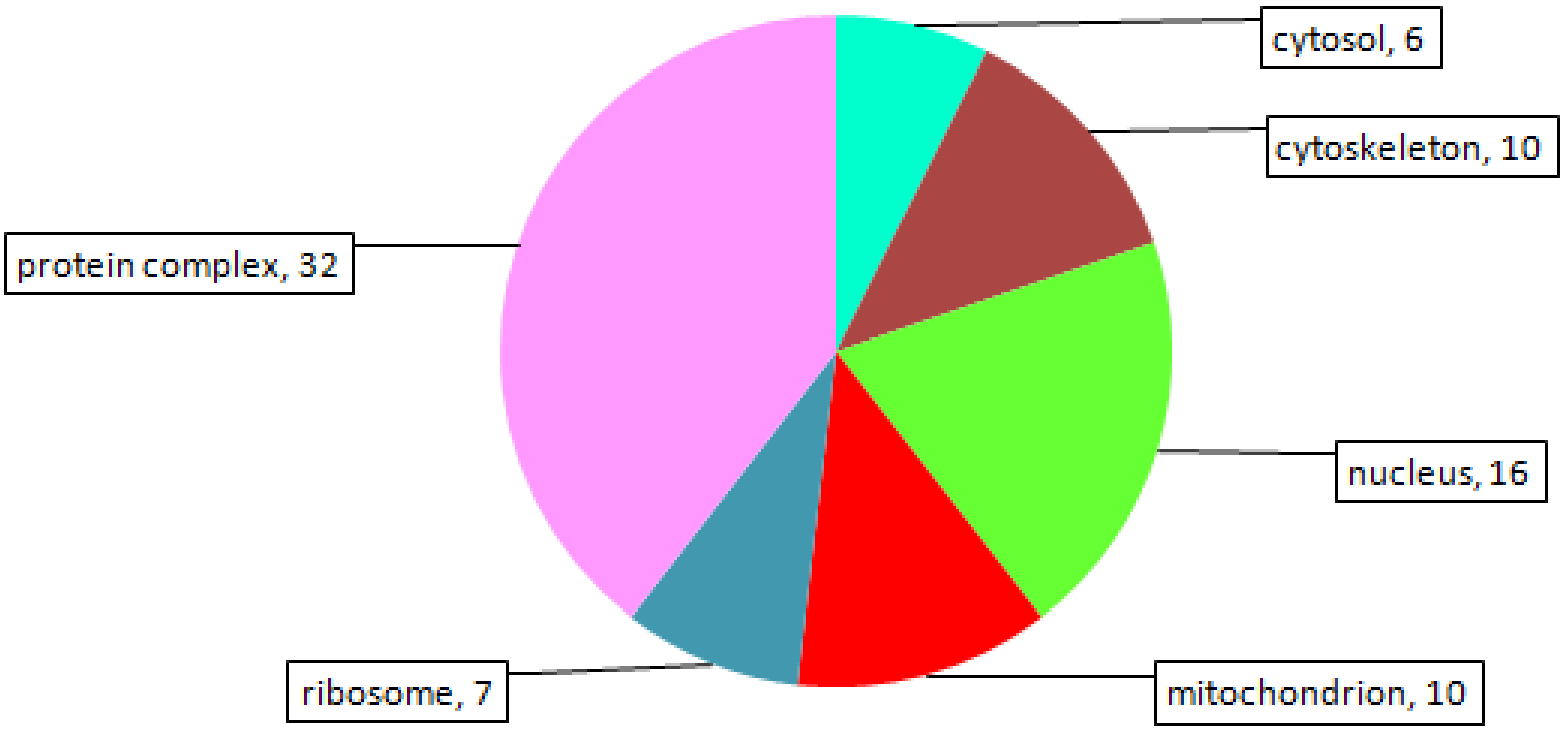

Figure 4.12. Cellular Component. GO multilevel representation of *A. mellea* mycelial proteins fractionated by 2-DE followed by MALDI-ToF and LC-MS/MS analysis; identification of cellular component property domains defined by http://www.geneontology.org. Visualisation of GO annotation is from the lowest nodes of GO hierarchy, in the cellular component category. Numbers indicate the number of proteins in each category.

Figure 4.13 illustrates the distribution actual of proteins identified following 2-DE separation and MALDI and LC-MS/MS analysis compared with predicted *A. mellea* proteins based on theoretical M_r and p*I* data using software from Hiller *et al.* (2006) http://www.jvirgel.de. The genome map shows a grouping of low pH (pH 4 – 7) and a second less dense, smaller grouping at higher pH (pH 7.5 – 10.13). The theoretical p*I* range is pH 4.18 -10.13 and theoretical M_r range is 7 – 391 kDa (Figure 4.13).

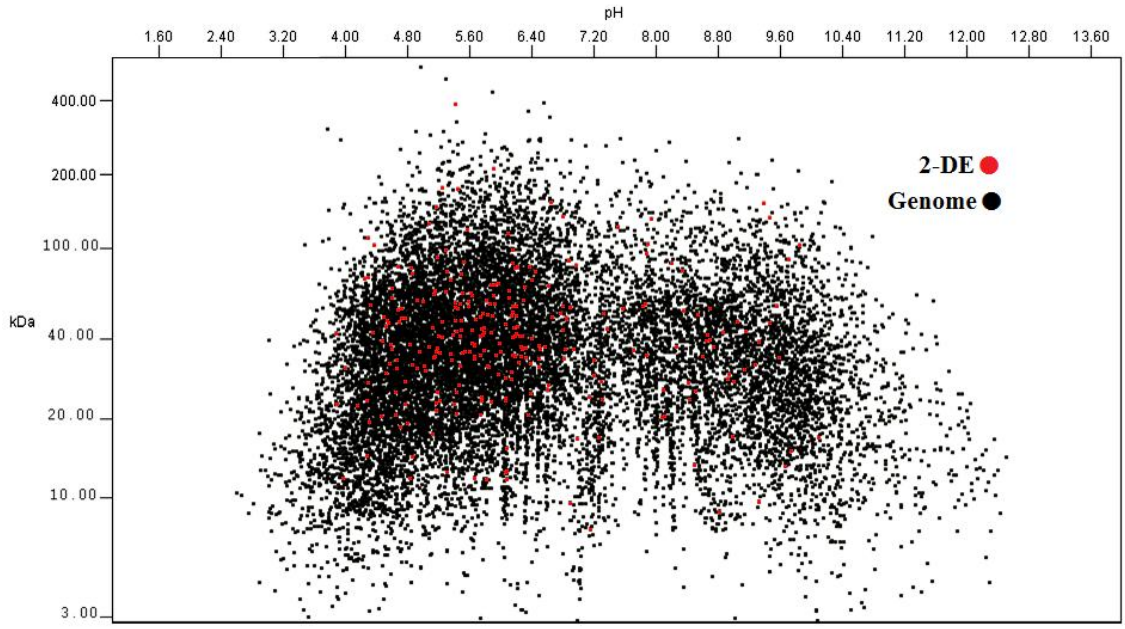

Figure 4.13. Alignment of theoretical M_r and p*I* from *A. mellea* genomic predicted proteins and 2-DE proteomic data. (Software: http://www.jvirgel.de (Hiller *et al.*, 2006)).

Representatives of some *A. mellea* gene categories described in the genome analysis of protein families (Section 3.2.3) were identified at protein level. CAZys identified were three each of GH, CE, plus one CBM (Am9123). Two proteins were categorised as metalloproteins (Am10231 and Am18955). Five oxygenases (Am7250, Am11579, Am14873, Am16713 and Am18657), three oxidoreductases (Am247, Am252 and Am13662) and three oxidases (Am9694, Am13458 and Am18337) were determined at protein level. Two proteins were recognised as 40S ribosomal proteins (Am16109 and Am17877) and one as a 60S ribosomal protein (Am19273). Three superoxide dismutases were distinguished (Am1068, Am17114 and Am18409) as were five peptidases. The complement of proteins grouped as "predicted proteins" (n = 6) were Am7248, Am8356, Am10757, Am12246, Am14569 and Am19891, and nineteen proteins were ranked as hypothetical, whose presence is now confirmed. Two proteins,

Am2320 and Am16969, were not identified by BLAST and can be classified as *A. mellea*-specific unknown function proteins.

4.2.4 Secretome protein identification by LC-MS/MS following SDS-PAGE.

A. mellea was grown for 3 - 6 weeks in liquid culture (Section 2.2.4.1), harvested, mycelia stored at – 70 °C and supernatant frozen at –20 °C prior to separation (Section 2.2.4.2). Protein was separated by SDS-PAGE (Section 2.2.7.5). Alternatively *A. mellea* was grown on solid media (Figure 4.1) (Section 2.2.3.3), protein extracted and solubilised (Section 2.2.7.7) prior to SDS-PAGE. Samples were subjected to gel electrophoresis (Section 2.2.8.1), stained (Section 2.1.6.11) and destained (Section 2.1.6.12). Gel bands were excised and digested (Section 2.2.15.2) prior to LC-MS/MS analysis (Section 2.2.15.2) using Program A (Table 2.6). Spectrum Mill software was used to analyse chromatograms from LC-MS/MS using the settings described in Section 2.2.15.3.

Overall 340 proteins were identified in *A. mellea* culture supernatants based on LC-MS/MS detection of 1019 peptides. Numbers of unique peptides per protein were as follows: single peptide (n = 178), 2-5 peptides (n = 128), 6-10 peptides (n = 30) and 11-15 peptides (n = 4).

With regard to structural features of supernatant proteins, 9% (n = 32) were determined to have transmembrane regions, SignalP 41% (n = 141) and SecretomeP 33% (n = 113) sequences were identified in this dataset of *A. mellea* supernatant proteins, therefore 74% of supernatant proteins had secretion signals. Twenty proteins had one transmembrane domain, six had two transmembrane domains and three, four, six, seven and nine domains were identified in one protein each. GRAVY scores indicated that 24% (n = 82) were hydrophobic proteins. Theoretical p*I* values were between pH 4.05 and 10.52. High scoring proteins from the cohort of secreted proteins is shown in Table 4.3 and a complete list of identified proteins and their associated data can be found in the Appendix A.3 A.4 (Accompanying CD file Master Tables Appendices.docx)..

Table 4.3. High scoring *A. mellea* culture supernatant proteins identified by SDS-PAGE followed by LC-MS/MS, uniquely identified by this method.

[a]Accession No.	[b]BLAST Annotation	[c]tM$_r$	[d]tp*I*	Coverage (%)	Unique Peptides	[e]SM Score	[f]GRAVY score	[g]TM	[h]SigP/ SecP	[i]TarP	[j]Method	[k]Extraction
Am19553	Af411251_1Cellulase, Cel6B	46891.4	4.54	19	7	123.23	-0.014		SigP		1D	Sn
Am5540	Alcohol Oxidase	63989.9	4.6	11	6	97.57	-0.079		SigP		1D	Sn
Am19545	Alpha Beta-Hydrolase	58494.9	4.37	11	4	78.62	0.112		SigP		1D	Sn
Am9991	Aspartic Peptidase A1	44506.6	5.4	12	4	69.26	0.006		SigP		1D	Sn
Am13346	Beta-Lactamase Transpeptidase-Like Protein	69309.3	4.92	4	2	46.4	-0.05		SigP		1D	Sn
Am14725	Carbohydrate Esterase Family 16	32583.4	4.19	31	5	101.79	0.001		SigP		1D	Sn
Am18408	Carbohydrate-Binding Module Family 1	35316.9	4.83	10	2	36.26	-0.253		SigP		1D	Sn
Am4493	Cellobiohydrolase I	48830.8	4.34	12	4	80.6	-0.338		SigP		1D	Sn
Am20101	Dyp-Type Peroxidase	56528.5	5.68	17	6	102.42	-0.293		SecP		1D	Sn
Am19126	Exo-β-Glucanase	81585.6	5.22	7	4	61.94	0.084		SigP		1D	Sn
Am17701	Exosome Component Rrp46	53733.3	5.2	13	4	83.91	-0.032		SigP		1D	Sn
Am11027	FAD FMN-Containing Dehydrogenase	56692.7	5.08	13	6	97.48	-0.005		SigP		1D	Sn

[a]Accession No.	[b]BLAST Annotation	[c]tM$_r$	[d]tp*I*	Coverage (%)	Unique Peptides	[e]SM Score	[f]GRAVY score	[g]TM	[h]SigP/ SecP	[i]TarP	[j]Method	[k]Extraction
Am12548	Family S53 Protease	68638	4.42	13	4	86.18	0.151		SigP		1D	Sn
Am10289	Glycoside Hydrolase Family 115	114008	4.55	2	2	40.53	-0.094		SigP		1D	Sn
Am17847	Glycoside Hydrolase Family 13	56284.6	4.94	5	3	58	-0.24		SigP		1D	Sn
Am14157	Glycoside Hydrolase Family 15	61191.1	4.56	11	4	68.88	0.016		SigP		1D	Sn
Am18038	Glycoside Hydrolase Family 16	39327.9	6.39	17	5	80.3	-0.114		SigP		1D	Sn
Am9564	Glycoside Hydrolase Family 20	59239.4	4.75	7	3	42.51	-0.083		SigP		1D	Sn
Am4117	Glycoside Hydrolase Family 3	66127.4	4.54	6	4	59.81	0.014	1	SecP		1D	Sn
Am14693	Glycoside Hydrolase Family 37	71119.8	4.35	6	3	44.78	-0.258		SigP		1D	Sn
Am13752	Glycoside Hydrolase Family 47	59389.7	4.97	32	15	282.75	-0.154		SigP		1D	Sn
Am15965	Glycoside Hydrolase Family 5	46113.4	4.8	25	6	108.18	-0.212		SigP		1D	Sn
Am18634	Glycoside Hydrolase Family 79	38585.2	4.86	19	5	84.99	-0.019		SecP		1D	Sn
Am17712	Glycoside Hydrolase Family 92	87085.9	4.84	15	7	112.69	-0.203		SigP		1D	Sn
Am7125	Glycoside Hydrolase Family 95	89157.1	4.8	13	8	125.65	-0.138				1D	Sn
Am16182	GMC Oxidoreductase	76670.5	4.83	16	7	114.65	-0.127		SigP		1D	Myc, Sn
Am13156	Hypothetical Protein Fommedraft_141224 [*Fomitiporia mediterranea* Mf3/22]	72243.6	4.96	25	10	177.07	-0.065		SigP		1D	Sn

[a]Accession No.	[b]BLAST Annotation	[c]tM$_r$	[d]tp*I*	Coverage (%)	Unique Peptides	[e]SM Score	[f]GRAVY score	[g]TM	[h]SigP/ SecP	[i]TarP	[j]Method	[k]Extraction
Am712	Hypothetical Protein Fommedraft_167770 [*Fomitiporia mediterranea* Mf3/22]	25236.3	5.1	13	3	45.18	-0.16		SecP		1D	Sn
Am18468	Hypothetical Protein Punstdraft_133002 [*Punctularia strigosozonata* Hhb-11173 Ss5]	52294.9	4.19	36	10	162.51	-0.272		SigP		1D	Sn
Am15281	Hypothetical Protein Stehidraft_82680 [*Stereum hirsutum* Fp-91666 Ss1]	27023.3	4.74	17	2	42.8	-0.072		SigP		1D	Sn
Am18005	Hypothetical Protein Travedraft_135035 [*Trametes versicolor* Fp-101664 Ss1]	89492	5.2	5	3	51.09	-0.468				1D	Sn
Am380	Laccase	56590.2	4.6	10	4	62.73	-0.019		SigP		1D	Sn
Am12382	Laccase 5	74949.3	5.74	10	6	94.18	0.083		SigP		1D	Sn
Am4666	Laccase Lcc5	27495.1	5.03	17	3	63.52	-0.115		SecP		1D	Sn
Am10767	LCCL Domain-Containing Protein	96791.9	5.18	2	2	34.17	0.067	9	SecP		1D	Sn
Am9721	Metalloprotease MEP2	80032.8	4.81	10	5	63.33	-0.123		SigP		1D	Sn

[a]Accession No.	[b]BLAST Annotation	[c]tM$_r$	[d]tp*I*	Coverage (%)	Unique Peptides	[e]SM Score	[f]GRAVY score	[g]TM	[h]SigP/ SecP	[i]TarP	[j]Method	[k]Extraction
Am5632	*A. mellea* unknown function protein	16183.3	5.1	23	3	48.67	-0.519				1D	Sn
Am15498	Neutral Alkaline Non-lysosomal Ceramidase	88910.3	5.05	17	10	165.42	-0.095		SecP		1D	Sn
Am16332	Oxalate Decarboxylase	27226.4	4.45	14	3	48.74	-0.235		SecP		1D	Sn
Am9981	Peptidase S28	60574.4	4.59	16	7	123.41	-0.061		SigP		1D	Sn
Am711	PhoD-Like Protein [*Pholiota nameko*]	26324.3	5.18	23	4	75.25	-0.26				1D	Sn
Am5682	Polysaccharide Lyase Family 1 Protein	33293.1	5.36	44	7	131.31	0.011		SigP		1D	Sn
Am1482	Pore-Forming Toxin-Like Protein Hfr-2 [*Triticum aestivum*]	37463.6	5.08	12	3	51.79	-0.382	1			1D	Sn
Am18603	Predicted Protein [*Laccaria bicolor* S238N-H82] Predicted: Uncharacterized Protein Loc100241465 [*Vitis Vinifera*]	41446.1	5.39	10	3	53.86	-0.492				1D	Sn
Am16001	Rhamnogalacturonan Acetylesterase	63120.7	4.63	7	3	64.06	-0.119		SigP		1D	Sn

[a]Accession No.	[b]BLAST Annotation	[c]tM_r	[d]tp*I*	Coverage (%)	Unique Peptides	[e]SM Score	[f]GRAVY score	[g]TM	[h]SigP/ SecP	[i]TarP	[j]Method	[k]Extraction
Am16269	Serine Carboxypeptidase	49333.5	4.82	15	4	65.81	0.032		SigP		1D	Sn
Am9367	Serine Protease	39340.7	4.71	24	6	108.68	0.173		SigP		1D	Sn
Am20245	Subtilisin-Like Protein	65001	4.59	16	7	144.09	-0.105		SigP		1D	Sn
Am9695	SurE-Like Protein	32123	4.08	14	4	88.65	0.217		SigP		1D	Sn

[a]Accession number from *A. mellea* cDNA database; [b]Blast annotation following Blast2GO analysis of proteins identified from *A. mellea* cDNA database; [c]M_r, theoretical molecular mass; [d]tp*I*, theoretical isoelectric point; [e]SM score, Spectrum Mill protein score; [f]GRAVY score, grand average of hydropathy (Negative score indicates hydrophilicity while Positive score indicates hydrophobicity); [g]TM, number of transmembrane regions; [h]SigP, classical secretion signal peptide; SecP, non-classical secretion signal; [i]TarP, subcellular location of proteins, Mt, mitochondrial targeting peptide; [j]Method: 1D, SDS-PAGE prior to LC-MS/MS analysis; [k]Extraction: Sn, culture supernatant.

A range of culture conditions and media were used to induce the broadest possible spectrum of protein expression. However, as mentioned previously restricted carbon sources and shaking culture conditions were not conducive to protein identification, as melanin and polysaccharide contamination proved impossible to eliminate. There were greater numbers of proteins identified from cultures grown on rich media such as yeast extract (n = 60, peptides n = 141) and PDB (n = 69, peptides n = 208) than were identified from cultures grown on restricted media. In glucose media, the number of proteins identified in supernatants was low (n = 14, identified from peptides n = 30). Sequence coverage of between 3% and 59% was observed for proteins (n = 4) from culture supernatants of *A. mellea*, grown with xylan as sole carbon source and 5% coverage (one peptide) of one protein in lignin media. No secreted proteins were uniquely identified from *A. mellea* cultures grown on xylan or lignin. Culture supernatant proteins (n = 41; peptides n = 290) were identified from *A. mellea* grown on MEA media, although none was uniquely identified from this growth condition. One protein (Am1200, a cupredoxin) was uniquely identified from supernatant proteins of grapevine media.

In the supernatants protein cohort CAZys identified were: GH proteins (n = 50) from 23 families and CE (n = 7) from three families, one CBM (Am18404) and one PL (Am5682).

Ten oxidases were identified including four peroxidases (Am14136, Am14782, Am18093 and Am20201) and one oxygenase (Am12382). Five oxidoreductases (Am8112, Am14850, Am15833, Am16182 and Am18195) plus five laccases (Am380, Am2859, Am4665, Am4666 and Am12382) were distinguished in the secretome. Twelve peptidases were among the secreted proteins identified. Ribonuclease (Am15975), ribosomal (Am10216) and ribonuclease (Am15893) proteins were identified in the secretome dataset. Superoxide dismutase (SOD) (n = 4) Am1068, Am16731, Am18409 and Am19270 were identified in the secretome. *A. mellea* predicted proteins (n = 15) actually identified in culture supernatants were predominantly proteins (n = 12) that had been previously only predicted from a genome analysis of *L. bicolor*. Previously classed hypothetical proteins (n = 30) were also abundant in the secretome. Eight *A. mellea* specific proteins were identified within the secreted protein cohort (Am1874, Am2320, Am5632, Am9253, Am11032, Am11414, Am13545 and Am13611).

Proteins were identified from shaking cultures (n = 18), after LC-MS/MS analysis (Am11054, Am12518, Am13739, Am13890, Am14850, Am15111, Am15133, Am15833, Am15965, Am16182, Am16201, Am16331, Am17712, Am17847, Am18369, Am1857, Am19794, and Am4047), no proteins were uniquely identified from shaking cultures, therefore protein attributes are included with details of proteins identified from static cultures.

B2G, and GO were used to annotate secreted proteins under three categories: biological process, cellular component and molecular function. GO multilevel analysis of biological functions is illustrated in Figure 4.14. Consistent with the protein identification, carbohydrate metabolic process comprises almost 31% of the GO annotation. Catabolic process accounts for 24%, protein metabolism 16% and generation of precursor metabolites and energy (9%).

The balance of the proteins identified are involved in regulation and signalling: secondary metabolic process (7%), lipid metabolic process (6%), cellular amino acid and derivative metabolic process (6%), response to stress (5%), regulation of biological process (3%), ion transport (2%), homeostasis (2%), translation (2%) and transcription, cell cycle, response to abiotic stimulus, and cell component organisation were 1% each.

Multilevel cellular component annotation by GO (Figure 4.15), illustrate protein complex proteins which account for 34%, extracellular proteins 19%, nuclear proteins 13% and endoplasmic reticulum 9%. GO annotation shows equal proportions of ribosome, mitochondrial, cytosolic and cytoskeleton proteins (6%).

Multilevel GO representation of secreted proteins categorised by molecular function is shown in Figure 4.16. Peptidase activity is shown as the largest component (24%) and is represented by fifteen proteins (Am1995, carboxypeptidase cpdS precursor; Am3212, zinc metallopeptidase found in the cytoplasm and intermembrane space of mitochondria; Am5484, proteasome beta 4 subunit; Am6964, tripeptidyl peptidase A; Am7447, 26s proteasome regulatory subunit 6b; Am9367, serine protease; Am9991, aspartic peptidase A1; Am11985, carboxypeptidase 4; Am12548, family s53 protease-like protein; Am13286, pepsinogen 2; Am13665, proteasome subunit alpha type 5; Am15698, mitochondrial processing peptidase beta mitochondrial precursor (β-mpp); Am18243, tripeptidyl peptidase A; Am18773, aspartic peptidase A1; Am20245, tripeptidyl peptidase A). Nucleotide binding exhibits 23%, carbohydrate binding 15% and antioxidant activity 11%, representation under GO analysis of molecular function.

Nutrient reservoir, transporter and kinase followed, all at 5 %, nuclease proteins were at 3%. RNA binding, calcium ion binding, motor activity, actin-binding structural molecule activity and translation factor activity were portrayed at 2 %.

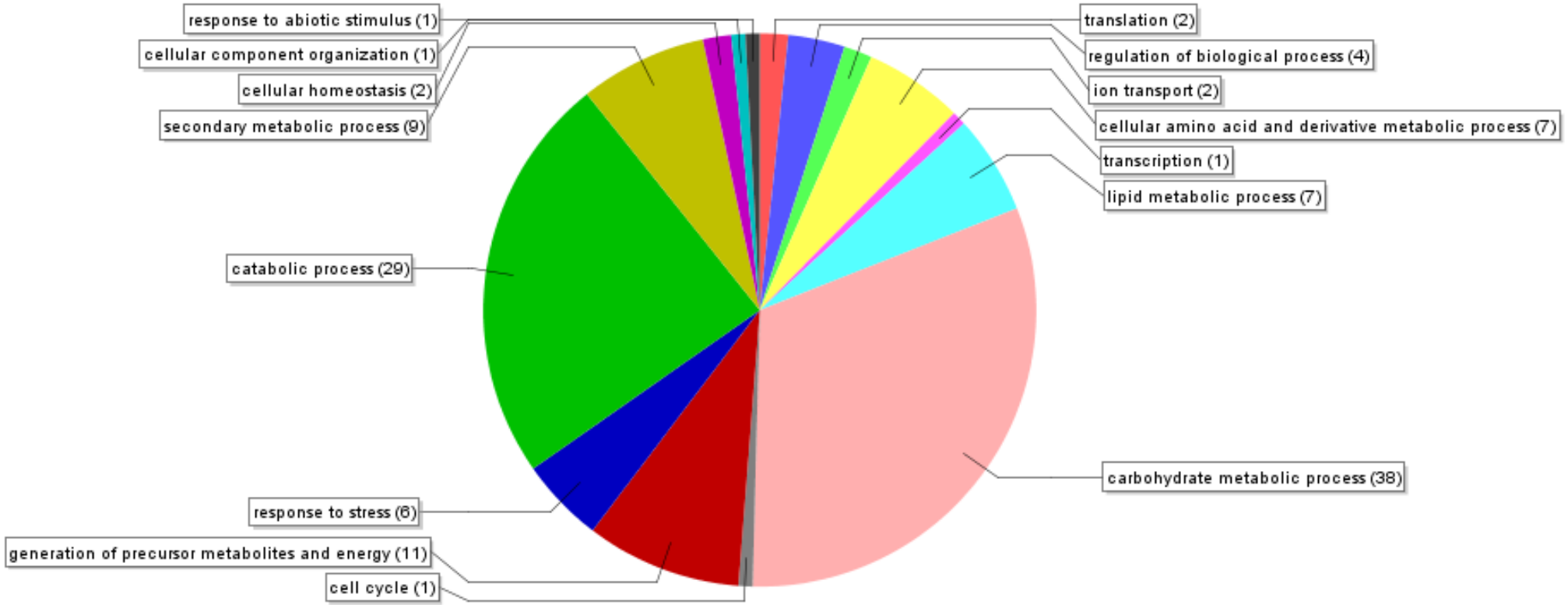

Figure 4.14. Biological process. GO annotation of *A. mellea* culture supernatant proteins fractionated by SDS-PAGE followed by LC-MS/MS analysis; identification of biological process property domains defined by http://www.geneontology.org. Visualisation of GO annotations is from the lowest nodes of GO hierarchy, in the category of biological process. Numbers in brackets indicate the number of proteins in each category.

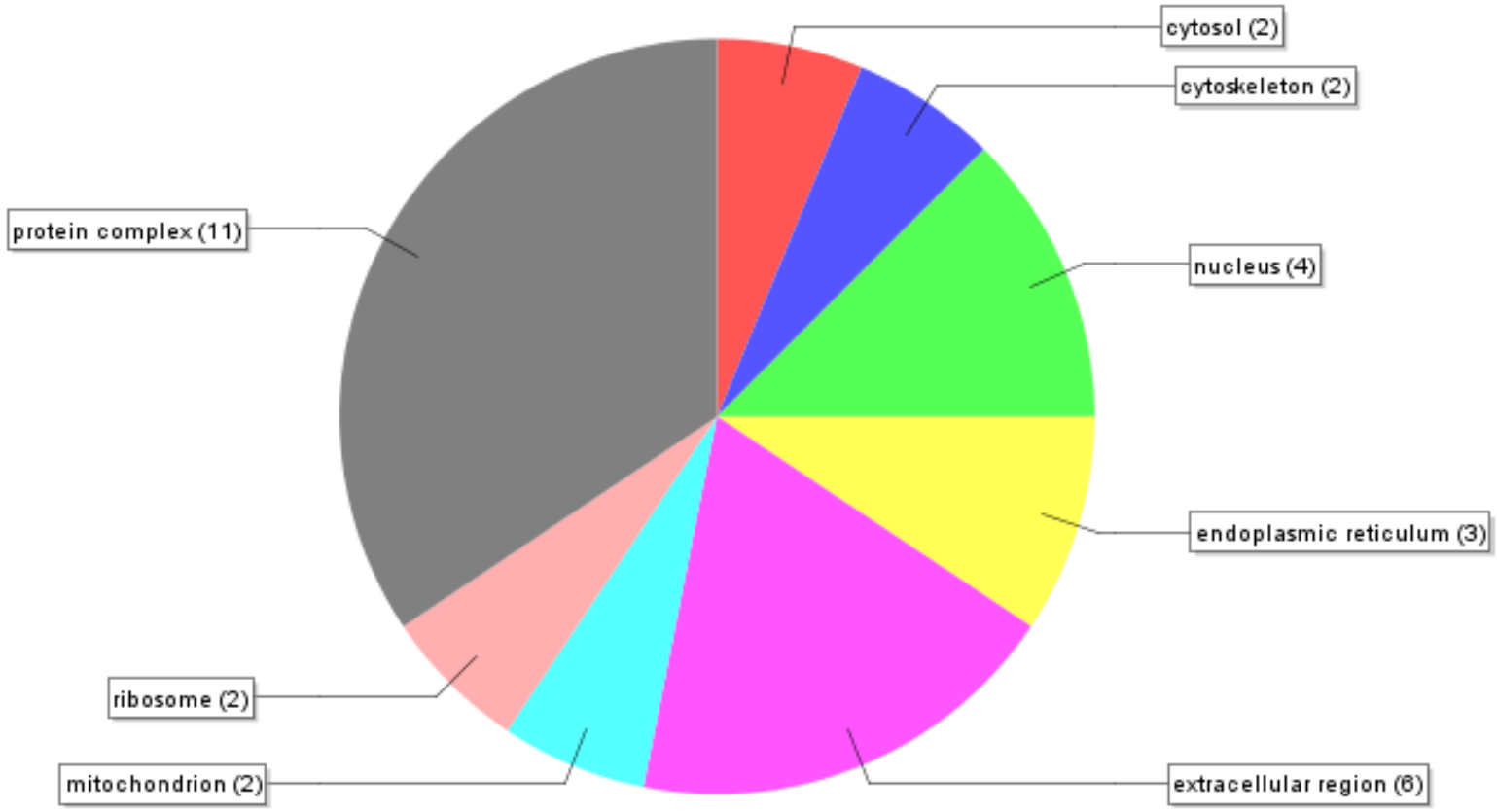

Figure 4.15. Cellular component. GO annotation of *A. mellea* mycelial protein fractionated by SDS-PAGE followed by LC-MS/MS analysis; identification of cellular component property domains defined by http://www.geneontology.org. Visualisation of GO annotations is from the lowest nodes of GO hierarchy, in the category of cellular component. Numbers in brackets indicate the number of proteins in each category.

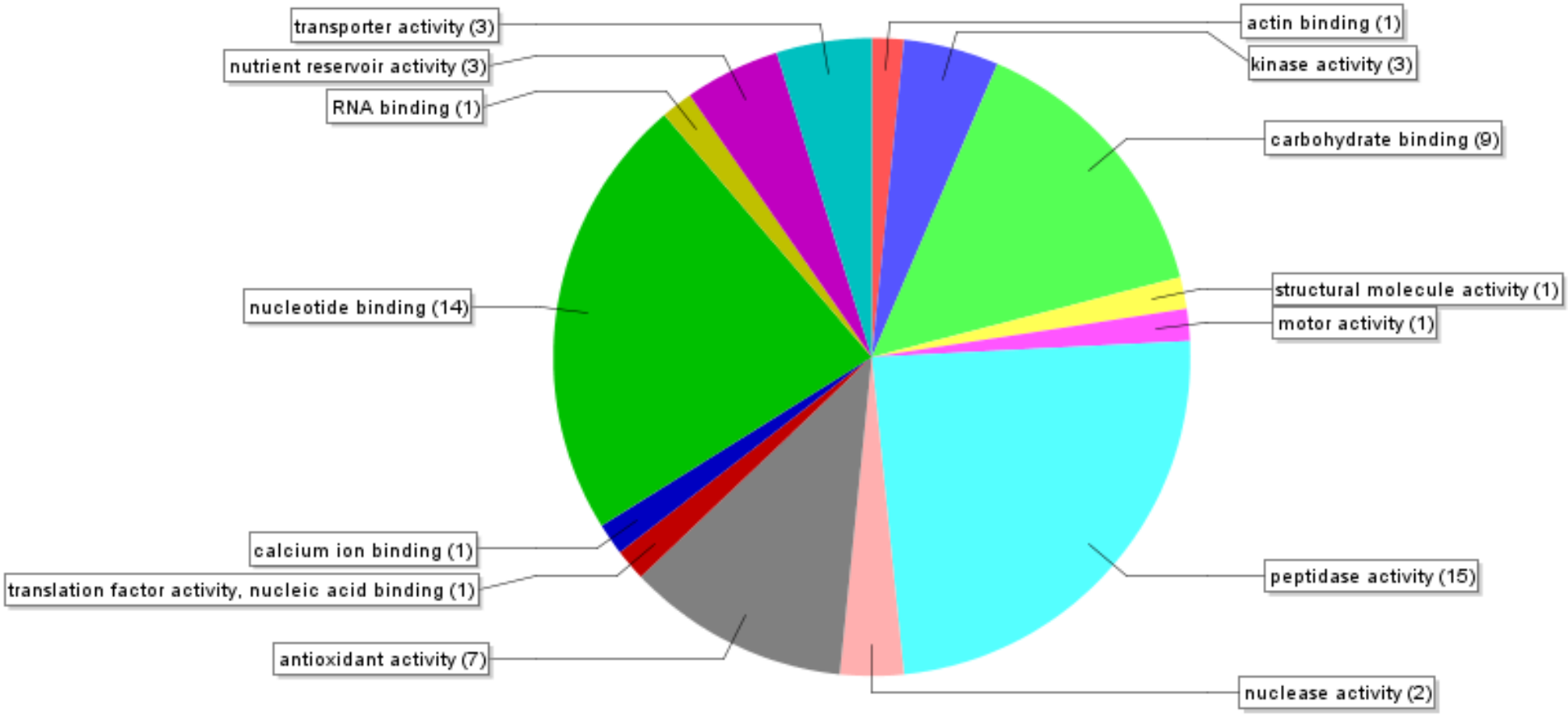

Figure 4.16. Molecular function. GO annotation of *A. mellea* mycelial protein fractionated by SDS-PAGE followed by LC-MS/MS analysis; identification of molecular function property domains defined by http://www.geneontology.org. The graph visualisation of GO annotations is from the lowest nodes of GO hierarchy, in the category of molecular function. Numbers in brackets indicate the number of proteins in each category.

A map of theoretical p*I* and M_r is shown in Figure 4.17. Theoretical molecular mass range of secreted proteins was between 7 and 397 kDa. Theoretical p*I* was between pH 3 and 10 with 10% of identified proteins > pH 7.5.

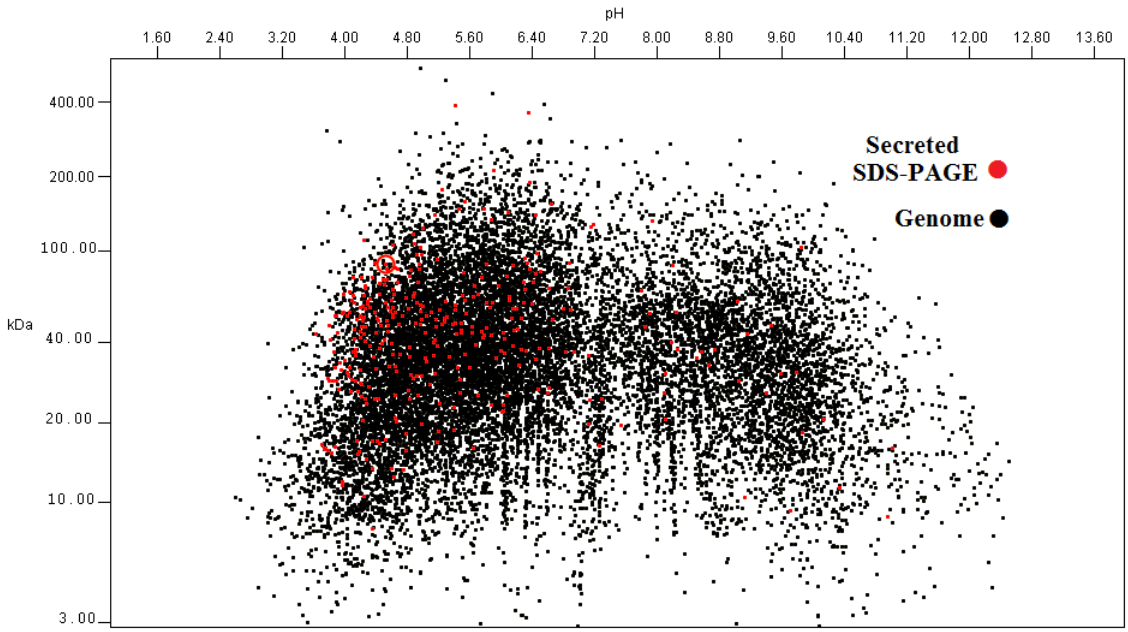

Figure 4.17. Map of theoretical M_r and p*I* of predicted proteins vs. secreted *A. mellea* proteins (Software: http://www.jvirgel.de (Hiller *et al.*, 2006)).

4.3 Discussion

Culture conditions for generation of *A. mellea* biomass and secreted proteins were optimised. The most effective means of generating mycelial biomass was in liquid culture in PDB, where cultures were incubated at 25 °C. Secreted proteins were more easily retrieved from static cultures than from shaking cultures under the same conditions. Two distinct morphologies are observed in *A. mellea* liquid cultures. Cultures with brown floating sclerotial mycelia were at least 90 % larger and protein identification from these was correspondingly greater than from white mycelia. Biomass generation on restricted carbon sources was slow, and thus supernatant protein available for analysis was reduced, with no *A. mellea* culture supernatant proteins uniquely identified from these sources. Nevertheless, the proteins which were identified are important in the study of lignocellulose degradation and nutrient scavenging under restricted conditions (Vanden Wymelenberg *et al.*, 2009, 2010; Hori *et al.*, 2012; Fernández-Acero *et al.*, 2010). Protein extraction methodologies from both mycelia and supernatants were optimised. Methods were developed using mechanical and chemical means of cell disruption to recover proteins from mycelia. Protein recovery from the secreteome was problematic and modification of protocols from Fragner *et al.* (2009) and Imanaka *et al.* (2010) were utilised to achieve this. The first 2-DE profile for *A. mellea* was established. Mycelial proteins were subjected to MALDI and LC-MS/MS analysis following 2-DE. Analysis of these results and interrogation of the *A. mellea* cDNA database identified proteins`(n = 279) of mycelial origin. Analysis by MALDI ToF proved much less sensitive than analysis by LC-MS/MS as > 98% of *A. mellea* mycelial proteins were determined by LC-MS/MS analysis. Three hundred and forty proteins from the *A. mellea* secretome were identified by interrogation of the *A. mellea* cDNA database after LC-MS/MS analysis following SDS-PAGE. Bioinformatic analysis of identified mycelial and secreted proteins was undertaken using a range of software tools to annotate identified proteins. A global map of *A. mellea* based on theoretical M_r and p*I* was produced and all mycelial (Figure 4.13) and secreted proteins identified (Figure 4.17) were plotted against this map.

Cultures of the fungus were grown on rich media and also media which restricted the carbon source available in order to induce expression of proteins across a broad spectrum of degradative activity. This approach was employed by (Sato *et al.* (2007), Vanden Wymelenberg *et al.* (2010, 2009) and Hori *et al.* (2012) in *P. chrysosporium* secretome analysis. Shaking and static cultures were also used to

induce breath of protein expression. However in this study, static cultures yielded 340 protein identifications and no proteins were uniquely identified from shaking cultures. *A. mellea* cultures produce mycelia with different morphologies under different conditions (Gao *et al.*, 2009) and even under the same conditions, two types of mycelia are formed, with substantial difference in biomass quantities. No proteins were uniquely identified from white submerged mycelia and no proteins were uniquely identified from supernatants of cultures grown on lignin or xylan. One secreted protein was uniquely identified from solid media utilising grapevine as sole carbon source, in a medium designed to induce lignocellulose degradation (Vanden Wymelenberg *et al.*, 2010).

Due to the robust nature of fungal cell walls, protein recovery from mycelia required mechanical methods, combining freezing in liquid nitrogen, grinding and sonication to lyse cells (Feofilova, 2010). This was followed by suspension of proteins in a lysis buffer and centrifugation to precipitate cell debris. This treatment was required prior to preparation for *A. mellea* mycelial protein separation by 2-DE.

Secreted proteins were more recalcitrant to separation and analysis (Fragner *et al.*, 2009; Sato *et al.*, 2007). A pellet of sticky polysaccharide was routinely obtained on centrifugation and in shaking cultures it was more abundant than in static cultures. High speed centrifugation proved efficacious in abstracting polysaccharides from secreted proteins samples. Subsequently prolonged centrifugation at a slower speed enabled protein precipitation, with ensuing solubilisation for separation by SDS-PAGE. Melanin, a phenolic pigment, was visible even after resolubilisation of protein (Sato *et al.*, 2007). SDS-PAGE served to remove this, whereby a brown material remained at the top of each well and proteins migrated into gels. Agar too appeared to assist in removal of melanin and polysaccharides as polysaccharide pellets retrieved from these cultures was smaller than those obtained in liquid cultures.

Gel electrophoresis coupled to MALDI-ToF or LC-MS/MS are well established methods for protein identification (Jungblut *et al.*, 1996). For *A. mellea*, MALDI-ToF proved to be much less sensitive than LC-MS/MS in identification of mycelial proteins. Proteins which are very large, hydrophobic or having extreme p*I*, are not suitable for 2-DE and gel free methods may be employed to analyse these (Vincent *et al.*, 2009), but nevertheless, it is a widely used method of protein separation and proved to be suitable for an initial survey of mycelial proteins, identifying a large number of mycelial proteins with good coverage. Actual mycelial proteins identified on a theoretical map of *A. mellea* proteins were mainly in the p*I* range < pH 7 (Figure 4.13) and clustered below

100 kDa. Analysis of these results and interrogation of the *A. mellea* cDNA database identified 279 proteins of mycelial origin; MALDI analysis uniquely identified 5, LC-MS/MS analysis uniquely identified 274 and 33 were common to both analyses (Figure 4.8). Twelve proteins had classical secretion signals and forty-seven were predicted to have non-classical secretion signals, 20 % in total. These proteins were largely hydrophilic (> 96 %) with ten proteins showing hydrophobicity and fourteen had transmembrane domains, although the transmembrane domains were not coincident with hydrophobicity. The protein whose predicted topology showed the greatest number (n = 5) of transmembrane domains had a GRAVY score (-0.327) which classed it as hydrophilic was Am11205, a previously hypothetical protein. Protein sequence coverage ranged between < 1 % and 81 % which is comparable with that obtained in a study of the basidiomycete *P. chrysosporium* (Matsuzaki *et al.*, 2008). Two heat shock 70 proteins, Am10845 and Am 7428 were identified by 25 and 22 peptides, respectively. Five proteins were uniquely identified by MALDI analysis, an sh3 domain protein (Am1181), a previously predicted protein (Am7248), a malate dehydrogenase (Am9971), an aldehyde dehydrogenase (Am13361) and a protein for which there was no homology and appears to be *A. mellea* specific (Am16969). Nineteen mycelial proteins which were previously "hypothetical" and five previously "predicted" proteins have been identified at protein level and can now be classified as *A. mellea* proteins of unknown function.

Functional categories of mycelial proteins included nucleotide and nucleic acid binding, protein binding, peptidase, kinase, transporter activity, DNA binding, electron carrier, antioxidant activity, catalytic activity, structural molecule activity and protein binding in descending order of numbers of proteins involved. Proteins originated from the nucleus, cytoskeleton, mitochondria, ribosome and cytosol in descending order of protein in each category. The biological processes in which mycelial proteins identified are: catabolic process, carbohydrate metabolism, precursor metabolites and energy, regulation, secondary metabolism, stress response, translation, ion transport, lipid metabolism, cellular component organisation, and homeostasis in desending order of the numbers of proteins in each process GO categories identified are broadly in line with those identified in *L. bicolor* (Vincent *et al.*, 2012).

The pH range of secreted *A. mellea* proteins was pH 4 – 10.5 although most were between pH 3.5 and pH 6.5 with a large cluster between pH 4 and pH 5 and M_r was largely below 100 kDa (Figure 4.17). Proteins from the *A. mellea* secretome

(*n* = 340) were identified using the *A. mellea* cDNA database for LC-MS/MS data interpretation following SDS-PAGE. One hundred and forty-one proteins from the secretome had classical secretion signals and one hundred and thirteen had non-classical secretion signals, a total of 74 % of secretome proteins identified. This is higher abundance than was identified in a study of *L. bicolor* (Vincent *et al.*, 2012). Mycelial proteins had lower abundance of proteins with secretion signals (53%) and were less acidic. Eighty-two proteins (24 %) had GRAVY scores indicating hydrophobicity. This is in contrast to mycelial proteins (< 12 %). Forty-seven proteins of supernatant origin were predicted to have transmembrane domains. A Zf-Parp-Domain-Containing Protein (Am19409) and a LCCL Domain-Containing Protein (Am10767) each had topology indicating nine transmembrane domains. Twelve hydrophobic supernatant proteins also had transmembrane domains. Secreted protein sequence coverage ranged from < 1% to 56%. A cobalamin-independent methionine synthase (Am17277), a valosin-containing protein (Am14558) and an ATP citrate synthase (Am16101) were identified by 24, 22 and 21 peptides, respectively. Proteins previously "hypothetical" (*n* = 26) and previously "predicted" proteins (*n* = 8) were identified in the *A. mellea* secretome at protein level and can now be classified as *A. mellea* proteins of unknown function. Eight secreted proteins had no homology to other organisms and can be classified as an *A. mellea* specific proteins of unknown function. Proteins of unknown function in *A. mellea* are low and this is due in part to the rapid growth in protein database repositories due to advances sequencing technology and project numbers in progress and study of *L. bicolor* secretome at protein level (Vincent *et al.*, 2012).

Secretome proteins were largely catalytic (~ 85%), large numbers of CAZys from many families were identified in the *A. mellea* secretome as were many from the *L. bicolor* secretome (Vincent *et al.*, 2012). However, the number of proteins and families were considerably increased compared to those identified in the *L. bicolor* secretome. Glycoside hydrolase enzymes (*n* = 46) from twenty-four families were most abundant, compared with twelve families from *L. bicolor* (Vincent *et al.*, 2012). Other CAZys identified were carbohydrate esterases (*n* = 8) from four families, one carbohydrate binding module protein, and three lyases. More CE families (*n* = 6) were identified in the *L. bicolor* secretome than in *A. mellea* (Vincent *et al.*, 2012). Protein-degrading enzymes (proteases, *n* = 3; peptidases, *n* = 15; metalloproteases, *n* = 4) were also identified. Peptidases were less abundant in *P. chrysosporium* and *L. bicolor* secretomes than in the *A. mellea* secretome (Vanden Wymelenberg *et al.*, 2006; Vincent *et al.*, 2012) Cellobiohydrolase (*n* = 3) enzymes which act in concert with

endoglucanases (n = 3) and exo-β-glucanases (Mattinen *et al.*, 2008) were identified in addition to the enumerated CAZy enzymes. Cellulase and enzymes modifiying xylan, xylose, xylulose which are involved in saccharification of plant cell wall material (Ryu *et al.*, 2011) also form part of the secretome of *A. mellea* and have biotechnological application. Laccases (n = 5), peroxidases (n = 5) and oxidases (n = 7) - other enzymes with potential for biotechnological applications, were also identified. There was an increased abundance of CAZys (Cantarel *et al.*, 2009) in the protein cohort identified in supernatants, compared with mycelia. Two superoxide dismutase enzymes (Am1068 and Am18409) were identified in mycelia as well as in supernatants. It is not unusual for proteins to have more than one function and to be found in different cell types (Jeffery, 1999, 2003; Kuees *et al.*, 2011; Gstaiger and Aebersold, 2009; Löwer *et al.*, 2008; Bendtsen *et al.*, 2005). One *A. mellea* protein (GenBank: AAD28627.1 Endo-Exonuclease) which was previously identified (Healy *et al.*, 1999), was identified in this study.

An initial survey has identified two hundred and ninety-seven proteins from the mycelial proteome and three hundred and forty proteins from the secretome of *A. mellea*, the first study of its kind. The functional range of identified proteins in *A. mellea* was comparable to the spectrum shown by Vincent *et al.* (2012), in a study of *L. bicolor*. High sequence coverage of the proteins is affirmation of the prediction of intron/exon splice sites and illustrates the quality of initial gene finding. This work will serve as a platform for further study of the organism's role as a saprotroph and necrotroph, and possible enzymatic applications of its proteins.

Chapter 5 Optimisation of shotgun the proteomic technique for *Armillaria mellea* mycelial and supernatant protein identification.

5.1 Introduction

At present, the complete or partial genome sequences of eighty-five basidiomycete species are available on the NCBI database (http://www.ncbi.nlm.nih.gov/genome/browse/ Accessed 25/02/2013). Specifically, complete genomic sequence data is available for 47, while sequence data for the remainder comprises raw sequencing data in a **S**equence **R**ead **A**rchive (SRA) (http://www.ncbi.nlm.nih.gov/Traces/sra/sra.cgi?view=studies Accessed 25/02/2013), obtained from various sequencing platforms (Henson *et al.*, 2012; Suzuki *et al.*, 2012). This compares unfavourably with the extensive amount of genomic sequence data available for 293 ascomycetes. Moreover, the exponential growth in fungal genome sequencing has not been matched by a corresponding increase in proteomic data (Doyle, 2011). *In silico* protein prediction from genome data, combined with experimentally verified proteomic data, is therefore essential for biological system profiling, since metabolic pathways, protein/protein and protein/metabolite interactions ultimately control both organism behaviour and function (François *et al.*, 2010). Consequently, a holistic system view is desirable to understand pathogenicity and virulence of *A. mellea* at a molecular level and to discover bioactive molecules with biotechnological application.

2-DE has been, until recently, the *de facto* standard for protein separation and analysis, whereby up to 10,000 proteins can be separated on a single 2-DE gel (Klose and Kobalz, 1995). However, high-throughput analysis of 2-DE gels by MS is laborious and time consuming. It is also unsuitable for identification of high molecular mass proteins, and those with extreme p*I* values. Analysis of intact hydrophobic proteins is also problematic due to their low solubility and aggregation (Lin *et al.*, 1999). Shotgun proteomics, analogous to shotgun genomics, by which total protein complement is fragmented by digestion into peptides, generating complex peptide mixtures, represents a solution to the problem of proteomic profiling of biological systems. This bottom-up approach can be used to establish a holistic blueprint of a system (Armengaud, 2012). One of the advantages of this method is that proteins which are unsuitable for gel electrophoresis are fragmented by digestion into peptides which do not have the undesirable biophysical characteristics of the parent protein. Proteins can then be identified from a fraction of their component peptides (Ernoult *et al.*, 2008; Hörth *et al.*,

2006; Chenau *et al.*, 2008). However, specimens prepared for shotgun proteomic analysis are, by definition, extremely complex since whole organism protein lysates are digested and analysed in a single LC-MS/MS run (Chenau *et al.*, 2008). This complexity may be overcome by sub-fractionation: for example, protein lysates may be enriched in extracellular or membrane proteins, or from a particular tissue type (Abdallah *et al.*, 2012), however the salient factor is that a large number of proteins are digested together and ultimate identification is derived from peptide sequence information (Ernoult *et al.*, 2008; Hörth *et al.*, 2006). This is specifically carried out whereby abundant peptide signals, from the peptide mixture, are isolated during initial MS scans, fragmented and re-analysed by MS^2 scans by a high resolution mass spectrometer (Gstaiger and Aebersold, 2009). However, LC-MS/MS systems are constrained by their peak (peptide) detection capacity (i.e., the number of peptides which can be separated or individually detected within the mixture under analysis), and their load capacity (i.e., the amount of material that can be analysed at any one time). Thus, as with 2-DE, an initial multi-dimensional separation prior to LC-MS/MS analysis can bring combinatorial optimisation of peptide resolution (Link, 2002; Giddings, 2005), however, it is still possible to successfully identify many proteins by direct analysis of peptides mixtures by LC-MS/MS (Chiu *et al.*, 2012).

To date, most proteomic investigations of fungi, particularly basidiomycetes, have been undertaken using electrophoretic gel-based approaches (Gonzalez-Fernandez *et al.*, 2010). Shotgun analysis of *L. bicolor* mycelia and secretome carried out by Vincent *et al.* (2012) utilised SDS-PAGE, 2-DE and an IPG-IEF technique similar to the indirect method described below, whereby peptides were eluted from an immobilised pH gradient strip rather than maintained in a liquid phase. *P. placenta* was grown on wood, secreted proteins prepared, digested, desalted by C_{18} solid-phase extraction and then subjected to direct shotgun/LC-MS/MS analysis (Ryu *et al.*, 2011). A multidimensional protein identification technology (MudPIT) technique was utilised by Manavalan *et al.* (2011) for the analysis of the *P. chrysosporium* secretome; here, peptides were iTRAQ labelled, then subjected to strong-cation exchange (SCX) and desalting prior to LC-MS/MS analysis.

Shotgun proteomic techniques that have been developed are: (i) direct shotgun, (ii) indirect shotgun and (iii) MudPIT (McDonald *et al.*, 2002; Washburn *et al.*, 2001; Michalski *et al.*, 2011; Alves *et al.*, 2007): (i) Direct shotgun analysis (single phase) is a technique whereby digested proteins are separated by their hydrophobicity via RP-

HPLC by application of an organic solvent gradient, and analysed by LC-MS/MS (Link *et al.*, 1999); (ii) Indirect shotgun analysis involves protein fractionation by a biophysical characteristic such as charge, size or affinity prior to separation by RP-HPLC and LC-MS/MS analysis. In one part of this study, proteins were digested and peptides separated based on their p*I* in a similar manner to gel electrophoresis, but in a liquid phase known as OFFGEL electrophoresis (Figure 5.1); (iii) Multidimensional protein identification technologies (MudPIT) are comprehensive systems whereby proteins, or peptides, are separated in several dimensions using iCAT (isotope coded affinity tags), SCX or IEF coupled to RP-HPLC and LC-MS/MS (Wall *et al.*, 2000; Link, 2002; Washburn *et al.*, 2001). Biphasic chromatography columns with the combined application of solvent gradients to strong cation exchange and reverse phase material has also been used for MudPIT (Washburn *et al.*, 2001).

As with high-throughput sequencing technology, shotgun proteomics exponentially increases the amount of data generated, which can present problems for the subsequent analysis and identification of constituent proteins (Peng *et al.*, 2003; Nesvizhskii, 2005). However, bioinformatic tools as described in Table 2.3 greatly assist in the automation of data mining. Nonetheless, complicating issues exist; for example, (i) a peptide may be identified in more than one protein in the database, (ii) alternative splicing or isoforms of a protein give rise to identical peptides and (iii) gene paralogs may have no peptide that is unique to a particular member of a gene family. Indeed, Nesvizhskii (2005), found that although eleven α-tubulin family peptides were identified in a dataset, none conclusively related to a distinct family member. Another complicating factor may result from truncated sequences and sequencing errors such as alternative sequences or sequences which have been given different accession numbers although they are the same gene. Amino acids with identical masses (Ile and Leu) or combinations amino acids with almost identical masses further complicate identification of peptides, and thus proteins, in instruments such as ion traps which have relatively low mass accuracy. LTQ-FT or Q-ToF instruments have high mass accuracy and can overcome this issue (Nesvizhskii, 2005). However, conservative analysis of shotgun proteomic data, allied to the use of commercially available and validated software for protein identification can surmount many, if not most, of these issues.

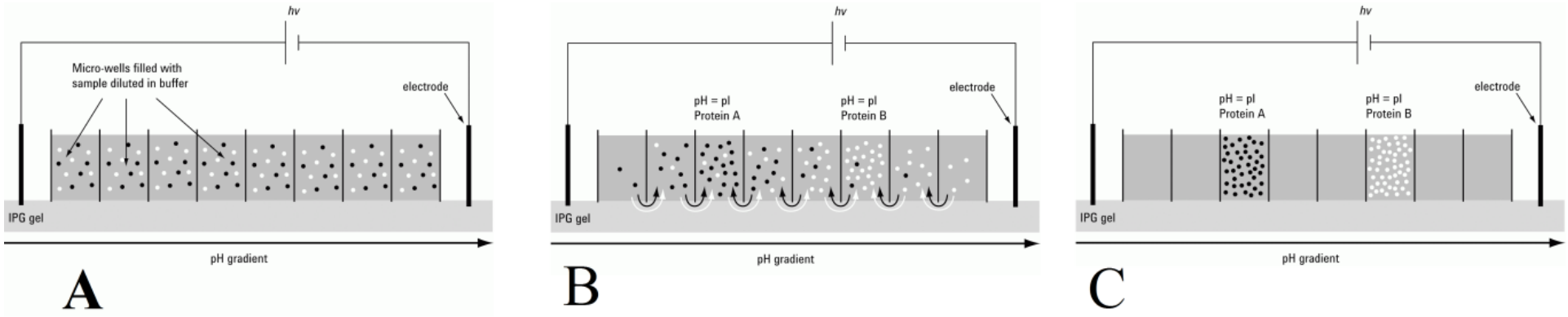

Figure 5.1. Schematic of the Agilent OFFGEL Fractionator: A compartmentalised plastic strip with eleven wells is sealed against a gel strip with an immobilised pH gradient. The wells are filled with sample (proteins, or a peptide mixture derived from mixed protein digest). A voltage is applied to both ends of the strip and proteins or peptides migrate through the gel to their isoelectric point. **A.** Sample is applied equally to all wells; **B.** Current is applied and proteins or peptides begin to migrate; **C.** Proteins or peptides reach their p*I* and samples are collected for LC-MS/MS analysis (Agilent Technologies, 2006).

Normally, peptide data derived from individual or multiple protein digestion is used to interrogate the NCBI database (http://www.ncbi.nlm.nih.gov/) using MASCOT software (http://www.matrixscience.com/) to enable protein identification. This was not possible for the present study as insufficient *A. mellea* genomic or cDNA data was available on NCBI. Thus, the *A. mellea* cDNA database (Chapter 3) used to facilitate protein identification in this thesis was interrogated using software termed Spectrum Mill, which is available from Agilent. Numerous studies have exploited the power of Spectrum Mill for high-throughput protein identification from other species (Hao *et al.*, 2006; Luo and Levine, 2009; Scruggs *et al.*, 2010; Bark *et al.*, 2012; Vanden Wymelenberg *et al.*, 2006).

Where shotgun proteomics is utilised, very large datasets of spectra are generated. These are reduced by software peptide validation, but as many ten or more spectra may be obtained for a particular peptide, thus yielding considerable amounts of data. Spectrum Mill software assigns a peptide to only one protein even when the same peptide is found in more than one protein in a database. Spectrum Mill has two summary modes: (i) a protein mode which identifies proteins from a database, but does not allow for peptide redundancy and eliminates any proteins from the identified dataset containing an identical peptide and (ii) analysis by peptide, whereby additional proteins may be identified where a second peptide is sufficient for positive identification. Ultimately, a score is applied to a peptide or protein hit based on database interrogation. Sequences between the peptide N- and C- termini are reversed, a score is applied to the reversed sequence and subtracted from the peptide score, thus an optimal value for the ΔForward-Reverse should be the same as the peptide score, but in every case should be more than 2. % SPI spectral peak intensity is the MS/MS peak-detected spectral ion current percentage of ion current based on the search and should be over 70 for positive identification. A combination of these parameters filters out poor quality spectra and results in high fidelity results. Sample duplicates and optimisation also generate multiple mass spectra with different scores which must be correlated to deduce the protein score and sequence coverage.

Overall, the aims of the work presented in this chapter were:

1. To develop a de novo LC-MS/MS strategy for direct shotgun proteomic identification of *A. mellea* proteins using Spectrum Mill and an in-house cDNA database.
2. To develop suitable methods for preparing *A. mellea* mycelial protein lysates for trypsinisation, and to optimise LC conditions for optimal peptide detection.
3. To study the effect of carbon source on *A. mellea* mycelial proteome and prepare protein lysates for trypsinisation, with LC conditions optimised for peptide detection.
4. To develop suitable methods for preparing *A. mellea* secretome protein lysates for trypsinisation, and to optimise LC conditions for optimal peptide detection.
5. To investigate the suitability of OFFGEL electrophoresis for *A. mellea* peptide fractionation prior to LC-MS/MS analysis.

5.2 Results

5.2.1 Optimisation of the shotgun LC-MS/MS technique

A. mellea was grown on solid (Section 2.2.3.3) or liquid (Section 2.2.4.1) media for 3 - 6 weeks and protein was extracted according to Method 2A WCL (Section 2.2.7.3), Method 2B WCL-lyophilised (Section 2.2.7.4) or secreted protein from agar cultures (Section 2.2.7.7). It was observed that 6 M guanidine-HCL, combined with DTT reduction, and subsequent IAA-mediated alkylation yielded optimal mycelial protein lysates for trypsinisation, once all denaturant had been removed by extensive dialysis. Protein lysates were prepared and digested as described in Section 2.2.10.1 or Section 2.2.10.2, diluted and used for direct LC-MS/MS analysis (Section 2.2.15.2). Initial LC-MS/MS analysis of shotgun peptide mixtures was undertaken using Method A (Table 2.6, Figure 5.2A), and it can be seen diagramatically that peptide elution was early and crowded, thereby impeding optimal peptide, and consequently protein, identification. Based on acetonitrile concentration (% B) at the time of peptide elution, the gradient slope and time were adjusted to give improved resolution prior to subsequent analyses. Schematically, Figure 5.2 illustrates elution of 5 identical peptides under two acetonitrile gradients A and B, showing optimised resolution by adjustment of acetonitrile gradient (Δ% B (acteonitrile)/min) in Figure 5.2B. If necessary, a third iteration was performed to produce optimum resolution of eluted peptides and, in general, peptides were generally eluted at < 40 % B. The number of spectra generated in an extended run was up to 33,000. This was reduced by peptide validation, but a single sample with replicates and optimisation generated up to 4000 valid peptides. Software analysis by protein was performed and further analysis of valid peptides was carried out.

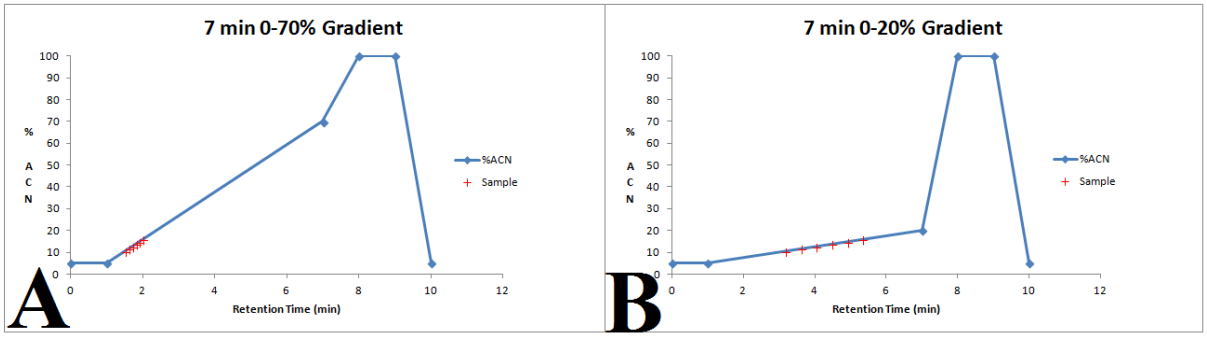

Figure 5.2. Schematic acetonitrile gradients illustrating elution of 5 identical peptides: **A.** Conditions: Δ 10% B/min with peptide retention time between 1.5 and 2 min; **B.**

Conditions: Δ 2.8 % B/min giving peptide retention time between 3 and 5.3 min with improved resolution.

5.2.2 Mycelial proteins from cultures on rich media analysed by direct shotgun LC-MS/MS analysis.

Proteins from 3 - 6 week *A. mellea* cultures grown on PDB (Section 2.2.4.2) were harvested and extracted according to Method 2A WCL (Section 2.2.7.3). Alkylated protein extracts were digested as described in Section 2.2.10.1, diluted and prepared for direct LC-MS/MS analysis (Section 2.2.15.2). After initial analysis the gradient was optimised as described in Section 5.2.1 above, and LC-MS/MS datafiles were analysed (Section 2.2.15.3) against the in-house *A. mellea* cDNA (protein) database using Spectrum Mill. Further analysis was carried out using the bioinformatic tools described in Table 2.3. Ultimately there were 518 proteins identified based on detection of 1856 peptides identified from PDB. The greatest number of peptides identified in one protein by this method was 15 (Am710, a heat shock protein Hss1) and highest percentage coverage was 51% (Am14466, a protease propeptide inhibitor). All high scoring *A. mellea* mycelial proteins uniquely identified by shotgun LC-MS/MS are given in Table 5.1. The complete list of identified proteins is to be found in Appendices A.2 and A.3 (Accompanying CD file Master Tables Appendices.docx).

Structural features of these proteins included hydrophobicity (n = 70), and transmembrane regions (n = 58), Two glycosyltransferase family 50 proteins (Am5593 and Am199) were predicted to have 11 and 12 regions, respectively and Am17215 (Duf221-Domain-Containing Protein) was predicted to contain 11 transmembrane regions. Secretion signals were identified in 47 % of these proteins (SignalP, n = 28 and SecretomeP, n = 220).

Table 5.1. High scoring *A. mellea* mycelial proteins identified by direct shotgun/LC-MS/MS analysis, not identified by other methods.

[a]Accession No.	[b]BLAST Annotation	[c]tM$_r$	[d]tp*I*	Coverage (%)	Unique Peptides	[e]SM Score	[f]GRAVY score	[g]TM	[h]SigP/ SecP	[i]TarP	[j]Method
Am17287	60S Ribosomal Protein L9	21384	9.49	16	2	33.08	-0.219				S
Am6581	Acbp From Moniliophthora Perniciosa	11791.4	6.3	27	2	36.09	-0.636		SecP		S
Am15570	Actin Depolymerizing Factor	15572.8	5.04	15	2	33.43	-0.397		SecP		S
Am8888	Apoptosis-Linked Protein 2	24903.9	4.98	15	3	36.07	-0.383		SecP		S
Am4833	Arm Repeat-Containing Protein	214933	5.14	<1	1	25.01	-0.037	1		Mt	S
m19878	Aspartate-tRNA Ligase	69006.9	5.97	4	2	33.89	-0.413	1			S
Am17958	Atp Synthase Subunit 5	22291.7	9.86	7	1	25.22	0.005		SecP	Mt	S
Am11736	Carbohydrate-Binding Module Family 13	80369.9	9.1	8	5	81.7	-0.936				S
Am18586	Clathrin Heavy Chain 1	189312	5.66	2	2	40.2	-0.174				S
Am13483	Cral Trio Domain-Containing Protein	50799.7	5.52	11	3	55.03	-0.043		SecP		S
Am16980	Dead-Domain-Containing Protein	45189.1	5.11	9	3	53.07	-0.209				S
Am15326	Dead-Domain-Containing Protein	62211.6	5.25	6	2	42.46	-0.135		SecP		S
Am18769	Disulfide Isomerase	96397.7	8.21	9	5	80.94	-0.441				S
Am8679	Duf1688-Domain-Containing Protein	46873.9	5.4	11	2	38.75	-0.131				S
Am14010	Farnesyl-Diphosphate Synthase	41462.9	5.1	8	2	39.2	-0.21				S
Am17077	Glutamate Decarboxylase	121212	5.4	7	5	79.94	-0.043	6	SecP		S
Am19909	Glycoside Hydrolase Family 16 Protein	147978	9.69	1	2	35.77	-0.157		SecP		S
Am18130	Glycosyltransferase Family 35 Protein	107817	6.51	3	2	40.23	-0.329				S

[a]Accession No.	[b]BLAST Annotation	[c]tM$_r$	[d]tp*I*	Coverage (%)	Unique Peptides	[e]SM Score	[f]GRAVY score	[g]TM	[h]SigP/ SecP	[i]TarP	[j]Method
Am5593	Glycosyltransferase Family 50 Protein	68987.1	9.06	4	2	27.94	0.302	11	SecP		S
Am9397	Gtp-Binding Protein Ypt1	22571.6	5.75	20	3	41.38	-0.289				S
Am19822	Heat Shock Protein	98414.4	6	5	3	46.1	-0.217				S
Am710	Heat Shock Protein Hss1	70591.5	5.1	35	15	260.66	-0.445				S
Am6607	Heme Peroxidase	110588	6.15	10	5	93.22	-0.254		SecP		S
Am18538	Histone H2A	18629.7	9.55	18	2	39.57	-0.112	2	SecP		S
Am19143	Histone H4	81543.6	8.53	4	3	49.91	-0.02				S
Am10761	Hypothetical Protein Lacbidraft_291634 [*Laccaria bicolor* S238N-H82]	104910	5.02	4	2	36.1	-0.605				S
Am19191	Hypothetical Protein Serla73Draft_143542 [*Serpula lacrymans* Var. Lacrymans S7.3]	9917.3	9.85	35	2	36.86	-0.816		SecP	Mt	S
Am17043	Leucyl Aminopeptidase	204008	6.18	2	3	53.33	-0.471	1			S
Am15243	L-Glutamine D-Fructose 6-Phosphate Amidotansferase	76220.8	6.23	21	10	168.62	-0.142				S
Am17403	Linoleate Diol Synthase	111234	6.13	15	9	164.16	-0.317	1	SecP		S
Am11730	Mitochondrial Carrier Protein	125072	6.87	4	3	48.1	0.13	8	SecP		S
Am13172	*A. mellea* unknown function protein	45328.5	5.6	24	8	135.18	-0.277	2			S
Am16113	NAD Binding Dehydrogenase	56738.2	7.12	7	2	28.03	-0.308				S
Am14849	NAD -Binding Protein	34440.9	8.72	10	2	34.33	-0.206		SecP		S
Am14903	Nuclear Transport Factor 2	13975	4.5	26	2	26.87	-0.014		SecP		S

[a]Accession No.	[b]BLAST Annotation	[c]tM$_r$	[d]tp*I*	Coverage (%)	Unique Peptides	[e]SM Score	[f]GRAVY score	[g]TM	[h]SigP/ SecP	[i]TarP	[j]Method
Am17955	Peptidase C1B Bleomycin Hydrolase	102204	5.72	3	2	32.72	-0.221	1	SecP		S
Am19506	Peroxisomal Copper Amine Oxidase	92337.9	6.05	7	4	64.48	-0.292				S
Am13744	Plasma-Membrane Proton-E	131565	5.25	5	3	55.2	0.025	1	SecP		S
Am10922	Prolyl-tRNA Synthetase	140248	6	3	3	60.81	-0.305				S
Am14466	Protease Propeptide Inhibitor	8111.1	4.11	51	2	27.45	-0.149		SecP		S
Am11554	Pyruvate Carboxylase	133085	6.32	10	9	139.78	-0.134				S
Am18495	Rho Gdp-Dissociation Inhibitor	22078.9	5.67	18	2	33.16	-0.496		SecP		S
Am15760	Ribosomal Protein 60S	14433.9	4.36	24	2	36.35	-0.295				S
Am13389	Septin	48544.6	6.46	15	4	70.95	-0.633				S
Am19811	Ser Thr Protein Phosphatase 2A Regulatory Subunit A	66606.1	4.89	5	2	31.89	0.063		SecP		S
Am12839	Short-Chain Dehydrogenase	29597.3	6.9	16	2	31.73	0.301		SecP		S
Am17192	Small Heat Shock Protein	16732.8	5.6	16	2	30.32	-0.609		SecP		S
Am18403	Ste16 [*Coprinopsis cinerea* Okayama7#130]	166773	6.57	3	5	76.07	-0.282				S
Am13773	tRNA Synthetase Class Ii	124421	7	2	3	41.73	-0.51				S
Am19743	Tubulin Alpha	49008.4	4.99	17	5	85.57	-0.232		SecP		S
Am17356	Wd40 Repeat-Like Protein	98427	5.83	3	2	36.09	-0.294				S

[a]Accession number from *A. mellea* cDNA database; [b]BLAST annotation following Blast2GO analysis of proteins identified from *A. mellea* cDNA database; [c]M$_r$, theoretical molecular mass; [d]tp*I*, theoretical isoelectric point; [e]SM score, Spectrum Mill protein score; [f]GRAVY score, grand average of hydropathy (Negative score indicates hydrophilicity

while Positive score indicates hydrophobicity); [g]TM, number of transmembrane regions; [h]SigP, classical secretion signal peptide; SecP, non-classical secretion signal; [i]TarP, subcellular location of proteins, Mt, mitochondrial targeting peptide; [j]Method: S, direct shotgun LC-MS/MS analysis

5.2.3 Direct Shotgun LC-MS/MS analysis of cultures grown on restricted carbon sources.

A. mellea liquid cultures were individually grown for 21 days (Section 2.2.4.1), on restricted carbon sources including cellulose, lignin, rutin and xylan (Section 2.1.3.9). Cultures were harvested, mycelia lyophylised and culture supernatants frozen (Section 2.2.4.2). Protein was extracted (Section 2.2.7.4) and digested (Section 2.2.10.1) and peptide digests diluted to $^{1}/_{4}$ with LC-MS/MS Solvent A (Section 2.1.9.2) in preparation for LC-MS/MS analysis (3 µl of each digest was used for LC-MS/MS analysis (Section 2.2.15.1) which was performed (Section 2.2.15.3) using program F (Table 2.6).

Mycelial proteins (*n* = 365) were identified from peptides (*n* = 1558) by shotgun LC-MS/MS analysis. Extensive bioinformatic analyses using Protein GRAVY predicted a hydrophobic protein content of *n* = 49. Additionally, proteins with transmembrane domains (*n* = 32) were predicted by Phobius and secretion signals were predicted via SecP (*n* = 164) and SigP (*n* = 13) analyses, respectively, giving a total of 48% overall. Specifically, proteins (*n* = 161) were identified in mycelia grown on cellulose, supported by peptide detection (*n* = 952). Proteins (*n* = 194) were identified from *A. mellea* cultured on lignin from peptides (*n* = 1048). From cultures with rutin as the sole carbon source, proteins (*n* = 185), following detection of 1011 peptides, were identified. When xylan was used as sole carbon source, proteins (*n* = 188), supported by 1050 peptides, were identified. A complete listing of proteins identified from cultures grown on restricted carbon sources is provided in Appendix A.5 (Accompanying CD file Master Tables Appendices.docx) and Table 5.2 presents proteins uniquely identified following culture on a single carbon source. B2G analysis followed by GO annotation illustrates the breakdown of *A. mellea* mycelial proteins when grown on restricted carbon sources by biological process (Figure 5.3). The most abundant category is generation of precursor metabolites and energy (18%). Catabolic processes are slightly lower at 17%. Proteins involved in translation represent 15%, and nucleoside, nucleotide and nucleic acid metabolic processes, 12%. Protein modification, lipid and secondary metabolic process represent 4% each.

Table 5.2. *A. mellea* mycelial proteins uniquely identified by direct shotgun/LC-MS/MS analysis, following culture on a specific carbon source.

[a]Accession No.	[b]BLAST Annotation	[c]tM$_r$	[d]tp*I*	Coverage (%)	Unique Peptides	[e]SM Score	[f]GRAVY score	[g]TM	[h]SigP/ SecP	[i]Carbon Source
Am6728	2-Isopropylmalate Synthase	87719.3	5.48	4	2	37.19	-0.285			L
Am18132	2-Nitropropane Dioxygenase	36253.4	5.84	6	2	22.59	-0.021			R
Am10445	2-Oxoglutarate Dehydrogenase Complex E1 Component Mitochondrial Precursor	111386.6	6.39	1	1	15.55	-0.457		SecP	R
Am20292	3-Deoxy-7-Phosphoheptulonate Synthase	54302.9	6.22	3	1	13.45	-0.099			L
Am19922	60S Ribosomal Protein L22	13803.7	9.35	7	1	14.12	-0.742		SecP	C
Am15604	60S Ribosomal Protein L3	43834.1	10.22	9	2	21.09	-0.594			X
Am17432	60S Ribosomal Protein L31	19415.7	10.04	5	1	17.41	-0.447		SecP	R
Am12978	60S Ribosomal Protein L44	93132.9	6.63	1	1	11.03	-0.668			C
Am17763	Adhesion Regulating Molecule	35107.5	4.96	4	1	13.72	-0.362			L
Am20036	Aldehyde Dehydrogenase	53410.1	6.29	3	1	16.11	-0.141		SecP	R
Am11138	Alpha Beta-Hydrolase	72524.9	5.91	5	2	28.27	-0.247	1	SecP	R
Am11369	Alpha Beta-Hydrolase	48071.9	5.81	3	1	16.51	-0.219			L
Am14083	Alpha Beta-Hydrolase	17628.4	5.89	11	1	15.76	-0.109		SecP	X
Am7036	Alpha Beta-Hydrolase	19628.3	4.73	16	2	26.79	-0.397			X
Am698	Asparagine Synthase	66390.6	6.02	2	1	15.22	-0.316			L
Am1656	Bifunctional Purine Biosynthesis Protein Ade10	102880.7	6.68	2	1	13.28	-0.141			R
Am16195	Branched-Chain Amino Acid Aminotransferase Ii	50091.5	6.08	4	1	17.03	0.222		SecP	L
Am6781	Carbamoyl-Phosphate Synthase	128202.6	5.58	1	1	13.7	-0.107			C

[a]Accession No.	[b]BLAST Annotation	[c]tM_r	[d]tp*I*	Coverage (%)	Unique Peptides	[e]SM Score	[f]GRAVY score	[g]TM	[h]SigP/ SecP	[i]Carbon Source
Am11216	Clps-Like Protein [*Punctularia Strigosozonata* Hhb-11173 Ss5] 60S Ribosomal Protein L7/L12 [*Coprinopsis Cinerea* Okayama7#130]	19569.8	9.1	8	1	11.6	-0.114		SecP	L
Am10309	Cyanide Hydratase	36508.4	5.17	10	2	38.94	-0.293			L
Am19539	Cytochrome P450	59192.4	7.75	5	1	13.28	-0.202	1		X
Am17714	Duf926-Domain-Containing Protein	31943.7	10.34	5	1	11.49	-1.654			R
Am18443	Enoyl- Hydratase	28429.6	5.73	6	1	15.2	-0.14			R
Am17421	FAD Binding Domain-Containing Protein	71332.5	5.1	2	1	14.56	-0.458			X
Am19516	Fruit-Body Specific Gene A	22995.6	4.15	14	1	16.16	-0.335		SigP	X
Am6729	Glutamate-tRNA Ligase	82564.3	6.35	3	2	30.51	-0.313			L
Am12531	Glycyl-tRNA Synthetase	77477.6	5.69	2	1	14.07	-0.382			L
Am8695	Heme-Thiolate Peroxidase Aromatic Peroxygenase	30726.2	6.76	6	1	14.97	-0.356		SecP	X
Am9566	Hit-Like Protein	15174.7	6.43	10	1	13.27	-0.165		SecP	C
Am20185	Homocitrate Synthase	57413.3	5.81	2	1	13.82	-0.254			L
Am6826	Hypothetical Protein Afua_8G01330 [*Aspergillus Fumigatu*s Af293]	6811.8	9.52	24	1	19.01	-0.138		SecP	R
Am9905	Hypothetical Protein Cc1G_02316 [*Coprinopsis Cinerea* Okayama7#130]	46986.4	5.98	4	1	13.18	-0.155		SecP	X
Am15856	Hypothetical Protein Mper_05655 [*Moniliophthora Perniciosa* Fa553]	29393.2	5.89	7.664234	1	11.6	-0.132			L

[a]Accession No.	[b]BLAST Annotation	[c]tM_r	[d]tp*I*	Coverage (%)	Unique Peptides	[e]SM Score	[f]GRAVY score	[g]TM	[h]SigP/ SecP	[i]Carbon Source
Am1780	Hypothetical Protein Schcodraft_71214 [*Schizophyllum Commune* H4-8]	47200.1	6.2	4	1	22.58	-0.305		SecP	X
Am15083	Hypothetical Protein Serla73Draft_176155 [*Serpula Lacrymans* Var. Lacrymans S7.3]	31332.7	4.46	5	1	17.11	-0.942			C
Am10047	Hypothetical Protein Serla73Draft_183485 [*Serpula Lacrymans* Var. Lacrymans S7.3]	17599.3	4.88	7	1	17.85	-0.751	1		L
Am17641	Hypothetical Protein Stehidraft_124123 [*Stereum Hirsutum* Fp-91666 Ss1]	18458.2	5.94	17	1	14.53	-0.167		SigP	X
Am7778	Hypothetical Protein Stehidraft_132886 [*Stereum Hirsutum* Fp-91666 Ss1]	7398.4	6.7	22	1	22.18	-0.027		SecP	X
Am19827	Isopentenyldiphosphate Isomerase	110051.5	4.89	1	1	24.26	-0.444			X
Am15222	Long-Chain-Fatty-Acid- -Ligase	84686.2	6.08	3	1	18.12	-0.043			L
Am18223	Mas20-Domain-Containing Protein	52653.5	5.51	3	1	16.43	-0.417			L
Am10401	Mitochondrial Inner Membrane Protein	26247.7	9.55	5	1	17.69	0.345		SecP	X
Am17299	Mov34-Domain-Containing Protein	30235.8	6.46	6	1	13.74	-0.348		SecP	X
Am3068	Myosin Regulatory Light Chain Cdc4	14466.4	4.77	15	1	13.34	-0.443		SecP	L
Am11164	*A. mellea* unknown function protein	23393.5	11.58	9	1	13.01	-1.75			X
Am15839	*A. mellea* unknown function protein	18959.3	4.61	6	1	22.16	-0.003		SigP	C
Am17640	*A. mellea* unknown function protein	15273.3	3.58	9	1	11.87	-1.65		SecP	L
Am2493	*A. mellea* unknown function protein	11542.1	8.75	23	1	17	-0.57			X

[a]Accession No.	[b]BLAST Annotation	[c]tM_r	[d]tp*I*	Coverage (%)	Unique Peptides	[e]SM Score	[f]GRAVY score	[g]TM	[h]SigP/ SecP	[i]Carbon Source
Am4753	*A. mellea* unknown function protein	19856.9	5.25	6	1	12.42	-0.463		SecP	C
Am14843	NAD -Binding Protein	33921.3	8.86	3	1	16.98	-0.197		SecP	X
Am6130	NADH-Ubiquinone Oxidoreductase	80827.3	5.85	6	3	47	-0.179		SecP	L
Am15049	NADH-Ubiquinone Oxidoreductase Kda Subunit	30681	8.92	6	1	17.98	-0.457		SecP	L
Am1862	Pci-Domain-Containing Protein	144834.7	6.03	1	1	17.82	-0.25			L
Am17064	Pkinase-Domain-Containing Protein	44696.4	8.7	4	1	16.75	-0.164			R
Am13522	Predicted Protein [*Laccaria Bicolor* S238N-H82]	12745.6	7.54	10	1	16.59	-0.495			C
Am15661	Predicted Protein [*Laccaria Bicolor* S238N-H82]	28483.4	6.09	5	1	15.53	-0.361		SecP	L
Am1474	Predicted Protein [*Sclerotinia Sclerotiorum* 1980]	5325.2	6.28	29	1	12.29	0.2		SecP	R
Am2522	Predicted Protein [*Sclerotinia Sclerotiorum* 1980]	5942.9	6.09	45	2	30.72	-0.028		SecP	C
Am10040	Protein Transporter Sec13	36229.9	5.81	5	1	19.73	-0.259		SecP	L
Am15181	Protein Yeta	101770.7	4.91	1	1	16.13	-0.296		SecP	X
Am3012	Saccharopine Dehydrogenase	42570.9	5.51	3	1	17.78	-0.101			L
Am20201	Serine Threonine-Protein Phosphatase Pp1	38343.6	7.49	5	1	16.35	-0.32		SecP	R
Am12952	Short-Chain Dehydrogenase	38932.1	5.24	3	1	14.23	-0.118			R
Am15670	Short-Chain Dehydrogenase	29960.6	5.61	6	1	12.72	0.208		SecP	R
Am12832	Short-Chain Dehydrogenase Reductase Sdr	30125.6	9.34	6	1	18.63	0.14		SecP	R
Am9802	Ste Ste11 Cdc15 Protein Kinase	176778.7	9.31	1	2	25.35	-0.57			R
Am5280	Threonyl-tRNA Synthetase	89785.9	6.08	1	1	15.44	-0.457			L
Am15540	Tkl Tkl-Ccin Protein Kinase	148559.3	6.65	1	1	12.51	-0.431			R

[a]Accession No.	[b]BLAST Annotation	[c]tM$_r$	[d]tp*I*	Coverage (%)	Unique Peptides	[e]SM Score	[f]GRAVY score	[g]TM	[h]SigP/ SecP	[i]Carbon Source
Am17809	Translation Initiation Factor Eif2 Gamma Subunit	48629.4	7.58	4	1	12.89	-0.147			L
Am14779	Translation Initiation Factor Eif3A	118315.4	9.03	1	1	14.52	-0.64			L
Am15088	Ubiquinol-Cytochrome C Reductase Iron-Sulfur Subunit	33684.6	9.01	3	1	14.1	-0.122		SecP	X
Am17092	Ubiquitin Interaction Domain-Containing Protein Family Protein	38078.6	4.48	5	1	12.83	-0.381			C

[a]Accession number from *A. mellea* cDNA database; [b]BLAST annotation following Blast2GO analysis of proteins identified from *A. mellea* cDNA database; [c]M$_r$, theoretical molecular mass; [d]tp*I*, theoretical isoelectric point; [e]SM score, Spectrum Mill protein score; [f]GRAVY score, grand average of hydropathy (Negative score indicates hydrophilicity while Positive score indicates hydrophobicity); [g]TM, number of transmembrane regions; [h]SigP, classical secretion signal peptide; SecP, non-classical secretion signal; [i]Carbon Source, restricted carbon source; C, cellulose L, lignin; R, rutin; X, xylan.

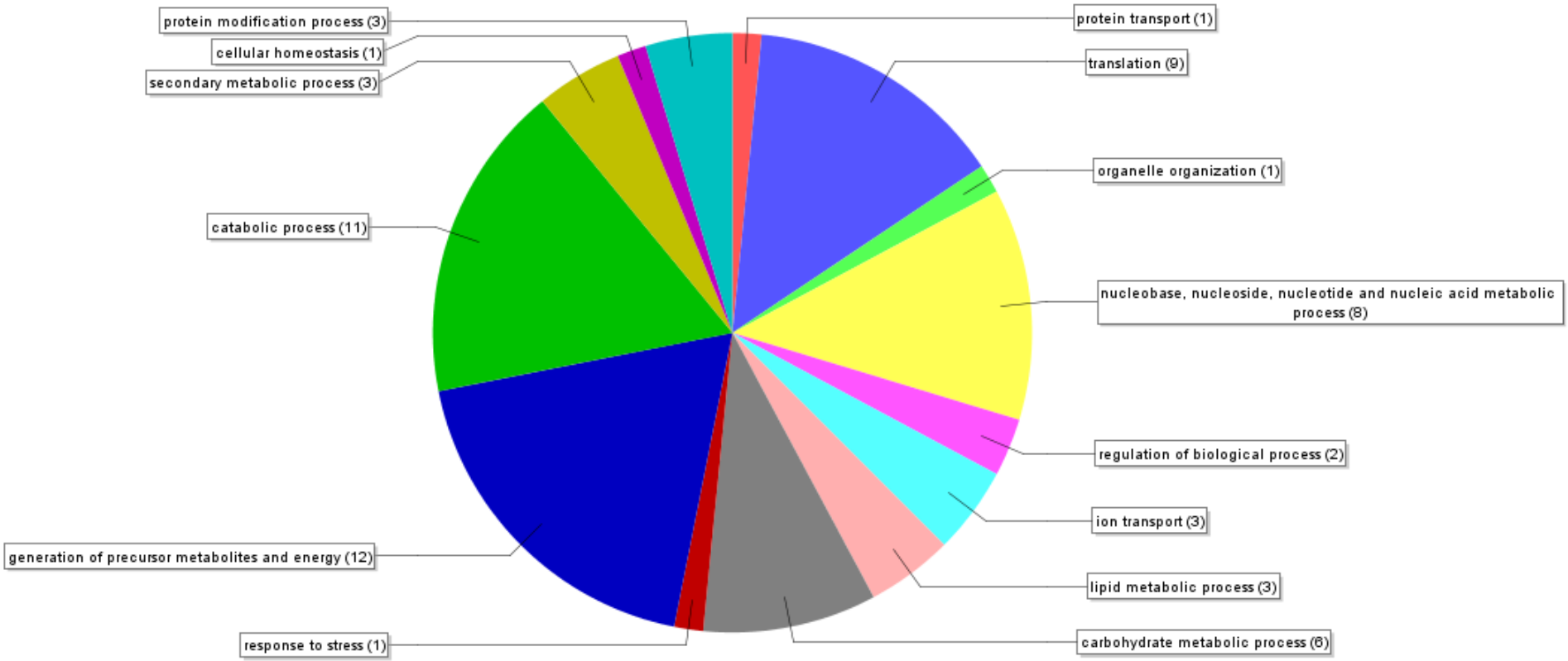

Figure 5.3. Biological process. GO categorisation by biological process of all *A. mellea* mycelial proteins, identified following growth on restricted carbon sources, and detected via shotgun LC-MS/MS. Numbers in brackets indicate the numbers of proteins in the GO category indicated.

5.2.4 *A. mellea* secreted protein from MEA culture: Shotgun LC-MS/MS identification and analysis.

Following *A. mellea* growth for 21 days on MEA (Section 2.2.3.3), conditioned agar was harvested as described in Section 2.2.7.7, following gentle maceration, proteins were extracted into 50 mM potassium phosphate pH 7.0 (Section 2.1.5.6) followed by TCA precipitation, washing and resuspension in trypsin digestion buffer (Section 2.1.5.11). Following direct LC-MS/MS analysis, 41 secreted proteins, from culture on MEA, were identified from peptides (n = 290). Almost 61% of the proteins identified possessed secretion signals SigP (n = 8) SecP (n = 17), and ten hydrophobic (24 %), and four transmembrane (10 %) proteins were detected. Total sequence coverage ranged from < 10 % (n = 8), to 10 - 20 % (n = 7), 20 - 50 % (n = 23) up to > 50 % (n = 3). Single peptides identified two proteins, Am10878 and Am13268, proteins (n = 19) were identified from 2 – 5 peptides, proteins (n = 12) 6 -10 peptides and >10 peptides (n = 8 proteins). All proteins identified by this shotgun approach were also identified by other methods, thus no protein was uniquely identified by shotgun proteomic analysis of *A. mellea* secretome following solid-phase culture on MEA agar. Nonetheless, a list of all proteins identified by this method is given in Table 5.3.

Table 5.3. *A. mellea* secreted proteins, identified by shotgun LC-MS/MS following extraction and trypsin digestion, from solid-phase culture on MEA.

[a]Accession No.	[b]BLAST Annotation	[c]tM_r	[d]tpI	Coverage (%)	Unique Peptides	[e]SM Score	[f]GRAVY score	[g]TM	[h]SigP/ SecP
Am13268	14-3-3 Protein	30042.7	8.91	4	1	14	-0.404		SecP
Am18230	14-3-3 Protein	34135.9	4.83	37	10	164.03	-0.35		
Am19381	Acetyl- Acetyltransferase	40335.3	6.26	42	11	212.23	0.088		SecP
Am15995	Aldo Keto Reductase	39486.6	8.58	18	5	87.18	-0.183		
Am18773	Aspartic Peptidase A1	44136.2	4.75	24	10	165.92	-0.055		SigP
Am14866	ATP Synthase F1 Gamma	32624.5	9.43	27	4	77.84	-0.167		SecP
Am3988	Carbohydrate Esterase Family 4 Protein	135875.9	5.93	3	2	45.32	-0.356		SigP
Am17600	Catalase	58498.8	6.75	39	13	243.76	-0.587		
Am16479	Class I Glutamine Amidotransferase-Like Protein	24213.5	5.38	11	2	29.79	-0.212		SecP
Am10627	Conjugated Polyketone Reductase C1	36926.4	5.96	27	8	126.92	-0.247		SecP
Am9269	Copper Radical Oxidase	84321.1	4.4	21	11	209.37	-0.093		SecP
Am3603	Dihydrolipoyl Dehydrogenase	53233.2	6.62	43	14	266.64	-0.103		SecP
Am20231	Enolase	47096.7	5.72	50	17	316.59	-0.108		
Am11987	Extracellular Solute-Binding Protein Family 1	45903.9	5.5	29	8	143.59	-0.003		SigP
Am18910	Glucose-6-Phosphate Isomerase	61249.8	6.38	5	2	45.54	-0.216		SecP
Am12863	Glyceraldehyde 3-Phosphate Dehydrogenase	39985.1	8.24	38	9	144.96	0.079		SecP
Am14135	Glycoside Hydrolase Family 27 Protein	47065	4.7	18	5	91.48	-0.182		
Am12215	Glycoside Hydrolase Family 3 Protein	148863.2	5.59	2	2	38.48	-0.211		SecP
Am5759	Glycoside Hydrolase Family 31 Protein	191108.2	6.39	2	4	60.82	-0.498	1	

[a]Accession No.	[b]BLAST Annotation	[c]tM$_r$	[d]tp*I*	Coverage (%)	Unique Peptides	[e]SM Score	[f]GRAVY score	[g]TM	[h]SigP/ SecP
Am15111	Glycoside Hydrolase Family 72 Protein	58531.8	4.34	11	5	84.6	-0.01		SigP
Am17793	Hcp-Like Protein	154493.3	6.64	3	3	48.33	-0.579		
Am3956	Heat Shock Protein	62575.8	5.15	44	19	340.81	-0.051		
Am15133	Hypothetical Protein Dicsqdraft_132490 [*Dichomitus Squalens* Lyad-421 Ss1]	14436.6	4.91	31	3	52.74	0.168		SigP
Am11329	Hypothetical Protein Dicsqdraft_170957 [*Dichomitus Squalens* Lyad-421 Ss1]	38549.9	5.64	23	4	74.13	0.032		SecP
Am3943	Hypothetical Protein Schcodraft_69684 [*Schizophyllum Commune* H4-8]	24157.7	4.6	22	3	59.58	-0.156	1	SecP
Am18369	Hypothetical Protein Travedraft_52018 [*Trametes Versicolor* Fp-101664 Ss1]	13690.6	4.47	17	3	64.53	0.174		SigP
Am13739	Malate Dehydrogenase	24250	6	19	3	65.65	0.314		SigP
Am3212	Mitochondrial Endopeptidase	75418.7	5.17	5	3	52.16	-0.451		
Am2320	*A. mellea* unknown function protein	15229.2	4.62	56	6	110.44	-0.483		
Am8112	NAD -Binding Protein	47400.2	8.82	43	15	250.81	0.017		
Am14376	NAD-Dependent Formate Dehydrogenase	39653.5	6.32	39	9	146.6	-0.207		SecP
Am10878	Peptidase S28	59821	5.19	2	1	19.36	-0.176		SigP
Am17796	Phosphoglycerate Kinase	46381.6	5.86	56	19	321.14	0.006	1	
Am12502	Phosphoglycerate Mutase-Like Protein	60386.3	6.2	26	10	188.36	-0.174	1	
Am13967	S-Adenosyl-L-Homocysteine Hydrolase	46819.9	5.59	27	9	121.04	-0.009		SecP

[a]Accession No.	[b]BLAST Annotation	[c]tM$_r$	[d]tp*I*	Coverage (%)	Unique Peptides	[e]SM Score	[f]GRAVY score	[g]TM	[h]SigP/ SecP
Am19945	Short Chain Type	32236.4	9.3	26	4	65.14	-0.029		SecP
Am4144	Tautomerase Mif	13091.1	4.99	46	3	55.53	0.071		SecP
Am16991	Transaldolase	34862.3	6.26	31	8	143.65	-0.141		
Am15936	Triose Phosphate Isomerase	25148	6.84	53	9	169.86	0.064		
Am15486	Tyrosinase	67594.7	5.75	18	8	127.39	-0.28		SecP
Am12436	Zb Protein	30612.3	5.1	25	5	86.75	-0.341		

[a]Accession number from *A. mellea* cDNA database; [b]BLAST annotation following Blast2GO analysis of proteins identified from *A. mellea* cDNA database; [c]M$_r$, theoretical molecular mass; [d]tp*I*, theoretical isoelectric point; [e]SM score, Spectrum Mill protein score; [f]GRAVY score, grand average of hydropathy (Negative score indicates hydrophilicity while Positive score indicates hydrophobicity); [g]TM, number of transmembrane regions; [h]SigP, classical secretion signal peptide; SecP, non-classical secretion signal.

5.2.5 Summary of mycelial and secreted proteins identified from direct shotgun LC-MS/MS.

In total, proteins (*n* = 613) were identified by optimised shotgun analysis following interrogation of the *A. mellea* cDNA database using 1995 peptides identified by LC-MS/MS. Approximately 47 % of identified proteins contained a signal sequence: SigP (*n* = 32) and SecP (*n* = 260). A number of hydrophobic proteins were identified (*n* = 80) and along with 63 proteins containing transmembrane regions. The breakdown of number of peptides by which proteins were identified is as follows: 1 peptide (*n* = 304), 2-5 peptides (*n* = 204), 6-10 peptides (*n* = 70), >11 (*n* = 35) with percentage coverage ranging from: < 10 % (*n* = 351), 10-20 % (*n* = 122), >20 % (*n* = 140).

B2G analysis of all mycelial proteins identified by shotgun LC-MS/MS, categorised by biological process, reveals that the largest quotient was classified as translation (45%). Breakdown of the other categories was as follows: nucleobase, nucleoside, nucleotide and nucleic acid metabolic process (11%); response to stress (8%); catabolic process (7%); Protein transport and carbohydrate metabolic process (5%) each; lipid metabolic process and signal transduction (3%) each (Figure 5.4). Complementary categorisation by cellular component (Figure 5.5) displays the breakdown as: ribosomal proteins (65%); protein complex (10%); nucleus (6%) and cytoskeleton (5%), while annotation via molecular process reveals involvement of proteins in structural molecule activity (42%), nucleotide binding (17%), RNA binding (7%) and enzyme regulator activity (4%) (Figure 5.6).

A theoretical M_r and p*I* map of the *A. mellea* proteome was constructed, from the in-house cDNA database, utilising JVirGel software (http://www.jvirgel.de) (Hiller *et al.*, 2006) and an overlay of the proteins actually identified by shotgun proteomics was carried out. The identified proteins encompassed all molecular mass and pH ranges compared to those predicted from the theoretical proteome (Figure 5.7).

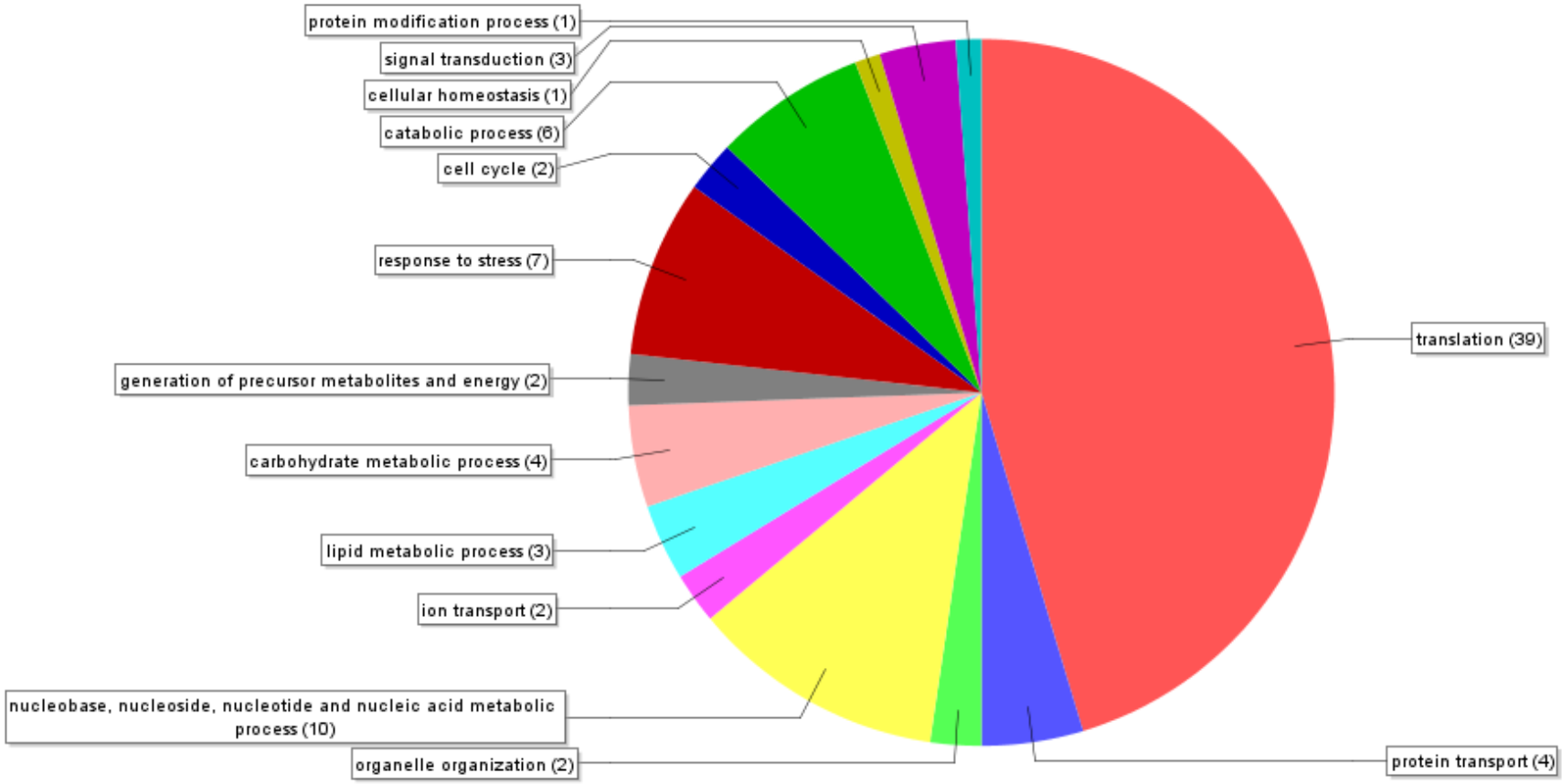

Figure 5.4. Biological process. GO multilevel graph of *A. mellea* mycelia analysed by shotgun LC-MS/MS; identification of biological process property domains defined by http://www.geneontology.org. The graph visualisation of GO annotations is from the lowest nodes of GO hierarchy, in the category of biological process. Numbers in brackets indicate the number of proteins in each category shown.

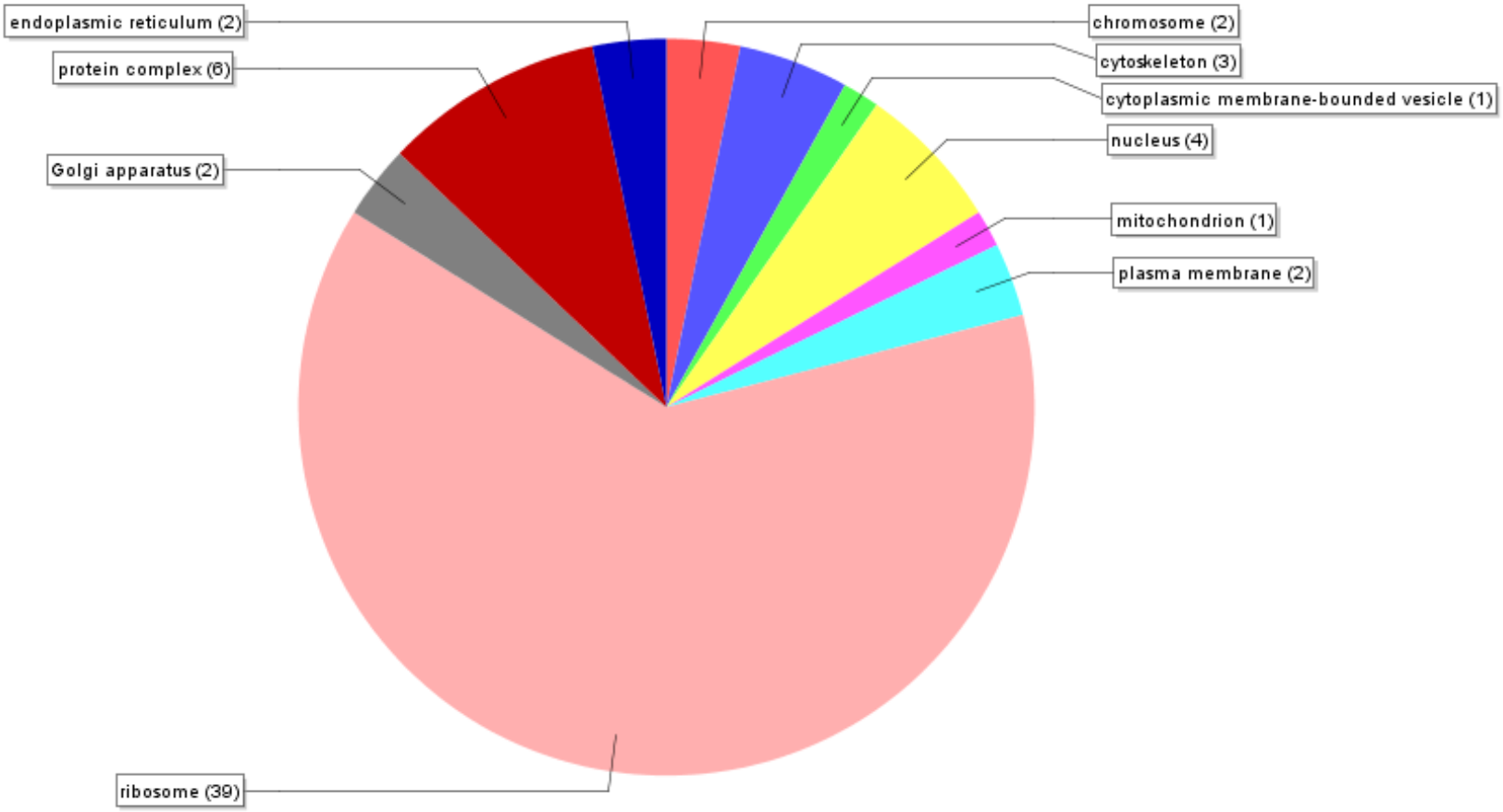

Figure 5.5. Cellular component. GO multilevel graph of *A. mellea* mycelia analysed by shotgun LC-MS/MS; identification of cellular component property domains defined by http://www.geneontology.org. The graph visualisation of GO annotations is from the lowest nodes of GO hierarchy, in the category of biological process. Numbers in brackets indicate the number of proteins in each category shown.

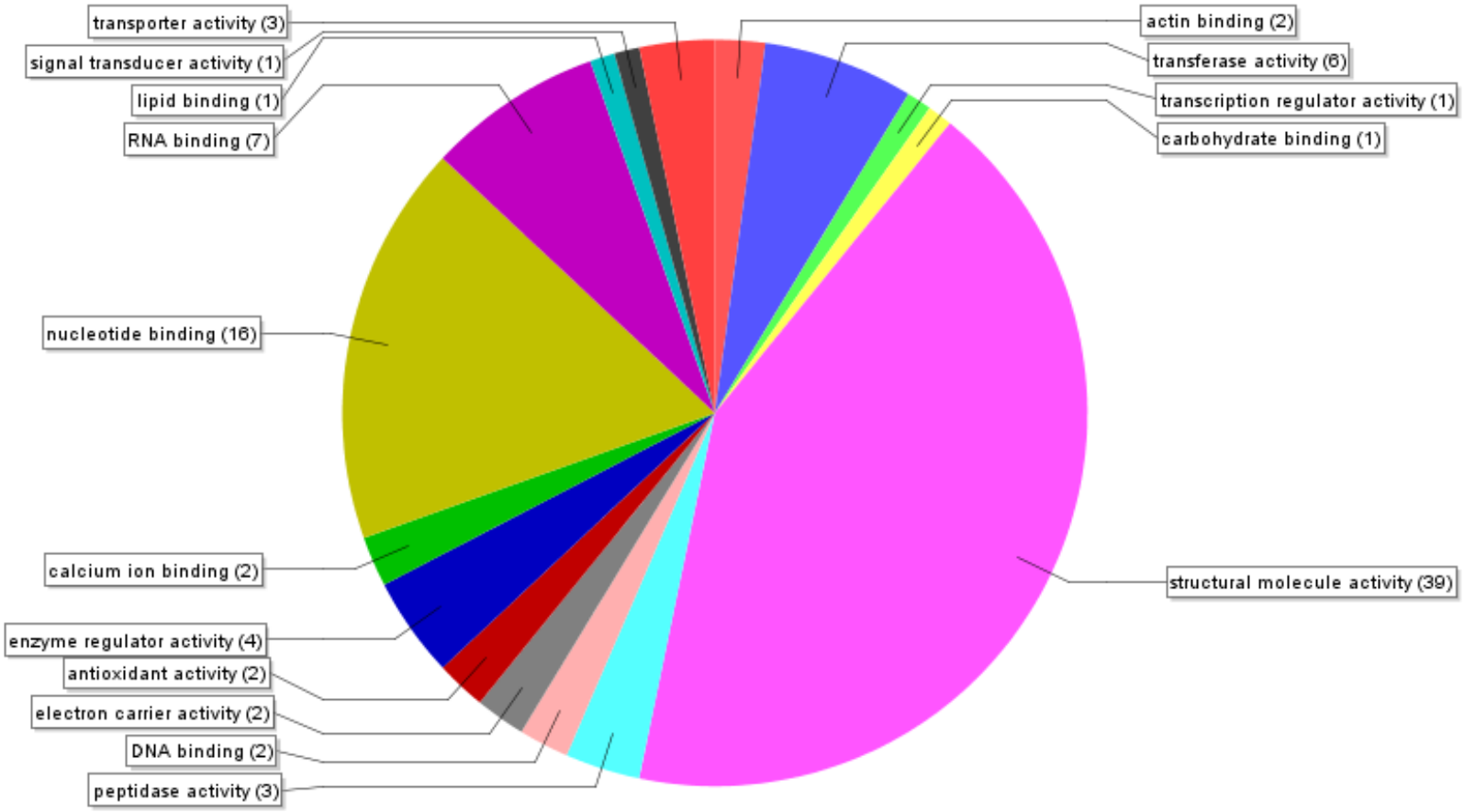

Figure 5.6. Molecular function. GO multilevel graph of *A. mellea* mycelia analysed by shotgun LC-MS/MS; identification of molecular function property domains defined by http://www.geneontology.org. The graph visualisation of GO annotations is from the lowest nodes of GO hierarchy, in the category of biological process. Numbers in brackets indicate the number of proteins in each category shown.

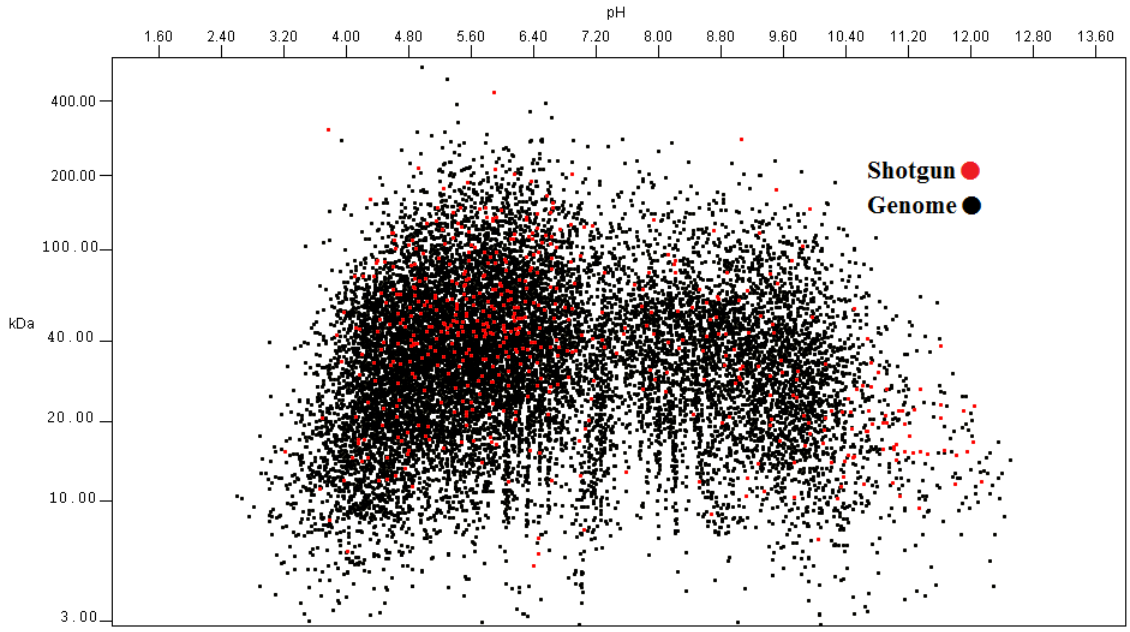

Figure 5.7. Superimposed theoretical M_r and p*I* of all observed proteins from shotgun analysis of mycelial proteins on those predicted from in silico analysis of the *A. mellea* proteome. Software from:http://www.jvirgel.de (Hiller *et al.*, 2006)

Ribosomal proteins (*n* = 63) were identified in *A. mellea* mycelia, and included those from the large 60S subunit (*n* = 36) and the small 40S eukaryotic subunit (*n* = 23). Only one ribosomal protein had a predicted transmembrane domain (Am16486). Thirty-one contained SecP signals and were identified from 1 - 8 peptides. Percentage coverage ranged from 1 % - 50 %. Eleven proteasome-related proteins were identified in mycelial extracts. Three (Am10604, Am14271 and Am15029) were the conserved 20S subunit and the remainder originated form the 26S proteasome complex proteins. Peptidases (*n* = 10), of which two were predicted to be of mitochondrial origin (Am3212 and Am15698), and NADH-ubiquinone oxidoreductases (Am6130 and Am15049) were identified in *A. mellea* mycelia by shotgun proteomics. Ribonucleases (*n* = 3) were identified in mycelia and Am1888 contained a SecP signal sequence and was hydrophobic. Am6779 was also hydrophobic and Am11553 was predicted to be hydrophilic in nature. Heat shock, heat shock-like and activator of Hsp proteins (*n* = 15) were identified from mycelia with 2% - 39 % coverage and Spectrum Mill scores of 16 – 433. The number of peptides identified per Hsp ranged from 1 - 25. Two metalloproteins (Am10231 and Am17617) were identified in mycelial extracts by detection of four and one peptides, respectively. Am10231 is hydrophobic while Am17617 contains a SecP signal peptide.

Alpha Beta-hydrolase proteins (n = 10) were identified in protein extracts from mycelia of *A. mellea* by shotgun proteomics. This family of proteins is one of the biggest superfamilies of structurally related proteins, with very diverse catalytic activity. There are currently more than 30,000 proteins in this group (Lenfant *et al.*, 2013, http://bioweb.ensam.inra.fr/esther), whose catalytic activity is derived from a common Nucleophile-His-Acid (Holmquist, 2000). Family members include lipases, esterases, peptidases hydrolases peroxidasese and lyases. Four of these proteins had SecP and one had SigP signal sequences, all had negative GRAVY scores, although two had one transmembrane region. Spectrum Mill scores for these proteins ranged from 16 – 39 with sequence coverage of 3 % - 16 % based on the detection of 1 or 2 peptides by LC-MS/MS. Eleven glycoside hydrolases (GH) from families 1, 2, 3, 16, 27, 31, 38 and 72 were identified by shotgun proteomics. Three proteins contained SecP and four SigP signal sequences. Four (Am5759, Am12215, Am14135 and Am15111) were identified in both mycelia and the secretome, while all other GH proteins were uniquely located. Sequence coverage ranged from 1 - 18 %, with between 1 - 5 peptides identified per protein, and Spectrum Mill scores ranging from 13 - 84. Five proteins from four families of glycosyltransferases (GT; 20, 32, 35 and 50) were identified at the protein level in mycelial extracts, two of which contained SecP secretion signals. Protein identification was based on detection of 1-2 unique peptides, and Spectrum Mill scores were in the range 16 - 44.

The substrate-specific carbohydrate binding module CBM12 (Am9123), was identified at protein level, as was CBM13 (Am11736); these proteins were identified by 6 and 5 peptides, respectively, and had Spectrum Mill scores of 81 and 114. Three carbohydrate esterase (CE) proteins from two families were detected by LC-MS/MS: CE1 (Am19807) was identified from 4 peptides and contained a SecP signal peptide, CE4 (Am3988) was identified in both mycelial and secretome extracts from 3 peptides, and another CE4 enzyme (Am6064) in a mycelial extract only was identified from 2 peptides. Both CE4 proteins possessed SigP signal peptides and overall, Spectrum Mill scores ranged from 45 – 74.

With regard to potential lignin degradation, no laccases were identified in the shotgun cohort of expressed proteins, but other proteins which may be implicated in lignin degradation were identified. For instance, a number of cytochrome P450s were identified, including Am19539 (1 transmembrane region) and Am5494 (a hydrophobic P450 with 2 transmembrane regions). A monooxygenase (Am16713) with a Spectrum

Mill score of 247 (from 14 peptides), a dioxygenase (Am18132) identified from 2 peptides and a peroxygenase (Am8695) with a SM score of 15 (from 1 peptide) were also identified in mycelia. Six peroxidases (Am13266, Am14119, Am14782, Am18006 Am6607 and Am14136) were identified at protein level from mycelia with Spectrum Mill scores from 12-250, as supported by 1-16 peptides. Three peroxidases possessed a SecP, and one a SigP, secretion sequence. A hydrophobic thioredoxin-dependent peroxidase (Am14136) was identified, which did not contain a transmembrane domain, while two others (Am13266 and Am14119) had predicted transmembrane domains.

A large number of proteins (n = 32) previously classified as "hypothetical proteins" were identified, which appear to exhibit homologs in 13 other fungal species. These re-categorised "unknown function proteins" were identified by Spectrum Mill scores between 11 and 247 (coverage ranged from 1-14 peptides). Four of these proteins were identified in the fungal secretome and mycelia. Seventeen predicted proteins were mycelial in origin, contained homologs in four fungal species, including 12 in *L. bicolor*. Two had one transmembrane region; Am15212, Am18801, while Am1474 and Am3995 were hydrophobic. Predicted proteins had Spectrum Mill scores ranging from 12 – 49 and were further identified by detection of 1 – 3 peptides/protein. Fifteen *A. mellea* specific proteins were identified in mycelia by shotgun LC-MS/MS. One (Am2320) was identified in both mycelia and the secretome. Six had SecP and two had SigP signal sequences, while four had transmembrane regions. All were identified by between 1 and 8 peptides and sequence coverage was 1% - 24%.

5.2.6 Indirect shotgun proteomics: LC-MS/MS following OFFGEL Electrophoresis.

Mycelial proteins from 3 - 6 week cultures were extracted according to Method 2A WCL (Section 2.2.7.3), digested as described in Section 2.2.10.4, subjected to fractionation by OFFGEL electrophoresis (Section 2.2.11), dried and reconstituted in Buffer A (Section 2.1.9.2). Samples were analysed by LC-MS/MS using several gradients (20 min – 600 min duration) and dilutions: $^{1}/_{100}$ dilution, $^{1}/_{10}$ dilution, 1 µl, 5 µl, 10 µl. It was found that sample volume of 1 µl using Program C (Table 2.6) gave optimum results in terms of protein identification.

Overall, 91 individual proteins were identified by a combination of OFFGEL electrophoresis and subsequent LC-MS/MS analysis and were supported by detection of 114 unique peptides. Four and 44 proteins, respectively, contained SigP and SecP secretion signals, and nine were identified as hydrophobic. Five proteins had 1-4 transmembrane regions. The p*I* ranges of peptides identified are given in Table 5.4, with the greatest number of peptides found in Well 1 of the OFFGEL electrophoresis chamber. Interestingly, no peptides were identified from wells 6, 11 and 12.

Proteins (*n* = 5; Am6080, Am7439, Am7452, Am17277 and Am19873) were identified from three peptides. With regard to Am19873, one of the peptides was identified in two wells and Am7452 three peptides were from the same well. Proteins (*n* = 9; Am6591 Am11036, Am11554, Am13413, Am14386, Am14558, Am15608, Am17796 and Am18706) were identified from two peptides. In the case of Am6591 and Am18706 both peptides were from Well 1, the remaining seven were from two different wells. Two proteins (Am14000 and Am20231) each were identified from one peptide present in two different wells (Table 5.5). It should be noted that ten *A. mellea* mycelial proteins were uniquely identified after OFFGEL electrophoresis fractionation and by LC-MS/MS (Table 5.6). Thus, although the overall number of proteins identified following OFFGEL fractionation was comparatively low, the potential to the technique to aid identification of selected proteins is noted.

Table 5.4. Number of peptides identified from each well following OFFGEL fractionation and LC-MS/MS of digested *A. mellea* mycelial protein

Well ID	Peptide p*I* range	No. Peptides
1	4 - 4.5	69
2	4.4 -5.2	7
3	4.2 - 5.8	2
4	5.2 -6	7
5	5.5 -6	5
6	-	N.D.*
7	6	1
8	6.7 -7.7	3
9	8.5 -9.2	2
10	8.5 - 9.75	8
11	-	N.D.*
12	-	N.D.*

*None detected

Table 5.5. *A. mellea* mycelial proteins identified by indirect shotgun proteomics (OFFGEL electrophoresis followed by LC-MS/MS).

[a]Accession No.	[b]BLAST Annotation	[c]SM Score	No. Peptides	Well ID
Am17277	5-methyltetrahydropteroyltriglutamate-homocysteine s-methyltransferase	53.05	3	W1, W10
Am6080	ATP synthase subunit beta	63.86	3	W1, W5
Am7452	Heat shock protein 90	37.31	3	W1
Am19873	Translation elongation factor 1a	56.88	3	W2, W8, W9, W10
Am7439	Trehalose synthase	60.31	3	W1, W2
Am6591	1-cys peroxiredoxin	37.04	2	W1
Am15608	40s ribosomal protein s7	28.2	2	W1, W10
Am18706	Act1_schco ame: full=actin-1 ame: full=beta-actin	35.94	2	W1
Am11036	Macrolide-binding protein fkbp12	23.41	2	W1, W10
Am17796	Phosphoglycerate kinase	23.98	2	W1, W10
Am11554	Pyruvate carboxylase	31.71	2	W1, W2
Am13413	Tubulin beta chain	38.32	2	W1, W2
Am14386	UTP-glucose-1-phosphate uridylyltransferase	32.53	2	W1
Am14558	Valosin-containing protein	41.98	2	W1
Am14000	6-phosphogluconate dehydrogenase	17.9	1	W9, W10
Am20231	Phosphopyruvate hydratase	19.64	1	W1, W2

[a]Accession number from *A. mellea* cDNA database; [b]BLAST annotation following Blast2GO analysis of proteins identified from *A. mellea* cDNA database; [c]SM score, Spectrum Mill protein score; No. of peptides, No of peptides identified from the protein; Well I.D., well number containing the relevant peptide.

Table 5.6. *A. mellea* mycelial proteins uniquely identified following prior fractionation of peptide mixtures using OFFGEL electrophoresis.

[a]Accession No.	Sample ID	[b]BLAST Annotation	[c]Protein tM*r*	[d]Protein tp*I*	[e]Peptide tp*I*	Coverage (%)	Unique Peptides	[f]SM Score	[g]GRAVY	Sequence
Am10358	W2	Adenylosuccinate synthase	46935.92	6.9	4.65	6	1	16.29	-0.041	(R)VGGGPFPTEQLNDVGVHLQEVGR(E)
Am10329	W2	Alcohol dehydrogenase superfamily protein	37847.44	6.16	4.65	5	1	15.99	0.152	(R)GVDHILEVGGPGTLEK(S)
Am14170	W1	C2H2 transcription factor	69190	8.6	9.7	3	1	13.37	-1.163	(R)IHnNDHnNITHHQPPKKTK(S)
Am13829	W4	Hypothetical protein SCHCODRAFT_107411 [*Schizophyllum commune* H4-8]	66530	6.02	5.96	4	1	13.24	-0.271	(R)NGIVVVRPDGIIGALVGGADGLK(E)
Am10368	W1	Ich1-like protein	51630	5.84	4.37	4	1	17.39	-0.113	(R)TLGSFIDLLGSEGWK(I)
Am16377	W1	Predicted protein [*Laccaria bicolor* S238N-H82]	25790	5.81	12.01	7	1	11.05	-0.65	(R)RFVGQKAPLFMPIR(T)
Am9598	W3	Protein	129540	6.38	4.23	2	1	13.14	-0.489	(R)EFILDVLEDVGKSLRDDILK(E)
Am11454	W3	Retrotransposable element tf2 155 kDa protein type 1-like	19200	4.87	5.84	9	1	11.88	-1.096	(K)GGmSIDTMVVnnK(N)

[a]Accession No.	Sample ID	[b]BLAST Annotation	[c]Protein tM*r*	[d]Protein tp*I*	[e]Peptide tp*I*	Coverage (%)	Unique Peptides	[f]SM Score	[g]GRAVY	Sequence
Am13023	W1	Ste ste7 protein kinase	52690	7.26	4.31	6	1	19.71	-0.391	(K)SASLPWSDDVLEQIASLGEG AGGAVHK(V)
Am5538	W10	Ubiquitin family protein	28300	6.58	9.72	6	1	16.62	-0.239	(R)VPVLPVPLPALPQR(K)

[a]Accession number from *A. mellea* cDNA database; [b]BLAST annotation following Blast2GO analysis of proteins identified from *A. mellea* cDNA database; [c]M_r, theoretical molecular mass; [d]Protein tp*I*, protein theoretical isoelectric point; [e]Peptide tp*I*, peptide theoretical iso electric point; [f]SM score, Spectrum Mill protein score; [g]GRAVY score, grand average of hydropathy (Negative score indicates hydrophilicity while Positive score indicates hydrophobicity); none of these proteins had transmembrane regions; none of these proteins had classical secretion signal peptides; Am5538, Am10329, Am10358, Am10368, Am3829 and Am16377 had non-classical secretion signals.

5.3 Discussion

No large-scale shotgun proteomic analysis of *Armillaria mellea* has been undertaken to date, primarily due to the dearth of genome sequence data available for the organism, and also because of the technical difficulties associated with obtaining sufficient protein for analysis and identification. Kim *et al.* (2007) predicted exponential growth in fungal proteomics which has largely come to pass, however to date, focus has been on particular sub-proteomic aspects of basidomycetes. In fact, only four large-scale basidiomycete mycelial proteomic analyses have been carried out in recent years: *Puccinia tritcina* (Rampitsch *et al.*, 2006), *Sparassis crispa* and *Hericium erinacum* (Horie *et al.*, 2008), *P. chrysosporium* (Matsuzaki *et al.*, 2008), and *L. bicolor* (Vincent *et al.*, 2012). Most studies of basidiomycetes have focussed on the secretome or sub-proteomic aspects of a particular fungus (Hori *et al.*, 2011; Vanden Wymelenberg *et al.*, 2010). Importantly, there has been no proteomic mycelial or secretome analysis of *A. mellea* carried out to date. The work presented in this Chapter used the *A. mellea* cDNA database described in Chapter 3 to overcome the first issue, while simultaneously developing protein isolation strategies, in parallel with extensive LC-MS/MS method development, to enable shotgun proteomic analysis of this plant pathogen. Using shotgun LC-MS/MS conditions optimised for analysis of complex protein digests, 613 unique proteins were identified from *A. mellea* mycelia and secretome, of which 32 had previously only been characterised as hypothetical proteins, and 17 as predicted proteins. Moreover, the identification of 15 proteins unique to *A. mellea* has been revealed by this analysis. There were a greater numbers of proteins (n = 518) and peptides (n = 1856) identified from PDB than from with restricted carbon sources. *A. mellea* growth on restricted carbon sources led to the identification of 74 proteins not found under any other culture condition. The direct shotgun proteomic analysis of the *A. mellea* secretome following solid-phase culture on MEA agar led to the successful identification of 41 proteins, which exhibited much greater occurrence of signal sequence (61%) compared to mycelial proteins (47%). Indirect shotgun proteomic analysis, via preliminary OFFGEL electrophoretic fraction of peptide digests was of limited success, yet resulted in the unique identification of ten *A. mellea* proteins. Combined, these data comprise the first output of unique proteome information from *A. mellea*

5.3.1 LC-MS/MS optimisation

A. mellea-specific LC-MS method development, combined with the shotgun proteomic approach for protein identification without prior fractionation, was the first time this strategy had been utilised at the host institution. The most effective means of optimisation of the direct shotgun technique in this study was gradient extension whose effect is shown in Figure 5.2B. Ion trap mass spectrometry is limited by the speed of processing of the machine used and thus the resolution of individual peptides is dependent on machine speed. Therefore, the number of identified peptides in an LC-MS/MS run is far less that the total number of peptides in samples. Michalski *et al.* (2011), using a high resolution MS system, detected more than 100,000 features (peptides) in a sample of which only 16 % were selected for fragmentation. These isopeptides could be detected at LC level but instrument speed is limiting and 10 -100 times increase would be required to detect all of these. Due to the lack of available protocols for large-scale proteomic analysis of basidiomycetes in general (Rampitsch *et al.*, 2006; Horie *et al.*, 2008; Matsuzaki *et al.*, 2008; Vincent *et al.*, 2012), and *A. mellea* in particular, future utilisation of protocols developed in this study represent a valuable strategy, not only for study of basidiomycetes, but also other organisms.

5.3.2 Mycelial proteins

PDB media yielded the greatest amount of biomass and also enabled the identification of the greatest number of proteins (n = 518). The maximum coverage of mycelial proteins identified by this method was somewhat lower (51 %), than that obtained by 2-DE (81%), but the number of proteins identified in a single sample was more than 150 in most cases. A large-scale study of *L. bicolor* identified 815 unique mycelial proteins by SDS-PAGE/ shotgun analysis, whereby mycelial proteins were first separated by SDS-PAGE, lanes cut into 16 divisions and digested and analysed by nanoLC-MS/MS, an instrument with very high sensitivity (Vincent *et al.*, 2012). A further 163 unique proteins were identified by 2-DE separation and nanoLC-MS/MS across three distinct pH ranges 3 – 11, 4 -7 and 7 -11 (Vincent *et al.*, 2012). This underlines the success achieved herein for protein identification from mycelia of *A. mellea* using an LC-MS instrument, theoretically of lower sensitivity, whereby 518 proteins were identified without prior fractionation. A 2-DE approach followed by MALDI-ToF-MS analysis, was used for proteome investigation of *P. chrysosporium* mycelia, with or without addition of exogenous benzoic acid, and 300 proteins were

identified. Coverage of differentially expressed proteins was up to 60% in that study (Matsuzaki *et al.*, 2008).

Hydrophobicity of identified mycelial proteins from shotgun/LC-MS/MS was 13%. To identify additional hydrophobic proteins from mycelia requires further method development, and techniques to isolate *A. mellea* membrane proteins would be one way of achieving this goal (Shary *et al.*, 2008; Shevchenko *et al.*, 2010). The molecular mass and pH distribution of proteins identified from the shotgun approach (Figure 5.7) was much wider than those identified by gel electrophoresis: 39% had pH >7 compared to 10% of those identified by 2-DE and 11% were >100 kDa compared to 7% of those identified by 2-DE. A large number of ribosomal proteins were identified by shotgun proteomics (n = 57) representing 11 % of the total, by far the most abundant group in this dataset. Ribosomal proteins are very abundant, but have extreme basic pH, and in fact 5 identified ribosomal proteins had p*I* values less than pH 6, and 51 were greater than pH 8.0 and so presented difficulties for fractionation by 2-DE (Tartaglia and Caflisch, 2007; Warner and McIntosh, 2009). Direct LC-MS/MS analysis following SCX separation of ribosomal proteins was used to identify >100 ribosomal proteins in a single run in *S. cerevisiae* (Link *et al.*, 1999). As *A. mellea* samples were more complicated mycelial samples the shogun approach highlights the efficacy of the method.

5.3.3 Restricted carbon sources

Culture of *A. mellea* on restricted carbon sources added considerably to the number of proteins identified. There were 365 proteins identified from mycelia obtained after growth on various restricted carbon sources, of which 74 proteins were uniquely identified in mycelia generated from these media. The numbers of mycelial proteins identified by culture on a single carbon source were: lignin, 194; xylan, 188; rutin, 185 and cellulose, 161. *P. chrysosporium*, a white rot fungus also showed increased growth on media containing cellulose and xylan compared to media only containing starch (Hori *et al.*, 2011, 2012). Cultures of *P. chrysosporium* were grown on oak in liquid or solid culture, and defined media (glucose and cellulose) liquid cultures (Abbas *et al.*, 2005; Sato *et al.*, 2007), to assess differential expression of secreted protein on different substrates and on solid and liquid media, by 2-DE and LC-MS/MS analysis. A total of fifty-eight secreted proteins were identified by a combination of SDS-PAGE and 2-DE protein separation, followed by LC-MS/MS analysis, in two studies (Abbas *et al.*, 2005; Sato *et al.*, 2007), however, no proteomic mycelial analysis was carried out. This is

consistent with *A. mellea* having lignocellulolystic attributes, but interestingly the proteins identified were of mycelial origin, although 48 % did display secretion signals. As with mycelial proteins identified when grown on PDB, a large number (n = 46) were ribosomal. The uniquely identified proteins of mycelia grown on restricted carbon sources included five ribosomal proteins. Five *A. mellea* specific proteins (Am2493, Am4753, Am11164, Am15839 and Am17640) were identified from mycelia generated under these restricted conditions. These proteins and the other 69 may be useful as enzymes with biotechnological application as replacement of glucose by glycerol as carbon source was shown by Li *et al.* (2011) to induce laccase activity in *G. lucidium.*

5.3.4 Direct LC-MS/MS analysis of secreted proteins.

Extracellular proteins are secreted in very small amounts and are difficult to quantify, as discussed in Section 4.2.2.2. Fragner *et al.* (2009), using their optimised protocol used gel electrophoresis to separate secreted protein. Secretome analysis of *Botrytis cinerea* an ascomycete, utilising restricted carbon sources and tomato cell walls was undertaken by Fernández-Acero *et al.*, (2010) but the approach was 2-DE followed by MALDI ToF/ToF analysis. Herein, development and application of the shotgun technique to analysis of secreted proteins from solid media although not uniquely identifying proteins was a novel application of the shotgun technique, which did identify 41 proteins of which 61% had a signal sequence and included four glycoside hydrolases from four families. The advantage of the shotgun proteomic technique is that protein identification was not constrained by the necessity to add detergent or SDS to solubilise protein and prevent aggregation as described by Lin *et al.* (1999), but in addition, polysaccharide and melanin were reduced, perhaps trapped in the agar, enabling the extraction of cleaner protein samples prior to preparation for direct LC-MS/MS analysis.

Table 5.7 lists proteomic studies of basidiomycete species that have been carried out in recent years. The two most extensively studied species are *L. bicolor* and *P. chrysosporium*, however few studies have focussed on a global organism analysis. Mycelial proteomic analysis of *P. tritcina* while generating a 2-DE map, targeted differential proteomics of host-pathogen interaction (Rampitsch *et al.*, 2006). Secretome analysis of basidomycetes, whether comparative or to optimise and analyse specific activity, comprises the largest sector of basidiomycete research. The main focus has been on identification of hydrolytic enzymes, with at least seventeen studies, compared to only four mycelial proteomic studies (Table 5.7). This highlights the importance of

the present work, where a combination of the genomic and proteomic data from *A. mellea* provides insight into this phytopathogenic fungus, thus enabling further exploration of its virulent and pathogenic mechanisms.

Table 5.7. List of proteomic studies of basidiomycete species.

Organism	**Category**	**Reference**
Laccaria bicolor	Mycelial proteome	Vincent *et al.*, 2012
Phanerochaete chrysosporium	Mycelial proteome	Matsuzaki *et al.*, 2008
Puccinia tritcina	Mycelial proteome	Rampitsch *et al.*, 2006
Sparassis crispa and *Hericium erinacum*	Mycelial proteome	Horie *et al.*, 2008
Phanerochaete carnosa	Secretome	Mahajan and Master, 2010
Phanerochaete chrysosporium	Secretome	Hori *et al.*, 2011, 2012
Phanerochaete chrysosporium	Secretome	Sato *et al.*, 2007
Postia placenta	Secretome	Martinez *et al.*, 2009
Postia placenta and *Phanerochaete chrysosporium*	Comparative secretome analysis	Vanden Wymelenberg *et al.*, 2010
Schitzophyllum commune and *Trichoderma viride*	Co-culture induced secretome	Ujor *et al.*, 2012
Tapinella panuoides	Atromentin proteins	Schneider *et al.*, 2008
Monoiliophthera pernicosa	Cellulolytic proteins	Ahamed and Vermette, 2009
Postia placenta	Cellulolytic proteins	Ryu *et al.*, 2011
Monoiliophthera pernicosa	Chitinase	Galante *et al.*, 2012
Coprinopsis cinerea	Laccase	Rühl *et al.*, 2013
Pleurotus ostreatus	Laccase	Castanera *et al.*, 2012
Ceriporiopsis subvermispora and *Phanerochaete chrysosporium*	Comparative laccase	Fernandez-Fueyo *et al.*, 2012
Phanerochaete chrysosporium	Laccase	Shary *et al.*, 2008
Ganoderma lucidium and *Candida spp.*	Co-culture induced laccase	Li *et al.*, 2011
Phanerochaete chrysosporium	Oxidative system	Kersten and Cullen, 2007

Organism	Category	Reference
Coprinopsis cinerea	Sesquiterpene synthase	Agger *et al.*, 2009

5.3.5 Indirect LC-MS/MS OFFGEL fractionation

Indirect LC-MS/MS whereby proteins were pre-fractionated by OFFGEL electrophoresis, identified 91 mycelial proteins, of which ten were uniquely identified using the indirect shotgun approach (Table 5.6). Separation of proteins was somewhat problematic as the distribution of peptides identified in fractions 2 – 12 (Table 5.4) was different to that observed by Chenau *et al.* (2008) (Figure 5.8). The numbers of peptides per well were also considerably lower, as Chenau *et al.* identified up to 150 unique peptides per well, compared to a maximum of 69 in this study. The volume of retrieved fractions from OFFGEL fractionation differs in each well and so at retrieval it appeared that fractions had focussed based on their volumes. Volumes in wells 4 – 8 representing pH 5 - 7 (Table 5.4) were greater than other wells and only a few microlitres were retrieved from well 11. Dried peptide samples were somewhat insoluble in sample buffer prior to purification on PepClean^{TM} C-$_{18}$ spin columns, hence the sonication step. Extended gradients were utilised as were a number of dilutions to improve the resolution of eluted peptides. The pH of the identified peptides was consistent with the fraction from which they were identified, but only from fraction W1 were a large number of peptides identified. According to a study by Chenau *et al.* (2008), the peptides in Well ID 10 (pH 8.5 – 9.75) would be expected to be less than 1% (Figure 5.8) of the total identified peptides (n = 104) while peptides identified in Well ID 2 represent 18% of the total (Table 5.4). Fractionation of *L. bicolor* secretome proteins by indirect shotgun approach identified 142 proteins (Vincent *et al.*, 2012), but no basidiomycete mycelial proteome has been analysed by this method to date. However if the technique could be further optimised the number of proteins identified could be greatly expanded, as pre-fractionation should greatly increase identification of proteins.

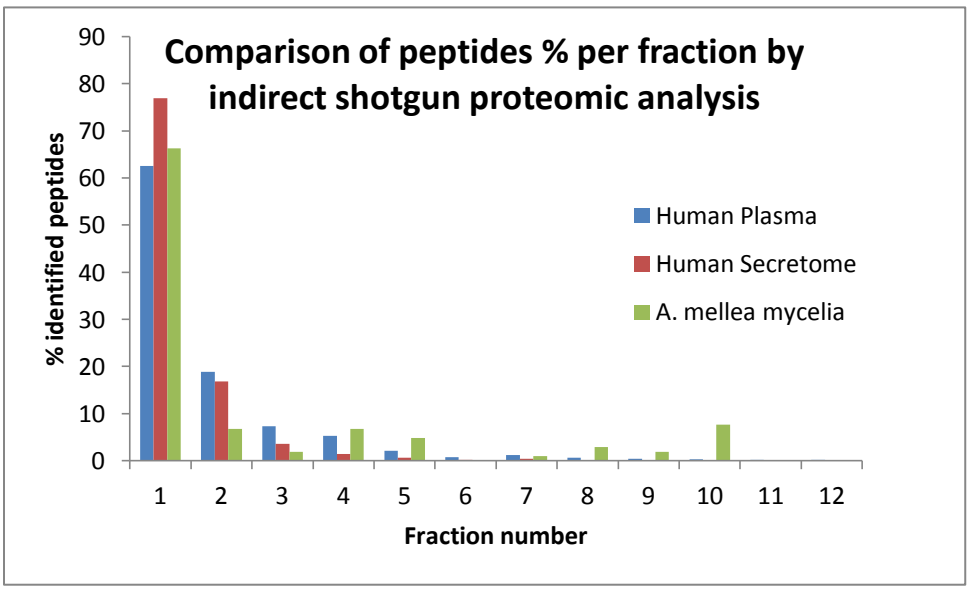

Figure 5.8. Percentages of identified peptides in sample fractions from indirect shotgun proteomic analysis. Human plasma and secretome percentages identified by Chenau *et al.* (2008), compared to analysis of *A. mellea* mycelial proteins.

In summary this method for large-scale protein identification proved very effective, as the substantial and tedious nature of extensive 2-DE in-gel digestion of protein spots is time consuming both in terms of preparation and sample analysis. Post LC-MS/MS data analysis, and organisation of the large datasets proved to be the most challenging part of the shotgun approach. This approach could be further optimised by pre-fractionation of proteins by organelle (e.g., ribosome or membrane), and OFFGEL electrophoresis prior to shotgun/LC-MS/MS analysis. The "hypothetical" (n = 33), "predicted" (n = 17) and *A. mellea* specific proteins (n = 15) identified are a valuable cohort of proteins for future defence, virulence and host-pathogen interaction studies. These aspects of *A. mellea* biology will be explored in the work presented in subsequent chapters.

Chapter 6 Differential proteomic investigation of the oxidative stress response in *Armillaria mellea*.

6.1 Introduction

Reactive oxygen species (ROS) are free radicals derived from the sequential reduction of molecular oxygen to water, and can be generated in organisms by aerobic respiration (Li *et al.*, 2009). ROS are localised in cellular compartments and are scavenged by antioxidants to maintain steady state levels (Heller and Tudzynski, 2011), but at high concentrations they cause wide-ranging cellular damage (Sharma *et al.*, 2008). They are also utilised as intracellular signalling molecules in symbiotic and pathogenic interactions (Heller and Tudzynski, 2011). Moreover, in certain basidiomycetes, extracellular lignin degradation is mainly achieved by oxidation reactions catalysed by extracellular oxidases and peroxidases, using hydrogen peroxide (H_2O_2) as a co-substrate (Syed and Yadav, 2012). Consequently, there are potentially three sources of ROS in *A. mellea* (i) intracellular ROS generated as a result of metabolism (ii) ROS generated by external stressors, hosts or pathogens, and (iii) ROS secreted by the organism as a means to degrade polymeric and aromatic substrates.

Intracellular ROS are generated in mitochondria during oxidative metabolism, as part of the routine generation of energy by all living organisms (Lushchak, 2011). As well as breakdown of substrates during metabolism, ROS have a protective function against pathogens, xenobiotics and proteotoxic moieties (Ray *et al.*, 2012). In phytopathogen fungal-plant interactions their main roles are in defence and signalling by the plant, but pathogens may induce and use ROS for their own benefit (Heller and Tudzynski, 2011). ROS, particularly hydroxyl radicals, interact non-specifically with all intracellular molecules: proteins, lipids, DNA, RNA and carbohydrates. When levels of ROS are elevated the organism is said to be under oxidative stress and an oxidative stress response is induced in order to maintain homeostasis (Heller and Tudzynski, 2011). Specifically, at a molecular level, oxidative stress causes DNA modification, oxidation of deoxyribose moieties, breakage, removal of nucleotides and formation of DNA-protein crosslinks. Lipids are cleaved and membranes become penetrable and fluid. Proteins are fragmented or modified, and enzymes are inactivated, leading to apoptosis and even tissue necrosis (Sharma *et al.*, 2012). Many organisms exhibit an oxidative stress response, which initiates a signalling cascade, leading to upregulation of transcription of antioxidant genes and alterations in cell membrane permeability (Ray *et al.*, 2012). ROS are scavenged by small soluble molecules such as polyamines,

glutathione, flavinoids and ascorbic acid which become oxidised by ROS, thus removing the damaging species. Enzymes upregulated under oxidative stress include superoxide dismutase (SOD) which dismutates $O_2^{\bullet -}$ to hydrogen peroxide, and catalase which degrades H_2O_2 to H_2O (Heller and Tudzynski, 2011).

Fungal degradation of organic material plays a vital part in recycling organic materials and the carbon cycle (Lundell *et al.*, 2010; Martin *et al.*, 2008). Indeed, fungi are particularly important in the degradation of lignocellulose (Dashtban *et al.*, 2009), and basidiomycetes secrete degradative enzymes, secondary metabolites, laccases, and peroxidases (Erjavec *et al.*, 2012) to effect this process. Cell wall degrading enzymes break down specific cell wall components, however lignin is one of the most problematic to degrade, due to its heterogeneous aromatic polymeric structure which crosslinks cellulose and hemicellulose, as well as phenolic compounds such as melanin, in the cell wall (Martinez *et al.*, 2004). There are two types of wood-degrading fungi, brown-rot fungi which digest cellulose and hemicellulose, and white-rot fungi such as *A. mellea* whose powerful enzyme activity degrades lignin (Lundell *et al.*, 2010). White rot fungi generate highly reactive ROS that react with lignin aromatic polymers, which are ultimately degraded to CO_2 and H_2O (Leonowicz *et al.*, 2001; Lundell *et al.*, 2010; Hammel and Cullen, 2008). Lignin modifying enzymes, laccases, heme-containing peroxidases, multicopper oxidases and metal-containing oxidoreducases are involved in a network of processes generating ROS to breakdown a wide range of aromatic compounds by oxidative processes. Brown-rot fungi generate radicals by the Haber-Weiss Reaction, also known as Fenton chemistry, to degrade cellulose (Martinez *et al.*, 2009).

Generation of ROS species by subjecting an organism to oxidative stress generally induces upregulation of genes involved in the stress response, and different stressors elicit upregulation of different stress responses (Pócsi *et al.*, 2005). In *A. nidulans*, three stressors, diamide which induces thiol-oxidation, H_2O_2 which increases intracellular peroxide, and menadione which generates superoxide anions, were compared, and were found to induce different patterns of cellular functional categories of RNA transcripts. From a total of 1986 genes identified from 10 functional categories, the observed distribution was diamide (n = 739), H_2O_2 (n = 631) and menadione (n = 1227) (Pócsi *et al.*, 2005). In *P. chrysosporium* exposed to 2, 4-dichlorophenol and cadmium, pollutants produced as a result of industrial activity which are known to cause widespread cellular damage, intracellular ROS increased and

antioxidant levels were upregulated. Most of the antioxidant response was dose-dependent and enzymes such as superoxide dismutase and catalase were upregulated in a dose-dependent manner as a response to the toxins. However, at high toxin levels, malondialdehyde, an indicator of increased intracellular ROS, thus indicating toxin levels at which damage was irreparable. This provides useful information for use of *P. chrysosporium* in bioremediation and its tolerance of industrial pollutants (Zeng *et al.*, 2012). Heavy metals such a cadmium and lead deplete cellular antioxidants, particularly thiols, leading to oxidative stress. White rot fungi are particularly tolerant of organic pollutants and heavy metals and *P. chrysosporium* was tolerant to 100 µM lead in liquid culture (Yildirim *et al.*, 2011). 2-DE followed by MALDI-ToF-MS was used to analyse differentially regulated proteins in *P. chrysosporium* subjected to 3 lead concentrations, and 14 upregulated proteins and 21 downregulated proteins were identified. Six of the upregulated proteins were induced by lead and two of these were only induced at higher concentrations. Among the down-regulated proteins, seven were cobalamin-independent methionine synthases (Yildirim *et al.*, 2011).

As different pathways are known to be induced under the influence of different stressors (Thorpe *et al.*, 2004), it was decided to undertake a comparative proteomic study of *A. mellea* using two complementary oxidative stress scenarios. Respiration pathways have been shown to be upregulated under H_2O_2-induced stress, but enzymes from the pentose phosphate pathway have been shown to be upregulated under menadione-induced stress in *A. nidulans,* with little overlap (Pócsi *et al.*, 2005). Respiratory chain complex III produces superoxide and it is thought that increased H_2O_2, together with superoxide generated from respiration would catalyse production of hydroxyl radicals by Haber-Weiss reaction, then metal ions reduced by superoxide anions would lead to hydroxyl radical formation from H_2O_2 (Thorpe *et al.*, 2004). Menadione, in a redox cycle, generates superoxide ions, which inhibits iron-sulphur proteins activities, which produces hydroxyl radicals (Pócsi *et al.*, 2005; Raha and Robinson, 2000; Toledano *et al.*, 2003). The two stressors are degraded differently, H_2O_2 generates hydroxyl radicals while menadione generates a range of ROS, by the Haber-Weiss reaction. The net Haber-Weiss reaction is formation of a hydroxyl radicals and a hydroxide ion with the release of oxygen. The reactivity of ROS increases consecutively: $O_2\bullet^-$, H_2O_2, and •OH (Lushchak, 2011). Oxidative stress induced by H_2O_2 in *A. nidulans*, increased levels of intracellular O_2^{2-} and $O_2\bullet^-$, whereas menadione-induced stress increased O_2^{2-} and $O_2\bullet^-$ levels but also promoted intracellular

accumulation of O_2^{2-}. Stress induced by H_2O_2 dissipated between 3 and 9 h but this was not the case where menadione was the stressor and oxidative stress continued to increase (Pócsi *et al.*, 2005).

Consequently, the aims of the work presented in this chapter were:

1. To subject *A. mellea* to two distinct oxidative stress conditions, namely H_2O_2 and menadione/Fe^{3+}, to mimic lignocellulolytic and infection conditions, respectively.
2. To carry out the first differential proteomic analyses, by 2-DE, of *A. mellea*, in response to these oxidative stress conditions.
3. To identify differentially-regulated *A. mellea* proteins following exposure to oxidative stress.
4. To use bioinformatic tools to elucidate hypotheses as to why specific metabolic systems, comprising differentially-expressed proteins, are altered subsequent to oxidative stress.

6.2 Results

A. mellea was grown for 28 days in PDB at 25 °C, and was subjected to two distinct oxidative stress conditions: 1 mM H_2O_2 or 0.5 mM Menadione/100 µM $FeCl_3$ for 3 h (Section 2.2.5). Two biological replicates per treatment were carried out. Cultures were harvested (Section 2.2.4.2), mycelia frozen in liquid N_2 and supernatant frozen at -20 °C. Mycelia were ground in liquid N_2 to effect lysis. Mycelial protein was extracted (Section 2.2.7.2) and quantified using the Bradford technique (Section 2.2.7.1). Proteins were separated by 2-DE (Table 2.4 and Section 2.2.8.3), gels stained with Colloidal Coomassie stain (Section 2.2.8.2) and were recorded as digital images using a CCD Scanner. Image quality was inspected, aligned, replicates grouped using SameSpots™ software (Section 2.2.9). Spots were selected for LC-MS/MS analysis based on a statitistically significant difference of $p < 0.05$ (Anova) from analysis and visual inspection. Spots were subjected to in-gel digestion (Section 2.2.10.3), LC-MS/MS analysis (Section 2.2.15.2), and identified following interrogation of the *A. mellea* cDNA database (Section 2.2.15.3).

An image of the 2-DE reference gel from extracted mycelial proteins of *A. mellea* under H_2O_2-induced stress is shown in Figure 6.1, with the differentially regulated, unambiguously identified spots outlined and numbered. There were ~1142 spots identified on the gels and thirty-four protein spots were found to be differentially regulated in the H_2O_2 dataset with 1.2 – 2.6 fold change (Table 6.1). After database interrogation a total of 45 distinct proteins were distinguished from these 34 spots, as multiple protein hits were detected from some spots (n = 16). Protein isoforms or modifications were also detected, as five proteins (Am6080, Am9508, Am11954, Am17277 and Am19873) were identified in more than one spot, whereas no protein hits were detected from three spots (Table 6.1). The 2-DE reference gel from extracted mycelial proteins of *A. mellea* under Menadione/$FeCl_3$-induced stress is shown in Figure 6.2, with differentially regulated and unambiguously identified spots outlined and numbered. In the Menadione/$FeCl_3$ dataset of ~1122 proteins which were visualised, 21 protein spots exhibited differential regulation whereby fold change ranged from 1.1 – 3.5 (Table 6.2). Under Menadione/$FeCl_3$-induced oxidative stress, 20 distinct proteins were identified from the 21 spots. There were seven spots from which there were multiple protein identifications. Isoforms or protein modifications of two proteins (Am18443 and Am19381) were identified, as they were both present in two spots and no proteins were distinguished in three of the spots (Table 6.2).

Four protein spots from the 2-DE analysis of the H_2O_2 stress condition and four from Menadione/$FeCl_3$ stress condition which were computationally identified as differentially regulated, were not selected for analysis as visual inspection deemed them too difficult to precisely excise for accurate identification.

Spots which contained more than one protein were excluded from further study as it was not possible to determine unambiguously which of the identified proteins was differentially regulated. One case in point is protein spot numbers 809 and 696 (Table 6.1), from which Am11954, a proliferation-associated 2g4 was identified. In spot number 809, this protein was computationally identified as upregulated 1.5 fold, and in spot number 696, it was down-regulated 1.7 fold. As the number of proteins identified from these spots were 5 and 2, respectively, it is not possible to determine which protein is differentially regulated. Another protein Am17277, a 5-methyltetrahydropteroyltriglutamate-homocysteine s-methyltransferase, was identified in spot numbers 339, 352 and 360 (Table 6.1). Spot number 339 was upregulated 2.7 fold, 352 was upregulated 1.8 fold and spot 360 was down-regulated 1.6 fold. In the case of spot numbers 339 and 352 only one protein was identified but in spot number 360, two proteins were identified. Therefore, spot numbers 339 and 352 were included in further study whereas spot number 360 was not. Hypothetical proteins and predicted proteins (Am11484, Am18005, Am11329, Am6889, Am15759, Am14065 and Am4394) (Table 6.1) identified from H_2O_2-induced stress and hypothetical proteins (Am14843 and Am18190) (Table 6.2), identified from Menadione/$FeCl_3$–induced stress identified in previous chapters were again confirmed at protein level as *A. mellea* proteins of unknown function. Interestingly, four proteins identified by a BLAST search, namely Am5280 (threonyl-tRNA synthetase) (Table 6.1), Am7428 (heat shock 70 protein) (Table 6.2), Am9185 (Hypothetical protein SCHCODRAFT_257557 [*Schizophyllum commune* H4-8]) (Table 6.2) and Am9232 (acetyl-acetyltransferase) (Table 6.2), have not been identified in any of the work presented in Chapters 3 - 5. Furthermore, Am9185 (Hypothetical protein SCHCODRAFT_257557 [*Schizophyllum commune* H4-8]) can now be reclassified as an unknown function protein as it has now been identified at protein level for the first time in *A. mellea*. Unambiguously differentially regulated proteins were subjected to further bioinformatic analysis: B2G, IPS, Phobius, ProteinGRAVY, SigP and SecP (Table 6.3 and Table 6.4) and will be summarised in Table 6.5 in the following order:

1. Proteins upregulated under H_2O_2–induced oxidative stress, in the order of most highly upregulated to least up-regulated.
2. Proteins downregulated under H_2O_2–induced oxidative stress, in the order of most highly downregulated to least downregulated.
3. Proteins up-regulated under Menadione/$FeCl_3$ –induced oxidative stress, in the order of most highly upregulated to least upregulated.
4. Proteins downregulated under Menadione/$FeCl_3$–induced oxidative stress, in the order of most highly downregulated to least downregulated.
5. Proteins upregulated under both oxidative stress conditions.
6. Proteins differentially regulated under each oxidative stress condition.

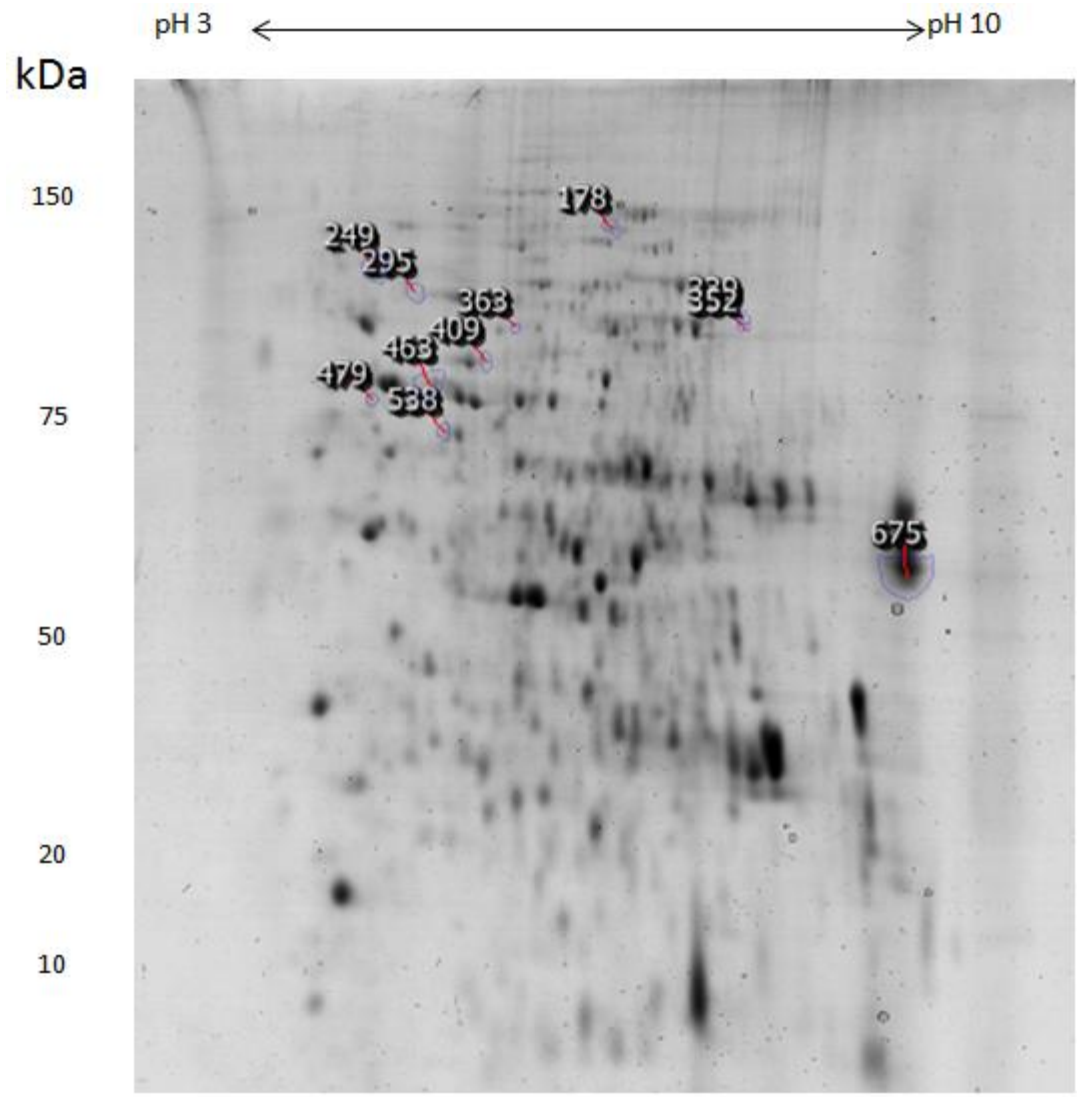

Figure 6.1. Reference gel image of 2-DE separation of *A. mellea* mycelial protein extracts following H_2O_2-induced oxidative stress for 3 h. There are 1142 proteins visualised on this gel, of which 34 showed differential regulation (3%). The image shows protein spot numbers from which a single differentially regulated protein was identified.

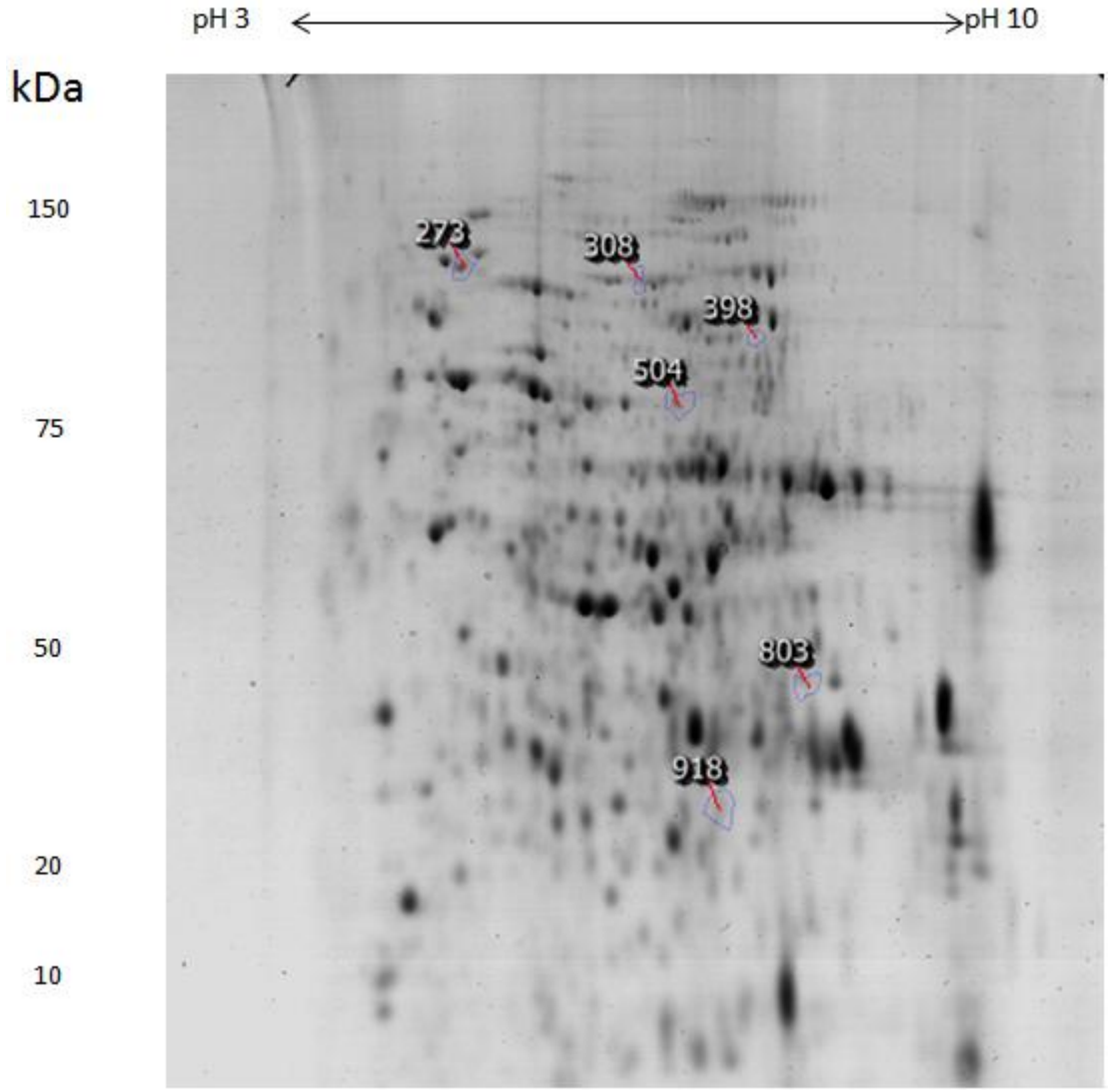

Figure 6.2. Reference gel image of 2-DE separation of *A. mellea* mycelial protein extracts following Menadione/$FeCl_3$-induced oxidative stress for 3 h. There are 1122 proteins visualised on this gel, of which 21 showed differential regulation (2%). The image shows protein spot numbers from which a single differentially regulated protein was identified.

Table 6.1. BLAST identification from *A. mellea* mycelial protein spots determined by SameSpots™ software to be differentially regulated following H_2O_2-induced oxidative stress for 3 h, following LC-MS/MS analysis. Overall, 34 spots were analysed and 45 distinct proteins identified. Isoforms or protein modifications were determined in five spots and sixteen spots showed multiple protein identification. Proteins are ranked by fold change in expression.

Spot No.	[a]Accession No.	[b]BLAST Description	Anova (*p*)	Fold change	[c]Expression$_2$	[d]No. Spectra	Unique Peptides	Coverage %	[e]SM Score
Up-regulated									
339	Am17277	5-methyltetrahydropteroyltriglutamate-homocysteine s-methyltransferase	0.032	2.7	↑	7	6	13	104.05
1001	Am17701	Exosome component rrp46	0.026	2.1	↑	1	1	3	24.68
	Am15133	[f]Predicted protein [*Laccaria bicolor* S238N-H82]				1	1	10	24.03
	Am12436	Zb protein				1	1	3	13.52
352	Am17277	5-methyltetrahydropteroyltriglutamate-homocysteine s-methyltransferase	0.005	1.8	↑	9	6	12	102.79
409	Am3212	Zinc metallopeptidase found in the cytoplasm and intermembrane space of mitochondria	0.008	1.8	↑	4	4	7	61.49

Spot No.	[a]Accession No.	[b]BLAST Description	Anova (*p*)	Fold change	[c]Expression$_2$	[d]No. Spectra	Unique Peptides	Coverage %	[e]SM Score
544	Am11484	[g]Hypothetical protein MPER_11943 [*Moniliophthora perniciosa* FA553]	0.049	1.8	↑	1	1	9	16.88
	Am18005	Expressed protein [*Schizophyllum commune* H4-8]				1	1	1	13.35
229	Am18817	Heat shock protein Hsp90	0.018	1.7	↑	5	4	7	60.61
	Am17043	Leucyl aminopeptidase				1	1	< 1 %	14.88
	Am17712	Glycoside hydrolase family 92 protein				1	1	1	13.23
255		Not selected for analysis	0.031	1.7	↑				
363	Am14050	Saccharopine dehydrogenase	0.036	1.7	↑	1	1	2	21.57
295	Am18454	Heat shock protein	0.032	1.6	↑	4	4	7	63.09
249	Am14558	Valosin-containing protein	0.017	1.6	↑	23	19	17	335.03
725	Am19936	Survival factor 1	0.008	1.6	↑	3	3	4	55.65
	Am20231	Phosphopyruvate hydratase				1	1	4	17.98
767		Not selected for analysis	0.03	1.6	↑				
809	Am5495	NAD-dependent epimerase	0.018	1.5	↑	7	6	21	89.41
	Am17808	Acid phosphatase				1	1	9	23.63
	Am20231	Phosphopyruvate hydratase				1	1	4	15.82
	Am11954	Proliferation-associated 2g4				1	1	6	15.26

Spot No.	[a]Accession No.	[b]BLAST Description	Anova (*p*)	Fold change	[c]Expression$_2$	[d]No. Spectra	Unique Peptides	Coverage %	[e]SM Score
	Am11329	[g]Hypothetical protein CC1G_11982 [*Coprinopsis cinerea* okayama7#130]				1	1	9	14.48
1083	Am9508	Short-chain dehydrogenase reductase sdr	0.006	1.5	↑	4	4	21	81.73
	Am6889	[g]Hypothetical protein SCHCODRAFT_35818 [*Schizophyllum commune* H4-8]				2	2	10	43.58
463	Am7160	Heat shock protein Hsp70	0.017	1.4	↑	10	9	17	153.55
644	Am6080	ATP synthase subunit β	0.004	1.4	↑	28	19	50	378.88
	Am13413	Tubulin beta chain				15	14	38	221.54
656	Am3638	Protein	0.014	1.4	↑	4	4	8	55.38
	Am19563	Argininosuccinate synthetase				3	3	9	45.66
	Am6080	ATP synthase subunit β				2	2	7	32.42
538	Am3211	Pyruvate decarboxylase	0.026	1.3	↑	5	4	11	81.3
988		Not selected for analysis	0.013	1.3	↑				
1079	Am19945	Short chain type	0.008	1.3	↑	6	5	24	94.61

Spot No.	[a]Accession No.	[b]BLAST Description	Anova (*p*)	Fold change	[c]Expression$_2$	[d]No. Spectra	Unique Peptides	Coverage %	[e]SM Score
	Am9508	Short-chain dehydrogenase/reductase SDR [*Coprinopsis cinerea* okayama7#130]				6	5	21	81.62
586	Am15966	UDP-n-acetylglucosamine diphosphorylase	0.045	1.2	↑	4	4	9	60.13
	Am16347	Ubiquitin activating enzyme				1	1	3	22.79
Down-regulated									
681	Am18930	Eukaryotic translation elongation factor 2	0.011	2.6	↓	4	3	3	60.16
	Am14000	6-phosphogluconate dehydrogenase				1	1	3	20.93
	Am17508	Chorismate synthase				1	1	2	19.83
	Am19873	Translation elongation factor 1a				1	1	3	16.47
178	Am16706	A-pheromone processing metallopeptidase ste23	0.044	2.3	↓	1	1	1	16.8
82	Am15759	[g]Hypothetical protein BC1G_06968 [*Botryotinia fuckeliana* B05.10]	0.033	1.9	↓	1	1	2	18.34
	Am17480	5-oxoprolinase				1	1	1	14.82
406	No Hit		0.011	1.9	↓				
1009		Not selected for analysis	0.033	1.9	↓				

Spot No.	[a]Accession No.	[b]BLAST Description	Anova (*p*)	Fold change	[c]Expression$_2$	[d]No. Spectra	Unique Peptides	Coverage %	[e]SM Score
675	Am19873	Translation elongation factor 1a	0.012	1.8	↓	13	11	35	186.6
424	Am15243	Glutamine-fructose-6-phosphate transaminase	0.037	1.7	↓	2	2	5	31.2
	Am5280	Threonyl-tRNA synthetase				1	1	1	17.42
696	Am11954	Proliferation-associated 2g4	0.026	1.7	↓	10	6	20	98.77
	Am19441	D-3-phosphoglycerate dehydrogenase 2				1	1	3	14.93
360	Am17277	5-methyltetrahydropteroyltriglutamate-homocysteine s-methyltransferase	0.023	1.6	↓	12	10	17	163.69
	Am7439	Trehalose synthase				9	9	17	154.58
520	No Hit		0.016	1.6	↓				
176	No Hit		0.01	1.5	↓				
479	Am7452	Heat shock protein 90	0.034	1.5	↓	8	7	12	97.18
1043	Am19533	GTP-binding nuclear protein ran	0.037	1.3	↓	8	7	34	117.9
	Am14065	[g]Hypothetical protein [*Tuber melanosporum* Mel28]				5	5	30	91.4
	Am4394	[f]Predicted protein [*Laccaria bicolor* S238N-H82]				1	1	4	13.76

[a]Accession number from *A. mellea* cDNA database; [b]BLAST annotation following B2G analysis of proteins identified from *A. mellea* cDNA database; [c]Expression, arrow direction denoted up-regulated or down-regulated; [e]No. spectra, the number of valid spectra from which the protein was identified; [e]SM score, Spectrum Mill protein score; [f]Prevously predicted protein, now identified at protein level; [g]Previously hypothetical protein, now identified at protein level.

Table 6.2. BLAST identification from *A. mellea* mycelial protein spots determined by SameSpots^{TM} software to be differentially regulated under Menadione/$FeCl_3$ oxidative stress for 3 h, following LC-MS/MS analysis. Overall, 21 spots were analysed and 20 distinct proteins were identified. Isoforms or protein modifications were determined in two spots and seven spots showed multiple protein identification. Proteins are ranked by fold change in expression.

Spot No	[a]Accession No.	[b]BLAST annotation	Anova (*p*)	Fold change	[c]Expression	[d]No. Spectra	Unique Peptides	Coverage %	[e]SM Score
Up-regulated									
209	Am18930	Eukaryotic translation elongation factor 2	0.045	3.5	↑	7	4	3	69.66
	Am9580	NAD-specific glutamate dehydrogenase				2	2	2	26.85
398	Am17277	5-methyltetrahydropteroyltriglutamate-homocysteine s-methyltransferase	0.028	2.6	↑	2	2	4	43.82
464		Not selected for analysis	0.008	1.5	↑				
473		Not selected for analysis	0.013	1.9	↑				
475	No Hits		0.031	1.8	↑				
803	Am19877	Glutamic oxaloacetic transaminase aat1	0.011	1.5	↑	6	6	17	79.56
987	Am4819	NAD-dependent epimerase dehydratase family protein	0.017	1.3	↑	6	4	24	86.44

Spot No	[a]Accession No.	[b]BLAST annotation	Anova (*p*)	Fold change	[c]Expression	[d]No. Spectra	Unique Peptides	Coverage %	[e]SM Score
	Am14843	[f]Hypothetical protein SERLA73DRAFT_183239 [*Serpula lacrymans* var. Lacrymans S7.3]				1	1	7	16.64
1096	Am16479	Domain-containing protein	0.027	1.2	↑	2	2	7	29.87
	Am7428	Heat shock protein				2	2	3	24.84
	Am18443	Enoyl hydratase				2	1	6	20.08
Down-regulated									
146		Not selected for analysis	0.022	2.1	↓				
326		Not selected for analysis	0.021	2	↓				
232	No Hits		0.028	1.5	↓				
185	No Hits		0.02	1.4	↓				
308	Am9629	Glycoside hydrolase family 3 protein	0.041	1.4	↓	3	3	5	41.54
1127	Am18443	Enoyl hydratase	0.025	1.4	↓	3	2	11	33.64
	Am19533	GTP-binding nuclear protein ran				1	1	3	16.43
918	Am19381	3-ketoacyl-CoA thiolase peroxisomal	0.024	1.4	↓	1	1	4	23.25
951	Am19874	Dienelactone hydrolase	0.006	1.3	↓	6	3	15	57.63
	Am18190	[f]Hypothetical protein SERLA73DRAFT_176091 [*Serpula lacrymans* var. Lacrymans S7.3]				4	3	16	47.89
	Am15995	D-xylose reductase				2	1	4	22.78
504	Am13458	Alcohol oxidase-like protein	0.025	1.3	↓	5	5	7	73.85

Spot No	[a]Accession No.	[b]BLAST annotation	Anova (*p*)	Fold change	[c]Expression	[d]No. Spectra	Unique Peptides	Coverage %	[e]SM Score
756	Am9232	Acetyl- acetyl transferase	0.013	1.3	↓	2	2	4	32.93
	Am17064	Glycogen synthase kinase				1	1	5	16.9
85	No Hits		0.022	1.2	↓				
273	Am14558	Valosin-containing protein	0.049	1.1	↓	15	14	11	241.76
835	Am19381	3-ketoacyl-CoA thiolase peroxisomal	0.005	1.1	↓	14	12	47	200.14
	Am9185	[f]Hypothetical protein SCHCODRAFT_257557 [*Schizophyllum commune* H4-8]				1	1	2	15.03

[a]Accession number from *A. mellea* cDNA database; [b]BLAST annotation following B2G analysis of proteins identified from *A. mellea* cDNA database; [c]Expression, arrow direction denoted upregulated or downregulated; [e]No. spectra, the number of valid spectra from which the protein was identified; [e]SM score, Spectrum Mill protein score; [f]Previously hypothetical protein, now identified at protein level.

Table 6.3. Summary and further details of unambiguously identified *A. mellea* mycelial proteins found to be differentially regulated following H_2O_2 oxidative stress for 3 h. Proteins from 2-DE identified by SameSpots™ software, analysed by LC-MS/MS with subsequent interrogation of the *A. mellea* cDNA database.

Spot No.	[a]Accession No.	[b]BLAST Description	Anova (*p*)	Fold Change	[c]Expression	[d]M_r (tM_r)	[e]p*I* (tp*I*)	No. Spectra	Unique Peptides	Coverage %	[f]SM Score	[g]GRAVY Score	[h]SigP/ SecP
Up-regulated													
339	Am17277	5-methyltetrahydropteroyltriglutamate-homocysteine s-methyltransferase	0.032	2.7	↑	95000 (84519)	7.4 (6.37)	7	6	13	104.05	-0.201	
352	Am17277	5-methyltetrahydropteroyltriglutamate-homocysteine s-methyltransferase	0.005	1.8	↑	95000 (84519)	7.4 (6.37)	9	6	12	102.79	-0.201	
409	Am3212	Zinc metallopeptidase found in the cytoplasm and intermembrane space of mitochondria	0.008	1.8	↑	85000 (75419)	5.1 (5.17)	4	4	7	61.49	-0.451	
363	Am14050	Saccharopine dehydrogenase	0.036	1.7	↑	90000 (82230)	5.6 (5.63)	1	1	2	21.57	-0.003	SecP

Spot No.	[a]Accession No.	[b]BLAST Description	Anova (*p*)	Fold Change	[c]Expression	[d]M_r (tM_r)	[e]p*I* (tp*I*)	No. Spectra	Unique Peptides	Coverage %	[f]SM Score	[g]GRAVY Score	[h]SigP/ SecP
249	Am14558	Valosin-containing protein	0.017	1.6	↑	12000 (178578)	4.3 (5.45)	23	19	17	335.03	-0.258	
295	Am18454	Heat shock protein	0.032	1.6	↑	78000 (93611)	4.75 (5.41)	4	4	7	63.09	-0.261	
463	Am7160	Heat shock protein hsp70	0.017	1.4	↑	80000 (74705)	4.78 (5.54)	10	9	17	153.55	-0.348	
538	Am3211	Pyruvate decarboxylase	0.026	1.3	↑	75000 (66203)	4.85 (5.62)	5	4	11	81.3	-0.151	
Down-regulated													
178	Am16706	A-pheromone processing metallopeptidase ste23	0.044	2.3	↓	15000 (136657)	6.5 (6.1)	1	1	1	16.8	-0.456	
675	Am19873	Translation elongation factor 1a	0.012	1.8	↓	60000 (49933)	8.9 (9.17)	13	11	35	186.6	-0.275	
479	Am7452	Heat shock protein 90	0.034	1.5	↓	78000 (86455)	4.3 (4.84)	8	7	12	97.18	-0.41	

[a]Accession number from *A. mellea* cDNA database; [b]BLAST annotation following B2G analysis of proteins identified from *A. mellea* cDNA database; [c]Expression, arrow direction denoted upregulated or downregulated [d]M_r (tM_r), molecular mass (theoretical molecular mass); [e]p*I* (tp*I*), isoelectric point (theoretical isoelectric point); [f]SM score, Spectrum Mill protein score; [g]GRAVY score, grand average of hydropathy (Negative score indicates hydrophilicity while Positive score indicates hydrophobicity); [h]SigP, classical secretion signal peptide; SecP, non-classical secretion signal.

Table 6.4. Summary and further details of unambiguously identified *A. mellea* mycelial proteins found to be differentially regulated following Menadione/$FeCl_3$-induced oxidative stress for 3 h. Proteins from 2-DE identified by SameSpots™ software, analysed by LC-MS/MS with subsequent interrogation of the *A. mellea* cDNA database.

Spot No.	[a]Accession No.	[b]BLAST annotation	Anova (*p*)	Fold Change	Expression	[c]M_r (tM_r)	[d]p*I* (tp*I*)	No. Spectra	Unique Peptides	Coverage %	[e]SM Score	[f]GRAVY Score	[g]SigP/ SecP
Upregulated													
398	Am17277	5-methyltetrahydropteroyltri glutamate-homocysteine s-methyltransferase	0.028	2.6	↑	10000 (84519)	4.8 (6.37)	2	2	4	43.82	-0.201	
803	Am19877	Glutamic oxaloacetic transaminase aat1	0.011	1.5	↑	45000 (45812)	8.0 (8.64)	6	6	17	79.56	-0.212	SecP
Downregulated													
918	Am19381	3-ketoacyl-CoA thiolase peroxisomal	0.024	1.4	↓	25000 (40335)	6.7 (6.26)	1	1	4	23.25	0.088	SecP
308	Am9629	Glycoside hydrolase family 3 protein	0.041	1.4	↓	120000 (94246)	6.5 (5.9)	3	3	5	41.54	-0.238	
504	Am13458	Alcohol oxidase-like protein	0.025	1.3	↓	80000 (68039)	6.6 (6.12)	5	5	7	73.85	-0.313	
273	Am14558	Valosin-containing protein	0.049	1.1	↓	130000 (178578)	4.8 (5.45)	15	14	11	241.76	-0.348	

[a]Accession number from *A. mellea* cDNA database; [b]BLAST annotation following B2G analysis of proteins identified from *A. mellea* cDNA database; [c]Expression, arrow direction denoted up-regulated or down-regulated; [d]M_r, theoretical molecular mass; [e]tp*I*, theoretical isoelectric point; [f]SM score, Spectrum Mill protein score; [g]GRAVY score, grand average of hydropathy (Negative score indicates hydrophilicity while Positive score indicates hydrophobicity); [h]SigP, classical secretion signal peptide; SecP, non-classical secretion signal.

Table 6.5. BLAST, InterProScan annotation and EC codes of differentially expressed proteins under both oxidative stress induced conditions.

[a]Accession No	[b]BLAST annotation	[c]InterProScan	[d]EC code	[e]H_2O_2	[f]Menadione $FeCl_3$
Am3212	Zinc metallopeptidase found in the cytoplasm and intermembrane space of mitochondria	Peptidase M3A/M3B.	EC:3.4.24.-	↑	
Am14050	Saccharopine dehydrogenase	Spermine/Spermidine synthase.	EC:2.5.1.16; EC:1.5.1.10	↑	
Am18454	Heat shock protein	Heat shock protein 70	-	↑	
Am7160	Heat shock protein hsp70	Heat shock protein Hsp70.	-	↑	
Am3211	Pyruvate decarboxylase	Thiamine pyrophosphate enzyme	EC:4.1.1.1	↑	
Am7452	Heat shock protein 90	Heat shock protein Hsp90	-	↓	
Am16706	A-pheromone processing metallopeptidase ste23	Peptidase M16.	EC:4.4.1.21	↓	

[a]Accession No	[b]BLAST annotation	[c]InterProScan	[d]EC code	[e]H_2O_2	[f]Menadione $FeCl_3$
Am19873	Translation elongation factor 1a	Translation elongation factor EF1A.	EC:3.6.5.1; EC:3.6.5.2; EC:3.6.5.3; EC:3.6.5.4	↓	
Am19877	Glutamic oxaloacetic transaminase aat1	Aminotransferase.	EC:2.6.1.1		↑
Am19381	3-ketoacyl-CoA -thiolase peroxisomal	Thiolase-like protein.	EC:2.3.1.16		↓
Am9629	Glycoside hydrolase family 3 protein	Glycoside hydrolase, family 3.	EC:3.2.1.21		↓
Am13458	Alcohol oxidase-like protein	GMC oxidoreductase	EC:1.1.99.1		↓
Am17277	5-methyltetrahydropteroyltriglutamate-homocysteine s-methyltransferase	Vitamin-B12 independent methionine synthase	EC:2.1.1.14	↑	↑
Am14558	Valosin-containing protein	Cytoskeleton-associated protein.	-	↑	↓

[a]Accession number from *A. mellea* cDNA database; [b]BLAST annotation following Blast2GO analysis of proteins identified from *A. mellea* cDNA database; [c]InterProScan annotation following Blast2GO analysis of proteins identified from *A. mellea* cDNA database; [d]EC code, the enzyme commission number for enzymes; [e]Expression under H_2O_2 stress, arrow direction denoted up-regulated or down-regulated; [f]Expression under Menadione/$FeCl_3$ stress, arrow direction denoted up-regulated or down-regulated.

6.2.1 Proteins upregulated under H_2O_2-induced oxidative stress.

A BLAST search identified Am3212 as a cytosolic and mitochondrial zinc M3 metalloproteinase which acts on small peptides (containing 9-17 amino acids) (Saric *et al.*, 2004) (Table 6.5) which was upregulated (1.8 fold) (Table 6.3) under H_2O_2-induced stress. M3 peptidases are also known as mitochondrial intermediate peptidases (MIP) which cleave pro-proteins imported into the mitochondria to their mature size in two steps, the first by mitochondrial processing peptidase (MPP) with subsequent cleavage by MIP, for proteins targeted to the mitochondrial inner membrane or matrix (Martin *et al.*, 2008).

Am14050 was identified by BLAST as a Saccharopine dehydrogenase (Table 6.5). It possesses a non-classical secretion signal and was upregulated (1.7 fold) (Table 6.3) under H_2O_2-induced stress. Further bioinformatic analysis identified it as a spermine/spermidine synthase; saccharopine dehydrogenase/homospermidine synthase, and $NAD(P)^+$ binding domain signatures were identified, as well as a motif with structural similarity to a viral methyltransferase (Vaccinia Virus protein VP39). Spermine/spermidine synthase is implicated in many metabolic pathways including methionine salvage, and polyamine metabolism (Rider *et al.*, 2007)**.** It is notable that polyamines play a non-enzymatic role in scavenging ROS (Heller and Tudzynski, 2011). Figure 6.3A, B and C show the activity of this protein. Saccharopine dehydrogenase activity is shown in Figure 6.3D and E.

BLAST identified Am18454 as a Hsp70 protein (Table 6.5), which was upregulated (1.6 fold) (Table 6.3) under H_2O_2-induced stress. Hsp70s are stress response proteins which have ATPase and substrate binding domains, and are found in cytosol and also in mitochondria. In order to further characterise this protein, a BlastP search was carried out against the Saccharomyces Genome Database (SGD) (http://www.yeastgenome.org/cgi-bin/blast-sgd.pl) which confirmed this protein as cytosolic with 42% identity to the *S. cerevisiae* orthologue. Hsp70 binds to a single molecule of substrate and does not effect global conformational changes, but refolds protein substrates in the immediate vicinity to the binding site (Bukau and Horwich, 1998). These Hsp70 proteins promote initial folding of nascent proteins which are subsequently passed to Hsp90s which facilitate further folding (Leach *et al.*, 2012). Am7160 was also identified as a Hsp70 protein (Table 6.5), a recognised stress response protein and a sensor of oxidative stress, by BLAST analysis. It too was upregulated (1.4 fold) (Table 6.3) under H_2O_2-induced oxidative stress. SGD analysis categorised this

protein as a component of an import motor protein of the mitochondrial membrane SSC1, with 68% identity to a *Saccharomyces* spp. ortholog, confirming it as a mitochondrial Hsp70.

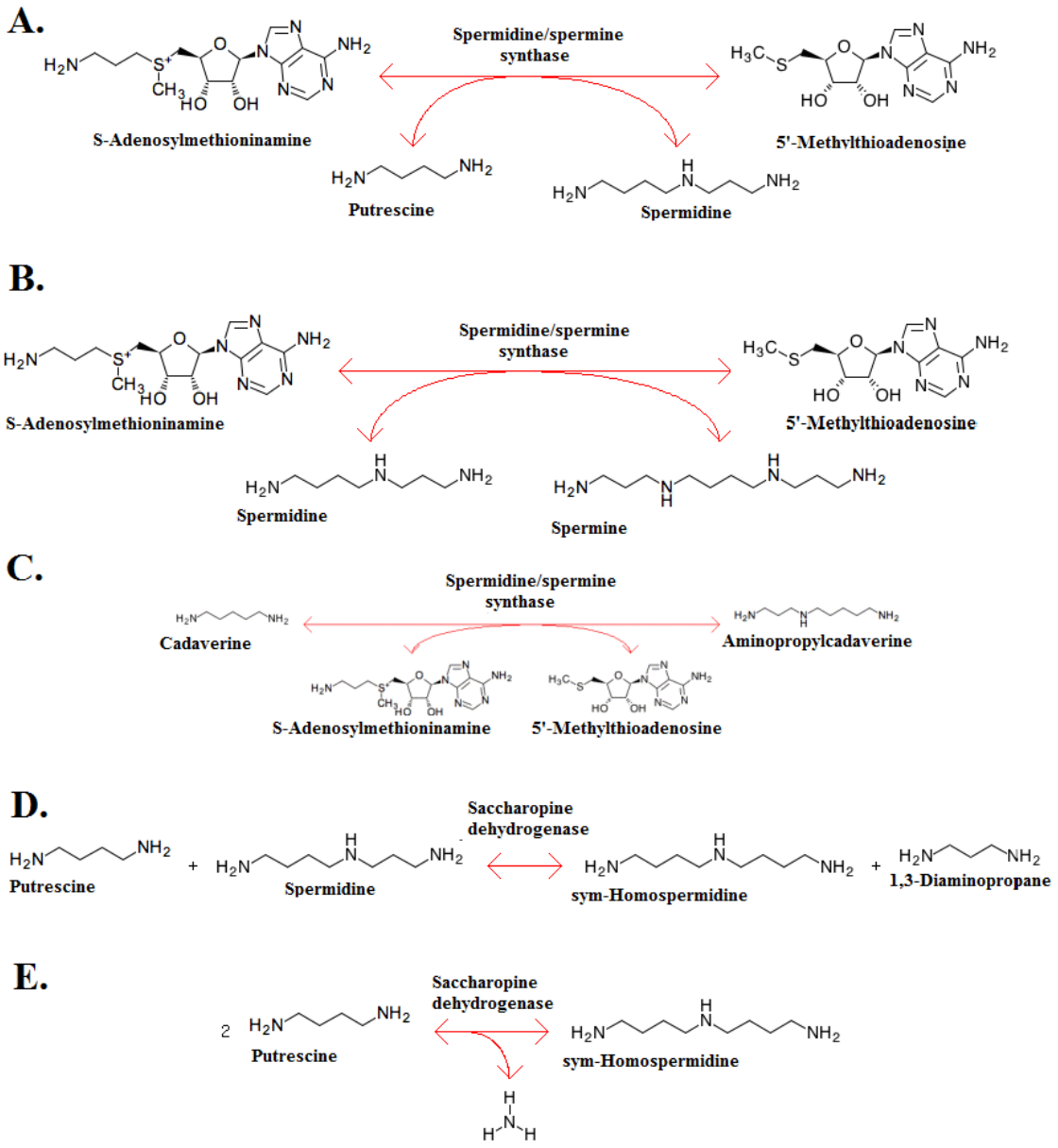

Figure 6.3. Reactions of Am14050 in polyamine biosythesis **Spermine/spermidine synthase A.** Formation of spermidine from putrescine by transfer of aminopropyl group from decarboxylated S-adenosylmethioniname (dcAdoMet) to putrescine, forming spermidine and 5'-methylthioadenosine (MTA) (http://www.kegg)**. B.** Transfer of aminopropyl group from dcAdoMet to spermidine (http://www.kegg.jp/). Metabolic pathways: Arginine and proline metabolism, cysteine/methionine metabolism and methionine salvage pathway, β-alanine pathway and glutathione pathway (KEGG

http://www.genome.jp/). **C**. Aminopropyl transfer from dcAdoMet to cadaverine forming MTA and aminopropylcadaverine. Metabolic pathway: Glutathione metabolism (KEGG http://www.genome.jp/). **Saccharopine dehydrogenase D**. Aminopropyl transfer from putrescine to spermidine forming sym-homospermidine and 1,3-diaminopropane. Metabolic pathways: Lysine metabolism; Secondary metabolites, pyrrolizidine alkaloid biosynthesis (KEGG http://www.genome.jp/). **E.** Aminopropyl transfer from putrescine one putresceine molecule to a second molecule sym-homospermidine with the release of an amino group. Metabolic pathways: Lysine metabolism; Secondary metabolites, pyrrolizidine alkaloidspyridine alkaloid biosynthesis (KEGG http://www.genome.jp/).

A BLAST search identified Am3211 as a pyruvate decarboxylase, a thiamine pyrophosphate (TPP)-utilising enzyme (Table 6.5). It was upregulated (1.3 fold) (Table 6.3) under H_2O_2-induced oxidative stress. Phobius protein topology search predicted a membrane region in this protein although it is hydrophilic in nature, as predicted by a ProteinGRAVY (**GR**and **AV**erage of hydropath**Y**) score of -0.15. Pyruvate decarboxylase, and a thiamine diphosphate co-factor, catalyses formation of acetaldehyde in two steps (Figure 6.4), and is involved in anaerobic fermentation or the production of oxo-acids for transamination.

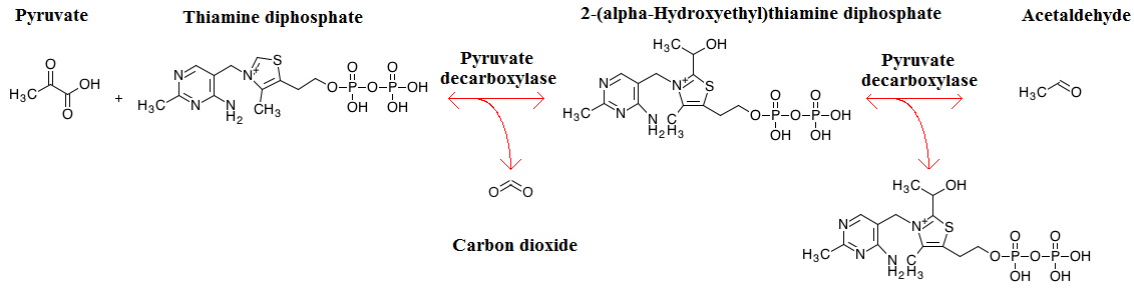

Figure 6.4. Pyruvate decarboxylase and a thiamine diphosphate co-factor, catalyses formation of carbon dioxide and acetaldehyde from pyruvate, in two steps (http://www.kegg.jp/).

6.2.2 Proteins downregulated under H_2O_2-induced oxidative stress.

A BLAST search identified Am16706 as an insulin degrading type M16 peptidase. It was downregulated (2.3 fold) (Table 6.3) under H_2O_2-induced oxidative stress (Table 6.5). Domains identified by bioinformatic analysis of this protein were M16 peptidase domain signatures, and a LuxS/M16 peptidase-like metal binding domain. LuxS catalyses cleavage of the thioester bond of S-ribosylhomocysteine (SRH), a product of

SAM methylation of macromolecules, to form homocysteine (HCys) (Figure 6.5). (Rajan *et al.*, 2005; Parveen and Cornell, 2011). S-adenosyl-L-homocysteine (SAH) is a product of SAM, which is involved in many methylation reactions. S-adenosyl-L-homocysteine hydrolase (sahH) in turn hydrolyses homocysteine from which methionine is synthesised, but sahH hydrolysis is reversible. SAH inhibits SAM-dependent methyl transferases and sahH hydrolysis of SAH is inhibited by high levels of homocysteine (Moffatt and Weretilnyk, 2001), thus downregulation of Am16706 could be occurring to prevent homocysteine formation.

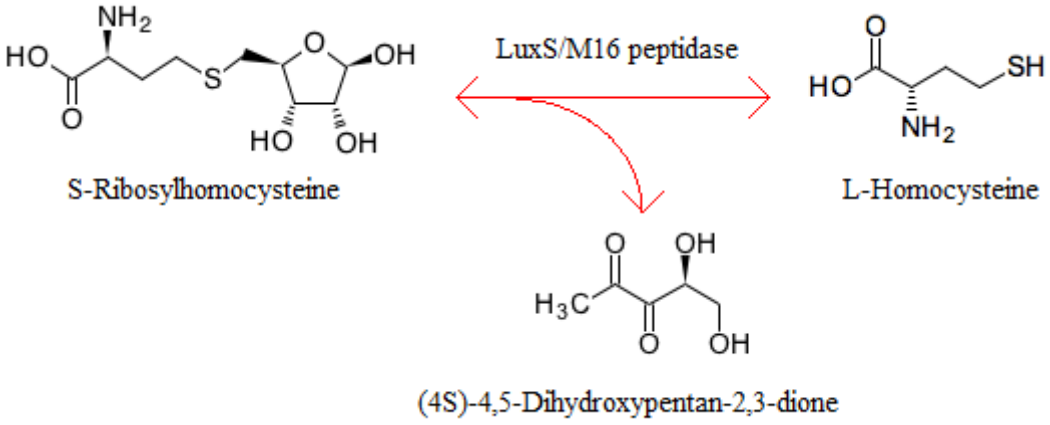

Figure 6.5. Reaction Lux/M16 peptidase: Cleavage of the thioester bond of S-ribosylhomocysteine (SAH) and formation of homocysteine. (KEGG http://www.genome.jp/).

A BLAST search identified Am19873 as a translation elongation factor 1a (EF1A/EF-Tu) (Table 6.5) which was downregulated (1.8 fold) (Table 6.3) under H_2O_2-induced oxidative stress. EF1A/EF-Tu is a G-protein, involved in protein biosynthesis, through binding of GTP and tRNA to the A site, prior to transport by a second protein, EF2, to the ribosomal P site. Am7452 was identified as a Hsp90 chaperone protein (Table 6.5) which was downregulated (1.5 fold) (Table 6.3) under H_2O_2-induced oxidative stress. Domain signatures identified by bioinformatic analysis were the N-terminal ATP binding domain and its conformational regulator, S5 domain 2-type fold which binds and refolds "client proteins" (Meyer *et al.*, 2004; Leach *et al.*, 2012).

6.2.3 Proteins upregulated under Menadione/$FeCl_3$-induced oxidative stress

BLAST analysis identified Am19877 as an aspartate aminotransferase (Table 6.5) which was upregulated (1.5 fold) (Table 6.4) under Menadione/$FeCl_3$-induced oxidative stress. This protein was identified by SecretomeP analysis as having a non-classical

secretion sequence and by TargetP analysis as being mitochondrial. This family of proteins play a central role in nitrogen metabolism. One activity of aspartate aminotransferase is the transamination of L-cysteine whose products are mercaptopyruvate and L-glutamate (Figure 6.6) (Akagi, 1982; Marienhagen and Kennerknecht, 2005). A pyridoxal 5'-phosphate (PLP), coenzyme acts as a catalyst in transamination (Eliot and Kirsch, 2004) and a PLP binding site motif in this protein was identified by bioinformatic analysis.

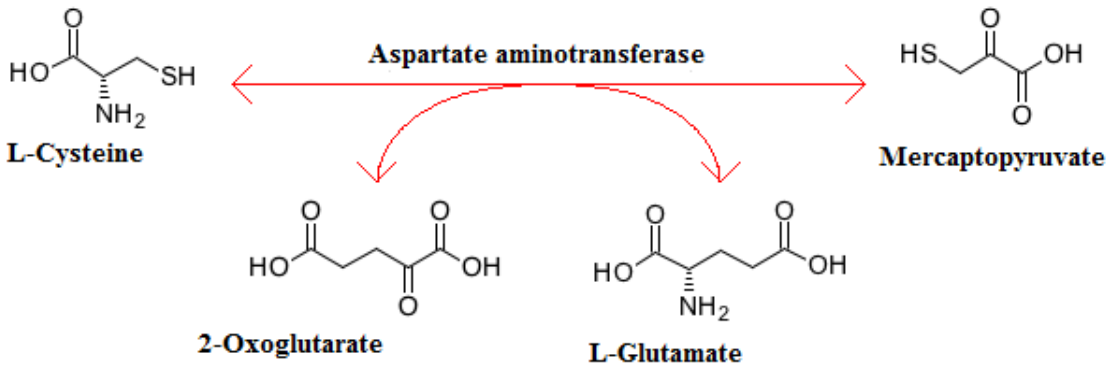

Figure 6.6. Aspartate aminotransferase reaction. Catalyses the reversible transfer of amine from L-glutamate to mecaptopyruvate to form L-cysteine. Metabolic pathway: cysteine and methionine metabolism (http://www.kegg.jp/).

6.2.4 Proteins down-regulated under Menadione/$FeCl_3$-induced oxidative stress

A BLAST search identified Am19381 as a peroxisomal 3-ketoacyl-CoA thiolase (Table 6.5) which was downregulated (1.4 fold) under Menadione/$FeCl_3$-induced oxidative stress 3-ketoacyl-CoA thiolase transfers a thiol group to CoA in the β-oxidation of fatty acids (Figure 6.7). SecretomeP analysis identified a non-classical secretion sequence and ProteinGRAVY search identified Am19381 as hydrophobic, although it does not have any transmembrane regions consistent with its amphipathic structure in peroxisomal membranes (Stolowich *et al.*, 2002). Am19381 may play a role in poly beta-hydroxybutyrate synthesis or steroid biogenesis, as a peroxisomal 3-ketoacyl-CoA thiolase.

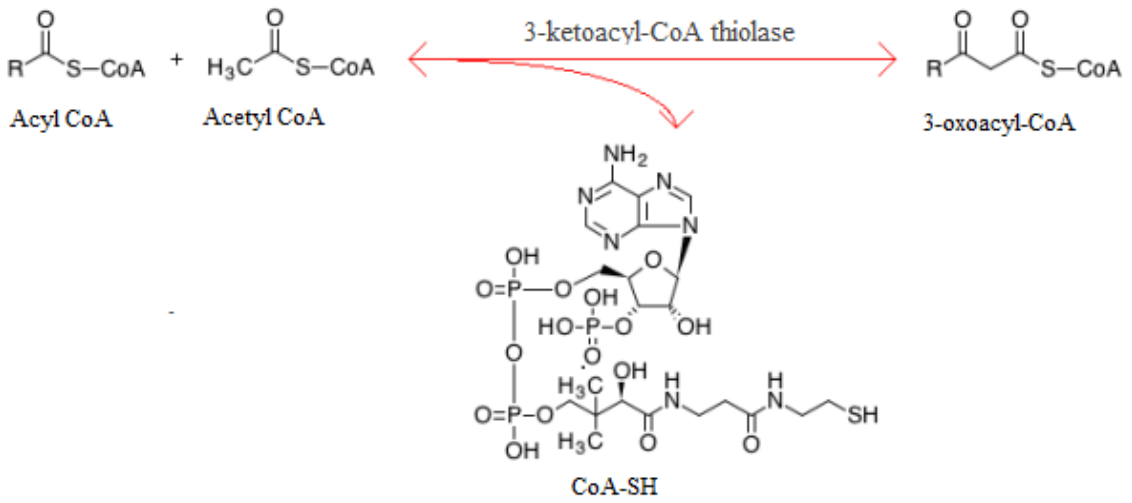

Figure 6.7. Reaction of 3-ketoacyl-CoA: Thiolytic cleavage of substrate with formation of 3-oxoacyl-CoA and transfer of thiol group to CoA (http://www.kegg.jp/).

A BLAST search identified Am9629 as a glycoside hydrolase family 3 (GH3) protein (Table 6.5) which was downregulated (1.4 fold) (Table 6.4) under Menadione/$FeCl_3$-induced oxidative stress. A protective antigen domain (PA14 domain) was identified in Am9629 by further bioinformatic analysis. A GH3, TIM (translocase of the inner membrane) α/β barrel catalytic site signature was identified in this protein, although not all PA14 enzymes have this (Rigden *et al.*, 2004). Expression of Am13458, identified by BLAST as an alcohol oxidase (Table 6.5), was downregulated (1.3 fold) (Table 6.4) under Menadione/$FeCl_3$-induced oxidative stress. These are usually extracellular enzymes required for lignolysis by white rot fungi, but this protein possesses neither classical nor non-classical secretion signals.

6.2.5 Proteins upregulated under both oxidative stress conditions.

A BLAST search identified Am17277 as a vitamin-B12 independent methionine synthase (Table 6.5) which was upregulated under both induced oxidative stress conditions. Under H_2O_2-induced oxidative stress, stress two isoforms were identified as up-regulated (2.7 fold and 1.8 fold) (Table 6.3), while under Menadione/$FeCl_3$-induced oxidative stress there was 2.6 fold upregulation. Vitamin-B12 independent methionine synthase activity is formation of L-methionine from L-homocysteine (Figure 6.8), and so this may represent a vehicle for the organism to reduce toxic levels of homocysteine. Methionine is a key substrate for production of S-adenosylmethionine, the universal cellular methyl donor which may be required for many reactions in the oxidative stress response.

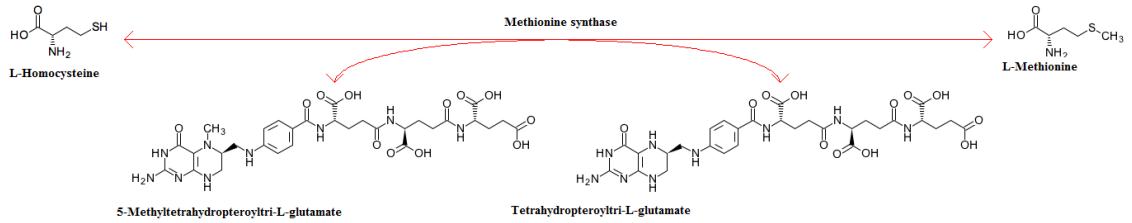

Figure 6.8. Vitamin B12 independent methionine synthase reaction: transfer of a methyl group from 5-methyltetrahydropteroyltri-L-glutamate to L-homocysteine in L-methionine synthesis (http://www.kegg.jp/). Metabolic pathway: Cysteine and methionine metabolism (http://www.genome.jp/).

6.2.6 Proteins up-regulated under H_2O_2 and down-regulated under Menadione/$FeCl_3$ stress.

BLAST identified Am14558 as a valosin-containing protein (VCP) (Table 6.5). VCP in higher eukaryotes is a key component of cellular processes involving protein ubiquitylation, both in proteasomal and in nonproteolytic pathways (Böhm *et al.*, 2011). Interestingly, its expression was upregulated under H_2O_2-induced oxidative stress (1.7 fold) (Table 6.3) and downregulated under Menadione/$FeCl_3$-induced oxidative stress (1.1 fold) (Table 6.4). Three transmembrane regions were predicted in Am14558 and this correlates to the functional localisation of VCP in both the endoplasmic reticulum and the Golgi. Bioinformatic analysis identified AAA^+ ATPase superfamily signatures. Domain signatures pertaining to protein degradation (Coles *et al.*, 1999), cytoskeleton (Li *et al.*, 2002) and membrane organisation (Liu, Siloto, *et al.*, 2011; Vajjhala *et al.*, 2008) were also identified in this protein.

6.3 Discussion

Differential proteomic analysis of *A. mellea* which had been independently subjected to two oxidative stress conditions, H_2O_2 and menadione/$FeCl_3$, respectively, was undertaken. Computational analysis identified 34 differentially regulated protein spots from H_2O_2-induced stress which exhibited statistical significance. Twenty-one upregulated spots had a fold change ranging 1.2 - 2.7 and thirteen protein spots were downregulated with a fold change ranging 1.3 - 2.6. Previously hypothetical and predicted proteins (n = 7), identified in previous chapters were expressed under H_2O_2-induced stress. Computational analysis identified 21 differentially regulated protein spots under menadione/$FeCl_3$-induced stress which exhibited statistical significance. Eight upregulated protein spots had a fold change ranging 1.2 - 3.5 and thirteen downregulated protein spots were down regulated 1.1 - 2.1 fold. Previously hypothetical proteins (n = 2) identified in previous chapters were expressed under menadione/$FeCl_3$-induced stress. Four proteins, one previously hypothetical were uniquely identified under menadione/$FeCl_3$-induced stress, the first instance of these proteins in *A. mellea*. Protein spots were excised from which there were no identifications may indicate limitiation or incompleteness of the database. A second and likely, alternative is that the protein modifications mean that the theoretical molecular mass does not coincide with the observed mass. A limitation of 2-DE is illustrated by spots which were identified as differentially regulated by computational analysis but could not be excised precisely and were therefore not selected for analysis. A means to address this is use of quantitative shotgun proteomics, as a complementary technique.

Forty-five proteins were identified following LC-MS/MS analysis of the protein spots under H_2O_2-induced stress and twenty proteins were identified following LC-MS/MS analysis of the protein spots under menadione/$FeCl_3$-induced stress. Protein isoforms or modifications were identified in five spots under H_2O_2 induced stress and two spots under menadione/$FeCl_3$ induced stress. Multiple proteins were identified from 16 spots under H_2O_2-induced stress and 7 spots under menadione/$FeCl_3$-induced stress. Four proteins were identified after LC-MS/MS analysis which had not previously been identified by methods described in previous chapters, one of which was a previously hypothetical protein now identified as being expressed at protein level in *A. mellea*.

Ten proteins from the H_2O_2-induced oxidative stress condition and six from the menadione/$FeCl_3$-induced oxidative stress condition were analysed in detail. Two proteins were common to both sets of data, one upregulated under both conditions and

one upregulated under H_2O_2-induced oxidative stress and downregulated under menadione/$FeCl_3$-induced oxidative stress.

6.3.1 Proteins upregulated under H_2O_2 stress

Am3212 was classified as a zinc M3 metallopeptidase. These enzymes are highly conserved and have been shown to contribute to the pathogenicity of *Mycosphaerella graminicola*, a wheat pathogen (Goodwin *et al.*, 2011). Although zinc M3 metallopeptidases can be secreted, in *A. mellea* no evidence of either classical or non-classical secretion signals was detectable. It is possible that increased expression of Am3212 is consequent to H_2O_2 presence, which mimics the host-defence environment that *A. mellea* experiences during plant infection. Alternatively, proteases may be produced during degradation of plant biomass, and although Am3212 may play no role in ligonocellulose degradation, its presence may be required to completely degrade plant proteinaceous material.

Am14050 is a spermine/spermidine synthase and was upregulated in *A. mellea* after H_2O_2-induced oxidative stress. Spermine is a polyamine contained in all eukaryotic cells, some prokaryotes and is crucial for survival (Pegg and McCann, 1982). Spermidine, is a mediator of cell proliferation and stabilises nucleic acids (Hashimoto *et al.*, 1998). Spermine/spermidine were shown to protect murine cells from H_2O_2 oxidative stress by scavenging ROS (Rider *et al.*, 2007). A saccharopine dehydrogenase/spermidine synthase signature is specific to basidiomycetes, and is a chimera of two genes without an intermediate stop codon or second initiation codon. This gene is multifunctional, with disparate roles in lysine and spermidine biosynthesis, and homologs have been identified in many basidiomycetes (León-Ramírez *et al.*, 2010). In a study of *Ustilago maydis* a regulatory role for this gene, in polyamine homeostasis by an unknown mechanism was proposed (Valdés-Santiago *et al.*, 2009). Mutant *Ustilago maydis* cells with deletion of the chimeric gene were more susceptible to stress, less virulent and morphology of cells grown in acidic conditions, normally filamentous, was yeast-like, and could not be restored by subsequent cultures at pH 3-7 (Valdés-Santiago *et al.*, 2009). In *A. mellea* upregulation of Am14050 in response stress and may also implicate it in virulence.

Both spermine and spermidine are scavengers of ROS, and as such prevent DNA damage and apoptosis, but spermine has shown to be the more active scavenger of peroxyl radicals even a low concentrations (Fujisawa and Kadoma, 2005; Rider *et al.*,

2007; Ha *et al.*, 1998; Newton *et al.*, 1997) (Figure 6.10). Exposure to exogenous spermidine was responsible for a wide range of gene upregulation, and in a polyamine-deficient mutant of *S. cerevisiae* exposed to spermidine, was responsible for methionine biosynthesis (Chattopadhyay *et al.*, 2009). A study in *A. fumigatus* challenged with H_2O_2, found upregulation in spermine synthase, but downregulation in methionine synthase (Lessing *et al.*, 2007). As both methionine synthase and spermine/spermidine synthase were upregulated in *A. mellea* under H_2O_2-induced oxidative stress, this may indicate upregulation of methionine biosynthesis by increased spermidine in *A. mellea*. Alternatively, increased methionine biosynthesis may be required to produce SAM, and possibly decarboxylated SAM (S-adenosylmethionamine), to facilitate polyamine biosynthesis (Figure 6.3), and its consequent antioxidant activity. Either way, this observation provides new insights into the interplay between oxidative stress response and polyamine biosynthesis in basidiomycetes, and *A. mellea*, in particular.

A third domain signature in Am14050 may indicate another role for this protein. A vaccinia virus protein (VP39) with this signature has methyltransferase activity and forms a complex with SAM and RNA (Hodel *et al.*, 1996) (Figure 6.9)

Am18454 is a cytosolic Hsp70 protein. Ssa a class of Hsp70 proteins, are necessary for cellular homeostasis in protein folding, translation (Kim *et al.*, 1998) translocation (Deshaies and Koch, 1988), and degradation in *S. cerevisiae* (Juretschke *et al.*, 2010). Ssa1/Ssa2, are inducible under stress conditions, Ssa3/4 are expressed only under stress conditions (Werner-Washburne, 1987). **Am7160** is homologous to mitochondrial Hsp70, a molecular chaperone that protects proteins from aggregation under stress conditions and ensures correct folding of nascent and misfolded proteins (Bukau and Horwich, 1998). The protein showed homology to *S. cerevisiae* Ssc1 including a mitochondrial targeting sequence that is cleaved when it is translocated to the inner mitochondrial matrix (Verghese *et al.*, 2012). It interacts with co-chaperones, DNAJ and GrpE, forming a complex which binds and refolds protein (Szabo *et al.*, 1994). Recognition of misfolded proteins is thought to be engendered by hydrophobic protein regions, normally interior in a correctly folded protein (Verghese *et al.*, 2012). Hsp70s have roles as chaperones of protein folding and stabilisation as proteins are transported through membranes (Morishima, 2005). Elevated Hsp70 levels in *A. mellea* are indicative of protein misfolding consequent to oxidative stress, and suggest that interference with this process could represent a possible antifungal strategy for inhibiting the stress response, and hence virulence of *A. mellea*.

Am3211, pyruvate decarboxylase, activity is cleavage or synthesis of C-C bonds (Sprenger and Pohl, 1999). It is the penultimate step of acetate synthesis, pyruvate decarboxylase catalyses formation of acetaldehyde, in the cytosol. Acetate may be expelled from the cell or assimilated into cytosolic acetyl-CoA, by-passing the mitochondrial pyruvate dehydrogenase step in formation of acetyl-CoA for the TCA cycle which is not as energy efficient, but this mechanism in *S. cerevisiae* utilises ethanol as an energy source (Pronk *et al.*, 1996).

6.3.2 Proteins down-regulated under H_2O_2-induced oxidative stress

Am16706 an M16 peptidase is functionally similar to mammalian insulin degrading enzyme (IDE) and homologous to fungal Ste23p a mating pheromone required for the mating and fusion of haploid cells in yeast (Kim *et al.*, 2005; Adames *et al.*, 1995). The LuxS motif in this protein is interesting (Figure 6.9), as it is the most important enzyme for quorum sensing in bacteria, with a role in biosynthesis of AI-2 (autoinducer-2), (Rajan *et al.*, 2005; Hilgers and Ludwig, 2001). Its cysteine residues are susceptible to oxidation (Hilgers and Ludwig, 2001), and in *Deinococcus* sp. this signalling gene is upregulated under oxidative stress, and induces upregulation of additional protective genes (Fernandez-Bunster *et al.*, 2012). Interestingly, Am16706 was downregulated under H_2O_2 stress in *A. mellea* possibly a protective measure, to reduce homocysteine levels consequent to S-ribosylhomocysteine degradation, due to H_2O_2-induced oxidative stress.

Am19873 a translation elongation factor 1a (EF1a/EF-Tu) and the domain architecture of this protein in *A. mellea* appears to be unusual. Four domain signatures were identified by bioinformatic analysis, yet the only organisms with this four domain arrangement, described on the EMBL-EBI site, are eleven methane-generating bacteria, which have selenospecific elongation factors, and a *Strongylocentrotus purpuratus* uncharacterised protein. A homolog of EF1a/EF-Tu protein was shown to be particularly susceptible to oxidative carbonylation in a study of stress response proteins in *E. coli* (Dukan and Nystrom, 1998). Downregulation of this protein in *A. mellea* may be a transcription suppression mechanism as protection against replication of DNA damaged cells, or alternatively, a protective strategy against oxidation of the EF1a/EF-Tu protein itself.

Am7452, a Hsp90 chaperone, assists in folding of newly synthesised proteins, re-folds proteins, promotes repair or degradation of proteins damaged by heat or oxidative stress (Leach *et al.*, 2012) and are thought to ameliorate protein mutations by

buffering their effects (Jarosz and Lindquist, 2010). Hsp90s are expressed constitutively and interact with 10% of all proteins (Leach *et al.*, 2012), and may be upregulated under stress. Hsp90 chaperone protein is responsible for advance of G_1/S phase of the cell cycle (Senn *et al.*, 2012). Protein misfolding was induced in yeast cells and resulted in activation of heat shock transcription factors (HSF) which in turn blocked cyclin expression causing G_1 arrest (Trotter and Berenfeld, 2001). Hsp90 was depleted in a *S. cerevisiae* mutant lacking a HSF transcriptional activation domain, with consequent cell cycle arrest (Morano and Santoro, 1999). As inhibition of Hsp90 arrests the cell cycle, downregulation of this protein in *A. mellea* may be protection against replication of cells with DNA damage as a result of oxidative stress (Verghese *et al.*, 2012). Hsp90 depletion in *C. albicans* resulted in cells whose morphology indicated that there were cell defects resultant from incomplete mitosis and cell cycle arrest at G_1/S and G_2/M stages of the cell cycle (Morano and Santoro, 1999; Senn *et al.*, 2012). DNA damage from oxidative stress includes oxidation of deoxyribose monomers, strand breakage, modification of DNA and formation of DNA/protein crosslinks (Sharma *et al.*, 2012). In summary, reduced expression of Am19381 may indicate downregulation of cell cycle progression in order to protect against defective DNA replication in *A. mellea*.

6.3.3 Proteins upregulated under Menadione/$FeCl_3$ stress

Am19877 is an aspartate aminotransferase catalyses reactions in many metabolic and biosynthetic pathways pathways, plays a central role in nitrogen metabolism (Sung *et al.*, 1990) and has been shown to be involved in amino acid transport regulation in *S. cerevisiae* (Garrett, 1989). Aspartate aminotransferase with its PLP co-factor catabolises L-cysteine in a reversible reaction (Akagi, 1982; Marienhagen and Kennerknecht, 2005; Han *et al.*, 2010). Homocysteine is synthesised from L-cysteine in two further steps which provide substrate for the synthesis of methionine as part of the S-adenosyl methionine (SAM) cycle. SAM in turn is a co-substrate with putrescine for synthesis of spermidine and spermine (Figure 6.9), thus a possible role for aspartate aminotransferase in *A. mellea* under menadione/$FeCl_3$-induced oxidative stress is regulation of homocysteine availability for methionine synthesis.

6.3.4 Proteins downregulated under Menadione/$FeCl_3$ stress

Am19381 is a peroxisomal 3-ketoacyl-CoA thiolase, involved in lipid β-oxidation and long chain fatty acid conversion to sucrose (Lee, Kim, *et al.*, 2009). A dual role was proposed for this protein in *S. cerevisiae* as thiolase and peroxisomal defense protein (Lee, Kim, *et al.*, 2009). Given that Am19381 functionality may also play a role in poly

beta-hydroxybutyrate synthesis, diminution of its expression in response to oxidative stress may be linked to reduced energy storage and a concomitant increase in utilisation of cellular energy stores. In this regard, Jendrossek (2009) noted that poly beta-hydroxybutyrate is a universal storage compound of carbon and energy in prokaryotes. Thus, diminished expression of a 3-ketoacyl-CoA thiolase in *A. mellea*, in response to oxidative stress, could indicate a downregulation of energy storage mechanisms due to immediate energy requirements.

Am9629 is a Family 3 glycoside hydrolase with wide specificity, which cleaves β1-4 glycosidic bonds between carbohydrates and between carbohydrate and non-carbohydrate substrates. GH3 family enzymes are implicated in the growth of fungal hyphae (Slámová *et al.*, 2012). One of the domain signatures in this protein is a protective antigen PA14 domain is found in many proteins including bacterial toxins and functions of this domain include signalling, toxin activation and adhesion (Rigden *et al.*, 2004). The presence of this domain in *Dictyostelium discoideum* GH enzymes was observed to have a signalling role in morphological change of the organism (Kawata *et al.*, 2004).

Am13458 an alcohol oxidase is a member of the GMC oxidoreductases, which have lignolytic functions and produce extracellular H_2O_2 (Daniel *et al.*, 2007). Alcohol oxidase accumulated in peroxisomes of *Candida boidinii* which had been grown on methanol as sole carbon source and in cultures without methanol could barely be detected (Goodman and Scott, 1984). Under induced oxidative stress, its function as a mediator of extracellular H_2O_2 production may be attenuated in *A. mellea* in the presence of Menadione/$FeCl_3$. In this way, *A. mellea* could minimise its sensitivity to elevated environmental stress, by reducing extracellular H_2O_2 production due to the presence of elevated superoxide levels resulting from menadione exposure.

6.3.5 Proteins up-regulated under both stressors

Am17277, is a vitamin-B12 independent methionine synthase. Methionine protects proteins from oxidative stress (Cowie *et al.*, 1959; Luo and Levine, 2009), and was shown to be essential in *C. albicans,* as mutants lacking the methionine synthase (MET6) gene were non-viable even when supplemented with exogenous methionine (Suliman *et al.*, 2007). Methionine residues are readily oxidised by many ROS and scavenge ROS to form methionine sulfoxide, which in turn can be reduced by methionine reductase, found in the majority of cells, to form methionine (Luo and Levine, 2009). Clearly, the involvement of **Am17277** in methionine biosynthesis, along

with simultaneous homocysteine utilisation, provides a clear rationale for the observed increased expression under both oxidative stress conditions. Methionine also can donate methyl groups whereby DNA is methylated to prevent gene expression, and, as noted above, is required for SAM biosynthesis, essential for polyamine synthesis via spermidine/spermine synthase (**Am14050**) (Figure 6.9). This observation clearly suggests interplay between methionine biosynthesis and polyamine production in *A. mellea*, to produce ROS-scavenging metabolites as a protective mechanism against cellular damage.

6.3.6 Proteins up-regulated under H_2O_2 and down-regulated under Menadione/$FeCl_3$ stress

Am14558, VCP has homologues in yeast (Cdc48) and mammals (p97) and is a member of the AAA^+ ATPase superfamily whose activities include proteolysis, DNA replication and membrane fusion (Ogura and Wilkinson, 2001). VCP is implicated in endoplasmic reticulum stress (Wójcik *et al.*, 2006), ubiquitin regulatory processes, mitosis, and DNA/RNA repair, interacting with a broad range of proteins (Dreveny *et al.*, 2004). In mammalian cells when VCP levels were reduced, diamine acetyltransferase/Spermidine/spermine N(1)-acetyltransferase (SSAT)- a cytosolic enzyme which catalyses back conversion of spermine to spermidine and spermidine to putrescine, was upregulated (Wójcik *et al.*, 2006). SSAT reaction products are putrescine, spermidine and H_2O_2 (Wallace *et al.*, 2003). Putrescine must be exported from cells if levels rise, as high levels are toxic to cells (Tome *et al.*, 1997). Polyamine synthesis via SSAT and polyamine oxidase, generates H_2O_2 and initiates upregulation of SSAT, signalling apoptosis (Wallace *et al.*, 2003). When VCP was downregulated in mammalian cells, SSAT activity was upregulated, by which spermine is back-converted to spermidine and putrescine and H_2O_2. This suggests that under Menadione/$FeCl_3$-induced oxidative stress in *A. mellea*, downregulation of VCP has a role in back-conversion of polyamides, and under H_2O_2-induced oxidative stress in *A. mellea* back-conversion of polyamides is reduced (Figure 6.10).

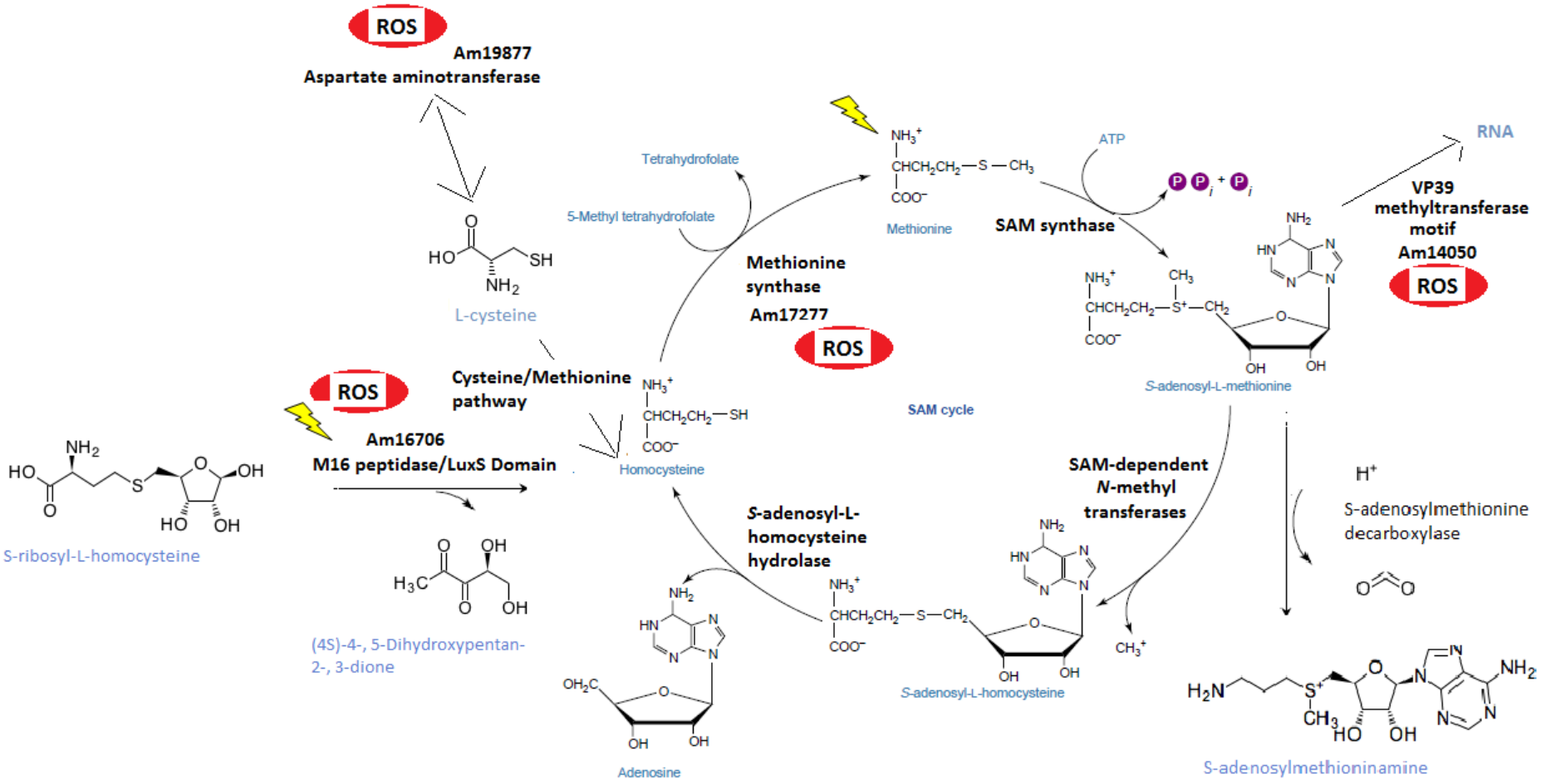
ROS
Am19877
Aspartate aminotransferase
L-cysteine
Tetrahydrofolate
5-Methyl tetrahydrofolate
Methionine synthase
Am17277
ROS
Methionine
ATP
SAM synthase
RNA
VP39 methyltransferase motif
Am14050
ROS
S-adenosyl-L-methionine
SAM cycle
Cysteine/Methionine pathway
ROS
Am16706
M16 peptidase/LuxS Domain
Homocysteine
S-ribosyl-L-homocysteine
(4S)-4-, 5-Dihydroxypentan-2-, 3-dione
S-adenosyl-L-homocysteine hydrolase
SAM-dependent N-methyl transferases
S-adenosyl-L-homocysteine
Adenosine
H+
S-adenosylmethionine decarboxylase
S-adenosylmethioninamine

Figure 6.9. Schematic of targets of ROS and enzymes differentially regulated in the SAM cycle. Proteins which have been identified in this study are indicated by their Am number and red elipse. Details of differentially regulated proteins: **(Am19877)** Aspartate aminotransferase from the cysteine/methionine pathway, is involved in synthesis of homocysteine which enters the SAM cycle, was up-regulated under menadione/$FeCl_3$-induced oxidative stress. **(Am17277)** Methionine synthase which was upregulated under both stress conditions. Methionine, the product of methionine synthase, is a precursor to polyamine synthesis and a ROS scavenger (Luo and Levine, 2009). (**Am14050)** A methyltransferase domain identified in Am14050 which was upregulated under H_2O_2-induced stress, can form a complex with SAM and bind RNA (Hodel *et al.*, 1996). **(Am16706),** down-regulated under H_2O_2-induced stress, a LuxS domain motif which is susceptible to oxidation, may catalyse the synthesis of homocysteine which enters the SAM cycle (Rajan *et al.*, 2005). Blue type indicates substrates/products, black type indicates enzymes. Species susceptible to oxidation or which scavenge ROS are shown with a yellow flash. Illustration adapted from Ashihara and Crozier (2001).

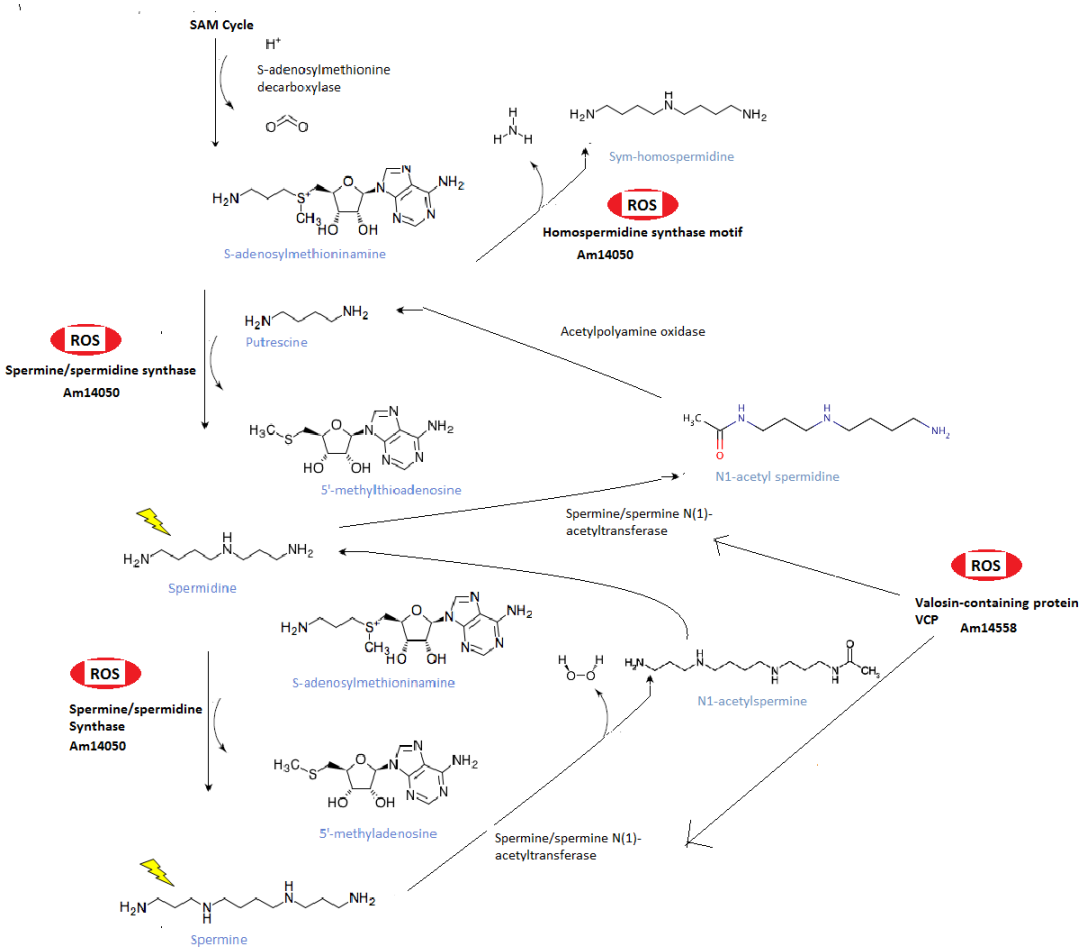

Figure 6.10. Schematic of targets of ROS and enzymes differentially regulated in the SAM cycle. Details of differentially regulated proteins: **(Am14050)** spermine/spermidine synthase was up-regulated under H_2O_2-induced oxidative stress. Spermidine and spermidine both scavenge ROS and spermine has been shown to signal upregulation of methionine production (Chattopadhyay *et al.*, 2009). **(Am14558)** A VCP protein was down-regulated under menadione/$FeCl_3$-induced oxidative stress and upregulated under H_2O_2-induced oxidative stress. In concert with SSAT, it catalyses the back conversion of spermine and spermidine with H_2O_2 as a by-product (Wójcik *et al.*, 2006). **(Am14050)** A homospermidine domain catalyses synthesis of sym-homospermidine, from putrescine and may play a regulatory role in polyamine biosynthesis (Valdés-Santiago *et al.*, 2009). Substrates/ products are in blue type, enzymes are in black type. Species susceptible to oxidation or which scavenge ROS are shown with a yellow flash.

In summary, differential proteomic investigation of *A. mellea* under distinct oxidative stress conditions has revealed extensive proteome remodelling within a 3 h

period. Metabolic systems involved in methionine biosynthesis, homocysteine dissipation and polyamine biosynthesis are affected to enable production of methionine, possibly as a free-radical scavenger, and ROS-scavenging polyamines. We postulate that methionine synthesis, regulated by LuxS and AAT homeostasis of homocysteine with concomitant spermine/spermidine upregulation and scavenging mitigate against cellular damage under conditions of oxidative stress.

This is the first differential proteomic study of oxidative stress in *A. mellea*. Further investigation of the secretome and metabolome of *A. mellea* under induced oxidative stress by LC-MS/MS analysis and quantitative shotgun proteomics would be valuable resources to further illuminate investigation of pathogenicity in *A. mellea,* as would application of other techniques such as RNAseq to study the transcriptome of the organism. An infection study in the ensuing Chapter will provide more insight into mechanisms of this virulent pathogen at a molecular level.

Chapter 7 Discovery and investigation of the fungicidal effect of *Armillaria mellea* on *Candida albicans* during co-culture

7.1 Introduction

Antagonistic interactions between microorganisms can induce defence responses and pathogenic phenotypes in both organisms. Indeed, co-culture of organisms is used to explore these responses and expression or upregulation of proteins is one way of identifying proteins involved in pathogenicity and virulence.

The subterranean filamentous network of *A. mellea* is subjected to constant ingress and depredation from animals, plants, bacteria and other fungi (Heaton *et al.*, 2012; Baumgartner *et al.*, 2011; Czederpiltz *et al.*, 2001). Its habitat dictates that it forages widely for nutrition, and exists as a facultative necrotroph and sacrotroph. *A. mellea* is even parasitized by plants (Williams *et al.*, 1989; Baumgartner *et al.*, 2011). *A. mellea* is a putative mycoparasite of *Wynnea* (Fukuda *et al.*, 2003) and in turn other fungi are mycoparasites of *A. mellea* (Czederpiltz *et al.*, 2001; Baumgartner *et al.*, 2011). Thus, the role of *A. mellea* as a mycoparasite and phytopathogen may necessitate a fungal response to depredation via exploitation of its arsenal of defensive proteins.

Biocontrol, by application of an antagonistic organism against a pathogenic species has been widely used, and *Trichoderma* spp. comprise 90% of biocontrol agents (Benítez *et al.*, 2004). Biocontrol of phytopathogens has focussed on the interaction of the biocontrol agent (BCA) and pathogen from the perspective of the antagonist rather than the pathogen, and thus antagonist genes their mechanisms and metabolites are known. The pathogen, and its interaction with the antagonist is much less studied, and there has been little analysis of pathogen response to its adversary (Duffy *et al.*, 2003). *Trichoderma* spp. have been used extensively as BCA (Benítez *et al.*, 2004) but *modi operandi* are different in individual species, even at a morphological level, and differentially regulated proteins are correspondingly diverse between species, in mycoparasitism against *Rhizoctonia solani* (Atanasova *et al.*, 2013).

As proteins are induced or upregulated in co-cultures, dual cultures have been used to produce enzymes with biotechnological application, *Ganoderma lucidum* and *Candida* spp. were co-cultured together with glucose as a carbon source. *Candida* utilised glucose and produced ethanol and glycerol, the glycerol was then utilised by *G. lucidum* as a carbon source to overproduce laccase (Li *et al.*, 2011). A novel utilisation of co-culture was the immobilisation of *Saccharomyces cerevisiae* for wine

production on a scaffold formed by the hyphae of *Penicillium chrysogenum* which was killed by *S. cerevisiae* during fermentation (García-Martínez *et al.*, 2011). Co-cultures have been used to induce synthesis of secondary metabolites. Taxol, the anticancer drug, was synthesised by *Paraconiothyrium* SSM001 in liquid cultures and its biosynthesis was increased eightfold by co-culture with two ascomycetes *Alternaria* and *Phomopsis* (Soliman and Raizada, 2013). This approach was also used to generate bioactive compounds from *Aspergillus fumigatus* in co-culture with other organisms for drug discovery (Zuck *et al.*, 2011). Another co-culture approach taken by Ahamed and Vermette (2008), was generation sugars through synergistic activity of *Trichoderma reesei* and *Aspergillus niger* on agro-industrial waste to produce cheap ethanol for bio-fuel.

One fungal strategy to protect against pathogens is secretion of secondary metabolites, many of which are toxins. *A. mellea* is known to secrete many metabolites and small molecules such as melanin and aryl esters, with antibiotic, antifungal and cytotoxic activities (Sonnenbichler *et al.*, 1997; Cremin *et al.*, 2000; Donnelly, *et al.*, 1985; Donnelly and Hutchinson, 1990). Indeed, the toxicity of these metabolites has been linked to fungal virulence (Peipp and Sonnenbichler, 1992; Bohnert *et al.*, 2011; Misiek and Hoffmeister, 2008). Different *Armillaria* species in co-culture are known to secrete compounds that are not secreted in mono-culture and which inhibit growth of each culture (Sonnenbichler *et al.*, 1997). Growth of *A. mellea* which had been labelled with ^{13}C, was inhibited by *Trichoderma atroviride* SC1, in co-culture and *T. atrovirde* was shown to have absorbed metabolites secreted by *A. mellea* (Pellegrini *et al.*, 2012). *Candida parapsilosis* inhibited aflatoxin production in *Aspergillus* spp., although it did not inhibit growth of *Aspergillus*, and Niknejad *et al.* (2012), proposed *C. parapsilosis* as a fungal biocontrol mechanism against aflatoxins.

Efflux pumps are used by fungi to reduce the concentration of toxins produced by pathogenic organisms. *A. fumigatus* was shown to be resistant to gliotoxin whereas *C. albicans* was not, but the number of efflux transporters in the *A. fumigatus* genome (n = 320) is more than three times that of *C. albicans* (n = 106) thereby conferring more likelihood of resistance to endogenous and exogenous toxins (Coleman *et al.*, 2011; Coleman and Mylonakis, 2009). Cytochrome P450 enzymes (Section 3.2.3.8), of which *A. mellea* possesses a large cohort, degrade xenobiotics produced by competing organisms, as well as environmental pollutants (Syed and Yadav, 2012) and cytochrome

P450 enzymes were upregulated in *T. reesei* co-culture with *R. solani* (Atanasova *et al.*, 2013).

A detailed proteomic analysis of *S. commune* and *T. viride* in co-culture identified 284 proteins differentially regulated in *S. commune* and 30 proteins differentially regulated in *T. viride*. Proteins involved in transcription and translation were most predominant, at 61% and 30%, respectively. Stress-related proteins accounted for 67% of the upregulated proteins in *S. commune* in co-culture with *T. viride*, which related to transcription and translation (61%), proteins pertaining to cell wall integrity (17%) and metabolism (22%). Functional classifications of proteins downregulated in *S. commune* in co-culture with *T. viride*, were related to metabolism (64%), transcription and translation (22%) and other activities (14%). Proteins differentially regulated in *T. viride* were two glyceraldehyde-3-phosphate dehydrogenases, an aspartyl protease, two elongation factor proteins and a transcription regulator, which were downregulated (Ujor *et al.*, 2012).

Given that *A. mellea* is a significant plant pathogen, and also exists in nature amidst a range of ascomycete and basidiomycete fungi, it was hypothesised that co-culture studies may further inform on organismal biology. Thus, this chapter presents information of an investigation into the (myco)parasitic action of, or predation by, *A. mellea* using co-culture of *A. mellea* with *C. albicans* as an infection model.

Specifically, the aims of the work presented in this chapter were:

1. To evaluate the reciprocal effects of *A. mellea* co-culture with other fungal, and bacterial, species; and to specifically investigate the effects of *A. mellea*/*Candida albicans* co-culture-derived extracts on the subsequent growth of *C. albicans* in monoculture.
2. To undertake assessment of *C. albicans* viability by fluorophore dye uptake and growth assays, respectively, following co-culture with *A. mellea*- compared to mono-culture conditions.
3. To analyse the *A. mellea* secretome by LC-MS/MS to identify the nature of the proteins secreted by *A. mellea* following co-culture with *C. albicans* in a novel infection model system.

.

7.2 Results

7.2.1 Co-culture with pathogenic species

Co-cultures of *A. mellea* and pathogenic microorganisms: *C. albicans* (Section 2.2.6.4), *P. aeruginosa* (Section 2.2.6.5), *S. aureus* (Section 2.2.6.6), MRSA (Section 2.2.6.7) and *E. coli* (Section 2.2.6.8) were carried out, however no inhibition of either *A. mellea* or any pathogenic species was observed, except in the case of *C. albicans*, which was overgrown by *A. mellea* mycelia until it was no longer visible. Dark crustose *A. mellea* rhizomorphs were clearly visible at *C. albicans* inoculation points (Figure 7.1).

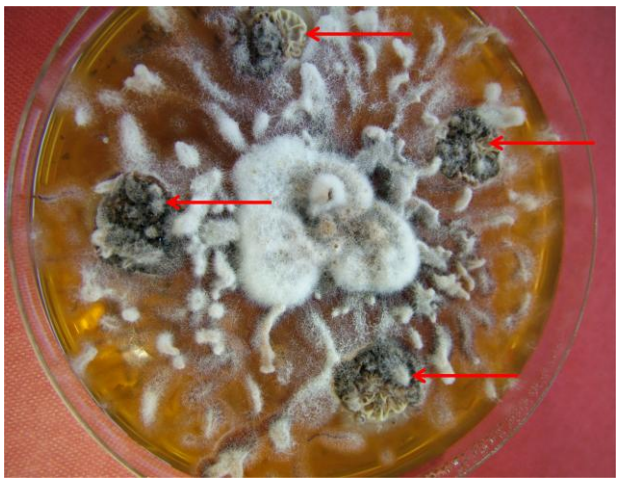

Figure 7.1. *A. mellea* and *C. albicans* co-culture on MEA at 21 days post-inoculation with *C. albicans*. Red arrows indicate *C. albicans* inoculation points which can be seen clearly due to crustose thickening of *A. mellea* mycelia and brown secretions (possibly melanin).

Interestingly, contamination of *A. mellea* culture by an unidentified environmental filamentous fungus on MEA appeared to show *A. mellea* mycelial growth inhibition and a zone of inhibition around the mycelia (Figure 7.2). This apparent inhibition could not be replicated in *A. mellea* co-cultures with conidia from this plate. Co-cultures of *A. mellea* and the filamentous pathogen *A. fumigatus* (Section 2.2.6.1) showed no inhibition of either fungus.

Figure 7.2. *A. mellea* culture contaminated with an unidentified fungus. The culture had been grown for 15 days and appeared to show a zone of inhibition around *A. mellea* mycelia.

7.2.1.1 Workflow of *A. mellea* and *C. albicans* co-cultures.

As co-culture of *A. mellea* with *C. albicans* had shown inhibition of *C. albicans*, an infection model was set up to assess the viability of *C. albicans* cells taken from co-cultures and identify proteins that were secreted in co-cultures of the fungi.

A flow diagram of co-culture protocols followed by LC-MS/MS analysis of supernatants, cultures of *C. albicans* cells removed from co-culture plates and cell viability staining for confocal microscopy is shown in Figure 7.3.

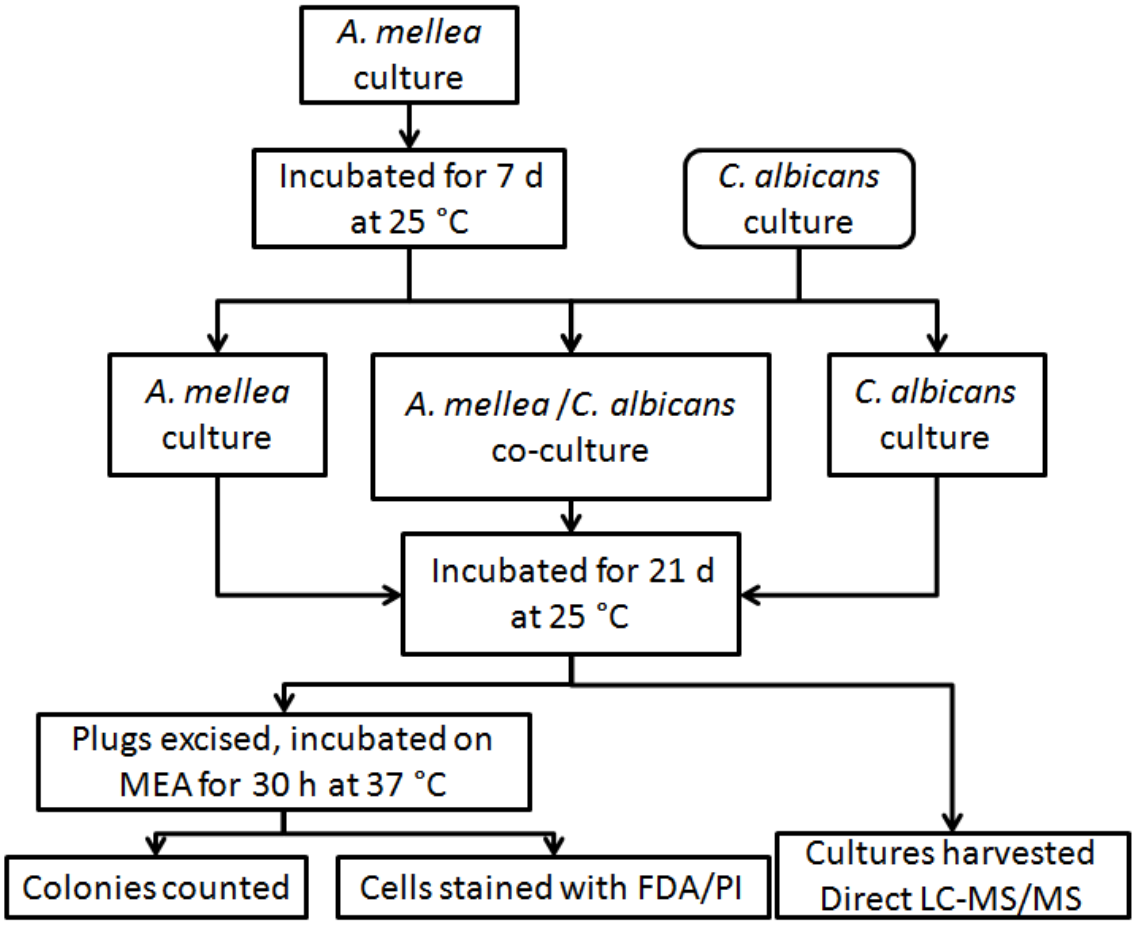

Figure 7.3. Flow diagram of *A. mellea/C. albicans* co-cultures. Plates containing mono-culture of *A. mellea* were inoculated with *C. albicans* after 7 d incubation at 25 °C prior to further incubation for 21 d at 25 °C. Cultures were (i) harvested for direct LC-MS/MS of agar supernatant, or (ii) plugs from *C. albicans* colonies were excised and used to inoculate MEA, cultured for 30 h at 37 °C prior to assessment of cell viability.

7.2.1.2 Co-culture of *A. mellea* and *C. albicans* on MEA.

Plates of MEA were inoculated with *A. mellea* and incubated for 7 d at 25 °C, after which they were further inoculated with *C. albicans* and grown for 21 d at 25 °C (Section 2.2.6.2). There was no differential growth of either species observed, whether in mono-cultures or co-cultures until *A. mellea* hyphae made contact with the *C. albicans* colonies (10 d post-inoculation), after which *C. albicans* colonies reduced in size (Figure 7.4). *A. mellea* hyphae did not preferentially grow towards *C. albicans* colonies, but once *A. mellea* hyphae reached *C. albicans* colonies, *A. mellea* hyphal growth into the *C. albicans* colonies increased and a brown exudate was apparent. *C. albicans* colonies were overgrown by *A. mellea* until they were no longer visible,

although inoculation points were clearly visible, due to crustose thickening and brown exudates of *A. mellea* (Figure 7.1). Light microscopy of cells from inoculation points revealed the presence of *C. albicans* cells which appeared to be intact.

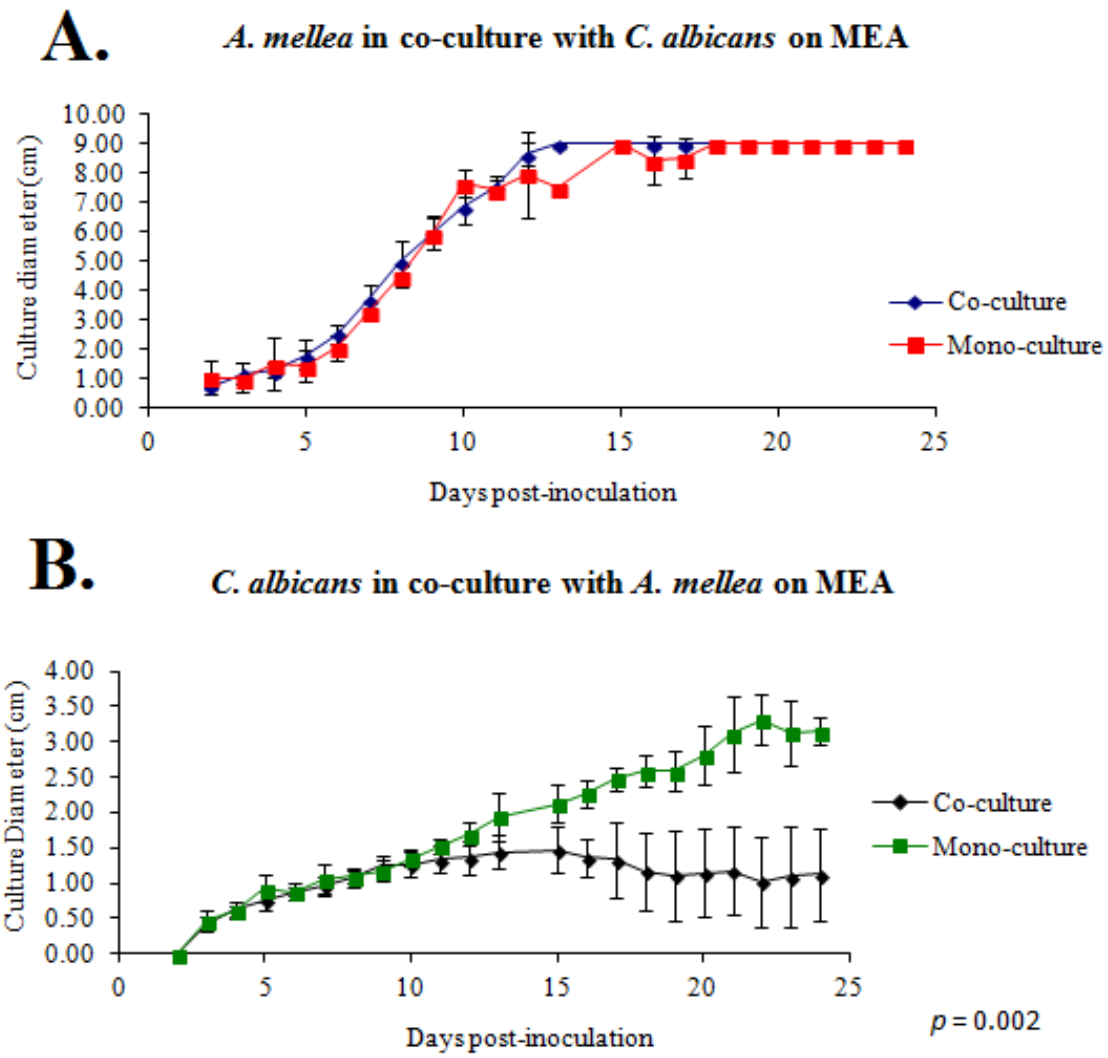

Figure 7.4. Comparison of colony growth: Mono-cultures of *A. mellea* and co-cultures of *A. mellea* with *C. albicans*. **A**. *A. mellea* culture diameter in mono-culture and in co-culture with *C. albicans*. **B.** *C. albicans* culture diameter in mono-culture and in co-culture with *A. mellea*. Significant reduction of *C. albicans* growth is evident when *A. mellea* is present.

7.2.1.3 Culture of *A. mellea* on MEA with autoclaved *C. albicans.*

To study the effect of dead *C. albicans* cells on culture of *A. mellea*, *C. albicans* cells which had been autoclaved prior to inoculation were put onto *A. mellea* cultures in four separate places (Section 2.2.6.2). When *A. mellea* mycelia overgrew *C. albicans* inoculation points, the dead cells did not elicit any response in *A. mellea*, either in rate of growth, or formation and accumulation of crustose hyphae seen in co-cultures with live cells. Cultures grown in a 9 cm petri dish reached a diameter of 9 cm within 12 d, which was the growth rate routinely observed in *A. mellea* mono-cultures.

In an attempt to establish if *A. mellea* was using *C. albicans* as a nutrient source, *C. albicans* (10^7 cells/ml) were added to MEA prior to autoclaving, plates were inoculated with *A. mellea* and incubated at 25 °C for two weeks to establish if growth rate or morphology were affected by addition of *C. albicans* cells to media. Control plates of MEA inoculated with *A. mellea* were also grown (Section 2.2.3.3). The cultures showed no differences in growth rates or morphology and all cultures reached a diameter of 9 cm within 12 d. No colour difference was observed in the agar supernatants which would have possibly indicated melanin-type exudate against *C. albicans* by *A. mellea*.

7.2.2 Growth inhibition study of *C. albicans* by mono and co-culture supernatants.

In order to establish if (i) *A. mellea* supernatants showed fungicidal activity or (ii) *A. mellea* and *C. albicans* co-culture supernatants elicited fungicidal activity, an evaluation of *C. albicans* grown with lyophilised supernatant in MeOH (Coleman *et al.*, 2011) was carried out (Section. 2.2.6.12) at ranges of 1 – 10 mg (supernatant lyophilisate or volume equivalents of MeOH). There was no specific inhibition of *C. albicans* at any of the amounts applied (Figure 7.5).

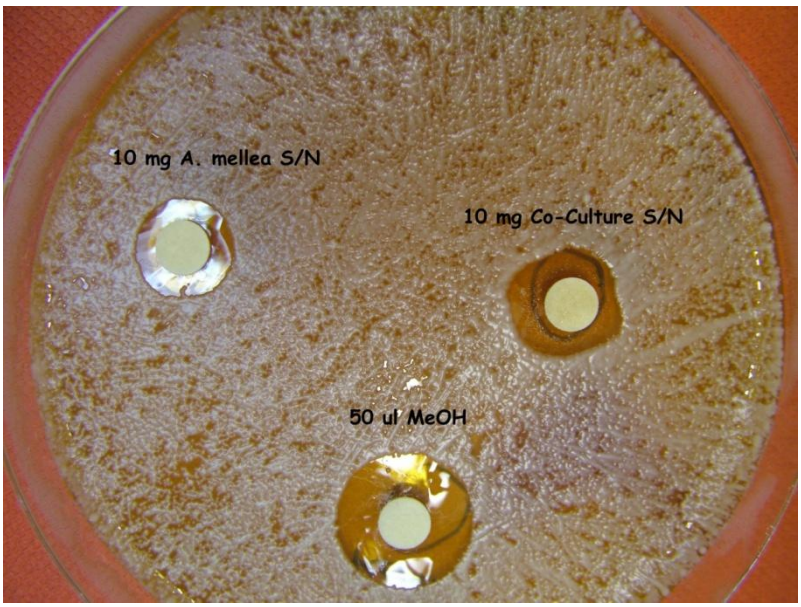

Figure 7.5. Inhibition study of *C. albicans* by *A. mellea* supernatants. *C. albicans* (10^6 cells) cultures were incubated at 37 °C for 24 h with lyophilised supernatants from mono-cultures of *A. mellea*, co-cultures of *A. mellea* with *C. albicans* (20 d) resuspended in MeOH or MeOH control. No specific inhibition of *C. albicans* was apparent indicating that there was no fungicidal activity in *A. mellea* culture supernatants against *C. albicans*.

7.2.3 Development of fluorescent staining protocol for *Candida albicans* cells to assess viability following co-culture.

Cell staining is widely used determine cell viability, to enumerate either live or dead cells, or both live/dead cells, in cell survival studies (Tsai *et al.*, 2010) and cidal activity against pathogens (Nomanbhoy *et al.*, 2002). Viability staining relies on physiological and morphological changes which differentiate live and dead cells as a result of changed cell membrane permeability. Two fluorescent dyes are used regularly for viability assays, propidium iodide (PI) which stains dead cells red, and fluorescein diacetate (FDA) which stains live cells green. PI stain binds to DNA in dead cells by migrating through damaged cell membranes and is excluded from live cells by intact cell membranes. FDA is lipid-soluble and non-fluorescent and can permeate cell membranes, where it is cleaved by cytoplasmic esterases to yield a fluorescent product, which is retained in the cytoplasm by cell membranes (Coder, 1997). Dual staining with both PI and FDA to assess numbers of live and dead has been used in many studies (Jones and Senft, 1985; Nomanbhoy *et al.*, 2002; Tsai *et al.*, 2010). Dual staining of *C. albicans* which had been excised after co-culture with *A. mellea* was undertaken. However, staining of live cells proved problematic as there was efflux of FDA from the

cells as had previously been reported in a multi-drug resistant strain of *C. albicans* (Yang *et al.*, 2001). A protocol whereby cells were simultaneously stained with PI and FDA and dried prior to visualisation was adopted (Jones and Senft, 1985). *C. albicans* cells were excised from inoculation points of *A. mellea*/*C. albicans* co-culture and simultaneously stained with PI and FDA (Section 2.2.15.6). Glass slides for microscopy were prepared from (i) freshly harvested cultures of *C. albicans* cells, (ii) from *C. albicans* cells killed by autoclaving (Section 2.2.15.5), (iii) *C. albicans* mono-culture control samples which had been grown for 21 d (Section 2.2.15.5), and (iv) *C. albicans* cells excised from co-cultures of *C. albicans* with *A. mellea* (Section 2.2.15.6). All glass slides were thoroughly air dried in darkness prior to microscopy.

Cells were visualised by confocal microscopy to determine their viability (Section 2.2.15.7). Live cells stained green (FDA) and dead cells stained red (PI). Figure 7.6 shows a confocal image of stained cells: **1.** Freshly cultured live *C. albicans* which has been stained with FDA/PI, all cells are stained green, denoting viable cells; **2.** Freshly cultured *C. albicans* killed by autoclaving and stained with FDA/PI, all cells are stained red, denoting non-viable cells; **3.** *C. albicans* from 21 d culture stained with FDA/PI, most cells are stained green, indicating viability; **4.** *C. albicans* from co-culture of *A. mellea* and *C. albicans* stained with FDA/PI, most of these cells are stained red, with only a few stained green indicating that most of these cells are not viable. *C. albicans* from mono-cultures (21 d) had a bloated irregular appearance and revealed some filamentous growth when compared to cells from fresh cultures. *C. albicans* from co-cultures had the same bloated irregular appearance as the cells from mono-cultures when viewed under a light microscope, but were more fragile than cells from mono-culture (21 d) as centrifugation and washing reduced the cell numbers by ~ 90 %, therefore, the number of *C. albicans* cells necessary for staining was 150 times greater than the number of mono-culture (21 d) *C. albicans* cells required for visualisation by microscopy.

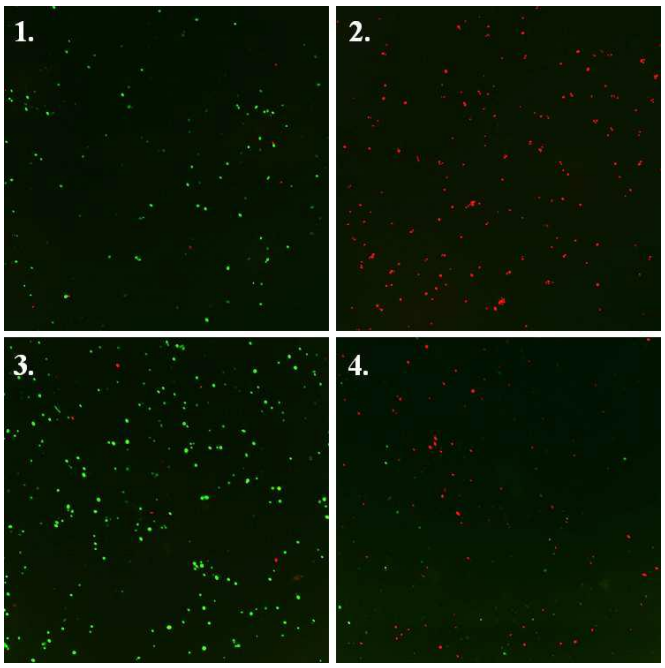

Figure 7.6. Fluorescent determination of *C. albicans* viability by simultaneous FDA (live) and PI (dead) cell staining of *C. albicans* cells: **1**. *C. albicans* from live cultures (24 h); **2.** *C. albicans* cells killed by autoclaving; 3. *C. albicans* from plates which had been inoculated with *C. albicans* excised from mono-cultures (21 d) and grown at 37 °C for 24 h; **4.** *C. albicans* from plates inoculated with *C. albicans* excised from co-cultures (21 d) with *A. mellea* and grown at 37 °C for 24 h. Magnification: 20X.

7.2.4 Viability plate assay of *C. albicans* cells excised from co-cultures

Dilutions of *C. albicans* cells which had been excised from co-cultures grown at 25 °C for 21 d (Section 2.2.6.3), were used to inoculate plates of MEA and incubated at 37 °C for 24 - 48 h. Dilutions of *C. albicans* cells from mono-cultures incubated at 25 °C for 21 d were excised and grown in the same manner (Section 2.2.6.3). Plates of all dilutions were inspected after 24 h for colony growth and density. Dilutions of 1/10000 were deemed to be most suitable for colony counting, which was carried out using SynGene GeneTools (v4.2) software (Figure 7.7). Graphical representation and a t-test were carried out from three replicates using Microsoft Excel® (Figure 7.8). The viability of *C. albicans* cells retrieved from mono-cultures was set to 100 % and the viability of cells retrieved from co-cultures was ~ 2% (p = 0.0004), representing a kill rate of 98 %.

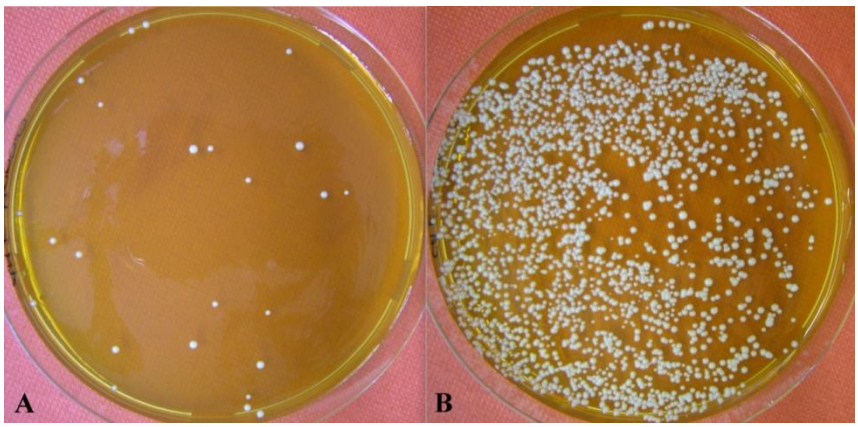

Figure 7.7. Viability assay 30 h post-inoculation of *C. albicans* retrieved from co-cultures and mono-cultures. Both plates are from $^{1}/_{10000}$ dilutions of recovered cells. **A.** Colonies of cells excised from previously *A. mellea* co-cultured *C. albicans*, **B.** Colonies of cells excised from previously mono-cultured *C. albicans* cells.

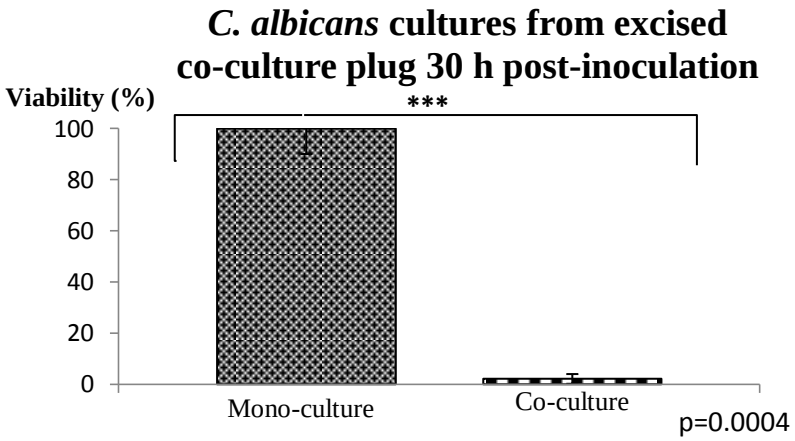

Figure 7.8. Viability of *C. albicans* cells retrieved from mono-cultures and co-cultures. The colony count values were adjusted to percentage viability rates. Thus, cell viability from mono-cultures was 100 %, and cell viability from co-cultures was ~2 %.

7.2.5 LC-MS/MS and bioinformatic analysis of fungal co-culture matrices.

C. albicans database was downloaded from the Candida genome database (http://www.candidagenome.org/ Accessed 02.03.2012) and added to the *A. mellea* database to create a chimeric protein database.

Protein extraction (Section 2.2.7.7), digestion (Section 2.2.10.2) and direct LC-MS/MS analysis (Section 2.2.15.1) of co-culture agar supernatants were undertaken. This was followed by interrogation of the *A. mellea/C. albicans* cDNA database by Spectrum Mill. *A. mellea* proteins (n = 205) (Appendix A.6 (Accompanying CD file Master Tables Appendices.docx)) were identified as well as *C. albicans* proteins (n = 11). B2G

was used to annotate all proteins identified and *C. albicans* proteins identified by BLAST and IPS is shown in Table 7.1. A subset of *A. mellea* proteins which were uniquely identified (n = 30) from agar supernatants of co-cultures of *A. mellea* with *C. albicans* is shown in Table 7.2.

A. mellea proteins were classified after BLAST search as (i) proteins with known functions (90%), (ii) hypothetical proteins (6%), (iii) predicted proteins (3%) and (iv) *A. mellea* specific (1%) (Figure 7.9). Further analysis by SecretomeP showed 26% (n = 54) with classical secretion signals and 40% (n = 83) with non-classical secretion signals, giving a total of 66% exhibiting secretion signals. ProteinGRAVY analysis showed that 19% (n = 38) were hydrophobic proteins and Phobius revealed proteins that 13% (n = 27) incorporated transmembrane domains.

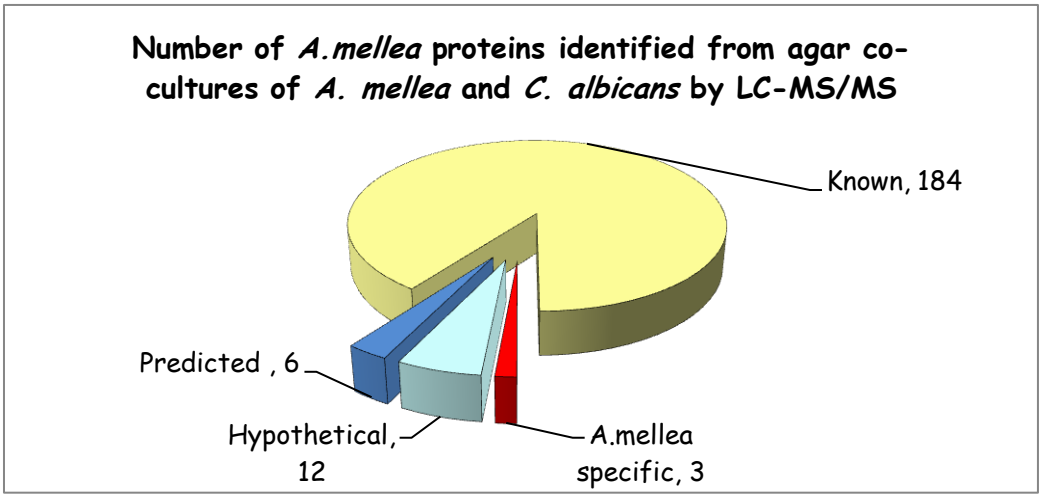

Figure 7.9. Categories and numbers of proteins identified from the *A. mellea* cDNA database and BLAST search following direct LC-MS/MS analysis of agar supernatant from co-cultures of *A. mellea* and *C. albicans*.

Combined DAGs from *A. mellea* proteins were constructed by B2G and multilevel graphs of the data from all the secreted proteins visualised the GO annotation analysis of biological process (Figure 7.10), cellular component (Figure 7.11) and molecular function (Figure 7.12).

The largest category in the biological process was catabolic process (21%) which was followed by carbohydrate metabolism (16%) and generation of precursor metabolites and energy (14%). Nucleotide, nucleobase and nucleic acid GO were the next most abundant (12%) and the balance was comprised of translation (8%), ion transport (6%), lipid metabolic process (5%), response to stress (4%), cellular homeostasis (2%) and

cellular component organisation (2%) (Figure 7.10). There were four GO cellular component categories; ribosome (33%), protein complex (31%), mitochondrion (25%) and nucleus (6%) (Figure 7.11). The largest class of GO in the molecular function visualisation was nucleotide binding (27%), followed by protein binding (15%). The next two categories were structural molecule activity (12%), transporter activity (11%) and peptidase activity (11%). The GO classes with the lowest abundance were RNA binding (7%), electron carrier activity and antioxidant activity, each 5%; carbohydrate binding and kinase activity, both 4% (Figure 7.12).

Table 7.1. *C. albicans* proteins from co-culture matrices following direct LC-MS/MS analysis, identified from interrogation of a combined *A. mellea/C. albicans* database.

Accession No.	BLAST Description	Enzyme Codes	InterProScan Annotation
orf19.3997	Alcohol dehydrogenase	EC:1.1.1.1	IPR002085; IPR002328; IPR011032; IPR013149; IPR013154; IPR016040; IPR020843; G3DSA:3.90.180.10 (GENE3D), PTHR11695:SF295 (PANTHER), seg (SEG), SSF51735 (SUPERFAMILY)
orf19.2619	Acid phosphatase	EC:3.1.3.2	IPR000560; IPR016274; G3DSA:3.40.50.1240 (GENE3D), PTHR20963 (PANTHER), PTHR20963:SF9 (PANTHER), SSF53254 (SUPERFAMILY)
orf19.3499	Hypothetical LDG family protein 8		no IPS match
orf19.6814	Glyceraldehyde-3-phosphate dehydrogenase	EC:1.2.1.12	IPR006424; IPR016040; IPR020828; IPR020829; IPR020830; IPR020831; G3DSA:3.30.360.10 (GENE3D), SSF51735 (SUPERFAMILY), SSF55347 (SUPERFAMILY)
orf19.5180	Mitochondrial peroxiredoxin prx1	EC:1.11.1.15; EC:1.11.1.7	IPR000866; IPR012336; IPR019479; IPR024706; G3DSA:3.30.1020.10 (GENE3D), PTHR10681 (PANTHER), PTHR10681:SF17 (PANTHER), seg (SEG)

Accession No.	BLAST Description	Enzyme Codes	InterProScan Annotation
orf19.395	Enolase 1	EC:4.2.1.11	IPR000941; IPR020809; IPR020810; IPR020811; G3DSA:3.20.20.120 (GENE3D), G3DSA:3.30.390.10 (GENE3D), seg (SEG), SSF51604 (SUPERFAMILY), SSF54826 (SUPERFAMILY)
orf19.6081	Protein EPD1 precursor	-	IPR004886; IPR012946; IPR013781; IPR017853
orf19.357	Prohibitin-like protein	-	IPR000163; IPR001107; coil (COIL), seg (SEG), SSF117892 (SUPERFAMILY)
orf19.3708	Secretory aspartyl proteinase sap2p	EC:3.4.23.0	IPR001461; IPR001969; IPR009007; IPR021109; PTHR13683:SF94 (PANTHER)
orf19.2623	Potential fungal zinc cluster transcription factor	-	IPR001138
orf19.3680	Hypothetical protein cao19.3680 [*Candida albicans* SC5314]	-	IPR000038; IPR002078; G3DSA:3.40.50.300 (GENE3D), PTHR18884:SF22 (PANTHER), SSF52540 (SUPERFAMILY)

[a]Accession number from *C. albicans* protein database; [b]BLAST annotation following Blast2GO analysis of proteins identified from *C. albicans* protein database; [c]Enzyme Code, (Internation Union of Biochemistry and Molecular biology (IUBMB) Enzyme Nomenclature following Blast2GO analysis of proteins identified from *C. albicans* protein database (http://www.enzyme-database.org/); [d]InterProScan Annotation, IPS motifs and families following Blast2GO analysis of proteins identified from *C. albicans* protein database.

Table 7.2. *A. mellea* proteins uniquely identified from co-culture matrices of *A. mellea* with *C. albicans*.

[a]Accession Number	[b]BLAST annotation	[c]tM_r	[d]tp*I*	Coverage %	Peptides	[e]SM Score	[f]GRAVY score	[g]TM	[h]SigP/ SecP	[i]Method	[j]Source
Am5344	60s ribosomal protein l10a	12603.7	9.6	10.7	1	11.51	-0.7		SecP	S	SN
Am12506	Aryl-alcohol oxidase	64088.4	4.7	2.7	1	16.33	-0.1		SigP	S	SN
Am17545	Coproporphyrinogen iii oxidase	103512.9	9.5	15.7	4	79.77	-0.1	2.0		S	SN
Am10593	Cys 2 peroxiredoxin	22242.4	5.2	6.5	1	12.87	-0.2		SecP	S	SN
Am9607	Cytochrome c oxidase subunit v	24861.9	9.7	7.5	1	20.74	-0.3	2.0	SecP	S	SN
Am19980	F_1F_0-ATPsyn f	15435.1	10.5	14.5	1	19.06	-0.1	1.0	SecP	S	SN
Am16128	Glycerol-3-phosphate o-acyltransferase	64013.5	9.8	3.3	1	13.13	0.0	3.0		S	SN
Am13890	Glycosyl hydrolase 53 domain-containing protein	21828.7	6.9	14.7	1	18.79	0.0		SigP	S	SN
Am13814	Hypothetical protein CC1G_12365 [*Coprinopsis cinerea* okayama7#130]	8166.3	5.8	18.7	1	18.59	-0.3			S	SN
Am13829	Hypothetical protein SCHCODRAFT_107411 [*Schizophyllum commune* H4-8]	66976.6	6.0	7.9	2	26.2	-0.3		SecP	S	SN

[a]Accession Number	[b]BLAST annotation	[c]tM$_r$	[d]tp*I*	Coverage %	Peptides	[e]SM Score	[f]GRAVY score	[g]TM	[h]SigP/ SecP	[i]Method	[j]Source
Am18856	Hypothetical protein SCHCODRAFT_237540 [*Schizophyllum commune* H4-8]	30601.9	9.5	6.1	1	13.69	0.4	4.0	SigP	S	SN
Am12218	Hypothetical protein SERLADRAFT_459096 [*Serpula lacrymans* var. Lacrymans S7.9]	56022.9	4.6	4.1	1	14.46	-0.2		SigP	S	SN
Am12353	Iron-sulfur protein subunit	30797.5	8.7	9.7	1	13.5	-0.5		SecP	S	SN
Am19926	Lipoic acid synthase	67338.7	9.6	3.3	1	16.04	-0.2	1.0		S	SN
Am16692	*A. mellea* unknown function protein	25812.9	4.6	6.5	1	17.44	-0.4			S	SN
Am13379	NADH dehydrogenase	61958.6	9.3	3.2	1	15	-0.2	2.0	SecP	S	SN
Am14001	Prohibitin phb1	26007.0	6.9	7.9	1	20.8	0.1		SigP	S	SN
Am20343	Protein	10943.5	9.1	21.2	1	13.75	-0.3		SecP	S	SN
Am3423	Protein	13693.7	4.6	18.1	1	20.53	0.2		SigP	S	SN
Am6084	Protein	32823.9	5.7	9.8	1	13.81	-0.5		SecP	S	SN
Am20304	Proteolysis and peptidolysis-related protein	22016.4	8.7	6.6	1	15.62	-0.2		SecP	S	SN

[a]Accession Number	[b]BLAST annotation	[c]tM$_r$	[d]tp*I*	Coverage %	Peptides	[e]SM Score	[f]GRAVY score	[g]TM	[h]SigP/ SecP	[i]Method	[j]Source
Am17796	Secreted protein	46381.6	5.9	12.1	2	36.22	0.0			S	SN
Am18628	Subunit vib of cytochrome c oxidase	10044.2	5.3	15.1	1	12.99	-0.8		SecP	S	SN
Am15086	Succinate-semialdehyde dehydrogenase	74240.9	8.5	2.0	1	15.07	0.1	4.0	SecP	S	SN
Am16124	Sulfide-quinone oxidoreductase	118017.6	8.7	4.0	2	33.19	-0.4	2.0		S	SN
Am7929	Thioredoxin	13706.0	4.7	15.6	1	15.39	0.1			S	SN
Am14705	Twin-arginine translocation pathway signal	63826.1	5.8	4.9	1	16.77	0.0		SecP	S	SN
Am2793	Ubiquitin domain-containing	37237.5	5.2	6.4	1	16.2	-0.2			S	SN
Am18503	Uracil phosphoribosyltransferase	19530.7	4.9	10.3	1	15.46	0.2		SecP	S	SN
Am14973	Urea hydro-lyase cyanamide hydratase	28060.0	5.7	8.4	1	19.82	-0.2		SecP	S	SN

[a]Accession number from *A. mellea* cDNA database; [b]BLAST annotation following Blast2GO analysis of proteins identified from *A. mellea* cDNA database; [c]M$_r$, theoretical molecular mass; [d]tp*I*, theoretical isoelectric point; [e]SM score, Spectrum Mill protein score; [f]GRAVY score, grand average of hydropathy (Negative score indicates hydrophilicity while Positive score indicates hydrophobicity); [g]TM, number of transmembrane regions; [h]SigP, classical secretion signal peptide; SecP, non-classical secretion signal; [i]Method: S, direct LC-MS/MS analysis, s. [j]Source, SN culture supernatant extracts.

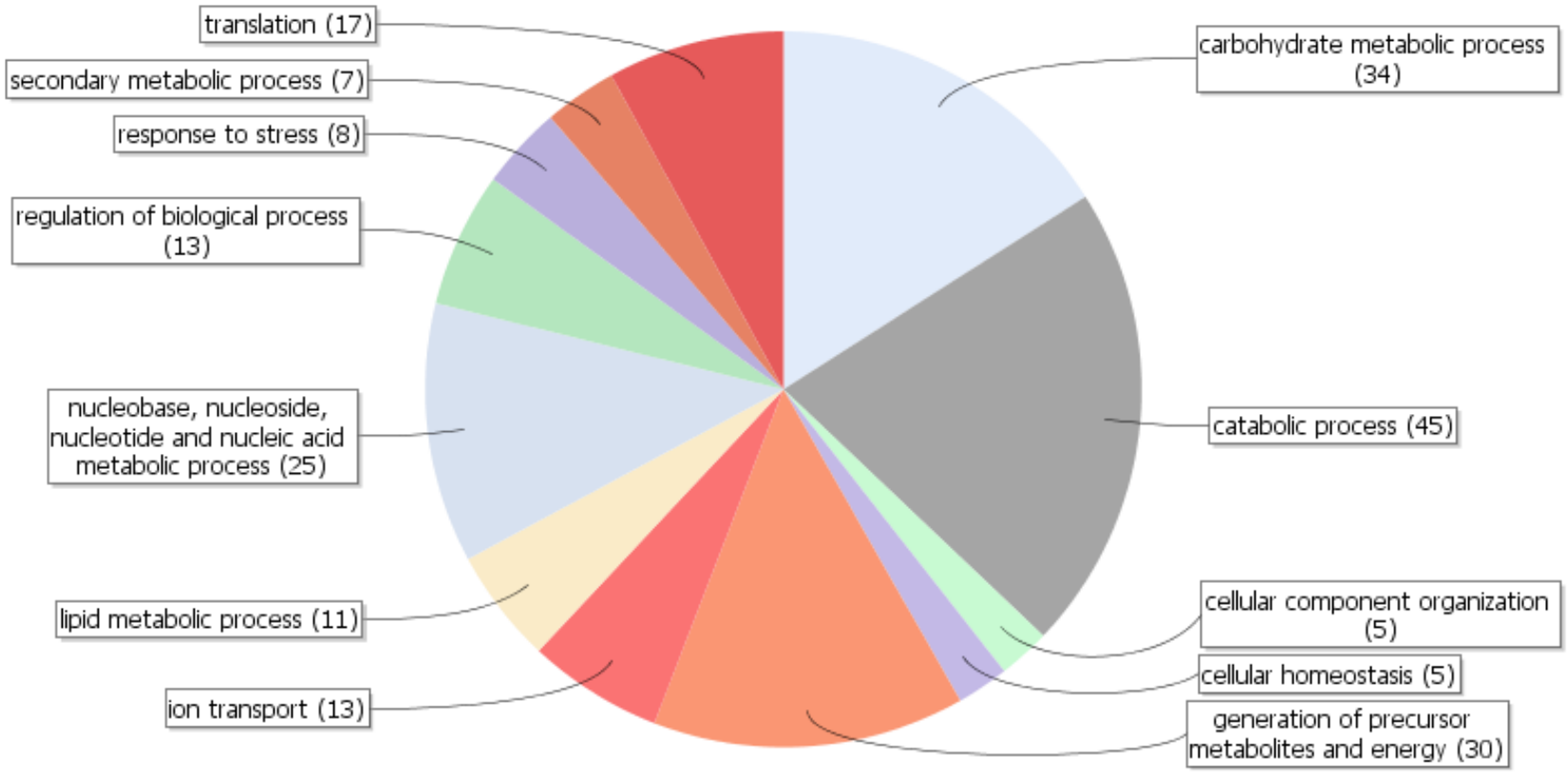

Figure 7.10. Biological process. GO multilevel graph of *A. mellea* secreted proteins from co-cultures of *A. mellea* with *C. albicans* analysed by direct LC-MS/MS; identification of biological process property domains defined by http://www.geneontology.org. The graph visualisation of GO annotations is from the lowest nodes of GO hierarchy, in the category of biological process. Numbers in brackets indicate the number of proteins in each category shown.

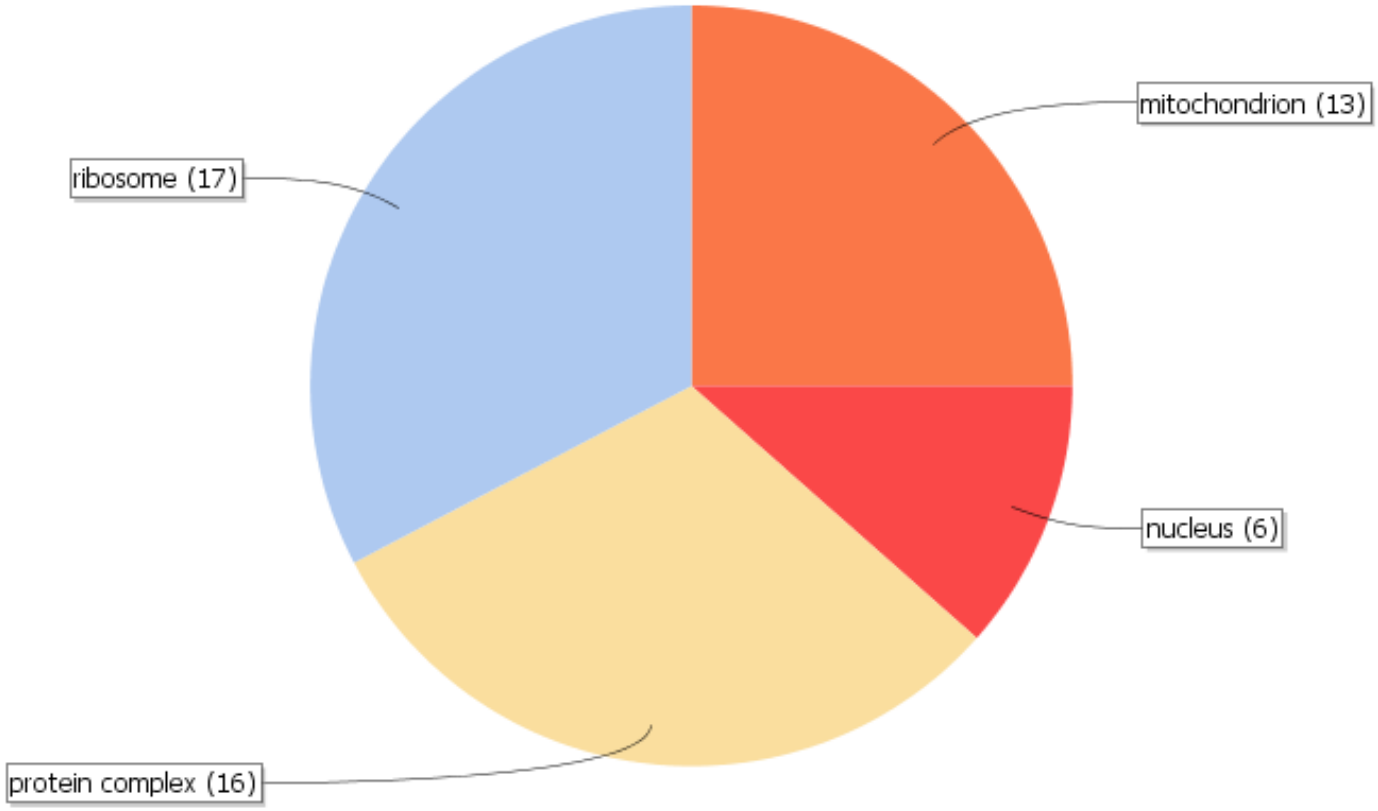

Figure 7.11. Cellular component. GO multilevel graph of *A. mellea* secreted proteins from co-cultures of *A. mellea* with *C. albicans* analysed by direct LC-MS/MS; identification of cellular component property domains defined by http://www.geneontology.org. The graph visualisation of GO annotations is from the lowest nodes of GO hierarchy, in the category of biological process. Numbers in brackets indicate the number of proteins in each category shown.

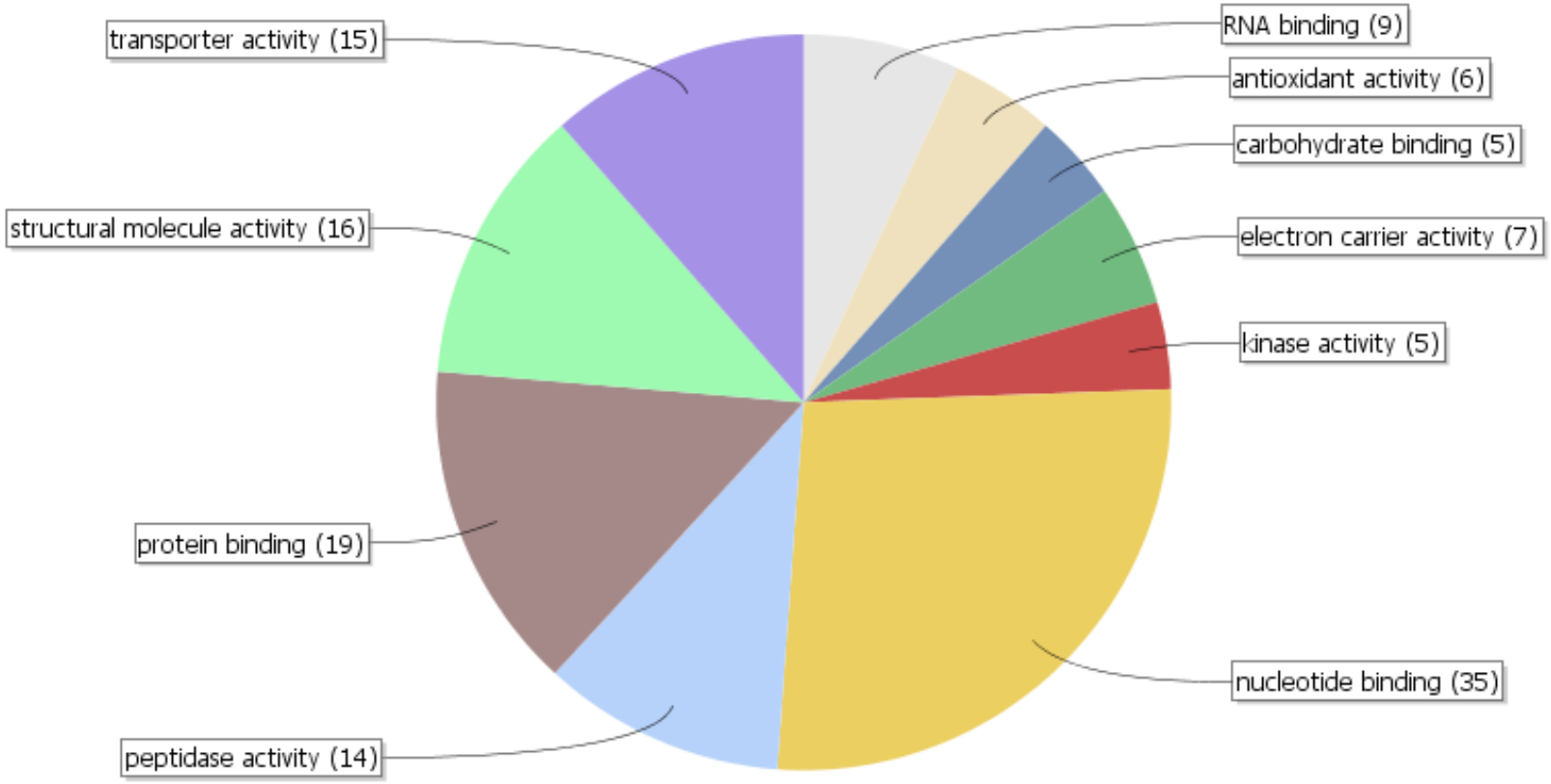

Figure 7.12. Molecular Function. GO multilevel graph of *A. mellea* secreted proteins from co-cultures of *A. mellea* with *C. albicans* analysed by direct LC-MS/MS; identification of molecular function property domains defined by http://www.geneontology.org. The graph visualisation of GO annotations is from the lowest nodes of GO hierarchy, in the category of biological process. Numbers in brackets indicate the number of proteins in each category shown.

7.2.5.1 Proteins uniquely identified from co-culture supernatants of *A. mellea* and *C. albicans* following direct LC-MS/MS analysis

Twenty-one of the 30 proteins uniquely identified from co-cultures (70%) possess either classical (n = 6) or non-classical (n = 15) secretion signals. Six proteins (20%) uniquely identified from co-cultures of *A. mellea* with *C. albicans* were predicted to be hydrophobic and eight (27%) were predicted to have transmembrane domains. Each *A. mellea* protein uniquely identified in co-cultures of *A. mellea* and *C. albicans* is described below:

Am5344 which possesses a non-classical secretion signal, was identified by BLAST as a 60S ribosomal protein L10a, ubiquitous across all organisms; these proteins regulate and assemble 80S ribosomes from 40S and 60S subunits. **Am12506** which possesses a classical secretion signal, was identified by BLAST as an aryl-alcohol oxidase (AAO). AAO are extracellular flavoproteins that generate H_2O_2 by aldehyde redox-cycling (Figure 7.13).

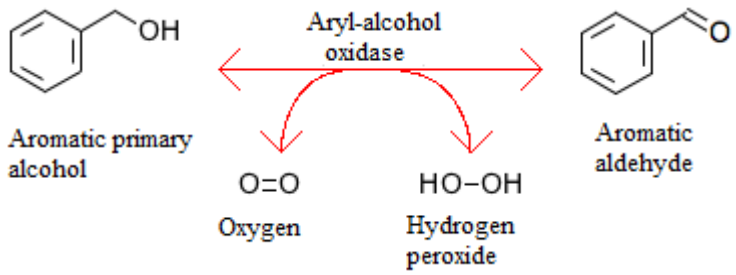

Figure 7.13. Reaction of aryl-alcohol oxidase which generates H_2O_2 from a primary alcohol and molecular oxygen (http://www.kegg.jp/).

Am17454 was identified by BLAST search as a coproporphyrinogen III oxidase, and is found in mitochondria in higher eukaryotes, but in the cytosol in yeast (Franken *et al.*, 2011). These enzymes, active in the presence of O_2, are involved in haem biosynthetic processses, where they catalyse the oxidation of coproporhyrinogen III, the product of which is protoporphyrinogen IX, with the concomitant release of CO_2 and H_2O (Figure 7.14).

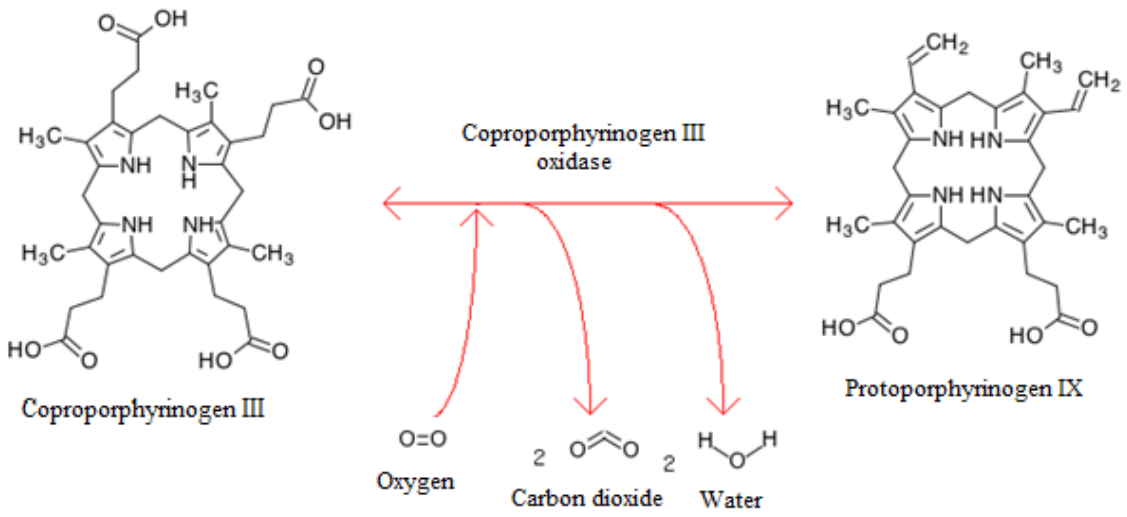

Figure 7.14. Reaction catalysed by coproporphyrinogen III oxidase. Coproporphyrinogen III and O_2 form protoporphyrinogen IX, releasing carbon dioxide and water in the haem biosynthetic pathway (http://www.kegg.jp/).

Am10593 was identified by BLAST search as a Cys-2 peroxiredoxin in which a non-classical secretion signal was predicted. These proteins are involved in oxidative stress response and signalling, through oxidation and reduction of cysteine residues of compounds in the cytosol of eukaryotes (Aran *et al.*, 2009) (Figure 7.15). Bioinformatic analysis identified an alkyl hydroperoxide reductase (AhpC) domain signature in Am10593. Cys-2 peroxiredoxins are decameric proteins containing five AhpC homodimers. This conformation is seen in reduced or overoxidised enzymes, but an oligomeric dissociation to the dimeric form exists in the oxidised enzyme, which is responsible for reducing a range of organic hydroperoxides (Wood *et al.*, 2003).

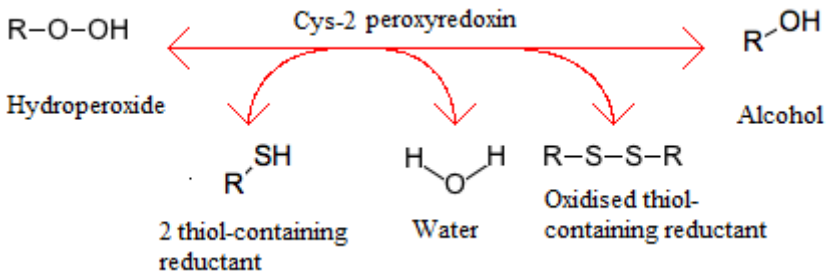

Figure 7.15. Reaction of Cys-2 peroxiredoxin oxidises hydroperoxide and two thiol-containing reductant moieties to water, an oxidised disulphide thiol-containing reductant and an alcohol (http://www.kegg.jp/).

Am9607 was identified by BLAST search as Cytochrome *c* oxidase subunit V. Cytochrome *c* oxidase is a complex of 13 proteins which regulates energy production in

eukaryotes, reduces molecular oxygen to water and plays a key role in metabolism (Cumsky *et al.*, 1987) of which subunit V is a highly conserved zinc binding protein (Tsukihara *et al.*, 2013). Am9607 was predicted to have two transmembrane domains and a non-classical secretion signal. **Am19980** was identified by BLAST search as mitochondrial F_1F_0-ATP synthase, subunit F, containing a predicted transmembrane domain and a non-classical secretion signal. Am19980 is a subunit of the highly conserved ATP synthase complex which drives the final step of ATP synthesis in the oxidative phosphorylation pathway. **Am16128** was identified by BLAST search as a glycerol-3-phosphate o-acyltransferase (GPAT). These enzymes catalyse esterification of 3-glycerol phosphate to lysophosphatic acid in the first step of glycerolipid synthesis (Figure 7.16) (Mishra and Kamisaka, 2001; Bratschi *et al.*, 2009). Am16128 is predicted to contain three transmembrane regions. Glycerol-3-phosphate o-acyltransferase enzymes, which are involved in glycerolipid synthesis, are located in mitochondria and the endoplasmic reticulum but their substrate specificity is different. Mitochondrial GPAT is specific for saturated fatty acyl-CoA and GPAT in endoplasmic reticulum membranes has broad specificity for acyl-CoA (Mishra and Kamisaka, 2001).

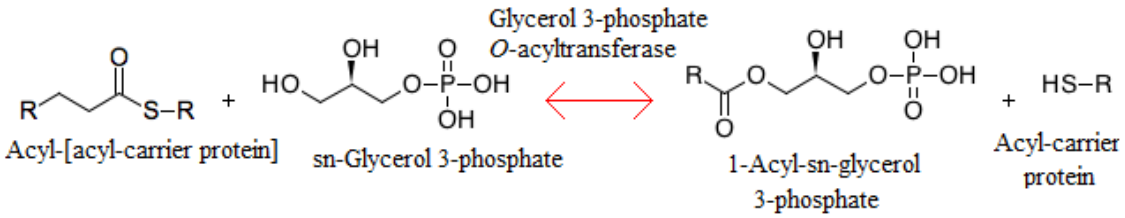

Figure 7.16. Reaction of glycerol-3-phosphate O-acyltransferase. Catalysis of 3-glycerol phosphate esterification to 1-acyl glycerol 3-phosphate in the first step of glycerolipid biosynthesis (http://www.kegg.jp/).

Am13890 was identified by BLAST search as glycosyl hydrolase 53 domain-containing protein, is a β-1,3-glucanase. Search of the CAZy database identified it as a GH128, a newly characterised GH family (Sakamoto *et al.*, 2011). Am13890 is homologous to hypothetical proteins from other basidiomycete species, as well as a GH128 protein characterised in *L. elodes* which showed high specificity for laminarin, a glucose polysaccharide, substrate (Sakamoto *et al.*, 2011). Am13890 is predicted to have a classical secretion signal. **Am13814** was identified by BLAST search as a hypothetical protein; bioinformatic analysis identified a conserved fungal domain of unknown function (DUF2611). **Am13829** was identified by BLAST search as a hypothetical protein. Further bioinformatic analysis identified it as an aromatic-ring hydroxylase-

like, FAD-binding monooxygenase, from the FAD/NAD(P)-binding superfamily. Am13829 protein also contained a thioredoxin-like fold and non-classical secretion signal.

Am18856 was identified by BLAST search as a hypothetical protein. Bioinformatic analysis identified an actin cortical patch SUR7/pH-response regulator PalI protein. Am18856 protein is predicted to be hydrophobic with four transmembrane domains, and a classical secretion signal, which is typical of SUR7 proteins. Normally, SUR7 family proteins encode three transmembrane domains (Yan *et al.*, 2012), however Am18856 is predicted to possess four. Actin cortical patch SUR7/pH-response regulator PalI proteins have been identified in many fungi. There are two types, a longer (~450 - 700 aa) and a shorter (~200 - 400 aa). *A. mellea* contains one of the former (Am15913, a rim9 protein), and five of the latter (Am686, Am3252 Am15113, Am17983 and Am18856) which are predicted or hypothetical proteins. **Am12218** was identified by BLAST search as hypothetical protein. Further bioinformatic analysis identified cytosolic zinc-dependent M28 exopeptidase domains and predicted Am12218 to possess a classical secretion signal. **Am12353** was identified by BLAST search as an iron-sulfur protein subunit. Further analysis identified an α-helical 2Fe-2S ferredoxin-type domain, typical of fumarate reductase. 2Fe-2S ferredoxins, comprise two iron atoms, each attached to the thiols of two cysteines and bridged by two sulphide ions. These proteins mediate electron transfer in many redox reactions (Figure 7.17). A non-classical secretion signal was identified in this protein.

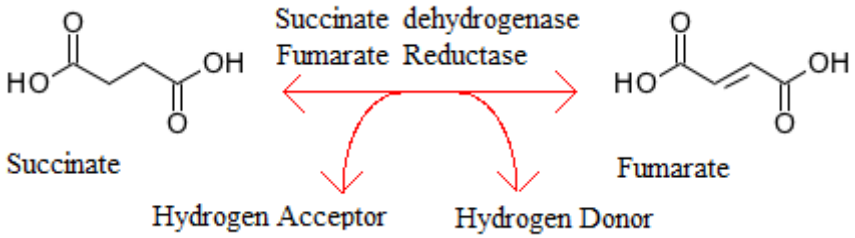

Figure 7.17. Fumarate reductase mediated transfer of electrons from succinate to fumarate (http://www.kegg.jp/).

Am19926 was identified by BLAST search as lipoic acid synthetase, elongator protein 3/MiaB/NifB. Further bioinformatic analysis identified the protein as containing a peroxisomal biogenesis factor 11 (PEX 11) domain, which is consistent with the transmembrane region which was also identified. Lipoic acid synthetase generates an essential lipoyl cofactor from a saturated fatty acid (Figure 7.18).

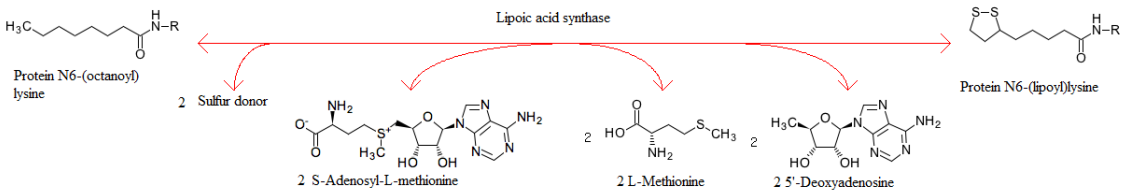

Figure 7.18. Reaction of lipoic acid synthethase, a SAM radical enzyme which catalyses the transfer of two sulphur atoms to a saturated fatty acid, whose product lipoic acid, is a essential cofactor involved oxidative metabolism (Cicchillo and Booker, 2005; Miller *et al.*, 2000) (http://www.kegg.jp/).

Am16692 was identified by BLAST search as an *A. mellea* unknown function protein, and no further annotation was possible by other bioinformatic analysis. **Am13379,** identified by BLAST search as NADH dehydrogenase, and a FAD-dependent pyridine nucleotide-disulphide oxidoreductase domain was also identified in Am13379. FAD flavoproteins from this family include glutathione reductase, trypanothione reductase, lipoamide dehydrogenase, mercuric reductase and thioredoxin reductase. Two transmembrane domains were predicted in this protein. **Am14001** was identified by BLAST search as prohibitin phb1, which possesses a classical secretion signal and is predicted to be a hydrophobic protein. These proteins have roles in signalling, development, senescence and are negative regulators of proliferation (McClung *et al.*, 1995; Nadimpalli *et al.*, 2000; Zhou and Qin, 2013). **Am20343** was identified by BLAST search as a protein with unknown function; a NAD(P)-binding Rossmann-fold domain was identified from bioinformatic analysis. NAD(P) proteins are involved in many redox reactions. Am20343 is also predicted to have a non-classical secretion signal. **Am3423** was identified by BLAST search as a protein of unknown function, however further bioinformatic analysis of domain signatures revealed a cell wall (1→6)-β-glucan synthesis protein. (1→6)-β-glucan synthesis proteins include haustorially expressed secreted proteins, which are avirulence proteins of *Melampsora lini*, a rust which infects flax; it is secreted into the plant from haustoria and causes necrosis in host tissue (Catanzariti and Dodds, 2006). A transmembrane domain was identified by B2G and classical secretion signal by SigP. Two proteins **Am6084** and **Am17996** were identified by BLAST as proteins of unknown function. A low complexity region was identified by IPS in Am6084, and BLAST predicted Am17996 to be secreted, which was confirmed by B2G analysis which identified a classical secretion signal. B2G identified a transmembrane region, although neither SignalP nor Phobius searches identified these domains. **Am20304** was identified by BLAST search

as a proteolysis and peptidolysis-related protein, a Band 7, prohibitin domain signature was identified by bioinformatic analysis, as in Am14001 above. **Am18628** was identified by BLAST as a subunit VIb of cytochrome *c* oxidase, in the oxidative phosphorylation pathway. This region is the haem-binding subunit, VIb, which is encoded in the nucleus (Fontanesi *et al.*, 2008), and this protein exhibited a non-classical secretion signal. **Am15086** was identified by BLAST as a succinate-semialdehyde dehydrogenase and further bioinformatic analysis detected aldehyde dehydrogenase domain signatures. This is a large superfamily which catalyses $NAD(P)^+$dependent oxidation of aldehydes, generated by peroxidation of lipids, amino acid catabolism and xenobiotics. Aldehyde dehydrogenase enzymes are implicated in mitigation of oxidative stress by hydrolysis of lipid peroxidation-derived aldehyde stressors (Marchitti *et al.*, 2008). Further analysis identified Am15086 as hydrophobic with four transmembrane regions and a non-classical secretion signal. **Am16124** was identified by BLAST as a sulfide-quinone oxidoreductase. Sulphide quinone-reductases are thioredoxin dependent enzymes (Theissen and Martin, 2008), described mainly in bacteria but also identified in eukaryotes, including fungi. These enzymes are FAD/NAD(P) dependent. Inner nuclear membrane protein (MAN1), helix extended loop helix domain (HeH/LEM) domain signatures) and two transmembrane domains were predicted in Am16124. **Am7929** was identified by BLAST as a thioredoxin, with antioxidant properties predicted by further analysis; GRAVY predicted Am7929 to be a hydrophobic protein. **Am14705** was identified by BLAST as a twin-arginine translocation (TAT) pathway signal protein (Palmer and Berks, 2012) from the α/β hydrolase superfamily, it possesses a non-classical secretion signal. TAT proteins transport fully folded proteins through cell membranes by mechanisms which are not fully understood (Palmer and Berks, 2012). TAT proteins are associated with virulence in bacterial pathogens (De Buck *et al.*, 2008). **Am2793** was identified by BLAST as ubiquitin domain-containing protein. Bioinformatic analysis identified ubiquitin-associated/translation elongation factor EF1β and heat shock chaperonin-binding domains in Am2793. EF1β is a nucleotide exchange factor which reactivates an elongation factor complex (EF1α-GDP) to the active EF1α-GTP during protein synthesis (Andersen *et al.*, 2003). **Am18503** was identified by BLAST as a uracil phosphoribosyltransferase. Phosphoribosyltransferase-like domain enzymes are involved in the synthesis of uracil from uridine monophosphate and a diphosphate in the pyrmidine pathway (http://www.kegg.jp/) (Figure 7.19). Am18503 is predicted to be hydrophobic and carry a non-classical secretion signal.

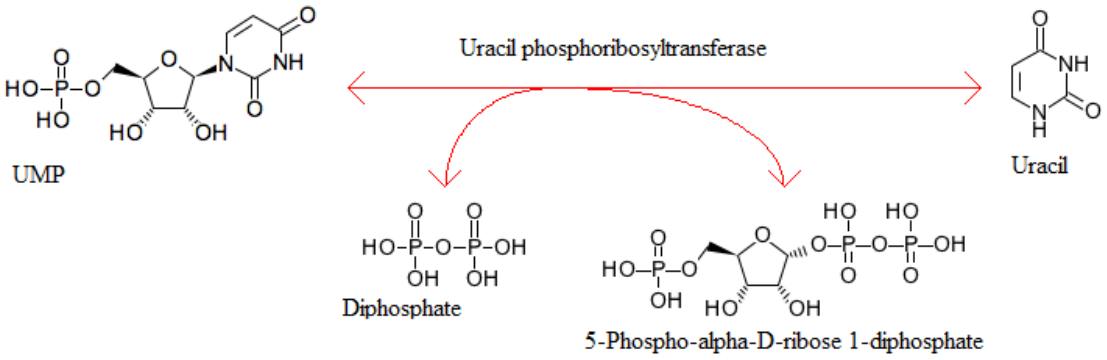

Figure 7.19. Reaction of uracil phosphoribosyltransferase which transfers a diphosphate to uridine monophosphate from which uracil and 5-phospho-α-D-ribose 1-diphosphate are produced (http://www.kegg.jp/).

Am14973 identified by BLAST as a urea hydro-lyase cyanamide hydratase, it has a non-classical secretion signal. This protein has previously been isolated from a *Myrothecium verrucaria* a soil fungus and converts toxic cyanamide into urea (Figure 7.20) (Maier-Greiner *et al.*, 1991).

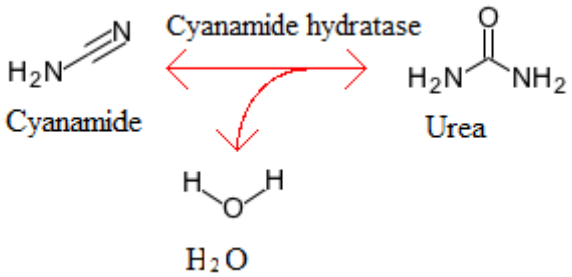

Figure 7.20. Cyanamide hydratase converts cyanamide a phytotoxin, into urea (Maier-Greiner *et al.*, 1991)(http://www.kegg.jp/).

7.3 Discussion

A. mellea was co-cultured with a five pathogenic microorganisms to study the reciprocal effects on the organisms in co-culture. The organisms selected were *C. albicans, P. aeruginosa, S. aureus,* MRSA and *E. coli*. Only *C. albicans* elicted any visible response by *A. mellea*, which showed crustose mycelia at the inoculation points of *C. albicans*. Two filamentous fungi, *Aspergillus fumigatus* and an environmental isolate of unknown origin, were also co-cultured with *A. mellea* and neither showed reproducible inhibition of *A. mellea* nor was their own growth inhibited. Co-cultures of *A. mellea* with dead *C. albicans* cells showed no apparent interaction between the organisms either pathogenic nor as a nutrient source. Lyophilised culture supernatants of either *A. mellea* in monoculture or in co-culture with *C. albicans* applied to *C. albicans* monocultures did not inhibit *C. albicans* growth. Further investigation of *A. mellea* and *C. albicans* co-cultures showed significant inhibition of *C. albicans* growth by *A. mellea* but no inhibition of *A. mellea*. *C. albicans* removed from co-cultures showed a preponderance of dead cells revealed by fluorescent staining, and re-culture of *C. albicans* showed only 2% of cells were live, a kill rate of 98% ($p = 0.0004$). LC-MS/MS analysis of proteins from co-cultures of *A. mellea* with *C. albicans* identified eleven *C. albicans* proteins and two hundred and five *A. mellea* proteins. Thirty of the 205 *A. mellea* proteins were uniquely identified from co-cultures of *A. mellea* with *C. albicans*.

Many bacteria exhibit antifungal activity against such human fungal pathogens such as *Cryptococcus*, *Aspergilli*, *Candida* spp. as well as many phytopathogens (Kerr, 1999). *Armillaria* spp. are known to produce secondary metabolites which have antifungal activity, including armillaric acid which has activity against *C. albicans* (Engels *et al.*, 2011; Obuchi *et al.*, 1990). In this study, *A. mellea* was co-cultured with a number of pathogenic species and no inhibition of pathogen growth was observed in any of the species with the exception of *C. albicans,* in which case the colonies became brown, ceased to grow, and were eventually overgrown to such an extent they were no longer visible.

Aspergillus spp. have shown antifungal activity against phytopathogens; a protein purified from *Aspergillus giganteus* termed antifungal protein (AFP) was highly potent against a number of phytopathogens, with highest activity against *Magnaporthe grisea* (Vila *et al.*, 2001), and *Aspergillus japonicas* was shown to be antagonistic to *A. mellea* inhibiting *A. mellea* growth (Pellegrini *et al.*, 2013). *A. mellea* altered

morphology was observed in co-culture with fungal isolates from soil, in biocontrol agent (BCA) studies (Pellegrini *et al.*, 2013) but no inhibition of either *A. mellea* or *A. fumigatus* was observed from dual cultures of these species in this study

Hyphal morphologies of *A. mellea* were not altered in the case of co-cultures with *P. aeruginosa, S. aureus*, MRSA or *E. coli*, but *A. mellea* morphology altered once hyphae came in contact with *C. albicans*, whereupon they became dense and crustose, although directional growth was not stimulated by the presence of *C. albicans*, an indication that *A. mellea* was not foraging for nutrients from *C. albicans*. Basidiomycete species, including *A. mellea*, have been shown to respond to the presence of a nutrient source by directional growth toward the nutrient source (Dowson *et al.*, 1988; Mihail and Bruhn, 2005). In fact, *A. mellea* and to a lesser extent *N. crassa*, were shown to respond to the presence of a nutrient source by organism-wide intracellular electrical signalling, similar to that of central nervous systems in animals (Olsson, 1995; Slayman *et al.*, 1976). Co-culture of *A. mellea* with dead *C. albicans* cells elicited no increased growth or exudate response by *A. mellea*.

Disk assays of lyophilised culture supernatants from *A. mellea* and co-culture supernatants of *A. mellea* with *C. albicans* were added to *C. albicans* agar plates, but growth of *C. albicans* was not inhibited by these, which was surprising, as many compounds secreted by *A. mellea* and other basidiomycetes exhibit antimicrobial activity. Supernatants of *Armillaria* spp. in co-culture with each other exhibited antifungal activity against other basidiomycetes such as *Heterobasidion annosum* and *Gloeophyllum ahietinum*, and against the bacteria, *E. coli* and *S. aureus* (Sonnenbichler *et al.*, 1997). Indeed secondary metabolites extracted from *A. tabescens* solid state fermentations on brown rice had fungistatic activity against *C. albicans* (Herath *et al.*, 2012). Mycelia from *A. mellea* inhibited bacterial growth of *E. coli*, *Salmonella typhimurium* and *Sarcina lutea* as well as *C. albicans* in a study of antimicrobial activity of ten edible fungal species, although *C. albicans* inhibition by *A. mellea* was among the lowest of the ten species (Kalyoncu *et al.*, 2010), a confirmation of *A. mellea* mycelial anti-*Candida* activity described earlier by Obuchi *et al.* (1990).

Plugs from inoculation points of *C. albicans* in co-culture with *A. mellea* were excised and dual stained with fluorescent dyes prior to confocal microscopy to identify viable and non-viable *C. albicans* cells (Jones and Senft, 1985). This method for assessment of viability has been used to assess the viability of *Echinpora* oocytes after treatment with cryoprotectants (Tsai *et al.*, 2010). FDA staining was used to investigate

microbial activity of soil organisms in an investigation of *Phytopthora* biocontrol (Richter *et al.*, 2011). Few viable *C. albicans* cells were observed from *A. mellea* co-cultures, whereas *C. albicans* controls were mainly viable. In addition, *C. albicans* removed from co-cultures, while appearing intact under light microscopy were less robust than *C. albicans* controls, as 150 times the number of cells from co-cultures were required to prepare samples for microscopy. A second approach to assess viablility of *C. albicans* removed from inoculation points of co-cultures of *A. mellea* with *C. albicans,* involved re-culture of excised cells on MEA and a 98% ($p = 0.0004$) kill rate of *C. albicans* cells in co-culture was determined, confirming the results obtained from confocal microscopy. Overall, this *A. mellea* infection model represents a new system for *A. mellea* virulence studies, and may complement virulence models which use plant material (Baumgartner and Rizzo, 2006; Baumgartner and Warnock, 2006a).

Proteins were extracted from agar supernatants of co-cultures of *A. mellea* with *C. albicans* and subjected to LC-MS/MS analysis. A composite database of *A. mellea* and *C. albicans* was interrogated to identify proteins from the supernatants. Eleven *C. albicans* proteins were identified from these supernatants. Interestingly some proteins identified from *C. albicans* in supernatants: glyceraldehyde-3-phosphate dehydrogenase, an aspartyl proteinase and a transcription factor, were proteins differentially regulated in *T. viride* in response to a challenge by *S. commune* (Ujor *et al.*, 2012). Other *C. albicans* proteins identified included an alcohol dehydrogenase, a peroxiredoxin, an enolase, a protein essential for pseudohyphal growth (EPD1) (Nakazawa and Horiuchi, 1998), a prohibitin and two hypothetical proteins. Two hundred and five *A. mellea* proteins were identified from co-culture supernatants of *A. mellea* with *C. albicans,* 90% of which were annotated with functions. Eighteen proteins which were previously "predicted" or "hypothetical", are now reclassified as proteins of unknown function and three proteins for which no homologs are evident, appear to be *A. mellea*-specific proteins of unknown function. Sixty-six percent of the identified proteins had secretion signals and eighty-one percent were hydrophilic.

GO annotation of identified proteins revealed a broad spectrum of protein functions. Proteins identified in the biological process category were largely related to carbohydrate metabolism ($n = 34$), catabolic process ($n = 45$) and energy generation ($n = 30$). Seventeen glycoside hydrolase proteins from 14 different families were identified. Previously, fungal co-cultures of *F. oxysporum* and *A. niger* have been used in stimulation of cellulase and xylanase activity (Kaushal *et al.*, 2012) as have pairing of

T. reesei and *A. niger* (Ahamed and Vermette, 2008) in lignocellulose degradation. Nucleobase, nucleoside and nucleic acid metabolism (n = 25) and translation (n = 17) also had high representation and eight proteins were classified as stress response proteins. *S. commune* stress response proteins in co-culture of *S. commune* with *T. viride* were differentially regulated and comprised 64% of the twelve differentially regulated proteins from co-culture of the two fungi (Ujor *et al.*, 2012). Sixteen *A. mellea* proteins characterised as protein complex members were annotated by GO. Proteins annotated by GO as binding proteins (n = 68) made up a large proportion of molecular function categories and nucleotide (n = 35), protein (n = 19), RNA (n = 9) and carbohydrate (n = 5) binding proteins were in this category. Transporter (n = 15) and electron carrier (n = 7) activity protens were identified, as were six proteins annotated by GO with antioxidant activity, these included a copper radical oxidase and three peroxidases. Interestingly, non-pathogenic and ectomycorrhizal basidiomycete species co-cultured with *Sinapis alba* L. (White mustard) elicited upregulation of oxidase and peroxidase secretion in both species pairs, in the case of *A. porphyrizon* with *Sinapis alba* L., oxidase activity was increased 2300 fold (Gramss and Mascher, 2011).

Thirty proteins were uniquely identified from culture co-culture supernatants of *A. mellea* with *C. albicans* and these will be grouped according to activity: 1. Stress response; 2. Virulence; 3. Redox; 4. Energy and 5. Other proteins.

1. Stress response: Am12506 AAO are extracellular flavoproteins that generate H_2O_2 by aldehyde redox-cycling as substrate for peroxidases in ligninolytic degradation of wood (Hernández-Ortega *et al.*, 2012). Their reactivity and ability to oxidise aromatic and aliphatic polyunsaturated alcohols in substrates makes them unique (Martínez *et al.*, 2005) and a constant source of reactive oxidative species for ligninolytic degradation (Ruiz-Dueñas *et al.*, 2006). **Am18856** is an actin cortical patch SUR7/pH-response regulator PalI protein, which has been identified in many fungi. Am18856 is a short (279 aa) protein, and Yan *et al.* (2012) propose that if a fungus possesses both long and short members of this gene family, the short version is critical in response to pH stress and xenobiotic stress (Denison *et al.*, 2001), an indication that Am18556 may be a stress response protein in *A. mellea* against *C. albicans*. **Am16128,** a glycerol-3-phosphate o-acyltransferase enzyme, which is involved in glycerolipid synthesis, is sensitive to oxidation (Mishra and Kamisaka, 2001) and can be inactivated by lipid peroxidation (Thomas and Poznansky, 1990), thus indicating that *A. mellea* while under stress, has not been subjected to lipid peroxidation. **Am15086,** an aldehyde

dehydrogenase enzyme, is implicated in mitigation of oxidative stress by hydrolysis of lipid peroxidation-derived aldehydes (Marchitti *et al.*, 2008). Further analysis identified Am15086 as hydrophobic with four transmembrane regions and a non-classical secretion signal. **Am19926,** a lipoic acid synthase is a SAM radical enzyme generating lipoic acid (LA) which is an essential cofactor in oxidative metabolism. LA and its reduced form, dihydroxylipoic acid, have antioxidant activity, scavenging a range of ROS and chelating metals (Packer *et al.*, 2001; Miller *et al.*, 2000). Secretion of the enzyme in *A. mellea* in co-culture with *C. albicans* may be a protective measure against ROS generated by *C. albicans* and thus protect *A. mellea* from damage. Alternatively, the enzyme may be employed to generate LA as a means to scavenge and chelate metals from *C. albicans*.

2. Virulence: Am13890, a β-1,3-glucanase, had a classical secretion signal. β-1, 3-glucanase from *Streptomyces torulosus* was shown to have antifungal activity, inhibiting hyphal growth of *Phytophthora capsici* and *Rhizoctonia solani* (Park *et al.*, 2012), and β-1,3-glucanase accumulation in the leaves of *Solanum tubersum* infected with *Phytophthora infestans* was proposed to play a pathogenesis-related role in plant defence against the fungus (Kombrink *et al.*, 1988). The substrate of this enzyme is laminarin which is found in algae, but β-1,3-glucans are virulence factors also found in fungal cell walls and elicit immune response in insects. In an infection study of *Drosophila* with *C. albicans*, an immune response protein was found to recognise fungal β-1,3-glucans, following which a β-1,3-glucanase with a signal peptide binds to this substrate (Gottar *et al.*, 2006). In *A. mellea/C. albicans* co-culture, this β-1,3-glucanase may be a stress response, which degrades β-1,3-glucans in *C. albicans* cell walls. **Am14001,** a prohibitin phb1 and **Am20304,** a proteolysis and peptidolysis-related protein with a prohibitin domain, are *A. mellea* proteins with putative roles in signalling, development, senescence and negative regulators of cell proliferation (McClung *et al.*, 1995; Nadimpalli *et al.*, 2000; Zhou and Qin, 2013). Interestingly, a prohibitin from *C. albicans* (orf19.357) was also identified in co-culture supernatants from *A. mellea* with *C. albicans* suggesting a competitive inhibition by both species. **Am3423** is a (1→6)-β-glucan synthesis protein. These proteins are haustorially-expressed secreted proteins, involved in cell wall synthesis. (1→6)-β-glucans synthesis proteins are avirulence factors which cause necrosis in host tissue (Catanzariti and Dodds, 2006) and may be secreted by *A. mellea* as suppression of *C. albicans* defences. **Am14705** a twin-arginine translocation (TAT) pathway signal protein, is associated with virulence in bacteria. The TAT pathway has been identified in eukaryotes; plant

chloroplasts (Fröbel *et al.*, 2012), algae and sponges (Gazave *et al.*, 2010) but is reputed to be absent from fungi (Palmer and Berks, 2012), although an alternate, an AAA ATPase with translocation functionality, has been identified in *S. cerevisiae* (Wagener *et al.*, 2011). Therefore, identification of this protein in *A. mellea* is the first instance of identification of a TAT pathway signal protein in fungi. **Am18503,** a uracil phosphoribosyltransferase, is an enzyme involved in purine biosynthesis, which is implicated in pathogenicity (Islam *et al.*, 2012). In *A. fumigatus* a phosphoribosyltransferase was upregulated when the organism was subjected to H_2O_2-induced oxidative stress (Lessing *et al.*, 2007).

3. Redox: Several proteins with peroxidase or oxidioreductase activity were identified. **Am7929,** a thioredoxin peroxidase protein whose activity is antioxidant interaction with radical species (Belozerskaya and Gessler, 2007). **Am16124,** a sulfide-quinone oxidoreductase, enzymes that require both thioredoxin and FAD/NAD(P) as co-factors (Theissen and Martin, 2008), and reduce sulphides by a mechanism that has not been fully characterised, to elemental sulphur (Cherney *et al.*, 2012), in sulphide detoxification. **Am13829,** is a hypothetical FAD-binding monooxygenase containing a thioredoxin-like fold. **Am13379** is an oxidoreductase, enzymes involved in many redox reactions, but no further specificity of the enzyme could be determined. **Am12353,** 4Fe-4S ferredoxin, with a 2Fe-2S iron binding domain classified as a succinate dehydrogenase/fumarate reductase a ubiquitous iron binding protein. **Am10593,** is a Cys-2 peroxiredoxin, containing an alkyl hydroperoxide reductase subunit. Alkyl hydroperoxide reductase was shown to be the primary scavenger of extracellular H_2O_2 in *E. coli* (Costa Seaver and Imlay, 2001). This peroxidase activity recycles sulphenic acid to a thiol, acting as a protective antioxidant in all cells (Wood *et al.*, 2003). **Am17454,** a coproporphyrinogen III oxidase, may be involved in haem biosynthesis and usually requires oxygen as substrate, although oxygen was found not to be required for activity under stress conditions in *S. cerevisiae* (Hoffman *et al.*, 2003). Transcription of this enzyme is regulated by a heme-dependent complex in *S. cerevisiae* (Klinkenberg and Mennella, 2005) and its activity may be subject to post-translational modification (Franken *et al.*, 2011). Study of heme biosynthesis and regulation in filamentous fungi has focussed mainly on *Aspergilli* and *N. crassa* (Franken *et al.*, 2011) and there is little known on its synthesis and regulation in basidiomycetes, despite the key role played by heme in peroxidase activities. **Am20343** a protein with unknown function with a NAD(P)-binding Rossmann-fold; the latter involved in many redox reactions.

4. Energy: Am9607 cytochrome c oxidase subunit V, **Am18628** cytochrome c oxidase, subunit VIb and **Am19980** F_1F_0-ATP synthase were identified within the group of supernatant proteins uniquely identified from co-cultures of *A. mellea* with *C. albicans*. These enzymes are usually mitochondrial and involved in generation of energy. Am9607 and Am18628 have transmembrane domains and all three have non-classical secretion signals. It is likely that increased energy is required by *A. mellea* in defence/virulence against *C. albicans*. In a yeast stress study against ROS it was suggested energy was required to provide defence against lipid peroxidation (Thorpe *et al.*, 2004). ATPases are found in many phyla and although this ATPase was predicted to be mitochondrial there are also extracellular ATPases, cell surface proteins, which hydrolyse extracellular ATP (Caldwell *et al.*, 2001).

5. Other proteins: Am5344 is a highly conserved protein involved in ribosomal assembly. **Am14973,** is a cyanamide hydratase and these enzymes degrade cyanamide to urea. Cyanamide is a known toxin and antifungal compound (Zhang *et al.*, 2005), it is a fertiliser used in agriculture and is chemically synthesised. In nature, it occurs in plant *Vicia* spp. but is not known to be synthesised by fungi (Kamo *et al.*, 2008), therefore it is unclear why *A. mellea* should express this enzyme or what its role might be. **Am2793** a ubiquitin-associated/translation elongation factor EF1B. **Am12218,** a cytosolic zinc-dependent M28 exopeptidase.

There were four proteins from co-culture of *A. mellea* with *C. albicans* which could not be further annotated: **Am13814,** a fungal protein of unknown function (DUF2611); **Am6084,** an unknown function protein; **Am17996,** a conserved secreted fungal protein of unknown function and **Am16692,** and an *A. mellea* specific protein of unknown function.

Two recent co-culture studies may provide further insight into host-pathogen interactions and provide targets for further study. Firstly, phytoplankton inhibition in co-culture with a white-rot fungus *Trichaptum abietinum,* a basidiomycete, which does not secrete antibiotics was investigated by Jia *et al.* (2010). In co-cultures with *T. abietinum,* chlorophyll-a concentration of four phytoplankton species was reduced to zero over 48 h, killing the organisms by unknown means, as no cell debris or turbidity was observed in the media. Interestingly *C. albicans* cells which have been killed by *A. mellea* remain largely intact and their morphology under light microscopy was unchanged which coincides with the results obtained by Jia *et al.* (2010). Secondly, oxylipids are derived from oxygenated lipids and are involved in signalling both

intracellularly and between host and pathogen, as well as facilitating pathogen attack (Christensen and Kolomiets, 2011). Complex host pathogen interactions are also facilitated by oxylipids.

C. albicans modulates cytokine production and cell proliferation in host species by oxylipin production although their synthetic pathway is not known. Fungal oxylipins have homology to eicosanoids in humans (Noverr, 2003). These oxylipins are effective at very low concentrations, making detection difficult. They are involved in host immune response, and both host- and pathogen-derived oxylipins are proposed to facilitate host-pathogen interaction and augment virulence mechanisms (Noverr, 2003). This is confirmed in a review by Brodhagen and Keller (2006) who conclude that plant oxylipins upregulate secondary metabolite synthesis in *Aspergillu*s spp. (Burow and Nesbitt, 1997). In *C. albicans*, oxylipins alter morphology and are intracellularly located; oxylipins are found at high levels during the transition from sexual to asexual phase during ascosporogenesis in *Dipodascaceae*, implicating them in life cycle control (Noverr, 2003). A mechanism proposed by Christensen and Kolomiets (2011), whereby fungal lipases are secreted into plant cells together with lipoxygenases to generate plant oxylipins, which are in turn secreted and activate fungal G-protein coupled receptors (GPCR). This then regulates growth, mycotoxin production and sporulation (Figure 7.21). In the co-culture of *A. mellea* with *C. albicans*, a similar mechanism may induce upregulation of mycotoxin secretion in *A. mellea* by lipase secretion and oxylipin signalling. This is an avenue for further investigation in the *A. mellea*/*C. albicans* pathosystem.

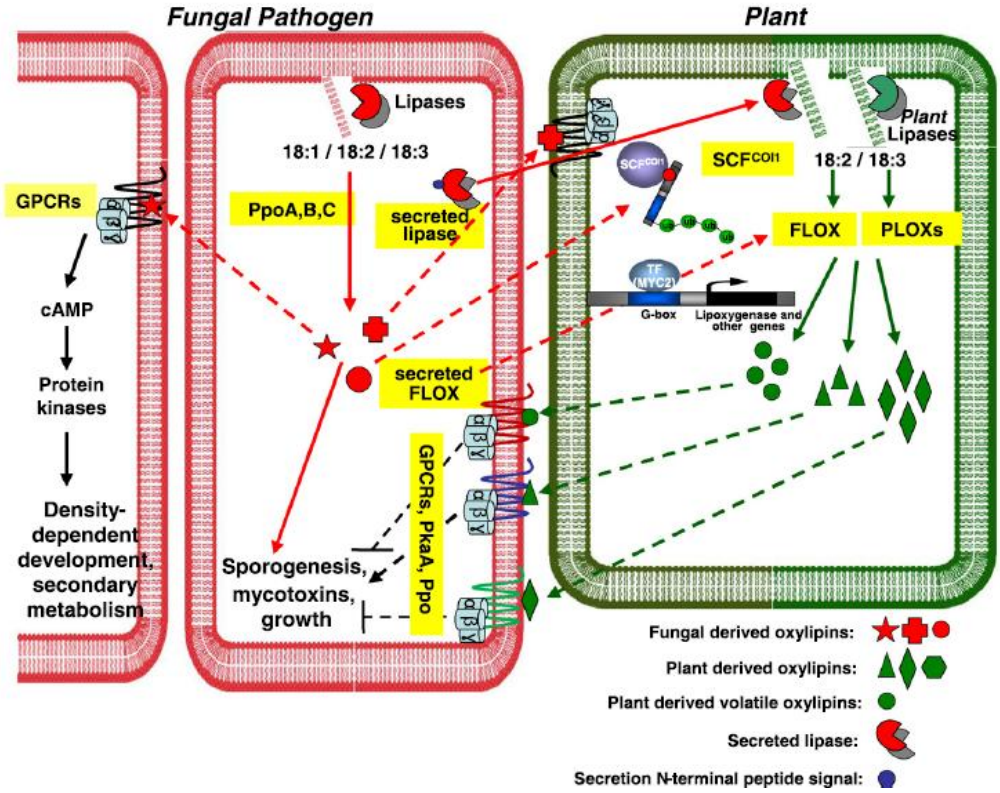

Figure 7.21. A schematic of a hypothetical mechanism for oxylipin mediated communication between fungal and plant cells, whereby fungal oxylipins couple to plant GPCRs. Fungal lipases are secreted into plant cells and with plant endogenous lipases, generate plant oxylipins which are secreted, and couple to fungal GPCRs moderating sporogenesis and growth, and upregulating mycotoxin synthesis. Biosynthetic pathogen and host oxylipin enzymes recognised by both species are highlighted in yellow. Abbreviations: LOX, lipoxygenase (FLOX, fungal LOX; PLOX, plant LOX); GPCR, G-protein coupled receptor; PpoA/B/C, oxylipin oxygenases; Pka, protein kinase A; SCFCOI1, SCF-type E3 ubiquitin ligase. Fungal oxylipins are shown in red and plant oxylipins are green. Hypothetical interactions are indicated by broken lines while solid lines are proven interactions (Christensen and Kolomiets, 2011).

Chapter 8 Discussion.

8.1 Overall summary

When this study commenced, very little genomic or proteomic data relevant to *A. mellea* was either known or in the public domain. Thus, the data presented in this thesis represents the first large-scale genomic and proteomic study of the phytopathogen *A. mellea*. Specifically, genome annotation and large-scale bioinformatic-led functional analysis has revealed that *A. mellea* protein families include CAZys and cytochrome P450 enzymes, which have been described in detail (Chapter 3). Genomic comparisons shown in this work, between *A. mellea* and other species have enabled detection of proteins involved in biopolymer degradation, metabolism, stress and virulence. This will inform future studies of organismal pathogenicity, and facilitate assessment of differences between pathogenic and non-pathogenic species of basidiomycetes, in general, and also between individual *Armillaria* species. Identification of sequence motifs within open reading frames encoding hypothetical and predicted proteins has been used to assign putative functions to the many hitherto unknown function proteins which exist within *A. mellea*. In general, large-scale genomic sequencing is in the ascendancy and has greatly increased our knowledge of basidiomycete species, with the initiation of several new basidiomycete genome sequencing projects (Eastwood *et al.*, 2011; Fernández-Fueyo *et al.*, 2012; Kämper *et al.*, 2006; Ohm *et al.*, 2010; Olson *et al.*, 2012; Martin *et al.*, 2008; Martinez *et al.*, 2009). Resultant genomic data has been complemented by extensive protein studies of *A. mellea*, under conditions of nutrient restriction, stress and pathogenic interactions which have facilitated identification of proteins from both mycelia and the secretome on a large-scale (Chapters 4 - 7). Indeed, 980 gene products were identified, thereby confirming their existence at proteomic level, as well as confirming the quality of the *A. mellea* cDNA database. Methodologies have also been developed throughout this study for identification of mycelial and secretome proteins which has addressed the deficit in proteomic techniques for basidiomycete study, and in particular the study of *Armillaria* spp (Chapter 4 - 7). Both the differential proteomic (Chapter 6) and infection studies (Chapter 7) are of particular importance, as they revealed fourteen proteins differentially expressed by *A. mellea* under oxidative stress, and 205 proteins in the secretome of *A. mellea* in co-culture, of which 30 were unique to this condition, and provide new insights into the virulence and pathogenicity of *A. mellea*.

8.1.1 Extracting biological information from large datasets

Combined with high-throughput sequence analysis, the advent of software tools for genome mining, the occurrence of many genomic and proteomic studies, and the consequent deposition of proteomic data into publicly accessible databases, have exponentially increased proteomic knowledge in recent years (Conesa and Gotz, 2009; Götz *et al.*, 2008; Cantarel *et al.*, 2009; Hall, 1999; Conesa *et al.*, 2005; Zdobnov and Apweiler, 2001). The ability to functionally annotate hypothetical proteins has also greatly increased. During the early part of this project, a BLAST survey of the *A. mellea* genome classified more than 67% of *A. mellea* genes identified at proteomic level as hypothetical or predicted, whereas the current percentage of genes identified at the proteomic level, classified as hypothetical or predicted, has now fallen to approximately 25%. However, studies of basidiomycetes, and *Armillaria* spp. in particular, have lagged behind studies pertaining to other phyla and genera. Notably, analysis via Web of Knowledge^{SM} shows the citations relating to *Aspergillus* spp., basidiomycetes and *Armillaria* spp. at 10-year intervals (Figure 8.1). Citation numbers of *Armillaria* spp. are approximately 4% of those of the *Aspergilli* and basidiomycetes; while the numbers of citations have actually fallen for *Armillaria* spp. and basidiomycetes since high-throughput methods have become available. PubMedCentral (PMC) only lists 188 articles relating to *Armillaria* spp. and so the present study goes some way towards addressing this deficit by adding to the body of knowledge concerning basidiomycetes in general, and *Armillaria* spp. in particular.

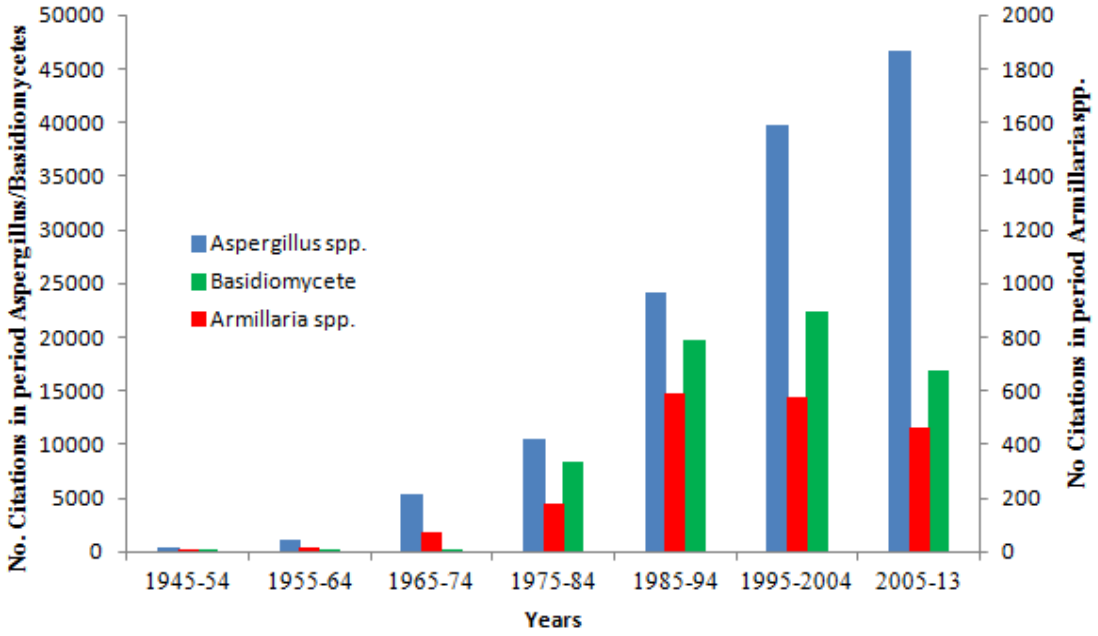

Figure 8.1. Web of Knowledge[SM] citation index search for *Aspergillus* spp., Basidiomycete and *Armillaria* spp., for which data is available, showing 10 year intervals*. Note the *Armillaria* spp. scale on the secondary axis. * 9 year interval (2005-13).

8.1.2 The power of fungal proteomics

The shotgun method of protein identification has been shown to be an efficient means of protein identification, with 435 *A. mellea* proteins uniquely identified by this method. Very few shotgun proteomic studies have been published to date; *P. placenta* whereby 231 proteins were identified (Ryu *et al.*, 2011) and *P. chrysosporium* in which 300-400 proteins were found (per sample) (Shary *et al.*, 2008). The further development and optimisation of shotgun fungal proteomic approaches will provide a valuable resource for future study of the pathogen, and subcellular fractionation, combined with this approach will enable new large-scale studies of *A. mellea*. Nevertheless, it is clear that multiple approaches to protein identification are important since 102 *A. mellea* mycelial proteins were uniquely identified by 2-DE and a further 78 proteins were common to both gel -based and shotgun identification of mycelial proteins. MALDI-ToF proved to be the least effective method of protein identification, although three *A. mellea* proteins were uniquely identified by this method. A majority of *A. mellea* secreted proteins (n = 205) were uniquely identified following SDS-PAGE fractionation, as shotgun proteomics could not be carried out on the fungal secretome, due to severe polysaccharide contamination which was recalcitrant to removal and interfered with protein recovery. However, a shotgun approach proved possible for

analysis of the *A. mellea* secretome in cultures on solid media, and in the case of the infection studies, 205 *A. mellea* secreted proteins were identified. It is important to note however, that multiple approaches to *A. mellea* protein identification are important as only eleven proteins were identified by all of the methods described in this work.

8.1.3 *A. mellea* contains enzymes for biotechnological exploitation

Many proteins identified in this study have potential biotechnological applications, particularly the degradative enzymes, such as glycoside hydrolases, pectin lyases and laccases. Bio-fuel and bioremediation are areas that are currently of particular interest, as laccases from *A. mellea* have already been identified and purified (Rehman, 1992; Billal and Thurston, 1996). Molecular technologies may be used for overexpression of *A. mellea* genes; as the activities of enzymes secreted by basidiomycetes is higher, and the quantities are greater than those secreted by other fungi (Alves and Record, 2004). *A. mellea* has also been shown to metabolise polyaromatic hydrocarbons (PAH), persistant pollutants from a variety of industrial processes (Hadibarata and Kristanti, 2012b, 2012a; Hadibarata *et al.*, 2012, 2013). Gene manipulation could be used to over-produce enzymes involved in PAH degradation. Further genome mining will provide a more targeted approach and inform studies of NRPS and PKS genes for investigation of potentially valuable secondary metabolites produced by *A. mellea*, which have bio-medical applications (Schneider *et al.*, 2008; Misiek *et al.*, 2009; Misiek and Hoffmeister, 2010; Misiek *et al.*, 2011; Lackner *et al.*, 2012; Martins and Carvalho, 2007; Wang *et al.*, 2013).

8.1.4 *A. mellea* responds to oxidative stress by proteome alterations

This work demonstrates the first study of *A. mellea* differential regulation of proteins in *A. mellea* under oxidative stress and it is revealed that proteome remodelling occurs over a short interval under the separate influence of two different stressors. Only two differentially regulated proteins were common to both conditions, one methionine synthase, was upregulated under both stress conditions and the second a VCP was upregulated under one stressor (H_2O_2) and downregulated under the second (Menadione/$FeCl_3$). *A. mellea* proteins differentially regulated under stress largely related to increased capacity to scavenge ROS which cause widespread cellular damage. DNA strand breakages and oxidation, protein inactivation and lipid peroxidation are but a few of the negative effects of ROS. We have found that upregulation of methionine synthase with concomitant upregulation of spermine/spermidine synthase, both of

which generate products with ROS scavenging properties, under the regulation of LuxS and AAT, maintain cellular homeostasis, while also protecting the cell from damage.

8.1.5 How does *A. mellea* perceive *C. albicans*?

Fungal-fungal interaction studies have become the focus of intense investigation particularly between pathogenic species (Rodriguez Estrada *et al.*, 2012; Foulongne-Oriol *et al.*, 2011; Moree *et al.*, 2012), and the virulence model of phytopathogen interaction with a human pathogen, detailed in this study, represents a new approach to the study of fungal-fungal interactions. Metabolites from *Armillaria* spp. were shown previously to have a fungistatic effect on *C. albicans* (Herath *et al.*, 2012). Although no fungicidal or fungistatic activity was determined against *C. albicans* from metabolites in this study, HPLC analysis of metabolites showed a large number of secreted compounds whose composition was not determined, including several autofluorescent compounds (data not shown). Production of *A. mellea* enzymes, with potential against *C. albicans* was shown in this study to be conceivably responsible for fungicidal activity, and thus, *A. mellea* may be sensing *C. albicans* presence, as it does a plant host, rather than perceiving it as a fungus. Thus, proteins (n = 30) uniquely expressed by *A. mellea* in co-culture with *C. albicans* are potential targets for future research. Although the precise mechanism remains to be established, sensing may involve signalling by effectors or small molecules (Christensen and Kolomiets, 2011; Jia *et al.*, 2010). SAM radical enzymes, which are involved in antioxidant activity were upregulated in co-cultures of *A. mellea*/*C. albicans.* SAM radical enzymes are involved in polyamine regulation, and oxidative stress elements of the virulence model mirrors antioxidant enzyme activity, in *A. mellea* under oxidative stress. Upregulation of both cys-2 peroxiredoxin and thioredoxin, a redox system for dismutation of H_2O_2, may be an *A. mellea* response to *C. albicans* defences, or alternatively a response to products of *C. albicans* cell wall degradation induced by *A. mellea*.

8.2 For the future

Proteins that were previously hypothetical or predicted, together with *A. mellea* unknown function proteins are possibly the most interesting proteins in the *A. mellea* proteome. Of particular interest are *A. mellea*-specific proteins which (i) may have novel activities and thus be suitable for biotechnological applications or (ii) proteins that may determine *A. mellea* pathogenicity. Therefore, identifying the functions of these proteins is a challenging but lucrative proposition and strategies which can be

employed in the future to do this are shown in Figure 8.2. Indeed, some of these strategies have been employed in the course of work presented in this thesis.

Use of bioinformatic software tools, to deduce function through homology, topology, protein signature motifs and signal peptides are valuable resources (Figure 8.2). Bioinformatic tools have been used to analyse proteins in *A. mellea* through homology and motif recognition, where whole proteins are not homologous to those found in other organisms. As described in Chapter 3, nineteen percent of *A. mellea* genes were classified by BLAST search as unique, but eleven percent of these had motifs to which an IPS search attributed some functionality based on other protein signatures. For example, domains identified in *A. mellea* specific proteins include F-box and hydrophobin motifs, transmembrane regions and signal peptides. Further genome mining using these tools will more precisely identify novel proteins from the *A. mellea* genome and proteome, and inform and catalyse research. It should be noted that while topology analysis and secretion signals give some indication of cellular location and motif recognition, protein functionality must still be verified experimentally, because proteins may have different functions in different organisms, or indeed even in the same organism (Jeffery, 1999).

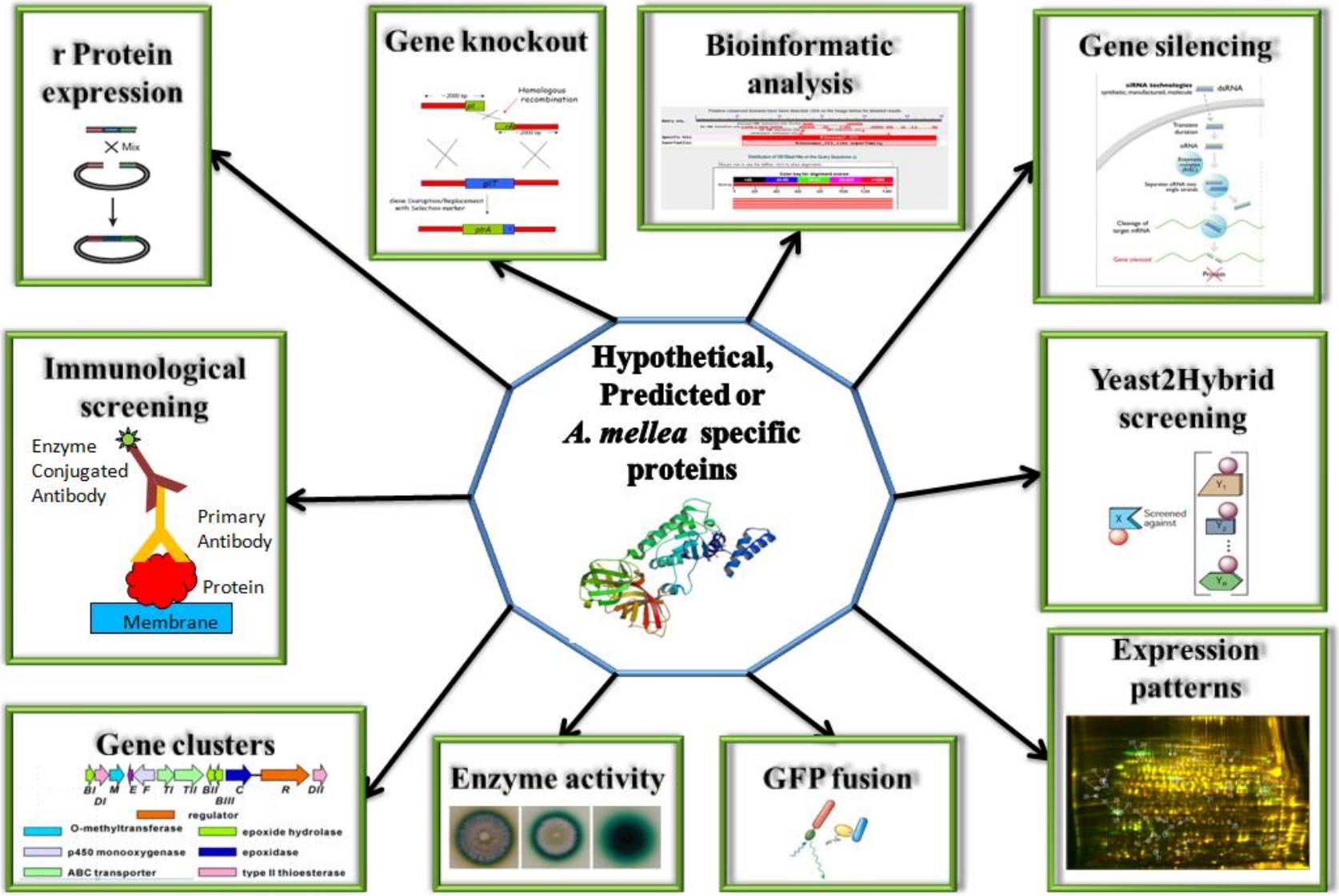
r Protein expression
Mix
Gene knockout
Homologous recombination
Bioinformatic analysis
Gene silencing
siRNA technologies
dsRNA
siRNA
Immunological screening
Enzyme Conjugated Antibody
Primary Antibody
Protein
Membrane
Hypothetical, Predicted or A. mellea specific proteins
Yeast2Hybrid screening
X
Screened against
Gene clusters
BI M E F TI TII BII C R DII
DI
BIII
regulator
O-methyltransferase
epoxide hydrolase
p450 monooxygenase
epoxidase
ABC transporter
type II thioesterase
Enzyme activity
GFP fusion
Expression patterns

Figure 8.2. Methods potentially applicable to study the function of hypothetical, predicted and *A. mellea* unknown function proteins. Clockwise from top, Bioinformatic analysis, using software tools to deduce function through homology, topology, motifs and signal peptides; Gene silencing, using RNAi to cleave or inactivate mRNA in transient interference of protein expression; Yeast 2 Hybrid, a reporter gene is activated by the binding of transcription factor to the protein of interest and interaction with activation domain attached to potential binding partner proteins, whereby transcription of the reporter occurs when the proteins attached to the transcription factor and activation domains interact; Expression patterns, using comparative and quantitative proteomics to identify proteins differentially expressed under stress/xenobiotic; GFP fusion, attachment of GFP to proteins to deduce their precise cellular locations; Enzyme activity assays, assay of enzyme activity to determine enzyme activity by measurement of substrate consumption; Gene clustering, to identify genome proteins that may be co-expressed and are therefore under the control of a single regulator; Immunological screening, use of anti-sera to identify immobilised proteins; Recombinant protein expression, expression of protein in another organism; Gene knockout, gene inactivation and phenotype analysis (Vitagliano *et al.*, 2001; Phizicky *et al.*, 2003; Jiang *et al.*, 2012; Mander *et al.*, 2006; Muszkieta *et al.*, 2013; (Images: http://blast.ncbi.nlm.nih.gov/Blast.cgi?PAGE=Proteins; www.sereassembly.ie/docs/seanddoyle.researchday.pdf; www.benitec.com/rnai-gene-silencing.php).

Gene silencing, (Figure 8.2) by the use of RNAi to cleave or inactivate mRNA is a method which has been successfuly employed to silence virulence genes in *P. triticina*, and the novel method of RNAi delivery to *P. triticina* by means of *A. tumefaciens*-mediated transformation of its host, wheat, which interferes with RNA shows promise as a means of transient silencing of genes in a phytopathogen such as *A. mellea* (Figure 8.3)(Panwar *et al.*, 2013). Unknown function *A. mellea* genes, from the infection model described in this work, present suitable targets for RNAi in both *A. mellea* and less pathogenic *Armillaria* spp.

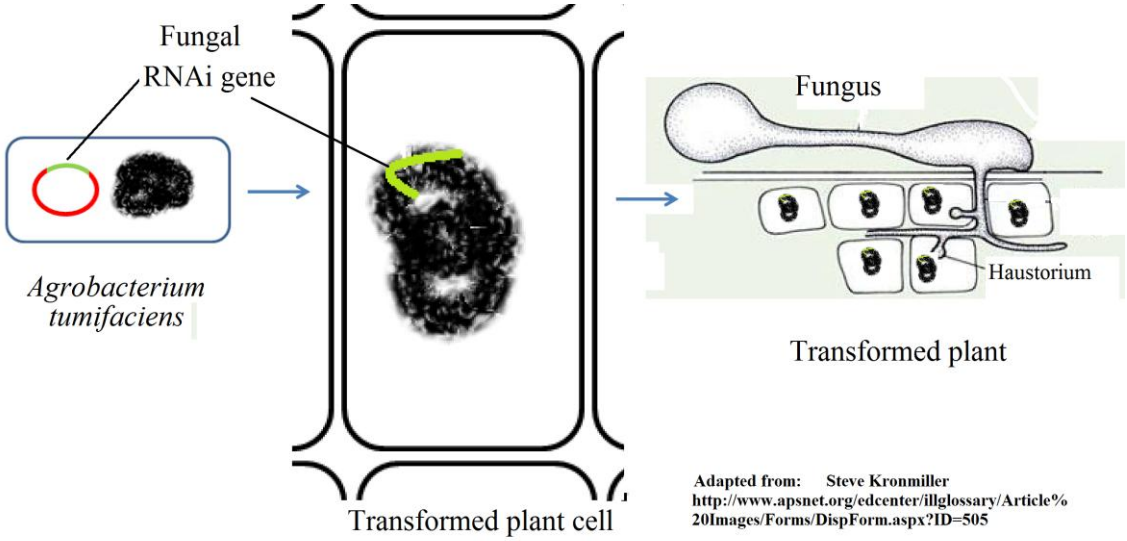

Figure 8.3. Transient RNAi in *P. triticina*. *Agrobacterium tumefaciens* plasmids are constructed, incorporating a fungal RNAi gene; *A. tumefaciens* mediated plant cell transformation is carried out; fungal RNAi occurs in haustoria of *P. triticina* (Panwar *et al.*, 2013).

A yeast two-hybrid system identifies interactions between two proteins (Figure 8.2), and was used to identify the unknown binding partner of a transcription regulator in *L. edodes*, a basidiomycete (Nakazawa *et al.*, 2008). A novel protein with an unusual binding mechanism was identified by this method, and, as one partner protein has homologues in other basidiomycetes it provided insight into possible interaction and mechanisms in other species (Nakazawa *et al.*, 2008), and application of this technique to *A. mellea* unknown function proteins may enable functional identification, particularly of proteins involved in virulence. Proteins uniquely identified in the infection model for which no function or motifs were determined would certainly be suitable for yeast two-hybrid study, as interaction partners would enable elucidation of their functions.

In addition to four proteins uniquely expressed in the virulence study (Chapter 7), there are a further 25 proteins previously classified as predicted or hypothetical, which were identified in the infection model, whose functions have not been established, and the expression these proteins may be differentially regulated during pathogenic interactions. Differential proteomic studies (Figure 8.2), involving quantitative shotgun proteomics, in the new infection model could be used to further inform *A. mellea* virulence mechanisms through fractionation and quantification of proteins (Figure 8.4).

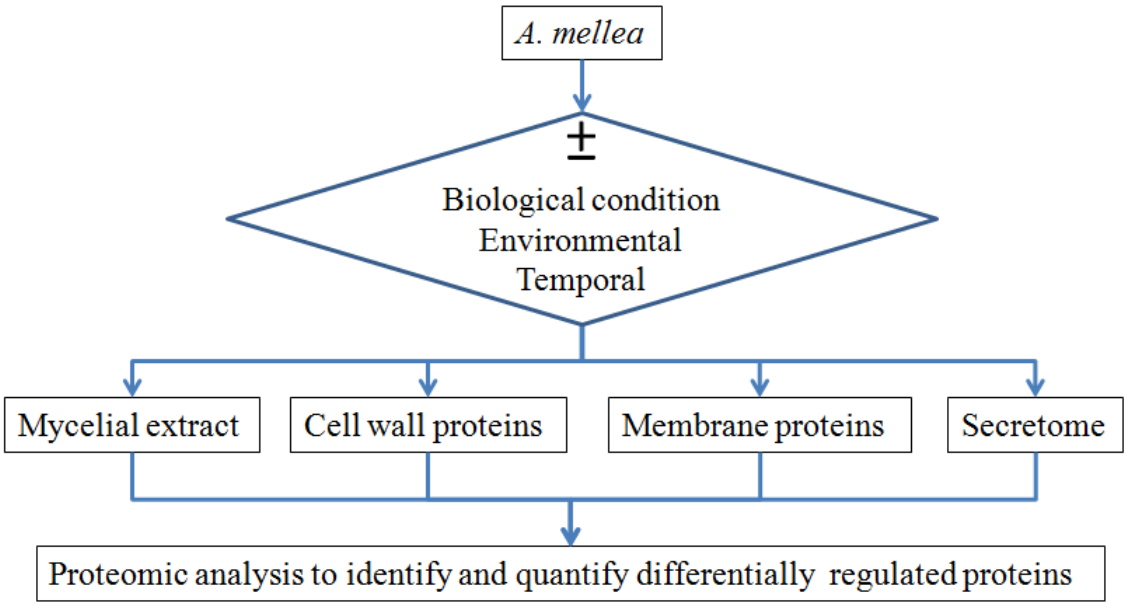

Figure 8.4. Subcellular fractionation combined with quantitative differential proteomic analysis of *A. mellea* proteins under different parameters: a strategy which could be employed to identify proteins involved in virulence and pathogenicity.

Transgene expression of GFP (Figure 8.2) in *A. mellea* hyphae has been carried out to visualise hyphal penetration of roots (Baumgartner *et al.*, 2008), but the protein expression was transient and after one month the protein was no longer expressed. Nonetheless this was a proof of concept experiment, which showed that the protein could be expressed in *A. mellea* and further application of GFP expression could be employed to identify localisation of unknown function proteins especially within infection structures such as haustoria. Activity of *A. mellea* enzymes, particularly enzymes which have hydrolytic activity, and thus may be suitable for biotechnological applications, may possess higher levels of activity or may have unique specificity for particular substrates. Preliminary activity assays (data not shown) have revealed increased laccase activity with lignin as sole carbon source, compared to other

substrates, and highest superoxide dismutase activity in cultures where xylan was sole carbon source. However, these are only preliminary studies and levels of activity compared to other basidiomycetes have yet to be determined. Gene clusters which encode enzymes for the synthesis of secondary metabolites have been described in *Aspergillus* spp, and other Ascomycetes, to be under the control of a single transcriptional regulator (Bok and Keller, 2004). Gene clusters have not been described in *Armillaria* spp. or in basidiomycetes. However, NRPS and PKS have been shown to be encoded in the *A. mellea* genome and their consecutive accession number annotation may indicate clusters of these genes. The newly sequenced *A. mellea* genome will enable further investigation of these genes, and related ORFs which have chromosomal proximity to these clusters.

Use of immunological screening, combined with recombinant protein expression, may also help to reveal protein function in *A. mellea*. One strategy which may provide immunoreagents is as follows: Rabbit immunisation with whole protein mycelial lysates, or secretome lysates, from *A. mellea* would yield a heterogenous population of antibodies against *A. mellea* proteins. This would essentially represent an *A. mellea* antisera reagent. Individual *A. mellea* recombinant proteins, resulting from expression of selected genes, could then by immobilised on Sepharose beads and used to facilitate immunoaffinity purification of *A. mellea* protein-monospecific antibodies from the *A. mellea* antisera. These immunoaffinity -purified antibodies could in turn be used for immunlocalisation studies in *A. mellea* or to complement quantitative protein expression studies using mycelial, cell wall, membrane fractions (Figure 8.5). Ultimately, this approach would enable the identification of *A. mellea* proteins in infected plants and thus identify *A. mellea* proteins involved in infection mechanisms, which is especially important for those proteins not hitherto known to be involved in infection. Importantly, the data resulting from the work undertaken as part of this PhD thesis, provides a unique platform from which to launch these immunological investigations of *A. mellea*. Finally, immunological analysis (Figure 8.2) of plant extracts, to detect *A. mellea*-specific proteins could be undertaken using the *A. mellea* antisera or immunoaffinity purified from the rabbit antisera.

Expression of *A. mellea* unknown function proteins, in other organisms such a *S. cerevisiae,* may enable identification of functionality, based on enzyme activity. Screening for catalytic, cytotoxic, antioxidant or antibiotic activities may identify novel

enzymes. Of particular interest for this type of study would be proteins/enzymes from *A. mellea* which are organism-specific or have no known homologs in other species.

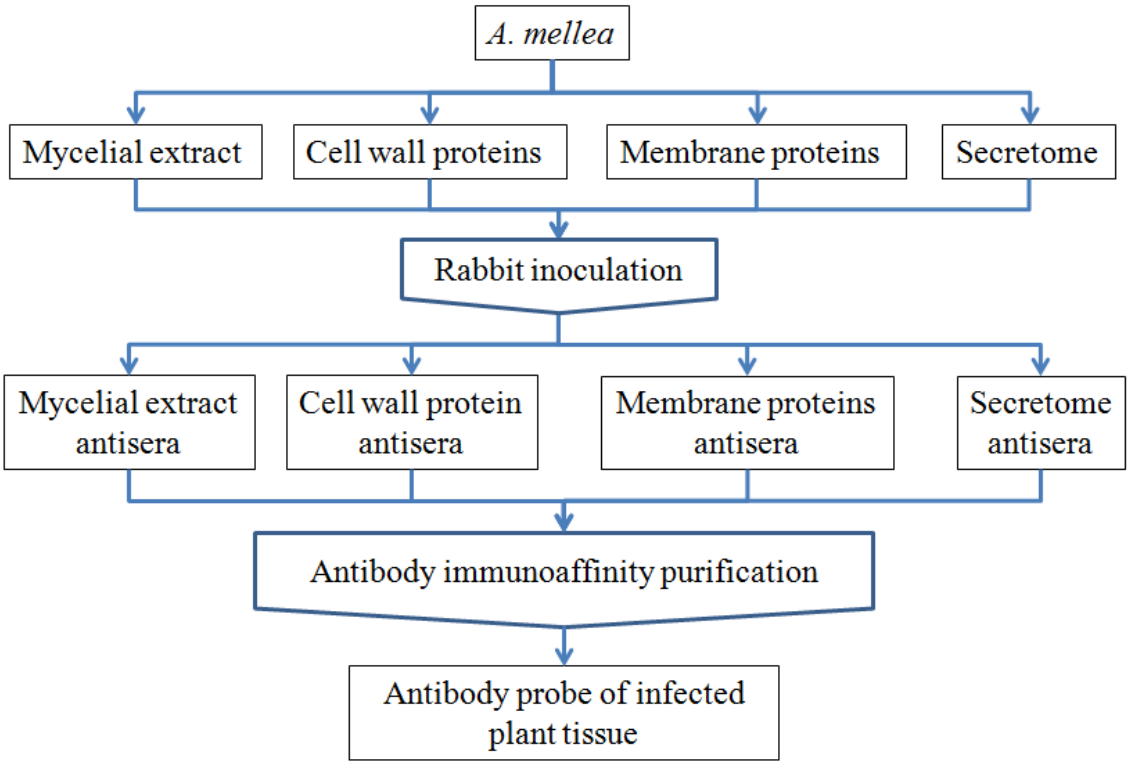

Figure 8.5. Strategy for immunological analysis of plant material infected with *A. mellea*. Subcellular fractions of *A. mellea* proteins could be used to inoculate rabbits, thus raising antisera. Following antibody immunoaffinity purification, resultant monospecific antibodies could, in turn, be used to probe *A. mellea* infected plant tissue thereby enabling identification of *A. mellea* proteins involved in pathogenicity and virulence.

Alternatively, over-expression of the proteins in *A. mellea* may also contribute to identification of function. Gene knock-out allows gene inactivation and phenotype analysis of transformed organism (Schrettl *et al.*, 2010). A technique has been developed for transformation of *A. mellea* with *A. tumefaciens* as a proof of concept (Baumgartner *et al.*, 2010). Although this technique is in the developmental stage and there has been no documented gene knockout in *A. mellea* thus far, deletion of unknown function proteins already identified in *A. mellea* - particularly in the infection model system – may elucidate the function of proteins involved in virulence and pathogenicity of *A. mellea*, and of basidiomycetes in general, as "hypothetical" and "predicted" proteins in *A. mellea* have homologues in other species.

8.3 Concluding remarks

To conclude, this thesis presents significant new information about the molecular nature of the phytopathogen *Armillaria mellea*, in terms of genome annotation, constituent gene families, the intra- and extra-cellular proteome, proteins involved in redox stress and, most interestingly, its anti-*Candida* activity. Moreover, the thesis describes, in detail, novel experimental strategies for dissection and study of *A. mellea* and elucidates valid strategies for further study of this most virulent plant pathogen. The proteins involved in the threat that *Armillaria mellea* poses to the environment may well be the selfsame proteins that are its buried treasure.

BIBLIOGRAPHY

Abbas, A., Koc, H., Liu, F., and Tien, M. (**2005**). Fungal degradation of wood: initial proteomic analysis of extracellular proteins of *Phanerochaete chrysosporium* grown on oak substrate. *Current Genetics* **47**: 49–56.

Abbott, E.P., Ianiri, G., Castoria, R., and Idnurm, A. (**2013**). Overcoming recalcitrant transformation and gene manipulation in Pucciniomycotina yeasts. *Applied Microbiology and Biotechnology* **97**: 283–95.

Abdallah, C., Sergeant, K., Guillier, C., Dumas-Gaudot, E., Leclercq, C.C., and Renaut, J. (**2012**). Optimization of iTRAQ labelling coupled to OFFGEL fractionation as a proteomic workflow to the analysis of microsomal proteins of *Medicago truncatula* roots. *Proteome Science* **10**: 37.

Adames, N., Blundell, K., Ashby, M.N., and Boone, C. (**1995**). Role of yeast insulin-degrading enzyme homologs in propheromone processing and bud site selection. *Science* **270**: 464–7.

Adaskaveg, J.E., Forster, H., Wade, L., Thompson, D.F., and Connell, J.H. (**1999**). Efficacy of sodium tetrathiocarbonate and propiconazole in managing *Armillaria* root rot of almond on peach rootstock. *Plant Disease* **83**: 240–246.

Agger, S., Lopez-Gallego, F., and Schmidt-Dannert, C. (**2009**). Diversity of sesquiterpene synthases in the basidiomycete *Coprinus cinereus. Molecular Microbiology* **72**: 1181–95.

Agilent, T. Agilent 3100 OFFGEL Fractionator User Manual. *Control*.

Agranoff, D. and Krishna, S. (**2002**). Metal ion homeostasis and intracellular parasitism. *Molecular Microbiology* **28**: 403–412.

Aguín, O., Mansilla, J.P., and Sainz, M.J. (**2006**). In vitro selection of an effective fungicide against *Armillaria mellea* and control of white root rot of grapevine in the field. *Pest Management Science* **62**: 223–8.

Ahamed, A. and Vermette, P. (**2009**). Effect of culture medium composition on *Trichoderma reesei*'s morphology and cellulase production. *Bioresource Technology* **100**: 5979–5987.

Ahamed, A. and Vermette, P. (**2008**). Enhanced enzyme production from mixed cultures of *Trichoderma reesei* RUT-C30 and *Aspergillus niger* LMA grown as fed batch in a stirred tank bioreactor. *Biochemical Engineering Journal* **42**: 41–46.

Akagi, R. (**1982**). Purification and characterization of cysteine aminotransferase from rat liver cytosol. *Acta Medica Okayama* **36**: 187–197.

Albrecht, D. and Guthke, R. (**2010**). Integrative analysis of the heat shock response in *Aspergillus fumigatus*. *BMC Genomics* **11**: 1–17.

Alcalde, M., Bulter, T., and Arnold, F.H. (**2002**). Colorimetric assays for biodegradation of polycyclic aromatic hydrocarbons by fungal laccases. *Journal of Biomolecular Screening* **7**: 547–53.

Allgaier, S., Weiland, N., Hamad, I., and Kempken, F. (**2010**). Expression of ribonuclease A and ribonuclease N1 in the filamentous fungus *Neurospora crassa*. *Applied Microbiology and Biotechnology* **85**: 1041–9.

Altschul, S., Gish, W., and Miller, W. (**1990**). Basic local alignment search tool. *Journal of Molecular Biology* **215**: 403–410.

Altschul, S.F., Madden, T.L., Schäffer, a a, Zhang, J., Zhang, Z., Miller, W., and Lipman, D.J. (**1997**). Gapped BLAST and PSI-BLAST: a new generation of protein database search programs. *Nucleic Acids Research* **25**: 3389–402.

Alves, A. and Record, E. (**2004**). Highly efficient production of laccase by the basidiomycete *Pycnoporus cinnabarinus*. *Applied and Environmental Microbiology* **70**: 6379–6384.

Alves, P., Arnold, R.J., Novotny, M. V, Radivojac, P., Reilly, J.P., and Tang, H. (**2007**). Advancement in protein inference from shotgun proteomics using peptide detectability. *Pacific Symposium on Biocomputing.* **420**: 409–20.

Amselem, J., Cuomo, C. a, van Kan, J. a L., Viaud, M., Benito, E.P., Couloux, A., Coutinho, P.M., de Vries, R.P., Dyer, P.S., Fillinger, S., Fournier, E., Gout, L., Hahn, M., Kohn, L., Lapalu, N., Plummer, K.M., Pradier, J.-M., Quévillon, E., Sharon, A., Simon, A., *et al.* (**2011**). Genomic analysis of the necrotrophic fungal pathogens *Sclerotinia sclerotiorum* and *Botrytis cinerea*. *PLoS genetics* **7**: e1002230.

Andersen, G.R., Nissen, P., and Nyborg, J. (**2003**). Elongation factors in protein biosynthesis. *Trends in Biochemical Sciences* **28**: 434–41.

Anderson, J., Petsche, D., and Smith, M. (**1987**). Restriction fragment polymorphisms in biological species of *Armillaria mellea*. *Mycologia* **79**: 69–76.

Anderson, J. and Stasovski, E. (**1992**). Molecular phylogeny of northern hemisphere species of *Armillaria*. *Mycologia* **84**: 505–516.

Anderson, J. and Ullrich, R. (**1979**). Biological Species of *Armillaria mellea* in North-America. *Mycologia* **71**: 402–414.

Ansorge, W. (**2009**). Next-generation DNA sequencing techniques. *New Biotechnology* **25**.

Antonin, V., Tomsovsky, M., Sedlak, P., Majek, T., and Jankovsky, L. (**2009**). Morphological and molecular characterization of the *Armillaria cepistipes - A. gallica* complex in the Czech Republic and Slovakia. *Mycological Progress* **83**: 259–271.

Apweiler, R. (**2001**). Functional information in SWISS-PROT: the basis for large-scale characterisation of protein sequences. *Briefings in Bioinformatics* **2**: 9–18.

Aran, M., Ferrero, D.S., Pagano, E., and Wolosiuk, R. a (**2009**). Typical 2-Cys peroxiredoxins--modulation by covalent transformations and noncovalent interactions. *The FEBS journal* **276**: 2478–93.

Arantes, V., Jellison, J., and Goodell, B. (**2012**). Peculiarities of brown-rot fungi and biochemical Fenton reaction with regard to their potential as a model for bioprocessing biomass. *Applied Microbiology and Biotechnology* **94**: 323–38.

Aravind, L. and Koonin, E. V (**1998**). Phosphoesterase domains associated with DNA polymerases of diverse origins. *Nucleic Acids Research* **26**: 3746–52.

Archie, J. (**1989**). A randomization test for phylogenetic information in systematic data. *Systematic Biology* **38**: 239–252.

Armengaud, J. (**2012**). Microbiology and proteomics, getting the best of both worlds! *Environmental microbiology*.

Arnone, A., Cardillo, R., Nasini, G., and Valdo Meille, S. (**1988**). Secondary mould metabolites. Part 19. Structure elucidation and absolute configuration of melledonals B and C, novel antibacterial sesquiterpenoids from *Armillaria mellea*. X-Ray molecular structure of melledonal C. *Journal of the Chemical Society, Perkin Transactions 1* **3**: 503–510.

Ashburner, M., Ball, C., and Blake, J. (**2000**). Gene Ontology: tool for the unification of biology. *Nature Genetics* **25**: 25–29.

Ashihara, H. and Crozier, A. (**2001**). Caffeine: a well known but little mentioned compound in plant science. *Trends in Plant Science* **6**: 407–13.

Atanasova, L., Crom, S., Gruber, S., Coulpier, F., Seidl-Seiboth, V., Kubicek, C.P., and Druzhinina, I.S. (**2013**). Comparative transcriptomics reveals different strategies of *Trichoderma* mycoparasitism. *BMC Genomics* **14**: 121.

Baginsky, S. and Gruissem, W. (**2006**). *Arabidopsis thaliana* proteomics: from proteome to genome. *Journal of Experimental Botany* **57**: 1485–91.

Baker, L.G. and Specht, C.A. (**2009**). Chitinases Are Essential for Sexual Development but not Vegetative Growth in *Cryptococcus neoformans*. *Eukaryotic Cell* **8**: 1692–1705.

Baldauf, S. and Palmer, J. (**1993**). Animals and fungi are each other's closest relatives: congruent evidence from multiple proteins. *Proceedings of the National Academy of Sciences of the United States of America* **90**: 11558–11562.

Baldrian, P. (**2006**). Fungal laccases - occurrence and properties. *FEMS Microbiology Reviews* **30**: 215–242.

Baldrian, P. and Valásková, V. (**2008**). Degradation of cellulose by basidiomycetous fungi. *FEMS Microbiology Reviews* **32**: 501–521.

Bao, W., Fukushima, Y., Jensen, K. a, Moen, M. a, and Hammel, K.E. (**1994**). Oxidative degradation of non-phenolic lignin during lipid peroxidation by fungal manganese peroxidase. *FEBS Letters* **354**: 297–300.

Bark, S.J., Wegrzyn, J., Taupenot, L., Ziegler, M., O'Connor, D.T., Ma, Q., Smoot, M., Ideker, T., and Hook, V. (**2012**). The protein architecture of human secretory vesicles reveals differential regulation of signaling molecule secretion by protein kinases. *PloS ONE* **7**: e41134.

Barrett, L.G. and Heil, M. (**2012**). Unifying concepts and mechanisms in the specificity of plant-enemy interactions. *Trends in Plant Science* **17**: 282–92.

Barry, F.P., Doonan, S., and Ross, C. (**1981**). Cleavage by trypsin and by the proteinase from Armillaria mellea at epsilon-N-formyl-lysine residues. *Biochemical Journal* **193**: 737–42.

Baumgartner, K. (**2004**). Root collar excavation for postinfection control of *Armillaria* root disease of grapevine. *Plant Disease* **88**: 1235–1240.

Baumgartner, K., Bailey, A., Foster, G.D., and Kilaru, S. (**2008**). Transgene expression in the basidiomycete root pathogen *Armillaria mellea*. *Phytopathology* **98**: S19–S19.

Baumgartner, K., Bhat, R., and Fujiyoshi, P. (**2010**). A rapid infection assay for *Armillaria* and real-time PCR quantitation of the fungal biomass in planta. *Fungal Biology* **114**: 107–119.

Baumgartner, K., Coetzee, M.P.A., and Hoffmeister, D. (**2011**). Secrets of the subterranean pathosystem of *Armillaria*. *Molecular Plant Pathology* **12**: 515–534.

Baumgartner, K., Fujiyoshi, P., Browne, G.T., Leslie, C., and Kluepfel, D.A. (**2013**). Evaluating Paradox Walnut Rootstocks for Resistance to *Armillaria* Root Disease. *Horticultural Science* **48**: 68–72.

Baumgartner, K., Fujiyoshi, P., Foster, G.D.D., and Bailey, A.M.M. (**2010**). *Agrobacterium tumefaciens*-Mediated Transformation for Investigation of Somatic Recombination in the Fungal Pathogen *Armillaria mellea*. *Applied and Environmental Microbiology* **76**: 7990–7996.

Baumgartner, K. and Rizzo, D.M. (**2001a**). Ecology of *Armillaria* spp. in mixed-hardwood forests of California. *Plant Disease* **85**: 947–951.

Baumgartner, K. and Rizzo, D.M. (**2006**). Relative resistance of grapevine rootstocks to *Armillaria mellea* root disease. *American Journal of Enology and Viticulture* **57**: 408–414.

Baumgartner, K. and Rizzo, D.M.M. (**2001b**). Distribution of *Armillaria* species in California. *Mycologia* **93**: 821–830.

Baumgartner, K. and Warnock, A.E. (**2006a**). Biological control of *Armillaria* root disease of grapevine. *Phytopathology* **96**: S10–S11.

Baumgartner, K. and Warnock, A.E.E. (**2006b**). A soil inoculant inhibits *Armillaria mellea* in vitro and improves productivity of grapevines with root disease. *Plant Disease* **90**: 439–444.

Belozerskaya, T. a. and Gessler, N.N. (**2007**). Reactive oxygen species and the strategy of antioxidant defense in fungi: A review. *Applied Biochemistry and Microbiology* **43**: 506–515.

Del Bem, L.E. V and Vincentz, M.G. a (**2010**). Evolution of xyloglucan-related genes in green plants. *BMC Evolutionary biology* **10**: 341.

Bendtsen, J., Jensen, L., and Blom, N. (**2004**). Feature-based prediction of non-classical and leaderless protein secretion. *Protein Engineering* **17**: 349–356.

Bendtsen, J.D., Kiemer, L., Fausboll, A., and Brunak, S. (**2005**). Non-classical protein secretion in bacteria. *BMC Microbiology* **5**.

Bendtsen, J.D., Nielsen, H., von Heijne, G., and Brunak, S. (**2004**). Improved prediction of signal peptides: SignalP 3.0. *Journal of Molecular Biology* **340**: 783–95.

Benítez, T., Rincón, A.M., Limón, M.C., and Codón, A.C. (**2004**). Biocontrol mechanisms of *Trichoderma* strains. *International microbiology : the official journal of the Spanish Society for Microbiology* **7**: 249–60.

Bentley, D.R., Balasubramanian, S., Swerdlow, H.P., Smith, G.P., Milton, J., Brown, C.G., Hall, K.P., Evers, D.J., Barnes, C.L., Bignell, H.R., Boutell, J.M., Bryant, J., Carter, R.J., Keira Cheetham, R., Cox, A.J., Ellis, D.J., Flatbush, M.R., Gormley, N. a, Humphray, S.J., Irving, L.J., *et al.* (**2008**). Accurate whole human genome sequencing using reversible terminator chemistry. *Nature* **456**: 53–9.

Billal, F. and Thurston, C.F. (**1996**). Purification of laccase II from *Armillaria mellea* and comparison of its properties with those of laccase I. *Mycological Research* **100**: 1099–1105.

Birkinshaw, J.H., Stickings, C.E., and Tessier, P.L.A. (**1948**). Biochemistry of the wood-rotting fungi: 5. The production of d-threitol (l-erythritol) by *Armillaria mellea* (Vahl) Quélet. *Biochemical Journal* **42**: 329–32.

Biswas, D., Datt, M., Aggarwal, M., and Mondal, A.K. (**2013**). Molecular cloning, characterization, and engineering of xylitol dehydrogenase from *Debaryomyces hansenii*. *Applied Microbiology and Biotechnology* **97**: 1613–23.

Blair, D.E., Schüttelkopf, A.W., MacRae, J.I., and van Aalten, D.M.F. (**2005**). Structure and metal-dependent mechanism of peptidoglycan deacetylase, a streptococcal virulence factor. *Proceedings of the National Academy of Sciences of the United States of America* **102**: 15429–34.

Boerjan, W., Ralph, J., and Baucher, M. (**2003**). Lignin biosynthesis. *Annual Review of Plant Biology* **54**: 519–46.

Böhm, S., Lamberti, G., Fernández-Sáiz, V., Stapf, C., and Buchberger, A. (**2011**). Cellular functions of Ufd2 and Ufd3 in proteasomal protein degradation depend on Cdc48 binding. *Molecular and Cellular Biology* **31**: 1528–39.

Bohnert, M., Miethbauer, S., Dahse, H.M., Ziemen, J., Nett, M., and Hoffmeister, D. (**2011**). In vitro cytotoxicity of melleolide antibiotics: structural and mechanistic aspects. *Bioorganic & Medicinal Chemistry Letters* **21**: 2003–2006.

Bok, J.W. and Keller, N.. (**2004**). LaeA, a regulator of secondary metabolism in *Aspergillus* spp. *Eukaryotic Cell* **3**: 527–535.

Boraston, A., Bolam, D., and Gilbert, H. (**2004**). Carbohydrate-binding modules: fine-tuning polysaccharide recognition. *Biochemical Journal* **781**: 769–781.

Bouws, H., Wattenberg, A., and Zorn, H. (**2008**). Fungal secretomes--nature's toolbox for white biotechnology. *Applied Microbiology and Biotechnology* **80**: 381–8.

Bowman, S.M. and Free, S.J. (**2006**). The structure and synthesis of the fungal cell wall. *BioEssays* **28**: 799–808.

Braaksma, M., Martens-Uzunova, E.S., Punt, P.J., and Schaap, P.J. (**2010**). An inventory of the Aspergillus niger secretome by combining in silico predictions with shotgun proteomics data. *BMC Genomics* **11**: 584.

Bratschi, M.W., Burrowes, D.P., Kulaga, A., Cheung, J.F., Alvarez, A.L., Kearley, J., and Zaremberg, V. (**2009**). Glycerol-3-phosphate acyltransferases gat1p and gat2p are microsomal phosphoproteins with differential contributions to polarized cell growth. *Eukaryotic cell* **8**: 1184–96.

Brazee, N.J. and Wick, R.L. (**2009**). *Armillaria* species distribution on symptomatic hosts in northern hardwood and mixed oak forests in western Massachusetts. *Forest Ecology and Management* **258**: 1605–1612.

Breuer, U. and Harms, H. (**2006**). *Debaryomyces hansenii*--an extremophilic yeast with biotechnological potential. *Yeast* **23**: 415–37.

Van den Brink, J. and de Vries, R.P. (**2011**). Fungal enzyme sets for plant polysaccharide degradation. *Applied Microbiology and Biotechnology* **91**: 1477–92.

Broadbent, D., Turner, R.W., and Walton, P.L. (**1972**). Enzymes - Patent GB1263956.

Brodhagen, M. and Keller, N. (**2006**). Signalling pathways connecting mycotoxin production and sporulation. *Molecular Plant Pathology* **7**: 285–301.

Bruhn, J., Wetteroff, J., and Mihail, J. (**2000**). Distribution of *Armillaria* species in upland Ozark Mountain forests with respect to site, overstory species composition and oak decline. *European Journal of Forest Pathology* **30**: 43–60.

De Buck, E., Lammertyn, E., and Anné, J. (**2008**). The importance of the twin-arginine translocation pathway for bacterial virulence. *Trends in Microbiology* **16**: 442–53.

Bukau, B. and Horwich, A.L. (**1998**). The Hsp70 and Hsp60 chaperone machines. *Cell* **92**: 351–66.

Burow, G. and Nesbitt, T. (**1997**). Seed lipoxygenase products modulate *Aspergillus* mycotoxin biosynthesis. *Molecular Plant-Microbe Interactions* **10**: 380–387.

Butler, D.K., All, O., Goffena, J., Loveless, T., Wilson, T., and Toenjes, K. a (**2006**). The GRR1 gene of *Candida albicans* is involved in the negative control of pseudohyphal morphogenesis. *Fungal Genetics and Biology* **43**: 573–82.

Buzzini, P. and Martini, A. (**2001**). Large-scale screening of selected *Candida maltosa, Debaryomyces hansenii* and *Pichia anomala* killer toxin activity against pathogenic yeasts. *Medical Mycology*: 479–482.

Caboche, S., Pupin, M., Leclère, V., Fontaine, A., Jacques, P., and Kucherov, G. (**2008**). NORINE: a database of nonribosomal peptides. *Nucleic Acids Research* **36**: D326–31.

Cai, D. and Tien, M. (**1992**). Kinetic studies on the formation and decomposition of compounds II and III. Reactions of lignin peroxidase with H_2O_2. *Journal of Biological Chemistry* **1**: 5–11.

Caldwell, C.C., Hornyak, S.C., Pendleton, E., Campbell, D., and Knowles, a F. (**2001**). Regulation of chicken gizzard ecto-ATPase activity by modulators that affect its oligomerization status. *Archives of Biochemistry and Biophysics* **387**: 107–16.

Camps, M., Nichols, A., and Arkinstall, S. (**2000**). Dual specificity phosphatases: a gene family for control of MAP kinase function. *FASEB Journal* **14**: 6–16.

Cantarel, B.L., Coutinho, P.M., Rancurel, C., Bernard, T., Lombard, V., and Henrissat, B. (**2009**). The Carbohydrate-Active EnZymes database (CAZy): an expert resource for Glycogenomics. *Nucleic Acids Research* **37**: D233–8.

Carberry, S., Neville, C.M., Kavanagh, K.A., and Doyle, S. (**2006**). Analysis of major intracellular proteins of Aspergillus fumigatus by MALDI mass spectrometry: Identification and characterisation of an elongation factor 1B protein with glutathione transferase activity. *Biochemical and Biophysical Research Communications* **341**: 1096–1104.

Carfi, A., Pares, S., Duée, E., Galleni, M., Dues, C., Frère, J., and Dideberg, O. (**1995**). The 3-D structure of a zinc metallo-β-lactamase from Bacillus cereus reveals a new type of protein fold. *The EMBO journal* **14**: 4914–21.

Castanera, R., Pérez, G., Omarini, A., Alfaro, M., Pisabarro, A.G., Faraco, V., Amore, A., and Ramírez, L. (**2012**). Transcriptional and enzymatic profiling of *Pleurotus ostreatus* laccase genes in submerged and solid-state fermentation cultures. *Applied and Environmental Microbiology* **78**: 4037–45.

Castresana, J. (**2000**). Selection of conserved blocks from multiple alignments for their use in phylogenetic analysis. *Molecular Biology and Evolution* **17**: 540–52.

Catanzariti, A. and Dodds, P. (**2006**). Haustorially expressed secreted proteins from flax rust are highly enriched for avirulence elicitors. *The Plant Cell* **18**: 243–256.

Caufrier, F., Martinou, A., Dupont, C., and Bouriotis, V. (**2003**). Carbohydrate esterase family 4 enzymes: substrate specificity. *Carbohydrate Research* **338**: 687–692.

Chapple, C., Ladisch, M., and Meilan, R. (**2007**). Loosening lignin's grip on biofuel production. *Nature Biotechnology* **25**: 746–8.

Chattopadhyay, M., Chen, W., and Poy, G. (**2009**). Microarray studies on the genes responsive to the addition of spermidine or spermine to a *Saccharomyces cerevisiae* spermidine synthase mutant. *Yeast*: 531–544.

Cheah, I.K. and Halliwell, B. (**2012**). Ergothioneine; antioxidant potential, physiological function and role in disease. *Biochimica et Biophysica Acta* **1822**: 784–93.

Chen, C.-C., Cheng, J.-J., and Shen, C.-C. (**2011**). Protoilludance Norsesquiterpenoid Esters and Uses therof. United States Patent Application 20110262561.

Chen, S., Xu, J., Liu, C., Zhu, Y., Nelson, D.R., Zhou, S., Li, C., Wang, L., Guo, X., Sun, Y., Luo, H., Li, Y., Song, J., Henrissat, B., Levasseur, A., Qian, J., Li, J., Luo, X., Shi, L., He, L., *et al.* (**2012**). Genome sequence of the model medicinal mushroom *Ganoderma lucidum. Nature Communications* **3**: 913.

Chenau, J., Michelland, S., and Sidibe, J. (**2008**). Peptides OFFGEL electrophoresis: a suitable pre-analytical step for complex eukaryotic samples fractionation compatible with quantitative iTRAQ labeling. *Proteome Science* **8**: 1–8.

Cherney, M.M., Zhang, Y., James, M.N.G., and Weiner, J.H. (**2012**). Structure-activity characterization of sulfide:quinone oxidoreductase variants. *Journal of Structural Biology* **178**: 319–28.

Chillali, M., Idder-Ighili, H., Guillaumin, J.J., Mohammed, C., Escarmant, B.L., and Botton, B. (**1998**). Variation in the ITS and IGS regions of ribosomal DNA among the biological species of European *Armillaria*. *Mycological Research* **102**: 533–540.

Chiu, C.-W., Chang, C.-L., and Chen, S.-F. (**2012**). Evaluation of peptide fractionation strategies used in proteome analysis. *Journal of Separation Science* **35**: 3293–301.

Choi, D., Cha, W., Park, N., Kim, H., and Lee, J. (**2011**). Purification and characterization of a novel fibrinolytic enzyme from fruiting bodies of Korean *Cordyceps militaris*. *Bioresource Technology*.

Christensen, S. a and Kolomiets, M. V (**2011**). The lipid language of plant-fungal interactions. *Fungal Genetics and Biology* **48**: 4–14.

Cicchillo, R.M. and Booker, S.J. (**2005**). Mechanistic investigations of lipoic acid biosynthesis in *Escherichia coli*: both sulfur atoms in lipoic acid are contributed by the same lipoyl synthase polypeptide. *Journal of the American Chemical Society* **127**: 2860–1.

Coder, D.M. (**1997**). Assessment of Cell Viability. In *Current Protocols in Cytometry*, K. Chambers and J.P. Robinson, eds, pp. 1–14.

Coder, K.D. and Daniel, B. (**1999**). Foxfire: Bioluminescence in the Forest (University of Georgia, DB Warnell School of Forest Resources).

Coetzee, M.P., Wingfield, B.D., Harrington, T.C., Steimel, J., Coutinho, T.A., and Wingfield, M.J. (**2001**). The root rot fungus *Armillaria mellea* introduced into South Africa by early Dutch settlers. *Molecular Ecology* **10**: 387–96.

Coetzee, M.P.A., Bloomer, P., Wingfield, M.J., and Wingfield, B.D. (**2011**). Paleogene Radiation of a Plant Pathogenic Mushroom. *PLoS ONE* **6**: e28545.

Coetzee, M.P.A., Maphosa, L., Mwenje, E., Wingfield, M.J., Wingfield, B.D., and others (**2009**). Characterisation of *Armillaria* species based on pectic isozyme analyses. *Fungal Diversity* **36**: 9–16.

Coetzee, M.P.A., Wingfield, B.D., Bloomer, P., and Wingfield, M.J. (**2005**). Phylogenetic analyses of DNA sequences reveal species amongst isolates of Armillaria from Africa. *Mycological Research* **109**: 1223–1234.

Coetzee, M.P.A., Wingfield, B.D., and Coutinho, T.A. (**2000**). Identification of the causal agent of *Armillaria* root rot of *Pinus* species in South Africa. *Mycologia* **92**: 777–785.

Coetzee, M.P.A., Wingfield, B.D., Kirisits, T., Chhetri, D.B., Bloomer, P., and Wingfield, M.J. (**2005**). Identification of *Armillaria* isolates from Bhutan based on DNA sequence comparisons. *Plant Pathology* **54**: 36–45.

Coleman, J.J., Ghosh, S., Okoli, I., and Mylonakis, E. (**2011**). Antifungal activity of microbial secondary metabolites. *PloS One* **6**: e25321.

Coleman, J.J. and Mylonakis, E. (**2009**). Efflux in fungi: la pièce de résistance. *PLoS Pathogens* **5**: e1000486.

Coles, M., Diercks, T., Liermann, J., Gröger, A., Rockel, B., Baumeister, W., Koretke, K.K., Lupas, A., Peters, J., and Kessler, H. (**1999**). The solution structure of VAT-N reveals a "missing link" in the evolution of complex enzymes from a simple β-α-β-β element. *Current Biology* **9**: 1158–68.

Collakova, E., Yen, J.Y., and Senger, R.S. (**2012**). Are we ready for genome-scale modeling in plants? *Plant Science* **191-192**: 53–70.

Conesa, A. and Gotz, S. (**2009**). Blast2Go Tutorial. *Centro de Genómica IVIA*.

Conesa, A., Gotz, S., Garcia-Gomez, J.M., Terol, J., Talon, M., and Robles, M. (**2005**). Blast2GO: a universal tool for annotation, visualization and analysis in functional genomics research. *Bioinformatics* **21**: 3674–3676.

Cosgrove, D.J. (**2000**). Loosening of plant cell walls by expansins. *Nature* **407**: 321–6.

Costa Seaver, L. and Imlay, J. (**2001**). Alkyl hydroperoxide reductase is the primary scavenger of endogenous hydrogen peroxide in *Escherichia coli*. *Journal of Bacteriology* **183**: 7173–7181.

Coutinho, P.M., Deleury, E., Davies, G.J., and Henrissat, B. (**2003**). An Evolving Hierarchical Family Classification for Glycosyltransferases. *Journal of Molecular Biology* **328**: 307–317.

Cowie, D.B., Cohen, G.N., Bolton, E.T., and De Rrobichon-Szulmajster H (**1959**). Amino acid analog incorporation into bacterial proteins. *Biochimica et Biophysica Acta* **34**: 39–46.

Cox, K.D., Scherm, H., and Riley, M.B. (**2006**). Characterization of *Armillaria* spp. from peach orchards in the southeastern United States using fatty acid methyl ester profiling. *Mycological Research* **110**: 414–422.

Cox, P.W. and Hooley, P. (**2009**). Hydrophobins: New prospects for biotechnology. *Fungal Biology Reviews* **23**: 40–47.

Creevey, C.J., Fitzpatrick, D.A., Philip, G.K., Kinsella, R.J., O'Connell, M.J., Pentony, M.M., Travers, S.A., Wilkinson, M., and McInerney, J.O. (**2004**). Does a tree-like phylogeny only exist at the tips in the prokaryotes? *Proceedings Royal Society Biological Sciences* **271**: 2551–8.

Cremin, P., Donnelly, D., Wolfender, J., and Hostettmann, K. (**1995**). Liquid chromatographic-thermospray mass spectrometric analysis of sesquiterpenes of *Armillaria* (Eumycota : Basidiomycotina) species. *Journal of Chromatography A* **710**: 273–285.

Cremin, P., Guiry, P., and Wolfender, J. (**2000**). A liquid chromatography–thermospray ionisation–mass spectrometry guided isolation of a new sesquiterpene aryl ester from *Armillaria novae-zelandiae*. *Journal of the Chemical Society, Perkin Transactions 1*: 2325–2329.

Creze, C., Castang, S., Derivery, E., Haser, R., Hugouvieux-Cotte-Pattat, N., Shevchik, V.E., and Gouet, P. (**2008**). The crystal structure of pectate lyase peli from soft rot pathogen *Erwinia chrysanthemi* in complex with its substrate. *The Journal of Biological Chemistry* **283**: 18260–8.

Cumsky, M.G., Trueblood, C.E., Ko, C., and Poyton, R.O. (**1987**). Structural analysis of two genes encoding divergent forms of yeast cytochrome c oxidase subunit V. *Molecular and Cellular Biology* **7**: 3511–9.

Czederpiltz, D., Volk, T., and Jr, H.B. (**2001**). Field observations and inoculation experiments to determine the nature of the carpophoroids associated with *Entoloma abortivum* and *Armillaria*. *Mycologia* **93**: 841–851.

Dai, C., Tao, J., Xie, F., Dai, Y., and Zhao, M. (**2007**). Biodiesel generation from oleaginous yeast *Rhodotorula glutinis* with xylose assimilating capacity. *African Journal of Biotechnology* **6**: 2130–2134.

Dalili, S.A.R.A.R., Nanagulyan, S.G.G., Alavi, S. V, and Razavi, M. (**2010**). Investigation of the wood destroying activity of *Armillaria mellea* on horticultural and forest plants species. *Australian Journal of Crop Science* **4**: 209–215.

Daniel, G., Volc, J., Filonova, L., Plíhal, O., Kubátová, E., and Halada, P. (**2007**). Characteristics of *Gloeophyllum trabeum* alcohol oxidase, an extracellular source of H_2O_2 in brown rot decay of wood. *Applied and Environmental Microbiology* **73**: 6241–53.

Dashtban, M., Schraft, H., and Qin, W. (**2009**). Fungal bioconversion of lignocellulosic residues; opportunities & perspectives. *International Journal of Biological Sciences* **5**: 578–595.

Davari, M. and Askari, B. (**2005**). *Armillaria mellea* as a cause of oak decline in Hatam-baigh forest of Iran. *Communications in Agricultural and Applied Biological Sciences* **70**: 295–304.

Denison, S., Negrete-Urtasun, S., Mingot, J., Tilburn, J., Mayer, W., Goel, A., Espeso, E., Peñalva, M., and Arst, H. (**2001**). Putative membrane components of signal transduction pathways for ambient pH regulation in *Aspergillus* and meiosis in *Saccharomyces* are homologous Addendum. *Molecular Microbiology* **39**: 211.

Deshaies, R. and Koch, B. (**1988**). A subfamily of stress proteins facilitates translocation of secretory and mitochondrial precursor polypeptides. *Nature* **332**: 800–805.

Dhiman, S.S., Kalyani, D., Jagtap, S.S., Haw, J.-R., Kang, Y.C., and Lee, J.-K. (**2012**). Characterization of a novel xylanase from *Armillaria gemina* and its immobilization onto SiO(2) nanoparticles. *Applied Microbiology and Biotechnology* **97**: 1081–1091.

Djamei, A. and Kahmann, R. (**2012**). *Ustilago maydis*: dissecting the molecular interface between pathogen and plant. *PLoS Pathogens* **8**: e1002955.

Djamei, A., Schipper, K., Rabe, F., Ghosh, A., Vincon, V., Kahnt, J., Osorio, S., Tohge, T., Fernie, A.R., Feussner, I., Feussner, K., Meinicke, P., Stierhof, Y.-D., Schwarz, H., Macek, B., Mann, M., and Kahmann, R. (**2011**). Metabolic priming by a secreted fungal effector. *Nature* **478**: 395–8.

Doddapaneni, H., Chakraborty, R., and Yadav, J.S. (**2005**). Genome-wide structural and evolutionary analysis of the P450 monooxygenase genes (P450ome) in the white rot fungus *Phanerochaete chrysosporium*: evidence for gene duplications and extensive gene clustering. *BMC Genomics* **6**: 92.

Dohm, J.C., Lottaz, C., Borodina, T., and Himmelbauer, H. (**2008**). Substantial biases in ultra-short read data sets from high-throughput DNA sequencing. *Nucleic Acids Research* **36**: e105.

Donnelly, D., Abe, F., Coveney, D., Fukuda, N., O'Reilly, J., Polonsky, J., Prang, T., Prangé, T., Oreilly, J., and Prange, T. (**1985**). Antibacterial sesquiterpene aryl esters from *Armillaria mellea*. *Journal of Natural Products* **48**: 10–16.

Donnelly, D., Coveney, D., and Polonsky, J. (**1985**). Melledonal and Melledonal, Sesquiterpene Esters from *Armillaria mellea*. *Tetrahedron Letters* **26**: 5343–5344.

Donnelly, D., Konishi, T., and Dunne, O. (**1997**). Sesquiterpene aryl esters from *Armillaria tabescens*. *Phytochemistry* **44**: 3–8.

Donnelly, D., Sanada, S., and O'Reilly, J. (**1982**). Isolation and structure (X-ray analysis) of the orsellinate of armillol, a new antibacterial metabolite from *Armillaria mellea*. *Journal of the Chemical Society, Chemical Communications*: 135–137.

Donnelly, D.M.X., Coveney, D.J., Fukuda, N., and Polonsky, J. (**1986**). New Sesquiterpene Aryl Esters from *Armillaria mellea*. *Journal of Natural Products* **49**: 111–116.

Donnelly, D.M.X. and Hutchinson, R.M. (**1990**). Armillane, a Saturated Sesquiterpene Ester from *Armillaria mellea*. *Phytochemistry* **29**: 179–182.

Donnelly, D.M.X., Hutchinson, R.M., Coveney, D., and Yonemitsu, M. (**1990**). Sesquiterpene Aryl Esters from *Armillaria mellea*. *Phytochemistry* **29**: 2569–2572.

Donnelly, D.M.X., Quigley, P.F., Coveney, D.J., and Polonsky, J. (**1987**). 2 New Sesquiterpene Esters from *Armillaria mellea*. *Phytochemistry* **26**: 3075–3077.

Doonan, S. and Fahmy, H.M. (**1975**). Specific enzymic cleavage of polypeptides at cysteine residues. *European Journal of Biochemistry* **56**: 421–6.

Dowson, C., Rayner, A., and Boddy, L. (**1988**). Foraging patterns of *Phallus-impudicus, Phanerochaete-laevis* and *Steccherinum-fimbriatum* between discontinuous resource units in soil. *FEMS Microbiology Ecology* **53**: 291–298.

Doyle, S. (**2011**). Fungal proteomics: from identification to function. *FEMS Microbiology Letters* **321**: 1–9.

Dreveny, I., Pye, V.E., Beuron, F., Briggs, L.C., Isaacson, R.L., Matthews, S.J., McKeown, C., Yuan, X., Zhang, X., and Freemont, P.S. (**2004**). P97 and Close Encounters of Every Kind: a Brief Review. *Biochemical Society Transactions* **32**: 715–20.

Duffy, B., Schouten, A., and Raaijmakers, J.M. (**2003**). Pathogen self-defense: mechanisms to counteract microbial antagonism,. *Annual review of Phytopathology* **41**: 501–38.

Dukan, S. and Nystrom, T. (**1998**). Bacterial senescence: stasis results in increased and differential oxidation of cytoplasmic proteins leading to developmental induction of the heat shock regulon. *Genes & Development* **12**: 3431–3441.

Dunford, H.B. (**1999**). Haem peroxidases (Wiley-VCH: New York).

Duplessis, S., Cuomo, C.A., Lin, Y.-C., Aerts, A., Tisserant, E., Veneault-Fourrey, C., Joly, D.L., Hacquard, S., Amselem, J., Cantarel, B.L., Chiu, R., Coutinho, P.M., Feau, N., Field, M., Frey, P., Gelhaye, E., Goldberg, J., Grabherr, M.G., Kodira, C.D., Kohler, A., *et al.* (2011). Obligate biotrophy features unraveled by the genomic analysis of rust fungi. *Proceedings of the National Academy of Sciences of the United States of America* **108**: 9166–9171.

Dwivedi, U.N., Singh, P., Pandey, V.P., and Kumar, A. (2011). Structure-function relationship among bacterial, fungal and plant laccases. *Journal of Molecular Catalysis B-Enzymatic* **68**: 117–128.

Eastwood, D.C., Floudas, D., Binder, M., Majcherczyk, A., Schneider, P., Aerts, A., Asiegbu, F.O., Baker, S.E., Barry, K., Bendiksby, M., Blumentritt, M., Coutinho, P.M., Cullen, D., de Vries, R.P., Gathman, A., Goodell, B., Henrissat, B., Ihrmark, K., Kauserud, H., Kohler, A., *et al.* (2011). The plant cell wall-decomposing machinery underlies the functional diversity of forest fungi. *Science* **333**: 762–5.

Edgar, R.C. (2004). MUSCLE: multiple sequence alignment with high accuracy and high throughput. *Nucleic Acids Research* **32**: 1792–7.

Eliot, A.C. and Kirsch, J.F. (2004). Pyridoxal phosphate enzymes: mechanistic, structural, and evolutionary considerations. *Annual Review of Biochemistry* **73**: 383–415.

Emanuelsson, O., Brunak, S., and Heijne, G. von (2007). Locating proteins in the cell using TargetP, SignalP and related tools. *Nature Protocols* **2**: 953–971.

Engels, B., Heinig, U., Grothe, T., Stadler, M., and Jennewein, S.C.-P. (2011). Cloning and characterization of an *Armillaria gallica* cDNA encoding protoilludene synthase, which catalyzes the first committed step in the synthesis of antimicrobial melleolides. *Journal of Biological Chemistry* **286**: 6871–8.

Enright, A.J., Van Dongen, S., and Ouzounis, C.A. (2002). An efficient algorithm for large-scale detection of protein families. *Nucleic Acids Research* **30**: 1575–84.

Erjavec, J., Kos, J., Ravnikar, M., Dreo, T., and Sabotic • , J. (2012). Proteins of higher fungi–from forest to application. *Trends in Biotechnology* **30**: 259–273.

Ernoult, E., Gamelin, E., and Guette, C. (2008). Improved proteome coverage by using iTRAQ labelling and peptide OFFGEL fractionation. *Proteome Science* **13**: 1–13.

Ewing, B. and Green, P. (1998). Base-calling of automated sequencer traces using Phred. II. error probabilities. *Genome Research* **8**: 186–194.

Faith, D. and Cranston, P. (1991). Could a cladogram this short have arisen by chance alone?: on permutation tests for cladistic structure. *Cladistics*.

Feldbrügge, M., Kämper, J., Steinberg, G., and Kahmann, R. (2004). Regulation of mating and pathogenic development in *Ustilago maydis*. *Current Opinion in Microbiology* **7**: 666–72.

Fenn, J., Mann, M., and Meng, C. (**1989**). Electrospray ionization for mass spectrometry of large biomolecules. *Science* **246**: 64–71.

Feofilova, E.P. (**2010**). The fungal cell wall: Modern concepts of its composition and biological function. *Microbiology* **79**: 711–720.

Ferguson, B.A., Dreisbach, T.A., Parks, C.G., Filip, G.M., and Schmitt, C.L. (**2003**). Coarse-scale population structure of pathogenic *Armillaria* species in a mixed-conifer forest in the Blue Mountains of northeast Oregon. *Canadian Journal of Forest Research-Revue Canadienne De Recherche Forestiere* **33**: 612–623.

Fernández-Acero, F.J., Colby, T., Harzen, A., Carbú, M., Wieneke, U., Cantoral, J.M., and Schmidt, J. (**2010**). 2-DE proteomic approach to the *Botrytis cinerea* secretome induced with different carbon sources and plant-based elicitors. *Proteomics* **10**: 2270–80.

Fernandez-Bunster, G., Gonzalez, C., Barros, J., and Martinez, M. (**2012**). Quorum Sensing Circuit and Reactive Oxygen Species Resistance in *Deinococcus* sp. *Current Microbiology* **65**: 719–25.

Fernandez-Fueyo, E., Ruiz-Dueñas, F.J., Ferreira, P., Floudas, D., Hibbett, D.S., Canessa, P., Larrondo, L.F., James, T.Y., Seelenfreund, D., Lobos, S., Polanco, R., Tello, M., Honda, Y., Watanabe, T., Watanabe, T., San, R.J., Kubicek, C.P., Schmoll, M., Gaskell, J., Hammel, K.E., *et al.* (**2012**). Comparative genomics of *Ceriporiopsis subvermispora* and *Phanerochaete chrysosporium* provide insight into selective ligninolysis. *Proceedings of the National Academy of Sciences of the United States of America* **109**: 5458–5463.

Fernández-Fueyo, E., Ruiz-Dueñas, F.J., Miki, Y., Martínez, M.J., Hammel, K.E., and Martínez, A.T. (**2012**). Lignin-degrading peroxidases from genome of selective ligninolytic fungus *Ceriporiopsis subvermispora*. *The Journal of Biological Chemistry* **287**: 16903–16.

Fetzner, S. (**2002**). Oxygenases without requirement for cofactors or metal ions. *Applied Microbiology and Biotechnology* **60**: 243–57.

Findley, K., Sun, S., Fraser, J.A., Hsueh, Y.-P., Averette, A.F., Li, W., Dietrich, F.S., and Heitman, J. (**2012**). Discovery of a modified tetrapolar sexual cycle in *Cryptococcus amylolentus* and the evolution of MAT in the *Cryptococcus* species complex. *PLoS genetics* **8**: e1002528.

Fisher, M.C., Henk, D.A., Briggs, C.J., Brownstein, J.S., Madoff, L.C., McCraw, S.L., and Gurr, S.J. (**2012**). Emerging fungal threats to animal, plant and ecosystem health. *Nature* **484**: 186–194.

Fitzkee, N.C., Fleming, P.J., and Rose, G.D. (**2005**). The Protein Coil Library: a structural database of nonhelix, nonstrand fragments derived from the PDB. *Proteins* **58**: 852–4.

Fitzpatrick, D.A., Logue, M.E., Stajich, J.E., and Butler, G. (**2006**). A fungal phylogeny based on 42 complete genomes derived from supertree and combined gene analysis. *BMC Evolutionary Bology* **6**: 99.

Fontanesi, F., Soto, I.C., and Barrientos, A. (**2008**). Cytochrome c oxidase biogenesis: new levels of regulation. *IUBMB Life* **60**: 557–68.

Foulongne-Oriol, M., Rodier, A., Rousseau, T., Largeteau, M., and Savoie, J.-M. (**2011**). Quantitative genetics to dissect the fungal-fungal interaction between *Lecanicillium verticillium* and the white button mushroom *Agaricus bisporus*. *Fungal biology* **115**: 421–31.

Fraga, B.M. (**2003**). Natural sesquiterpenoids. *Natural Product Reports* **20**: 392.

Fraga, B.M. (**2001**). Natural sesquiterpenoids. *Natural Product Reports* **17**: 650–673.

Fraga, B.M. (**1995**). Natural sesquiterpenoids. *Natural Product Reports* **12**: 303.

Fraga, B.M. (**2012**). Natural sesquiterpenoids. *Natural product reports* **29**: 1334–66.

Fragner, D., Ku, U., Zomorrodi, M., Kues, U., and Majcherczyk, A. (**2009**). Optimized protocol for the 2-DE of extracellular proteins from higher basidiomycetes inhabiting lignocellulose. *Electrophoresis* **30**: 2431–2441.

François, J.M., Guais, O., and Toulouse, F.- (**2010**). Genomic and proteomics analyses provide insights into the potential of filamentous fungi for biomass degradation. In *Mycofactories*, Ana Lucia Leitao, ed (Bentham Science Publishers), pp. 60–77.

Franken, A.C.W., Lokman, B.C., Ram, A.F.J., Punt, P.J., van den Hondel, C. a M.J.J., and de Weert, S. (**2011**). Heme biosynthesis and its regulation: towards understanding and improvement of heme biosynthesis in filamentous fungi. *Applied Microbiology and Biotechnology* **91**: 447–60.

Fröbel, J., Rose, P., Lausberg, F., Blümmel, A.-S., Freudl, R., and Müller, M. (**2012**). Transmembrane insertion of twin-arginine signal peptides is driven by TatC and regulated by TatB. *Nature Communications* **3**: 1311.

Fujisawa, S. and Kadoma, Y. (**2005**). Kinetic evaluation of polyamines as radical scavengers. *Anticancer Research* **25**: 965–9.

Fukuda, M., Nakashima, E., Hayashi, K., and Nagasawa, E. (**2003**). Identification of the biological species of *Armillaria* associated with *Wynnea* and *Entoloma abortivum* using PCR-RFLP analysis of the intergenic region (IGR) of ribosomal DNA. *Mycogical Research* **107**: 1435–41.

Galante, R.S., Taranto, A.G., Koblitz, M.G.B., Góes-Neto, A., Pirovani, C.P., Cascardo, J.C.M., Cruz, S.H., Pereira, G. a G., and Assis, S. a De (**2012**). Purification, characterization and structural determination of chitinases produced by *Moniliophthora perniciosa*. *Anais da Academia Brasileira de Ciências* **84**: 469–86.

Gao, J.M., Yang, X., Wang, C.Y., and Liu, J.K. (**2001**). Armillaramide, a new sphingolipid from the fungus *Armillaria mellea*. *Fitoterapia* **72**: 858–864.

Gao, L.W., Li, W.Y., Zhao, Y.L., and Wang, J.W. (**2009**). The cultivation, bioactive components and pharmacological effects of *Armillaria mellea*. *African Journal of Biotechnology* **8**: 7383–7390.

Gao, L.W. and Wang, J.W. (**2012**). Antioxidant Potential and DNA Damage Protecting Activity of Aqueous Extract From *Armillaria mellea*. *Journal of Food Biochemistry* **36**: 139–148.

Garcia-Conesa, M.T., Kroon, P.A., Ralph, J., Mellon, F.A., Colquhoun, I.J., Saulnier, L., Thibault, J.F., and Williamson, G. (**1999**). A cinnamoyl esterase from *Aspergillus niger* can break plant cell wall cross-links without release of free diferulic acids. *European Journal of Biochemistry* **266**: 644–52.

García-Martínez, T., Peinado, R.A., Moreno, J., García-García, I., and Mauricio, J.C. (**2011**). Co-culture of *Penicillium chrysogenum* and *Saccharomyces cerevisiae* leading to the immobilization of yeast. *Journal of Chemical Technology & Biotechnology* **86**: 812–817.

Garrett, J. (**1989**). Characterization of AAT1: a gene involved in the regulation of amino acid transport in *Saccharomyces cerevisiae*. *Journal of General Microbiology* **135**: 2429–2431.

Gaskell, S. (**1997**). Electrospray: principles and practice. *Journal of Mass Spectrometry* **32**: 677–688.

Gautam, P., Madan, T., Gade, W., and Sarma, P. (**2006**). Immunoproteomic analysis of secretory proteins of *Aspergillus fumigatus* with specific IGE immunoreactivity. *Indian Journal of Clinical Biochemistry* **21**: 12–19.

Gavnholt, B., Larsen, K., and Rasmussen, S. (**2002**). Isolation and characterisation of laccase cDNAs from meristematic and stem tissues of ryegrass (*Lolium perenne*). *Plant Science* **162**: 873–885.

Gazave, E., Lapébie, P., Renard, E., Vacelet, J., Rocher, C., Ereskovsky, A. V, Lavrov, D. V, and Borchiellini, C. (**2010**). Molecular phylogeny restores the supra-generic subdivision of homoscleromorph sponges (*Porifera, Homoscleromorpha*). *PloS ONE* **5**: e14290.

Giddings, J. (**2005**). Concepts and comparisons in multidimensional separation. *Journal of High Resolution Chromatography* **10**: 319–323.

Godio, R.P., Fouces, R., Gudiña, E.J., and Martín, J.F. (**2004**). *Agrobacterium tumefaciens*-mediated transformation of the antitumor clavaric acid-producing basidiomycete *Hypholoma sublateritium*. *Current Genetics* **46**: 287–94.

Gonzalez-Fernandez, R. and Jorrin-Novo, J. V (**2012**). Contribution of proteomics to the study of plant pathogenic fungi. *Journal of Proteome Research* **11**: 3–16.

González-Fernández, R. and Novo, J. (**2010**). Proteomics of fungal plant pathogens: the case of *Botrytis cinerea*. In *Current Research, Technology and Education Topics in Applied Microbiology and Microbial Biotechnology*, A. Mendez-Villas,

ed (Formatex Research Center C/ Zurbaran 1, 2nd Floor, Office 1, 06002 Badajoz, Spain: Badajoz, Spain), pp. 205–217.

Gonzalez-Fernandez, R., Prats, E., and Jorrin-Novo, J. V (**2010**). Proteomics of Plant Pathogenic Fungi. *Journal of Biomedicine and Biotechnology* **2010**: 1–36.

Goodman, J. and Scott, C. (**1984**). Alcohol oxidase assembles post-translationally into the peroxisome of *Candida boidinii*. *Journal of Biological Chemistry* **259**: 8485–8493.

Goodwin, S.B., M'barek, S. Ben, Dhillon, B., Wittenberg, A.H.J., Crane, C.F., Hane, J.K., Foster, A.J., Van der Lee, T. a J., Grimwood, J., Aerts, A., Antoniw, J., Bailey, A., Bluhm, B., Bowler, J., Bristow, J., van der Burgt, A., Canto-Canché, B., Churchill, A.C.L., Conde-Ferràez, L., Cools, H.J., *et al.* (**2011**). Finished genome of the fungal wheat pathogen *Mycosphaerella graminicola* reveals dispensome structure, chromosome plasticity, and stealth pathogenesis. *PLoS Genetics* **7**: e1002070.

Gottar, M., Gobert, V., Matskevich, A. a, Reichhart, J.-M., Wang, C., Butt, T.M., Belvin, M., Hoffmann, J. a, and Ferrandon, D. (**2006**). Dual detection of fungal infections in *Drosophila* via recognition of glucans and sensing of virulence factors. *Cell* **127**: 1425–37.

Götz, S., Garcia-Gómez, J.M., Terol, J., Williams, T.D., Nagaraj, S.H., Nueda, M.J., Robles, M., Talón, M., Dopazo, J., and Conesa, A. (**2008**). High-throughput functional annotation and data mining with the Blast2GO suite. *Nucleic Acids Research* **36**: 3420–3435.

Gramss, G. and Mascher, R. (**2011**). Mutual influence of soil basidiomycetes and white mustard plants on their enzymatic and catabolic activities. *Journal of Basic Microbiology* **51**: 40–51.

Gregory, S.C. (**1985**). The use of potato tubers in pathogenicity studies of *Armillaria* isolates. *Plant Pathology* **34**: 41–48.

Grigoriev, I., Cullen, D., and Goodwin, S. (**2011**). Fueling the future with fungal genomics. *Mycology* **2**: 192–209.

Grigoriev, I. V, Nordberg, H., Shabalov, I., Aerts, A., Cantor, M., Goodstein, D., Kuo, A., Minovitsky, S., Nikitin, R., Ohm, R. a, Otillar, R., Poliakov, A., Ratnere, I., Riley, R., Smirnova, T., Rokhsar, D., and Dubchak, I. (**2012**). The genome portal of the Department of Energy Joint Genome Institute. *Nucleic Acids Research* **40**: D26–32.

Grillo, R., Korhonen, K., Hantula, J., and Hietala, A.M.M. (**2000**). Genetic evidence for somatic haploidization in developing fruit bodies of Armillaria tabescens. *Fungal Genetics and Biology* **30**: 135–45.

Gstaiger, M. and Aebersold, R. (**2009**). Applying mass spectrometry-based proteomics to genetics, genomics and network biology. *Nature reviews. Genetics* **10**: 617–27.

Guillaumin, J.J., Lung, B., Romagnesi, H., Marxmuller, H., Lamoure, D., Durrieu, G., Berthelay, S., and Mohammed, C. (**1985**). The Systematics of the *Armillaria mellea* Complex - Phytopathological Consequences. *European Journal of Forest Pathology* **15**: 268–277.

Guindon, S. and Gascuel, O. (**2003**). A Simple, Fast, and Accurate Algorithm to Estimate Large Phylogenies by Maximum Likelihood. *Systematic Biology* **52**: 696–704.

Guo, W.J. and Guo, S.X. (**2008**). Steroids from *Armillaria mellea* Rhizomorphs. *Chemistry of Natural Compounds* **44**: 403–403.

Ha, H.C., Yager, J.D., Woster, P.A., and Casero, R.A. (**1998**). Structural specificity of polyamines and polyamine analogues in the protection of DNA from strand breaks induced by reactive oxygen species. *Biochemical and Biophysical Research Communications* **244**: 298–303.

Hadibarata, T. and Kristanti, R. (**2012a**). Biodegradation and metabolite transformation of pyrene by basidiomycetes fungal isolate *Armillaria* sp. F022. *Bioprocess and Biosystems Engineering* **36**: 461–468.

Hadibarata, T. and Kristanti, R.A. (**2012b**). Fate and cometabolic degradation of benzo[a]pyrene by white-rot fungus *Armillaria* sp. F022. *Bioresource Technology* **107**: 314–8.

Hadibarata, T., Yusoff, A.R.M., Aris, A., and Kristanti, R.A. (**2012**). Identification of naphthalene metabolism by white rot fungus *Armillaria* sp. F022. *Journal of Environmental Sciences* **24**: 728–732.

Hadibarata, T., Zubir, M.M.F.A., Rubiyatno, Chuang, T.Z., Yusoff, A.R.M., Salim, M.R., Fulazzaky, M.A., Seng, B., and Nugroho, A.E. (**2013**). Degradation and transformation of anthracene by the white-rot fungus Armillaria spp. F022. *Folia Microbiol (Praha)*: Epub ahead of print.

Hahn, M. (**2000**). The rust fungi. Cytology, physiology and molecular biology of infection. In *Fungal Pathology*, J. Kronstadt, ed (Kluwer Academic Publisher: Dordrecht), pp. 267–306.

Hakala, T.K., Maijala, P., Konn, J., and Hatakka, A. (**2004**). Evaluation of novel wood-rotting polypores and corticioid fungi for the decay and biopulping of Norway spruce (*Picea abies*) wood. *Enzyme and Microbial Technology* **34**: 255–263.

Hall, T. (**1999**). BioEdit: a user-friendly biological sequence alignment editor and analysis program for Windows 95/98/NT. *Nucleic Acids Symposium Series* **41**: 95–98.

Halliwell, G. (**1965**). Catalytic decomposition of cellulose under biological conditions. *Biochemical Journal* **95**: 35–40.

Hamel, L.-P., Nicole, M.-C., Duplessis, S., and Ellis, B.E. (**2012**). Mitogen-activated protein kinase signaling in plant-interacting fungi: distinct messages from conserved messengers. *The Plant Cell* **24**: 1327–51.

Hammel, K.E. and Cullen, D. (**2008**). Role of fungal peroxidases in biological ligninolysis. *Current Opinion in Plant Biology* **11**: 349–355.

Han, Q., Cai, T., Tagle, D. a, and Li, J. (**2010**). Structure, expression, and function of kynurenine aminotransferases in human and rodent brains. *Cellular and Molecular Life Sciences* **67**: 353–68.

Han, Y.-K., Kim, M.-D., Lee, S.-H., Yun, S.-H., and Lee, Y.-W. (**2007**). A novel F-box protein involved in sexual development and pathogenesis in *Gibberella zeae*. *Molecular Microbiology* **63**: 768–79.

Hao, G., Derakhshan, B., Shi, L., Campagne, F., and Gross, S.S. (**2006**). SNOSID, a proteomic method for identification of cysteine S-nitrosylation sites in complex protein mixtures. *Proceedings of the National Academy of Sciences of the United States of America* **103**: 1012–7.

Harrington, T.C., Worrall, J.J., and Baker, F.A. (**1992**). Techniques for Selected Genera of Soilborne Fungi. In *Methods for Research on Soilborne Phytopathogenic Fungi*, L.L. Singleton, J.D. Mihail, and C.M. Rush, eds (American Phytopathological Society.: St. Paul, MN), pp. 81–85.

Harris, P. V, Welner, D., McFarland, K.C., Re, E., Navarro Poulsen, J.-C., Brown, K., Salbo, R., Ding, H., Vlasenko, E., Merino, S., Xu, F., Cherry, J., Larsen, S., and Lo Leggio, L. (**2010**). Stimulation of lignocellulosic biomass hydrolysis by proteins of glycoside hydrolase family 61: structure and function of a large, enigmatic family. *Biochemistry* **49**: 3305–16.

Hashimoto, T., Tamaki, K., Suzuki, K., and Yamada, Y. (**1998**). Molecular cloning of plant spermidine synthases. *Plant & cell physiology* **39**: 73–9.

Hatakka, A. (**1994**). Lignin-modifying Enzymes from Selected White-rot Fungi - Production and role in Lignin Degradation. *FEMS Microbiology Reviews* **13**: 125–135.

Hayaishi, O. (**2005**). An odyssey with oxygen. *Biochemical and Biophysical Research Communications* **338**: 2–6.

Healy, V., Doonan, S., and McCarthy, T. V (**1999**). Purification, characterization and cDNA cloning of an endo-exonuclease from the basidiomycete fungus Armillaria mellea. *Biochemical Journal* **339 (Pt 3**: 713–20.

Healy, V., O'Connell, J., McCarthy, T. V, and Doonan, S. (**1999**). The lysine-specific proteinase from Armillaria mellea is a member of a novel class of metalloendopeptidases located in basidiomycetes. *Biochemical and Biophysical Research Communications* **262**: 60–3.

Heaton, L., Obara, B., Grau, V., Jones, N., Nakagaki, T., Boddy, L., and Fricker, M.D. (**2012**). Analysis of fungal networks. *Fungal Biology Reviews* **26**: 12–29.

Heller, J. and Tudzynski, P. (**2011**). Reactive Oxygen Species in Phytopathogenic Fungi: Signaling, Development, and Disease. *Annual Review of Phytopathology* **40**: 369–390.

Henrissat, B. (**1991**). A classification of glycosyl hydrolases based on amino acid sequence similarities. *Biochemical Journal* **280**: 309–316.

Henrissat, B. and Bairoch, A. (**1993**). New families in the classification of glycosyl hydrolases based on amino acid sequence similarities. *The Biochemical Journal* **293**: 781–8.

Henson, J., Tischler, G., and Ning, Z. (**2012**). Next-generation sequencing and large genome assemblies. *Pharmacogenomics* **13**: 901–915.

Herath, H.M.T.B., Jacob, M., Wilson, Ad., Abbas, H.K., and Nanayakkara, N.P.D. (**2012**). New secondary metabolites from bioactive extracts of the fungus *Armillaria tabescens*. *Natural Product Research*: 37–41.

Hernández-Ortega, A., Ferreira, P., and Martínez, A.T. (**2012**). Fungal aryl-alcohol oxidase: a peroxide-producing flavoenzyme involved in lignin degradation. *Applied Microbiology and Biotechnology* **93**: 1395–410.

Herron, S. and Benen, J. (**2000**). Structure and function of pectic enzymes: virulence factors of plant pathogens. *Proceedings of the National Academy of Sciences of the United States of America* **97**: 8762–8769.

Hesami, S., Metcalf, D.S., Lumsden, J.S., and Macinnes, J.I. (**2011**). Identification of cold-temperature-regulated genes in *Flavobacterium psychrophilum*. *Applied and Environmental Microbiology* **77**: 1593–600.

Hibbett, D.S., Binder, M., Bischoff, J.F., Blackwell, M., Cannon, P.F., Eriksson, O.E., Huhndorf, S., James, T., Kirk, P.M., Lücking, R., Thorsten Lumbsch, H., Lutzoni, F., Matheny, P.B., McLaughlin, D.J., Powell, M.J., Redhead, S., Schoch, C.L., Spatafora, J.W., Stalpers, J. a, Vilgalys, R., *et al.* (**2007**). A higher-level phylogenetic classification of the Fungi. *Mycological research* **111**: 509–47.

Higuchi, T., Hattori, M., Tanaka, Y., Ishitani, R., and Nureki, O. (**2009**). Crystal structure of the cytosolic domain of the cation diffusion facilitator family protein. *Proteins* **76**: 768–71.

Hilgers, M.T. and Ludwig, M.L. (**2001**). Crystal structure of the quorum-sensing protein LuxS reveals a catalytic metal site. *Proceedings of the National Academy of Sciences of the United States of America* **98**: 11169–74.

Hiller, K., Grote, A., Maneck, M., Münch, R., and Jahn, D. (**2006**). JVirGel 2.0: computational prediction of proteomes separated via two-dimensional gel electrophoresis under consideration of membrane and secreted proteins. *Bioinformatics* **22**: 2441–3.

Himmel, M.E. and Bayer, E. a (**2009**). Lignocellulose conversion to biofuels: current challenges, global perspectives. *Current Opinion in Biotechnology* **20**: 316–7.

Hodel, A.E., Gershon, P.D., Shi, X., and Quiocho, F.A. (**1996**). The 1.85 A structure of vaccinia protein VP39: a bifunctional enzyme that participates in the modification of both mRNA ends. *Cell* **85**: 247–56.

Hoegger, P.J., Navarro-González, M., Kilaru, S., Hoffmann, M., Westbrook, E.D., and Kües, U. (**2004**). The laccase gene family in *Coprinopsis cinerea (Coprinus cinereus)*. *Current Genetics* **45**: 9–18.

Hoffman, M., Góra, M., and Rytka, J. (**2003**). Identification of rate-limiting steps in yeast heme biosynthesis. *Biochemical and Biophysical Research Communications* **310**: 1247–1253.

Hofrichter, M. (**2002**). Review: lignin conversion by manganese peroxidase (MnP). *Enzyme and Microbial Technology* **30**: 454–466.

Holmquist, M. (**2000**). α/β-Hydrolase Fold Enzymes Structures, Functions and Mechanisms. *Current Protein & Peptide Science* **1**: 209–235.

Hood, I., Petrini, L., and Gardner, J. (**2008**). Colonisation of woody material in *Pinus radiata* plantations by *Armillaria novae-zelandiae* basidiospores. *Australasian Plant Pathology* **37**: 347–352.

Hood, I.A., Gardner, J.F., and Sandberg, C.J. (**2002**). *Armillaria* root disease of *Pinus radiata* in New Zealand. 1: Basidiospore dispersal. *New Zealand Journal of Forestry Science* **32**: 94–102.

Hori, C., Igarashi, K., Katayama, A., and Samejima, M. (**2011**). Effects of xylan and starch on secretome of the basidiomycete *Phanerochaete chrysosporium* grown on cellulose. *FEMS Microbiology Letters* **321**: 14–23.

Hori, C., Suzuki, H., Igarashi, K., and Samejima, M. (**2012**). Transcriptional response of the cellobiose dehydrogenase gene to cello- and xylooligosaccharides in the basidiomycete *Phanerochaete chrysosporium*. *Applied and Environmental Microbiology* **78**: 3770–3.

Horie, K., Rakwal, R., Hirano, M., Shibato, J., Nam, H.W., Kim, Y.S., Kouzuma, Y., Agrawal, G.K., Masuo, Y., and Yonekura, M. (**2008**). Proteomics of two cultivated mushrooms *Sparassis crispa* and *Hericium erinaceum* provides insight into their numerous functional protein components and diversity. *The Journal of Proteome Research* **7**: 1819–1835.

Hörth, P., Miller, C.A.C. a, Preckel, T., and Wenz, C. (**2006**). Efficient fractionation and improved protein identification by peptide OFFGEL electrophoresis. *Molecular & Cellular Proteomics* **5**: 1968–1974.

Huisman, M.M., Fransen, C.T., Kamerling, J.P., Vliegenthart, J.F., Schols, H. a, and Voragen, a G. (**2001**). The CDTA-soluble pectic substances from soybean meal are composed of rhamnogalacturonan and xylogalacturonan but not homogalacturonan. *Biopolymers* **58**: 279–94.

Hung, C., Seshan, K., and Yu, J. (**2005**). A metalloproteinase of *Coccidioides posadasii* contributes to evasion of host detection. *Infection and Immunity* **73**: 6889–6703.

Hunneyball, I.M. and Stanworth, D.R. (**1975**). Fragmentation of human IgG by a new protease isolated from the basidiomycete *Armillaria mellea*. *Immunology* **29**: 921–31.

Hunt, C.G., Houtman, C.J., Jones, D.C., Kitin, P., Korripally, P., and Hammel, K.E. (**2013**). Spatial mapping of extracellular oxidant production by a white rot basidiomycete on wood reveals details of ligninolytic mechanism. *Environmental Microbiology* **15**: 956–66.

Hunter, S., Jones, P., Mitchell, A., Apweiler, R., Attwood, T.K., Bateman, A., Bernard, T., Binns, D., Bork, P., Burge, S., de Castro, E., Coggill, P., Corbett, M., Das, U., Daugherty, L., Duquenne, L., Finn, R.D., Fraser, M., Gough, J., Haft, D., *et al.* (**2012**). InterPro in 2011: new developments in the family and domain prediction database. *Nucleic Acids Research* **40**: D306–12.

Ichinose, H. (**2013**). Cytochrome P450 of wood-rotting basidiomycetes and biotechnological applications. *Biotechnology and applied biochemistry* **60**: 71–81.

Ide, M., Ichinose, H., and Wariishi, H. (**2012**). Molecular identification and functional characterization of cytochrome P450 monooxygenases from the brown-rot basidiomycete *Postia placenta*. *Archives of Microbiology* **194**: 243–53.

Idnurm, A., Bahn, Y.-S., Nielsen, K., Lin, X., Fraser, J. a, and Heitman, J. (**2005**). Deciphering the model pathogenic fungus *Cryptococcus neoformans*. *Nature reviews. Microbiology* **3**: 753–64.

Illumina Inc. (**2012**). An Introduction to Next-Generation Sequencing Technology Welcome to Next-Generation Sequencing.

Illumina Inc. (**2010**). Illumina Sequencing Technology.

Illumina Inc. (**2011**). TruSeq ™ RNA and DNA Sample Preparation Kits v2. 2–5.

Imanaka, H., Tanaka, S., Feng, B., Imamura, K., and Nakanishi, K. (**2010**). Cultivation characteristics and gene expression profiles of Aspergillus oryzae by membrane-surface liquid culture, shaking-flask culture, and agar-plate culture. *Journal of Bioscience and Bioengineering* **109**: 267–273.

Iqbal, A., Arunlanantham, H., Brown, T., Chowdhury, R., Clifton, I.J., Kershaw, N.J., Hewitson, K.S., McDonough, M.A., and Schofield, C.J. (**2010**). Crystallographic and mass spectrometric analyses of a tandem GNAT protein from the clavulanic acid biosynthesis pathway. *Proteins* **78**: 1398–407.

Islam, M.S., Haque, M.S., Islam, M.M., Emdad, E.M., Halim, A., Hossen, Q.M.M., Hossain, M.Z., Ahmed, B., Rahim, S., Rahman, M.S., Alam, M.M., Hou, S., Wan, X., Saito, J.A., and Alam, M. (**2012**). Tools to kill: genome of one of the most destructive plant pathogenic fungi *Macrophomina phaseolina*. *BMC Genomics* **13**: 493.

Jahnke, K.D., Bahnweg, G., and Worrall, J.J. (**1987**). Species Delimitation in the *Armillaria mellea* Complex by analysis of Nuclear and Mitochondrial DNAs. *Transactions of the British Mycological Society* **88**: 572–575.

James, T.Y. (**2012**). Ancient yet fast: rapid evolution of mating genes and mating systems in fungi. In *Rapidly Evolving Genes and Genetic Systems*, R.S. Singh, J. Xu, and R.J. Kulanthinal, eds, pp. 187–198.

Janeček, Š., Svensson, B., and MacGregor, E.A. (**2011**). Structural and evolutionary aspects of two families of non-catalytic domains present in starch and glycogen binding proteins from microbes, plants and animals. *Enzyme and Microbial Technology* **49**: 429–40.

Jang, M.-K., Kong, B.-G., Jeong, Y.-I., Lee, C.H., and Nah, J.-W. (**2004**). Physicochemical characterization of α-chitin, β-chitin, and γ-chitin separated from natural resources. *Journal of Polymer Science Part A: Polymer Chemistry* **42**: 3423–3432.

Jarosz, D.F. and Lindquist, S. (**2010**). Hsp90 and environmental stress transform the adaptive value of natural genetic variation. *Science* **330**: 1820–4.

Jeffery, C.J. (**1999**). Moonlighting proteins. *Trends in Biochemical Sciences* **24**: 8–11.

Jeffery, C.J. (**2003**). Moonlighting proteins: old proteins learning new tricks. *Trends in Genetics* **19**: 415–7.

Jendrossek, D. (**2009**). Polyhydroxyalkanoate granules are complex subcellular organelles (carbonosomes). *Journal of Bacteriology* **191**: 3195–202.

Jeon, J.-R., Kim, E.-J., Murugesan, K., Park, H.-K., Kim, Y.-M., Kwon, J.-H., Kim, W.-G., Lee, J.-Y., and Chang, Y.-S. (**2010**). Laccase-catalysed polymeric dye synthesis from plant-derived phenols for potential application in hair dyeing: Enzymatic colourations driven by homo- or hetero-polymer synthesis. *Microbial Biotechnology* **3**: 324–35.

Jerez, C.A. (**2007**). Biomining in the post-genomic age: Advances and perspectives. *Biohydrometallury: from the Single Cell to the Environment* **20-21**: 389–400.

Jerez, C.A. (**2008**). The use of genomics, proteomics and other OMICS technologies for the global understanding of biomining microorganisms. *Hydrometallurgy* **94**: 162–169.

Jia, Y., Wang, Q., Chen, Z., Jiang, W., Zhang, P., and Tian, X. (**2010**). Inhibition of phytoplankton species by co-culture with a fungus. *Ecological Engineering* **36**: 1389–1391.

Jiang, C., Wang, H., Kang, Q., Liu, J., and Bai, L. (**2012**). Cloning and characterization of the polyether salinomycin biosynthesis gene cluster of Streptomyces albus XM211. *Applied and Environmental Microbiology* **78**: 994–1003.

Johannes, C. and Majcherczyk, A. (**2000**). Natural mediators in the oxidation of polycyclic aromatic hydrocarbons by laccase mediator systems. *Applied and Environmental Microbiology* **66**: 524.

Johnson, E.A. (**2013**). Biotechnology of non-*Saccharomyces* yeasts--the ascomycetes. *Applied Microbiology and Biotechnology* **97**: 503–17.

Jones, K.H. and Senft, J.A. (**1985**). An improved method to determine cell viability by simultaneous staining with fluorescein diacetate-propidium iodide. *Journal of Histochemistry & Cytochemistry* **33**: 77–79.

Jones, T. and Federspiel, N. (**2004**). The diploid genome sequence of Candida albicans. *Proceedings of the National Academy of Sciences of the United States of America* **101**: 7329–7334.

Jonkers, W., Van Kan, J.A.L., Tijm, P., Lee, Y.W., Tudzynski, P., Rep, M., and Michielse, C.B. (**2011**). The *FRP1* F- • box gene has different functions in sexuality, pathogenicity and metabolism in three fungal pathogens. *Molecular Plant Pathology* **12**: 548–563.

Jonkers, W., Rodriguez Estrada, A.E., Lee, K., Breakspear, A., May, G., and Kistler, H.C. (**2012**). Metabolome and transcriptome of the interaction between *Ustilago maydis* and *Fusarium verticillioides* in vitro. *Applied and Environmental Microbiology* **78**: 3656–67.

Jungblut, P., Thiede, B., Zimny-Arndt, U., Müller, E.C., Scheler, C., Wittmann-Liebold, B., and Otto, a (**1996**). Resolution power of two-dimensional electrophoresis and identification of proteins from gels. *Electrophoresis* **17**: 839–47.

Juretschke, J., Menssen, R., Sickmann, A., and Wolf, D.H. (**2010**). The Hsp70 chaperone Ssa1 is essential for catabolite induced degradation of the gluconeogenic enzyme fructose-1,6-bisphosphatase. *Biochemical and Biophysical Research Communications* **397**: 447–52.

Käll, L., Krogh, A., and Sonnhammer, E.L.L. (**2004**). A combined transmembrane topology and signal peptide prediction method. *Journal of Molecular Biology* **338**: 1027–36.

Kalyoncu, F., Oskay, M., Sağlam, H., Erdoğan, T.F., and Tamer, A.U. (**2010**). Antimicrobial and antioxidant activities of mycelia of 10 wild mushroom species. *Journal of Medicinal Food* **13**: 415–9.

Kamo, T., Endo, M., Sato, M., Kasahara, R., Yamaya, H., Hiradate, S., Fujii, Y., Hirai, N., and Hirota, M. (**2008**). Limited distribution of natural cyanamide in higher plants: occurrence in *Vicia villosa subsp. varia, V. cracca*, and *Robinia pseudo-acacia*. *Phytochemistry* **69**: 1166–72.

Kämper, J., Kahmann, R., Bölker, M., Ma, L.-J., Brefort, T., Saville, B.J., Banuett, F., Kronstad, J.W., Gold, S.E., Müller, O., Perlin, M.H., Wösten, H. a B., de Vries, R., Ruiz-Herrera, J., Reynaga-Peña, C.G., Snetselaar, K., McCann, M., Pérez-Martín, J., Feldbrügge, M., Basse, C.W., *et al.* (**2006**). Insights from the

genome of the biotrophic fungal plant pathogen *Ustilago maydis*. *Nature* **444**: 97–101.

Kanehisa, M. and Goto, S. (**2000**). KEGG: kyoto encyclopedia of genes and genomes. *Nucleic Acids Research* **28**: 27–30.

Kanehisa, M., Goto, S., Sato, Y., Furumichi, M., and Tanabe, M. (**2012**). KEGG for integration and interpretation of large-scale molecular data sets. *Nucleic Acids Research* **40**: D109–14.

Kang, K.-H., Dec, J., Park, H., and Bollag, J.-M. (**2002**). Transformation of the fungicide cyprodinil by a laccase of *Trametes villosa* in the presence of phenolic mediators and humic acid. *Water Research* **36**: 4907–15.

Kaufmann, R. (**1995**). Matrix-assisted laser desorption ionization (MALDI) mass spectrometry: a novel analytical tool in molecular biology and biotechnology. *Journal of Biotechnology* **41**: 155–175.

Kaushal, R., Sharma, N., and Tandon, D. (**2012**). Cellulase and xylanase production by co-culture of *Aspergillus niger* and *Fusarium oxysporum* utilizing forest waste. *Turkish Journal of Biochemistry* **37**: 35–41.

Kawata, T., Nakagawa, M., Shimada, N., Fujii, S., and Oohata, A. a (**2004**). A gene encoding, prespore-cell-inducing factor in *Dictyostelium discoideum. Development, Growth & Differentiation* **46**: 383–92.

Keane, T., Naughton, T., and McInerney, J. (**2004**). ModelGenerator: amino acid and nucleotide substitution model selection. *... ://bioinf. nuim. ie/software/modelgenerator*.

Kerr, J.R. (**1999**). Bacterial inhibition of fungal growth and pathogenicity. *Microbial Ecology in Health and Disease* **11**: 129–142.

Kersten, P. and Cullen, D. (**2007**). Extracellular oxidative systems of the lignin-degrading Basidiomycete *Phanerochaete chrysosporium. Fungal Genetics and Biology* **44**: 77–87.

Keum, Y.S. and Li, Q.X. (**2004**). Fungal laccase-catalyzed degradation of hydroxy polychlorinated biphenyls. *Chemosphere* **56**: 23–30.

Kile, G. and Watling, R. (**1988**). Identification and occurrence of Australian Armillaria species, including A. pallidula sp. nov. and comparative studies between them and non-Australian. *Transactions of the British Mycological Society* **91**: 305–315.

Kim, M. and Klopfenstein, N. (**2000**). Characterization of North American *Armillaria* species by nuclear DNA content and RFLP analysis. *Mycologia* **5**: 874–883.

Kim, S., Lapham, A.N., Freedman, C.G.K., Reed, T.L., and Schmidt, W.K. (**2005**). Yeast as a tractable genetic system for functional studies of the insulin-degrading enzyme. *The Journal of Biological Chemistry* **280**: 27481–90.

Kim, S., Park, S., Min, T., and Yu, K. (**1999**). Antioxidant Activity of Ergosterol Peroxide (5,8-Epidioxy-5 ,8 -ergosta-6,22E-dien-3 -ol) in *Armillariella mellea*. *Bulletin of the Korean Chemical Society* **20**: 819–823.

Kim, S., Schilke, B., Craig, E.A., and Horwich, A.L. (**1998**). Folding in vivo of a newly translated yeast cytosolic enzyme is mediated by the SSA class of cytosolic yeast Hsp70 proteins. *Proceedings of the National Academy of Sciences of the United States of America* **95**: 12860–5.

Kim, S.K., Im, J., Yun, C.-H., Son, J.Y., Son, C.G., Park, D.K., and Han, S.H. (**2008**). *Armillariella mellea* induces maturation of human dendritic cells without induction of cytokine expression. *Journal of Ethnopharmacology* **119**: 153–9.

Kim, Y., Nandakumar, M., and Marten, M.R. (**2007**). Proteomics of filamentous fungi. *Trends in biotechnology* **25**: 395–400.

King, B.C., Waxman, K.D., Nenni, N. V, Walker, L.P., Bergstrom, G.C., and Gibson, D.M. (**2011**). Arsenal of plant cell wall degrading enzymes reflects host preference among plant pathogenic fungi. *Biotechnology for Biofuels* **4**: 4.

Klinkenberg, L. and Mennella, T. (**2005**). Combinatorial repression of the hypoxic genes of Saccharomyces cerevisiae by DNA binding proteins Rox1 and Mot3. *Eukaryotic Cell* **4**: 649–660.

Klose, J. and Kobalz, U. (**1995**). 2-Dimensional electophoresis of proteins - an updated proteocol and implications for a functional analysis of the genome. *Electrophoresis* **16**: 1034–1059.

Kniemeyer, O. (**2011**). Proteomics of eukaryotic microorganisms: The medically and biotechnologically important fungal genus *Aspergillus*. *Proteomics* **11**: 3232–43.

Koenigs, J. (**1974**). Hydrogen peroxide and iron: a proposed system for decomposition of wood by brown-rot basidiomycetes. *Wood and Fiber Science* **6**: 66–79.

Köllner, T.G., O'Maille, P.E., Gatto, N., Boland, W., Gershenzon, J., and Degenhardt, J. (**2006**). Two pockets in the active site of maize sesquiterpene synthase TPS4 carry out sequential parts of the reaction scheme resulting in multiple products. *Archives of Biochemistry and Biophysics* **448**: 83–92.

Kombrink, E., Schroder, M., and Hahlbrock, K. (**1988**). Several "pathogenesis-related" proteins in potato are 1, 3-β-glucanases and chitinases. *Proceedings of the National Academy of Sciences of the United States of America* **85**: 782–786.

Korhonen, K. (**1978**). Infertility and clonal size in the Armillariella mellea complex. *Karstenia* **18**: 31–42.

Korhonen, K. and Hintikka, V. (**1974**). Cytological evidence for somatic diploidization in dikaryotic cells of *Armillariella mellea*. *Archives of Microbiology* **95**: 187–192.

Kozarewa, I., Ning, Z., Quail, M.A., Sanders, M.J., Berriman, M., Turner, D.J., and America, N. (**2009**). Amplification-free Illumina sequencing-library

preparation facilitates improved mapping and assembly of (G + C) -biased genomes. *Nature Methods* **6**: 291–295.

Kozubowski, L. and Heitman, J. (**2012**). Profiling a killer, the development of *Cryptococcus neoformans. FEMS microbiology reviews* **36**: 78–94.

Kristan, K. and Rižner, T.L. (**2012**). Steroid-transforming enzymes in fungi. *The Journal of Steroid Biochemistry and Molecular Biology* **129**: 79–91.

Kuees, U., Ruehl, M., Kües, U., and Rühl, M. (**2011**). Multiple Multi-Copper Oxidase Gene Families in Basidiomycetes - What for? *Current Genomics* **12**: 72–94.

Kummer, P. (**1871**). Der Führer in die Pilzkunde (Zerbst : Verlag von E. Luppe's Buchhandlung).

Kunamneni, A., Plou, F.J., Ballesteros, A., and Alcalde, M. (**2008**). Laccases and their applications: a patent review. *Recent Patents on Biotechnology* **2**: 10–24.

Kwan, D.H. and Schulz, F. (**2011**). The stereochemistry of complex polyketide biosynthesis by modular polyketide synthases. *Molecules* **16**: 6092–115.

Labbé, J., Murat, C., Morin, E., Tuskan, G. a, Le Tacon, F., and Martin, F. (**2012**). Characterization of transposable elements in the ectomycorrhizal fungus *Laccaria bicolor. PloS ONE* **7**: e40197.

Lacadena, J., Alvarez-García, E., Carreras-Sangrà, N., Herrero-Galán, E., Alegre-Cebollada, J., García-Ortega, L., Oñaderra, M., Gavilanes, J.G., and Martínez del Pozo, A. (**2007**). Fungal ribotoxins: molecular dissection of a family of natural killers. *FEMS microbiology reviews* **31**: 212–37.

Lackner, G., Misiek, M., Braesel, J., and Hoffmeister, D. (**2012**). Genome mining reveals the evolutionary origin and biosynthetic potential of basidiomycete polyketide synthases. *Fungal Genetics and Biology* **49**: 996–1003.

Laemmli, U.K. (**1970**). Cleavage of Structural Proteins during the Assembly of the Head of Bacteriophage T4. *Nature* **227**: 680–685.

Lamoure, D. (**1985**). Le cycle caryologique des *Armillaires* du groupe *mellea*. *European Journal of Forest Pathology* **15**: 288–293.

Larkin, M.A., Blackshields, G., Brown, N.P., Chenna, R., McGettigan, P.A., McWilliam, H., Valentin, F., Wallace, I.M., Wilm, A., Lopez, R., Thompson, J.D., Gibson, T.J., and Higgins, D.G. (**2007**). Clustal W and Clustal X version 2.0. *Bioinformatics* **23**: 2947–8.

Laursen, L.S., Overgaard, M.T., Søe, R., Boldt, H.B., Sottrup-Jensen, L., Giudice, L.C., Conover, C. a, and Oxvig, C. (**2001**). Pregnancy-associated plasma protein-A (PAPP-A) cleaves insulin-like growth factor binding protein (IGFBP)-5 independent of IGF: implications for the mechanism of IGFBP-4 proteolysis by PAPP-A. *FEBS Letters* **504**: 36–40.

Leach, M.D., Klipp, E., Cowen, L.E., and Brown, A.J.P. (**2012**). Fungal Hsp90: a biological transistor that tunes cellular outputs to thermal inputs. *Nature reviews. Microbiology* **10**: 693–704.

Lee, I. (**2008**). Ranpirnase (Onconase), a cytotoxic amphibian ribonuclease, manipulates tumour physiological parameters as a selective killer and a potential enhancer for chemotherapy and radiation in cancer therapy. *Expert Opinion on Bological Therapy* **8**: 813–27.

Lee, J.R., Kim, S.Y., Chae, H.B., Jung, J.H., and Lee, S.Y. (**2009**). Antifungal activity of *Saccharomyces cerevisiae* peroxisomal 3-ketoacyl-CoA thiolase. *Biochemistry and Molecular Biology reports* **42**: 281–5.

Lee, J.S.J.-S., Oka, K., Watanabe, O., Hara, H., and Ishizuka, S. (**2010**). Immunomodulatory effect of mushrooms on cytotoxic activity and cytokine production of intestinal lamina propria leukocytes does not necessarily depend on β-glucan contents. *Food Chemistry* **126**: 1521–1526.

Lee, S.Y., Kim, J.S.E., Sapkota, K., Shen, M.H., Kim, S.J., Chun, H.S., Yoo, J.C., Choi, H.S., and Kim, M.K. (**2005**). Purification and characterization of fibrinolytic enzyme from cultured mycelia of *Armillaria mellea. Protein Expression and Purification* **43**: 10–17.

Lee, W., Park, E., Ahn, J., and Ka, K. (**2009**). Ergothioneine Contents in Fruiting Bodies and Their Enhancement in Mycelial Cultures by the Addition of Methionine. *Mycobiology* **37**: 43–47.

Lenfant, N., Hotelier, T., Velluet, E., Bourne, Y., Marchot, P., and Chatonnet, A. (**2013**). ESTHER, the database of the α/β-hydrolase fold superfamily of proteins: tools to explore diversity of functions. *Nucleic acids research* **41**: D423–9.

Leonowicz, A., Cho, N.S., Luterek, J., Wilkolazka, A., Wojtas-Wasilewska, M., Matuszewska, A., Hofrichter, M., Wesenberg, D., and Rogalski, J. (**2001**). Fungal laccase: properties and activity on lignin. *Journal of Basic Microbiology* **41**: 185–227.

León-Ramírez, C.G., Valdés-Santiago, L., Campos-Góngora, E., Ortiz-Castellanos, L., Aréchiga-Carvajal, E.T., and Ruiz-Herrera, J. (**2010**). A molecular probe for Basidiomycota: the spermidine synthase-saccharopine dehydrogenase chimeric gene. *FEMS microbiology letters* **312**: 77–83.

Lesburg, C., Caruthers, J., Paschall, C., and Christianson, D. (**1998**). Managing and manipulating carbocations in biology: terpenoid cyclase structure and mechanism. *Current Opinion in Structural Biology* **8**: 695–703.

Lessing, F., Kniemeyer, O., Wozniok, I., Loeffler, J., Kurzai, O., Haertl, A., and Brakhage, A. a (**2007**). The *Aspergillus fumigatus* transcriptional regulator AfYap1 represents the major regulator for defense against reactive oxygen intermediates but is dispensable for pathogenicity in an intranasal mouse infection model. *Eukaryotic Cell* **6**: 2290–302.

Lewis, W.G., Basford, J.M., and Walton, P.L. (**1978a**). Specificity and Inhibition Studies of *Armillaria mellea* Protease. *Biochimica et Biophysica Acta* **522**: 551–560.

Lewis, W.G., Basford, J.M., and Walton, P.L. (**1978b**). Specificity and inhibition studies of Armillaria mellea protease. *Biochimca Biophysica Acta* **522**: 551–60.

Li, J., Yu, L., Tian, Y., and Zhang, K.-Q. (**2012**). Molecular evolution of the deuterolysin (M35) family genes in *Coccidioides. PloS ONE* **7**: e31536.

Li, P., Wang, H., Liu, G., Li, X., and Yao, J. (**2011**). The effect of carbon source succession on laccase activity in the co-culture process of *Ganoderma lucidum* and a yeast. *Enzyme and Microbial Technology* **48**: 1–6.

Li, Q., Harvey, L.M., and McNeil, B. (**2009**). Oxidative stress in industrial fungi. *Critical Reviews in Biotechnology* **29**: 199–213.

Li, S., Finley, J., Liu, Z.-J., Qiu, S.-H., Chen, H., Luan, C.-H., Carson, M., Tsao, J., Johnson, D., Lin, G., Zhao, J., Thomas, W., Nagy, L. a, Sha, B., DeLucas, L.J., Wang, B.-C., and Luo, M. (**2002**). Crystal structure of the cytoskeleton-associated protein glycine-rich (CAP-Gly) domain. *The Journal of Biological Chemistry* **277**: 48596–601.

Lin, S.-X., Gangloff, A., Huang, Y.-W., and Xie, B. (**1999**). Electrophoresis of hydrophobic proteins. *Analytica Chimica Acta* **383**: 101–107.

Link, A.J. (**2002**). Multidimensional peptide separations in proteomics. *Trends in Biotechnology* **20**: S8–13.

Link, A.J., Eng, J., Schieltz, D.M., Carmack, E., Mize, G.J., Morris, D.R., Garvik, B.M., and Yates, J.R. (**1999**). Direct analysis of protein complexes using mass spectrometry. *Nature biotechnology* **17**: 676–82.

Liu, L., Li, Y., Li, S., Hu, N., He, Y., Pong, R., Lin, D., Lu, L., and Law, M. (**2012**). Comparison of Next-Generation Sequencing Systems. *Journal of Biomedicine and Biotechnology* **2012**: 1–11.

Liu, Q., Siloto, R.M.P., Snyder, C.L., and Weselake, R.J. (**2011**). Functional and topological analysis of yeast acyl-CoA:diacylglycerol acyltransferase 2, an endoplasmic reticulum enzyme essential for triacylglycerol biosynthesis. *The Journal of Biological Chemistry* **286**: 13115–26.

Liu, Q.P., Sulzenbacher, G., Yuan, H., Bennett, E.P., Pietz, G., Saunders, K., Spence, J., Nudelman, E., Levery, S.B., White, T., Neveu, J.M., Lane, W.S., Bourne, Y., Olsson, M.L., Henrissat, B., and Clausen, H. (**2007**). Bacterial glycosidases for the production of universal red blood cells. *Nature Biotechnology* **25**: 454–64.

Liu, T.-B., Wang, Y., Stukes, S., Chen, Q., Casadevall, A., and Xue, C. (**2011**). The F-Box protein Fbp1 regulates sexual reproduction and virulence in Cryptococcus neoformans. *Eukaryotic cell* **10**: 791–802.

Liu, T.-B. and Xue, C. (**2011**). The Ubiquitin-Proteasome System and F-box Proteins in Pathogenic Fungi. *Mycobiology* **39**: 243–8.

Liu, X., Tang, W.-H., Zhao, X.-M., and Chen, L. (**2010**). A network approach to predict pathogenic genes for *Fusarium graminearum. PloS ONE* **5**.

Liu, Y. and Dong, S. (**2007**). A biofuel cell harvesting energy from glucose-air and fruit juice-air. *Biosensors & Bioelectronics* **23**: 593–7.

Lombard, V., Bernard, T., Rancurel, C., Brumer, H., Coutinho, P.M., and Henrissat, B. (**2010**). A hierarchical classification of polysaccharide lyases for glycogenomics. *The Biochemical Journal* **432**: 437–44.

Lorenz, P. and Zinke, H. (**2005**). White biotechnology: differences in US and EU approaches? *Trends in Biotechnology* **23**: 570–574.

Losada, L., Ajayi, O., Frisvad, J.C.C., Yu, J.J., and Nierman, W.C.C. (**2009**). Effect of competition on the production and activity of secondary metabolites in *Aspergillus species. Medical Mycology* **47**: S88–S96.

Löwer, M., Weydig, C., Metzler, D., Reuter, A., Starzinski-Powitz, A., Wessler, S., and Schneider, G. (**2008**). Prediction of extracellular proteases of the human pathogen *Helicobacter pylori* reveals proteolytic activity of the Hp1018/19 protein HtrA. *PloS ONE* **3**: e3510.

Lubec, G., Afjehi-Sadat, L., Yang, J.-W., and John, J.P.P. (**2005**). Searching for hypothetical proteins: theory and practice based upon original data and literature. *Progress in Neurobiology* **77**: 90–127.

Lundell, T.K., Mäkelä, M.R., and Hildén, K. (**2010**). Lignin-modifying enzymes in filamentous basidiomycetes--ecological, functional and phylogenetic review. *Journal of Basic Microbiology* **50**: 5–20.

Lundquist, J.E. (**1993**). Spatial and Temporal Characteristics of Canopy Gaps Caused by *Armillaria* Root Disease and their Management Implications in Lowveld Forests of South-Africa. *European Journal of Forest Pathology* **23**: 362–371.

Lung, M.-Y. and Chang, Y.-C. (**2011**). Antioxidant Properties of the Edible Basidiomycete Armillaria mellea in Submerged Cultures. *International Journal of Molecular Sciences* **12**: 6367–6384.

Lung, M.Y. and Hsieh, C.W. (**2011**). Antioxidant property and production of exopolysaccharide from *Armillaria mellea* in submerged cultures: Effect of culture aeration rate. *Engineering in Life Sciences* **11**: 482–490.

Luo, S. and Levine, R.L. (**2009**). Methionine in proteins defends against oxidative stress. *Federation of American Societies for Experimental Biology* **23**: 464–72.

Lushchak, V.I. (**2011**). Adaptive response to oxidative stress: Bacteria, fungi, plants and animals. *Comparative Biochemistry and Physiology, Part C* **153**: 175–90.

Lynd, L.R., Laser, M.S., Brandsby, D., Dale, B.E., Davison, B., Hamilton, R., Himmel, M., Keller, M., McMillan, J.D., Sheehan, J., and Wyman, C.E. (**2008**). How biotech can transform biofuels. *Nature Biotechnology* **26**: 169–172.

Ma, L., Chen, H., Dong, P., and Lu, X. (**2013**). Anti-inflammatory and anticancer activities of extracts and compounds from the mushroom *Inonotus obliquus. Food Chemistry* **139**: 503–8.

Macaulay, J. (**1988**). Metabolites of *Armillaria mellea* and synthetic studies on a potention iron-binding fungal metabolite and analogues.

Machida, M., Asai, K., Sano, M., Tanaka, T., Kumagai, T., Terai, G., Kusumoto, K.-I., Arima, T., Akita, O., Kashiwagi, Y., Abe, K., Gomi, K., Horiuchi, H., Kitamoto, K., Kobayashi, T., Takeuchi, M., Denning, D.W., Galagan, J.E., Nierman, W.C., Yu, J., *et al.* (**2005**). Genome sequencing and analysis of *Aspergillus oryzae. Nature* **438**: 1157–61.

Mahajan, S. and Master, E.R. (**2010**). Proteomic characterization of lignocellulose-degrading enzymes secreted by *Phanerochaete carnosa* grown on spruce and microcrystalline cellulose. *Applied Microbiology and Biotechnology* **86**: 1903–1914.

Maier-Greiner, U.H., Obermaier-Skrobranek, B.M., Estermaier, L.M., Kammerloher, W., Freund, C., Wülfing, C., Burkert, U.I., Matern, D.H., Breuer, M., and Eulitz, M. (**1991**). Isolation and properties of a nitrile hydratase from the soil fungus *Myrothecium verrucaria* that is highly specific for the fertilizer cyanamide and cloning of its gene. *Proceedings of the National Academy of Sciences of the United States of America* **88**: 4260–4.

Mallett, K. (**1985**). *Armillaria* root rot in Alberta, pathogenicity,identification and detection. *Forest Science and Plant Science* **Ph.D**: 169.

Manavalan, A., Adav, S.S., and Sze, S.K. (**2011**). iTRAQ-based quantitative secretome analysis of *Phanerochaete chrysosporium. Journal of Proteomics*.

Mander, G.J., Wang, H., Bodie, E., Wagner, J., Vienken, K., Vinuesa, C., Foster, C., Leeder, A.C., Allen, G., Hamill, V., Janssen, G.G., Dunn-Coleman, N., Karos, M., Lemaire, H.G., Subkowski, T., Bollschweiler, C., Turner, G., Nüsslein, B., and Fischer, R. (**2006**). Use of laccase as a novel, versatile reporter system in filamentous fungi. *Applied and Environmental Microbiology* **72**: 5020–6.

Mapari, S.A.S., Meyer, A.S., Thrane, U., and Frisvad, J.C. (**2009**). Identification of potentially safe promising fungal cell factories for the production of polyketide natural food colorants using chemotaxonomic rationale. *Microbial Cell Factories* **8**: 1–15.

Marcais, B. and Wargo, P.M. (**2000**). Impact of liming on the abundance and vigor of *Armillaria* rhizomorphs in Allegheny hardwoods stands. *Canadian Journal of Forest Research* **30**: 1847–1857.

Marchitti, S. a, Brocker, C., Stagos, D., and Vasiliou, V. (**2008**). Non-P450 aldehyde oxidizing enzymes: the aldehyde dehydrogenase superfamily. *Expert Opinion on Drug Metabolism & Toxicology* **4**: 697–720.

Marienhagen, J. and Kennerknecht, N. (**2005**). Functional analysis of all aminotransferase proteins inferred from the genome sequence of *Corynebacterium glutamicum*. *Journal Of Bacteriology* **187**: 7639–7646.

Markussen, E.K. and P.E. Jensen (**2006**). Stabilisation of granules comprising active compounds - WO2006053564 A2.

Martin, F., Aerts, A., Ahren, D., Brun, A., Danchin, E.G.J., Duchaussoy, F., Gibon, J., Kohler, A., Lindquist, E., Pereda, V., Salamov, A., Shapiro, H.J., Wuyts, J., Blaudez, D., Buee, M., Brokstein, P., Canback, B., Cohen, D., Courty, P.E., Coutinho, P.M., *et al.* (**2008**). The genome of *Laccaria bicolor* provides insights into mycorrhizal symbiosis. *Nature* **452**: 88–92.

Martínez, A.T., Speranza, M., Ruiz-Dueñas, F.J., Ferreira, P., Camarero, S., Guillén, F., Martínez, M.J., Gutiérrez, A., and del Río, J.C. (**2005**). Biodegradation of lignocellulosics: microbial, chemical, and enzymatic aspects of the fungal attack of lignin. *International microbiology* **8**: 195–204.

Martinez, D., Challacombe, J., Morgenstern, I., Hibbett, D., Schmoll, M., Kubicek, C.P., Ferreira, P., Ruiz-Duenas, F.J., Martinez, A.T., Kersten, P., Hammel, K.E., Vanden Wymelenberg, A., Gaskell, J., Lindquist, E., Sabat, G., Bondurant, S.S., Larrondo, L.F., Canessa, P., Vicuna, R., Yadav, J., *et al.* (**2009**). Genome, transcriptome, and secretome analysis of wood decay fungus *Postia placenta* supports unique mechanisms of lignocellulose conversion. *Proceedings of the National Academy of Sciences of the United States of America* **106**: 1954–9.

Martinez, D., Larrondo, L.F., Putnam, N., Gelpke, M.D.S., Huang, K., Chapman, J., Helfenbein, K.G., Ramaiya, P., Detter, J.C., Larimer, F., Coutinho, P.M., Henrissat, B., Berka, R., Cullen, D., and Rokhsar, D. (**2004**). Genome sequence of the lignocellulose degrading fungus *Phanerochaete chrysosporium* strain RP78. *Nature Biotechnology* **22**: 695–700.

Martins, M.B. and Carvalho, I. (**2007**). Diketopiperazines: biological activity and synthesis. *Tetrahedron* **63**: 9923–9932.

Matsuzaki, F., Shimizu, M., and Wariishi, H. (**2008**). Proteomic and Metabolomic Analyses of the White-Rot Fungus Phanerochaete chrysosporium Exposed to Exogenous Benzoic Acid. *Journal of Proteome Research* **7**: 2342–2350.

Mattinen, M.-L., Kontteli, M., Kerovuo, J., Drakenberg, T., Annila, A., Linder, M., Reinikainen, T., and Lindeberg, G. (**2008**). Three-dimensional structures of three engineered cellulose-binding domains of cellobiohydrolase I from *Trichoderma reesei*. *Protein Science* **6**: 294–303.

McClung, J.K., Jupe, E.R., Liu, X.T., and Dell'Orco, R.T. (**1995**). Prohibitin: potential role in senescence, development, and tumor suppression. *Experimental Gerontology* **30**: 99–124.

McDonald, W.H., Ohi, R., Miyamoto, D.T., Mitchison, T.J., and Yates, J.R. (**2002**). Comparison of three directly coupled HPLC MS/MS strategies for identification of proteins from complex mixtures: single-dimension LC-MS/MS, 2-phase MudPIT, and 3-phase MudPIT. *International Journal of Mass Spectrometry* **219**: 245–251.

McLaughlin, D.J., Hibbett, D.S., Lutzoni, F., Spatafora, J.W., and Vilgalys, R. (**2009**). The search for the fungal tree of life. *Trends in Microbiology* **17**: 488–97.

Mehmood, M.A., Xiao, X., Hafeez, F.Y., Gai, Y., and Wang, F. (**2011**). Molecular characterization of the modular chitin binding protein Cbp50 from *Bacillus thuringiensis* serovar konkukian. *Antonie van Leeuwenhoek* **100**: 445–53.

Meyer, P., Prodromou, C., Liao, C., Hu, B., Mark Roe, S., Vaughan, C.K., Vlasic, I., Panaretou, B., Piper, P.W., and Pearl, L.H. (**2004**). Structural basis for recruitment of the ATPase activator Aha1 to the Hsp90 chaperone machinery. *The EMBO journal* **23**: 511–9.

Michalski, A., Cox, J., and Mann, M. (**2011**). More than 100,000 detectable peptide species elute in single shotgun proteomics runs but the majority is inaccessible to data-dependent LC-MS/MS. *Journal of Proteome Research* **10**: 1785–93.

Mieczkowski, P. a, Lemoine, F.J., and Petes, T.D. (**2006**). Recombination between retrotransposons as a source of chromosome rearrangements in the yeast Saccharomyces cerevisiae. *DNA Repair* **5**: 1010–20.

Mihail, J.D. (**2013**). Comparative bioluminescence dynamics among multiple *Armillaria gallica, A. mellea,* and *A. tabescens* genets. *Fungal biology* **117**: 202–10.

Mihail, J.D. and Bruhn, J.N. (**2007**). Dynamics of bioluminescence by *Armillaria gallica, A. mellea* and *A. tabescens*. *Mycologia* **99**: 341–350.

Mihail, J.D. and Bruhn, J.N. (**2005**). Foraging behaviour of *Armillaria* rhizomorph systems. *Mycological Research* **109**: 1195–207.

Miller, J.R., Busby, R.W., Jordan, S.W., Cheek, J., Henshaw, T.F., Ashley, G.W., Broderick, J.B., Cronan, J.E., and Marletta, M.A. (**2000**). *Escherichia coli* LipA is a lipoyl synthase: in vitro biosynthesis of lipoylated pyruvate dehydrogenase complex from octanoyl-acyl carrier protein. *Biochemistry* **39**: 15166–78.

Miller, R. (**1994**). Estimated peach tree losses from 1980 to 1992 in South Carolina, causes and economic impact. In *Proceedings of the 6th Stone Fruit Decline Workshop* (Fort Valley, GA), pp. 121–127.

Mishra, S. and Kamisaka, Y. (**2001**). Purification and characterization of thiol-reagent-sensitive glycerol-3-phosphate acyltransferase from the membrane fraction of an oleaginous fungus. *The Biochemical journal* **355**: 315–22.

Misiek, M., Braesel, J., and Hoffmeister, D. (**2011**). Characterisation of the ArmA adenylation domain implies a more diverse secondary metabolism in the genus *Armillaria*. *Fungal Biology* **115**: 775–781.

Misiek, M. and Hoffmeister, D. (**2008**). Processing sites involved in intron splicing of *Armillaria* natural product genes. *Mycological Research* **112**: 216–224.

Misiek, M. and Hoffmeister, D. (**2010**). Sesquiterpene aryl ester natural products in North American *Armillaria* species. *Mycological Progress* **11**: 7–15.

Misiek, M., Williams, J., Schmich, K., Hu ttel, W., Merfort, I., Salomon, C.E.E.C.E., Aldrich, C.C.C., Hoffmeister, D., and Huttel, W. (**2009**). Structure and Cytotoxicity of Arnamial and Related Fungal Sesquiterpene Aryl Esters. *Journal of Natural Products* **72**: 1888–1891.

Moffatt, B. and Weretilnyk, E. (**2001**). Sustaining S-adenosyl- L-methionine-dependent methyltransferase activity in plant cells. *Physiologia Plantarum* **113**: 435–442.

Mohan, R. and Venugopal, S. (**2012**). Computational structural and functional analysis of hypothetical proteins of *Staphylococcus aureus*. *Bioinformation* **8**: 722–8.

Momose, I., Sekizawa, R., Hosokawa, N., Iinuma, H., Matsui, S., Nakamura, H., Naganawa, H., Hamada, M., and Takeuchi, T. (**2000**). Melleolides K, L and M, new melleolides from *Armillariella mellea. The Journal of Antibiotics* **53**: 137–43.

Monteoliva, L. and Martinez-Lopez, R. (**2011**). Quantitative proteome and acidic subproteome profiling of Candida albicans yeast-to-hypha transition. *Journal of Proteome Research* **10**: 502–517.

Morano, K. and Santoro, N. (**1999**). A trans-activation domain in yeast heat shock transcription factor is essential for cell cycle progression during stress. *Molecular and Cellular Biology* **19**: 402–411.

Moree, W.J., Phelan, V. V, Wu, C.-H., Bandeira, N., Cornett, D.S., Duggan, B.M., and Dorrestein, P.C. (**2012**). Interkingdom metabolic transformations captured by microbial imaging mass spectrometry. *Proceedings of the National Academy of Sciences of the United States of America* **109**: 13811–13816.

Moreira-Neto, S.L., Mussatto, S.I., Machado, K.M.G., and Milagres, a M.F. (**2013**). Decolorization of salt-alkaline effluent with industrial reactive dyes by laccase-producing basidiomycetes strains. *Letters in Applied Microbiology* **56**: 283–90.

Morishima, N. (**2005**). Control of cell fate by Hsp70: more than an evanescent meeting. *Journal of Biochemistry* **137**: 449–53.

Morrison, D.J. (**1991**). Identity of *Armillaria* isolates used in studies of rhizomorph behaviour and pathogenicity. *Mycological Research* **95**: 1437–1438.

Morrison, D.J. (**2004**). Rhizomorph growth habit, saprophytic ability and virulence of 15 *Armillaria* species. *Forest Pathology* **34**: 15–26.

Morrison, D.J. (**1982**). Variation among British isolates of Armillaria mellea. *Transactions of the British Mycological Society* **78**: 459–463.

Motta, J. (**1969**). Cytology and morphogenesis in the rhizomorph of *Armillaria mellea*. *American Journal of Botany* **56**: 610–619.

Motta, J. (**1985**). Evidence for significant differences in nuclear DNA content between two geographically isolated clones of Armillaria mellea. *American Journal of Botany* **72**: 1307–1310.

Mulder, N.J. and Apweiler, R. (**2008**). The InterPro database and tools for protein domain analysis. In *Current Protocols in Bioinformatics*, p. Unit 2.7.

Mullen, J.R., Chen, C.-F., and Brill, S.J. (**2010**). Wss1 is a SUMO-dependent isopeptidase that interacts genetically with the Slx5-Slx8 SUMO-targeted ubiquitin ligase. *Molecular and Cellular Biology* **30**: 3737–48.

Murao, S., Arai, M., Tanaka, N., Ishikawa, H., and Matsumoto, K. (**1985**). A Method for Assaying of α-Glucosidase and α-Amylase Using Laccase. *Agricultural Biological Chemistry* **49**: 981–985.

Muszkieta, L., Beauvais, A., Pähtz, V., Gibbons, J.G., Anton Leberre, V., Beau, R., Shibuya, K., Rokas, A., Francois, J.M., Kniemeyer, O., Brakhage, A. a, and Latgé, J.P. (**2013**). Investigation of *Aspergillus fumigatus* biofilm formation by various "omics" approaches. *Frontiers in Microbiology* **4**: 13.

Muszyska, B., Maslanka, A., Ekiert, H., and Sulkowska-Ziaja, K. (**2011**). Analysis of indole compounds *Armillaria mellea* fruiting bodies. *Acta Poloniae Pharmaceutica* **68**: 93–97.

Mwenje, E. and Ride, J. (**1997**). The use of pectic enzymes in the characterization of *Armillaria* isolates from Africa. *Plant Pathology* **46**: 341–354.

Mwenje, E., Ride, J., and Pearce, R. (**1998**). Distribution of Zimbabwean *Armillaria* groups and their pathogenicity on cassava. *Plant pathology* **47**: 623–634.

Mwenje, E., Wingfield, B.D., Coetzee, M.P.A., Nemato, H., and Wingfield, M.J. (**2006**). *Armillaria* species on tea in Kenya identified using isozyme and DNA sequence comparisons. *Plant Pathology* **55**: 343–350.

Nadimpalli, R., Yalpani, N., Johal, G.S., and Simmons, C.R. (**2000**). Prohibitins, stomatins, and plant disease response genes compose a protein superfamily that controls cell proliferation, ion channel regulation, and death. *The Journal of Biological Chemistry* **275**: 29579–86.

Nakazawa, T. and Horiuchi, H. (**1998**). Isolation and characterization of EPD1, an essential gene for pseudohyphal growth of a dimorphic yeast, Candida maltosa. *Journal of Bacteriology* **180**: 2079–2086.

Nakazawa, T., Kaneko, S., Miyazaki, Y., Jojima, T., Yamazaki, T., Katsukawa, S., and Shishido, K. (**2008**). Basidiomycete *Lentinula edodes* CDC5 and a novel interacting protein CIPB bind to a newly isolated target gene in an unusual manner. *Fungal Genetics and Biology* **45**: 818–28.

Naumann, T.A., Wicklow, D.T., and Price, N.P.J. (**2011**). Identification of a chitinase-modifying protein from *Fusarium verticillioides*: truncation of a host resistance protein by a fungalysin metalloprotease. *The Journal of Biological Chemistry* **286**: 35358–66.

Nesvizhskii, A. (**2005**). Interpretation of shotgun proteomic data. *Molecular & Cellular Proteomics*: 1419–1440.

Newton, G., Aguilera, J., Ward, J., and Fahey, R. (**1997**). Effect of polyamine-induced compaction and aggregation of DNA on the formation of radiation-induced strand breaks: quantitative models for cellular radiation damage. *Radiation Research* **148**: 272–284.

Nicholson, R., Butler, L., and Asquith, T. (**1986**). Glycoproteins from *Colletotrichum graminicola* that bind phenols: Implications for survival and virulence of phytopathogenic fungi. *Phytopathology* **76**: 1315–1318.

Nierman, W.C., Pain, A., Anderson, M.J., Wortman, J.R., Kim, H.S., Arroyo, J., Berriman, M., Abe, K., Archer, D.B., Bermejo, C., Bennett, J., Bowyer, P., Chen, D., Collins, M., Coulsen, R., Davies, R., Dyer, P.S., Farman, M., Fedorova, N., Fedorova, N., *et al.* (**2005**). Genomic sequence of the pathogenic and allergenic filamentous fungus *Aspergillus fumigatus. Nature* **438**: 1151–6.

Niknejad, F., Zaini, F., Faramarzi, M., Amini, M., Kordbacheh, P., Mahmoudi, M., and Safara, M. (**2012**). *Candida parapsilosis* as a Potent Biocontrol Agent against Growth and Aflatoxin Production by *Aspergillus* Species. *Iranian Journal of Public Health* **41**: 72–80.

Nomanbhoy, F., Steele, C., and Yano, J. (**2002**). Vaginal and oral epithelial cell anti-*Candida* activity. *Infection and Immunity* **70**: 7081–7088.

Noverr, M. (**2003**). Production of Eicosanoids and other Oxylipins by Pathogenic Eukaryotic Microbes. *Clinical Microbiology Reviews* **16**: 517–533.

O'Hanlon, K. a, Gallagher, L., Schrettl, M., Jöchl, C., Kavanagh, K., Larsen, T.O., and Doyle, S. (**2012**). Nonribosomal peptide synthetase genes pesL and pes1 are essential for Fumigaclavine C production in Aspergillus fumigatus. *Applied and Environmental Microbiology* **78**: 3166–76.

Obuchi, T., Kondoh, H., Watanabe, N., Tamai, M., Omura, S., Yang, J.S., and Liang, X.T. (**1990**). Armillaric acid, a new antibiotic produced by *Armillaria mellea*. *Planta Med* **56**: 198–201.

Ogura, T. and Wilkinson, a J. (**2001**). AAA+ superfamily ATPases: common structure--diverse function. *Genes to cells : devoted to molecular & cellular mechanisms* **6**: 575–97.

Ohm, R.A., Feau, N., Henrissat, B., Schoch, C.L., Horwitz, B.A., Barry, K.W., Condon, B.J., Copeland, A.C., Dhillon, B., Glaser, F., Hesse, C.N., Kosti, I., LaButti, K., Lindquist, E.A., Lucas, S., Salamov, A.A., Bradshaw, R.E., Ciuffetti, L., Hamelin, R.C., Kema, G.H.J., *et al.* (**2012**). Diverse lifestyles and

strategies of plant pathogenesis encoded in the genomes of eighteen Dothideomycetes fungi. *PLoS Pathogens* **8**: e1003037.

Ohm, R.A., de Jong, J.F., Lugones, L.G., Aerts, A., Kothe, E., Stajich, J.E., de Vries, R.P., Record, E., Levasseur, A., Baker, S.E., Bartholomew, K.A., Coutinho, P.M., Erdmann, S., Fowler, T.J., Gathman, A.C., Lombard, V., Henrissat, B., Knabe, N., Kues, U., Lilly, W.W., *et al.* (**2010**). Genome sequence of the model mushroom *Schizophyllum commune*. *Nature Biotechnology* **28**: 957–U10.

De Oliveira, B. V, Teixeira, G.S., Reis, O., Barau, J.G., Teixeira, P.J.P.L., do Rio, M.C.S., Domingues, R.R., Meinhardt, L.W., Paes Leme, A.F., Rincones, J., and Pereira, G. a G. (**2012**). A potential role for an extracellular methanol oxidase secreted by *Moniliophthora perniciosa* in Witches' broom disease in cacao. *Fungal Genetics and Biology* **49**: 922–32.

Olson, A., Aerts, A., Asiegbu, F., Belbahri, L., Bouzid, O., Broberg, A., Canbäck, B., Coutinho, P.M., Cullen, D., Dalman, K., Deflorio, G., van Diepen, L.T. a, Dunand, C., Duplessis, S., Durling, M., Gonthier, P., Grimwood, J., Fossdal, C.G., Hansson, D., Henrissat, B., *et al.* (**2012**). Insight into trade-off between wood decay and parasitism from the genome of a fungal forest pathogen. *The New Phytologist* **194**: 1001–13.

Olsson, S. (**1995**). Action potential-like activity found in fungal mycelia is sensitive to stimulation. *Naturwissenschaften* **82**: 0–1.

Onsando, J., Wargo, P., and Waudo, S. (**1997**). Distribution, severity, and spread of *Armillaria* root disease in Kenya tea plantations. *Plant disease* **Feb**: 133–137.

Van Ooyen, A.J.J., Dekker, P., Huang, M., Olsthoorn, M.M. a, Jacobs, D.I., Colussi, P. a, and Taron, C.H. (**2006**). Heterologous protein production in the yeast Kluyveromyces lactis. *FEMS Yeast Research* **6**: 381–92.

Orndorff, S.A. (**1984**). Enzymatic catalyzed biocide system - US4478683 A.

Osma, J.F., Toca-Herrera, J.L., and Rodríguez-Couto, S. (**2010**). Uses of laccases in the food industry. *Enzyme research* **2010**: 918761.

Ota, Y., Fukuda, K., and Suzuki, K. (**1998**). The nonheterothallic life cycle of Japanese *Armillaria mellea*. *Mycologia* **90**: 396–405.

Otieno, W., Sierra, A.P.P., and Termorshuizen, A. (**2003**). Characterization of *Armillaria* isolates from tea (*Camellia sinensis*) in Kenya. *Mycologia* **95**: 160–75.

Packer, L., Kraemer, K., and Rimbach, G. (**2001**). Molecular aspects of lipoic acid in the prevention of diabetes complications. *Nutrition* **17**: 888–95.

Page, R. (**1998**). GeneTree: comparing gene and species phylogenies using reconciled trees. *Bioinformatics* **14**: 819–820.

Palmer, T. and Berks, B.C. (**2012**). The twin-arginine translocation (Tat) protein export pathway. *Nature Reviews Microbiology* **10**: 483–96.

Pannecoucque, J. and Höfte, M. (**2009**). Interactions between cauliflower and *Rhizoctonia anastomosis* groups with different levels of aggressiveness. *BMC Plant Biology* **9**: 95.

Panwar, V., McCallum, B., and Bakkeren, G. (**2013**). Endogenous silencing of *Puccinia triticina* pathogenicity genes through in planta-expressed sequences leads to the suppression of rust diseases on wheat. *The Plant Journal* **73**: 521–32.

Papanikolaou, S. and Aggelis, G. (**2011**). Lipids of oleaginous yeasts. Part II: Technology and potential applications. *European Journal of Lipid Science and Technology* **113**: 1052–1073.

Papanikolaou, S., Chevalot, I., Komaitis, M., Marc, I., and Aggelis, G. (**2002**). Single cell oil production by Yarrowia lipolytica growing on an industrial derivative of animal fat in batch cultures. *Applied Microbiology and Biotechnology* **58**: 308–12.

Park, E., Lee, W., and Kim, S. (**2010**). Ergothioneine accumulation in a medicinal plant *Gastrodia elata*. *Journal of Medicinal Plants Research* **4**: 1141–1147.

Park, J.K., Kim, J.-D., Park, Y. Il, and Kim, S.-K. (**2012**). Purification and characterization of a 1,3-β-d-glucanase from Streptomyces torulosus PCPOK-0324. *Carbohydrate Polymers* **87**: 1641–1648.

Parveen, N. and Cornell, K. (**2011**). Methylthioadenosine/S-adenosylhomocysteine nucleosidase, a critical enzyme for bacterial metabolism. *Molecular Microbiology* **79**: 7–20.

Paszkiewicz, K. and Studholme, D.J. (**2010**). De novo assembly of short sequence reads. *Briefings in Bioinformatics* **11**: 457–72.

Pegg, A. and McCann, P. (**1982**). Polyamine metabolism and function. *American Journal of Cell Physiology* **243**: C212–C221.

Peipp, H. and Sonnenbichler, J. (**1992**). Secondary fungal metabolites and their biological activities, II. Occurrence of antibiotic compounds in cultures of *Armillaria ostoyae* growing in the presence of an antagonistic fungus or host plant cells. *Biological Chemistry Hoppe Seyler* **373**: 675–83.

Pel, H.J., Winde, J.H. De, Archer, D.B., Dyer, P.S., Hofmann, G., Schaap, P.J., Turner, G., Vries, R.P. De, Albang, R., Albermann, K., Andersen, M.R., Bendtsen, J.D., Benen, J.A.E., Berg, M. Van Den, Breestraat, S., Caddick, M.X., Contreras, R., Cornell, M., Coutinho, P.M., Danchin, E.G.J., *et al.* (**2007**). Genome sequencing and analysis of the versatile cell factory *Aspergillus niger* CBS 513.88. *Nature Biotechnology* **25**: 221–231.

Pelaez, F. (**2005**). Biological activities of fungal metabolites. In *Handbook of Industrial Mycology* (Crc Press-Taylor & Francis Group: Boca Raton, Florida), pp. 49–92.

Pellegrini, A., Corneo, P.E., Camin, F., Ziller, L., Tosi, S., and Pertot, I. (**2013**). Isotope ratio mass spectrometry identifies soil microbial biocontrol agents having

trophic relations with the plant pathogen *Armillaria mellea*. *Applied Soil Ecology* **64**: 142–151.

Pellegrini, A., Corneo, P.E., Camin, F., Ziller, L., Tosi, S., and Pertot, I. (**2012**). Studying trophic interactions between a plant pathogen and two different antagonistic microorganisms using a ^{13}C-labeled compound and isotope ratio mass spectrometry. *Rapid Communications in Mass Spectrometry* **26**: 510–516.

Peng, J., Elias, J., and Thoreen, C. (**2003**). Evaluation of multidimensional chromatography coupled with tandem mass spectrometry (LC/LC-MS/MS) for large-scale protein analysis: the yeast proteome. *Journal of Proteome Research* **2**: 43–50.

Peng, R.-H., Xiong, A.-S., Xue, Y., Fu, X.-Y., Gao, F., Zhao, W., Tian, Y.-S., and Yao, Q.-H. (**2008**). Microbial biodegradation of polyaromatic hydrocarbons. *FEMS Microbiology Reviews* **32**: 927–55.

Perazzolli, M., Bampi, F., Faccin, S., Moser, M., De Luca, F., Ciccotti, A.M., Velasco, R., Gessler, C., Pertot, I., and Moser, C. (**2010**). *Armillaria mellea* Induces a Set of Defense Genes in Grapevine Roots and One of Them Codifies a Protein with Antifungal Activity. *Molecular Plant-Microbe Interactions* **23**: 485–496.

Pérez-Sierra, A., Guillaumin, J., Spooner, B., and Bridge, P. (**2004**). Characterization of *Armillaria heimii* from Africa. *Plant Pathology* **53**: 220–230.

Pertot, I., Gobbin, D., De Luca, F., and Prodorutti, D. (**2008**). Methods of assessing the incidence of *Armillaria* root rot across viticultural areas and the pathogen's genetic diversity and spatial-temporal pattern in northern Italy. *Crop Protection* **27**: 1061–1070.

Petersen, T.N., Brunak, S., von Heijne, G., and Nielsen, H. (**2011**). SignalP 4.0: discriminating signal peptides from transmembrane regions. *Nature Methods* **8**: 785–6.

Phizicky, E., Bastiaens, P.I.H., Zhu, H., Snyder, M., and Fields, S. (**2003**). Protein analysis on a proteomic scale. *Nature* **422**: 208–15.

Piacentini, L., Fanti, L., Berloco, M., Perrini, B., and Pimpinelli, S. (**2003**). Heterochromatin protein 1 (HP1) is associated with induced gene expression in Drosophila euchromatin. *The Journal of Cell Biology* **161**: 707–14.

Pisani, D., Cotton, J.A., and McInerney, J.O. (**2007**). Supertrees disentangle the chimerical origin of eukaryotic genomes. *Molecular Biology and Evolution* **24**: 1752–60.

Plett, J.M., Gibon, J., Kohler, A., Duffy, K., Hoegger, P.J., Velagapudi, R., Han, J., Kües, U., Grigoriev, I. V, and Martin, F. (**2012**). Phylogenetic, genomic organization and expression analysis of hydrophobin genes in the ectomycorrhizal basidiomycete *Laccaria bicolor*. *Fungal Genetics and Biology* **49**: 199–209.

Pócsi, I., Miskei, M., Karányi, Z., Emri, T., Ayoubi, P., Pusztahelyi, T., Balla, G., and Prade, R.A. (**2005**). Comparison of gene expression signatures of diamide, H_2O_2 and menadione exposed *Aspergillus nidulans* cultures--linking genome-wide transcriptional changes to cellular physiology. *BMC Genomics* **6**: 182.

Pontoppidan, M.-B., Himaman, W., Hywel-Jones, N.L., Boomsma, J.J., and Hughes, D.P. (**2009**). Graveyards on the move: the spatio-temporal distribution of dead *Ophiocordyceps*-infected ants. *PloS ONE* **4**: e4835.

Pronk, J., Steensma, H., and Dijken, J. Van (**1996**). Pyruvate metabolism in *Saccharomyces cerevisiae*. *Yeast* **12**: 1607–1633.

Punt, P.J., Biezen, N. Van, Conesa, A., Albers, A., Mangnus, J., and Hondel, C. Van Den (**2002**). Filamentous fungi as cell factories for heterologous protein production. *Trends in Biotechnology* **20**: 200–206.

Punta, M., Coggill, P.C., Eberhardt, R.Y., Mistry, J., Tate, J., Boursnell, C., Pang, N., Forslund, K., Ceric, G., Clements, J., Heger, A., Holm, L., Sonnhammer, E.L.L., Eddy, S.R., Bateman, A., and Finn, R.D. (**2012**). The Pfam protein families database. *Nucleic Acids Research* **40**: D290–301.

Raabe, R. (**1972**). Variation in pathogenicity and virulence in single-spore isolates of *Armillaria mellea*. *Mycologia* **64**: 1154–1159.

Raabe, R.D. (**1962**). Host list of the root rot fungus *Armillaria mellea. Hilgardia* **33**: 25–88.

Raabe, R.D. (**1966**). Testing plants for resistance to oak root fungus. *California Agriculture* **20**: 12–13.

Rafiqi, M., Ellis, J.G., Ludowici, V. a, Hardham, A.R., and Dodds, P.N. (**2012**). Challenges and progress towards understanding the role of effectors in plant-fungal interactions. *Current Opinion in Plant Biology* **15**: 477–82.

Raha, S. and Robinson, B.H. (**2000**). Mitochondria, oxygen free radicals, disease and ageing. *Trends in Biochemical Sciences* **25**: 502–8.

Raja, M.R., Waterman, S.R., Qiu, J., Bleher, R., Williamson, P.R., and O'Halloran, T. V (**2013**). A copper hyperaccumulation phenotype correlates with pathogenesis in *Cryptococcus neoformans. Metallomics* **5**: 363–371.

Rajan, R., Zhu, J., Hu, X., Pei, D., and Bell, C. (**2005**). Crystal structure of S-ribosylhomocysteinase (LuxS) in complex with a catalytic 2-ketone intermediate. *Biochemistry* **44**: 3745–3753.

Rampitsch, C., Bykova, N. V, McCallum, B., Beimcik, E., and Ens, W. (**2006**). Analysis of the wheat and *Puccinia triticina* (leaf rust) proteomes during a susceptible host-pathogen interaction. *Proteomics* **6**: 1897–907.

Ray, P.D., Huang, B.-W., and Tsuji, Y. (**2012**). Reactive oxygen species (ROS) homeostasis and redox regulation in cellular signaling. *Cellular Signalling* **24**: 981–90.

Raziq, F. (**1998**). Biological and integrated control of the root rot caused by *Armillaria mellea.*

Redfern, D.B. (**1975**). The influence of food base on rhizomorph growth and pathogenicity of *Armillaria mellea* isolates. In *Biology and Control of Soil-Borne Plant Pathogens.*, G.W. Breuhl, ed (The American Phytopathological Society: St Paul, MN), pp. 69–73.

Rehman, A. (**1992**). Purification of laccase I from *Armillaria mellea*. *Journal of General Microbiology*: 1251–1257.

Reithner, B., Ibarra-Laclette, E., Mach, R.L., and Herrera-Estrella, A. (**2011**). Identification of mycoparasitism-related genes in *Trichoderma atroviride. Applied and Environmental Microbiology* **77**: 4361–70.

Renzetti, S., Courtin, C.M., Delcour, J.A., and Arendt, E.K. (**2010**). Oxidative and proteolytic enzyme preparations as promising improvers for oat bread formulations: Rheological, biochemical and microstructural background. *Food Chemistry* **119**: 1465–1473.

Richter, B.S., Ivors, K., Shi, W., and Benson, D.M. (**2011**). Cellulase activity as a mechanism for suppression of phytophthora root rot in mulches. *Phytopathology* **101**: 223–30.

Rider, J.E., Hacker, A., Mackintosh, C.A., Pegg, A.E., Woster, P.M., and Casero, R.A. (**2007**). Spermine and spermidine mediate protection against oxidative damage caused by hydrogen peroxide. *Amino acids* **33**: 231–40.

Riffle, M. and Eng, J. (**2009**). Proteomics data repositories. *Proteomics* **9**: 4653–4663.

Rigden, D.J., Mello, L. V, and Galperin, M.Y. (**2004**). The PA14 domain, a conserved all-β domain in bacterial toxins, enzymes, adhesins and signaling molecules. *Trends in biochemical sciences* **29**: 335–9.

Rioux, R., Manmathan, H., Singh, P., de los Reyes, B., Jia, Y., and Tavantzis, S. (**2011**). Comparative analysis of putative pathogenesis-related gene expression in two *Rhizoctonia solani* pathosystems. *Current genetics* **57**: 391–408.

Rishbeth, J. (**1982**). Species of *Armillaria* in southern England. *Plant Pathology* **31**: 9–17.

Rizzo, D.M., Whiting, E.C., and Elkins, R.B. (**1998**). Spatial distribution of *Armillaria mellea* in pear orchards. *Plant Disease* **82**: 1226–1231.

Robinson-Bax, C. and Fox, R. (**2002**). Root rots of herbaceous plants caused by *Armillaria mellea*. *Mycologist* **16**: 21–2.

Rodríguez Couto, S. and Toca Herrera, J.L. (**2006**). Industrial and biotechnological applications of laccases: a review. *Biotechnology Advances* **24**: 500–13.

Rodriguez Estrada, A.E., Jonkers, W., Kistler, H.C., and May, G. (**2012**). Interactions between *Fusarium verticillioides, Ustilago maydis*, and *Zea mays*: an

endophyte, a pathogen, and their shared plant host. *Fungal genetics and biology* **49**: 578–87.

Rossman, A.Y. and Palm-Hernandez, M.E. (**2008**). Systematics of plant pathogenic fungi: why it matters. *Plant disease* **92**: 1376–1386.

Rühl, M., Majcherczyk, A., and Kües, U. (**2013**). Lcc1 and Lcc5 are the main laccases secreted in liquid cultures of *Coprinopsis cinerea* strains. *Antonie van Leeuwenhoek*.

Ruiz-Duenas, F., Guillen, F., Camarero, S., Perez-Boada, M., Martinez, M.J., and Martinez, A.T. (**1999**). Regulation of peroxidase transcript levels in liquid cultures of the ligninolytic fungus *Pleurotus eryngii*. *Applied and Environmental Microbiology* **65**: 4458.

Ruiz-Dueñas, F.J., Ferreira, P., Martínez, M.J., and Martínez, A.T. (**2006**). In vitro activation, purification, and characterization of *Escherichia coli* expressed aryl-alcohol oxidase, a unique H_2O_2-producing enzyme. *Protein Expression and Purification* **45**: 191–9.

Ruiz-Dueñas, F.J. and Martínez, A.T. (**2009**). Microbial degradation of lignin: how a bulky recalcitrant polymer is efficiently recycled in nature and how we can take advantage of this. *Microbial Biotechnology* **2**: 164–77.

Ryu, J.S., Shary, S., Houtman, C.J., Panisko, E. a, Korripally, P., St John, F.J., Crooks, C., Siika-Aho, M., Magnuson, J.K., and Hammel, K.E. (**2011**). Proteomic and functional analysis of the cellulase system expressed by *Postia placenta* during brown rot of solid wood. *Applied and Environmental Microbiology* **77**: 7933–41.

Sainz-Oses, M. (**2004**). *Armillaria* species infesting vineyards in northwestern Spain. *European journal of Plant Pathology*: 683–687.

Sakamoto, T., Tsujitani, Y., Fukamachi, K., Taniguchi, Y., and Ihara, H. (**2010**). Identification of two GH27 bifunctional proteins with β-L-arabinopyranosidase/α-D-galactopyranosidase activities from *Fusarium oxysporum*. *Applied Microbiology and Biotechnology* **86**: 1115–24.

Sakamoto, Y., Nakade, K., and Konno, N. (**2011**). Endo-β-1,3-glucanase GLU1, from the fruiting body of *Lentinula edodes*, belongs to a new glycoside hydrolase family. *Applied and Environmental Microbiology* **77**: 8350–4.

Saloheimo, M., Paloheimo, M., Hakola, S., Pere, J., Swanson, B., Nyyssönen, E., Bhatia, A., Ward, M., and Penttilä, M. (**2002**). Swollenin, a *Trichoderma reesei* protein with sequence similarity to the plant expansins, exhibits disruption activity on cellulosic materials. *European Journal of Biochemistry* **269**: 4202–4211.

Saric, T., Graef, C.I., and Goldberg, A.L. (**2004**). Pathway for Degradation of Peptides Generated by Proteasomes. *Journal of Biological Chemistry* **279**: 46723–46732.

Sasidharan, R., Voesenek, L.A., and Pierik, R. (**2011**). Cell Wall Modifying Proteins Mediate Plant Acclimatization to Biotic and Abiotic Stresses. *Critical Reviews in Plant Sciences* **30**: 548–562.

Sato, S., Liu, F., Koc, H., and Tien, M. (**2007**). Expression analysis of extracellular proteins from *Phanerochaete chrysosporium* grown on different liquid and solid substrates. *Microbiology* **153**: 3023–3033.

Schneider, P., Misiek, M., and Hoffmeister, D. (**2008**). In vivo and in vitro production options for fungal secondary metabolites. *Molecular Pharmaceutics* **5**: 2334–242.

Schrettl, M., Carberry, S., Kavanagh, K., Haas, H., Jones, G.W., O'Brien, J., Nolan, A., Stephens, J., Fenelon, O., and Doyle, S. (**2010**). Self-protection against gliotoxin--a component of the gliotoxin biosynthetic cluster, GliT, completely protects *Aspergillus fumigatus* against exogenous gliotoxin. *PLoS Pathogens* **6**: e1000952.

Schulze, S. and Bahnweg, G. (**1995**). Identification of European *Armillaria* species by restriction fragment length polymorphisms of ribosomal DNA. *European Journal of Forest Pathology* **25**: 214–223.

Schuster, A. and Schmoll, M. (**2010**). Biology and biotechnology of *Trichoderma*. *Applied Microbiology and Biotechnology* **87**: 787–799.

Schweiger, P., Rouhier, H., and Söderström, B. (**2002**). Visualisation of ectomycorrhizal rhizomorph structure using laser scanning confocal microscopy. *Mycological Research* **106**: 349–354.

Scruggs, S.B., Reisdorph, R., Armstrong, M.L., Warren, C.M., Reisdorph, N., Solaro, R.J., and Buttrick, P.M. (**2010**). A novel, in-solution separation of endogenous cardiac sarcomeric proteins and identification of distinct charged variants of regulatory light chain. *Molecular & Cellular Proteomics* **9**: 1804–18.

Sekizaki, H., Kuninaga, S., Yamamoto, M., Asazu, S.N., Sawa, S., Kojoma, M., Yokosawa, R., and Yoshida, N. (**2008**). Identification of *Armillaria nabsnona* in gastrodia tubers. *Biological & Pharmaceutical Bulletin* **31**: 1410–4.

Senn, H., Shapiro, R.S., and Cowen, L.E. (**2012**). Cdc28 provides a molecular link between Hsp90, morphogenesis, and cell cycle progression in Candida albicans. *Molecular Biology of the Cell* **23**: 268–83.

Sharma, A.K., Zhaxybayeva, O., Papke, R.T., and Doolittle, W.F. (**2008**). Actinorhodopsins: proteorhodopsin-like gene sequences found predominantly in non-marine environments. *Environmental Microbiology* **10**: 1039–1056.

Sharma, P., Jha, A.B., Dubey, R.S., and Pessarakli, M. (**2012**). Reactive Oxygen Species, Oxidative Damage, and Antioxidative Defense Mechanism in Plants under Stressful Conditions. *Journal of Botany* **2012**: 1–26.

Shary, S., Kapich, A.N., Panisko, E. a, Magnuson, J.K., Cullen, D., and Hammel, K.E. (**2008**). Differential expression in *Phanerochaete chrysosporium* of

membrane-associated proteins relevant to lignin degradation. *Applied and Environmental Microbiology* **74**: 7252–7.

Shaw III, C.G. and Kile, G.A. (**1991**). *Armillaria* root disease. Agricultural Handbook No. 691. C.G.I. Shaw and G.A. Kile, eds (USDA Forest Service: Washington, DC).

Shendure, J. and Ji, H.L. (**2008**). Next-generation DNA sequencing. *Nature Biotechnology* **26**: 1135–1145.

Shevchenko, A., Tomas, H., Havlis, J., Olsen, J.V. V, Mann, M., and Henrik Tomas, J.H. (**2007**). In-gel digestion for mass spectrometric characterization of proteins and proteomes. *Nature protocols* **1**: 2856–2860.

Shevchenko, G.M., Sj din, M., Malmstr M, D., Wetterhall, M., Bergquist, J., Sjodin, M.O.D., and Malmstrom, D. (**2010**). Cloud-Point Extraction and Delipidation of Porcine Brain Proteins in Combination with Bottom-Up Mass Spectrometry Approaches for Proteome Analysis. *Journal of Proteome Research* **9**: 3903–3911.

Shieh, J.-C., White, A., Cheng, Y.-C., and Rosamond, J. (**2005**). Identification and functional characterization of *Candida albicans* CDC4. *Journal of Biomedical Science* **12**: 913–24.

Sicoli, G., Fatehi, J., and Stenlid, J. (**2003**). Development of species-specific PCR primers on rDNA for the identification of European *Armillaria* species. *Forest Pathology* **33**: 287–297.

Singer, R. (**1986**). Agaricales in Modern Taxonomy, 4th ed., 4th ed. (Koenigstein, FRG: Koeltz Scientific Books).

Sirota, F.L., Batagov, A., Schneider, G., Eisenhaber, B., Eisenhaber, F., and Maurer-Stroh, S. (**2012**). Beware of moving targets: reference proteome content fluctuates substantially over the years. *Journal of Bioinformatics and Computational Biology* **10**: 1250020.

Sivashankari, S. and Shanmughavel, P. (**2006**). Functional annotation of hypothetical proteins–A review. *Bioinformation* **18**: 335–338.

Slámová, K., Bojarová, P., Gerstorferová, D., Fliedrová, B., Hofmeisterová, J., Fiala, M., Pompach, P., and Křen, V. (**2012**). Sequencing, cloning and high-yield expression of a fungal β-N-acetylhexosaminidase in *Pichia pastoris*. *Protein Expression and Purification* **82**: 212–7.

Slayman, C., Long, W., and Gradmann, D. (**1976**). Action potentials in*Neurospora-crassa* , a mycelial fungus. *Biochimica et Biophysica Acta* **426**: 732–744.

Slowinski, J. and Page, R. (**1999**). How should species phylogenies be inferred from sequence data? *Systematic Biology* **48**: 814–825.

Smedsgaard, J. (**1997**). Micro-scale extraction procedure for standardized screening of fungal metabolite production in cultures. *Journal of Chromatography A* **760**: 264–270.

Smith, M.L., Duchesne, L.C., Bruhn, J.N., and Anderson, J.B. (**1990**). Mitochondrial genetics in a natural population of the plant pathogen *Armillaria*. *Genetics* **126**: 575–82.

Society, A.P. (**2008**). Microbial Genomic Sequencing Perspectives of the American Phytopathological Society. *American Phytopathological Society*.

Soliman, S.S.M. and Raizada, M.N. (**2013**). Interactions between Co-Habitating fungi Elicit Synthesis of Taxol from an Endophytic Fungus in Host Taxus Plants. *Frontiers in microbiology* **4**: 3.

Song, X., Rampitsch, C., Soltani, B., Mauthe, W., Linning, R., Banks, T., McCallum, B., and Bakkeren, G. (**2011**). Proteome analysis of wheat leaf rust fungus, *Puccinia triticina*, infection structures enriched for haustoria. *Proteomics* **11**: 944–963.

Sonnenbichler, J., Dietrich, J., and Peipp, H. (**1994**). Secondary fungal metabolites and their biological activities, V. Investigations concerning the induction of the biosynthesis of toxic secondary metabolites in basidiomycetes. *Biological Chemistry Hoppe Seyler* **375**: 71–9.

Sonnenbichler, J., Guillaumin, J.J.J., Peipp, H., and Schwarz, D. (**1997**). Secondary metabolites from dual cultures of genetically different *Armillaria* isolates. *European Journal of Forest Pathology* **27**: 241–249.

Spectrum Mill MS Proteomics Workbench *Agilent Technologies*.

Sprenger, G. a. and Pohl, M. (**1999**). Synthetic potential of thiamin diphosphate-dependent enzymes. *Journal of Molecular Catalysis B: Enzymatic* **6**: 145–159.

Sprockett, D.D., Piontkivska, H., and Blackwood, C.B. (**2011**). Evolutionary analysis of glycosyl hydrolase family 28 (GH28) suggests lineage-specific expansions in necrotrophic fungal pathogens. *Gene* **479**: 29–36.

Srivatsan, A., Han, Y., Peng, J., Tehranchi, A.K., Gibbs, R., Wang, J.D., and Chen, R. (**2008**). High-precision, whole-genome sequencing of laboratory strains facilitates genetic studies. *PLoS genetics* **4**: e1000139.

Stack, D., Neville, C., and Doyle, S. (**2007**). Nonribosomal peptide synthesis in Aspergillus fumigatus and other fungi. *Microbiology* **153**: 1297–306.

Stajich, J.E., Wilke, S.K., Ahrén, D., Hang, C., Birren, B.W., Borodovsky, M., Burns, C., James, T.Y., Kamada, T., Kilaru, S., Kodira, C., Kües, U., Kupfer, D., and Kwan, H.S. (**2010**). Insights into evolution of multicellular fungi from the assembled chromosomes of the mushroom*Coprinopsis cinerea (Coprinus cinereus). Proceedings of the National Academy of Sciences of the United States of America* **107**.

Stanke, M. and Waack, S. (**2003**). Gene prediction with a hidden Markov model and a new intron submodel. *Bioinformatics* **19**: ii215–ii225.

Stergiopoulos, I. and de Wit, P.J.G.M. (**2009**). Fungal effector proteins. *Annual Review of Phytopathology* **47**: 233–63.

Sticklen, M.B. (**2008**). Plant genetic engineering for biofuel production: towards affordable cellulosic ethanol. *Nature reviews. Genetics* **9**: 433–43.

Stolowich, N., Petrescu, A., and Huang, H. (**2002**). Sterol carrier protein-2: structure reveals function. *Cellular and Molecular Life Sciences* **59**: 193–212.

Stothard, P. (**2000**). The sequence manipulation suite: JavaScript programs for analyzing and formatting protein and DNA sequences. *Biotechniques* **28**.

Stoytchev, I. and Nerud, F. (**2000**). Ligninolytic enzyme complex of *Armillaria* spp. *Folia Microbiol (Praha)* **45**: 248–50.

Strieker, M., Tanović, A., and Marahiel, M. a (**2010**). Nonribosomal peptide synthetases: structures and dynamics. *Current Opinion in Sructural Bology* **20**: 234–40.

Strong, P.J. and Claus, H. (**2011**). Laccase: A Review of Its Past and Its Future in Bioremediation. *Critical Reviews in Environmental Science and Technology* **41**: 373–434.

Suliman, H., Appling, D., and Robertus, J. (**2007**). The gene for cobalamin-independent methionine synthase is essential in *Candida albicans*: A potential antifungal target. *Archives of Biochemistry and Biophysics* **467**: 218–226.

Sun, Y., Liang, H., Zhang, X., Tong, H., and Liu, J. (**2009**). Structural elucidation and immunological activity of a polysaccharide from the fruiting body of *Armillaria mellea*. *Bioresource Technology* **100**: 1860–3.

Sunde, M., Kwan, A.H.Y., Templeton, M.D., Beever, R.E., and Mackay, J.P. (**2008**). Structural analysis of hydrophobins. *Micron* **39**: 773–84.

Sung, M.H., Tanizawa, K., Tanaka, H., Kuramitsu, S., Kagamiyama, H., and Soda, K. (**1990**). Purification and characterization of thermostable aspartate aminotransferase from a thermophilic Bacillus species. *Journal of Bacteriology* **172**: 1345–51.

Suzuki, H., Macdonald, J., Syed, K., Salamov, A., Hori, C., Aerts, A., Henrissat, B., Wiebenga, A., Vankuyk, P. a, Barry, K., Lindquist, E., Labutti, K., Lapidus, A., Lucas, S., Coutinho, P., Gong, Y., Samejima, M., Mahadevan, R., Abou-Zaid, M., de Vries, R.P., *et al.* (**2012**). Comparative genomics of the white-rot fungi, *Phanerochaete carnosa* and *P. chrysosporium*, to elucidate the genetic basis of the distinct wood types they colonize. *BMC Genomics* **13**: 444.

Sweigard, J., Carroll, A.M., Farrall, L., Chumley, F.G., and Valent, B. (**1998**). *Magnaporthe grisea* pathogenicity genes obtained through insertional mutagenesis. *Molecular Plant-Microbe Interactions* **11**: 404–12.

Syed, K., Doddapaneni, H., Subramanian, V., Lam, Y.W., and Yadav, J.S. (**2010**). Genome-to-function characterization of novel fungal P450 monooxygenases oxidizing polycyclic aromatic hydrocarbons (PAHs). *Biochemical and Biophysical Research Communications* **399**: 492–7.

Syed, K. and Yadav, J.S. (**2012**). P450 monooxygenases (P450ome) of the model white rot fungus *Phanerochaete chrysosporium. Critical Reviews in Microbiology* **38**: 339–63.

Szabo, a, Langer, T., Schröder, H., Flanagan, J., Bukau, B., and Hartl, F.U. (**1994**). The ATP hydrolysis-dependent reaction cycle of the *Escherichia coli* Hsp70 system DnaK, DnaJ, and GrpE. *Proceedings of the National Academy of Sciences of the United States of America* **91**: 10345–9.

Szewczak, A.A., Moore, P.B., Chang, Y.L., and Wool, I.G. (**1993**). The conformation of the sarcin/ricin loop from 28S ribosomal RNA. *Proceedings of the National Academy of Sciences of the United States of America* **90**: 9581–5.

Takahashi, K. (**1988**). The amino acid sequence of ribonuclease N1, a guanine-specific ribonuclease from the fungus *Neurospora crassa*. *Journal of biochemistry* **104**: 375–382.

Talbot, N. and Kershaw, M. (**1996**). MPG1 encodes a fungal hydrophobin involved in surface interactions during infection-related development of *Magnaporthe grisea*. *The Plant Cell* **8**: 985–999.

Tartaglia, G. and Caflisch, A. (**2007**). Computational analysis of the S. cerevisiae proteome reveals the function and cellular localization of the least and most amyloidogenic proteins. *Proteins: Structure, Function, and Bioinformatics* **278**: 273–278.

Taylor, A., Smith, B., and Kitada, S. (**2001**). Crystal structures of mitochondrial processing peptidase reveal the mode for specific cleavage of import signal sequences. *Structure* **9**: 615–25.

Taylor, J.W., Spatafora, J., and Berbee, M. (**2006**). Ascomycota. Sac Fungi. Version 09 October 2006 (under construction). http://tolweb.org/Ascomycota/20521/2006.10.09 in The Tree of Life Web Project, http://tolweb.org/. *The Tree of Life Web Project*.

The Schistosoma japonicum Genome Sequencing and Functional Analysis Consortium (**2009**). The *Schistosoma japonicum* genome reveals features of host-parasite interplay. *Nature* **460**: 345–51.

Theissen, U. and Martin, W. (**2008**). Sulfide : quinone oxidoreductase (SQR) from the lugworm *Arenicola marina* shows cyanide- and thioredoxin-dependent activity. *The FEBS journal* **275**: 1131–9.

Thind, T.S. and Aggarwal, R. (**2008**). Characterization and Pathogenic Relationships of*Rhizoctonia solani* Isolates in a Potato-Rice System and their Sensitivity to Fungicides. *Journal of Phytopathology* **156**: 615–621.

Tholl, D. (**2006**). Terpene synthases and the regulation, diversity and biological roles of terpene metabolism. *Current opinion in plant biology* **9**: 297–304.

Thomas, H., Roberts, C., and Amstutz, A. (**1948**). Rootstock Susceptibilty to *Armillaria mellea*. *Phytopathology* **38**: 152–154.

Thomas, P. and Poznansky, M. (**1990**). Lipid peroxidation inactivates rat liver microsomal glycerol-3-phosphate acyl transferase. Effect of iron and copper salts and carbon tetrachloride. *Journal of Biological Chemistry* **265**.

Thomidis, T. and Exadaktylou, E. (**2012**). Effectiveness of cyproconazole to control *Armillaria* root rot of apple, walnut and kiwifruit. *Crop Protection* **36**: 49–51.

Thomson, J., Rankin, H., Ashcroft, G., Yates, C., McQueen, J., and Cummings, S. (**1982**). The Treatment of Depression in General-Practice - A Comparison of L-Tryptophan, Amitriptyline, and a Ccombination of L-Tryptphan and Amitriptyline with Placebo. *Psychological Medicine* **12**: 741–751.

Thorpe, G.W., Fong, C.S., Alic, N., Higgins, V.J., and Dawes, I.W. (**2004**). Cells have distinct mechanisms to maintain protection against different reactive oxygen species: oxidative-stress-response genes. *Proceedings of the National Academy of Sciences of the United States of America* **101**: 6564–9.

Tokai, T., Koshino, H., Takahashi-Ando, N., Sato, M., Fujimura, M., and Kimura, M. (**2007**). *Fusarium* Tri4 encodes a key multifunctional cytochrome P450 monooxygenase for four consecutive oxygenation steps in trichothecene biosynthesis. *Biochemical and Biophysical Research Communications* **353**: 412–7.

Toledano, M.B., Delaunay, A., Biteau, B., Spector, D., and Azevedo, D. (**2003**). Oxidative stress responses in yeast. In *Yeast stress responses*, S. Hohmann and W.H. Mager, eds (Springer-Verlag New York Inc., 175 Fifth Avenue, New York, NY, 10010-7858, USA Heidelberger Platz 3, D-14197, Berlin, Germany), pp. 241–303.

Tome, M., Fiser, S., Payne, C., and Gerner, E. (**1997**). Excess putrescine accumulation inhibits the formation of modified eukaryotic initiation factor 5A (eIF-5A) and induces apoptosis. *Biochemical Journal* **328**: 847–854.

Travadon, R., Smith, M.E., Fujiyoshi, P., Douhan, G.W., Rizzo, D.M., and Baumgartner, K. (**2011**). Inferring dispersal patterns of the generalist root fungus *Armillaria mellea*. *New Phytologist* **193**: 1–11.

Tremblay, A., Hosseini, P., Alkharouf, N.W., Li, S., and Matthews, B.F. (**2010**). Transcriptome analysis of a compatible response by Glycine max to *Phakopsora pachyrhizi* infection. *Plant Science* **179**: 183–193.

Trotter, E. and Berenfeld, L. (**2001**). Protein misfolding and temperature up-shift cause G1 arrest via a common mechanism dependent on heat shock factor in Saccharomyces cerevisiae. *Proceedings of the National Academy of Sciences of the United States of America* **98**: 7313–7318.

Tsai, S., Spikings, E., Kuo, F.W., Lin, N.C., and Lin, C. (**2010**). Use of an adenosine triphosphate assay, and simultaneous staining with fluorescein diacetate and propidium iodide, to evaluate the effects of cryoprotectants on hard coral (*Echinopora* spp.) oocytes. *Theriogenology* **73**: 605–611.

Tsopelas, P. (**1999**). Distribution and ecology of *Armillaria species* in Greece. *European Journal of Forest Pathology* **29**: 103–116.

Tsukihara, T., Aoyama, H., Yamashita, E., Tomizaki, T., Shinzawa-itoh, K., Nakashima, R., Yaono, R., and Yoshikawa, S. (**2013**). The Whole Structure of the 12-subunit Oxidized Cytochrome c Oxidase at 2.8 Å. *Science* **272**: 1136–1144.

Tuomela, M., Vikman, M., Hatakka, A., and Itavaara, M. (**2000**). Biodegradation of lignin in a compost environment: a review. *Bioresource Technology* **72**: 169–183.

Ujor, V.C., Peiris, D.G., Monti, M., Kang, a S., Clements, M.O., and Hedger, J.N. (**2012**). Quantitative proteomic analysis of the response of the wood-rot fungus, *Schizophyllum commune*, to the biocontrol fungus, *Trichoderma viride*. *Letters in Applied Microbiology* **54**: 336–43.

USDA Forest Service (**2011**). *Armillaria* Root Disease. *Forest Health protection - Rocky Mountain Region* **l**: 1–3.

Vajjhala, P.R., Nguyen, C.H., Landsberg, M.J., Kistler, C., Gan, A.-L., King, G.F., Hankamer, B., and Munn, A.L. (**2008**). The Vps4 C-terminal helix is a critical determinant for assembly and ATPase activity and has elements conserved in other members of the meiotic clade of AAA ATPases. *The FEBS Journal* **275**: 1427–49.

Valdés-Santiago, L., Cervantes-Chávez, J. a, and Ruiz-Herrera, J. (**2009**). *Ustilago maydis* spermidine synthase is encoded by a chimeric gene, required for morphogenesis, and indispensable for survival in the host. *FEMS Yeast Research* **9**: 923–35.

Veness, R.G. (**1991a**). Hydrogen peroxide as a controlling factor in Armillaria mellea pathogenicity (ProQuest Dissertations and Thesis dx96645).

Veness, R.G. (**1991b**). Hydrogen peroxide as a controlling factor in Armillaria mellea pathogenicity. *October*.

Verbeke, J., Coutinho, P., Mathis, H., Quenot, A., Record, E., Asther, M., and Heiss-Blanquet, S. (**2009**). Transcriptional profiling of cellulase and expansin-related genes in a hypercellulolytic *Trichoderma reesei*. *Biotechnology letters* **31**: 1399–405.

Verghese, J., Abrams, J., Wang, Y., and Morano, K. a (**2012**). Biology of the Heat Shock Response and Protein Chaperones: Budding Yeast (*Saccharomyces cerevisiae*) as a Model System. *Microbiology and Molecular Biology Reviews* **76**: 115–58.

Vila, L., Lacadena, V., Fontanet, P., Martinez del Pozo, A., and San Segundo, B. (**2001**). A protein from the mold *Aspergillus giganteus* is a potent inhibitor of fungal plant pathogens. *Molecular Plant-Microbe Interactions* **14**: 1327–31.

Vincent, D., Balesdent, M.H.H., Gibon, J., Claverol, S., Lapaillerie, D., Lomenech, A.M.M., Blaise, F., Rouxel, T., Martin, F., Bonneu, M., others, Amselem, J., Dominguez, V., Howlett, B.J., Wincker, P., Joets, J., Lebrun, M.H., and Plomion, C. (**2009**). Hunting down fungal secretomes using liquid-phase IEF prior to high resolution 2-DE. *Electrophoresis* **30**: 4118–4136.

Vincent, D., Kohler, A., Claverol, S., Solier, E., Joets, J., Gibon, J., Lebrun, M.-H., Plomion, C., and Martin, F. (**2012**). Secretome of the free-living mycelium from the ectomycorrhizal basidiomycete *Laccaria bicolor*. *Journal of Proteome Research* **11**: 157–71.

Vitagliano, L., Masullo, M., Sica, F., Zagari, A., and Bocchini, V. (**2001**). The crystal structure of *Sulfolobus solfataricus* elongation factor 1α in complex with GDP reveals novel features in nucleotide binding and exchange. *The EMBO Journal* **20**: 5305–11.

Voelkerding, K. V, Dames, S. a, and Durtschi, J.D. (**2009**). Next-generation sequencing: from basic research to diagnostics. *Clinical chemistry* **55**: 641–58.

Volk, T. and Burdsall, H. (**1995**). A nomenclatural study of *Armillaria* and *Armillariella* species (Eko-trykk A/S, Førde, Norway).

Vries, R. De and Michelsen, B. (**1997**). The faeA genes from *Aspergillus niger* and *Aspergillus tubingensis* encode ferulic acid esterases involved in degradation of complex cell wall polysaccharides. *Applied and Environmental Microbiology* **63**: 4638–4644.

Wagener, N., Ackermann, M., Funes, S., and Neupert, W. (**2011**). A pathway of protein translocation in mitochondria mediated by the AAA-ATPase Bcs1. *Molecular cell* **44**: 191–202.

Wainright, P.O., Hinkle, G., Sogin, M.L., and Stickel, S.K. (**1993**). Monophyletic origins of the metazoa: an evolutionary link with fungi. *Science* **260**: 340–2.

Waldron, K.J., Rutherford, J.C., Ford, D., and Robinson, N.J. (**2009**). Metalloproteins and metal sensing. *Nature* **460**: 823–830.

Wall, D.B., Kachman, M.T., Gong, S., Hinderer, R., Parus, S., Misek, D.E., Hanash, S.M., and Lubman, D.M. (**2000**). Isoelectric focusing nonporous RP HPLC: a two-dimensional liquid-phase separation method for mapping of cellular proteins with identification using MALDI-TOF mass spectrometry. *Analytical Chemistry* **72**: 1099–111.

Wallace, H.M., Fraser, A. V, and Hughes, A. (**2003**). A perspective of polyamine metabolism. *Biochemical Journal* **14**: 1–14.

Wang, Y.-C., Zhang, Y.-W., Zheng, L.-H., Bao, Y.-L., Wu, Y., Yu, C.-L., Sun, L.-G., Zhang, Y., Huang, Y.-X., Sun, Y., and Li, Y.-X. (**2013**). A new compound from liquid fermentation broth of *Armillaria mellea* and the determination of its absolute configuration. *Journal of Asian Natural Products Research*: 37–41.

Warner, J.R. and McIntosh, K.B. (**2009**). How common are extraribosomal functions of ribosomal proteins? *Molecular Cell* **34**: 3–11.

Washburn, M.P., Wolters, D., and Yates, J.R. (**2001**). Large-scale analysis of the yeast proteome by multidimensional protein identification technology. *Nature Biotechnology* **19**: 242–7.

Watling, R., Kile, G.A., and M, G.N. (**1982**). Nomenclature, typification, the identity of Armillaria-mellea and species differentiation. *Transactions of the British Mycological Society* **78**: 271–285.

Weckwerth, W. (**2011**). Green systems biology - From single genomes, proteomes and metabolomes to ecosystems research and biotechnology. *Journal of Proteomics* **75**: 284–305.

Wehe, A., Bansal, M.S., Burleigh, J.G., and Eulenstein, O. (**2008**). DupTree: a program for large-scale phylogenetic analyses using gene tree parsimony. *Bioinformatics* **24**: 1540–1.

Weitz, H.J., Ballard, A.L.L., Campbell, C.D.D., and Killham, K. (**2001**). The effect of culture conditions on the mycelial growth and luminescence of naturally bioluminescent fungi. *FEMS Microbiology Letters* **202**: 165–170.

Weitz, H.J., Campbell, C.D., and Killham, K. (**2002**). Development of a novel, bioluminescence-based, fungal bioassay for toxicity testing. *Environmental Microbiology* **4**: 422–9.

Werner-Washburne, M. (**1987**). Complex interactions among members of an essential subfamily of hsp70 genes in *Saccharomyces cerevisiae*. *Molecular and Cellular Biology* **7**: 2568–2577.

West, C.M., Nguyen, P., van der Wel, H., Metcalf, T., Sweeney, K.R., Blader, I.J., and Erdos, G.W. (**2009**). Dependence of stress resistance on a spore coat heteropolysaccharide in *Dictyostelium*. *Eukaryotic Cell* **8**: 27–36.

West, J. and Hughes, C. (**2000**). *Armillaria mellea* can infect the perennial weed, *Rumex obtusifolius*, in the UK. *Plant Pathology*: 2000.

Whiteford, J.R., Lacroix, H., Talbot, N.J., and Spanu, P.D. (**2004**). Stage-specific cellular localisation of two hydrophobins during plant infection by the pathogenic fungus *Cladosporium fulvum*. *Fungal Genetics and Biology* **41**: 624–34.

Williams, R.E., Shaw III, C.G., Wargo, P.M., and Sites, W.H. (**1989**). *Armillaria* root disease. *Forest Insect and Disease Leaflet 78*.

Williamson, M.P. (**1994**). The structure and function of proline-rich regions in proteins. *The Biochemical Journal* **297**: 249–60.

Williams-Woodward, J. (**2001**). 2000 Georgia Plant Disease Loss Estimates [http://www.caes.uga.edu/publications/pubDetail.cfm?pk_ID=7340]. *University of Georgia*.

Wingfield, M. and Knox-Davies, P. (**1980**). Association of *Diplodia pinea* with a root disease of pines in South Africa. *Plant Disease*: 221–223.

De Wit, P., Mehrabi, R., Van den Burg, H., and Stergiopoulous, I. (**2009**). Fungal effector proteins: past, present and future. *Molecular Plant Pathology* **10**: 735–747.

Wójcik, C., Rowicka, M., Kudlicki, A., Nowis, D., McConnell, E., Kujawa, M., and DeMartino, G.N. (**2006**). Valosin-containing protein (p97) is a regulator of endoplasmic reticulum stress and of the degradation of N-end rule and ubiquitin-fusion degradation pathway substrates in mammalian cells. *Molecular Biology of the Cell* **17**: 4606–4618.

Wong, D. (**2008**). Enzymatic deconstruction of backbone structures of the ramified regions in pectins. *The Protein Journal* **27**: 30–42.

Wood, Z.A., Schröder, E., Robin Harris, J., and Poole, L.B. (**2003**). Structure, mechanism and regulation of peroxiredoxins. *Trends in Biochemical Sciences* **28**: 32–40.

Wootton, J. and Federhen, S. (**1996**). Computer methods for macromolecular sequence analysis. (Academic Press Inc.,: San Diego, CA).

Worlock, A. and Smith, R. (**2002**). ZntB is a novel Zn2+ transporter in *Salmonella enterica* serovar *Typhimurium*. *Journal of bacteriology* **184**.

Wösten, H.A., van Wetter, M.A., Lugones, L.G., van der Mei, H.C., Busscher, H.J., and Wessels, J.G. (**1999**). How a fungus escapes the water to grow into the air. *Current Biology* **9**: 85–8.

Wright, J., Sugden, D., and Francis-McIntyre, S. (**2009**). Exploiting proteomic data for genome annotation and gene model validation in *Aspergillus niger*. *BMC Genomics* **14**: 1–14.

Wu, S., Tsai, J., Lai, M., and Ng, L. (**2007**). *Armillariella mellea* shows anti-inflammatory activity by inhibiting the expression of NO, iNOS, COX-2 and cytokines in THP-1 cells. *The American Journal of Chinese Medicine* **35**: 507–516.

Vanden Wymelenberg, A., Gaskell, J., Mozuch, M., Kersten, P., Sabat, G., Martinez, D., and Cullen, D. (**2009**). Transcriptome and secretome analysis of *Phanerochaete chrysosporium* reveal complex patterns of gene expression. *Applied and Environmental Microbiology* **75**: 4058–4068.

Vanden Wymelenberg, A., Gaskell, J., Mozuch, M., Sabat, G., Ralph, J., Skyba, O., Mansfield, S.D., Blanchette, R.A., Martinez, D., Grigoriev, I., Kersten, P.J., and Cullen, D. (**2010**). Comparative transcriptome and secretome analysis of wood decay fungi *Postia placenta* and *Phanerochaete chrysosporium. Applied and Environmental Microbiology* **76**: 3599–610.

Vanden Wymelenberg, A., Minges, P., Sabat, G., Martinez, D., Aerts, A., Salamov, A., Grigoriev, I., Shapiro, H., Putnam, N., Belinky, P., Dosoretz, C., Gaskell, J., Kersten, P., and Cullen, D. (**2006**). Computational analysis of the *Phanerochaete chrysosporium* v2.0 genome database and mass spectrometry

identification of peptides in ligninolytic cultures reveal complex mixtures of secreted proteins. *Fungal Genetics and Biology* **43**: 343–56.

Xu, J., Linning, R., Fellers, J., Dickinson, M., Zhu, W., Antonov, I., Joly, D.L., Donaldson, M.E., Eilam, T., Anikster, Y., Banks, T., Munro, S., Mayo, M., Wynhoven, B., Ali, J., Moore, R., McCallum, B., Borodovsky, M., Saville, B., and Bakkeren, G. (**2011**). Gene discovery in EST sequences from the wheat leaf rust fungus *Puccinia triticina* sexual spores, asexual spores and haustoria, compared to other rust and corn smut fungi. *BMC Genomics* **12**: 161.

Yafetto, L., Davis, D.J.J., and Money, N.P.P. (**2009**). Biomechanics of invasive growth by *Armillaria* rhizomorphs. *Fungal Genetics and Biology* **46**: 688–69.

Yajima, W. and Kav, N.N. V (**2006**). The proteome of the phytopathogenic fungus *Sclerotinia sclerotiorum*. *Proteomics* **6**: 5995–6007.

Yan, L., Côte, P., Li, X.-X., Jiang, Y.-Y., and Whiteway, M. (**2012**). PalI domain proteins of *Saccharomyces cerevisiae* and *Candida albicans. Microbiological Research* **167**: 422–32.

Yang, H., Mikami, Y., Imai, T., and Taguchi, H. (**2001**). Extrusion of fluorescein diacetate by multidrug • resistant *Candida albicans*. *Mycoses* **374**: 368–374.

Yang, J., Chen, Y., Feng, X., Yu, D., He, C., Zheng, Q., and Liang, X. (**1989**). Isolation and structure elucidation of armillaricin1. *Planta Medica* **55**: 564–5.

Yang, J.S., Su, Y., Wang, Y., Feng, X., Yu, D., Cong, P., Tamai, M., Obuchi, T., Kondoh, H., and Liang, X. (**1989**). Isolation and structures of two new sesquiterpenoid aromatic esters: armillarigin and armillarikin1. *Planta Medica* **55**: 479–81.

Yang, J.S., Su, Y.L., Wang, Y.L., Feng, X.Z., Yu, D.Q., and Liang, X.T. (**1990**). Studies on the chemical constituents of *Armillaria mellea* mycelium. V. Isolation and characterization of armillarilin and armillarinin. *Yao Xue Xue Bao* **25**: 24–8.

Yang, X.Q., Zhao, X.X., Liu, C.Y., Zheng, Y., and Qian, S.J. (**2009**). Decolorization of azo, triphenylmethane and anthraquinone dyes by a newly isolated *Trametes* sp. SQ01 and its laccase. *Process Biochemistry* **44**: 1185–1189.

Yates, J.R. (**1998**). Mass Spectrometry and the Age of the Proteome. *Journal of Mass Spectrometry* **33**: 1–19.

Yildirim, V., Özcan, S., Becher, D., Büttner, K., and Özcengiz, G. (**2011**). Characterization of proteome alterations in *Phanerochaete chrysosporium* in response to lead exposure. *Proteome Science* **9**: 12.

Yoo, C., Ahn, K., Park, J.E., Kim, M.-J., and Jo, S.A. (**2010**). An aminopeptidase from *Streptomyces* sp. KK565 degrades β amyloid monomers, oligomers and fibrils. *FEBS Letters* **584**: 4157–62.

Yoon, H., Mikami, B., Hashimoto, W., and Murata, K. (**1999**). Crystal Structure of Alginate Lyase A1-III from *Sphingomonas* Species A1 at 1.78 angstrom Resolution. *Journal of Molecular Biology* **290**: 505–514.

Young, S.N. (**2007**). How to increase serotonin in the human brain without drugs. *Journal of Psychiatry & Neuroscience* **32**: 394–9.

Yuen, K., Chan, C., and Chan, K. (**2001**). Characterization of AFMP1: a novel target for serodiagnosis of aspergillosis. *Journal of Clinical Microbiology* **39**: 3830–3837.

Zdobnov, E.M. and Apweiler, R. (**2001**). InterProScan-an integration platform for signature-recognition methods in InterPro. *Bioinformatics* **17**: 847–848.

Zeng, G.-M., Chen, A.-W., Chen, G.-Q., Hu, X.-J., Guan, S., Shang, C., Lu, L.-H., and Zou, Z.-J. (**2012**). Responses of *Phanerochaete chrysosporium* to toxic pollutants: physiological flux, oxidative stress, and detoxification. *Environmental Science & Technology* **46**: 7818–25.

Zerbino, D.R. and Birney, E. (**2008**). Velvet: algorithms for *de novo* short read assembly using de Bruijn graphs. *Genome Research* **18**: 821–9.

Zhang, X.-H., Zhong, W.Q., and Widholm, J.M. (**2005**). Expression of a fungal cyanamide hydratase in transgenic soybean detoxifies cyanamide in tissue culture and in planta to provide cyanamide resistance. *Journal of Plant Physiology* **162**: 1064–73.

Zheng, A., Lin, R., Zhang, D., Qin, P., Xu, L., Ai, P., Ding, L., Wang, Y., Chen, Y., Liu, Y., Sun, Z., Feng, H., Liang, X., Fu, R., Tang, C., Li, Q., Zhang, J., Xie, Z., Deng, Q., Li, S., *et al.* (**2013**). The evolution and pathogenic mechanisms of the rice sheath blight pathogen. *Nature Communications* **4**: 1424.

Zhou, T.-B. and Qin, Y.-H. (**2013**). Signaling pathways of prohibitin and its role in diseases. *Journal of Receptor and Signal Transduction Research* **33**: 28–36.

Zhu, Z., Gao, Y., Zhu, Z., Yu, Y., Zhang, X., Zang, J., Teng, M., and Niu, L. (**2009**). Structural basis of the autolysis of AaHIV suggests a novel target recognizing model for ADAM/reprolysin family proteins. *Biochemical and Biophysical Research Communications* **386**: 159–64.

Zuck, K., Shipley, S., and Newman, D. (**2011**). Induced Production of N-Formyl Alkaloids from *Aspergillus fumigatus* by Co-culture with *Streptomyces peucetius*. *Journal of Natural Products* **74**: 1653–1657.